INTERDISCIPLINARY APPROACHES TO IMPROVE QUALITY OF SOFT FRUIT BERRIES

EDITED BY: Brian Farneti, Francesco Emanuelli, Kevin M. Folta, Chad Elliott Finn, Lara Giongo, Massimo Iorizzo and Peter Toivonen

PUBLISHED IN: Frontiers in Plant Science

frontiers Research Topics

ISSN 1664-8714
ISBN 978-2-88966-135-0
DOI 10.3389/978-2-88966-135-0

About Frontiers

Frontiers is more than just an open-access publisher of scholarly articles: it is a pioneering approach to the world of academia, radically improving the way scholarly research is managed. The grand vision of Frontiers is a world where all people have an equal opportunity to seek, share and generate knowledge. Frontiers provides immediate and permanent online open access to all its publications, but this alone is not enough to realize our grand goals.

Frontiers Journal Series

The Frontiers Journal Series is a multi-tier and interdisciplinary set of open-access, online journals, promising a paradigm shift from the current review, selection and dissemination processes in academic publishing. All Frontiers journals are driven by researchers for researchers; therefore, they constitute a service to the scholarly community. At the same time, the Frontiers Journal Series operates on a revolutionary invention, the tiered publishing system, initially addressing specific communities of scholars, and gradually climbing up to broader public understanding, thus serving the interests of the lay society, too.

Dedication to Quality

Each Frontiers article is a landmark of the highest quality, thanks to genuinely collaborative interactions between authors and review editors, who include some of the world's best academicians. Research must be certified by peers before entering a stream of knowledge that may eventually reach the public - and shape society; therefore, Frontiers only applies the most rigorous and unbiased reviews.
Frontiers revolutionizes research publishing by freely delivering the most outstanding research, evaluated with no bias from both the academic and social point of view. By applying the most advanced information technologies, Frontiers is catapulting scholarly publishing into a new generation.

What are Frontiers Research Topics?

Frontiers Research Topics are very popular trademarks of the Frontiers Journals Series: they are collections of at least ten articles, all centered on a particular subject. With their unique mix of varied contributions from Original Research to Review Articles, Frontiers Research Topics unify the most influential researchers, the latest key findings and historical advances in a hot research area! Find out more on how to host your own Frontiers Research Topic or contribute to one as an author by contacting the Frontiers Editorial Office: researchtopics@frontiersin.org

INTERDISCIPLINARY APPROACHES TO IMPROVE QUALITY OF SOFT FRUIT BERRIES

Topic Editors:
Brian Farneti, Fondazione Edmund Mach, Italy
Francesco Emanuelli, Fondazione Edmund Mach, Italy
Kevin M. Folta, University of Florida, United States
Chad Elliott Finn, United States Department of Agriculture (USDA), United States
Lara Giongo, Fondazione Edmund Mach, Italy
Massimo Iorizzo, North Carolina State University, United States
Peter Toivonen, Agriculture and Agri-Food Canada (AAFC), Canada

Citation: Farneti, B., Emanuelli, F., Folta, K. M., Finn, C. E., Giongo, L., Iorizzo, M., Toivonen, P., eds. (2020). Interdisciplinary Approaches to Improve Quality of Soft Fruit Berries. Lausanne: Frontiers Media SA. doi: 10.3389/978-2-88966-135-0

Table of Contents

frontiers in Plant Science

EDITORIAL
published: 10 September 2020
doi: 10.3389/fpls.2020.592222

Editorial: Interdisciplinary Approaches to Improve Quality of Soft Fruit Berries

Brian Farneti[1], Francesco Emanuelli[1], Lara Giongo[1], Peter Toivonen[2], Massimo Iorizzo[3], Kevin Folta[4] and Chad Finn[5]*

[1] Genomics and Biology of Fruit Crop Department, Fondazione Edmund Mach, San Michele all'Adige, Italy, [2] Summerland Research and Development Centre, Agriculture and Agri-Food Canada, Summerland, BC, Canada, [3] Department of Horticultural Science, North Carolina State University, Raleigh, NC, United States, [4] Horticultural Sciences Department, University of Florida, Gainesville, FL, United States, [5] Horticultural Crops Research Unit, Agricultural Research Service, United States Department of Agriculture, Corvallis, OR, United States

Keywords: quality, breeding, omics analyses, vaccinium, rubus, fragaria, postharvest, nutraceutical

Editorial on the Research Topic

Interdisciplinary Approaches to Improve Quality of Soft Fruit Berries

OPEN ACCESS

Edited by:
Nadia Bertin,
INRA Plantes et Système de cultures Horticoles, France

Reviewed by:
Zhanwu Dai,
Chinese Academy of Sciences, China
Bruno Mezzetti,
Marche Polytechnic University, Italy

****Correspondence:***
Brian Farneti
Brian.farneti@fmach.it

Specialty section:
This article was submitted to Crop and Product Physiology, a section of the journal Frontiers in Plant Science

Received: *06 August 2020*
Accepted: *26 August 2020*
Published: *10 September 2020*

Citation:
Farneti B, Emanuelli F, Giongo L, Toivonen P, Iorizzo M, Folta K and Finn C (2020) Editorial: Interdisciplinary Approaches to Improve Quality of Soft Fruit Berries. Front. Plant Sci. 11:592222. doi: 10.3389/fpls.2020.592222

Improving the fruit quality is a chief target to support the rising global economic importance of berry crops (Di Vittori et al., 2018). Quality of soft fruit berries is a complex trait, which includes visual attractiveness (color, size, and shape), overall flavor (taste and texture), and nutritional properties. Among these traits, texture, flavor, and appearance directly impact postharvest performance and consumer appreciation and therefore fruit marketability. Although the importance of these factors can hardly be underestimated, breeding efforts have historically been mainly oriented to improve fruit appearance and storability. However, selection for improved shelf-life and appearance properties, and inappropriate postharvest strategies, may have unintended negative consequences on other fruit quality traits, for instance, aroma and nutritional value. This quality decline can be heightened by the fact that breeding selection for flavor occurs nearly by chance (not assisted), since flavor and nutraceutical content are currently not considered as a discriminating trait in the early selection phase (Klee and Tieman, 2018). This limitation is also reinforced by the fact that complex and time-consuming phenotyping protocols are ordinarily used, making the analytical screening of large populations plant material unrealistic (Folta and Klee, 2016). This Research Topic has aimed to collect the most recent advances on scientific progress concerning the quality of soft fruit berries, in particular strawberry (*Fragaria ananassa*), blueberry (*Vaccinium* spp.), and raspberry (*Rubus idaeus*). These studies focused on innovative technologies and multidisciplinary approaches of quality management throughout the entire production chain, from breeding selection to consumer consumption.

In this article collection authors have discussed the importance of developing chemical and molecular markers to assist breeding selection, in particular for three main features: controlling of the flowering period (Jibran et al.), improving quality and storability (Farneti et al.), and increasing the nutraceutical content (Mengist et al.). The study of Jibran et al. focused on raspberry (*Rubus idaeus*) and blackberry (*Rubus* subgenus *Rubus*) segregating populations and discovered that two major loci (RiAF3 and RiAF4) and a region located on the upper arm of LG7 are controlling the annual-fruiting (AF) trait in *Rubus*. AF varieties of *Rubus* are able to flower and fruit in one growing season, without the occurring dormant period required in biennial-fruiting varieties. Molecular

assisted selection of accessions with the AF trait would be beneficial for a more sustainable and schedulable *Rubus* production.

The studies of Farneti et al. and Mengist et al. were mainly focused on discovery the metabolic and quality variability among blueberry (*Vaccinium* spp.) genotypes, to provide a framework to uncover the genetic basis of bioactive compounds and fruit quality traits useful to advance blueberry-breeding programs focusing on integrating these traits. The exploitation of the genetic variability existing within the blueberry germplasm collection allowed Farneti et al. to identify the best performing cultivars to be used as superior parental lines for future breeding programs, based on texture and volatile organic compounds (VOCs) variability. In particular, the comprehensive characterization of blueberry aroma by direct injection mass spectrometry technique allowed the identification of a wide array of VOCs that can be used as putative biomarkers to rapidly evaluate the blueberry aroma variations related to genetic differences and storability.

Mengist et al. assessed the variability of different nutraceutical metabolites among blueberry accessions of three ploidy levels (diploid, tetraploid, and hexaploid). Results of that study revealed a moderate to high broad sense heritability for many metabolites, suggesting a strong role of genetic factors in controlling these traits in blueberry fruit. In addition, despite a relevant fruit size-dependent variation for anthocyanin content, metabolite concentrations and fruit size, to a certain degree, can be improved simultaneously in breeding programs. Regulation of anthocyanin production in blueberry fruit was further investigated by Günther et al. By linking the accumulation patterns of phenolic metabolites with gene transcription in Northern Highbush (*Vaccinium corymbosum*) and Rabbiteye (*Vaccinium virgatum*) blueberry, they found that flavonoid production was generally lower in fruit flesh compared with skin and concentrations further declined during maturation. A common set of structural genes was identified across both species, indicating that tissue-specific flavonoid biosynthesis was dependent on co-expression of multiple pathway genes and limited by the phenylpropanoid pathway in combination with CHS, F3H, and ANS as potential pathway bottlenecks. Moreover, they identified several candidate transcriptional regulators that were co-expressed with structural genes, including the activators MYBA, MYBPA1, and bHLH2 together with the repressor MYBC2, which suggested an interdependent role in anthocyanin regulation.

Anthocyanin content was considerably improved with preharvest agronomic practices in grapevine berry and strawberry in the studies of Pereira et al. and Zuñiga et al., respectively. Pereira et al. found that trunk girdling applied at veraison, in "Cabernet Sauvignon" wine grapes (*Vitis vinifera* L.) increased anthocyanin and flavonol concentrations in skin/pulp tissues of grape berries without affecting primary metabolites. Trunk girdling trials might be applied to change the source-sink relationship on blueberry as already reported by Jorquera-Fontena et al. (2016). Zuñiga et al. demonstrated that increasing the number of methyl jasmonate preharvest applications (maximum three treatments) on strawberry (*Fragaria ananassa* "Camarosa") improved the anthocyanin, proanthocyanidin, and ascorbic acid content of the fruit, as well as the antioxidant-related enzymatic activity during postharvest storage.

Improving the storability and the acceptance period of berry fruit is of chief importance, being the short commercial life one of the strong limiting factor of berries. Even if fruit storability is often regulated by genetic differences (Farneti et al.) and/or preharvest agronomic practices (Zuniga et al.) optimized postharvest methods are needed. Tosetti et al. elucidated the role of ethylene in strawberry postharvest physiology. Continuous exposure to ethylene induced an accumulation of abscisic acid in the receptacle tissue, followed by an increase in CO_2 production. Ethylene also elicited sucrose hydrolysis and malic acid catabolism, with the major effect seen after 4 days of ethylene exposure. Additionally, ethylene treatment induced an accumulation of phenolics (epicatechin and chlorogenic acid). Ethylene can intensely affect quality of harvested products. These effects can be beneficial or deleterious depending on the product, its ripening stage, and its desired use. Thus, new strategies for controlling ethylene production are needed. Shu et al. proved that 1-MCP treatment could effectively maintain the quality of the "Laiyang" pear during cold storage, and the additional application of ethephon on fruits during shelf-life managed to restore volatile aromas in pear fruits after long-term storage. Postharvest storability of blueberry, instead, was significantly improved by the development of an innovative controlled atmosphere (CA) approach, proposed by Falagán et al., based on gradually reaching the optimal storage concentrations (GCA). This methodology allowed the reduction of blueberry respiratory metabolism when compared to standard CA and control treatments. This had a positive impact on quality parameters such as sugars, organic acids, firmness and decay incidence.

Understanding the stability of each quality trait during different storage and/or agronomical conditions may allow a better definition of future breeding strategies aimed at the selection of accessions suitable to improve distinct market sector performance. For this purpose, comprehensive investigations and a tight synergy of analytical approaches, from different branches of knowledge, are needed. The expanded use of inexpensive, high-quality, and high throughput omics techniques is expected to soon provide elucidation of the genetic and physiological regulation of fruit quality.

The completion of this work is overshadowed by the tragic loss of one of its co-editors. In his 26 years, Dr. Chad Finn served as a world-renowned berry-crop breeder, contributing to the release of 51 cultivars in blackberry, red and black raspberry, strawberry, blueberry, and other crops as part of the USDA-ARS and Oregon State University. We will miss his internationally respected collegiality and work ethic, his industry-leading cultivars, and professional contributions to the discipline. But most of all, we will miss his kind guidance and mentoring, his booming laugh, and his bone-crushing hugs. We dedicate this Research Topic in Dr. Chad Finn's memory.

AUTHOR CONTRIBUTIONS

All authors listed have made a substantial, direct, and intellectual contribution to the work and approved it for publication.

REFERENCES

Di Vittori, L., Mazzoni, L., Battino, M., and Mezzetti, B. (2018). Pre-harvest factors influencing the quality of berries. *Sci. Hortic.* 233, 310–322. doi: 10.1016/j.scienta.2018.01.058

Folta, K. M., and Klee, H. J. (2016). Sensory sacrifices when we mass-produce mass produce. *Hort. Res.* 3, 16032. doi: 10.1038/hortres.2016.32

Jorquera-Fontena, E., Alberdi, M., Reyes-Díaz, M., and Franck, N. (2016). Rearrangement of leaf traits with changing source-sink relationship in blueberry (Vaccinium corymbosum L.) leaves. *Photosynthetica* 54, 508–516. doi: 10.1007/s11099-016-0207-9

Klee, H. J., and Tieman, D. M. (2018). The genetics of fruit flavour preferences. *Nat. Rev. Genet.* 19, 347–356. doi: 10.1038/s41576-018-0002-5

Conflict of Interest: The authors declare that the research was conducted in the absence of any commercial or financial relationships that could be construed as a potential conflict of interest.

frontiers in Plant Science

ORIGINAL RESEARCH
published: 25 October 2019
doi: 10.3389/fpls.2019.01341

Two Loci, *RiAF3* and *RiAF4*, Contribute to the Annual-Fruiting Trait in *Rubus*

*Rubina Jibran[1], Jessica Spencer[2], Gina Fernandez[2], Amparo Monfort[3,4], Mourad Mnejja[3,4], Helge Dzierzon[1], Jibran Tahir[1], Kevin Davies[1], David Chagné[1] and Toshi M. Foster[1]**

[1] The New Zealand Institute for Plant & Food Research Limited, Palmerston North Research Centre, Palmerston North, New Zealand, [2] Department of Horticultural Science, North Carolina State University, Raleigh, NC, United States, [3] IRTA (Institut de Recerca I Tecnologia Agroalimentàries), Barcelona, Spain, [4] Centre for Research in Agricultural Genomics (CRAG) CSIC-IRTA-UAB-UB, Barcelona, Spain

Most *Rubus* species have a biennial cycle of flowering and fruiting with an intervening period of winter dormancy, in common with many perennial fruit crops. Annual-fruiting (AF) varieties of raspberry (*Rubus idaeus* and *Rubus occidentalis* L.) and blackberry (*Rubus* subgenus *Rubus*) are able to flower and fruit in one growing season, without the intervening dormant period normally required in biennial-fruiting (BF) varieties. We used a red raspberry (*R. idaeus)* population segregating for AF obtained from a cross between NC493 and 'Chilliwack' to identify genetic factors controlling AF. Genotyping by sequencing (GBS) was used to generate saturated linkage maps in both parents. Trait mapping in this population indicated that AF is controlled by two newly identified loci (*RiAF3* and *RiAF4*) located on *Rubus* linkage groups (LGs) 3 and 4. The location of these loci was analyzed using single-nucleotide polymorphism (SNP) markers on independent red raspberry and blackberry populations segregating for the AF trait. This confirmed that AF in *Rubus* is regulated by loci on LG 3 and 4, in addition to a previously reported locus on LG 7. Comparative RNAseq analysis at the time of floral bud differentiation in an AF and a BF variety revealed candidate genes potentially regulating the trait.

Keywords: marker-assisted selection, primocane, floricane, comparative mapping, RNA sequencing, annual-fruiting, biennial-fruiting

OPEN ACCESS

Edited by:
Lara Giongo,
Fondazione Edmund Mach, Italy

Reviewed by:
Tae Kyung Hyun,
Chungbuk National University, South Korea
Maria Manuela Rigano,
University of Naples Federico II, Italy

****Correspondence:***
Toshi M. Foster
Toshi.Foster@plantandfood.co.nz

Specialty section:
This article was submitted to Crop and Product Physiology, a section of the journal Frontiers in Plant Science

Received: *11 June 2019*
Accepted: *26 September 2019*
Published: *25 October 2019*

Citation:
Jibran R, Spencer J, Fernandez G, Monfort A, Mnejja M, Dzierzon H, Tahir J, Davies K, Chagné D and Foster TM (2019) Two Loci, RiAF3 and RiAF4, Contribute to the Annual-Fruiting Trait in Rubus. Front. Plant Sci. 10:1341. doi: 10.3389/fpls.2019.01341

INTRODUCTION

The *Rosoideae* subfamily of Rosaceae contains many economically important soft berry crops, including red and black raspberry (*Rubus idaeus* and *Rubus occidentalis* L. respectively), blackberry (*Rubus* subgenus *Rubus*) and strawberry (*Fragaria* species), which are renowned for their taste and health properties (Potter et al., 2007; Hummer and Janick, 2009; Shi et al., 2013; Simpson, 2018). Raspberry (*Rubus* sp.) is a shrub that initiates shoots (canes) from a perennial root system (Keep, 1988; Carew et al., 2000; Sønsteby and Heide, 2009; Heide et al., 2013; Graham and Simpson, 2018). Biennial-fruiting (BF) raspberry varieties (also called floricane-fruiting or summer-fruiting) initiate axillary floral buds toward autumn of the first year of growth, but these do not develop into fruit until spring/summer of the following year. Annual-fruiting (AF) varieties (also called primocane-fruiting or autumn-fruiting) initiate flowers in late spring/early summer that develop into fruit from summer until late autumn of the same year. In both AF and BF varieties, flowering and fruiting

initiate from the shoot tip and develop basipetally after vegetative growth has stopped. The key developmental difference between the two flowering phenologies is that AF floral buds are initiated earlier and progress directly to fruit set, whereas floral initiation is normally followed by dormancy in BF types (Keep, 1988; Carew et al., 2000; Sønsteby and Heide, 2009; Heide et al., 2013).

Flowering time is controlled by complex interactions among endogenous factors, such as developmental pathways and hormones, as well as environmental cues, such as temperature and day length (Simpson and Dean, 2002; Song et al., 2018; Tabas-Madrid et al., 2018; Kinmonth-Schultz et al., 2019; Kozlov et al., 2019). A number of genes that integrate specific signals and either repress or activate flowering have been identified and characterized in model species, such as *Arabidopsis* and *Antirrhinum* (Simpson and Dean, 2002; Wigge et al., 2005; Khan et al., 2014; Blumel et al., 2015; Sasaki et al., 2015). Among these, CONSTANS (CO), FLOWERING LOCUS T (FT), SUPPRESSOR OF OVEREXPRESSION OF CONSTANS 1 (SOC1), FLOWERING LOCUS C (FLC), AGAMOUS1 (AG1), and LEAFY (LFY) are the best characterized flowering integrators (Yanofsky et al., 1990; Blazquez et al., 1997; Kardailsky et al., 1999; Kobayashi et al., 1999; Michaels and Amasino, 1999; Yoo et al., 2007; Deng et al., 2011; Pin and Nilsson, 2012; Song et al., 2018; Tabas-Madrid et al., 2018). For example, CO activates flowering under long days in both FLC-dependent and independent manners by activating flower promoters *FT* and *SOC1* (Kim et al., 2008; Michaels and Amasino, 2001). FLC regulates floral transition by repressing the key genes of flowering pathway, for example, *FT* and *SOC1* (Simpson and Dean, 2002; Crevillen and Dean, 2011). FLC antagonizes the flowering pathway in a dose-dependent manner, with FLC abundance being regulated by an interplay between epigenetic factors and RNA-processing factors, such as polyadenylation and splicing (Simpson, 2004). Recently, it was shown that CO accelerates flowering under long days but represses flowering under very short days (3 hours light) by regulating *FT* expression (Luccioni et al., 2019).

Although there is little information on the genes controlling flowering in raspberry, more is known about the environmental cues that stimulate flowering. For example, floral induction in BF varieties is triggered by a combination of decreased temperatures and shorter photoperiod (Fejer and Spangelo, 1974; Dale and Daubeny, 1987; Carew et al., 2000; Sønsteby and Heide, 2009; Hodnefjell et al., 2018). Although there is no absolute requirement for AF varieties to experience chilling in the prior season to initiate flowering, as newly initiated canes can progress through fruiting in a single season, the expression of AF in terms of floral consistency across canes and the total number of flowers is strongly influenced by chilling (Sønsteby and Heide, 2009).

Modern AF varieties of red and black raspberry have complex pedigrees because of interspecific hybridization with other *Rubus* species during their development, including *R. arcticus*, *R. odoratus*, and *R. spectabilis* (Keep, 1988; Lewers et al., 2005; Dossett et al., 2012). Many studies have been conducted to study the genetic inheritance of AF in raspberry and blackberry, along with an analogous continuous flowering trait in strawberry. Continuous or perpetual flowering in commercial strawberry (*Fragaria* × *ananassa*) is controlled by quantitative trait loci (QTLs) on linkage groups (LGs) 3, 4, and 7 (Gaston et al., 2013; Perrotte et al., 2016; Hackett et al., 2018), whereas AF in blackberry and red raspberry was suggested to be controlled by a recessive monogenic trait (Lewis, 1939; Haskell, 1960; Lopez-Medina et al., 2000). Castro et al. (2013) reported that in auto-tetraploid blackberry, this recessive locus was located on LG7.

Lewis (1939) demonstrated that the AF trait is controlled by a single recessive locus, later named "af" (Haskell, 1960). However, trait segregation analysis performed on various AF populations suggested an alternative possibility of multiple loci having minor effects on the expression of AF (Slate, 1940; Waldo and Darrow, 1941; Oberle and Moore, 1952; Ourecky, 1976; Fejer, 1977; Barrientos and Rodriguez, 1980). For example, Barrientos and Rodriguez (1980) suggested the possibility of partial dominance for the AF cultivar 'Malling Exploit.' Similarly, Fejer (1977) reported that inheritance of AF in mapping populations raised from a series of diallelic crosses among seven red raspberry cultivars was predominately additive and proposed that the genetic control for the trait could not be recessive. Thus, the genetic regulation of AF in raspberry is still unclear.

To address this issue, we constructed saturated linkage maps for the AF accession NC493 and the BF cultivar 'Chilliwack' to map genetic loci associated with control of AF. Trait mapping in this population indicated that AF is controlled by two newly identified loci (*RiAF3* and *RiAF4*) located on *Rubus* LGs 3 and 4. The location of these loci was verified in independent red raspberry and blackberry populations segregating for AF. In addition, we compared the transcriptomes of AF and BF axillary buds to identify candidate genes involved with the transcriptional regulation of the AF trait.

MATERIALS AND METHODS

Plant Material and Assessment of Fruiting Phenotype

A segregating population of 131 F_1 individuals was developed from a controlled cross made in 2004 between AF accession NC493 (*R. parvifolius* x *R. idaeus* 'Cherokee') and BF 'Chilliwack' (CW) (*R. idaeus*). The seedling population was planted in 2006 at the Sandhills Research Station, Jackson Springs, NC, USA. In 2008, the 131 NC493 x CW progeny were assessed biweekly from July to September for the presence or absence of AF by determining whether flowers or fruits were present on the primocanes (canes initiated that season). The population was again evaluated in 2009 for AF on a weekly to biweekly basis from June to August, except for two individuals that died over the winter.

Three families of red raspberry (*R. idaeus*), x16.093, x16.109, and x16.111 of 47, 55, and 49 individuals, respectively, were developed from controlled crosses between AF and BF parents within the Plant & Food Research (PFR) breeding program and planted in 2017 at the PFR site located at Motueka, New Zealand. These populations were phenotyped for the presence of AF in 2018.

A tetraploid blackberry (*R.* subgenus *Rubus*) mapping population (C1) was generated from a cross between BF RM44 and AF RM63 from the IRTA-PLANASA breeding program. The population was planted in 2015 at Cartaya, Spain. The parents and progeny were phenotyped for the presence of AF in 2016 and 2017.

Genotyping by Sequencing

High molecular weight DNA was extracted from 100 mg of leaf tissue from each individual in the 131 progeny in the NC493 x CW family using a standard CTAB protocol (Doyle and Doyle, 1987). The genotyping by sequencing (GBS) method of Elshire et al. (2011) was used to obtain reduced representation of the genomes for the two parents and progeny of 83 individuals. The GBS library preparation protocol was first optimized for the red raspberry genome by digesting DNA from a few individuals with *Ape*K1, as described by Elshire et al. (2011). GBS libraries were then constructed for 83 individuals and the two parents. The libraries from 83 individuals were combined to make the final pooled library. The quantity and quality checks of the individual libraries and the pooled library were performed using a Qubit Fluorometer and a Fragment analyser, respectively. The pooled DNA library was dried and sent to the Australian Genome Research Facility for sequencing on two lanes of the Illumina HiSeq2500 platform using single-end sequencing chemistry.

The sequencing reads were demultiplexed based on GBS library preparation bar codes using the ea-utils.1.1.2-537 package (Richardson, 2013), and those reads starting with the approved bar code immediately followed by the remnant of the *Ape*K1 cleavage site sequence were retained for further analysis. The bar coded reads meeting the initial read quality criteria were aligned to the *R. occidentalis* genome assembly of ORUS 4115-3 v3.0 (Vanburen et al., 2018) (https://www.rosaceae.org/analysis/268) using Burrows-Wheeler Aligner (bwa/0.7.17) (Li and Durbin, 2009). Single-nucleotide polymorphism (SNP) calling and GBS data filtering were performed using the GATK pipeline (gatk/3.8.0) (McKenna et al., 2010) using default parameters. The GBS pipeline used to create a set of markers is available on Github at https://jupyterhub.powerplant.pfr.co.nz/user/cfprxj/notebooks/cfprxj/bioinf_Braspberry_GBS/Variant_calls_Braspberry_GATK_pipeline.ipynb. GATK_GBS analysis yielded a total of 284,146 SNPs between the two parents.

Preparation of GBS Markers for Linkage Analysis

The SNP data were filtered and formatted for appropriate genetic segregation codes using MS Excel (Microsoft Corporation, USA). Markers segregating abxaa, aaxab, and abxab were selected for each parent using GATK and MS Excel. Homozygous SNP calls, such as A/A, G/G, T/T, and C/C, were converted into *aa* marker type, whereas heterozygous SNP calls (such as A/G, A/T, C/T, etc.) were converted into the *ab* marker type. Joinmap v5.0® (Van Ooijen and Voorrips, 2001) was used to develop genetic linkage maps for each parent of the NC493 x CW population. A LOD score >6 was employed for grouping. Due to the high number of markers on each linkage group, the markers were then filtered based on chi-square values ranging from 0.1 to 7.0, and these selected loci were subsequently used to reconstruct the maps using regression mapping (Kosambi mapping function).

Trait Mapping

Trait mapping was initially performed by including the AF phenotypes of both years in the GBS data set using Joinmap v5.0® (Van Ooijen and Voorrips, 2001). As the phenotypes in the CW x NC493 population were scored as a presence-absence of AF, which is not quantitative and cannot be used for QTL mapping with methods such as interval mapping, a chi-square test was performed on all GBS markers that were heterozygous in only one parent to identify markers linked to AF. Chi-square values for the significant differences between the expected allelic frequencies and the observed allelic frequencies were calculated with the formula:

$$X^2 = \Sigma^k i = 1\ [\left(\text{observed value}_i - \text{expected value}_i\right)^2 / \text{expected value}_i]$$

GBS markers with chi-square test values between 5 and 20 and p values <0.05 were selected for identification of QTLs controlling to the trait. This filtering criterion yielded 26,925 abxaa markers that are heterozygous for the NC493 parent and 6,571 aaxab markers that are heterozygous for the CW parent. The markers that are heterozygous for one parent and homozygous for other parent were used for QTL mapping.

Further mapping was performed using abxaa markers (heterozygous for AF parent) located around the AF loci on the NC493 parental map. The phase of these markers was calculated using Joinmap v5.0® (Van Ooijen and Voorrips, 2001), and they were ordered according to their physical location on the ORUS 4115-3 v3.0 *R. occidentalis* genome assembly (Vanburen et al., 2018). Bins of 10 to 12 markers within focal points spanning no more than 100 kb physical intervals were manually inspected. Focal points were evenly spaced throughout the region flanking the *RiAF4* locus at 0.1, 2, 3.1, 3.6, 3.8, 4.1, 4.5, 6, and 8 megabase pairs (Mb). Likely genotypic errors due to allelic dropout, a common feature in GBS data for heterozygous species and detectable as a single change in phase within a linked focal point, were manually corrected. A consensus genotype was then imputed for each focal point and compared to the neighboring focal points. The linkage between each focal point and the AF phenotype was examined to delimitate the most likely genomic interval flanking the AF loci.

High-Resolution Melting Marker Development

SNPs that were closely associated with the AF loci were selected from the GBS data set for the NC493 x CW population for transformation into high-resolution melting (HRM) quantitative PCR markers. PCR primer pairs were designed to span amplicons ranging from 70 to 150 basepairs (bp) flanking the selected SNPs using Primer3 (http://frodo.wi.mit.edu/primer3/). The following criteria were employed for primer pair design: max self-complementarity and max 3' self-complementarity were set to 4 and 1, respectively; GC content of the primers ranged from 40 to 55%. SNP analysis (Liew et al., 2004) was performed on a LightCycler480 instrument (Roche Diagnostics), and amplifications were performed using the PCR mix and conditions described in Guitton et al. (2011). Outputs were analyzed using the LightCycler480 SW1.5 software. Heterozygous genotypes were identified as having a lower melting temperature in comparison with homozygous genotypes and a shoulder in

the melting peaks. HRM markers, which were heterozygous and homozygous for the AF and BF parent, respectively, were screened over the x16.093, x16.109, and x16.111 populations, and association between the HRM genotypes and the presence of the AF trait was assessed using a chi-square test.

Simple Sequence Repeat Marker Development and Screening

PCR primers for simple sequence repeats (SSRs) from *Rubus* were developed close to the chromosomal regions associated with the loci of interest identified in the NC493 x CW raspberry population, as well as the LG 7 locus identified in blackberry by Castro et al. (2013). SSRs were screened over the C1 blackberry population using a Hitachi ABI3500 Applied Biosystems genetic analyzer (Foster City, CA, USA). Association between the SSR alleles and the presence of the AF trait was determined using a chi-square test.

RNAseq and Differential Gene Expression Analysis

Total RNA was extracted from axillary buds 5–10 nodes below the apex of 'Heritage' and 'Wakefield,' which are AF and BF, respectively. The cultivars were grown together in the field under standard conditions at the PFR orchard at Motueka, New Zealand. Bud samples were collected on November 5 (spring/early summer). Tissue was snap-frozen in liquid nitrogen, and total RNA was extracted from three biological replicates of each cultivar, as described in Janssen et al. (2008). The quality and concentration of the RNA samples were assessed using a Fragment Analyzer (Agilent, Santa Clara, CA, USA), and only samples with an RNA Integrity Number higher than 8 were sequenced. Library preparation was completed at the Australian Genome Research Facility using the TruSeq Stranded kit, and subsequent paired-end Illumina® sequencing employed the NovaSeq6000 platform, with the S2 flow cell. An average of ~19 million, 150-bp paired-end reads was retrieved for each sample (~6 Gb of data). Read sequences of low-quality ribosomal RNA and adaptors were filtered out using Trimmomatic (Bolger et al., 2014) and SortMeRna (Kopylova et al., 2012). RNAseq reads were aligned to the *R. occidentalis* reference gene models (Vanburen et al., 2018) using Spliced Transcripts Alignment to a Reference (STAR), and differential expression analysis was performed using DESeq2 (Love et al., 2014). All RNAseq data, read statistics, and differentially expressed genes (DEGs) are deposited in NCBI's Gene Expression Omnibus (Edgar et al., 2002) and are accessible through GEO Series accession number GSE135907 (https://www.ncbi.nlm.nih.gov/geo/query/acc.cgi?acc = GSE135907). Significant DEGs were selected using a threshold of $\alpha < -0.005$ with an adjusted p value of <0.01 and a $|\log2 \text{ fold change}| > 1$. *Arabidopsis* orthologues were determined by BLAST against the TAIR database.

RESULTS

Phenotypic Segregation for AF in Raspberry

The segregating population of 131 F_1 individuals from the NC493 x CW (AF x BF) cross was assessed for the AF trait over two consecutive years. The observed segregation ratio for AF : BF phenotypes were 55:76 and 66:65 in 2008 and 2009, respectively. Thirty-three phenotypes were inconsistent between years. The subset of the population with consistent AF and BF phenotypes between years was used for GBS analysis. Out of 98 individuals sampled, five did not yield sufficient DNA for GBS and could not be analyzed further. The final set (93 individuals) used for GBS library preparation contained 42 and 51 with AF and BF phenotypes, respectively (**Table S1**).

GBS of the NC493 x 'Chilliwack' Segregating Population

Two lanes of Illumina HiSeq2500 single-end 100 bp reads generated a total amount of 50,515,918,100 bp sequences and 505,159,381 total reads. The removal of adapters and filtering of low-quality reads yielded 46,822,022,484 bp (92% of the total data). The GBS libraries for eight individuals failed to produce any sequencing data. In total, 85 GBS libraries from the progeny and two duplicates of each parent yielded an average number of ~5.8 million reads per individual that were used for read alignment against the *R. occidentalis* genome assembly ORUS 4115-3 v3.0 (Vanburen et al., 2018) (https://www.rosaceae.org/analysis/268). SNP calling identified 284,146 SNPs in total (**Table 1**). Further filtering of the SNP data was applied to remove loci that had more than 10% missing data and were monomorphic or ambiguous. These filtering criteria yielded a total of 48,002 abxaa and 16,440 aaxab SNPs heterozygous for NC493 and CW, respectively. An additional 5,821 abxab type markers were generated between the parents, resulting in 70,263 SNP markers in total.

Map Construction

Linkage maps were constructed for both parents (**Figures 1** and **2**; **Table 2**). The NC493 map comprised 473 markers that spanned the seven LGs, and extended over 378.1 cM, with an average distance of 0.8 cM between markers (**Figure 1**). LG4 had the greatest number of markers (80), LG5 had the fewest number of markers (33), and LG4 was the longest (108.7 cM). The CW parental map was constructed from 419 markers that spanned the seven *Rubus* LGs and covered 251.6 cM, with an average distance of 0.6 cM between markers (**Figure 2**). LG5 had the greatest number of markers (74), and LG7 had fewest markers (27). LG5 was the longest group, with 74 markers covering 75.96 cM.

TABLE 1 | Summary of single-nucleotide polymorphism (SNP) markers obtained by genotyping by sequencing of a mapping population derived from NC493 x 'Chilliwack' (CW).

Parents	Total SNPs identified by GBS between parents	Monomorphic SNPs + markers with 10% missing data	abxaa SNPs	abxab SNPs
NC493	284,146	230,323	48,002	5,821
CW		261,885	16,440	

abxaa type markers are heterozygous in one parent and homozygous in the other parent. abxab type markers are heterozygous for both parents.

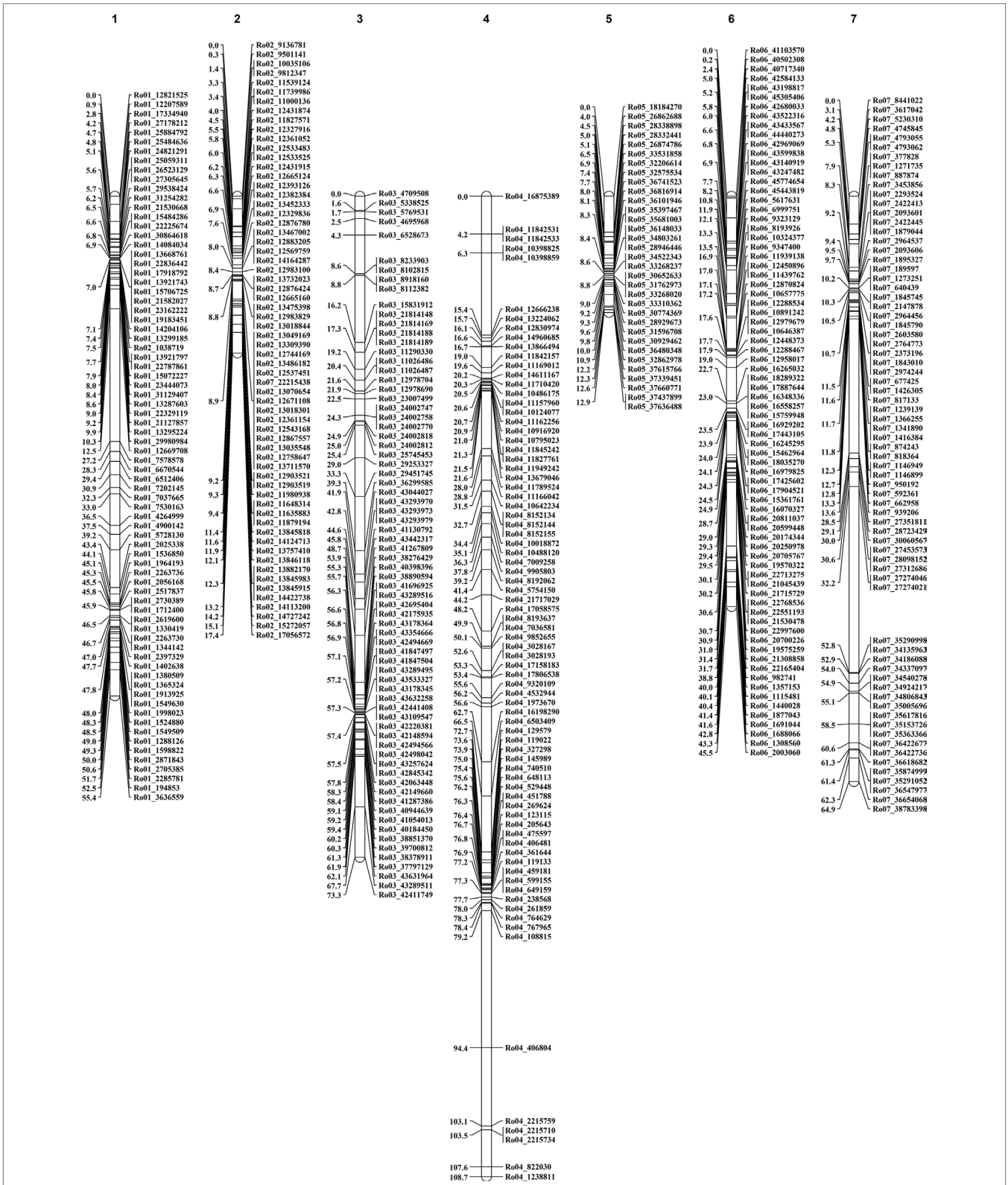

FIGURE 1 | *Rubus idaeus* genetic map for Annual-Fruiting (AF) parent NC493. The vertical bars represent linkage groups, and the lines across the bars represent genotyping by sequencing (GBS) marker position in the map. The scale on the left represents the genetic distance in centiMorgans (cMs). Only markers that segregated according to the Mendelian ratio at $p < 0.005$ were employed for the map construction with Joinmap v5.0® (Van Ooijen and Voorrips, 2001). Each SNP marker was named according its physical position (right-hand side) in the genome.

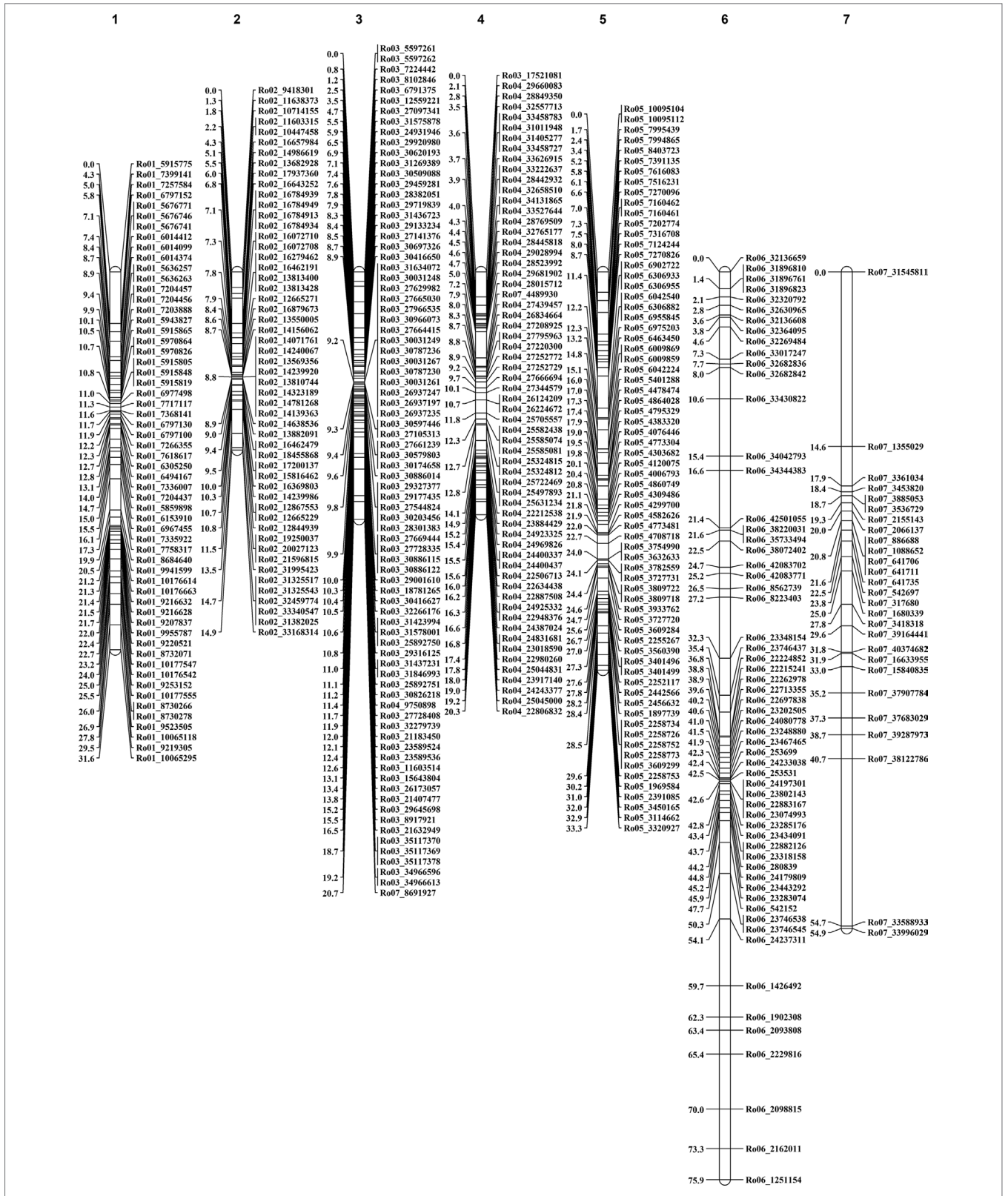

FIGURE 2 | *Rubus idaeus* linkage map for Biennial-Fruiting (BF) parent 'Chilliwack'. Each linkage group (represented by a vertical bar) was constructed using SNP loci generated by genotyping by sequencing (GBS). The lines across the bars represent marker positions in the map, and the scale on the right represents the genetic distance in centiMorgan (cM). All markers segregated according to the Mendelian ratio at $p < 0.005$, and markers were named according to their physical positions in the genome (right-hand side of each LG). The maps were generated in Joinmap v5.0® (Van Ooijen and Voorrips, 2001).

TABLE 2 | Summary of the linkage groups (LG) constructed for NC493 (Annual-Fruiting, AF) and 'Chilliwack' (CW, Biennial-Fruiting, BF) parents and the number of markers identified per LG.

Linkage groups	Number of loci mapped in the NC493 map	Number of loci mapped in the CW map
1	75	58
2	64	53
3	73	83
4	80	64
5	33	74
6	76	60
7	72	27
Total markers	473	419

The LGs were constructed by using the SNP markers obtained from a NC493 x 'Chilliwack' mapping population.

Trait Locus Mapping for AF

The AF trait was not significantly associated with any markers on the saturated CW (BF) linkage map when the AF phenotypes for both years were included in the GBS data set used in map construction. Because the phenotypes were scored qualitatively as presence–absence of AF, they could not be used for interval mapping of QTLs. Hence, the chi-square test was performed on heterozygous GBS markers for each parent to identify markers linked to the AF phenotype (**Table S2**). The analysis of markers heterozygous for NC493 identified two genomic regions, located on LGs 3 and 4, that were significantly associated (LOD > 4) with AF (**Figure 3**). These two new loci were named *RiAF3* and *RiAF4* for *R. idaeus* AF, located on LGs 3 and 4 of NC493, respectively. The GBS markers chr3_41,124,650 and chr4_4,076,592 are those most significantly linked to *RiAF3* and *RiAF4*, respectively. A third locus on LG5 may be present; however, none of the markers were associated with the trait with a LOD score greater than 4. No linkage with phenotype was found for the markers that were informative for CW.

Examination of the genotypes of 85 individuals over segments of chromosomes 3 and 4 spanning the SNP markers with the most significant LOD scores enabled us to determine the genotypes of the population between 35.1 to 43.7 Mb of chromosome 3 and 0 to 8 Mb of chromosome 4. The mapping analysis using a bin map based on the number of recombinants over a window of 8 Mb indicated that *RiAF4* is located in an interval between 3.50 Mb and 4.38 Mb (**Figure 4**). We were unable to perform similar mapping analysis for *RiAF3* because the order of markers on the linkage map was not colinear with the ORUS 4115-3 v3.0 genome.

Analysis of *QTLs* in Three Independent Populations of Red Raspberry

The phenotypes of parents and number of progeny in the three independent populations segregating for the AF trait are shown in **Table 3**. HRM-based markers were developed by designing PCR

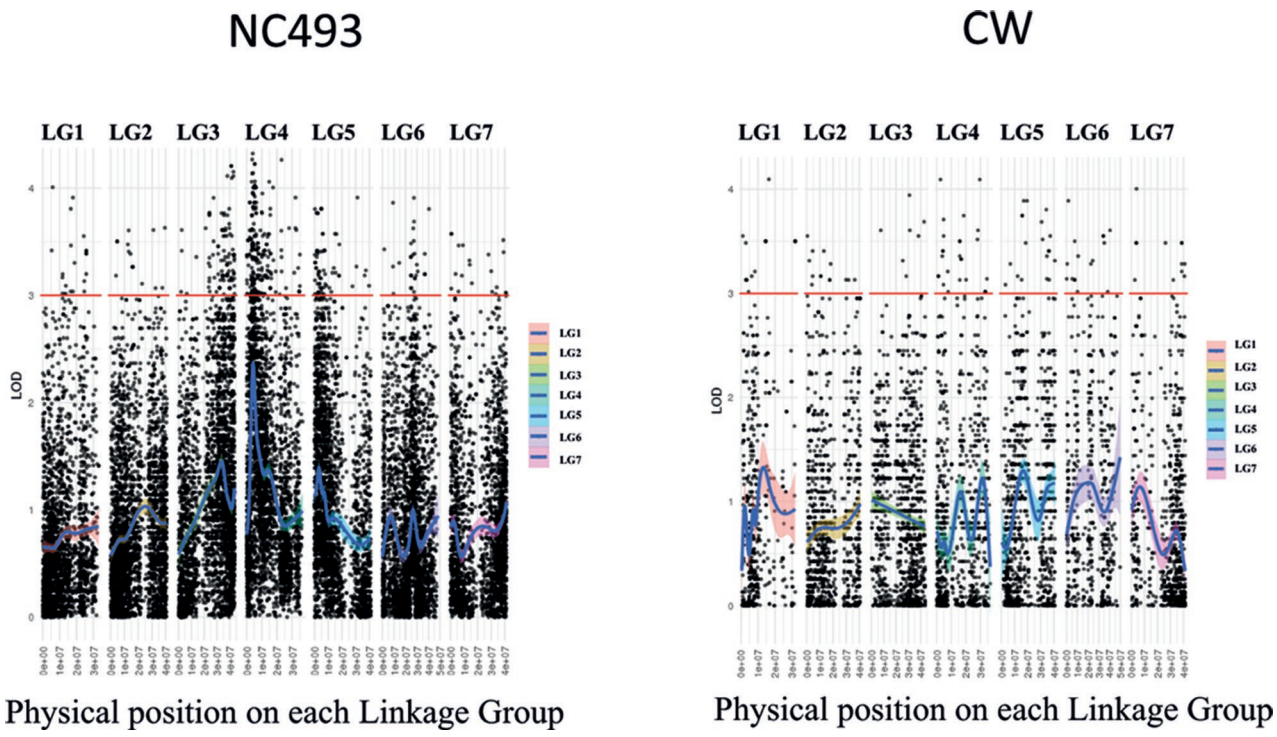

FIGURE 3 | Manhattan plot showing genomic regions associated with Annual-Fruiting (AF) in *Rubus idaeus*. Genotyping by sequencing (GBS)-based single-nucleotide polymorphism (SNP) markers significantly linked to the trait was identified by the chi-square test using markers that were heterozygous in NC493 (AF) and homozygous in 'Chilliwack' (Biennial-Fruiting, BF). The x-axis shows LOD scores, and the y-axis indicates the physical position of markers (black points) in the genome divided into seven linkage groups (LGs). The names and the physical position of the markers associated with control of AF are given in **Supplementary Table S2**. CW = 'Chilliwack'.

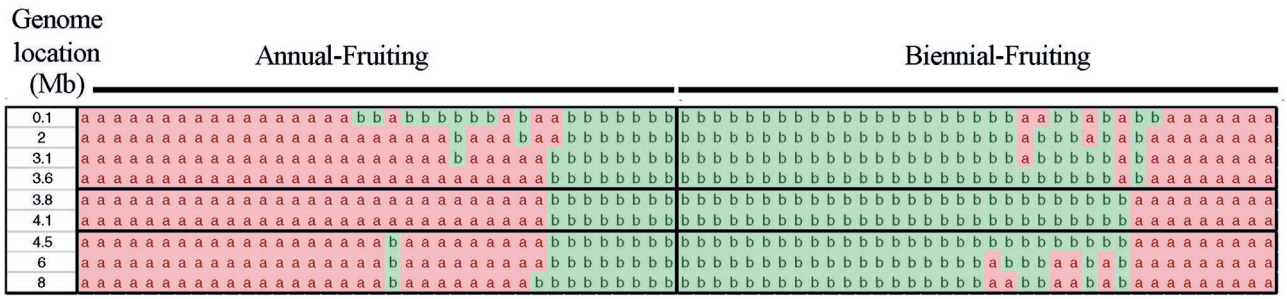

FIGURE 4 | Fine mapping the *RiAF4* locus. A bin map was created by analyzing the genotypes of individuals over small genomic regions located within 0–8 Mb of LG4. Each column represents genotypic data from a single individual, either Annual-Fruiting (AF) or Biennial-Fruiting (BF). The allele of single-nucleotide polymorphisms (SNPs) in the genomic region of LG4 listed in the first column is indicated as a or b. The "a" allele (in pink) and "b" allele (in green) are linked to AF and BF, respectively. Recombination breakpoints are visible as a change in color and narrow the *RiAF4* locus to the region located between 3.6 and 4.1Mb indicated by black horizontal lines.

TABLE 3 | Summary of red raspberry (*R. idaeus*) populations segregating for the Annual-Fruiting (AF) trait.

Population	Female parent	Male parent	Total progeny size	AF individuals in progeny	BF individuals in progeny	Chi-square value	P value
x16.093	Z12041-2 (AF)	Z12022-7 (BF)	47	23	24	.01	.950
x16.109	Z12027-13 (AF)	Z12022-7 (BF)	55	32	23	.73	.75
x16.111	Z12027-13 (AF)	Z12011-8 (BF)	49	30	19	1.23	.75

These populations were used for validating RiAF3 and RiAF4 loci. Seedlings were planted in spring of 2017 at the Plant & Food Research site located at Motueka, New Zealand, and were scored for AF in the summer of 2018. BF, Biennial-Fruiting.

primer pairs that flanked the most closely linked SNPs on LG3 and LG4 and near the Rubus285a maker on LG7 (**Table S3**). These markers were screened over the three populations (**Figure 5**). In x16.093 and x16.109 populations, the chr3-9,188,040 marker is associated with the AF trait, with chi-square tests significant at 95% and 99% (d.f. = 1), respectively. In population x16.111, ch4-7,738,811 and chr7-4,042,651 markers are associated with the AF trait with chi-square test significance of 95% and 99% (d.f. = 1), respectively.

Screening of SSR Markers for *RiAF3*, *RiAF4*, and the LG7 locus in a Blackberry (*R.* subgenus *Rubus*) Population

To verify the two newly identified loci, we analyzed markers linked to AF in a tetraploid blackberry population (C1) segregating for the AF trait. In this population, 76 progenies were scored over two consecutive years as 12 AF and 64 BF (**Table S4**). The C1 population was screened with SSR markers from *R. idaeus* LGs 3, 4, and 7 (Castro et al., 2013), and only the LG3 marker Rubus285a was associated with AF (**Figure 6**). The data show that the 244-bp allele of Rubus285a from BF parent is linked to the BF phenotype. This allele is not present in the AF parent. No association between marker and phenotype was identified for markers located on LGs 4 and 7.

Candidate Genes Underlying *RiAF3* and *RiAF4*

The region of the ORUS 4115-3 v3.0 genome spanning from 35.1 to 43.7 Mb on LG3 contains 1,276 predicted gene models, and the region from 0 to 8 Mb on LG4 contains 1,399 gene models (**Table S5**). A number of genes in these intervals are involved with flowering time.

DEGs Between AF and BF Axillary Buds

To identify genes potentially involved with the transcriptional regulation of AF, we compared gene expression in axillary buds of AF 'Heritage' and BF 'Wakefield' in late spring. Of the DEG genes with a |log2fold change| > 1, 443 (2.22%) were upregulated, and 363 (1.8%) were downregulated in AF compared with BF. The majority of the DEGs are orthologues of genes identified in other species as being involved in reproduction, flower development, and defence responses against biotic and abiotic stress.

Table S6 shows the relative expression of all genes within the genomic intervals spanning the *RiAF3* and *RiAF4* loci. The genomic locations and biological functions of some of the most promising differentially expressed candidate genes are listed in **Table 4**. Within the *RiAF3* interval, a gene orthologous to *Arabidopsis JUMONJI 14* (*JMJ14*) was expressed 2-fold higher in AF relative to BF. In the *RiAF4* region, *PHYTOCHROME AND FLOWERING TIME 1* (*PFT*1), *FLOWERING LOCUS A* (*FCA*), and *AGAMOUS-LIKE 24* (*AGL24*) genes were all upregulated in AF, with *AGL24* having 5-fold higher transcript levels in AF relative to BF (**Figure 7**).

DISCUSSION

We report that AF is a complex genetic trait regulated by at least two loci on *R. idaeus* LGs 3 and 4, *RiAF3* and *RiAF4*. These novel loci are syntenic to QTLs identified in strawberry for control of

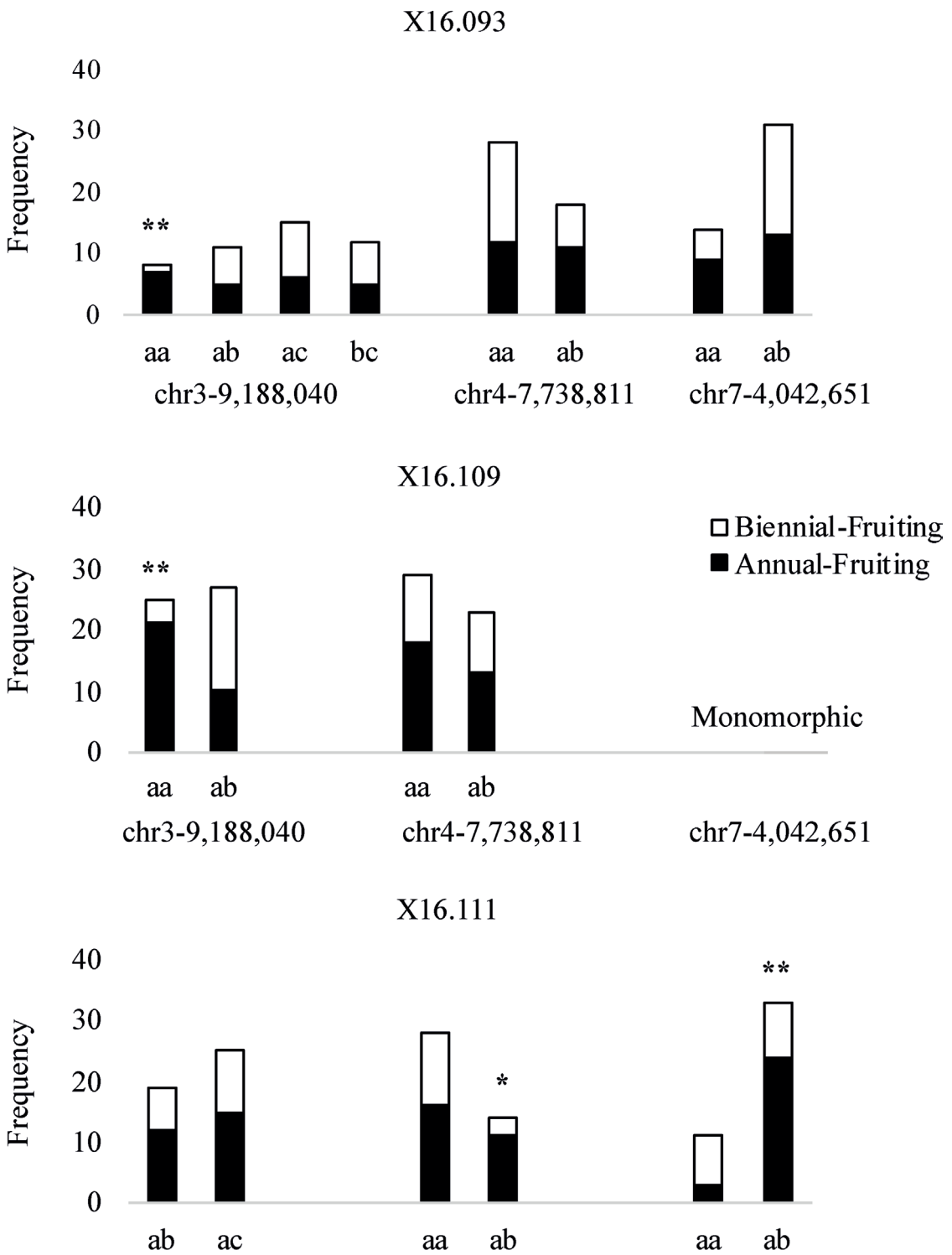

FIGURE 5 | Histograms showing allelic frequencies of SNP-based markers underlying quantitative trait loci in three independent red raspberry populations segregating for the Annual-Fruiting trait. The marker names indicate their chromosome and physical positions (in bp) on the *Rubus occidentalis* genome (Vanburen et al., 2018). The * and ** represent chi-square test significance of 95% and 99% (d.f. = 1), respectively. The marker chr7-4,042,651 was monomorphic in the x16.109 population.

A

Alleles present (frequency)	195 bp	197 bp	201 bp	244 bp	265 bp
AF parent	absent	present	present	absent	present
BF parent	present	present	present	present	absent
AF progeny (N=11)	6 (54%)	11 (100%)	6 (54%)	1 (9%)	7 (63%)
BF progeny (N=55)	25 (40%)	55 (100%)	42 (90%)	33 (55%)	38 (63%)

B

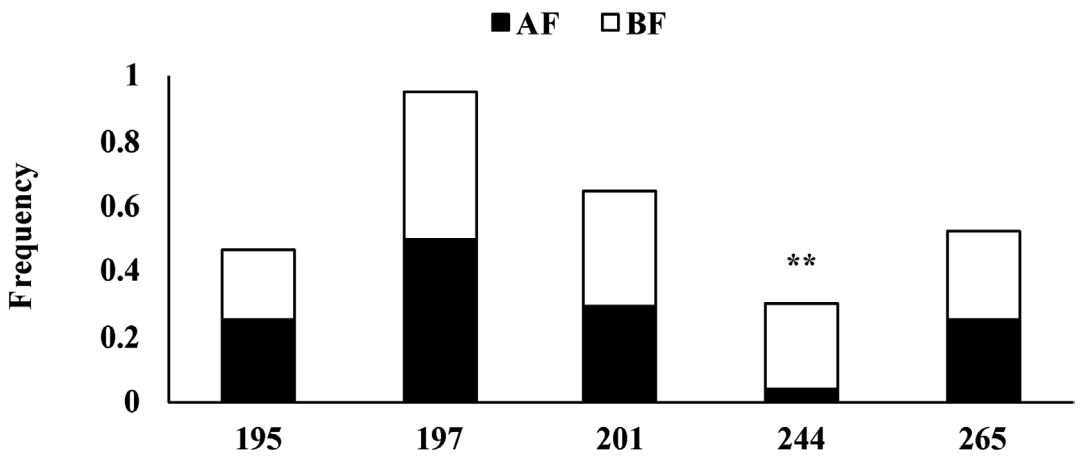

FIGURE 6 | Rubus285a marker segregation in a tetraploid blackberry mapping population segregating for Annual-Fruiting (AF). **(A)** Table showing the presence or absence of alleles in parents and the numbers of AF and Biennial-Fruiting (BF) progeny with each allele and the percentage in parentheses. The AF parent has three alleles with PCR product sizes of 197, 201, and 265 bp. The BF parent has four alleles with sizes of 195, 197, 201, and 244 bp. **(B)** Histogram showing allelic frequencies of the Rubus285a marker in the C1 blackberry population. The 244-bp allele is linked with BF trait with chi-square test significance of 99% (d.f. = 1) indicated by **.

recurrent flowering, suggesting conserved function across the *Rosoideae* subfamily. Markers linked to the newly discovered loci and to a locus previously identified on LG7 (Castro et al., 2013) were tested in independent raspberry and blackberry populations segregating for AF. In addition, we identified DEGs that may be involved in regulating the AF trait in *Rubus*.

Development of a High-Density Genetic Map of *R. idaeus*

GBS technology has greatly facilitated SNP discovery and genotyping for crop genetics (Crossa et al., 2013; He et al., 2014; İpek et al., 2016; Hackett et al., 2018). We used GBS-based SNP markers to develop a high-density genetic map of red raspberry. This new map is constructed with 70,263 SNP markers and is aligned with the genome assembly of black raspberry. In a previous study, a blackberry genetic map developed with 119 SSR markers in a mapping population segregating for AF (Castro et al., 2013) was employed to identify three markers linked to AF. However, one marker was 71cM from AF and, hence, unlinked. Furthermore, none of their LG7 markers mapped on the black raspberry genetic map of Bushakra et al. (2012) and the blackberry LG7 was assigned by default. It is possible that one of the other six LGs could have split and been mistakenly designated LG7 by Castro et al. (2013).

AF Is a Complex Genetic Trait

Castro et al. (2013) proposed that AF in blackberry was controlled by a single locus located on LG7. We were unable to map the AF phenotype as a single locus in the NC493 x CW population. A chi-square test of the thousands of markers detected by GBS identified two novel loci on LGs 3 and 4 for control of AF in red raspberry. The previous single locus hypothesis was largely based on the 3:1 (BF : AF) phenotypic

TABLE 4 | Differentially expressed candidate genes that underlie RiAF3 and RiAF4 loci.

***Rubus* gene model**	**Location in genome (bp)**	**Log2Foldchange (BF/AF)**	***Arabidopsis* hom ologue**	**Description**
Ro04_G19915	8,594,128	-0.28	AT4G16280	Flowering Control Locus A (FCA)
Ro04_G02642	4,485,423	-0.51	AT1G25540	Phytochrome and Flowering Time 1
Ro04_G36356	8,736,093	-1.75	AT4G24540	Agamous-like 24 (AGL24)
Ro03_G05776	35,959,751	-0.001	AT3G12680	Hua1, Enhancer of Ag-4 1
Ro03_G15781	37,388,564	-1.08	AT4G20400	Jumonji 14 (JMJ14)
Ro03_G33037	38,575,123	-0.88	AT1G30330	Auxin Response Factor 6 (ARF6)
Ro03_G13396	39,438,396	1.43	AT1G29390	Cold regulated thylakoid membrane
Ro03_G13391	39,478,286	-0.03	AT4G18130	Phytochrome E
Ro03_G05247	40,252,833	0.50	AT2G42610	Light Sensitive Hypocotyls 10
Ro03_G06544	40,834,857	-0.5	AT1G28330	Dormancy-Associated Protein-like 1
Ro03_G06488	41,189,726	-0.16	AT4G04920	Sensitive to Freezing 6

RNAseq was performed on axillary buds from three biological replicates each of 'Heritage' (Annual-Flowering) and 'Wakefield' (Biennial-Flowering). The physical location of each R. occidentalis gene model is given in bps (ORUS 4115-3 v3.0, Vanburen et al., 2018). The log2 fold change of 'Wakefield' relative to that of 'Heritage' is presented.

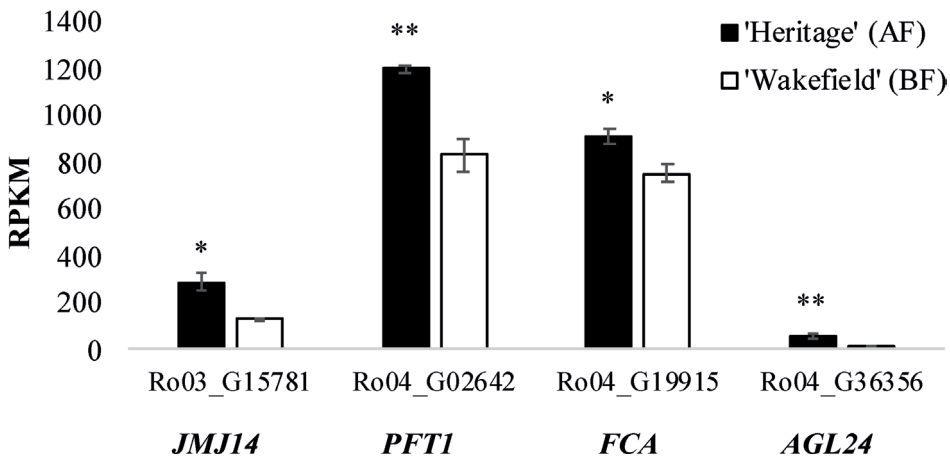

FIGURE 7 | Expression of flowering time genes located in *RiAF3* and *RiAF4* mapping intervals. RNA was collected from axillary buds in late spring from 'Heritage' (Annual-Fruiting, AF) and 'Wakefield' (Biennial-Flowering, BF). The x-axis shows RPKM (Reads Per Kilobase Million) for Ro03_G15781 (orthologous to *JUMONJI 14*, *JMJ14*), Ro04_G02642 (orthologous to *PHYTOCHROME AND FLOWERING TIME 1*, *PFT1*), Ro04_G19915 (orthologous to *FLOWERING CONTROL LOCUS A*, *FCA*), and Ro04_G36356 (orthologous to *AGAMOUS-LIKE 24*, *AGL24*). The columns represent the means of three biological replicates, and error bars are standard error of the mean. * and **indicate statistically significant differences ($P < 0.05$ and $P < 0.01$, respectively) between AF and BF using Student's *t*-test.

ratio observed in several populations but is unsupported by molecular marker data (Oberle and Moore, 1952; Keep, 1961). On the basis of the phenotypic data collected from intercrossing or selfing AF individuals, some studies have suggested a complex genetic basis for the trait (Lewis, 1939; Waldo and Darrow, 1941; Haskell, 1960; Fejer and Spangelo, 1974; Fejer, 1977). Various studies concluded that AF is controlled by a number of minor genes with predominant evidence that AF is a complex genetic trait controlled by loci on three LGs (*RiAF3*, *RiAF4*, and LG7). Recently, linkage analysis of 'Glen Moy' x 'Latham' raspberry population identified flower development QTLs on LGs 3, 5, and 7 (Hackett et al., 2018). These QTLs harbored genes involved in regulating flowering time. For example, FKF1, a regulator of CO expression, was mapped to LG7. Similarly, FT, EFL7 (a regulator of FLC levels), and COL9 (a regulator of CO levels) were mapped to LG3.

In this study, we found that LGs 3, 4, and 7 HRM markers were linked to the AF trait in red raspberry (**Figure 5**). An LG3 SSR marker (Rubus285a) was linked to the BF trait in blackberry (**Figure 6**). We were unable to verify all three loci in all of the populations, which could be due to one or more loci being fixed in a homozygous state in the parents, hence preventing detection of polymorphic markers linked to AF.

Our GBS data indicated that *RiAF3* is located at the bottom of chromosome 3 (**Figure 3**). However, the HRM marker that was developed from the most closely linked SNP is located on the upper arm of chromosome 3 (chr3-9,188,040). This discrepancy is likely due to errors in the assembly, and it is possible that the HRM marker position is incorrect. The populations used for the QTL analysis were relatively small, which would reduce the possibility of detecting several loci. This analysis should be repeated in one or more large

populations to more precisely identify the genomic intervals linked to AF.

RiAF3 and *RiAF4* Are Syntenic With Two Loci for Control of Recurrent Flowering in Strawberry

To extend the fruiting season, many international strawberry breeding programs are focusing on developing early, late, and perpetual (continuous) flowering cultivars. Comparative genomic studies between strawberry and raspberry have revealed a high degree of synteny between the genomes of two species (Bushakra et al., 2012; Jibran et al., 2018). Results from molecular studies also support a common molecular mechanism for control of flowering time among different Rosaceae species (Gaston et al., 2013; Honjo et al., 2016; Perrotte et al., 2016; Samad et al., 2017). Floral repressors, such as *Perpetual Flowering 1* and *Terminal Flower 1*, control perpetual flowering habits in strawberry. Seasonal flowering (SF) strawberry plants produce flowers only in autumn, whereas perpetual flowering (PF) plants flower over an extended time. The strawberry PF habit is under the control of a major QTL named *FaPFRU*, located on the lower arm of LG4 called LG4b-F (Gaston et al., 2013). This mapped region contains a floral activator gene orthologous to *Flowering Time* (*FT*) (Yoo et al., 2005). Perrotte et al. (2016) investigated the effect of *FaPFRU* on PF habit in 28 strawberry genotypes and found that the locus was linked to PF when analysis was carried out in both PF and SF genotypes. However, the analysis involving only PF genotypes did not detect linkage of *FaPFRU* with the PF trait; instead, a QTL located on LG3c-F (LG3c), associated with a late PF-intense phase, was identified. Hence, the authors concluded that PF in strawberry is regulated by multiple loci. It was postulated that *FaPFRU* regulates the switch between PF and SF, whereas the LG3c locus controls the intensity of flowering. Furthermore, Albani et al. (2004) suggested that the PF trait in woodland strawberry (*Fragaria vesca* L.) and cultivated strawberry are regulated by different genetic components. In woodland strawberry, two early flowering QTLs were identified on the upper and lower arm of LG4 (Samad et al., 2017).

The two novel loci *RiAF3* and *RiAF4* identified from the NC493 x CW population colocalize with the previously identified QTLs related to PF in strawberry. *FaPFRU* is located on the lower arm of LG4, whereas *RiAF4* locus is located at the upper arm of LG4. The difference in the genome positions between species might well be because parts of LG4 are inverted in raspberry compared to strawberry (Vanburen et al., 2018).

Candidate Genes Underlying *RiAF3* and *RiAF4*

JMJ14 is the best candidate for *RiAF3*. JMJ14 is a histone H3 lysine 4 (H3K4) demethylase, and H3K4 methylation is linked to transcription of key flowering time genes (Lu et al., 2010; Lu et al., 2011; Cui et al., 2016). The *Arabidopsis jmj14-1* mutant flowers early under short day conditions and has elevated levels of *LFY*, *FT*, and *AP1* transcripts (Jeong et al., 2009). Previous studies have indicated that demethylases are involved with the regulation of flowering time. Yang et al. (2012) found that *Arabidopsis* plants overexpressing *JMJ15*, a member of the *H3K4 demethylase JARID1* family, had accelerated flowering time. The early flowering phenotypes of the overexpression lines were associated with an increased *FT* expression and a decrease in H3K4me3 at the *FLC* locus that cause FLC repression. It has also been shown that *JMJ14* is required for gene silencing (Searle et al., 2010). Similarly, Zheng et al. (2019) found that *JMJ13* is a floral repressor that regulates *Arabidopsis* flowering timing in a temperature- and light-dependent manner.

The genomic region underlying the *RiAF4* locus contains three key genes that promote flowering, *PFT1* (Ro04_G02642), *FCA* (Ro04_G19915), and *AGL24* (Ro04_G36356) (Simpson et al., 2003; Turck et al., 2008; Michaels et al., 2003; Torti and Fornara, 2012). PFT1 is a nuclear protein that integrates various environmental cues into plant flowering pathway both in a *CO*-dependent and -independent manner (Liu et al., 2017). *PFT1* regulates flowering by increasing the transcript abundance of *CO* and *FT* (Iñigo et al., 2012). *FCA* is an RNA binding protein that downregulates expression of the floral repressor FCA by methylating central parts of the FLC gene (Liu et al., 2007). Reduced *FCA* function results in late flowering due to increased FLC activity, whereas overexpression of *FCA* causes early flowering, both in long and short day photoperiods (Liu et al., 2007). *AGL24* is a MADS-box transcription factor that regulates flower timing by inducing expression of the floral integrator SOC1 (Liu et al., 2008). *AGL24* loss-of-function mutants and plants with reduced *AGL24* transcript levels showed delayed flowering phenotypes, whereas overexpression of AGL24 resulted in early flowering phenotypes (Michaels et al., 2003; Yu et al., 2002). It was suggested that AGL24 controls flower timing in a dosage-dependent manner (Yu et al., 2002). Our finding that the raspberry orthologues of *PFT1, FCA*, and *AGL24* are upregulated in AF buds relative to BF makes each of them promising candidate genes in the control of AF.

CONCLUSION

We have presented the first evidence of loci linked to control of AF in *R. idaeus*. Our results suggest that two major loci *RiAF3* and *RiAF4* and a region located on the upper arm of LG7 control AF in *Rubus*. Additionally, we identified putative flowering time genes as candidates for functional validation. The genetic loci identified will be of value for marker-assisted selection of AF raspberries and blackberries following further validation in breeding germplasm.

DATA AVAILABILITY STATEMENT

All datasets for this study are included in the article/ **Supplementary Material**.

AUTHOR CONTRIBUTIONS

RJ, substantial contributions to the conception or design of the work; or the acquisition, analysis or interpretation of data for the work. JS, contribution to labwork and fieldwork. GH, acquisition, analysis or interpretation of data for the work. AM, acquisition, analysis or interpretation of data for the work. MM, contribution to labwork and fieldwork. HD, contribution to data analysis. JT, contribution to data analysis. KD, comments to the manuscript. DC, substantial contributions to the conception or design of the work; or

the acquisition, analysis or interpretation of data for the work. TF, substantial contributions to the conception or design of the work; or the acquisition, analysis or interpretation of data for the work.

ACKNOWLEDGMENTS

This project was funded by New Zealand Ministry of Business Innovation and Employment (MBIE) Strategic Science Investment Fund (SSIF) allocated to Plant & Food Research as part of the Discovery Science programs.

SUPPLEMENTARY MATERIAL

The Supplementary Material for this article can be found online at: https://www.frontiersin.org/articles/10.3389/fpls.2019.01341/full#supplementary-material

REFERENCES

Albani, M., Battey, N., and Wilkinson, M. (2004). The development of ISSR-derived SCAR markers around the SEASONAL FLOWERING LOCUS (SFL) in Fragaria vesca. *Theor. Appl. Genet.* 109, 571–579. doi: 10.1007/s00122-004-1654-4

Barrientos, F., and Rodriguez, J. A. (1980). "Transgressive segregation for winter chilling requirement in the red raspberry cultivar Malling Exploit", in: *Symposium on Breeding and Machine Harvesting of Rubus 112*, 21-24. doi: 10.17660/ActaHortic.1980.112.2

Blazquez, M. A., Soowal, L. N., Lee, I., and Weigel, D. (1997). LEAFY expression and flower initiation in Arabidopsis. *Development* 124, 3835–3844.

Blumel, M., Dally, N., and Jung, C. (2015). Flowering time regulation in crops - what did we learn from Arabidopsis? *Curr. Opin. Biotechnol.* 32, 121–129. doi: 10.1016/j.copbio.2014.11.023

Bolger, A. M., Lohse, M., and Usadel, B. (2014). Trimmomatic: a flexible trimmer for Illumina sequence data. *Bioinformatics* 30, 2114–2120. doi: 10.1093/bioinformatics/btu170

Bushakra, J. M., Stephens, M. J., Atmadjaja, A. N., Lewers, K. S., Symonds, V. V., Udall, J. A., et al. (2012). Construction of black (Rubus occidentalis) and red (R. idaeus) raspberry linkage maps and their comparison to the genomes of strawberry, apple, and peach. *Theor. Appl. Genet.* 125, 311–327. doi: 10.1007/s00122-012-1835-5

Carew, J. G., Gillespie, T., White, J., Wainwright, H., Brennan, R., and Battey, N. H. (2000). The control of the annual growth cycle in raspberry. *J. Hortic. Sci. Biotechnol.* 75, 495–503. doi: 10.1080/14620316.2000.11511275

Castro, P., Stafne, E., Clark, J., and Lewers, K. (2013). Genetic map of the primocane-fruiting and thornless traits of tetraploid blackberry. *Theor. Appl. Genet.* 126, 2521–2532. doi: 10.1007/s00122-013-2152-3

Crevillen, P., and Dean, C. (2011). Regulation of the floral repressor gene FLC: the complexity of transcription in a chromatin context. *Curr. Opin. Plant Biol.* 14, 38–44. doi: 10.1016/j.pbi.2010.08.015

Crossa, J., Beyene, Y., Kassa, S., Pérez, P., Hickey, J. M., Chen, C., et al. (2013). Genomic prediction in maize breeding populations with genotyping-by-sequencing. *G3: Genes, Genomes, Genet.* 3, 1903–1926. doi: 10.1534/g3.113.008227

Cui, X., Lu, F., Qiu, Q., Zhou, B., Gu, L., Zhang, S., et al. (2016). REF6 recognizes a specific DNA sequence to demethylate H3K27me3 and regulate organ boundary formation in Arabidopsis. *Nat. Genet.* 48, 694. doi: 10.1038/ng.3556

Dale, A., and Daubeny, H. A. (1987). Flower-Bud Initiation in Red Raspberry (Rubus-Idaeus L) in 2 Environments. *Crop Res.* 27, 61–66.

Deng, W. W., Ying, H., Helliwell, C. A., Taylor, J. M., Peacock, W. J., and Dennis, E. S. (2011). FLOWERING LOCUS C (FLC) regulates development pathways throughout the life cycle of Arabidopsis. *Proc. Natl. Acad. Sci. U.S.A.* 108, 6680–6685. doi: 10.1073/pnas.1103175108

Dossett, M., Bassil, N. V., Lewers, K. S., and Finn, C. E. (2012). Genetic diversity in wild and cultivated black raspberry (Rubus occidentalis L.) evaluated by simple sequence repeat markers. *Genetic Res. Crop Evol.* 59, 1849–1865. doi: 10.1007/s10722-012-9808-8

Doyle, J., and Doyle, J. (1987). Genomic plant DNA preparation from fresh tissue-CTAB method. *Phytochem. Bull.* 19, 11–15.

Edgar, R., Domrachev, M., and Lash, A. E. (2002). Gene Expression Omnibus: NCBI gene expression and hybridization array data repository. *Nucleic Acids Res.* 30, 207–210. doi: 10.1093/nar/30.1.207

Elshire, R. J., Glaubitz, J. C., Sun, Q., Poland, J. A., Kawamoto, K., Buckler, E. S., et al. (2011). A Robust, Simple Genotyping-by-Sequencing (GBS) approach for high diversity species. *PLoS One* 6, e19379. doi: 10.1371/journal.pone.0019379

Fejer, S. (1977). Inheritance of yield, yield components, and fall-fruiting habit in red raspberry diallel crosses. *Can. J. Genet. Cytol.* 19, 1–13. doi: 10.1139/g77-001

Fejer, S., and Spangelo, L. (1974). Three generations of inbreeding and S2 factorial test crosses in red raspberry cultivars. *Can. J. Genet. Cytol.* 16, 419–432. doi: 10.1139/g74-044

Gaston, A., Perrotte, J., Lerceteau-Kohler, E., Rousseau-Gueutin, M., Petit, A., Hernould, M., et al. (2013). PFRU, a single dominant locus regulates the balance between sexual and asexual plant reproduction in cultivated strawberry. *J. Exp. Bot.* 64, 1837–1848. doi: 10.1093/jxb/ert047

Graham, J., and Simpson, C. (2018). "Developmental transitions to fruiting in red raspberry," in *The Genomes of Rosaceous Berries and their Wild Relatives. Compendium of Plant Genomes*. Eds. T. Hytonen, J. Graham, and R. Harrison (Cham: Springer), 199–212. Chapter 14. doi: 10.1007/978-3-319-76020-9_14

Guitton, B., Kelner, J.-J., Velasco, R., Gardiner, S. E., Chagne, D., and Costes, E. (2011). Genetic control of biennial bearing in apple. *J. Exp. Bot.* 63, 131–149. doi: 10.1093/jxb/err261

Hackett, C. A., Milne, L., Smith, K., Hedley, P., Morris, J., Simpson, C. G., et al. (2018). Enhancement of Glen Moy x Latham raspberry linkage map using GbS to further understand control of developmental processes leading to fruit ripening. *BMC Genet.* 19, 59. doi: 10.1186/s12863-018-0666-z

Haskell, G. (1960). The raspberry wild in Britain. *Watsonia* 4, 238–255.

He, J., Zhao, X., Laroche, A., Lu, Z.-X., Liu, H., and Li, Z. (2014). Genotyping-by-sequencing (GBS), an ultimate marker-assisted selection (MAS) tool to accelerate plant breeding. *Front. Plant Sci.* 5, 484. doi: 10.3389/fpls.2014.00484

Heide, O., Stavang, J., and Sønsteby, A. (2013). Physiology and genetics of flowering in cultivated and wild strawberries–a review. *J. Hortic. Sci. Biotechnol.* 88, 1–18. doi: 10.1080/14620316.2013.11512930

Hodnefjell, R., Heide, O. M., Rivero, R., Remberg, S. F., and Sonsteby, A. (2018). Control of growth cessation and floral initiation in red raspberry (Rubus idaeus L.) cultivars of diverse origin in controlled and natural environments. *Sci. Hortic.* 233, 412–420. doi: 10.1016/j.scienta.2018.02.011

Honjo, M., Nunome, T., Kataoka, S., Yano, T., Hamano, M., Yamazaki, H., et al. (2016). Simple sequence repeat markers linked to the everbearing flowering gene in long-day and day-neutral cultivars of the octoploid cultivated strawberry Fragaria× ananassa. *Euphytica* 209, 291–303. doi: 10.1007/s10681-015-1626-6

Hummer, K. E., and Janick, J. (2009). "Rosaceae: taxonomy, economic importance, genomics," in *Genetics and genomics of Rosaceae* (New York: Springer), 1–17. doi: 10.1007/978-0-387-77491-6_1

Iñigo, S., Alvarez, M. J., Strasser, B., Califano, A., and Cerdán, P. D. (2012). PFT1, the MED25 subunit of the plant Mediator complex, promotes flowering through CONSTANS dependent and independent mechanisms in Arabidopsis. *Plant J.* 69, 601–612. doi: 10.1111/j.1365-313X.2011.04815.x

İpek, A., Yılmaz, K., Sıkıcı, P., Tangu, N. A., Öz, A. T., Bayraktar, M., et al. (2016). SNP discovery by GBS in olive and the construction of a high-density genetic linkage map. *Biochem. Genet.* 54, 313–325. doi: 10.1007/s10528-016-9721-5

Janssen, B. J., Thodey, K., Schaffer, R. J., Alba, R., Balakrishnan, L., Bishop, R., et al. (2008). Global gene expression analysis of apple fruit development from the floral bud to ripe fruit. *BMC Plant Biol.* 8, 16. doi: 10.1186/1471-2229-8-16

Jeong, J.-H., Song, H.-R., Ko, J.-H., Jeong, Y.-M., Kwon, Y. E., Seol, J. H., et al. (2009). Repression of FLOWERING LOCUS T chromatin by functionally redundant histone H3 lysine 4 demethylases in Arabidopsis. *PLoS one* 4, e8033. doi: 10.1371/journal.pone.0008033

Jibran, R., Dzierzon, H., Bassil, N., Bushakra, J. M., Edger, P. P., Sullivan, S., et al. (2018). Chromosome-scale scaffolding of the black raspberry (Rubus

occidentalis L.) genome based on chromatin interaction data. *Hortic. Res.* 5, 8. doi: 10.1038/s41438-017-0013-y

Jung, S., Ficklin, S. P., Lee, T., Cheng, C.-H., Blenda, A., Zheng, P., et al. (2013). The genome database for Rosaceae (GDR): year 10 update. *Nucleic Acids Res.* 42, D1237–D1244. doi: 10.1093/nar/gkt1012

Kardailsky, I., Shukla, V. K., Ahn, J. H., Dagenais, N., Christensen, S. K., Nguyen, J. T., et al. (1999). Activation tagging of the floral inducer FT. *Science* 286, 1962–1965. doi: 10.1126/science.286.5446.1962

Keep, E. (1961). Autumn-fruiting in raspberries. *J. Hortic. Sci.* 36, 174–185. doi: 10.1080/00221589.1961.11514013

Keep, E. (1988). Primocane (autumn)-fruiting raspberries - a review with particular reference to progress in breeding. *J. Hortic. Sci.* 63, 1–18. doi: 10.1080/14620316.1988.11515821

Khan, M. R., Ai, X. Y., and Zhang, J. Z. (2014). Genetic regulation of flowering time in annual and perennial plants. *Wiley Interdiscip. Rev. RNA* 5, 347–359. doi: 10.1002/wrna.1215

Kim, S. Y., Yu, X., and Michaels, S. D. (2008).). Regulation of CONSTANS and FLOWERING LOCUS T expression in response to changing light quality. *Plant Physiol.* 148, 269–279. doi: 10.1104/pp.108.122606

Kinmonth-Schultz, H. A., Macewen, M. J., Seaton, D. D., Millar, A. J., Imaizumi, T., and Kim, S.-H. (2019). An explanatory model of temperature influence on flowering through whole-plant accumulation of FT in Arabidopsis thaliana. *In Silico Plants*. 1, 1–22. doi: 10.1093/insilicoplants/diz006

Kobayashi, Y., Kaya, H., Goto, K., Iwabuchi, M., and Araki, T. (1999). A pair of related genes with antagonistic roles in mediating flowering signals. *Science* 286, 1960–1962. doi: 10.1126/science.286.5446.1960

Kopylova, E., Noé, L., and Touzet, H. (2012). SortMeRNA: fast and accurate filtering of ribosomal RNAs in metatranscriptomic data. *Bioinformatics* 28, 3211–3217. doi: 10.1093/bioinformatics/bts611

Kozlov, K., Singh, A., Berger, J., Bishop-Von Wettberg, E., Kahraman, A., Aydogan, A., et al. (2019). Non-linear regression models for time to flowering in wild chickpea combine genetic and climatic factors. *BMC Plant Biol.* 19, 94. doi: 10.1186/s12870-019-1685-2

Lewers, K., Styan, S., Hokanson, S., and Bassil, N. (2005). Strawberry GenBank-derived and genomic simple sequence repeat (SSR) markers and their utility with strawberry, blackberry, and red and black raspberry. *J. Am. Soc. Hortic. Sci.* 130, 102–115. doi: 10.21273/JASHS.130.1.102

Lewis, D. (1939). Genetical studies in cultivated raspberries. *J. Genet.* 38, 367–379. doi: 10.1007/BF02982182

Lewis, D. (1941). The relationship between polyploidy and fruiting habit in the cultivated raspberry. *Proc. 7th Int. Genet. Cong. Edinburgh, UK.* 1939, 190.

Li, H., and Durbin, R. (2009). Fast and accurate short read alignment with Burrows–Wheeler transform. *Bioinformatics* 25, 1754–1760. doi: 10.1093/bioinformatics/btp324

Liew, M., Pryor, R., Palais, R., Meadows, C., Erali, M., Lyon, E., et al. (2004). Genotyping of single-nucleotide polymorphisms by high-resolution melting of small amplicons. *Clin. Chem.* 50, 1156–1164. doi: 10.1373/clinchem.2004.032136

Liu, C., Chen, H., Er, H. L., Soo, H. M., Kumar, P. P., Han, J.-H., et al. (2008). Direct interaction of AGL24 and SOC1 integrates flowering signals in Arabidopsis. *Development* 135, 1481. doi: 10.1242/dev.020255

Liu, F., Quesada, V., Crevillén, P., Bäurle, I., Swiezewski, S., and Dean, C. (2007). The Arabidopsis RNA-binding protein FCA requires a lysine-specific demethylase 1 homolog to downregulate FLC. *Mol. Cell* 28, 398–407. doi: 10.1016/j.molcel.2007.10.018

Liu, J., Cheng, X. L., Liu, P., Li, D. Y., Chen, T., Gu, X. F., et al. (2017). MicroRNA319-regulated TCPs interact with FBHs and PFT1 to activate CO transcription and control flowering time in Arabidopsis. *PLoS Genet.* 13 (5), e1006833. doi: 10.1371/journal.pgen.1006833

Lopez-Medina, J., Moore, J. N., and McNew, R. W. (2000). A proposed model for inheritance of primocane fruiting in tetraploid erect blackberry. *J. Am. Soc. Hortic. Sci.* 125, 217–221.

Love, M. I., Huber, W., and Anders, S. (2014). Moderated estimation of fold change and dispersion for RNA-seq data with DESeq2. *Genome Biol.* 15, 550. doi: 10.1186/s13059-014-0550-8

Lu, F., Cui, X., Zhang, S., Jenuwein, T., and Cao, X. (2011). Arabidopsis REF6 is a histone H3 lysine 27 demethylase. *Nat. Genet.* 43, 715. doi: 10.1038/ng.854

Lu, F., Cui, X., Zhang, S., Liu, C., and Cao, X. (2010). JMJ14 is an H3K4 demethylase regulating flowering time in Arabidopsis. *Cell Res.* 20, 387. doi: 10.1038/cr.2010.27

Luccioni, L., Krzymuski, M., Sánchez-Lamas, M., Karayekov, E., Cerdán, P. D., and Casal, J. J. (2019). CONSTANS delays Arabidopsis flowering under short days. *Plant J.* 97, 923–932. doi: 10.1111/tpj.14171

McKenna, A., Hanna, M., Banks, E., Sivachenko, A., Cibulskis, K., Kernytsky, A., et al. (2010). The Genome Analysis Toolkit: a MapReduce framework for analyzing next-generation DNA sequencing data. *Genome Res.* 20, 1297–1303. doi: 10.1101/gr.107524.110

Michaels, S. D., and Amasino, R. M. (1999). FLOWERING LOCUS C encodes a novel MADS domain protein that acts as a repressor of flowering. *Plant Cell* 11, 949–956. doi: 10.1105/tpc.11.5.949

Michaels, S. D., and Amasino, R. M. (2001). Loss of FLOWERING LOCUS C activity eliminates the late-flowering phenotype of FRIGIDA and autonomous pathway mutations but not responsiveness to vernalization. *Plant Cell* 13, 935–941. doi: 10.1105/tpc.13.4.935

Michaels, S. D., Ditta, G., Gustafson-Brown, C., Pelaz, S., Yanofsky, M., and Amasino, R. M. (2003). AGL24 acts as a promoter of flowering in Arabidopsis and is positively regulated by vernalization. *Plant J.* 33, 867–874. doi: 10.1046/j.1365-313X.2003.01671.x

Oberle, G., and Moore, R. (1952). "Transmission of the autumn-fruiting character in crosses of red and black raspberries", in: Proceedings of the American Society for Horticultural Science, 235-237.

Ourecky, D. K. (1976). "Fall-bearing red raspberries, their future and potential", in: *Symposium on Breeding and Machine Harvesting of Rubus and Ribes 60*, 135-144. doi: 10.17660/ActaHortic.1976.60.18

Perrotte, J., Gaston, A., Potier, A., Petit, A., Rothan, C., and Denoyes, B. (2016). Narrowing down the single homoeologous FaPFRU locus controlling flowering in cultivated octoploid strawberry using a selective mapping strategy. *Plant Biotechnol. J.* 14, 2176–2189. doi: 10.1111/pbi.12574

Pin, P. A., and Nilsson, O. (2012). The multifaceted roles of FLOWERING LOCUS T in plant development. *Plant Cell Environ.* 35, 1742–1755. doi: 10.1111/j.1365-3040.2012.02558.x

Potter, D., Eriksson, T., Evans, R. C., Oh, S., Smedmark, J., Morgan, D. R., et al. (2007). Phylogeny and classification of Rosaceae. *Plant Syst. Evol.* 266, 5–43. doi: 10.1007/s00606-007-0539-9

Richardson, S. (2013). *"BioStudio"*. Lawrence Berkeley National Laboratory.

Samad, S., Kurokura, T., Koskela, E., Toivainen, T., Patel, V., Mouhu, K., et al. (2017). Additive QTLs on three chromosomes control flowering time in woodland strawberry (Fragaria vesca L.). *Hortic. Res.* 4, 17020. doi: 10.1038/hortres.2017.20

Sasaki, E., Zhang, P., Atwell, S., Meng, D., and Nordborg, M. (2015). MissingG x E variation controls flowering time in Arabidopsis thaliana. *PLoS Genet.* 11, e1005597. doi: 10.1371/journal.pgen.1005597

Searle, I. R., Pontes, O., Melnyk, C. W., Smith, L. M., and Baulcombe, D. C. (2010). JMJ14, a JmjC domain protein, is required for RNA silencing and cell-to-cell movement of an RNA silencing signal in Arabidopsis. *Genes Dev.* 24, 986–991. doi: 10.1101/gad.579910

Shi, S., Li, J., Sun, J., Yu, J., and Zhou, S. (2013). Phylogeny and classification of Prunus sensu lato (Rosaceae). *J. Integr. Plant Biol.* 55, 1069–1079. doi: 10.1111/jipb.12095

Simpson, D. (2018). "The Economic Importance of Strawberry CropsChapter 1," in *The Genomes of Rosaceous Berries and their Wild Relatives. Compendium of Plant Genomes*. Eds. T. Hytonen, J. Graham, and R. Harrison (Cham: Springer), 17–23. doi: 10.1007/978-3-319-76020-9_1

Simpson, G. G. (2004). The autonomous pathway: epigenetic and post-transcriptional gene regulation in the control of Arabidopsis flowering time. *Curr. Opin. Plant Biol.* 7, 570–574. doi: 10.1016/j.pbi.2004.07.002

Simpson, G. G., and Dean, C. (2002). Arabidopsis, the Rosetta stone of flowering time? *Science* 296, 285–289. doi: 10.1126/science.296.5566.285

Simpson, G. G., Dijkwel, P. P., Quesada, V., Henderson, I., and Dean, C. (2003). FY is an RNA 3′ end-processing factor that interacts with FCA to control the Arabidopsis floral transition. *Cell* 113, 777–787. doi: 10.1016/S0092-8674(03)00425-2

Slate, G. L. (1940). "Breeding autumn-fruiting raspberries", in: *Proceedings of the American Society for Horticultural Science*), 574-578.

Song, Y. H., Kubota, A., Kwon, M. S., Covington, M. F., Lee, N., Taagen, E. R., et al. (2018). Molecular basis of flowering under natural long-day conditions in Arabidopsis. *Nat. Plants* 4, 824. doi: 10.1038/s41477-018-0253-3

Song, Y., Gao, Z., and Luan, W. (2012). Interaction between temperature and photoperiod in regulation of flowering time in rice. *Sci. China Life Sci.* 55, 241–249. doi: 10.1007/s11427-012-4300-4

Sønsteby, A., and Heide, O. M. (2009). Effects of photoperiod and temperature on growth and flowering in the annual (primocane) fruiting raspberry (Rubus idaeus L.) cultivar 'Polka'. *J. Hortic. Sci. Biotechnol.* 84, 439–446. doi: 10.1080/14620316.2009.11512546

Tabas-Madrid, D., Méndez-Vigo, B., Arteaga, N., Marcer, A., Pascual-Montano, A., Weigel, D., et al. (2018). Genome-wide signatures of flowering adaptation to climate temperature: Regional analyses in a highly diverse native range of Arabidopsis thaliana. *Plant Cell Environ.* 41, 1806–1820. doi: 10.1111/pce.13189

Torti, S., and Fornara, F. (2012). AGL24 acts in concert with SOC1 and FUL during Arabidopsis floral transition. *Plant Signaling Behav.* 7, 1251–1254. doi: 10.4161/psb.21552

Turck, F., Fornara, F., and Coupland, G. (2008). Regulation and identity of florigen: FLOWERING LOCUS T moves center stage. *Annu. Rev. Plant Biol.* 59, 573–594. doi: 10.1146/annurev.arplant.59.032607.092755

Van Ooijen, J., and Voorrips, R. (2001). *"JoinMap 3.0, Software for the Calculation of Genetic Linkage Maps, Plant Research International"*. The Netherlands: Wageningen).

Vanburen, R., Wai, C. M., Colle, M., Wang, J., Sullivan, S., Bushakra, J. M., et al. (2018). A near complete, chromosome-scale assembly of the black raspberry (Rubus occidentalis) genome. *GigaScience* 7, giy094. doi: 10.1093/gigascience/giy094

Waldo, G. F., and Darrow, G. M. (1941). "Breeding autumn-fruiting raspberries under Oregon conditions", in: *Proceedings of the American Society for Horticultural Science*), 263-267.

Wigge, P. A., Kim, M. C., Jaeger, K. E., Busch, W., Schmid, M., Lohmann, J. U., et al. (2005). Integration of spatial and temporal information during floral induction in Arabidopsis. *Science* 309, 1056–1059. doi: 10.1126/science.1114358

Yang, H., Mo, H., Fan, D., Cao, Y., Cui, S., and Ma, L. (2012). Overexpression of a histone H3K4 demethylase, JMJ15, accelerates flowering time in Arabidopsis. *Plant cell Rep.* 31, 1297–1308. doi: 10.1007/s00299-012-1249-5

Yanofsky, M. F., Ma, H., Bowman, J. L., Drews, G. N., Feldmann, K. A., and Meyerowitz, E. M. (1990). The protein encoded by the arabidopsis homeotic gene agamous resembles transcription factors. *Nature* 346, 35–39. doi: 10.1038/346035a0

Yoo, S. K., Chung, K. S., Kim, J., Lee, J. H., Hong, S. M., Yoo, S. J., et al. (2005). Constans activates suppressor of overexpression of constans 1 through Flowering Locus T to promote flowering in Arabidopsis. *Plant Physiol.* 139, 770–778. doi: 10.1104/pp.105.066928

Yoo, S. Y., Kim, Y., Kim, S. Y., Lee, J. S., and Ahn, J. H. (2007). Control of flowering time and cold response by a NAC-domain protein in Arabidopsis. *PLoS One* 2 (7), e642. doi: 10.1371/journal.pone.0000642

Yu, H., Xu, Y., Tan, E. L., and Kumar, P. P. (2002). AGAMOUS-LIKE 24, a dosage-dependent mediator of the flowering signals. *Proc. Natl. Acad. Sci. U.S.A* 99, 16336–16341. doi: 10.1073/pnas.212624599

Zheng, S., Hu, H., Ren, H., Yang, Z., Qiu, Q., Qi, W., et al. (2019). The Arabidopsis H3K27me3 demethylase JUMONJI 13 is a temperature and photoperiod dependent flowering repressor. *Nat. Commun.*10, 1303 doi: 10.1038/s41467-019-09310-x

Conflict of Interest: Author RJ is employed by The New Zealand Institute for Plant & Food Research Limited. The remaining authors declare that the research was conducted in the absence of any commercial or financial relationships that could be construed as a potential conflict of interest.

frontiers in Plant Science

ORIGINAL RESEARCH
published: 12 March 2020
doi: 10.3389/fpls.2020.00174

Continuous Exposure to Ethylene Differentially Affects Senescence in Receptacle and Achene Tissues in Strawberry Fruit

*Roberta Tosetti, Fardusa Elmi, Inmaculada Pradas, Katherine Cools and Leon A. Terry**

Plant Science Laboratory, Cranfield University, Bedfordshire, United Kingdom

Strawberry shelf life is limited, and little is known about the postharvest regulation of senescence in different fruit tissues. Strawberry is classified as a non-climacteric fruit, yet it is known that ethylene affects strawberry ripening. Here the effects of continuous exogenous ethylene (50 μl l^{-1}) were investigated in cold stored strawberry (5°C). The physiological and biochemical responses of ripe strawberry were evaluated across 6 days, together with hormonal profiles of the whole fruit and individual tissues (achenes and receptacle). Continuous exposure to ethylene induced as a first response an accumulation of abscisic acid (ABA) in the receptacle tissue, followed by an increase in CO_2 production. Ethylene also elicited sucrose hydrolysis and malic acid catabolism, with the major effect seen after 4 days of ethylene exposure. Additionally, accumulation of phenolics (epicatechin and chlorogenic acid) were also observed in ethylene treated strawberry. Achenes did not exhibit a response to ethylene, yet catabolism of both ABA and auxins increased by two thirds during air storage. In contrast, ethylene induced ABA accumulation in the receptacle tissue without ABA catabolism being affected. This hormonal disequilibrium in response to ethylene between the two tissues was maintained during storage, and therefore might be the precursor for the following biochemical variations reported during storage.

Keywords: abscisic acid homeostasis, invertase, non-climacteric fruit, senescence precursor, ethylene

OPEN ACCESS

Edited by:
Brian Farneti, Fondazione Edmund Mach, Italy

Reviewed by:
Lida Fuentes-Viveros, Centro Regional de Estudios en Alimentos Saludables-CREAS, Chile
Amnon Lichter, Agricultural Research Organization (ARO), Israel

***Correspondence:**
Leon A. Terry
l.a.terry@cranfield.ac.uk

Specialty section:
This article was submitted to Crop and Product Physiology, a section of the journal Frontiers in Plant Science

Received: *28 November 2019*
Accepted: *05 February 2020*
Published: *12 March 2020*

Citation:
Tosetti R, Elmi F, Pradas I, Cools K and Terry LA (2020) Continuous Exposure to Ethylene Differentially Affects Senescence in Receptacle and Achene Tissues in Strawberry Fruit. Front. Plant Sci. 11:174. doi: 10.3389/fpls.2020.00174

INTRODUCTION

The high perishability of strawberry represents a bottleneck for expanding the fresh market supply chain (Terry et al., 2011). Strawberry is classified as a non-climacteric fruit and its ripening is mainly regulated by the abscisic acid (ABA)/auxins ratio (Moya-León et al., 2019). In particular, auxins have been associated with ripening inhibition, while ABA accumulation has been linked with promotion of strawberry fruit ripening (Jia et al., 2011; Symons et al., 2012; Leng et al., 2014; Chen et al., 2015; Chen et al., 2016; Giné-Bordonaba and Terry, 2016; Jia et al., 2016; Li et al., 2016b; Medina-Puche et al., 2016). Despite this, an increasing number of studies have highlighted that ethylene does affect the late stages of ripening (Gu et al., 2019). Confirmations of ethylene involvement in strawberry ripening are also supported by research using the ethylene binding

inhibitor, 1-methylcyclopropene (1-MCP) (Ku et al., 1999; Jiang et al., 2001; Bower et al., 2003; Villarreal et al., 2010; Villareal et al., 2016).

Ethylene plays a key role in the development of strawberry color, in the accumulation of taste-related compounds (flavonoids, phenolics, organic acids, and sugars), and in the softening process (Villarreal et al., 2010; Merchante et al., 2013; Li et al., 2016a; Villareal et al., 2016; Moya-León et al., 2019). Moreover, it has been reported that ethylene biosynthesis and signaling genes are differentially expressed during ripening of strawberry, and that some Ethylene Response Factors (ERFs) showed an expression pattern similar to those found in a climacteric fruit (Trainotti et al., 2005; Sun et al., 2013; Sánchez-Sevilla et al., 2017). Nowadays, it is well understood that ripening involves cross-talk among different hormones rather than single hormone action (Chang et al., 2013; Chen et al., 2015). However, the complexity of ripening regulation in strawberry is also attributable to the peculiar anatomy of the fruit, which is composed of achenes (true fruit) and a swollen fleshy receptacle. The two tissues are different in terms of origin, physiological and biochemical roles, and metabolic networks (Fait et al., 2008; Csukasi et al., 2011; Symons et al., 2012; Gu et al., 2019). It has been demonstrated that endogenous ethylene production in ripening strawberry is mainly attributable to the achenes (Iannetta et al., 2006). Nevertheless, a recent study describing the transcriptional and hormonal profiles of the two tissues highlighted that ethylene related genes were upregulated in the receptacle only (Sánchez-Sevilla et al., 2017). Strawberry ripening seems therefore to depend on how the achenes and receptacle differentially respond and synergistically interplay with one another (Merchante et al., 2013).

Despite increasing knowledge about strawberry ripening, it is surprising that little work has evaluated the postharvest hormonal regulation of strawberry physiology. Previous evidence has suggested that ethylene and the control thereof can have both positive and negative effects during postharvest storage of strawberry (Terry et al., 2007a), but the interplay between exogenous ethylene and ABA during postharvest is still unknown. One of the consequences of this paucity of information is also reflected in the limitation of strawberry shelf life management strategies.

To better characterise the role of ethylene, the postharvest effects of continuous exogenous ethylene (50 μl l^{-1}) exposure were investigated. The physiological and biochemical responses of ripe strawberry were evaluated across 6 days of cold storage, together with the hormonal profiles of whole fruit and individual tissues (achenes and receptacle).

MATERIALS AND METHODS

Plant Material and Ethylene Treatment

Ripe strawberry fruit (cv. Sonata, n = 252) were purchased from a local grower (H & H Duncalfe in Cambs., UK). Plants were grown under standard commercial conditions (Spanish tunnels), and fruit harvested on 6th August before being transferred to Cranfield University within 2 h. On arrival, disease-free fruits of similar size and weight were selected, placed in plastic punnets and subjected to two different storage environments: continuous air (control), continuous ethylene supplementation (50 μl l^{-1}). Each punnet contained n = 12 fruit and for each treatment there were n = 5 punnets (n = 60 fruit per treatment). The punnets were placed inside labeled 13 L sealed plastic boxes stored at 5°C for 6 days to simulate shelf life conditions in a domestic refrigerator, and constantly flushed to avoid the creation of modified atmosphere. Continuous exposure to ethylene was achieved by flushing ethylene in air (50 μl l^{-1}, 250 ml min^{-1}) using a blower manifold (Amoah et al., 2017) (custom built and supplied by Air Equipment, Beds., UK). After 2 h from the beginning of treatment the concentration of ethylene (50 μl l^{-1}) was quantified as previously described (Terry et al., 2007a). Control strawberries were constantly flushed with cleaned air (250 ml min^{-1}) from a cylinder of pure air to ensure complete air exchange within the boxes and to prevent the creation of a modified atmosphere.

Fruit Sampling

At each sampling time (0 d; days of storage, 1 d, 2 d, 4 d, 6 d), the 13 l boxes were opened for few seconds and 12 fruit from each treatment (n = 12) were collected. They were separated into three blocks (n = 4 fruit) and assessed for CO_2 and ethylene production, weight loss and color changes. Each of these parameters was assessed on three replicates per treatments. After the physiological measurements, the fruit were longitudinally halved. Following division, fruit were immediately snap frozen and freeze dried for further analysis. One half was used as whole fruit and the other was divided into achenes and receptacle tissues (Terry et al., 2007b). The receptacle tissue and achenes were manually separated from freeze dried material, using a pair of tweezers. All the achenes from four halves of strawberry fruit per treatment (* 3 blocks) were collected at each time point. Fruit assessed on day zero, before continuous ethylene exposure, were used for baseline measurements.

Physiological Assessments

CO_2 Production Measurement and Weight Loss

Real time CO_2 production rate of strawberries were measured *in situ* (5°C) connecting the 13 l boxes to a Sable Respirometer System (Model 1.3.8 Pro, Sable Systems International, NV, USA) according to Alamar et al. (2017). The blocks (four fruits) for each treatment were weighed before each measurement. The weight was used to calculate the CO_2 production per kg of fruit, and the percentage of weight loss.

Ethylene Production Rate

Real time ethylene production was continuously monitored (for 3 h) *ex situ* (20°C) with a laser-based photoacoustic ethylene detector ETD-300 (Sensor Sense B.V., Nijmegen, The Netherlands) as previously described (Salman et al., 2009).

Color Measurements

Objective color (lightness; L*), chroma index (color saturation; C*), hue angle (H°) was determined for each fruit (n = 12) per

treatment as previously reported (Terry et al., 2007a). Measurements were obtained using a Minolta CR-400 colorimeter and DP-400 data processor (Minolta Co. Ltd., Japan).

Biochemical Analysis

Sugars and Organic Acids Extraction and Quantification

Sugars and organic acids were extracted from whole fruit samples as previously reported (Terry et al., 2007a) and quantified using an Agilent 1200 series HPLC binary pump system (Agilent, Berks., UK) coupled with either an Agilent refractive index detector (RID) G1312A for sugars or a G1364C/G1315D photodiode array for organic acids. The concentration of glucose, fructose and sucrose, and citric, ascorbic and malic acids were calculated by comparison against an external calibration curve prepared with authentic standards (Sigma-Aldrich, Dorset, UK) and the results expressed as g kg^{-1} of dry weight.

Phenolic Compounds Extraction and Quantification

Phenolic compounds were extracted from whole fruit samples as previously described (Terry et al., 2007b). Concentrations of total anthocyanins, pelargonidin-3-glucoside, pelargonidin-3-glucoside derivative, cyanidin-3-glucoside, quercetin-3-glucoside, catechin, epicatechin, ellagic and chlorogenic acids (Sigma-Aldrich, Dorset, UK or Extrasynthese, Lyon, France) were calculated against authentic standards and expressed as mg kg^{-1} of dry weight.

Extraction and Quantification of Strawberry Phytohormones

Phytohormones were extracted from both whole fruit and individual tissues (achenes and receptacle) and analyzed as previously described (Ordaz-Ortiz et al., 2015). An Agilent 6540 Ultra High Definition Accurate Mass Q-TOF LC-MS System was used to quantify abscisic acid (ABA), 7'OH-abscisic acid (7'OH-ABA), indole-3-acetic acid (IAA) and indole-3-acetylaspartic acid (IAAsp). Calibration curves for the four compounds were generated by plotting the known concentration of the calibration level (ABA and 7'-OH ABA were purchased from National Research Council of Canada-Plant Biotechnology Institute, Ottawa, Canada. IAA and IAAsp were purchased from OlchemIm Ltd, Olomouc, Czech Republic) against the relative response calculated for each calibration level. Quantification analysis was carried out using an Agilent MassHunter Quantitative Analysis Software B.05.00. Endogenous phytohormones concentration was calculated as μg kg^{-1} of dry weight.

Statistical Analysis

Statistical analysis of results was performed using STATISTICA software for Windows (Dell Inc., 2015. Dell Statistica, version 12). Data were checked for residuals distribution, and tested with ANOVA, followed by a comparison of the means according to a least significant difference (LSD) test at $p < 0.05$.

RESULTS

Physiological Assessments

The physiological parameters of respiration activity in terms of CO_2 production, weight loss and color changes of strawberry fruit were assessed. Significant variations relating to continuous ethylene exposure were identified in the production of CO_2 and weight loss (**Figure 1**), while color parameters were more affected by the storage time.

Ethylene treated fruit exhibited a more than 2-fold increase in CO_2 production compared to the control fruit during the storage (**Figure 1A**). However, by the end storage (6 d) the CO_2 production of control fruit was similar to ethylene treated fruit. The ethylene treated fruit showed a total weight loss of circa 35% at the end of storage, while the difference in weight in control fruit was around 20% (**Figure 1B**).

The color evolution assessment showed that the chroma index (C*) and the hue angle (H°) decreased during the storage and exhibited a more marked decline in ethylene treated fruit. However, significant differences were identified only in relation with the storage day ($p < 0.0000$ and $p < 0.0052$, respectively) (**Table 1**), while the lightness (L*) did not change (*data not shown*).

Biochemical Changes Induced by Continuous Ethylene Exposure: Sugars/ Organic Acids, and Phenolics Compounds

Sugars data showed significant differences related to both treatment and storage day (**Figure 2**). Ethylene induced sucrose hydrolysis and accumulation of reducing sugars. In particular, ethylene treated strawberries showed increased sucrose hydrolysis from day 4 of storage, and by 6d, ethylene treated fruit had halved their initial sucrose values. In contrast, sucrose concentrations in control fruit decreased by *ca.* 25% compared to the initial amounts (**Figure 2A**). Concomitantly, ethylene-treated also induced the accumulation of reducing sugars in treated fruit (glucose 1.05-fold increase, fructose 1.1-fold increase) (**Figures 2B, C**, respectively).

Of the organic acids analyzed, ethylene only had a significant impact on malic acid, and this effect was similar to the response for sucrose in treated fruit (**Figure 3A**). Citric and ascorbic acid content were affected by the storage time only (**Figure 3B**). At the beginning of storage, the most abundant organic acid was citric acid (67 g kg^{-1}), followed by the malic (38 g kg^{-1}), oxalic (6.7 g kg^{-1}) and ascorbic acid (4.3 g kg^{-1}), respectively; despite these variations in initial organic acids levels, an overall decline was observed at the end of the storage.

Total anthocyanins and three specific anthocyanins, cyanidin-3-glucoside, pelargonidin-3-glucoside, and pelargonidin-3-glucoside derivative, were analyzed. Significant differences were identified for total anthocyanins and pelargonidin-3-glucoside content, and were due to the storage day only ($p < 0.0203$ and $p < 0.0047$, respectively). Both compounds *ca.* increased 1.1-fold during storage without marked differences between ethylene and air (**Supplemental Figure 1**).

Besides anthocyanins, other phenolic compounds were also quantified (quercetin-3-glucoside, catechin, epicatechin,

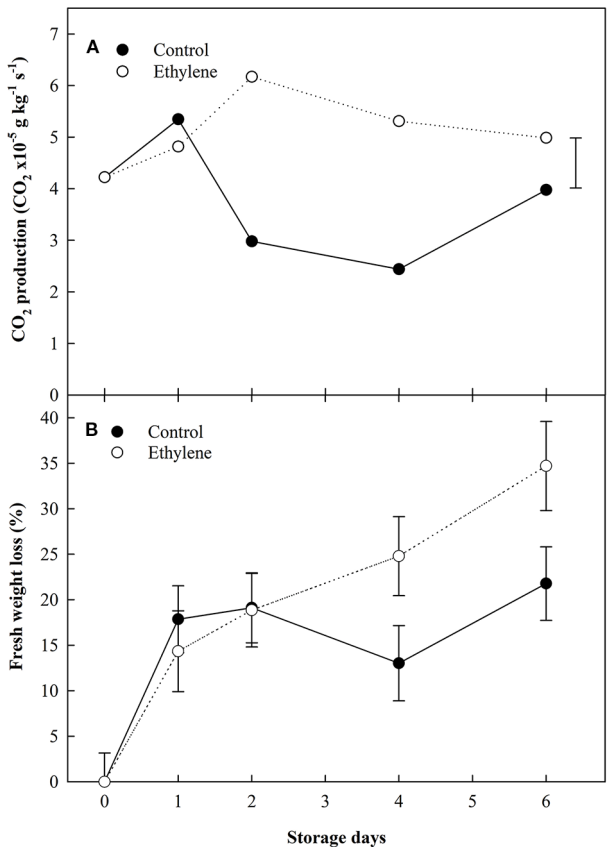

FIGURE 1 | The effect of ethylene (continuous exposure) on CO_2 production ($CO_2 \times 10^{\times 5}$ g kg^{-1} s^{-1}) and fresh weight variation (kg) of strawberries, cv. Sonata, stored at 5°C for 6 d. **(A)** CO_2 production. Vertical bar represents the LSD ($p < 0.05$). **(B)** Fresh weight variation. Vertical bars represent the Standard Error.

chlorogenic and ellagic acids). Among them, quercetin-3-glucose did not show any significant difference; catechin and ellagic acid showed quite steady levels during all the storage (400–450 mg kg^{-1} and 35.8–36.1 mg kg^{-1}, respectively. *Data not shown*). In contrast, epicatechin and chlorogenic acid levels were significantly affected by ethylene supplementation (**Figure 4**). Ethylene induced a gradual accumulation of epicatechin in the first four days of ethylene exposure (**Figure 4A**), while a sudden increase was observed for chlorogenic acid from day 1 until the end of storage (50% more than untreated fruit) (**Figure 4B**).

TABLE 1 | The effect of ethylene (continuous exposure) on chroma index (C*) and the hue angle (H°) of strawberries, cv. Sonata, stored at 5°C for 6. d. LSD ($p < 0.05$) for the overall means of the significant variable "storage day".

Storage day	C*			H°		
	Control	Ethylene	LSD	Control	Ethylene	LSD
0	48.22			36.13		
1	51.04	51.63		37.16	37.88	
2	47.89	49.57		34.26	36.55	
4	47.59	45.61		35.75	34.24	
6	48.34	44.30		35.24	34.84	
			2.24			1.58

Phytohormones

The effect of continuous ethylene exposure on phytohormone profile was studied. The *ex-situ* (20°C) monitoring of endogenous ethylene production showed a significant difference only according to the storage time, and overall the endogenous ethylene production increased during storage by 2.6-fold (**Supplemental Figure 2**).

The quantification of two phytohormones and two metabolites thereof [abscisic acid (ABA), 7'OH-abscisic acid (7'-OHABA), indole-3-acetic acid (IAA), indole-3-acetylaspartic acid (IAAsp)] was carried out, using LC-MSMS, in the whole strawberry fruit as well as in individual tissues. Continuous ethylene exposure increased ABA content in the whole fruit and in the receptacle throughout storage (**Figure 5A**). ABA content was 4-times higher in receptacle tissue (only) than achenes at the beginning of storage, and the ethylene-induced ABA increase in the receptacle showed a steady difference of *ca.* 1.2-fold from day 1 in comparison with the untreated fruit content (**Figure 5B**). Achenes did not exhibit a response to ethylene, yet catabolism of ABA and auxins increased by two thirds during air storage (**Figure 6**).

7'OH-ABA content was more affected by storage duration than by ethylene treatment. An overall increase in 7'OH-ABA was found in all the tissues analyzed. 7 OH-ABA levels in whole fruit showed a mean increase of 1.71-fold (**Figure 5A**), while in the receptacle tissues no significant differences were identified (*data not shown*). In the achenes, 7'OH-ABA exhibited *ca.* 3-fold increase compared to the beginning of storage (**Figure 6**).

Auxins (IAA and IAAsp) content were detected only in the achenes, since the concentration of these phytohormones in the whole fruit and in the receptacle was below the quantification limit. IAA levels showed significant variations relating to storage days only. An overall 2-fold decrease in IAA content was reported across storage, although the major changes happened during the first two days. IAAsp exhibited an increasing trend (*ca.* 2.4-fold) in both control and ethylene treated fruit but a significant variation was not identified (**Figure 6**).

DISCUSSION

Previous studies investigating the effect of high level of ethylene (100 µl l^{-1}) did not report a clear mechanism of response in cold stored strawberry (Siriphanich, 1980; Terry et al., 2007a). As consequence, it has been suggested that high concentration of ethylene would not impact on strawberry shelf life, while very low concentration (<1 µl l^{-1}) have been reported to promote decay and softening (Wills and Kim, 1995). To better understand whether and how high level of ethylene can affect the postharvest quality of strawberry, the current work describes the responses induced by continuous ethylene exposure (50 µl l^{-1}) in cold stored ripe strawberry.

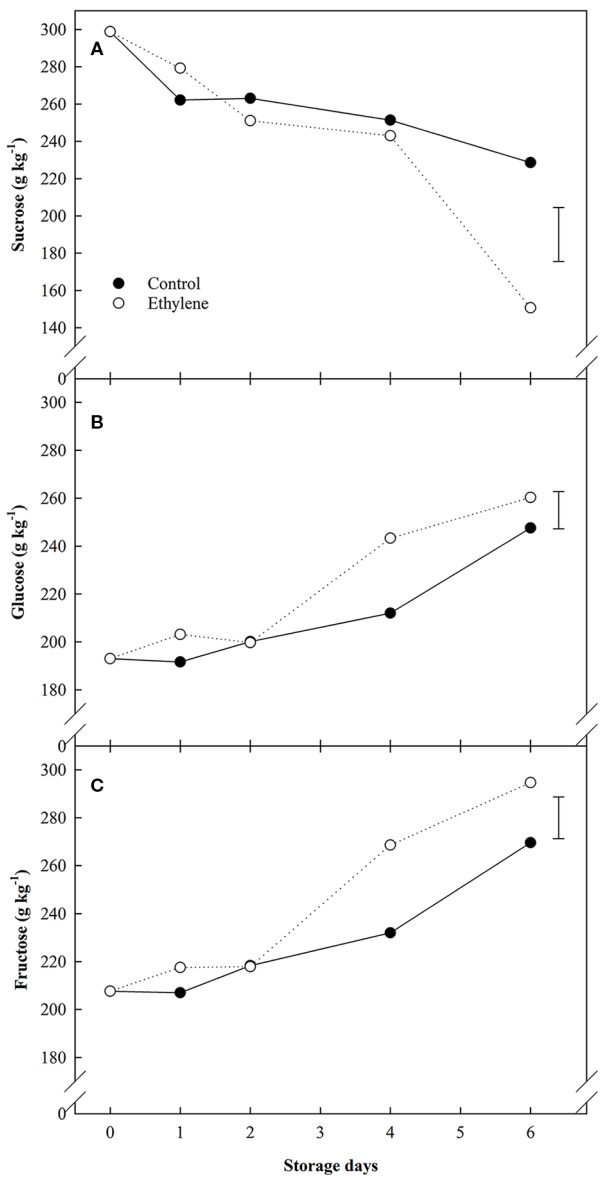

FIGURE 2 | The effect of ethylene (continuous exposure) on sugars content (g kg^{-1}) of strawberries, cv. Sonata, stored at 5°C for 6 d. **(A)** Sucrose content. **(B)** Glucose content. **(C)** Fructose content. Vertical bar represents LSD ($p < 0.05$) for the overall means of the significant variable "treatment".

Strawberry is classified as a non-climacteric fruit even though an increasing number of studies highlight that the receptacle exhibits some ripening features similar to a climacteric fruit. Although strawberry does not show the typical ethylene climacteric rise in respiration, it has been reported that ethylene biosynthesis and signaling pathways are differentially affected during strawberry ripening, and these changes are mainly localized in the receptacle (Trainotti et al., 2005; Iannetta et al., 2006; Merchante et al., 2013; Sun et al., 2013; Sánchez-Sevilla et al., 2017). Besides this transcriptional activation, the role of ethylene in modulating sugars/organic acid ratio, promoting anthocyanins accumulation and softening during strawberry ripening has been reported (Villarreal et al., 2010; Merchante et al., 2013; Villareal et al., 2016; Gu et al., 2019; Moya-León et al., 2019). Ethylene has been linked with increased CO_2 production and water loss in ripening strawberry fruit (Tian et al., 2000); this being in agreement with results herein. Opazo and colleagues (2013) reported differential effects of ethylene and 1-MCP on the expression of the softening-related gene xyloglucan endotransglycosylase/hydrolase 1 (*XTH1*), due to the presence of ethylene responsive elements in the promoter region. The finding was confirmed by Villareal and colleagues (2016) who described the response to ethylene of several strawberry cell-wall metabolic genes. It has also been extensively reported that ethylene treatment elicited anthocyanins accumulation in ripening strawberry (Ku et al., 1999; Bower et al., 2003; Villarreal et al., 2010; Merchante et al., 2013; Sun et al., 2013; Lopes et al., 2015). In addition, Sun and colleagues (2013) demonstrated that the expression of *FaSAMS1*(S-adenosyl-L-methionine synthase 1) and *FaCTR1* (constitutive triple response 1) genes played a significant role in the softening and red-color development of strawberry fruit. The results herein did not show any effect of ethylene exposure on anthocyanins content; this difference may be explained since the fruit used in the current study were already at red ripe stage. In addition, the fruit were kept in cold storage, rather than 20°C, as indicated in previous works.

Lopes and colleagues (2015) reported that ethephon treatment increased sugars content in strawberry fruit both when applied in the field, and during postharvest. The results herein confirmed the propensity of ethylene to elicit an accumulation of reducing sugars, together with a concomitant decline in sucrose content during postharvest, as previously described (Li et al., 2019). In blueberry, ethylene can positively influence sucrose metabolism and invertase enzymes activity (Wang et al., 2020), and Jia and colleagues (2016) reported the key role of acid invertase during strawberry ripening. This may explain the activation of sucrose hydrolysis described here. Nevertheless, the taste and quality of strawberry fruit are linked to the sugars/organic acids ratio rather than sugars content alone (Giné-Bordonaba and Terry, 2009). Although both citric and malic acids are important compounds influencing strawberry acidity, malic acid is the main acid responsible for changes in pH regulation (Fait et al., 2008). The data of this work showed that malic acid catabolism was positively affected by continuous ethylene exposure, and developed concomitantly with the sucrose decline. These similar variations of malic acid and sucrose, and the role of malic acid in pH regulation seemed to suggest an ethylene-induced upregulation of different members of the invertase family activated by the changes in pH, and/or an upregulation of invertase members not localized in the cytoplasm (e.g. cell wall invertase). All these changes in water loss, respiration, and variations of fruit pH and reducing sugars can be linked to the progression of senescence (Alkan and Fortes, 2015). Taken together, the data supports the role of ethylene in promoting senescence in strawberry fruit.

It is well documented that the ABA/auxins ratio plays a major role in regulating strawberry fruit ripening (Iannetta et al., 2006; Jia et al., 2011; Symons et al., 2012; Chen et al., 2015; Chen et al., 2016;

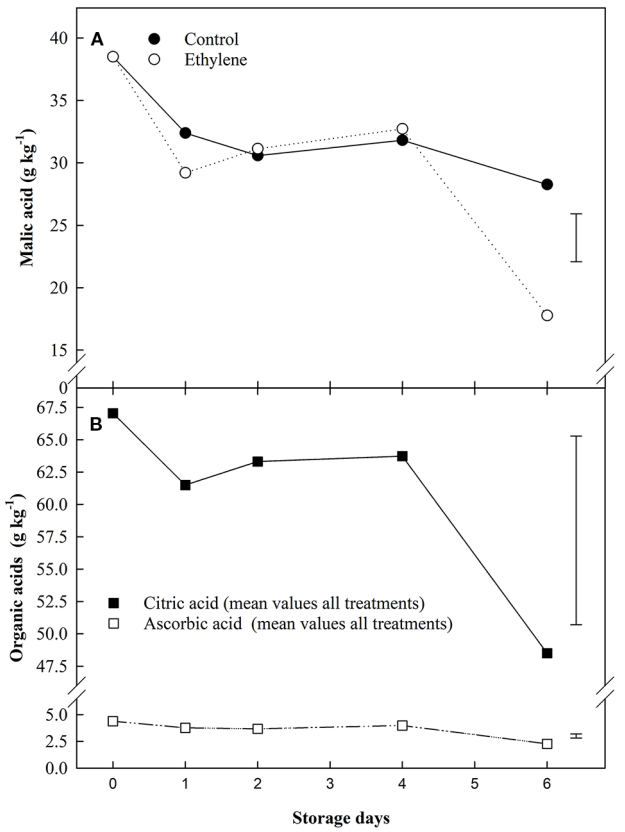

FIGURE 3 | The effect of ethylene (continuous exposure) on organic acids content (g kg^{-1}) of strawberries, cv. Sonata, stored at 5°C for 6 d. **(A)** Malic acid content (g kg^{-1}) of strawberries, cv. Sonata, stored at 5°C for 6 d. Vertical bar represents LSD ($p < 0.05$) for the overall means of the significant variable "treatment". **(B)** Ascorbic and citric acids. The represented values show the mean of all treatments (control and ethylene treated fruit) content. ■ citric acid. □ ascorbic acid. Vertical bar represents LSD ($p < 0.05$) for the overall means of the significant variable "Storage day".

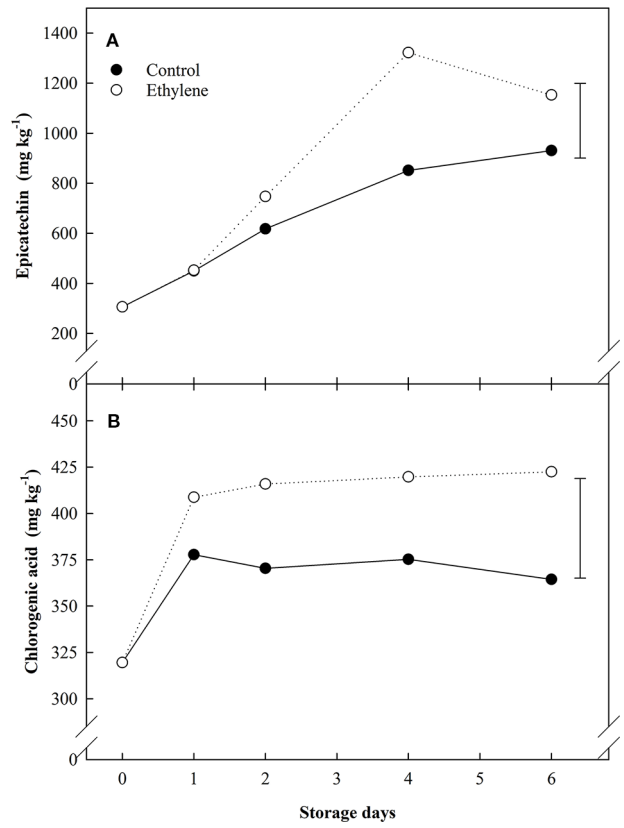

FIGURE 4 | The effect of ethylene (continuous exposure) on phenolics content (mg kg^{-1}) of strawberries, cv. Sonata, stored at 5°C for 6 d. **(A)** Epicatechin. **(B)** Cholorogenic acid. Vertical bar represents LSD ($p < 0.05$) for the overall means of the significant variable "treatment".

Medina-Puche et al., 2016; Moya-León et al., 2019); despite this, there is a lack of information about the role of ABA during storage (Terry et al., 2007a). Results of this study highlighted that continuous exposure to exogenous ethylene did not affect ABA and auxins metabolism in achenes. In contrast, ethylene induced a marked increase in ABA content in the receptacle as a first response (within 24 h), which was sustained through storage (50% higher ABA content than untreated fruit at the end of the storage). In the same tissue, auxins and IAAsp levels were too low to be detectable, and the ABA metabolite 7'OH-ABA did not show any response to ethylene exposure. A study on hormonal content in different strawberry fruit tissues during ripening reported higher ABA amounts in the achenes than in the receptacle (Symons et al., 2012). However, the more recent work of Gu and colleagues (2019) highlighted that ABA content in the receptacle markedly increased with the progression of the ripening and reached a maximum level only at the red stage. The presented data confirmed that in ripe (red) strawberry, ABA concentration 4-times higher in the receptacle tissue compared to achenes through storage. Furthermore, continuous ethylene exposure induced a constant upregulation of the ABA receptacle content (1.24-fold) compared to the control. These findings seemed to suggest a synergistic action of ethylene and ABA: ethylene-induced disequilibrium in the receptacle ABA homeostasis might be a trigger for, and participate in, the regulation of the senescence-related changes observed during storage.

Li and colleagues (2014) described that following UV-C stress, ABA can induce ethylene biosynthesis in unripe detached strawberry, and that ABA levels were inversely correlated to ethylene content. In contrast, the presented data showed a positive correlation between ethylene exposure and ABA content. Moreover, the increasing trend exhibited by ABA throughout storage indicated that the selected ethylene concentration (50 µl l^{-1}) was able to keep a positive regulation on ABA accumulation in the receptacle tissue.

ABA is well-known to be also involved in water stress, and following deficit irrigation an increase in phenolic compounds was found in strawberry fruit (Terry et al., 2007b; Weber et al., 2016). Accordingly, samples exposed to ethylene showed higher weight loss, higher ABA content, and higher phenolics accumulation than untreated fruit. This positive effect of ABA on the flavonoid/phenylpropanoid pathway has been explained

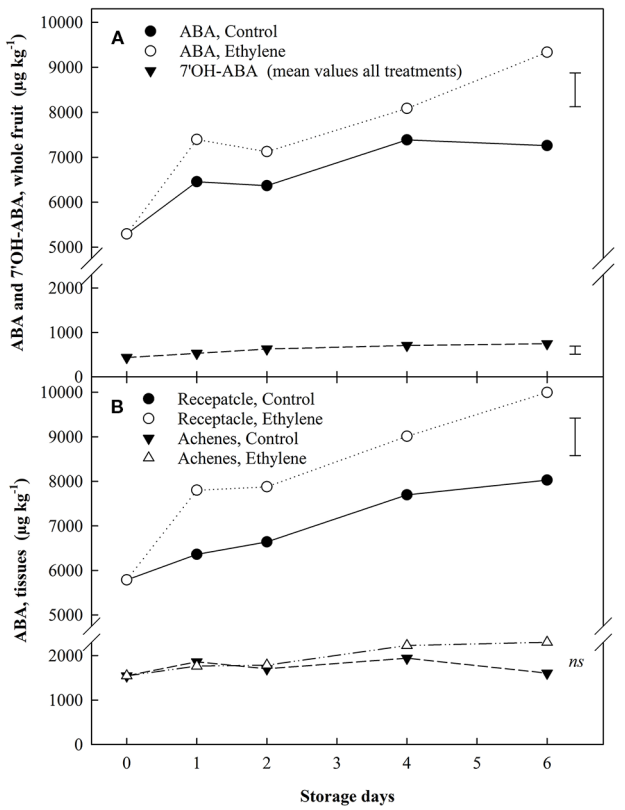

FIGURE 5 | The effect of ethylene (continuous exposure) on ABA and the metabolite 7'OH-ABA content (µg kg^{-1}) of strawberries, cv. Sonata, stored at 5°C for 6 d. **(A)**, ABA and the metabolite 7'OH-ABA content in the whole fruit. For the metabolite 7'OH-ABA the represented values show the mean of all treatments (control and ethylene treated fruit) content. **(B)**, ABA in individual tissues. Vertical bar represents LSD ($p < 0.05$) for the overall means of the significant variable "treatment" for ABA in both graphs and of the significant variable "Storage day" for 7'OH-ABA (whole fruit); ns, not significant.

with the ABA-induced upregulation of *FaSCL8* (*SCARECROW-LIKE 8*) and *FaMYB10* expression (Medina-Puche et al., 2014; Pillet et al., 2015). These two genes have been proposed as key elements for the flavonoid/phenylpropanoid pathway regulation during the ripening of strawberry fruit. The results of the present study showed that epicatechin and chlorogenic acid content were positively affected by ethylene supplementation. Moreover, the sharp increase found in chlorogenic acid at day 1 of storage, and during storage resembled the trend found in ABA content following ethylene exposure. This seemed to support the idea that there is interplay between ethylene and ABA, and that both phytohormones regulate strawberry ripening/senescence during postharvest (**Supplemental Figure 3**).

In conclusion, in this study it is proposed that strawberry postharvest senescent decline is induced by ethylene through ABA action in the receptacle tissue, and that a better understanding of the role of ethylene and ABA and their interplay in mediating senescence would allow better design of shelf life management strategies.

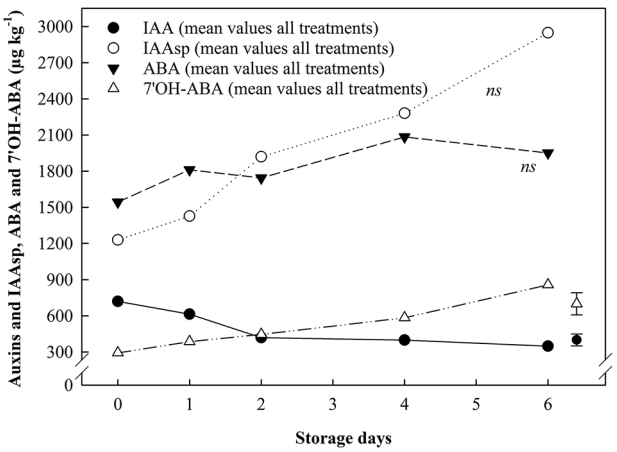

FIGURE 6 | The effect of ethylene (continuous exposure) on auxins and ABA, and their catabolites, content (µg kg^{-1}) in achenes of strawberries, cv. Sonata, stored at 5°C for 6 d. The represented values show the mean of all treatments (control and ethylene treated fruit) content. Vertical bar represents LSD ($p < 0.05$) for the overall means of the significant variable "Storage day" for IAA and 7'OH-ABA; ns, not significant.

DATA AVAILABILITY STATEMENT

Data underlying this paper can be accessed at https://doi.org/10.17862/cranfield.rd.11876544.v1.

AUTHOR CONTRIBUTIONS

LT conceived and designed the experiments. FE, IP, and KC performed the experiments. RT performed data analysis and wrote the manuscript with the help of LT. All authors contributed to the discussion, revised and approved the final manuscript.

FUNDING

Engineering and Physical Sciences Research Council (EPSRC) and Johnson Matthey Plc (case number: 09000987).

ACKNOWLEDGMENTS

The authors would like to thank both the Engineering and Physical Sciences Research Council (EPSRC; 09000987) and Johnson Matthey Plc for financial and Case studentship support. IP would like to thank the Institute of Agricultural and Fisheries Research and Training (IFAPA) and the European Social Fund (Programa Operativo del Fondo Social Europeo de Andalucía 2007-2013) for the postdoctoral fellowship.

SUPPLEMENTARY MATERIAL

The Supplementary Material for this article can be found online at: https://www.frontiersin.org/articles/10.3389/fpls.2020.00174/full#supplementary-material

SUPPLEMENTAL FIGURE 1 | The effect of ethylene (continuous exposure) on total anthocyanins and pelargonidin-3-glucoside content (mg kg^{-1}) of strawberries, cv. Sonata, stored at 5° C for 6 d. The represented values show the mean (control and ethylene treated fruit) content. Vertical bar represents LSD ($p < 0.05$) for the overall means of the significant variable "Storage day".

SUPPLEMENTAL FIGURE 2 | The effect of ethylene (continuous exposure) on endogenous ethylene production (x10^{-11} g kg^{-1} s^{-1}) of strawberries, cv. Sonata, stored at 5° C for 6 d. Vertical bar represents LSD ($p < 0.05$) for the overall means of the significant variable "Storage day".

SUPPLEMENTAL FIGURE 3 | Graphical abstract of ethylene (continuous exposure) effect on senescence in receptacle and achene tissues in strawberry fruit.

REFERENCES

Alamar, M. C., Colling, E., Cools, K., and Terry, L. A. (2017). Impact of controlled atmosphere scheduling on strawberry and imported avocado fruit. *Postharvest Biol. Technol.* 134, 6–86. doi: 10.1016/j.postharvbio.2017.08.003

Alkan, N., and Fortes, A. M. (2015). Insights into molecular and metabolic events associated with fruit response to post-harvest fungal pathogens. *Front. Plant Sci.* 6, 1–14. doi: 10.3389/fpls.2015.00889

Amoah, R. S., Landahl, S., and Terry, L. A. (2017). Design and construction of a flexible laboratory-scale mixing apparatus for continuous ethylene supplementation of fresh produce. *Biosyst. Eng.* 157, 86–91. doi: 10.1016/j.biosystemseng.2017.02.010

Bower, J. H., Biasi, W. V., and Mitcham, E. J. (2003). Effects of ethylene and 1-MCP on the quality and storage life of strawberries. *Postharvest Biol. Technol.* 28, 417–423. doi: 10.1002/jsfa.3868

Chang, K. N., Zhong, S., Weirauch, M. T., Hon, G., Pelizzola, M., Li, H., et al. (2013). Temporal transcriptional response to ethylene gas drives growth hormone cross-regulation in Arabidopsis. *Elife* 2013, 1–20. doi: 10.7554/eLife.00675.001

Chen, J., Mao, L., Lu, W., Ying, T., and Luo, Z. (2015). Transcriptome profiling of postharvest strawberry fruit in response to exogenous auxin and abscisic acid. *Planta* 243, 183–197. doi: 10.1007/s00425-015-2402-5

Chen, J., Mao, L., Mi, H., Lu, W., Ying, T., and Luo, Z. (2016). Involvement of abscisic acid in postharvest water-deficit stress associated with the accumulation of anthocyanins in strawberry fruit. *Postharvest Biol. Technol.* 111, 99–105. doi: 10.1016/j.postharvbio.2015.08.003

Csukasi, F., Osorio, S., Gutierrez, J. R., Kitamura, J., Giavalisco, P., Nakajima, M., et al. (2011). Gibberellin biosynthesis and signalling during development of the strawberry receptacle. *New Phytol.* 191, 376–390. doi: 10.1111/j.1469-8137.2011.03700.x

Fait, A., Hanhineva, K., Beleggia, R., Dai, N., Rogachev, I., Nikiforova, V. J., et al. (2008). Reconfiguration of the achene and receptacle metabolic networks during strawberry fruit development. *Plant Physiol.* 148, 730–750. doi: 10.1104/pp.108.120691

Giné-Bordonaba, J., and Terry, L. A. (2009). Development of a glucose biosensor for rapid assessment of strawberry quality: relationship between biosensor response and fruit composition. *J. Agric. Food Chem.* 57, 8220–8226. doi: 10.1021/jf901596w

Giné-Bordonaba, J., and Terry, L. A. (2016). Effect of deficit irrigation and methyl jasmonate application on the composition of strawberry (*Fragaria* × *ananassa*) fruit and leaves. *Sci. Hortic.* 199, 63–70. doi: 10.1016/j.scienta.2015.12.026

Gu, T., Jia, S., Huang, X., Wang, L., Fu, W., Hou, G., et al. (2019). Transcriptome and hormone analyses provide insights into hormonal regulation in strawberry ripening. *Planta* ,250, 145–162. doi: 10.1007/s00425-019-03155-w

Iannetta, P. P. M., Laarhoven, L. J., Medina-Escobar, N., James, E. K., McManus, M. T., Davies, H. V., et al. (2006). Ethylene and carbon dioxide production by developing strawberries show a correlative pattern that is indicative of ripening climacteric fruit. *Physiol. Plant* 127, 247–259. doi: 10.1111/j.1399-3054.2006.00656.x

Jia, H.-F., Chai, Y.-M., Li, C.-L., Lu, D., Luo, J.-J., Qin, L., et al. (2011). Abscisic acid plays an important role in the regulation of strawberry fruit ripening. *Plant Physiol.* 157, 188–199. doi: 10.1104/pp.111.177311

Jia, H., Jiu, S., Zhang, C., Wang, C., Tariq, P., Liu, Z., et al. (2016). Abscisic acid and sucrose regulate tomato and strawberry fruit ripening through the abscisic acid-stress ripening transcription factor. *Plant Biotechnol. J.* 14, 2045–2065. doi: 10.1111/pbi.12563

Jiang, Y., Joyce, D. C., and Terry, L. A. (2001). 1-Methylcyclopropene treatment affects strawberry fruit decay. *Postharvest Biol. Technol.* 23 (3), 227–232. doi: 10.1016/S0925-5214(01)00123-5

Ku, V. V. V., Wills, R. B. H., and Ben-Yehoshua, S. (1999). 1-Methylcyclopropene can differentially affect the postharvest life of strawberries exposed to ethylene. *HortScience* 34, 119–120. doi: 10.21273/HORTSCI.34.1.119

Leng, P., Yuan, B., Guo, Y., and Chen, P. (2014). The role of abscisic acid in fruit ripening and responses to abiotic stress. *J. Exp. Bot.* 65, 4577–4588. doi: 10.1093/jxb/eru204

Li, D., Luo, Z., Mou, W., Wang, Y., Ying, T., and Mao, L. (2014). ABA and UV-C effects on quality, antioxidant capacity and anthocyanin content of strawberry fruit (*Fragaria* × *ananassa* Duch.). *Postharvest Biol. Technol.* 90, 56–62. doi: 10.1016/j.postharvbio.2013.12.006

Li, L., Lichter, A., Chalupowicz, D., Gamrasni, D., Goldberg, T., Nerya, O., et al. (2016a). Effects of the ethylene-action inhibitor 1-methylcyclopropene on postharvest quality of non-climacteric fruit crops. *Postharvest Biol. Technol.* 111, 322–329. doi: 10.1016/j.postharvbio.2015.09.031

Li, L., Li, D., Luo, Z., Huang, X., and Li, X. (2016b). Proteomic response and quality maintenance in postharvest fruit of strawberry (*Fragaria* × *ananassa*) to exogenous cytokinin. *Sci. Rep.* 6, 27094. doi: 10.1038/srep27094

Li, D., Zhang, X., Xu, Y., Li, L., Aghdam, M. S., and Luo, Z. (2019). Effect of exogenous sucrose on anthocyanin synthesis in postharvest strawberry fruit. *Food Chem.* 289, 112–120. doi: 10.1016/j.foodchem.2019.03.042

Lopes, P. Z., Fornazzari, I. M., Almeida, A. T., Galvão, C. W., Etto, R. M., and Inaba, J. (2015). Effect of ethylene treatment on phytochemical and ethylene-related gene expression during ripening in strawberry fruit *Fragaria* x *ananassa* cv. Camino Real. *Genet. Mol. Res.* 14, 16113–16125. doi: 10.4238/2015.December.7.23

Medina-Puche, L., Cumplido-Laso, G., Amil-Ruiz, F., Hoffmann, T., Ring, L., Rodríguez-Franco, A., et al. (2014). MYB10 plays a major role in the regulation of flavonoid/phenylpropanoid metabolism during ripening of *Fragaria* × *ananassa* fruits. *J. Exp. Bot.* 65, 401–417. doi: 10.1093/jxb/ert377

Medina-Puche, L., Blanco-Portales, R., Molina-Hidalgo, F. J., Cumplido-Laso, G., García-Caparrós, N., Moyano-Cañete, E., et al. (2016). Extensive transcriptomic studies on the roles played by abscisic acid and auxins in the development and ripening of strawberry fruits. *Funct. Integr. Genomics* 16, 671–692. doi: 10.1007/s10142-016-0510-3

Merchante, C., Vallarino, J. G., Osorio, S., Aragüez, I., Villarreal, N., Ariza, M. T., et al. (2013). Ethylene is involved in strawberry fruit ripening in an organ-specific manner. *J. Exp. Bot.* 64, 4421–4439. doi: 10.1093/jxb/ert257

Moya-León, M. A., Mattus-Araya, E., and Herrera, R. (2019). Molecular events occurring during softening of strawberry fruit. *Front. Plant Sci.* 10, 615. doi: 10.3389/fpls.2019.00615

Opazo, M. C., Lizana, R., Pimentel, P., Herrera, R., and Moya-León, M. A. (2013). Changes in the mRNA abundance of FcXTH1 and FcXTH2 promoted by hormonal treatments of Fragaria chiloensis fruit. *Postharvest Biol. Technol.* 77, 28–34. doi: 10.1016/j.postharvbio.2012.11.007

Ordaz-Ortiz, J. J., Foukaraki, S., and Terry, L. A. (2015). Assessing temporal flux of plant hormones in stored processing potatoes using high definition accurate mass spectrometry. *Hortic. Res.* 2, 15002. doi: 10.1038/hortres.2015.2

Pillet, J., Yu, H. W., Chambers, A. H., Whitaker, V. M., and Folta, K. M. (2015). Identification of candidate flavonoid pathway genes using transcriptome correlation network analysis in ripe strawberry (*Fragaria* × *ananassa*) fruits. *J. Exp. Bot.* 66, 4455–4467. doi: 10.1093/jxb/erv205

Sánchez-Sevilla, J. F., Vallarino, J. G., Osorio, S., Bonbarely, A., Posé, D., Merchante., C., et al. (2017). Gene expression atlas of fruit ripening and transcriptome assembly from RNA-seq data in octoploid strawberry (*Fragaria* × *ananassa*). *Sci. Rep.* 7, 13737. doi: 10.1038/s41598-017-14239-6

Salman, A., Filgueiras, H., Cristescu, S., Lopez-Lauri, F., Harren, F., and Sallanon, H. (2009). Inhibition of wound-induced ethylene does not prevent red

discoloration in fresh-cut endive (*Cichoriumintybus* L.). *Eur. Food Res. Technol.* 228, 651–657. doi: 10.1007/s00217-008-0974-z

Siriphanich, J. (1980). Postharvest deterioration of strawberries as influenced by ethylene and some other volatiles. *MS Thesis, University of California, 65*.

Sun, J.-H., Luo, J.-J., Tian, L., Li, C.-L., Xing, Y., and Shen, Y.-Y. (2013). New evidence for the role of ethylene in strawberry fruit ripening. *J. Plant Growth Regul.* 32, 461–470. doi: 10.1007/s00344-012-9312-6

Symons, G. M., Chua, Y.-J., Quittenden, L. J., Davies, N. W., and Reid, J. B. (2012). Hormonal changes during non-climacteric ripening in strawberry. *J. Exp. Bot.* 63, 4741–4750. doi: 10.1093/jxb/ers147

Terry, L. A., Ilkenhans, T., Poulston, S., Rowsell, L., and Smith, A. W. J. (2007a). Development of new palladium-promoted ethylene scavenger. *Postharvest Biol. Technol.* 45, 214–220. doi: 10.1016/j.postharvbio.2006.11.020

Terry, L. A., Chope, G. A., and Giné-Bordonaba, J. (2007b). Effect of water deficit irrigation and inoculation with *Botrytis cinerea* on strawberry (*Fragaria* × *ananassa*) fruit quality. *J. Agric. Food Chem.* 55, 10812–10819. doi: 10.1021/jf072101n

Terry, L., Mena, C., Williams, A., Jenney, N., and Whitehead, P. (2011). Fruit and vegetable resource maps: Mapping fruit and vegetable waste through the wholesale supply chain. *Wrap* 1–94.

Tian, M. S., Prakash, S., Elgar, H. J., Young, H., Burmeister, D. M., and Ross, G. S. (2000). Responses of strawberry fruit to 1-methylcyclopropene (1-MCP) and ethylene. *Plant Growth Regul.* 32 (1), 83–90. doi: 10.1023/A:1006409719333

Trainotti, L., Pavanello, A., and Casadoro, G. (2005). Different ethylene receptors show an increased expression during the ripening of strawberries: does such an increment imply a role for ethylene in the ripening of these non-climacteric fruits? *J. Exp. Bot.* 56, 2037–2046. doi: 10.1093/jxb/eri202

Villareal, N. M., Marina, M., Nardi, C. F., Civello, P. M., and Martínez, G. A. (2016). Novel insights of ethylene role in strawberry cell wall metabolism. *Plant Sci.* 252, 1–11. doi: 10.1016/j.plantsci.2016.06.018

Villarreal, N. M., Bustamante, C. A., Civello, P. M., and Martínez, G. A. (2010). Effect of ethylene and 1-MCP treatments on strawberry fruit ripening. *J. Sci. Food Agric.* 90, 683–689. doi: 10.1002/jsfa.3868

Wang, S., Zhou, Q., Zhou, X., Zhang, F., and Ji, S. (2020). Ethylene plays an important role in the softening and sucrose metabolism of blueberries postharvest. *Food Chem.* 310, 125965. doi: 10.1016/j.foodchem.2019.125965

Weber, N., Zupanc, V., Jakopic, J., Veberic, R., Mikulic-Petkovsek, M., and Stampar, F. (2016). Influence of deficit irrigation on strawberry (*Fragaria* × *ananassa* Duch.) fruit quality. *J. Sci. Food Agric*. 97, 849–857 doi: 10.1002/jsfa.7806

Wills, R. B. H., and Kim, G. H. (1995). Effect of ethylene on postharvest life of strawberries. *Postharvest Biol. Technol.* 6 (3-4), pp.249–pp.255. doi: 10.1016/0925-5214(95)00005-Q

Conflict of Interest: The authors declare that the research was conducted in the absence of any commercial or financial relationships that could be construed as a potential conflict of interest.

The reviewer AL declared a past co-authorship with one of the authors LT to the handling Editor.

frontiers in Plant Science

ORIGINAL RESEARCH
published: 17 March 2020
doi: 10.3389/fpls.2020.00221

Graduated Controlled Atmosphere: A Novel Approach to Increase "Duke" Blueberry Storage Life

*Natalia Falagán, Tiana Miclo and Leon A. Terry**

Plant Science Laboratory, Cranfield University, Cranfield, United Kingdom

Blueberries (*Vaccinium corymbosum* L.) are highly valued for their health-promoting potential, yet they are extremely perishable. Controlled atmosphere (CA) strategies reduce blueberry respiratory metabolism, slowing down senescence. However, the sudden change of atmosphere could elicit a physical abiotic stress in the fruit, negatively affecting quality. We propose an innovative approach based on controlled graduation to slowly reach optimum gas storage conditions as an alternative to standard CA. For two consecutive seasons, "Duke" blueberries were subjected to four different storage conditions: control (air); standard CA (sudden exposure to 5 kPa O_2 and 10 kPa CO_2 across the experiment); GCA3 and GCA7 (gradually reaching 5 kPa O_2 and 10 kPa CO_2 in 3 and 7 days, respectively). Fruit were stored for 28 days at 0 ± 0.5°C. Real-time respirometry provided an in-depth insight to the respiratory response of blueberries to their gas environment. Blueberries subjected to the graduated application of CA (GCA) treatments had a lower steady-state respiration rate compared to control and standard CA fruit. This indicated a reduction in metabolic activity that positively impacted quality and storage life extension. For example, GCA3 and GCA7 blueberries had a 25% longer storage life when compared to control, based on reduced decay incidence. In addition, GCA fruit were 27% firmer than control and CA fruit after 28 days of cold storage. GCA3 had a positive effect on maintaining individual sugars concentrations throughout the experiment, and both GCA treatments maintained ascorbic acid content close to initial values compared to a decrease of 44% in the control fruit at the end of the experiment. This work provides a paradigm shift in how CA could be applied and a better understanding of blueberry physiology and postharvest behavior.

Keywords: ***Vaccinium corymbosum*** **L, postharvest, quality, cold storage, controlled atmosphere**

OPEN ACCESS

Edited by:
Peter Toivonen, Agriculture and Agri-Food Canada, Canada

Reviewed by:
María Serrano, Universidad Miguel Hernández de Elche, Spain
Anna Spinardi, University of Milan, Italy
Claudia Moggia, University of Talca, Chile

***Correspondence:**
Leon A. Terry
l.a.terry@cranfield.ac.uk

Specialty section:
This article was submitted to Crop and Product Physiology, a section of the journal Frontiers in Plant Science

Received: *25 November 2019*
Accepted: *12 February 2020*
Published: *17 March 2020*

Citation:
Falagán N, Miclo T and Terry LA (2020) Graduated Controlled Atmosphere: A Novel Approach to Increase "Duke" Blueberry Storage Life. Front. Plant Sci. 11:221. doi: 10.3389/fpls.2020.00221

INTRODUCTION

Blueberries (*Vaccinium* spp.) have become a popular soft fruit because of their organoleptic characteristics and health-promoting compound content (Manganaris et al., 2014). Yet, blueberries are highly perishable. Their storage life at 0°C varies between 14 and 20 days depending on preharvest factors (i.e., cultivar, ripeness stage, harvest method) and storage conditions (Matiacevich et al., 2013). Slowing down respiration, the main process in fruit metabolism (Gomes et al., 2010), is key to delaying senescence. Respiration is mostly affected by temperature and the respiratory gaseous environment (Wang et al., 2019). Hence, the combination of low temperature

storage and controlled atmosphere (CA) technology has been used for many years to maintain physical and functional quality (Terry et al., 2009). For blueberries, a high concentration of carbon dioxide (CO_2) has a positive impact on decay suppression (Retamales and Hancock, 2018). Recommendations range between 10–12 kPa CO_2; higher levels elicit a negative effect on firmness, flavor, and titratable acidity (TA) content (Kader, 2003; Harb and Streif, 2004). Oxygen (O_2) concentration has less impact on blueberry quality, although lowering it to 2–5 kPa is advised (Kader, 2003). O_2 concentrations below 2 kPa lead to hypoxia and fermentation (Retamales and Hancock, 2018). However, applying standard CA can lead to abiotic stress derived from a sudden change in the surrounding atmosphere, negatively affecting quality (Falagán and Terry, 2018). The introduction of real-time respirometry has allowed the effects of CA to be monitored, reactivating research in this field. Previous studies have shown how targeted CA applications had a similar effect to continuous CA in extending shelf-life of onion, strawberry and avocado (Chope et al., 2007; Alamar et al., 2017). Based on these results, we hypothesized in this work that the graduated application of CA (GCA) could avoid this metabolic shock as it allows fresh produce to more slowly adapt to an optimal gaseous environment. This approach is based on the way modified atmosphere packaging (MAP) works, gradually reaching the respiratory equilibrium, instead of exposing the fresh produce to a sudden change in the atmosphere. Work on adaptive control of the gas diffusion in MAP has been successfully implemented before, e.g., preserving quality in blueberries and spinach (Lee et al., 2016). In this study, the MAP approach is translated to CA systems. The aim of this work was to study the benefits of GCA on the physiological and functional quality of "Duke" blueberries.

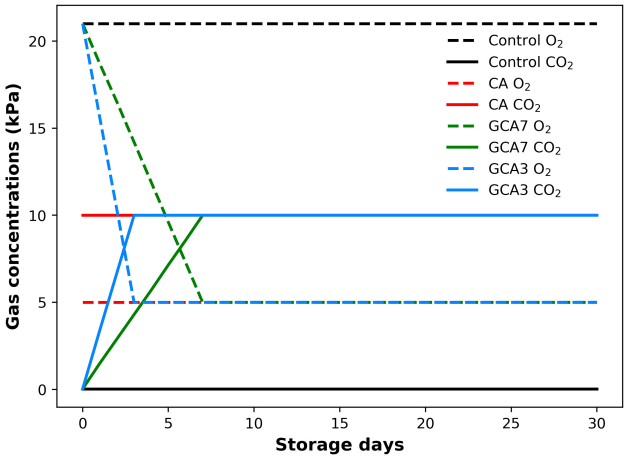

FIGURE 1 | Gas concentration (CO_2 and O_2; kPa) supply throughout 28 days of storage at 0°C and 90–95 RH%; air [control]; standard CA (10 kPa CO_2 + 5 kPa O_2); graduated CA 7 (GCA7; 7 days to achieve standard CA values); and GCA3 (3 days to achieve standard CA values).

MATERIALS AND METHODS

Plant Material

Blueberries (*Vaccinium corymbosum* L.) "Duke" were hand harvested at Cobrey Farms (Herefordshire, United Kingdom) on the 12 of July 2017 (season 1) and on the 27 of June 2018 (season 2) at their optimal maturity stage according to commercial standards defined by the company, considering color and maturity index. They were immediately transported in 600 g punnets to the Plant Science Laboratory at Cranfield University by refrigerated truck (2.5 h). Fruit were then directly transferred to the treatment boxes upon arrival at the laboratory and allowed to cool down for 24 h at 0°C prior treatment application.

Experimental Plan

Forty-eight 4 L air-tight polypropylene boxes (L&L Nordic OÜ, Estonia) were used to store 1 kg of sound fruit each. They were kept in a cold room at 0°C and 90–95% relative humidity (RH). Four treatments were considered: (i) Control, flushed with regular atmosphere gas concentrations (20.9 kPa O_2 and 0.03 kPa CO_2); (ii) standard CA (5 kPa O_2 and 10 kPa CO_2); (iii) graduated CA 3 (GCA3) flushed to reach the desired CA partial pressures in 3 days; and (iv) GCA7 gradually flushed to reach the standard CA conditions in 7 days (**Figure 1**). Each condition was performed in triplicate. The combination of 5 kPa O_2 and 10 kPa CO_2 was selected as optimal according to previous work (Kader, 2003; Harb and Streif, 2004; Retamales and Hancock, 2018). For each CA condition, boxes were connected to an ICA6000 (International Controlled Atmosphere Ltd., Paddock Wood, Kent, United Kingdom) via PVC tubes; gases were bubbled through water to maintain a high RH%. For each treatment, an extra empty box was used as a baseline to avoid cross-contamination and allow respirometry calculations. The ICA6000 included an automated sample sequencing system to measure and control the gas concentration introduced in CA environments. The system was regularly checked for calibration with both fresh air and bottled calibration gas. Both temperature and RH were monitored in real-time with RD Sens RFS-TH (Prodisei, Valencia, Spain). Sampling was carried out on days 0, 7, 14, 21, and 28. Day 0 (one day after harvest) analysis were considered as baseline and samples were taken before placing the fruit in the treatment boxes.

Fruit Quality Assessment

Respiration Rate

Real-time respiration rate was continuously recorded using a Sable Respirometry System (model 1.3.8 Pro, Sable Systems International, Nevada, United States) as described in Alamar et al. (2017) with slight modifications. Air from each box passed through a CA-10 (Firmware version 1.05) and a FC-10 sensor (Firmware version 3.0), which recorded CO_2 and O_2 partial pressures (kPa), respectively. For each treatment, an empty box was used as a baseline. These baseline boxes were sampled for 2 min between each replicate and for 6 min between each treatment to avoid cross-contamination. Baseline values were subtracted from sample values to obtain an accurate respiration rate expressed in mg kg^{-1} h^{-1}.

Decay and Weight Loss

Fruit presenting fungal development symptoms, leakage, or collapse were considered as decayed. Decay was assessed on 100 blueberries per replicate and results were expressed as percentages. Decay severity was evaluated using a scale, where 1 = 0%, 2 = 1 to 25%, 3 = 26 to 50%, 4 = 51 to 75%, and 5 = 76 to 100% of the decayed fruit. Fruit were counted and a percentage was attributed to each level of the scale. Weight was recorded weekly using a digital balance (Precisa Ltd., Buckinghamshire, United Kingdom) with 0.1 g resolution. The same boxes were measured throughout the experiment. Weight loss was expressed as the percentage of loss compared to the initial 1 kg weight (Paniagua et al., 2014).

Firmness

A non-destructive compression test was performed on ten fruit per replicate using a uniaxial texture analyzer (model 5542, Instron, Norwood, MA, United States) equipped with a 38 mm diameter flat steel disc and a calibrated 500 N load cell. Berries were compressed by 2 mm, equatorially, at a rate of 1.2 mm s^{-1} according to Schotsmans et al. (2007) with slight modifications. The peak force necessary to achieve the target distance was recorded. Firmness was expressed as Newton (N).

pH, Total Soluble Solids, and Titratable Acidity

The juice of 25 blueberries per replicate (Schotsmans et al., 2007) was extracted using a commercial blender (Moulinex, Berkshire, United Kingdom). pH was recorded using a pH-meter (model 3540, Jenway, Staffordshire, United Kingdom). Total soluble solids (TSS) were determined using a digital refractometer (model PR-32α, Atago Ltd., Tokyo, Japan). TA was determined by titrating a solution of 5 mL of juice diluted in 45 mL of distilled water to pH 8.4 using 0.1 N NaOH and an automatic titrator (Mettler Toledo Ltd., Leicestershire, United Kingdom), according to Zheng et al. (2008) with slight modifications. Results were expressed as g citric acid L^{-1} (Schotsmans et al., 2007).

Determination of Biochemistry Attributes

Sugar Content

For each replicate (n = 3), following Downes and Terry (2010) with modifications, freeze-dried blueberry powder (150 mg) was extracted and then analyzed in an HPLC (Agilent Technologies 1200 series, Berkshire, United Kingdom) with an evaporative light scattering detector (ELSD, Agilent Technologies 1200 Series, G1362A). Sugars were quantified using the external standards glucose, fructose and sucrose purchased from Sigma-Aldrich.

Organic Acids Content

For each replicate (n = 3), following Crespo et al. (2010) with modifications, freeze-dried blueberry powder (50 mg) was extracted and analyzed in an HPLC (Agilent Technologies 1200 series, Berkshire, United Kingdom) equipped with a diode array detector (DAD Agilent Technologies 1200 Series, G1315B) set at 210 nm was used to quantify ascorbic and citric acids (Sigma Aldrich, Kent, United Kingdom). Separation was performed on a prevail organic acid column of 250 mm × 4.6 mm, 5 μm particle size (Hichrom, United Kingdom; Part no. 88645). Mobile phase was 25 mM KH_2PO_4 in water, adjusted to pH 2.5 using meta-phosphoric acid. Organics acids were quantified using the external standards ascorbic and citric acids purchased from Sigma-Aldrich.

Statistical Analysis

Data were subjected to analysis of variance (ANOVA) using GenStat for Windows (8.1, VSN International Ltd., Hertfordshire, United Kingdom). ANOVA assumptions were tested and found to be valid for this dataset. The differences between treatments and storage times were studied. Also, the differences between the two seasons were analyzed. Least significant difference values (LSD; $p < 0.05$) were calculated from each analysis.

RESULTS

Respiratory Response to GCA

A peak in CO_2 production was observed for all treatments in both seasons; its intensity and timing varied depending on treatment. Blueberries subjected to standard CA conditions showed the earliest and highest CO_2 burst, while GCA7 was the most delayed and had the lowest peak. CO_2 production reached a plateau after *ca.* 60 h in both years; control samples presented the highest CO_2 production compared to any of the CA treatments during the plateau period (**Figure 2**).

Physiological Response to GCA

GCA3, GCA7 and CA blueberries showed a significantly lower decay incidence than the control (92, 89, and 75% less than control, respectively; mean values between Y1 and Y2 values) after 28 storage days (**Figure 3**). In the case of decay severity, both GCA treatments prevented the development of fungal growth (<1%), while CA reached an average incidence value of 3.09% after 28 days (data not shown). Fruit subjected to CA and GCA showed less weight loss compared to the control. Both GCA delayed decay incidence by 14 days, compared to control and CA treatments (**Figure 4**). No significant differences were found between seasons ($p < 0.05$).

At the end of the storage period, control and CA blueberries lost an average of 40 and 29% of their initial firmness in Y1 and Y2, respectively. Firmness of berries held under GCA3 and GCA7 showed a loss of 16% in the first season and no significant changes were observed during the second season (**Figure 5**). pH showed a decreasing trend in Y1 and Y2, triggered by the interaction of treatment and time in Y1 and time in Y2. No significant differences were found in TA across both years (**Supplementary Table 1**).

Biochemical Response to GCA

Total sugar content was 40% higher in Y2 compared to Y1, but showed a similar pattern during storage. CA, GCA3 and GCA7 maintained the concentration of sucrose and fructose across the experiment, while control blueberries presented a sharp decrease in sucrose (49% mean for Y1 and Y2) and fructose (12.5% mean for Y1 and Y2). Glucose concentrations were maintained

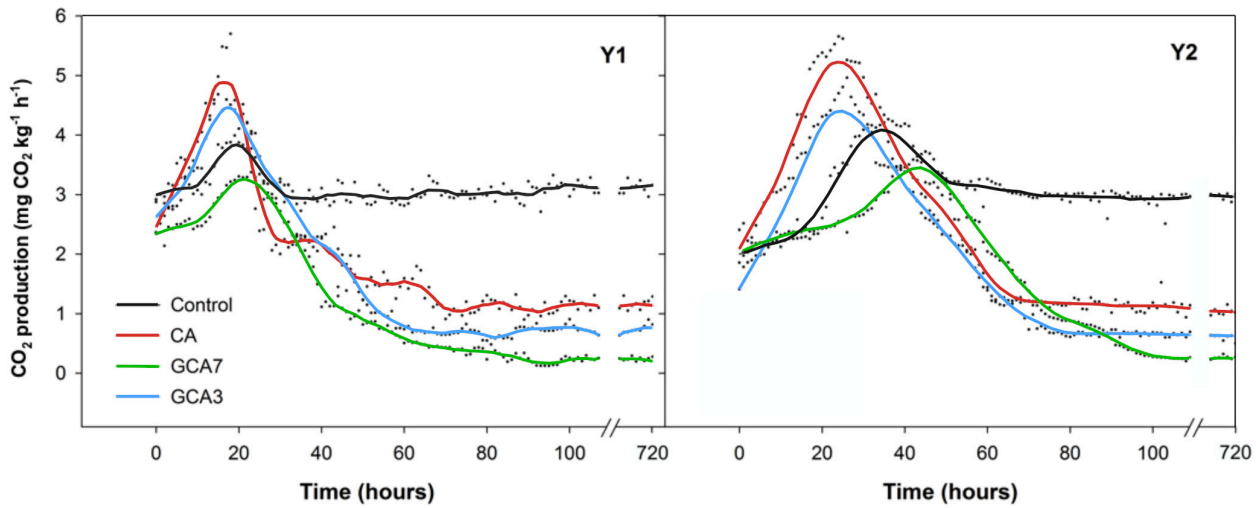

FIGURE 2 | Real-time respiration rate (CO_2 production expressed as mg kg^{-1} h^{-1}) of "Duke" blueberry fruit subjected to controlled atmosphere (CA) applications throughout 28 days of storage at 0°C and 90–95 RH%; air [control]; standard CA (10 kPa CO_2 + 5 kPa O_2); graduated CA 7 (GCA7; 7 days to achieve standard CA values); and GCA3 (3 days to achieve standard CA values). Two consecutive seasons are considered 2017 (year 1; Y1) and 2018 (Y2). Lines represent smooth fit curves.

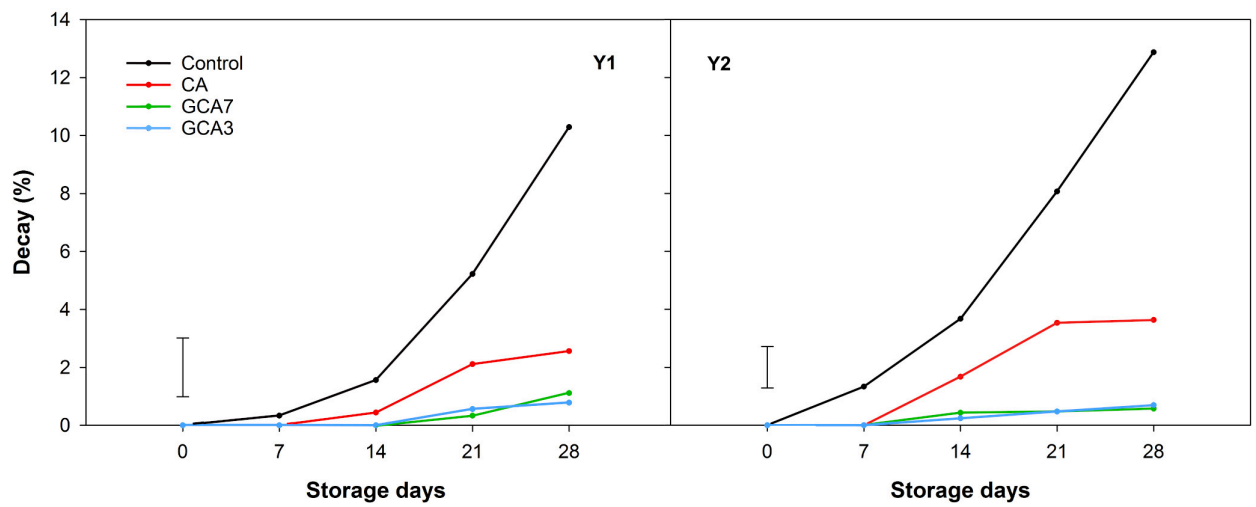

FIGURE 3 | Decay expressed as percentage (%) of "Duke" blueberry fruit subjected to controlled atmosphere (CA) applications throughout 28 days of storage at 0°C and 90–95 RH%; air [control]; standard CA (10 kPa CO_2 + 5 kPa O_2); graduated CA 7 (GCA7; 7 days to achieve standard CA values); and GCA3 (3 days to achieve standard CA values). Two consecutive seasons are considered 2017 (year 1; Y1) and 2018 (Y2). Data represents means (n = 300). Least Significant Differences (LSD) are included as $LSD_{treatment*time}$ = 1.0145 for Y1 and $LSD_{treatment*time}$ = 0.713 for Y2.

in CA and GCA treated fruit, whilst they slightly increased in control fruit (**Figure 6**). Ascorbic acid content degraded by 34, 29, and 41% during storage for CA, GCA, and control blueberries, respectively, for Y1; and 21, 29, and 44% during storage for CA, GCA, and control blueberries, respectively, for Y2 (**Figure 7**). In the case of citric acid, no significant differences were found among CA treatments and time during the experiment. CA treatments maintained the initial citric acid level, while control samples suffered a decrease of 45 and 31% in Y1 and Y2, respectively (**Figure 7**). Significant differences were observed between Y1 and Y2 for both ascorbic and citric acids contents (Ascorbic acid: $LSD_{Y1 \times Y2} = 1.56$; citric acid: $LSD_{Y1 \times Y2} = 0.23$; $p < 0.05$). Despite these differences, the response of blueberries to CA and GCA was the same in both seasons (**Figure 7**).

DISCUSSION

Fruit and vegetables undergo physiological and functional changes during senescence, which affect their quality and storage life (Terry, 2011). Most of these changes are linked to fruit respiration, which supports the many metabolic

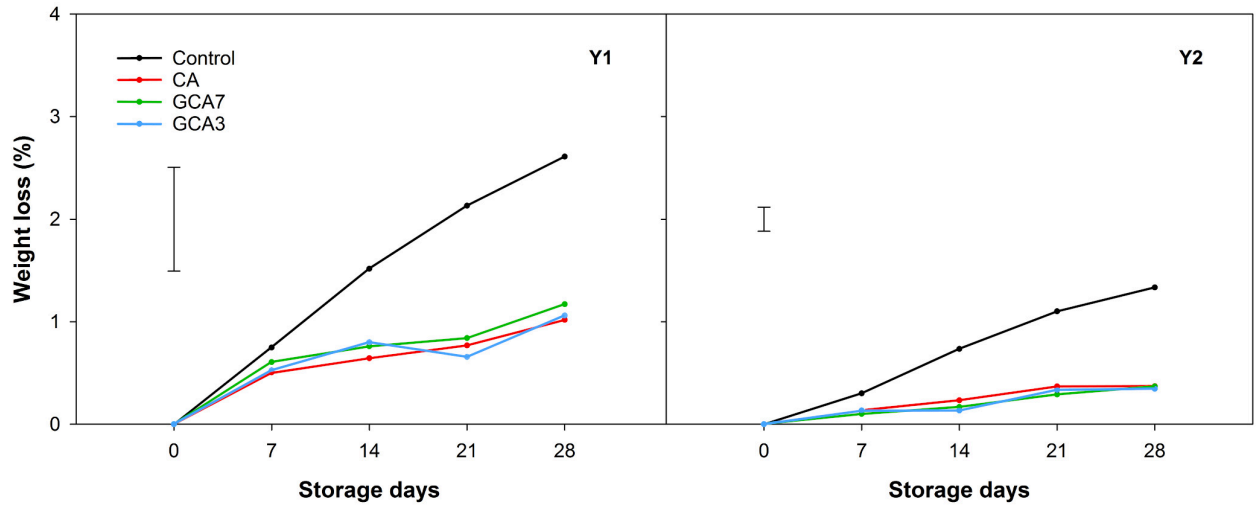

FIGURE 4 | Weight loss expressed as percentage (%) of "Duke" blueberry fruit subjected to controlled atmosphere (CA) applications throughout 28 days of storage at 0°C and 90–95 RH%; air [control]; standard CA (10 kPa CO_2 + 5 kPa O_2); graduated CA 7 (GCA7; 7 days to achieve standard CA values); and GCA3 (3 days to achieve standard CA values). Two consecutive seasons are considered 2017 (year 1; Y1) and 2018 (Y2). Data represents means (n = 3). Least Significant Differences (LSD) are included as: $LSD_{treatment*time}$ = 1.0145 for Y1 and $LSD_{treatment}$ = LSD_{time} = 0.2338 for Y2.

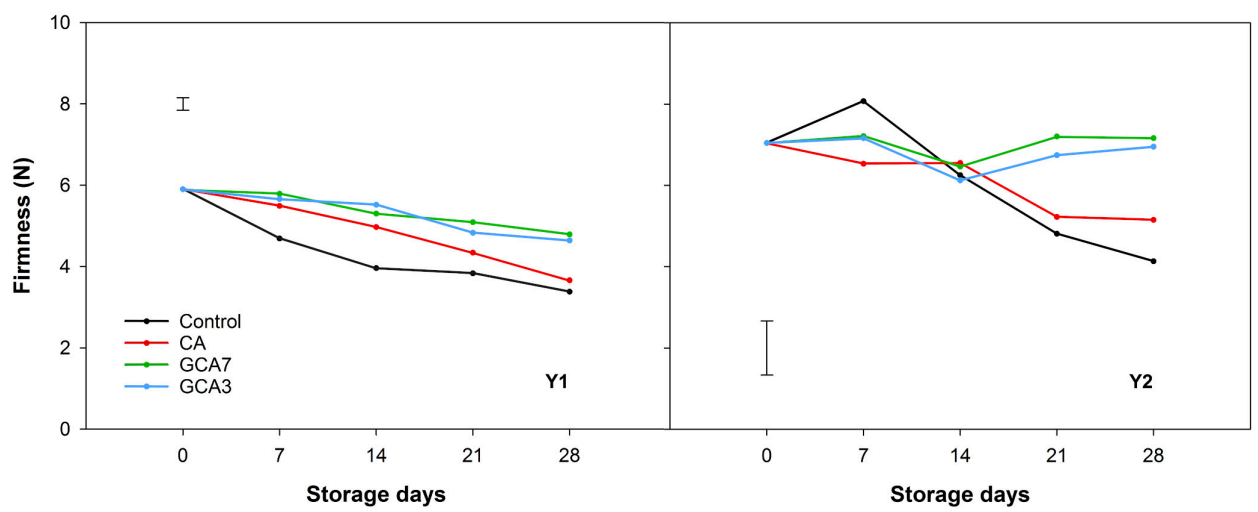

FIGURE 5 | Firmness expressed as Newton (N) of "Duke" blueberry fruit subjected to controlled atmosphere (CA) applications throughout 28 days of storage at 0°C and 90–95 RH%; air [control]; standard CA (10 kPa CO_2 + 5 kPa O_2); graduated CA 7 (GCA7; 7 days to achieve standard CA values); and GCA3 (3 days to achieve standard CA values). Two consecutive seasons are considered 2017 (year 1; Y1) and 2018 (Y2). Data represents means (n = 30). Least Significant Differences (LSD) are included as: $LSD_{treatment}$ = LSD_{time} = 0.310 for Y1 and $LSD_{treatment*time}$ = 1.335 for Y2.

reactions occurring in a cell (Saltveit, 2019). According to Van Hoorn (2004), the higher the respiration rate, the faster the fruit/vegetable metabolism, leading to early senescence. Until now, the main way to achieve lower blueberry respiration rate has been through cold storage and the modification of gas concentrations surrounding the fresh produce (lowering O_2 availability and increasing CO_2 concentration). This approach works because respiratory metabolism is affected by low O_2 concentrations due to limited gas transport (Armstrong and Beckett, 2011), triggering the active regulation of respiration (Gupta et al., 2009). In this study we proposed a novel application of CA, based on reaching the optimal CA gas concentrations in a gradual way, preventing abiotic stress that results from the sudden change in the gaseous environment. The observed CO_2 production bursts occurred at different times and were linked to the decrease of available O_2 in the storage environment. Blueberries subjected to CA were exposed to a sudden drop in the available O_2 from 21 to 5 kPa. In response to this change, CA samples presented a well-defined peak in CO_2 production. Following CA response, GCA3 blueberries increased

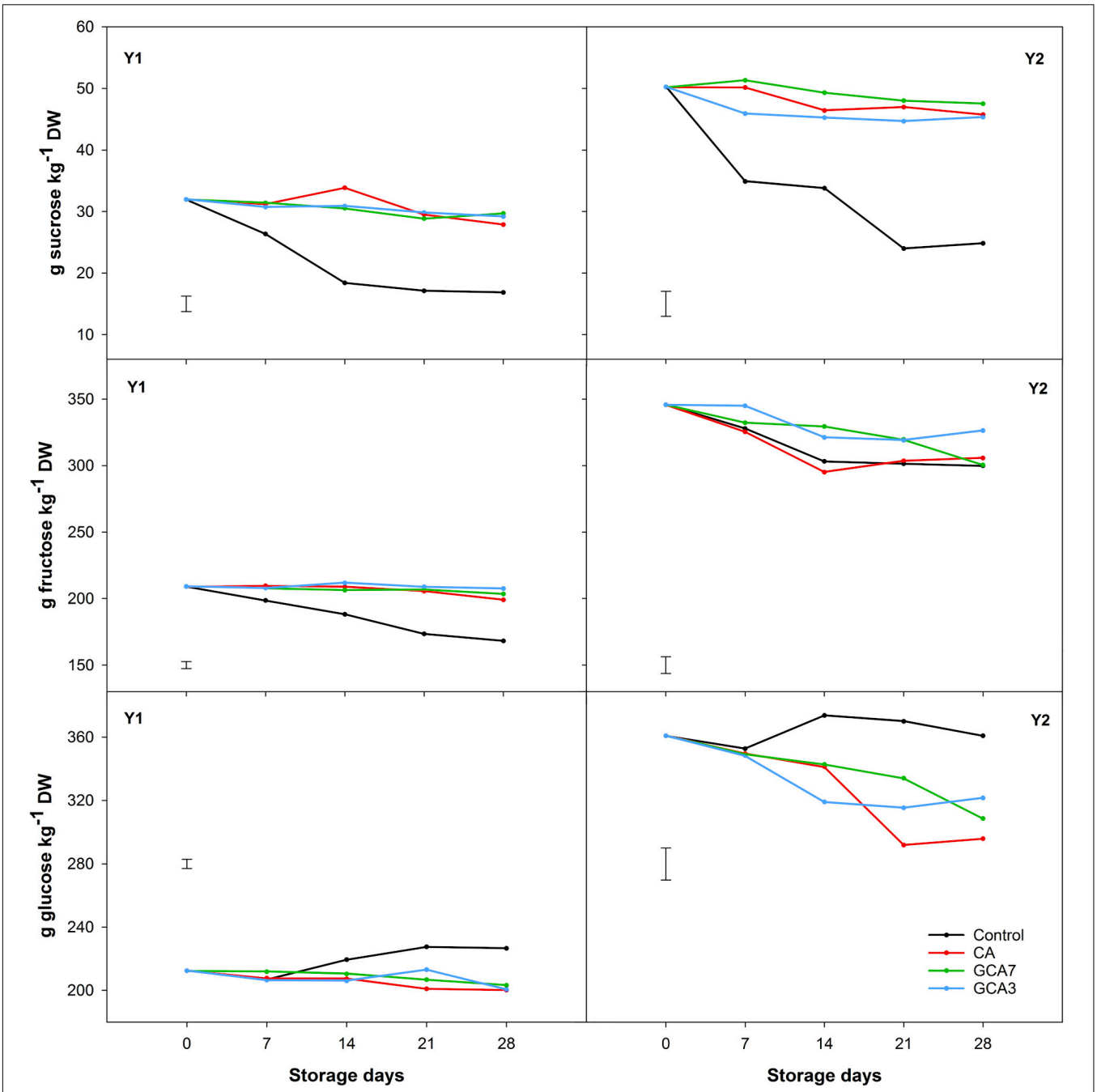

FIGURE 6 | Individual sugar concentration (sucrose, fructose, and glucose) expressed as g kg^{-1} dry weight (DW) of "Duke" blueberry fruit subjected to controlled atmosphere (CA) applications throughout 28 days of storage at 0°C and 90–95 RH%; air [control]; standard CA (10 kPa CO_2 + 5 kPa O_2); graduated CA 7 (GCA7; 7 days to achieve standard CA values); and GCA3 (3 days to achieve standard CA values). Two consecutive seasons are considered 2017 (year 1; Y1) and 2018 (Y2). Data represents means (n = 3). Least Significant Differences (LSD) are included as: (i) Sucrose – $LSD_{treatment}$ = LSD_{time} = 2.484 for Y1 and $LSD_{treatment}$ = 4.082 for Y2; Fructose – $LSD_{treatment*day}$ = 5.251 for Y1 and $LSD_{treatment}$ = LSD_{time} = 12.63 for Y2; and Glucose – $LSD_{treatment*day}$ = 5.848 for Y1 and $LSD_{treatment*time}$ = 20.26 for Y2.

their CO_2 production when the O_2 availability dropped from 21 to 15.6 kPa. In the case of GCA7, its peak was delayed, coinciding with an O_2 availability of *ca.* 15 kPa. Therefore, O_2 concentrations below 15 kPa were seen to induce an abiotic stress, and consequently an increase in CO_2 production. This finding agreed with Gupta et al. (2009) who highlighted the importance of the timescale in O_2 availability changes for respiratory metabolism. These peaks in CO_2 production represented an increase in respiration, interpreted as possible abiotic stress to the changing gaseous environment (Mathooko et al., 2001).

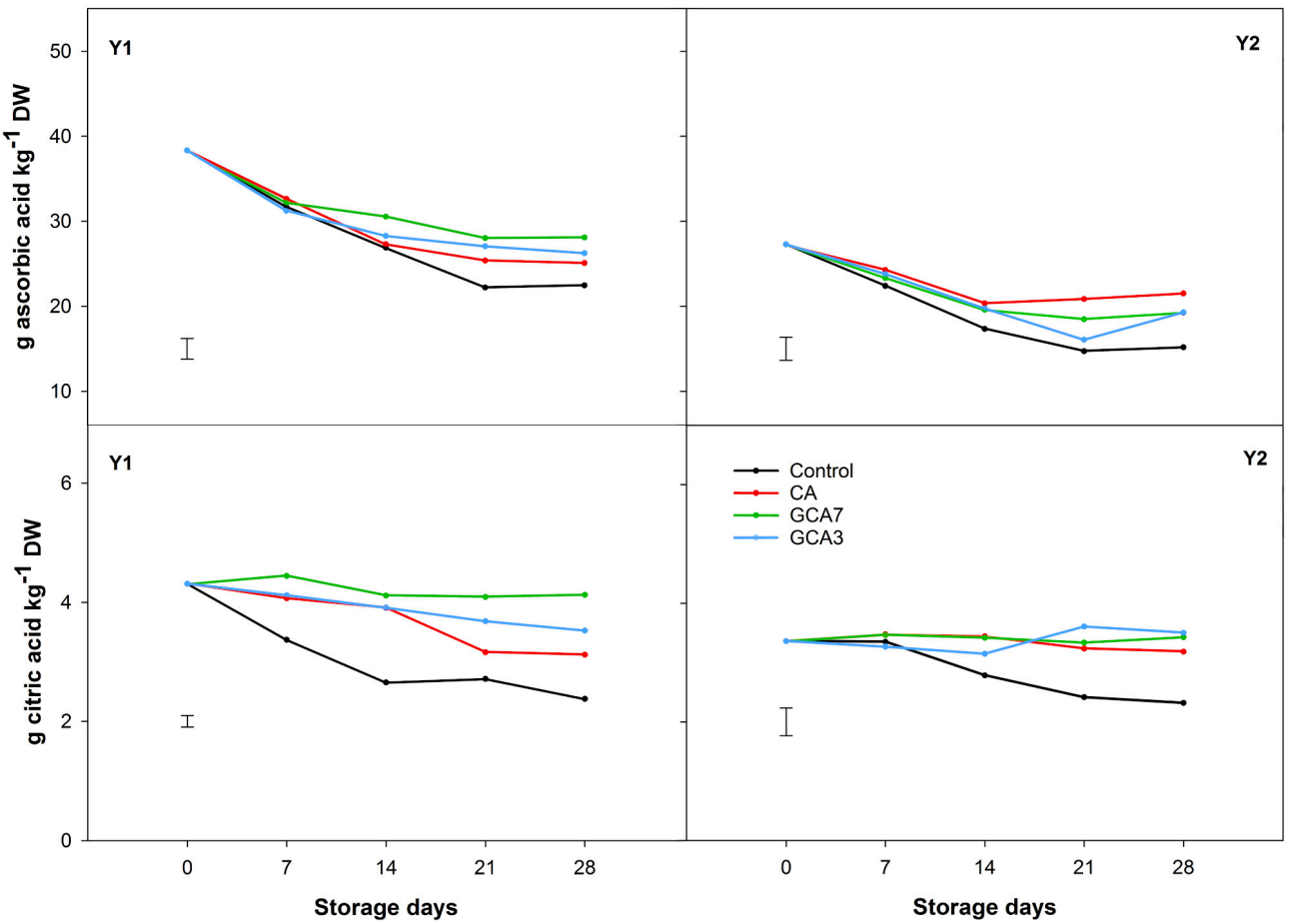

FIGURE 7 | Organic acid concentration (ascorbic and citric acids) expressed as g kg^{-1} dry weight (DW) of "Duke" blueberry fruit subjected to controlled atmosphere (CA) applications throughout 28 days of storage at 0°C and 90–95 RH%; air [control]; standard CA (10 kPa CO_2 + 5 kPa O_2); graduated CA 7 (GCA7; 7 days to achieve standard CA values); and GCA3 (3 days to achieve standard CA values). Two consecutive seasons are considered 2017 (year 1; Y1) and 2018 (Y2). Data represents means (n = 3). Least Significant Differences (LSD) are included as: (i) ascorbic acid – $LSD_{treatment}$ = LSD_{time} = 2.417 for Y1 and $LSD_{treatment}$ = 2.731 for Y2; and citric acid – $LSD_{treatment}$ = LSD_{time} = 0.1907 for Y1 and $LSD_{treatment}$ = 0.4680 for Y2.

Interestingly, control blueberries also showed a peak, although smaller than the treatments had provoked, before reaching a steady-state level. This phenomenon might be because of the handling procedure, which involved a change in temperature, RH and storage environment. More research is needed in this area to identify the mechanisms behind this response. Nevertheless, it is observed that a slower imposed GCA, such as GCA7, produced the most delayed and lowest peak in CO_2 production compared to standard CA, GCA3 and control (**Figure 2**). We herein hypothesized that GCA allowed the adaptive response of respiration to low O_2 availability, preventing the metabolic shock that could reduce the physical quality of the fruit (Armstrong and Beckett, 2011). Apart from preventing this abiotic stress, GCA achieved a lower respiration rate compared to standard CA and control treatments when it reached stability after *ca.* 7 days of storage.

In fresh produce, senescence is generally marked by changes in firmness, weight and decay incidence (Defraeye et al., 2015). The reduction in respiratory metabolism had a positive impact on firmness, which is a critical quality index for blueberry, as consumers associate it with freshness (Chiabrando and Giacalone, 2017). Changes in firmness are a consequence of primary cell wall component degradation, such as pectin, cellulose and hemicellulose (Liu et al., 2019). We speculated that low O_2 and high CO_2 storage environments inhibited the action of polygalacturonase and pectin methylesterase (Beaudry, 1999), which are the enzymes responsible for the catabolism of cell wall metabolism (Yang et al., 2018). This event was also observed in blueberries stored under standard CA conditions (Concha-Meyer et al., 2015). GCA regulated response and delayed firmness loss when compared to control and CA treatments. Previous studies showed that targeted CA application on strawberry maintained their color (flesh and calyx) and firmness when compared to control and standard CA (Alamar et al., 2017). Firmness loss is directly linked to weight loss and decay incidence, as observed in this study (Paniagua et al., 2014; Chen et al., 2017). In the case of weight loss, blueberries subjected to GCA showed the same response as

CA fruit, both significantly lower than control samples. Weight is generally lost through transpiration, the gradient of water vapor pressure in the cell tissues (Díaz-Pérez et al., 2007). In blueberries, transpiration generally happens through the stem scar rather than through the cuticle and it increases with temperature (Moggia et al., 2017). The blueberries herein were stored at 0°C, so that overall low weight loss percentages were observed. Although control samples showed a significantly higher weight loss than CA and GCA blueberries, it is considered that losses up to 4–5% do not affect fruit freshness (Mannozzi et al., 2017). In this study, higher weight and firmness loss contributed to greater decay in control samples when compared to CA and GCA. In general, CA with CO_2 concentrations over 6 kPa retard decay symptoms in blueberry fruit (Schotsmans et al., 2007; Rodríguez and Zoffoli, 2016). However, a long exposure to high CO_2 levels can cause internal damage to fruit leading to firmness and weight loss. We assumed that a graduated CA approach prevented this damage, providing better quality fruit than CA. GCA is an innovative approach to standard CA storage, and is analogous to a MAP strategy. Alternatives to standard CA include targeted CA application, which showed that 2.5 days of CA were sufficient to extend the shelf-life of strawberry by 3 days based on delayed decay incidence (Alamar et al., 2017).

Sugars and organic acids are considered the main substrates in the respiratory metabolism (Saltveit, 2019). Recent studies have considered that glucose and sucrose can play a role as signaling molecules in the stress responses (Huang et al., 2016), rather than just as a carbon source. It has also been reported that in non-climacteric fruit such as strawberry both sucrose and glucose promote fruit ripening and senescence (Jia et al., 2013; Cherian et al., 2014). In this study, control samples showed sucrose hydrolysis (**Figure 6**), likely through the action of invertase and sucrose synthase (Thomas et al., 2016). This process was not observed in CA nor GCA, indicating an inhibition of sugar degradation and delayed senescence. The different sugar profiles between the control and CA/GCA blueberries was linked to observed respiratory behavior, confirming the role of sugars as substrates in the respiratory metabolism. However, there was no evidence to support the hypothesis of sugars acting as signaling molecules in the stress responses of blueberries, this being in agreement with Karppinen et al. (2018). In this study, there was a poor correlation between sugar content and TSS, as described in Terry (2012). With respect to TA, neither time or treatments had an effect on its content. In contrast, Duarte et al. (2009) found that blueberries "Brigitta" treated with CA had a higher TA than control samples. Looking at ascorbic and citric acid concentrations, both were more stable in fruit subjected to GCA and CA berries than the control. This study showed the positive impact of GCA on preserving bioactive life of blueberry and potentially for other fresh produce by suppressing senescence decline. Both pH and TA remained stable across the experiment, while changes were observed in organic acid content. We acknowledged the lack of correlation among these parameters; this could be related to the lower sensitivity of pH and TA measurement methods, compared to HPLC.

The difference in the results between seasons 1 and 2 ($p < 0.05$) may be potentially attributable to variable environmental preharvest factors, particularly temperature as several heat waves were registered in June and July 2018 (Met Office, 2018).

CONCLUSION

Blueberries require advanced postharvest techniques to maintain their physiological and functional quality. The development of an innovative CA approach, based on gradually reaching the optimal storage concentrations (GCA) allowed the reduction of blueberry respiratory metabolism when compared to standard CA and control treatments. This had a positive impact on quality parameters such as firmness and decay incidence. The reduction in respiration was also evident as sugars and organic acids were better maintained, these being the main respiratory substrates. GCA could potentially be successfully applied to other blueberry cultivars. Further research is needed to better understand the mechanisms underlying this technique and the efficacy of its use on other fresh produce.

DATA AVAILABILITY STATEMENT

All datasets generated for this study can be accessed at https://doi.org/10.17862/cranfield.rd.11876544.v1.

AUTHOR CONTRIBUTIONS

NF and LT conceived and designed the experiments. NF and TM performed the experiments. NF wrote the manuscript with the help of LT. All authors contributed to the discussion, revised, and approved the final manuscript.

FUNDING

This work was supported by the Biotechnology and Biological Sciences Research Council (BBSRC; BB/P00492X/1) and Johnson Matthey Plc.

ACKNOWLEDGMENTS

The authors thank BBSRC and Johnson Matthey Plc. for financial support.

SUPPLEMENTARY MATERIAL

The Supplementary Material for this article can be found online at: https://www.frontiersin.org/articles/10.3389/fpls.2020.00221/full#supplementary-material

REFERENCES

Alamar, M. C., Collings, E., Cools, K., and Terry, L. A. (2017). Impact of controlled atmosphere scheduling on strawberry and imported avocado fruit. *Postharvest Biol. Technol.* 134, 76–86. doi: 10.1016/j.postharvbio.2017.08.003

Armstrong, W., and Beckett, P. M. (2011). Experimental and modelling data contradict the idea of respiratory down-regulation in plant tissues at an internal [O_2] substantially above the critical oxygen pressure for cytochrome oxidase. *New Phytol.* 190, 431–441. doi: 10.1111/j.1469-8137.2010.03537.x

Beaudry, R. M. (1999). Effect of O_2 and CO_2 partial pressure on selected phenomena affecting fruit and vegetable quality. *Postharvest Biol. Technol.* 15, 293–303. doi: 10.1016/S0925-5214(98)00092-1

Chen, Y. H., Hung, Y. C., Chen, M. Y., and Lin, H. T. (2017). Effects of acidic electrolyzed oxidizing water on retarding cell wall degradation and delaying softening of blueberries during postharvest storage. *LWT Food Sci. Technol.* 84, 650–657. doi: 10.1016/j.lwt.2017.06.0110023-6438

Cherian, S., Figueroa, C. R., and Nair, H. (2014). 'Movers and shakers' in the regulation of fruit ripening: a cross-dissection of climacteric versus non-climacteric fruit. *J. Exp. Bot.* 65, 4705–4722. doi: 10.1093/jxb/eru280

Chiabrando, V., and Giacalone, G. (2017). Quality evaluation of blueberries coated with chitosan and sodium alginate during postharvest storage. *Int. Food Res. J.* 24, 1553–1561.

Chope, G., Terry, L. A., and White, P. J. (2007). The effect of the transition between controlled atmosphere and regular atmosphere storage on bulbs of onion cultivars SS1, Carlos and Renate. *Postharvest Biol. Technol.* 49, 61–68. doi: 10.1016/j.postharvbio.2006.12.018

Concha-Meyer, A., Eifert, J. D., Williams, R. C., Marcy, J. E., and Welbaum, G. E. (2015). Shelf life determination of fresh blueberries (*Vaccinium corymbosum*) stored under controlled atmosphere and ozone. *Int. J. Food Sci.* 164143, 1–9. doi: 10.1155/2015/164143

Crespo, P., Bordonaba, J. G., Terry, L. A., and Carlen, C. (2010). Characterisation of major taste and health-related compounds of four strawberry genotypes grown at different Swiss production sites. *Food Chem.* 122, 16–24. doi: 10.1016/j.foodchem.2010.02.010

Defraeye, T., Cronjé, P., Berry, T., Opara, U. L., East, A., Hertog, M., et al. (2015). Towards integrated performance evaluation of future packaging for fresh produce in the cold chain. *Trends Food Sci. Technol.* 44, 201–225. doi: 10.1016/j.tifs.2015.04.008

Díaz-Pérez, J. C., Muy-Rangel, M. D., and Mascorro, A. G. (2007). Fruit size and stage of ripeness affect postharvest water loss in bell pepper fruit (*Capsicum annuum* L.). *J. Sci. Food Agric.* 87, 68–73. doi: 10.1002/jsfa.2672

Downes, K., and Terry, L. A. (2010). A new acetonitrile-free mobile phase method for LC–ELSD quantification of fructooligosaccharides in onion (*Allium cepa* L.). *Talanta* 82, 118–124. doi: 10.1016/j.talanta.2010.04.003

Duarte, C., Guerra, M., Daniel, P., Camelo, A. L., and Yommi, A. (2009). Quality changes of highbush blueberries fruit stored in CA with different CO_2 levels. *J. Food Sci.* 74, 154–159. doi: 10.1111/j.1750-3841.2009.01118.x

Falagán, N., and Terry, L. A. (2018). Recent advances in controlled and modified atmosphere of fresh produce. *Johnson Matthey Tech.* 62, 107–117. doi: 10.1595/205651318X696684

Gomes, M. H., Beaudry, R. M., Almeida, D. P. F., and Malcata, F. X. (2010). Modelling respiration of packaged fresh-cut 'Rocha' pear as affected by oxygen concentration and temperature. *J. Food Eng.* 96, 74–79. doi: 10.1016/j.jfoodeng.2009.06.043

Gupta, K. J., Zabalza, A., and van Dongen, J. T. (2009). Regulation of respiration when the oxygen availability changes. *Physiol. Plant.* 137, 383–391. doi: 10.1111/j.1399-3054.2009.01253.x

Harb, J., and Streif, J. (2004). Controlled atmosphere storage of highbush blueberries cv. '*Duke*'. *Eur. J. Hort. Sci.* 69, 66–72.

Huang, H., Xie, S., Xiao, Q., Wei, B., Zheng, L., Wang, Y., et al. (2016). Sucrose and ABA regulate starch biosynthesis in maize through a novel transcription factor, ZmEREB156. *Sci. Rep.* 6:27590. doi: 10.1038/srep27590

Jia, H., Wang, Y., Sun, M., Li, B., Han, Y., Zhao, Y., et al. (2013). Sucrose functions as a signal involved in the regulation of strawberry fruit development and ripening. *New Phytol.* 198, 453–465. doi: 10.1111/nph.12176

Kader, A. A. (2003). A summary of CA requirements and recommendations for fruits other than apples and pears. *Acta Hortic.* 600, 737–740. doi: 10.17660/ActaHortic.2003.600.112

Karppinen, K., Tegelberg, P., Häggman, H., and Jaakola, L. (2018). Abscisic acid regulates anthocyanin biosynthesis and gene expression associated with cell wall modification in ripening bilberry (*Vaccinium myrtillus* L.) fruits. *Front. Plant Sci.* 29:1259. doi: 10.3389/fpls.2018.01259

Lee, J. H., An, D. S., Song, J. M., Jung, Y. B., and Lee, D. S. (2016). An adaptively controlled modified atmosphere container system for fresh produce. *Biosyst. Eng.* 148, 11–17. doi: 10.1016/j.biosystemseng.2016.05.003

Liu, B., Wang, K., Shu, X., Liang, J., and Sun, L. (2019). Changes in fruit firmness, quality traits and cell wall constituents of two highbush blueberries (*Vaccinium corymbosum* L.) during postharvest cold storage. *Sci. Hortic.* 246, 557–562. doi: 10.1016/j.scienta.2018.11.042

Manganaris, G. A., Goulas, V., Vicente, A. R., and Terry, L. A. (2014). Berry antioxidants: small fruits providing large benefits. *J. Sci. Food Agric.* 94, 825–833. doi: 10.1002/jsfa.6432

Mannozzi, C., Cecchini, J. P., Tylewicza, U., Siroli, L., Patrignani, F., Lanciotti, R., et al. (2017). Study on the efficacy of edible coatings on quality of blueberry fruits during shelf-life. *LWT* Food Sci. Technol. 85, 440–444. doi: 10.1016/j.lwt.2016.12.056

Mathooko, F. M., Tsunashima, Y., Owino, W. Z. O., Kubo, Y., and Inaba, K. (2001). Regulation of genes encoding ethylene biosynthetic enzymes in peach (*Prunus persica* L.) fruit by carbon dioxide and 1-methylcyclopropene. *Postharvest Biol. Technol.* 21, 265–281. doi: 10.1016/S0925-5214(00)00158-7

Matiacevich, S., Cofré, D. C., Silva, P., Enrione, J., and Osorio, F. (2013). Quality parameters of six cultivars of blueberry using computer vision. *Int. J. Food Sci.* 419535*, doi: 10.1155/2013/419535

Met Office (2018). *Climate Summaries*. Available online at: https://www.metoffice.gov.uk/climate/uk/summaries (accessed: September 2, 2018).

Moggia, C., Beaudry, R. M., Retamales, J. B., and Lobos, G. A. (2017). Variation in the impact of stem scar and cuticle on water loss in highbush blueberry fruit argue for the use of water permeance as a selection criterion in breeding. *Postharvest Biol. Technol.* 132:8896. doi: 10.1016/j.postharvbio.2017.05.019

Paniagua, A. C., East, A. R., and Heyes, J. A. (2014). Interaction of temperature control deficiencies and atmosphere conditions during blueberry storage on quality outcomes. *Postharvest Biol. Technol.* 95, 50–59. doi: 10.1016/j.postharvbio.2014.04.006

Retamales, J. B., and Hancock, J. F. (2018). *Blueberries*. Wallingford: CABI.

Rodríguez, J., and Zoffoli, J. P. (2016). Effect of sulfur dioxide and modified atmosphere packaging on blueberry postharvest quality. *Postharvest Biol.Technol.* 117, 230–238. doi: 10.1016/j.postharvbio.2016.03.008

Saltveit, M. E. (2019). "Respiratory metabolism," in *Postharvest Physiology and Biochemistry of Fruits and Vegetables*, eds E. M. Yahia and A. Carrillo-López (Cambridge: Woodhead Publishing), 73–91.

Schotsmans, W., Molan, A., and MacKay, B. (2007). Controlled atmosphere storage of rabbiteye blueberries enhances postharvest quality aspects. *Postharvest Biol. Technol.* 44, 277–285. doi: 10.1016/j.postharvbio.2006.12.009

Terry, L. A. (2011). *Health-Promoting Properties of Fruits and Vegetables*. Wallingford: CABI.

Terry, L. A. (2012). "Soft Fruit," in *Crop Post-harvest: Science and Technology: Perishables*, eds D. Rees, G. Farrell, and J. Orchard (Hoboken, NJ: Wiley-Blackwell Publishing Ltd), 226–246.

Terry, L. A., Crisosto, C. H., and Forney, C. F. (2009). "Small fruit and berries," in *Modified and Controlled Atmospheres for the Storage, Transportation, and Packaging of Horticultural Commodities*, ed. E. M. Yahia (Boca Raton, CA: CRC Press), 364–388.

Thomas, B., Murphy, D. J., and Murray, B. G. (2016). *Encyclopaedia of Applied Plant Sciences*. Cambridge: Academic Press.

Van Hoorn, A. T. (2004). *Optimisation of Blueberry Postharvest Handling and Storage*. Master's thesis, University of Stellenbosch, Stellenbosch.

Wang, Y., Ji, S., Dai, H., Kong, X., Hao, J., Wang, S., et al. (2019). Changes in membrane lipid metabolism accompany pitting in blueberry during refrigeration and subsequent storage at room temperature. *Front. Plant Sci.* 10:829. doi: 10.3389/fpls.2019.00829

Yang, Y., Yu, Y., Liang, Y., Anderson, C. T., and Cao, J. (2018). A profusion of molecular scissors for pectins: classification, expression, and functions of plant polygalacturonases. *Front. Plant Sci.* 9:1208. doi: 10.3389/fpls.2018.01208

Zheng, Y., Yang, Z., and Chen, X. (2008). Effect of high oxygen atmospheres on fruit decay and quality in Chinese bayberries, strawberries and blueberries. *Food Control* 19, 470–474. doi: 10.1016/j.foodcont.2007.05.011

Conflict of Interest: The authors declare that the research was conducted in the absence of any commercial or financial relationships that could be construed as a potential conflict of interest.

frontiers in Plant Science

ORIGINAL RESEARCH
published: 03 April 2020
doi: 10.3389/fpls.2020.00370

Diversity in Metabolites and Fruit Quality Traits in Blueberry Enables Ploidy and Species Differentiation and Establishes a Strategy for Future Genetic Studies

Molla F. Mengist[1], Mary H. Grace[1], Jia Xiong[1], Colin D. Kay[1], Nahla Bassil[2], Kim Hummer[2], Mario G. Ferruzzi[1], Mary Ann Lila[1] and Massimo Iorizzo[1,3]**

[1] Plants for Human Health Institute, North Carolina State University, NCRC, Kannapolis, NC, United States, [2] USDA-ARS-National Clonal Germplasm Repository, Corvallis, OR, United States, [3] Department of Horticultural Science, North Carolina State University, Raleigh, NC, United States

Blueberry is well recognized as a rich source of health promoting phytochemicals such as flavonoids and phenolic acids. Multiple studies in blueberry and other crops indicated that flavonoids and phenolic acids function as bioactive compounds in the human body promoting multiple health effects. Despite their importance, information is limited about the levels of variation in bioactive compounds within and between ploidy level and species, and their association with fruit quality traits. Such information is crucial to define a strategy to study the genetic mechanisms controlling these traits and to select for these traits in blueberry breeding programs. Here we evaluated 33 health related phytochemicals belonging to four major groups of flavonoids and phenolic acids across 128 blueberry accessions over two years together with fruit quality traits, including fruit weight, titratable acidity, total soluble acids and pH. Highly significant variation between accessions, years, and accession by year interaction were identified for most of the traits. Cluster analysis grouped phytochemicals by their functional structure (e.g., anthocyanins, flavanols, flavonols, and phenolic acids). Multivariate analysis of the traits resulted in separation of diploid, tetraploid and hexaploid accessions. Broad sense heritability of the traits estimated in 100 tetraploid accessions, ranged from 20 to 90%, with most traits revealing moderate to high broad sense heritability ($H^2 > 40\%$), suggesting that strong genetic factors control these traits. Fruit size can be estimated as a proxy of fruit weight or volume and vice versa, and it was negatively correlated with content of most of phytochemicals evaluated here. However, size-independent variation for anthocyanin content and profile (e.g., acylated vs. non-acylated anthocyanin) exists in the tetraploid accessions and can be explored to identify other factors such as genes related to the biosynthetic pathway that control this trait. This result also suggests that metabolite concentrations and fruit size, to a certain degree can be improved simultaneously in breeding programs. Overall, the results of this study provide a framework to uncover the genetic basis of bioactive compounds and fruit quality traits and will be useful to advance blueberry-breeding programs focusing on integrating these traits.

Keywords: blueberry, health promoting phytochemicals, fruit size, ploidy, fruit quality, flavonoid pathway

OPEN ACCESS

Edited by:
Roberto Papa,
Marche Polytechnic University, Italy

Reviewed by:
Saleh Alseekh,
Max Planck Institute of Molecular Plant Physiology, Germany
Pasquale Tripodi,
Council for Agricultural Research and Economics (CREA), Italy

***Correspondence:**
Mary Ann Lila
mlila@ncsu.edu
Massimo Iorizzo
miorizz@ncsu.edu

Specialty section:
This article was submitted to Plant Breeding, a section of the journal Frontiers in Plant Science

Received: *20 December 2019*
Accepted: *16 March 2020*
Published: *03 April 2020*

Citation:
Mengist MF, Grace MH, Xiong J, Kay CD, Bassil N, Hummer K, Ferruzzi MG, Lila MA and Iorizzo M (2020) Diversity in Metabolites and Fruit Quality Traits in Blueberry Enables Ploidy and Species Differentiation and Establishes a Strategy for Future Genetic Studies. Front. Plant Sci. 11:370. doi: 10.3389/fpls.2020.00370

INTRODUCTION

Blueberry belongs to the Ericaceae family and the genus *Vaccinium* section Cyanococcus. Three blueberry species, that include the highbush blueberry (HB), *V. corymbosum* L., rabbiteye blueberry (RB), *V. ashei* Reade (syn. *Vaccinium virgatum* Ait) and native stands of lowbush blueberry (LB), *V. angustifolium* Ait, are commercially grown in the United States (Kalt et al., 2001; Lyrene et al., 2003; Hancock et al., 2008; Retamales and Hancock, 2018). Among these species, the HB blueberry is widely grown in the US, accounting for ∼95% of total blueberry production (Kalt et al., 2001; Wang et al., 2019). The HB cultivars are further classified into northern highbush (NHB) and southern highbush (SHB) blueberries based on chilling requirement and winter hardiness (Lyrene et al., 2003; Hancock et al., 2008; Retamales and Hancock, 2018). In addition to these species, a number of wild diploid blueberry species have been described and are used in breeding programs as sources for low chilling requirement, disease resistance (mummy berry disease), heat tolerance and adaptation to higher soil pH (Hancock et al., 2008; Lobos and Hancock, 2015; Retamales and Hancock, 2018; Wang et al., 2019). Studies have also focused on diploid wild blueberries as important sources of bioactive metabolites including flavonoids and phenolic acids (Kalt et al., 2001; Giovanelli and Buratti, 2009; Prencipe et al., 2014; Zoratti et al., 2015; Wang et al., 2019).

During the last decade, blueberry production and consumption have increased (Rodriguez-Saona et al., 2019) and the growing body of research supporting the health benefits associated with blueberry consumption have likely contributed to this growth (Norberto et al., 2013; Sun et al., 2019). Indeed, clinical evidence suggests that sufficient intake of blueberries provides multiple health benefits including lowering blood pressure, protecting against heart attack, preventing cancer, improving mental health and managing diabetes (Martineau et al., 2006; Krikorian et al., 2010; Stull et al., 2010; Norberto et al., 2013; Sun et al., 2019; Yang H. et al., 2019).

Important health–promoting bioactive metabolites, including flavonoids (anthocyanins, flavanols, and flavonols) and non-flavonoids such as phenolic acids, are found abundantly in blueberry (Kalt et al., 2001; Rodriguez-Mateos et al., 2012; Yousef et al., 2013, 2014; Gündüz et al., 2015; Scalzo et al., 2015; Li et al., 2017; Timmers et al., 2017; Grace et al., 2019; Wang et al., 2019). In blueberry, anthocyanins are the most abundant flavonoids, and are derivative of anthocyanidins (aglycones) by the addition of sugar moieties. The most common anthocyanidins in blueberry are delphinidin (Dp), cyanidin (Cyn), petunidin (Pet), peonidin (Peo), and malvidin (Mv). The anthocyanidins can be conjugated with sugar moieties like arabinoside, glucosides, and galactoside via the C3 hydroxyl group in ring C, and form structurally different anthocyanins. The conjugation of anthocyanidins with sugar moieties can be further modified through acylation (Norberto et al., 2013; Yousef et al., 2014; Li et al., 2017; Grace et al., 2019; Wang et al., 2019). Various patterns of conjugated sugar moieties, with or without acylation, can affect the chemical properties of anthocyanins, such as stability and bioavailability. Acylation of anthocyanins, through the addition of acyl groups such as organic acids (cinnamic and aliphatic acids) via ester bonds, improves color and tinctorial strength and increases the stability of anthocyanins at higher pH or under intense light and heat stress (Giusti and Wrolstad, 2003; Matera et al., 2015; Zhao et al., 2017; Strauch et al., 2019). Acylated anthocyanins are of special interest for use as a stable natural colorants in food industries (Giusti and Wrolstad, 2003; Matera et al., 2015; Zhao et al., 2017; Strauch et al., 2019).

Caffeic, ferulic, and chlorogenic acids are commonly reported phenolic acids. Of these, chlorogenic acid is the most abundant phenolic acid in blueberry (Grace et al., 2019; Wang et al., 2019). Similarly, flavanols (epi-catechin, catechin, proanthocyanidin B_1, and proanthocyanidin B_2) and flavonols (kaempferol, quercetin, and myricetin) are also commonly reported flavonoids in blueberry (Grace et al., 2019; Wang et al., 2019).

Differences in bioavailability between acylated and non-acylated anthocyanins have been reported in the literature (Kurilich et al., 2005; Charron et al., 2009; Oliveira et al., 2019). Charron et al. (2009) reported that non-acylated anthocyanins are better absorbed in the upper intestine compared to acylated anthocyanins. This effect may have been due, in part, to presence of phenolic acids as acylation agents on anthocyanins that serves to limit the transport efficiency or enzymatic conversion to aglycones in the upper intestine. While acylation does serve to stabilize anthocyanins to digestive conditions (McDougall et al., 2007; Correa-Betanzo et al., 2014), this would potentially serve to enhance their retention during intestinal passage and make them more available for catabolism by human microbiota in the large intestine (Fleschhut et al., 2006). As such, understanding factors promoting differences in acylation patterns could serve to better predict efficiencies of absorption, extent of host and microbial metabolism and ultimate health protective properties of anthocyanin rich foods.

Numerous studies have been conducted to examine genotype- or species-specific metabolites and fruit quality variability in blueberry (Kalt et al., 2001; Rodriguez-Mateos et al., 2012; Yousef et al., 2013, 2014; Gündüz et al., 2015; Scalzo et al., 2015; Li et al., 2017; Timmers et al., 2017; Wang et al., 2019). However, these studies targeted a small number of genotypes/accessions and provided limited insight into species and ploidy diversity of metabolite profiles and fruit quality traits. In addition, there is limited information about the association between metabolites with quality traits including fruit weight/size, pH, total soluble solid (TSS) and titratable acidity (TA) (Kalt et al., 2001; Rodriguez-Mateos et al., 2012; Yousef et al., 2013, 2014; Gündüz et al., 2015; Li et al., 2017; Wang et al., 2019). Most importantly, no studies have yet identified potential strategy to perform genetic analysis for these bioactive metabolites.

In this study, we profiled metabolites (anthocyanins, phenolic acids, flavanols, and flavonols) and fruit quality traits (pH, TA, TSS, fruit weight) in 128 blueberry accessions across three ploidy levels (diploid, tetraploid, and hexaploid) over two years. The main objectives of this study were to: (1) assess variability among the blueberry accessions for different metabolites and fruit quality traits; (2) investigate the association among metabolites, and between metabolites and fruit quality traits; and (3) establish a strategy to study the genetic basis controlling metabolite accumulation in highbush blueberry.

MATERIALS AND METHODS

Materials Collection and Preparation

A collection of 128 blueberry accessions was obtained from the National Clonal Germplasm Repository (NCGR), Corvallis, OR, United States. Information about these *Vaccinium* accessions, including name, collection sites, ploidy level and species is provided in **Supplementary Table S1**. The collection included 100 tetraploid (4×), 22 hexaploid (6×), and 6 diploid (2×) accessions, representing diversity in geographical origin and genetic background (**Supplementary Table S1**). Of the 100 tetraploid (4×) accessions, 98 accessions represent *V. corymbosum*, NHB, SHB, and hybrids between these two types of blueberry cultivars. Berries were harvested at ripening stage for two consecutive years (2017 and 2018). For each accession, fruit were harvested from two or three clones. Since amount of fruit available for each clone was not the same and in several case not sufficient to perform all the phenotyping assays, prior to processing, the fruits were combined and then separated into three technical replicates. The technical replicates could minimize errors associated with sample processing and fruit quality and metabolite traits phenotyping. After harvesting, the berries were stored at −80°C, shipped on dry ice to the Plants for Human Health Institute (PHHI), Kannapolis, North Carolina, United States, and stored at −80°C until processing. Frozen berries (approximately 10–30 g, three replicates), were then used for fruit quality and metabolite analyses.

Fruit Quality Trait Evaluation

Establishment of Phenotyping Method for Fruit Size

Image-based phenotyping is a powerful tool to estimate fruit quality attributes including fruit shape, size and color (Diaz-Garcia et al., 2016). While this method is high-throughput, it is also relatively time-consuming (sample set up, image acquisition and processing) if we are interested in phenotyping a single trait. Preliminary data from our lab suggested that image-based fruit volume estimation using the GiNA R package (Diaz-Garcia et al., 2016) and fruit weight were highly correlated. This association provides an opportunity to phenotype fruit size using fruit weight as a proxy for estimating fruit size, a faster phenotyping method as compared to fruit volume measurement. To verify this hypothesis, we selected 54 accessions varying in fruit weight. A minimum of 10 berries for each accession were used to estimate the fruit weight (g per fruit) of each berry. The same berries were scanned with a digital camera and the images were processed using the GiNA R package (Diaz-Garcia et al., 2016), which measured fruit volume and fruit surface area of each berry. Correlation was performed between all the measured parameters, to determine the relationship. To assess the agreement between the two measurements, fruit volume (cm^3) and fruit weight (g), Bland-Altman plot was created using excel (Bland and Altman, 1986). Bland-Altman plot determines the bias (mean of the differences) and limits of agreement [bias ± 2 × SD (standard deviation)].

Phenotyping of Fruit Quality Traits

Fruit weight (g per fruit) was recorded (10–30 berries, three replicates) for fruit harvested in 2017 and 2018. In addition to fruit weight, we evaluated TSS, pH and TA. The berries used to measure fruit weight were homogenized to a puree in a Waring Commercial Blender 7012G (Torrington, CT, United States). Homogenized samples were used to determine TSS, pH and TA and to quantify anthocyanins and non-anthocyanin bioactive metabolites using high-performance liquid chromatography (HPLC) and liquid chromatography–mass spectrometry (LC-MS).

Total soluble solid was estimated using a digital hand-held "pocket" refractometer PAL-1 (Atago, Tokyo, Japan) and the results were expressed as°Brix. pH and TA were measured using 1 g of homogenized sample diluted with 30 ml pre-boiled double distilled water. The pH was measured using Accumet AB15, pH-meter (Fisher Scientific, Waltham, MA, United States). Then, TA was determined with a Mettler DL15 Auto-Titrator (Columbus, OH, United States) at pH of 8.2 using 0.02 mol L^{-1} sodium hydroxide. TA was expressed as percentage of citric acid (wt/wt) per 1 g FW.

Extraction and Quantification of Anthocyanins and Non-anthocyanin Metabolites

Extraction and Sample Preparation for HPLC and LC-MS Analysis

An aliquot (3 g) of the homogenized blueberry puree was weighed in a 30-mL centrifuge tube. After the addition of 8 ml of 80% methanol in water (containing 5% formic acid), this mix was homogenized using a PRO0250 (PRO Scientific Inc., Oxford, CT, United States) for 2 min to extract polyphenols. The homogenate was centrifuged (Sorvall RC-6 plus, Asheville, NC, United States) for 2 min at 4,000 rpm. The supernatant was collected in a 25-ml volumetric flask. The residue was then extracted two more times, once with 8 ml of the same solvent, and then with 100% methanol. Supernatants were collected and brought to a final volume of 25 ml. About 1 ml of each sample was diluted with equal volume of methanol-water-formic acid, 65:35:5 and filtered (0.22 μm PTFE membrane) prior to HPLC-PDA analysis for anthocyanins and chlorogenic acid.

For LC-MS analysis of other phenolic compounds of low concentrations (flavonols, flavanols, and phenolic acids), a solid phase extraction (SPE) procedure was performed to remove sugars that may cause decrease in sensitivity of the MS system. An aliquot of 1–1.5 mL from each sample/replicate was centrifuged at 15,000 rpm for 5 min. In a 96-deep well plate (loading plate), 1.2 mL water (1% formic acid, FA), 10 μL fisetin (200 μg/mL, final concentration, 5 μg/mL), and 200 μL extract were mixed. The SPE plate (Phenomenex; StrataTM 96 Well Plate 10 mg/Well) was preconditioned with methanol (1% FA), then with water (1% FA). The samples were transferred from the loading plate to the SPE plate and drained by gravity. The 96-SPE well plate was washed 5 times with 600 μL water (1% FA) and dried about 20 min using positive pressure manifold. Finally, the samples from the SPE plate were eluted with 300 μL methanol (0.1% FA) to a 96-well collection plate. Then, 90 μL water (0.1% FA) and 10 μL internal standard (phlorizin 200 μg/mL, final concentration 5 μg/mL) was added to each

well. The collection plate was covered with a sealing mat and immediately transferred to the auto-sampler of the MS system for analysis.

HPLC Analysis

HPLC analysis was conducted to quantify anthocyanins and chlorogenic acid. Standards, cyanidin-3-galactoside, cyanidin-3-glucoside, and malvidin-3-galactoside, were obtained from Chromadex (Irvine, CA, United States). Delphinidin-3-glucoside was purchased from Cayman Chemicals (Ann Arbor, MI, United States). Delphinidin-3-galactoside, malvidin-3-glucoside, petunidin-3-glucoside, myricetin-3-glucoside, kaempferol-3-glucoside, and syringetin-3-glucoside were obtained from Extrasynthese (Genay Cedex, France). Cyanidin-3-arabinoside and peonidin-3-glucoside were obtained from Polyphenols (Sandnes, Norway).

Each of the nine anthocyanin reference compounds and chlorogenic acid standard were individually dissolved in methanol-water-formic acid, 65:35:5, at a concentration of 5 mg/mL. Equal volumes from each standard solution were mixed together and diluted with the solvent mix to prepare a standard stock mix solution (200 μg/mL). Eight standard working solutions, used for the calibration curve, were prepared by appropriate dilution of the stock mix solution (2–175 μg/mL). The reference standard mix dilutions were injected to generate an eight-point calibration curve for each compound, separately. Standard curves were linear with $R^2 > 0.9997 \pm 0.0007$.

The chromatography was conducted on an Agilent 1260 HPLC with diode array detector (DAD) (Agilent Technologies, Santa Clara, CA, United States). Separation of anthocyanins was performed on a Supelco C-18 column (25 cm × 4.6 mm × 5 μm), and the temperature of the column oven was maintained at 30°C. The eluents were water (formic acid 5%, v/v) (A) and methanol (B), with a gradient of 10–20% B (0–5 min), 20–25% B (5–20 min), 25–30% B (20–25 min), 30–35% B (25–30 min), 35–90% (30–43 min), and isocratic at 90% B (43–46 min). The column was then re-equilibrated for 4 min at 5% B, at the flow rate of 1 ml/min. Absorption was recorded at 520 nm for anthocyanins, and 280 nm for chlorogenic acid. Not all anthocyanins present in blueberry are commercially available; therefore, anthocyanins with no standard reference were quantified as their corresponding glucoside or galactoside equivalent. The lowest limit of detection (LLD) for all anthocyanins was in the range of 1.24–1.91 ppm, 0.96 ppm for chlorogenic acid (**Supplementary Table S2**).

LC-MS Analysis

LC-MS analysis was conducted to quantify non-anthocyanin compounds including flavonols, flavanols and phenolic acids. Standards, procyanidins B1 and B2, catechin, epicatechin, caffeic acid, 2,4-dihydroxybenzoic acid, quercetin glucoside and galactoside and quercetin arabinoside were purchased from Sigma-Aldrich (St. Louis, MO, United States). Phlorizin was used as an internal standard; Fesitin was used to measure the efficiency of SPE, and both were purchased from Sigma-Aldrich. The analysis was performed on a hybrid IT-TOF mass spectrometer (Shimadzu LC-MS-IT-TOF, Kyoto, Japan) equipped with two LC-20AD pumps, a SIL-20AC autosampler, a CTO-20A column oven, an SPD-M20A PDA detector, a CBM-20A system controller coupled to an IT-TOF-MS through an ESI interface. All data were processed by Shimadzu LCMS lab Solution Version 1.2. The mass spectrometer was programmed to carry out a full scan over *m/z* 70–100–700 (MS1) and *m/z* 70–500 (MS2) in the negative ionization mode. The heat block and curved desolvation line (CDL) temperature were maintained at 200°C; nitrogen was used as the nebulizing gas at a flow rate of 1.5 L/min, and as the drying gas at 75 kPa; the interface voltage was (+), 4.5 kV; (-), -3.5 kV; and the detector voltage was 1.80 kV.

The chromatography was performed on a Shim-pack XR-ODS column (50 mm × 3.0 mm × 2.2 μm) (Shimadzu, Japan), and the temperature of the column oven was maintained at 50°C. The eluents were water (FA 0.5%, v/v) (A) and methanol (B), with a gradient of 5–50% B (0–17 min), 50–80% B (17–18 min), and 80–5% B (18–19 min). The column was then re-equilibrated for 1 min at 5% B, at the flow rate of 0.6 mL/min. Compounds were quantified as their extracted-ion chromatograms (EIC) in the negative ion mode using phlorizin as an internal standard. The lowest limits of detection for all non-anthocyanin compounds ranged from 0.41 to 2.66 ppm as presented in **Supplementary Table S2**.

Data Processing and Statistical Analyses

Analysis of Variance, Trait Heritability, and Correlation Analyses

To assess the magnitude of variation within and between ploidy groups, we computed a minimum, maximum and range of variation for all metabolites and fruit quality traits. Fold-change values were calculated independently for each metabolite and fruit quality trait, dividing the maximum value by the minimum value of each trait within ploidy group. To normalize metabolite data, a log2 transformation was applied on quantified values. Analysis of variance (ANOVA) was performed to partition individual metabolites and fruit quality related trait according to ploidy, accession number, year, and accession by year interaction. Best linear unbiased estimate (BLUE) data obtained from the linear model were used as the phenotypic values for all subsequent analyses. Broad-sense heritability (H^2) was estimated using variance components calculated from the restricted maximum likelihood (REML), calculated as follows

$$H^2 = \frac{\delta_g^2}{(\delta_g^2 + \frac{\delta_{gy}^2}{y} + \frac{\delta_e^2}{ry})}$$

where, δ_g^2, δ_{gy}^2, and δ_e^2 are variance components of accessions, [genotype x environment] interaction, and residual variations, respectively; y is the number of environments (number of years in this study, 2) and r is the number of replications (3).

Pearson Coefficient of Correlation was performed to find the relationship among traits and for the two-year data,

independently. The correlation was visualized using the R package corrplot (Wei et al., 2017).

Multivariate Analysis of Metabolites and Fruit Quality Traits

BLUE data obtained from linear effects model were used as an input file for hierarchical clustering (HC), principal component analysis (PCA) and partial least square discriminant analysis (PLS-DA). HC combines similar individuals or variables into clusters and arranges these clusters into a hierarchy while PCA is a technique used to reduce dimensionality of the data by finding linear combinations (dimensions; in this case, the number of metabolite and fruit quality traits) of the data. HC was performed with the Spearman and Ward's methods, and were visualized as a heatmap with a dendrogram using the heatmap.2 R package (Warnes et al., 2016). PCA was performed using the R package FactoMiner (Lê et al., 2008) as a non-supervised method to identify key traits with the largest effect on the overall variability and to evaluate the effect of genetic background on fruit quality and metabolite profiles among different accessions. PLS-DA (supervised version of PCA) was performed using metaboanalyst (Chong et al., 2018) to examine the classification of accessions based on ploidy groups/species and also identify key features using variable importance for the projection (VIP) > 1. The model fitness was evaluated using model accuracy, Q^2 and R^2 values of the model as described (Szymańska et al., 2012).

RESULTS

Fruit Weight and Image-Based Volume Phenotyping Methods

Correlation analysis indicated that fruit weight and image-based volume measurements are highly ($P < 0.001$, $r = 0.99$) correlated (**Figure 1A**). Correlation provides information about the strength of the relationship between two measurements, but not agreement between the two measurements. Therefore, we assessed the agreement between the measurements, fruit volume (cm^3) and fruit weight (g per fruit) with the Bland–Altman plot (**Figure 1B**). Here, the mean difference (bias) is 0.08, where the limits of agreement are −0.0734 and 0.25, indicating that 95% of the differences between the two measurements are within this range. Only one observation lies outside the 95% confidence interval, suggesting that the two measurements have an acceptable level of agreement, meaning that the absolute value of the numerical scale used to express the two measurements agree. Therefore, fruit weight can be used as a proxy to estimate fruit volume. It is also important to note that fruit surface area and fruit volume are also highly ($r > 0.99$) correlated traits (**Figure 1C**), suggesting that both fruit volume and fruit surface area can be highly predictable based on fruit weight. Furthermore, we also estimated fruit volume from 12 accessions with other fruit volume estimation methods including water displacement and texture analyzer and found that both methods are strongly ($r > 0.99$) correlated with fruit weight (Data not shown).

Phenotypic Variability of Fruit Quality Traits

Phenotypic data for fruit quality traits including fruit weight, TA, pH and TSS, summarized by ploidy levels provided (**Supplementary Table S3** and **Supplementary Figure S1**). The accessions evaluated here exhibited a considerable phenotypic variation for all traits, within and between ploidy-groups. For example, fruit weight exhibited ca. 2, 16- and 6-fold variation in diploid, tetraploid and hexaploid species, respectively (**Figure 1D**, **Supplementary Table S3**, and **Supplementary Figure S1**). TA had ca. 4, 9-, and 3-fold changes for diploid, tetraploid and hexaploid species, respectively. However, for pH and TSS, the variation among accessions was relatively low, less than two-fold changes for all ploidy groups (**Supplementary Table S3** and **Supplementary Figure S1**). Overall, tetraploid accessions exhibited the highest level of variation for all fruit quality traits, probably due to the larger number of tetraploid samples evaluated in this study.

Combined analysis of variance showed significant ($P < 0.01$) effects for accession, year and accession by year interaction for all fruit quality traits except for pH, which did not show significant differences between years for any ploidy groups (**Supplementary Table S4**). Furthermore, broad sense heritability of fruit quality traits, estimated for tetraploid accessions (the largest group, $N = 100$), revealed a moderate to high (>40%) level of heritability (**Figure 2**). Fruit weight and TSS are highly heritable traits (>70%), suggesting these traits can be improved through phenotypic selection and that the genetic component may play a major effect on the observed variation.

Phenotypic Variability in Metabolites

We identified 33 metabolites including 20 anthocyanins, 6 flavonols, 4 flavanols and 3 phenolic acid compounds. Of the 20 anthocyanins identified, 14 were non-acylated anthocyanins and 6 were acylated anthocyanins (**Supplementary Table S2**). We observed a high degree of variability for all metabolites, with ca. 2-, 5-, and 2-fold variations for total anthocyanin in diploid, tetraploid and hexaploid species, respectively (**Supplementary Table S3**). Individual anthocyanins such as peonidin-3-glucoside, peonidin-3-(6-acetyl) galactoside and malvidin-3-(6-acetyl) galactoside exhibited more than 17 fold variation within ploidy levels (**Supplementary Table S3** and **Supplementary Figure S1**). Similarly, the degree of variability in total flavanol, total flavonol and total phenolic acid was examined between and within the different ploidy levels and it was found that tetraploid species had a higher degree of variability compared to diploid or hexaploid species (**Supplementary Table S3** and **Supplementary Figure S1**). Overall, the degree of variability was higher in tetraploid accessions, suggesting this material represents a wider pool of genetic diversity and could be used to study the genetic basis of these metabolites.

Combined analysis of variance was performed independently at ploidy level. For tetraploid accessions, combined analysis of variance for metabolites showed significant ($P < 0.01$) effects for accession, year and accession by year interaction for all traits except for cyanidin-3-(6-acetyl glucoside), malvidin-3-(6-acetyl

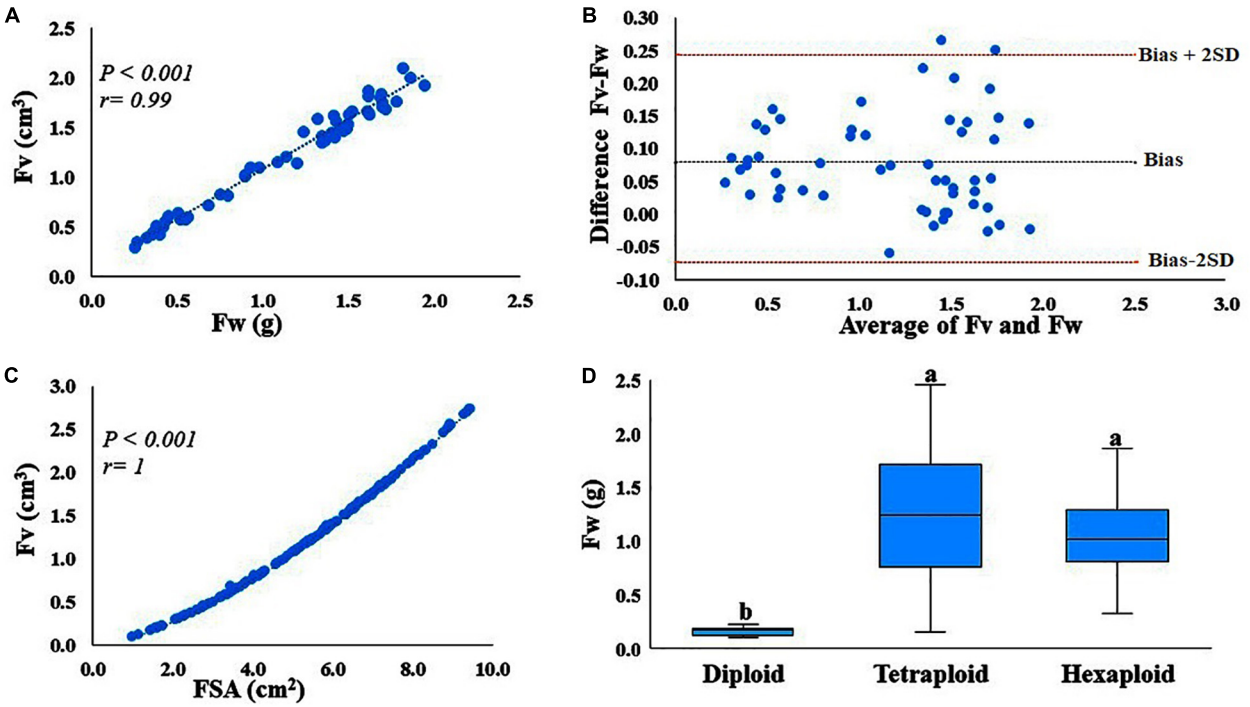

FIGURE 1 | Correlation and agreement between fruit volume (Fv) and fruit weight (Fw), and Fw variations within and between ploidy level. **(A)** Correlation between fruit volume (cm^3) measured using GiNA (image-based phenotyping) and fruit weight (g). **(B)** Agreement between the two measurements, Fv (cm^3) estimated by GiNA and Fw (g). Bias is the mean of the differences between the two measurements, whereas bias-2SD and bias + 2SD are the lower and upper limits of the interval agreement, respectively. SD is the standard deviation of the mean of the differences. **(C)** Correlation between the two fruit parameters, fruit surface area (cm^2) and fruit volume (cm^3) as estimated by GiNA (image-based phenotying). **(D)** Fw variation between and within ploidy level.

galactoside), peonidin-3-(6-acetyl glucoside), malvidin-3-(6-acetyl glucoside) and quercetin-3-rutinoside, which did not show significant differences between years (**Supplementary Table S4**). For hexaploid accessions, we observed significant ($P < 0.01$) effect of accession, year and accession by year for all traits except for delphinidin-3-arabinoside, peonidin-3-galactoside, malvidin-3-arabinoside, malvidin-3-(6-acetyl galactoside), catechin, quercetin-3-galactoside and kaempferol-7-glucoside, which did not exhibit significant year effects (**Supplementary Table S4**). Regarding diploid accessions, significant ($P < 0.01$) variations were exhibited among accessions for all metabolites except for delphinidin-3-glucoside and quercetin-3-rutinoside, while most of the metabolites were not significantly affected by year and year by accession interaction (**Supplementary Table S4**). The smaller sample size of the diploid accessions ($N = 6$) as compared to the hexaploid and tetraploid accessions, probably limited our ability to exploit the full spectrum of phenotypic variation (**Supplementary Figure S1**) for fruit quality and metabolite content naturally existing in this germplasm, and to determine year or year × accession interaction effects (**Supplementary Table S4**).

We also estimated the broad sense heritability of bioactive metabolite using tetraploid accessions. The results showed moderate to high (>40%) range of heritability for all anthocyanin metabolites (**Figure 2**), suggesting that a significant portion of these variations have a genetic basis. On the other hand, most of the flavanols, flavonols, and phenolic acids showed low heritability (<40%), suggesting that these traits may be highly influenced by environmental factors (**Figure 2**). Kaempferol-7-glucoside, catechin, epi-catechin, and chlorogenic acid exhibited moderate to high (>40%) broad sense heritability (**Figure 2**).

To compare the average composition of anthocyanidins relative to the total anthocyanins across different ploidy levels, means of the five-anthocyanidin classes, delphinidin, cyanidin, petunidin, peonidin, and malvidin, were calculated for each ploidy level. Regardless of ploidy levels, across all accessions malvidin and delphinidin were the two major anthocyanidin classes. Peonidin was the least abundant anthocyanin. Similarly, the flavanol, flavonol and phenolic acid profiles were compared for each ploidy level. For flavanol, the pattern of distribution is somewhat similar among the different ploidy levels. Catechin followed by procyanidin-B1 were the most abundant flavanols in blueberry whereas, epi-catechin and procyanidin-B2 were the least abundant flavanols (**Supplementary Figure S2**). Among phenolic acids, more than 95% of the total phenolic acids were represented by chlorogenic acid while caffeic acid and ferulic acid were detected at relatively low levels (**Supplementary Figure S2**).

To further examine the diversity of the different forms of anthocyanin for potential use in genetic studies we carried out a cluster analysis using the data from the tetraploid accessions. Cluster analysis identified two major anthocyanin

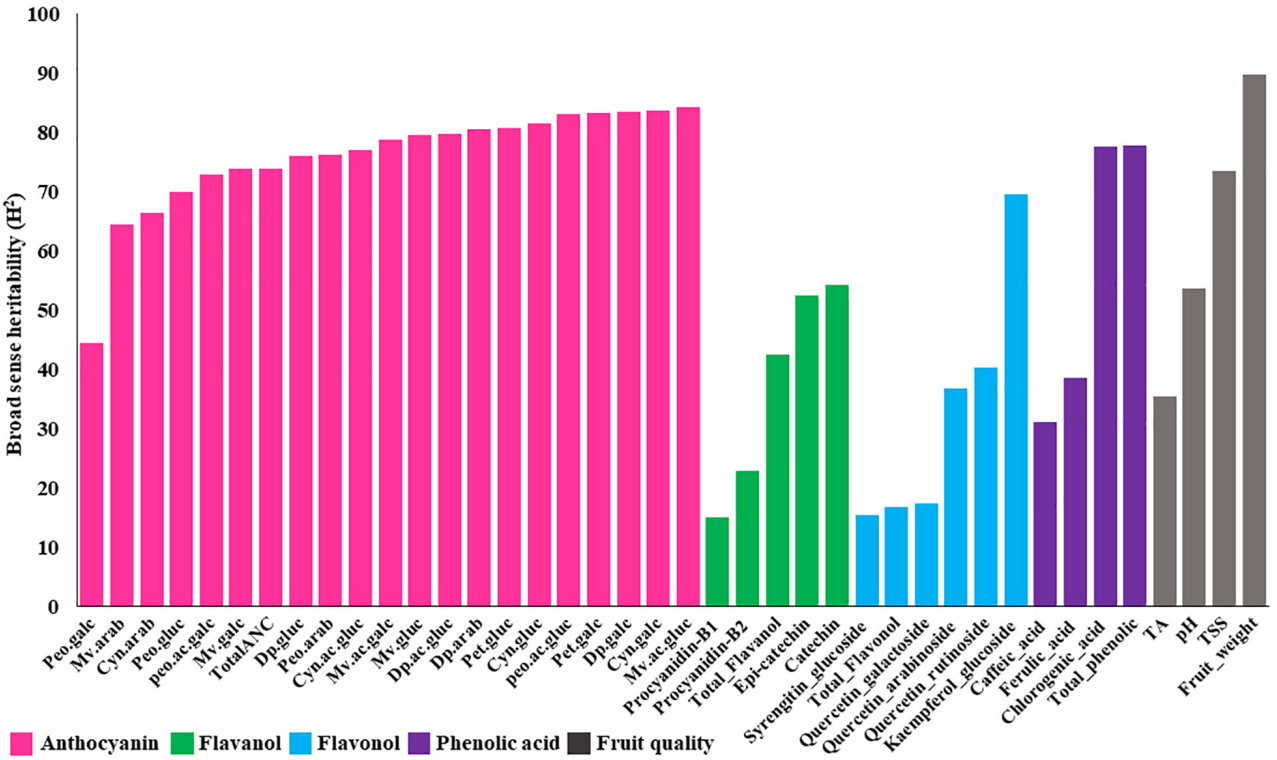

FIGURE 2 | Broad sense heritability estimates for metabolites and fruit quality traits across 100 tetraploid accessions over two years. Anthocyanin abbreviations: Dp, delphinidin; Cyn, cyanidin; Peo, peonidin; Mv, malvidin; Pet, petunidin; gluc, -3-glucoside; galc, -3-galactoside; arab, -3-arabinoside; ac.gluc, -3-(6-acetyl glucoside); ac.galc, -3-(6-acetyl galactoside).

clusters, one cluster containing the glucoside anthocyanins and the second cluster comprising the arabinoside and galactoside anthocyanins. Within each of these two clusters, acylated and non-acylated anthocyanins formed different sub-clusters. Another observation was that anthocyanidin aglycones clustered based upon their derivatives, petunidin clustered with malvidin, and delphinidin and peonidin clustered with cyanidin (**Supplementary Figure S3**).

Correlation Between Bioactive Metabolites and Fruit Quality Traits

Pearson coefficient of correlation analysis between metabolite and fruit quality traits was performed for all tetraploid and hexaploid accessions (**Figure 3** and **Supplementary Figures S4, S5**).

For the 2017 tetraploid phenotypic data, fruit weight was negatively ($P < 0.05$) correlated with TSS, anthocyanins, flavanols, and phenolic acids. Smaller-sized fruits tended to have greater anthocyanin, flavanol and phenolic acids concentrations than the larger-sized fruits. However, fruit weight did not show any significant correlation with flavonols except for quercetin-3-arabinoside (**Figure 3**). In contrast, TSS was positively and significantly ($P < 0.05$) correlated with most of the anthocyanins, flavanols, and phenolic aids. As expected, TA showed a significant ($P < 0.05$) negative correlation with pH. However, pH did not exhibit any significant correlation with TSS or fruit weight (**Figure 3**). Another interesting observation was that pH was positively associated with acylated anthocyanins (**Figure 3**). Higher-pH accessions tended to exhibit greater acylated anthocyanin concentrations than the lower-pH accessions. These results suggest that acylation could be a pH dependent process. Similar correlation patterns were established for the 2018 phenotypic data (**Figure 3**).

For hexaploid accessions, there were no significant correlations between fruit weight and TSS, anthocyanins, flavonols, flavanols, and phenolic acids except for petunidin-3-arabinoside. Furthermore, TSS did not show any correlations with other fruit quality traits, anthocyanins, and flavanols (**Supplementary Figure S4**). The patterns of correlations among traits in tetraploid and hexaploid accessions were different. Fruit quality traits, fruit weight and TSS, showed significant associations with most of the metabolites in tetraploid accessions, but the same relationship was not observed in the hexaploid accessions. For the diploid accessions, the results highlighted that fruit weight was negatively ($P < 0.05$) correlated with chlorogenic acid and phenolic acids for both years, while for total anthocyanin fruit weight showed a significant ($P < 0.05$) negative correlation only for the 2017 phenotypic data (**Supplementary Figure S5**).

To identify tetraploid accessions that have a fruit size and anthocyanin content larger and higher than the average, we examined the relationship between anthocyanin concentration

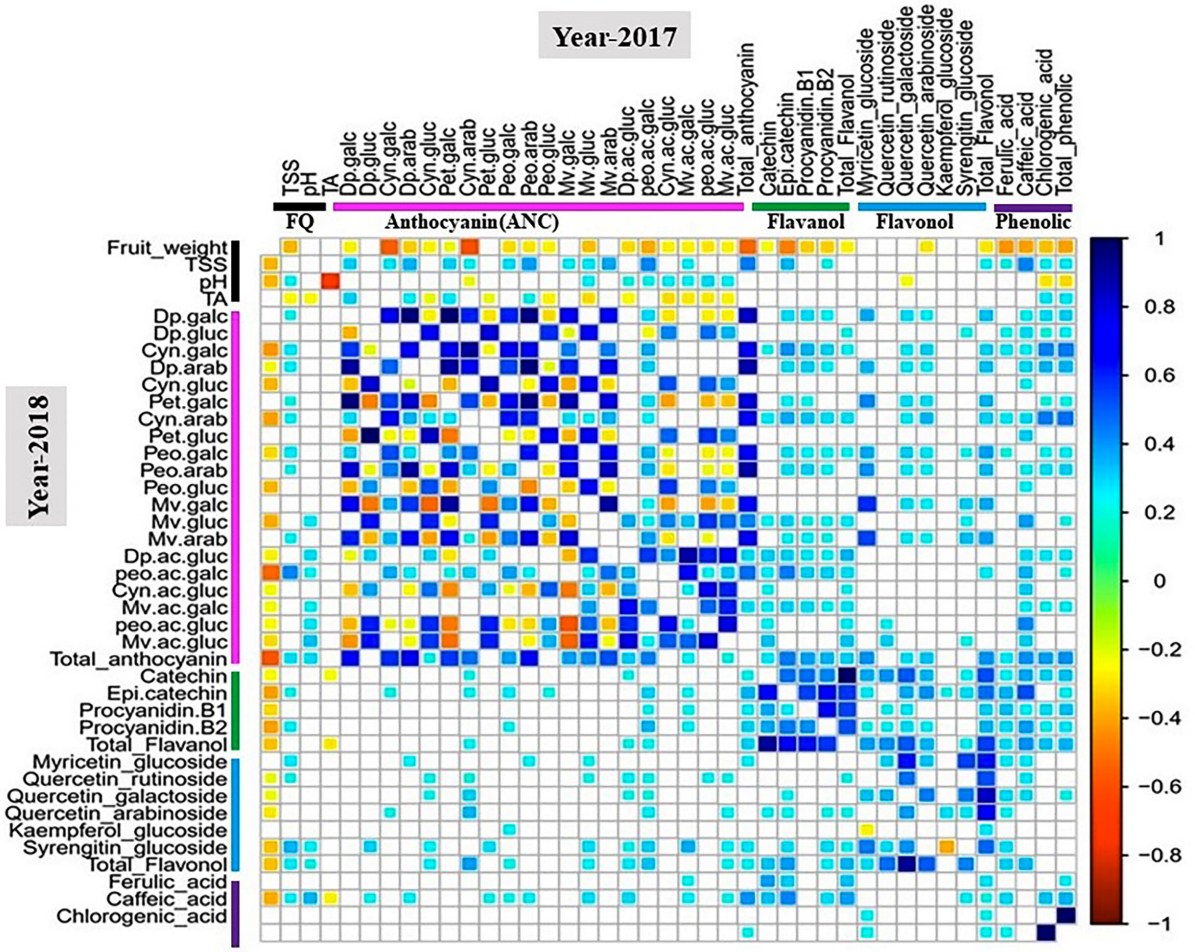

FIGURE 3 | Correlation analysis of metabolite and fruit quality traits for 100 tetraploid accessions. White boxes represent non-significant correlations. The color bar indicates metabolite classes and fruit quality traits. Cyan-to-blue and yellow-to-red colors show significant ($P < 0.05$) positive and negative correlation between traits, respectively. Abbreviation: FQ, fruit quality trait.

and fruit size based on the BLUE data. Accessions separated into four quadrants each representing the following phenotypes: (I) anthocyanin content higher than average and fruit size smaller than the average; (II) anthocyanin content and fruit size lower and smaller than the average; (III) anthocyanin content lower than the average and fruit size larger than the average; (IV) anthocyanin content and fruit size higher and larger than the average. As expected, a large number of accessions with high anthocyanin content and small fruit size were in quadrant I. However, four accessions with a fruit size and anthocyanin content larger than the average, were identified (**Supplementary Figure S6**).

Multivariate Analysis of Metabolites and Fruit Quality Traits

To provide an insight into the relationships/similarity among the different metabolites, a hierarchical clustering (HC) analysis was performed. The metabolites grouped largely into six major clusters (**Figure 4**), representing flavanols (cluster 2), flavonols (cluster 6), phenolic acids (cluster 3), and three clusters (1, 4, 5) representing the 20 anthocyanins (**Figure 4**). The three clusters of anthocyanins represent glucoside vs. galactoside/arabinoside anthocyanin (cluster 1 and 4, respectively) and acylated anthocyanins (cluster 5) (**Figure 4**).

Following HC analysis, we examined the data using PCA. The scree plot of the PCA demonstrated the variance explained for each component. Accordingly, the first five principal components (PCs) accounted for 63.8% of the variance (**Supplementary Figure S7**). Among these, the first three PCs accounted for 22.9, 17.3, and 12.8% of the variance, respectively (**Supplementary Figure S7**). To identify the key traits discriminating the different accessions, loading scores of the first two PCs were examined (**Supplementary Figure S8**) and metabolites with highest loading scores on PC1/2 were identified for all 128 accessions (**Supplementary Figure S9A**). Metabolites that contain galactoside sugar moieties (petunidin-3-galactoside, delphinidin-3-galactoside,

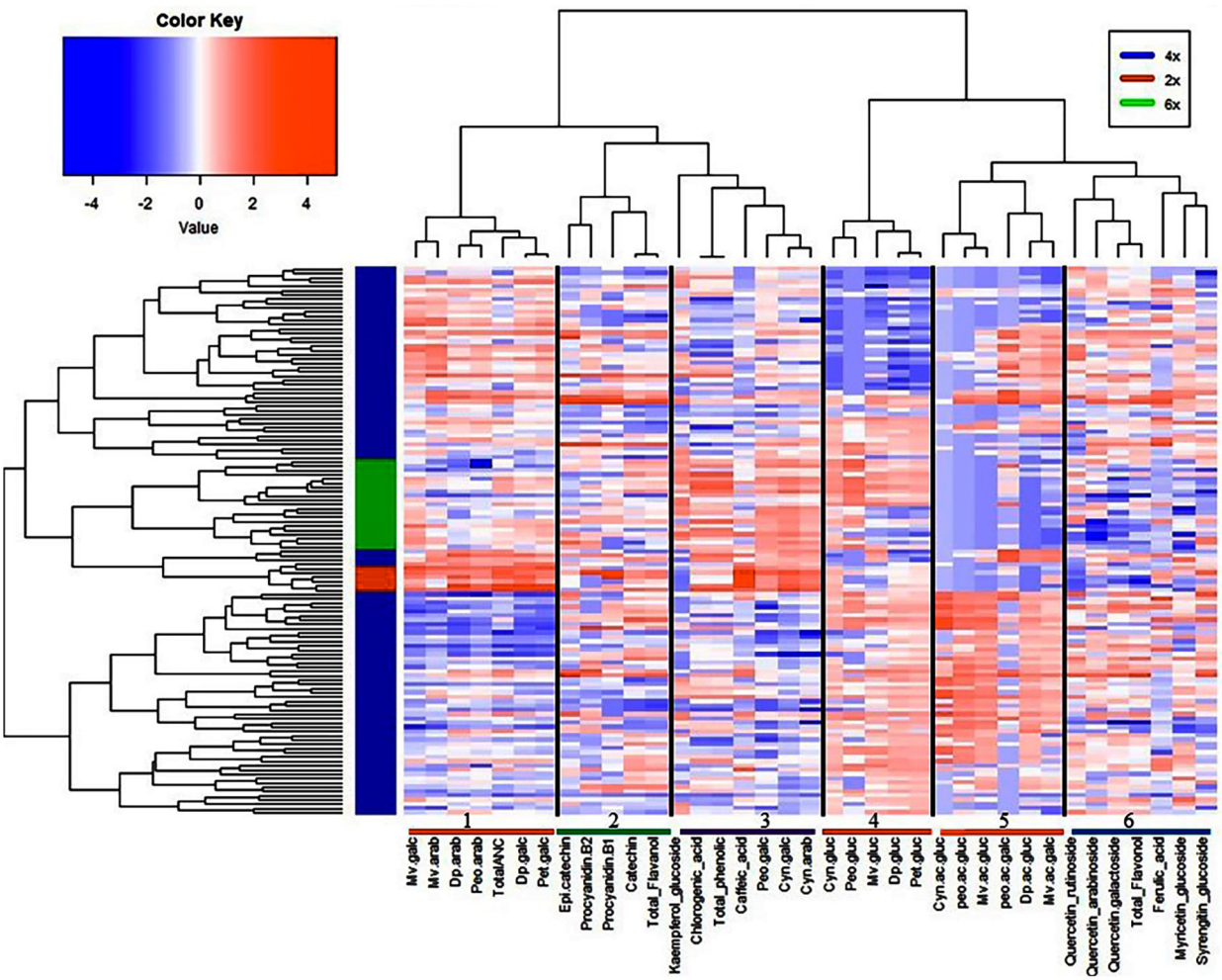

FIGURE 4 | Hierarchical clustering analysis of metabolites and fruit quality traits from all 128 accessions. Six clusters represent the different metabolite classes, anthocyanins (1, 4, 5); flavanols (2); phenolic acids (3); and flavonols (6).

cyanidin-3-galactoside and peonidin-3-galactoside) followed by arabinoside anthocyanins (cyanidin-3-arabinoside, cyanidin-3-arabinoside, delphinidin-3-arabinoisde and peonidin-3-arabinoside) showed the highest loading score in PC1. Whereas variables such as malvidin-3-(6-acetyl glucoside), malvinidin-3-glcuoside, total flavanol, delphinidin-3-(6-acetyl glucoside), malvidin-3-(6-acetyl glucoside), peonidin-3-(6-acetyl glucoside) and fruit weight explained most of the variability of the accessions in PC2 (**Supplementary Figure S9B**). A PCA biplot (**Supplementary Figure S10**) demonstrates the relationship between individuals and variables. For example, accessions PI554796, PI618230 and PI296406, and PI346623, PI554795 and PI267851 had high scores for the acylated anthocyanins and total anthocyanin concentrations, respectively. In contrast, accessions PI618099 and PI618193 had high fruit weight.

We examined whether metabolites and fruit quality data could discriminate accessions based on ploidy levels. PCA analysis revealed that diploid accessions clustered in a distinct group from other accessions (tetraploid and hexaploid), though no definitive separation was observed between hexaploid and tetraploid accessions for the first two PCs (**Figure 5A**). However, the first and third PCs of the PCA were able to separate all accessions by ploidy levels (**Figure 5B**). A supervised analysis, PLS-DA was applied to highlight separation of the accessions by ploidy levels and to identify key traits contributing to this separation. PLS-DA model on the first two PCs (accuracy = 0.95, R^2 = 0.75, and Q^2 = 0.70), separated accessions into their respective ploidy levels (**Figure 6**). Examination of variable importance projection (VIP > 1) suggests that the variables cyanidin-3-galactoside, delphinidin-3-(6-acetyl glucoside) and TSS significantly contributed to separate the accessions based on ploidy level (**Supplementary Figure S11**).

We compared the metabolite concentrations and fruit quality traits across ploidy levels and found that tetraploid accessions had higher pH, acylated anthocyanin and flavonols concentrations than diploid and hexaploid accessions (**Figure 7**). It is important

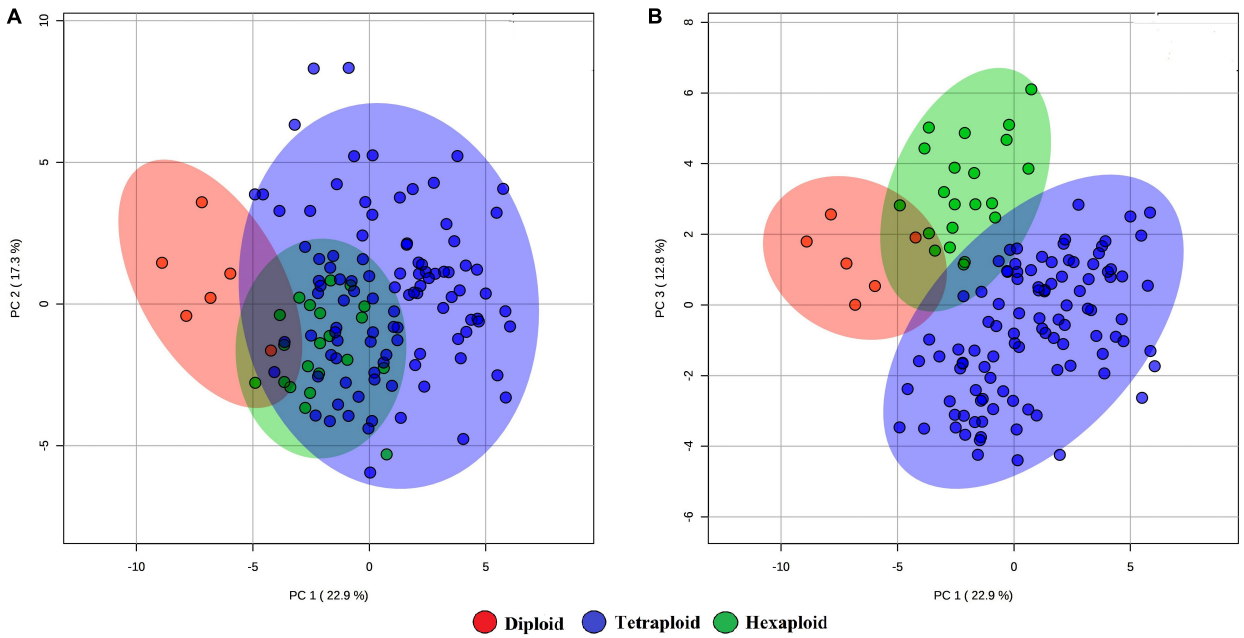

FIGURE 5 | PCA score plots of the first and second **(A)** and first and third **(B)** principal components. The data obtained from metabolites and fruit quality data of 128 blueberry accessions across three ploidy levels (diploid, tetraploid, and hexaploid).

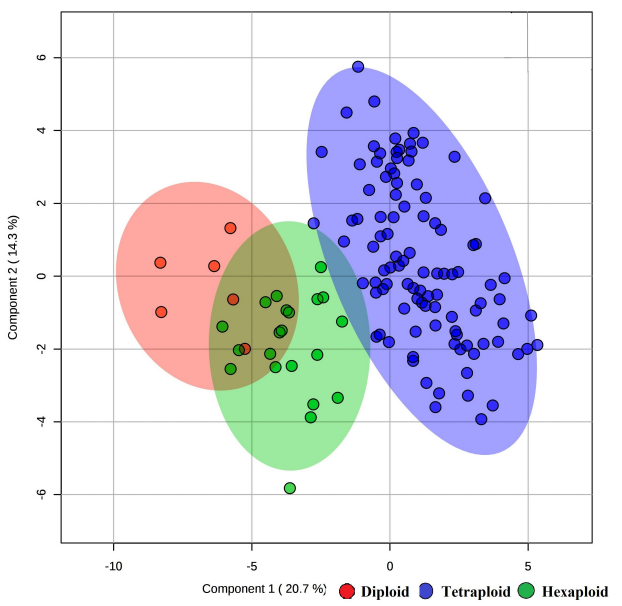

FIGURE 6 | PLS-DA model of metabolite and fruit quality data from 128 blueberry accessions in three ploidy levels (diploid, tetraploid, and hexaploid). The figure representing the first two components of the PLS-DA model.

to note that pH of tetraploid accession is positively associated with acylated anthocyanins (**Figure 3**). The higher pH of the tetraploid accessions may have resulted in higher acylated anthocyanins as opposed to diploid and hexaploid accessions. Non-acylated anthocyanins and flavanols content were higher in diploid than hexaploid or tetraploid accessions. In contrast, tetraploid accessions had low total phenolic acid content, as compared to diploid and hexaploid accessions. The level of phenolic acids was comparable between diploid and hexaploid groups (**Figure 7**).

To assess whether the metabolites composition and fruit quality traits differentiate accessions by species, we performed PCA and PLS-DA. The PCA analysis revealed that *V. elliottii* formed a distinct group in the first two PCs. However, hexaploid and tetraploid species did not form a distinctive group (**Figure 8A**). Results from the first and third PCs of the PCA analysis revealed that *V. virgatum* and V. *elliottii* formed distinct groups while other species including tetraploid hybrids, *V. angustifolium* and *V. corymbosum* clustered as a single group (**Figure 8**). PLS-DA models also separated the accessions into three groups corresponding to *V. elliottii*, *V. virgatum* and other tetraploid (*V. corymbosum, V. angustifolium* and hybrids). Both PCA and PLS-DA analyses did not separate accessions of the same ploidy level into their respective species (**Supplementary Figure S12**). Furthermore, the key traits (cyanidin-3-galactoside, delphinidin-3-(6-acetyl glucoside) and TSS) identified, as most the discriminatory variables for the species analysis were the same variables that separated the accessions by ploidy by PLS-DA analysis (**Supplementary Figure S11**). Further, both PCA and PLS-DA analyses did not separate the accessions according to SHB and NHB types (**Supplementary Figure S13**). Similarly, when the geographical collection site was used as a classifier, the accessions did not show any distinct grouping pattern, though accessions from Maine showed a tendency to cluster together (**Supplementary Figure S14**). Overall, our data demonstrate that the accessions

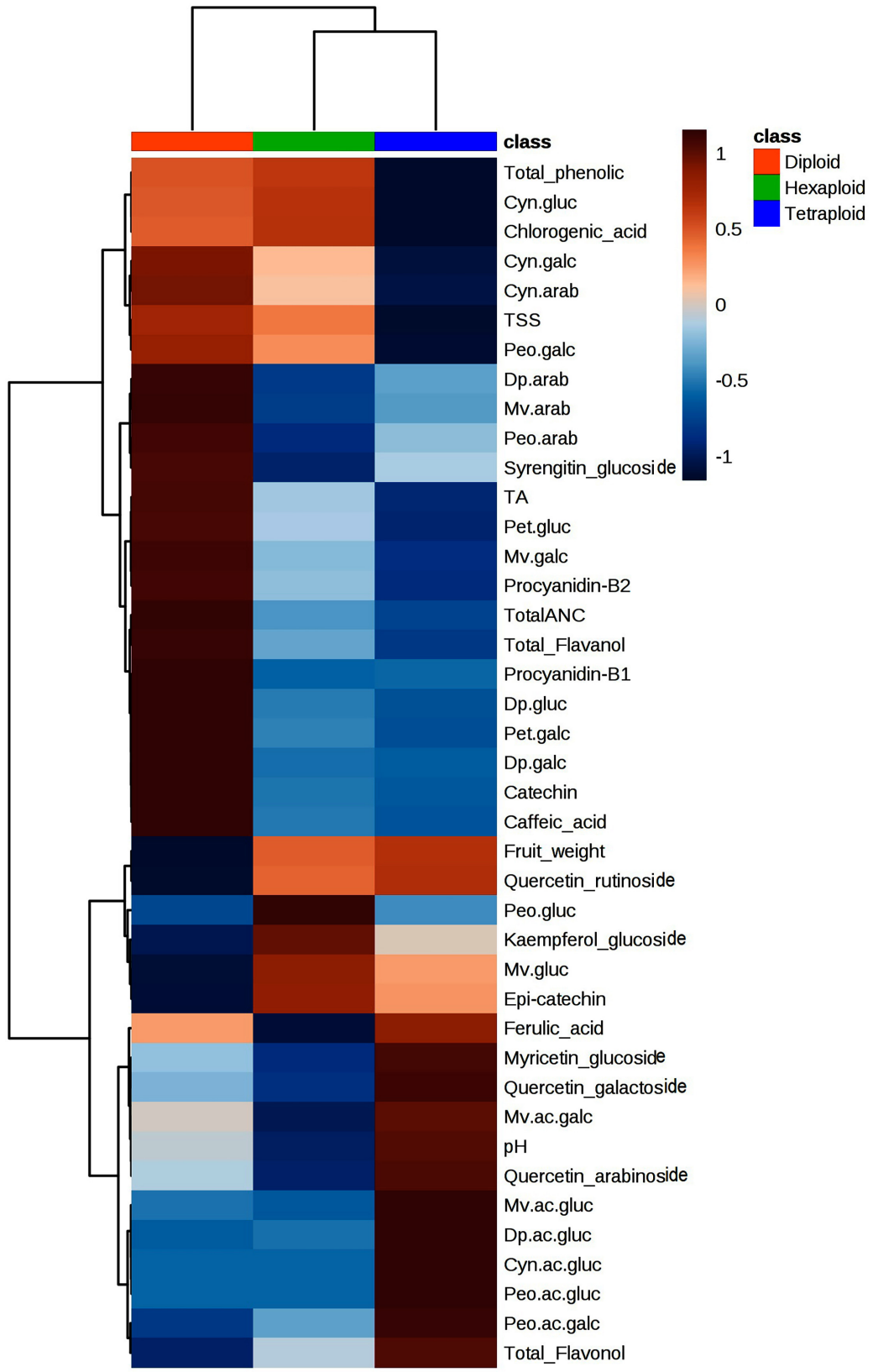

FIGURE 7 | Heatmap showing variation of metabolites and fruit quality traits across the three-ploidy levels. Red and blue colors indicate highest and lowest performance of the traits, respectively.

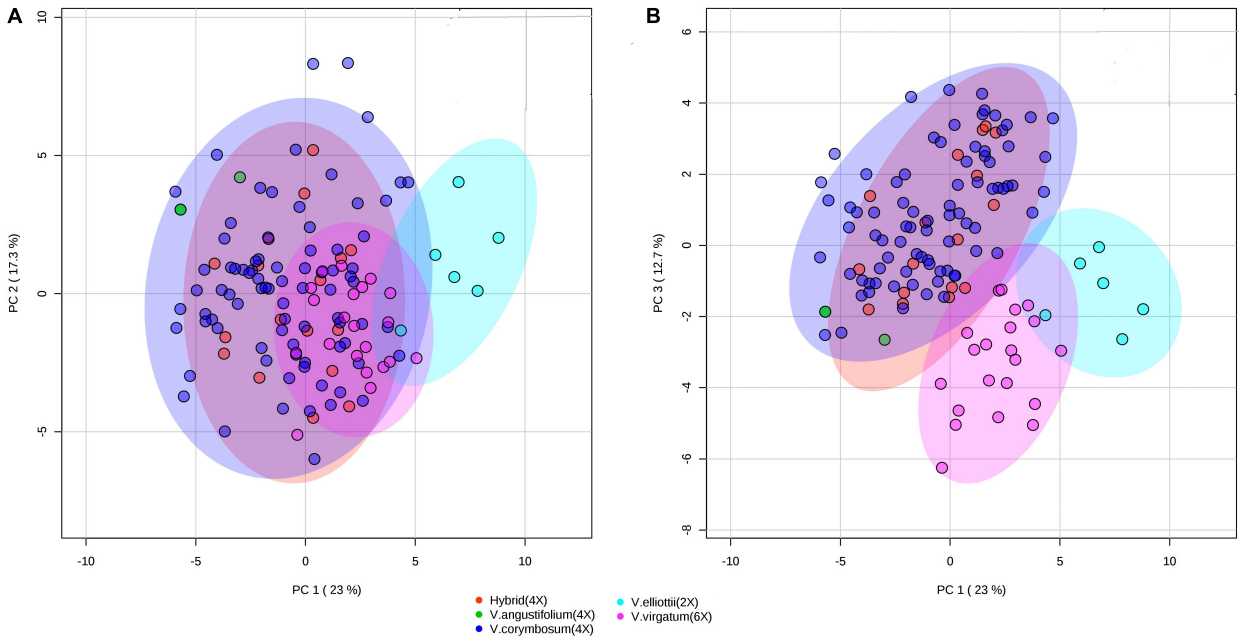

FIGURE 8 | PCA score plots of the first and second **(A)** and first and third **(B)** principal components. The data obtained from metabolites and fruit quality data of 128 blueberry accessions from five species (hybrid, *V. elliottii*, *V. virgatum*, *V. angustifolium*, and *V. corymbosum*).

could be grouped according to ploidy group, but not type (NHB vs. SHB) or geographical origin.

DISCUSSION

Blueberry is recognized globally for its health promoting properties that have in part contributed to a rapid increase in demand and production over the past 15 years (Rodriguez-Saona et al., 2019). Multiple studies in blueberry and other crops indicated that polyphenols function as bioactive compounds in the human body promoting multiple health effects (Krikorian et al., 2010; Stull et al., 2010; Norberto et al., 2013). Despite their importance, limited research has been conducted in blueberry to characterize the extent of variation of metabolites in tetraploid cultivated germplasm, and their association with other fruit quality traits. Previous studies also used a limited number of cultivated accessions, and often used material that is not directly accessible to breeders and scientists (Kalt et al., 2001; Scalzo et al., 2013, 2015; Yousef et al., 2013, 2014; Gündüz et al., 2015; Timmers et al., 2017; Wang et al., 2019). In this study, we characterized the concentration of three major flavonoids and phenolic acids, and four fruit quality traits across a large set of tetraploid cultivated blueberry accessions ($N = 100$) and a number ($N = 28$) of other species with different ploidy. These plant materials represent clones of blueberry accessions publicly available through the USDA-NCGR and searchable through the Germplasm Resources Information – Global Network (GRIN-Global) database. The results were used to identify a strategy to perform a genetic study for bioactive metabolites in blueberry.

Genotypic Effects Explain the Extensive Metabolite and Fruit Quality Traits Diversity Identified Within and Between Ploidy Groups

Extensive variation for concentrations and fruit quality traits was identified in this study, especially within the tetraploid accessions. Bioactive metabolite analysis identified 20 anthocyanins, 6 flavonols, 4 flavanols and 4 phenolic acids, in agreement with type and number of flavonoids and polyphenols observed in previous studies (Grace et al., 2019; Wang et al., 2019). We detected a pronounced accession, year and accession by year interaction effects on the metabolite concentrations. These interactions were expected since the metabolite concentration of a fruit crop, including blueberry, is governed by complex and interconnected enzymatic activities, each of which can react differently in response to the different growing environments (Chen et al., 2013; Wen et al., 2014; Matsuda et al., 2015; Colle et al., 2019). Similarly, there were significant effects of accession, year and year by environment interactions on fruit quality traits including fruit size, pH, TA and TSS. Similar results using a much smaller set of accessions were previously reported (Kalt et al., 2001; Yousef et al., 2014; Gündüz et al., 2015; Scalzo et al., 2015; Timmers et al., 2017).

Despite the significant accession by year interaction identified for most of the traits, the tetraploid accessions evaluated here, which are mostly cultivated and suitable for genetics studies, demonstrated moderate to high (>40%) broad sense heritability, indicating that genotypic effects explain most of the variability (Lourenço et al., 2017; Schmidt et al., 2019). To the best of our knowledge, this is the first study to estimate broad sense

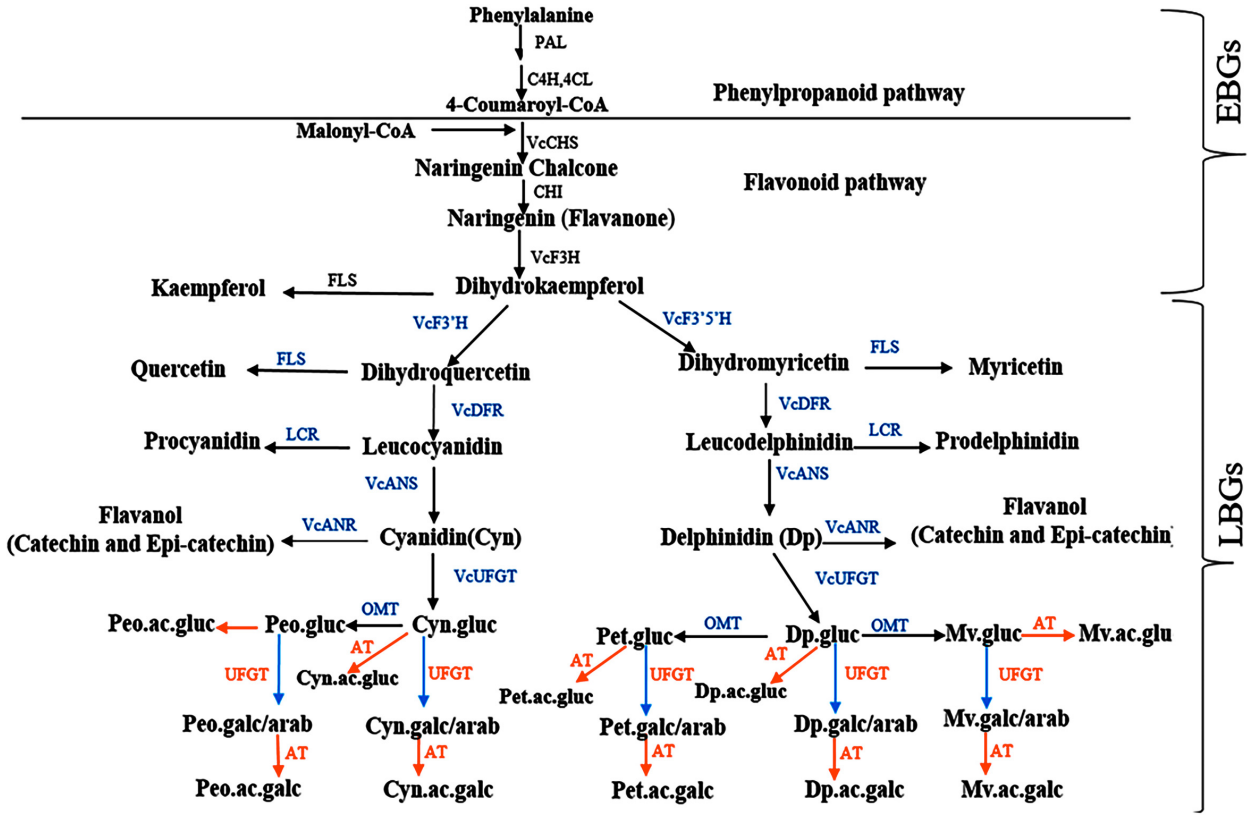

FIGURE 9 | A schematic representation of anthocyanin pathway in blueberry with slight modification from bilberry as described in Jaakola et al. (2002). Enzyme abbreviations: C4H, Cinnamate 4-hydroxylase4; 4CL, 4-coumaroyl:CoA ligase; CHI, chalcone isomerase; F3′H, flavonoid 3′ hydroxylase; F3′5′H, flavonoid 3′5′ hydroxylase; LCR, leucoanthocyanidin reductase; UFGT, UDP Glc-flavonoid 3-*O*-glucosyl transferase; OMT,O-methyltransferase. Sugar and anthocyanidins abbreviations: gluc, glucoside; arab, arabinoside; galc, galactoside; Mv, malvidin; Pet, petunidin; and Peo, peonidin. Pathway genes: EBGs, early biosynthesis genes; LBGs, late biosynthesis genes.

heritability for bioactive metabolites and fruit quality traits in blueberry and to provide preliminary insight for performing future genetic studies for these traits. The high level of broad sense heritability (>40%) detected here will help to improve QTL detection, especially in auto-polyploid species like blueberry (Bourke et al., 2019). Among the fruit quality traits, fruit weight had the highest broad sense heritability (>80%). Among the metabolites, the different forms of anthocyanins had the highest heritability followed by chlorogenic acid. As demonstrated by cluster analysis (**Supplementary Figure S3**), glycosylation and acylation, two enzymatic reactions that contribute to anthocyanin diversification in plants (Jaakola et al., 2002; Noguchi et al., 2009; Zifkin et al., 2012; Cheng et al., 2014; Le Roy et al., 2016) can explain the diversity observed within the tetraploid accessions. Previous studies described genes involved in flavonoid and more specifically anthocyanin biosynthesis in blueberry (Jaakola et al., 2002; Kurilich et al., 2005; Charron et al., 2009; Zifkin et al., 2012; Jaakola, 2013; Li et al., 2016; Lin et al., 2018; Colle et al., 2019). Here based on data from multiple studies (Jaakola et al., 2002; Zifkin et al., 2012; Jaakola, 2013; Colle et al., 2019), we reconstructed a scheme of the flavonoid pathway in blueberry (**Figure 9**) that includes early and late biosynthetic genes (EBGs and LBGs, respectively). The early anthocyanin genes (EBGs) are highly conserved across the plant kingdom including *Vaccinium* species (Jaakola et al., 2002; Zifkin et al., 2012; Jaakola, 2013; Li et al., 2016; Lin et al., 2018; Colle et al., 2019). However, the late anthocyanins biosynthesis genes (LBGs) have not fully explored in *Vaccinium*. Among the LBGs, the dihydroflavonol 4-reductase (DFR), anthocyanidin synthase (ANS), the (methyltransferase) OMT and a flavonoid 3-O-glucosyltransferase (*VcUFGT*) which play an important role into the diversification of the aglycone derivatives have been described (Jaakola et al., 2002; Zifkin et al., 2012). However, the LBGs regulating the downstream anthocyanin biosynthesis, including formation of galactoside, arabinoside, and the acylated derivatives, which contribute to the diversification of the anthocyanin, are still unknown. The results of this study highlight three aspects that can provide new insight in anthocyanin biosynthesis pathway in blueberry. First, the anthocyanidin aglycones were clustered based on their derivatives, petunidin and malvidin with delphinidin and peonidin with cyanidin (**Figure 4** and **Supplementary Figure S3**), which suggest that probably a flux effect, toward each branch exist. These results are in agreement with the previous report in bilberry

(Jaakola et al., 2002; Jaakola, 2013) and with the proposed pathway (**Figure 9**). Second, we observed clear clustering pattern between sugar moieties, glucoside vs. galactoside/arabinoside (**Supplementary Figure S3**). Previous study (Zifkin et al., 2012) reported that *Vc*UFGT gene product is involved in adding of glucoside on anthocyanidin structure in blueberry. However, no genes and genetic mechanisms have been described to regulate the formation of galactoside and arabinoside. Our cluster analysis suggests that one or more UFGT genes with major effect are most likely involved in catalyzing the synthesis of galactoside and/or arabinoside based anthocyanins. The third important point is that acylated anthocyanin also formed a subcluster (**Supplementary Figure S3**). Multiple families and types of acyltransferase (AT) have been described in plants (Giusti and Wrolstad, 2003; D'Auria, 2006; Matera et al., 2015) and could underlie the clear pattern of diversification observed here.

Studying the genetic mechanisms controlling anthocyanin diversification in blueberry is important since anthocyanin glycosylation contributes to anthocyanin stability and transport of anthocyanins to the vacuole (Jaakola et al., 2002; Noguchi et al., 2009; Zifkin et al., 2012; Jaakola, 2013; Cheng et al., 2014; Le Roy et al., 2016; Wang et al., 2018). Similarly, acylation contributes to stability under unfavorable conditions such as high pH, heat stress and intense light (Giusti and Wrolstad, 2003; D'Auria, 2006; Matera et al., 2015; Yang W. et al., 2019) and could be involved in bioaccessibility (Kurilich et al., 2005; Charron et al., 2009; Oliveira et al., 2019). Overall, the high broad sense heritability together with clear clustering patterns among the different anthocyanins based on sugar moieties and acylation suggest that key genetic factors/genes that have a relatively simple genetic inheritance are likely to be involved in the glycosylation and acylation of the different forms of anthocyanin in blueberry. Although this study does not identify specific genes involved in the anthocyanin diversification, the results provides a better understanding of the flux and underlying genetic effects controlling the downstream anthocyanin biosynthesis. This represent a solid framework for follow up genetic and functional analysis of this important pathway in blueberry. Similar levels of broad sense heritability were reported for metabolomes of diverse rice and maize accessions (Chen et al., 2013; Wen et al., 2014; Matsuda et al., 2015), or for fruit weight in cranberry (Georgi et al., 2013; Schlautman et al., 2015) and grape (Doligez et al., 2013), and were successfully used to dissect the genetic basis of these traits using genome-wide association analysis or QTL mapping.

Ploidy was the most distinctive descriptor to differentiate the germplasm evaluated here. Indeed, PCA and PLS-DA analyses clearly separated the three-ploidy groups (2×, 4×, and 6×). These results are consistent with previous studies reporting that HB (4×) blueberry differed from RB (6×) blueberry with respect to metabolite profile and fruit quality traits (Gündüz et al., 2015; Scalzo et al., 2015). Interestingly, traits with high level of heritability such as acylated anthocyanin, cyanidin derivatives, chlorogenic acid concentration or TSS had a high discriminatory importance, suggesting that a strong genetic footprint controlling these traits underlie the pattern of differentiation observed here across ploidy groups. In contrast, tetraploid species *V. corymbosum* and *V. angustifolium*, and blueberry types SHB and NHB were not differentiated, probably because they have a more uniform genetic makeup as compared to inter-ploidy groups. Indeed, hybridization between tetraploid NHB and LB is relatively common, as demonstrated by the high level of NHB and LB hybrids identified in invasive natural populations (Schepker and Kowarik, 1998), and their common use in breeding programs to develop the so-called tetraploid half-highbush cultivars like "Polaris," "Chippewa," "Northblue," or "Northcountry" to cite a few examples (Bian et al., 2014). Similarly, NHB and SHB hybrids are very easy to obtain and are commonly used in breeding programs (Ballington, 2009; Hancock et al., 2018; Retamales and Hancock, 2018). Consistent with these observations, two independent studies (Campa and Ferreira, 2018; Zong et al., 2019) that used molecular markers to characterize blueberry germplasm revealed that the different ploidy (2×, 4×, 6×) were clearly differentiated, while SHB, NHB and half-highbush cultivars were not separated into different groups.

Fruit Size Is a Key Factor to Study Genetic Mechanisms Controlling Flavonoids and Phenolic Acids in Blueberry

Our results demonstrated that not only fruit weight, surface area, and volume or size are very highly correlated (>0.99) but also that fruit weight and fruit volume measurements agreed. This information is relevant when planning phenotyping strategies to study the genetic mechanism controlling these traits. For instance, high-throughput phenotyping methods such as image analysis that can estimate fruit volume and number of fruits/plant, could be used to estimate fruit yield very accurately. Similarly, phenotyping instruments (e.g., texture analyzers) that integrate fruit weight measurements can be used to estimate fruit size.

Trait correlation analysis highlighted that in tetraploid accessions, fruit size was negatively correlated with anthocyanins, phenolic acids, flavanols and TSS content. Similar results for individual anthocyanins and total anthocyanin content, TSS and total phenolic acids were previously reported (Yousef et al., 2014; Gündüz et al., 2015; Scalzo et al., 2015). In contrast, significant correlation was not observed between fruit size and most of the metabolites including anthocyanins in hexaploid and in the diploid accessions, this negative correlation was observed for one year only. However, it is important to note that the different results across the ploidy groups are likely due to the low degree of variation in fruit size and total anthocyanin observed within these accessions, and most importantly the small set of accessions evaluated for these ploidy groups (diploid $N = 6$, hexaploid $N = 22$) (**Figure 1** and **Supplementary Table S2**). Overall, we propose that the results highlighted in the tetraploid accessions are robust and confirm that fruit size is negatively correlated with the metabolites evaluated in this study. Zifkin et al. (2012) localized accumulation anthocyanin and the expression of its biosynthetic genes, specifically in the skin of fully ripen fruits. In another study by Scalzo et al. (2015), anthocyanins

are primarily found in the skin of blueberry, so if anthocyanins are extracted from whole berries, small fruit are expected to have relatively higher skin surface area, and would results in higher concentration of metabolites. This would also assume a uniform skin thickness. The fact that in our study fruit surface area, volume and weight are highly correlated, confirms this hypothesis. It is important to note that in blueberry, anthocyanin accumulation in the pulp can occur, but this trait is specific to a small number of accessions or cultivars (Kalt et al., 1999; Ribera et al., 2010) that are not represented in our study. The negative correlation between fruit size and the bioactive metabolites evaluated here, implies that to perform GWAS or QTL mapping studies targeting these bioactive metabolites, estimating fruit size is important since it should be used as a co-factor in the analysis.

To examine the extent of size-independent phenotypic variation for total anthocyanin concentration, the anthocyanin concentration of the tetraploid accessions were normalized by fruit size. The size-independent data showed more than fivefold variation for total anthocyanin (**Supplementary Figure S15**), indicating the presence of size-independent factors that regulate anthocyanin concentration. The size independent phenotypic variation can be explored to identify other factors such as peel thickness or genes related to the biosynthetic pathway that control this trait. Also, as demonstrated by biplot analysis (**Supplementary Figure S4**), cultivated accessions with high anthocyanin content and large fruit could be identified. Positive associations were also observed between total anthocyanin with phenolic acid and other flavonoids such as total flavanols and total flavonols (**Figures 3**, **4**). These results suggest that metabolite content and fruit size can be improved simultaneously in breeding programs.

Overall, the results of our study highlighted that the tetraploid accessions evaluated here will be suitable to perform a genome wide association study to investigate the genetic basis controlling flavonoids and polyphenol accumulation for most of the fruit quality traits in this study. Fruit size can be estimated as a proxy of fruit weight or volume and vice versa, and it is a critical parameter to account for when performing genetic studies for the bioactive metabolites. Finally, since the blueberry accessions evaluated in this study represent a publicly available germplasm resource, and the phenotypic data will be made available through the GRIN-Global database, breeders and scientists will be able to use the results of this work as a basis for future genetic studies and in breeding programs.

AUTHOR'S NOTE

The content of this publication is solely the responsibility of the authors and does not necessarily represent the official views of FFAR.

DATA AVAILABILITY STATEMENT

The raw data supporting the conclusions of this article will be made available by the authors, without undue reservation, to any qualified researcher.

AUTHOR CONTRIBUTIONS

MI designed the study. NB and KH coordinated the fruit harvest and germplasm management. ML coordinated the HPLC and LC-MS analysis. MG and JX performed the HPLC and MS analysis. MM performed the fruit quality phenotyping and all statistical analysis; MM and MI interpreted the results, drafted the sections of the manuscript, prepared the figures and tables, and prepared the final version of the manuscript. MG, JX, CK, NB, KH, MF, and ML critically revised the manuscript. All authors read, reviewed, and approved the manuscript.

FUNDING

This research was supported by the Foundation for Food and Agriculture Research (FFAR) under award number 534667. MI and ML were also supported by the United States Department of Agriculture National Institute of Food and Agriculture, Hatch project 1008691 and the National Institute of Food and Agriculture, United States Department of Agriculture, under award number 2019-51181-30015, project "VacciniumCAP: Leveraging genetic and genomic resources to enable development of blueberry and cranberry cultivars with improved fruit quality attributes." MI was also supported by the United States Department of Agriculture National Institute of Food and Agriculture, Hatch project 1008691.

SUPPLEMENTARY MATERIAL

The Supplementary Material for this article can be found online at: https://www.frontiersin.org/articles/10.3389/fpls.2020.00370/full#supplementary-material

REFERENCES

Ballington, J. R. (2009). The role of interspecific hybridization in blueberry improvement. *Acta Hortic.* 810, 49–60. doi: 10.17660/ActaHortic.2009.810.2

Bian, Y., Ballington, J., Raja, A., Brouwer, C., Reid, R., Burke, M., et al. (2014). Patterns of simple sequence repeats in cultivated blueberries (*Vaccinium* section *Cyanococcus* spp.) and their use in revealing genetic diversity and population structure. *Mol. Breed.* 34, 675–689. doi: 10.1007/s11032-014-0066-7

Bland, J. M., and Altman, D. (1986). Statistical methods for assessing agreement between two methods of clinical measurement. *Lancet* 327, 307–310. doi: 10.1016/s0140-6736(86)90837-8

Bourke, P. M., Hackett, C. A., Voorrips, R. E., Visser, R. G. F., and Maliepaard, C. (2019). Quantifying the power and precision of QTL analysis in autopolyploids

under bivalent and multivalent genetic models. *G3* 9, 2107–2122. doi: 10.1534/g3.119.400269

Campa, A., and Ferreira, J. J. (2018). Genetic diversity assessed by genotyping by sequencing (GBS) and for phenological traits in blueberry cultivars. *PLoS One* 13:e0206361. doi: 10.1371/journal.pone.0206361

Charron, C. S., Kurilich, A. C., Clevidence, B. A., Simon, P. W., Harrison, D. J., Britz, S. J., et al. (2009). Bioavailability of anthocyanins from purple carrot juice: effects of acylation and plant matrix. *J. Agric. Food Chem.* 57, 1226–1230. doi: 10.1021/jf802988s

Chen, W., Gong, L., Guo, Z., Wang, W., Zhang, H., Liu, X., et al. (2013). A novel integrated method for large-scale detection, identification, and quantification of widely targeted metabolites: application in the study of rice metabolomics. *Mol. Plant* 6, 1769–1780. doi: 10.1093/mp/sst080

Cheng, J., Wei, G., Zhou, H., Gu, C., Vimolmangkang, S., Liao, L., et al. (2014). Unraveling the mechanism underlying the glycosylation and methylation of anthocyanins in peach. *Plant Physiol.* 166, 1044–1058. doi: 10.1104/pp.114.246876

Chong, J., Soufan, O., Li, C., Caraus, I., Li, S., Bourque, G., et al. (2018). MetaboAnalyst 4.0: towards more transparent and integrative metabolomics analysis. *Nucleic Acids Res.* 46, W486–W494. doi: 10.1093/nar/gky310

Colle, M., Leisner, C. P., Wai, C. M., Ou, S., Bird, K. A., Wang, J., et al. (2019). Haplotype-phased genome and evolution of phytonutrient pathways of tetraploid blueberry. *Gigascience* 8:giz012. doi: 10.1093/gigascience/giz012

Correa-Betanzo, J., Allen-Vercoe, E., McDonald, J., Schroeter, K., Corredig, M., and Paliyath, G. (2014). Stability and biological activity of wild blueberry (*Vaccinium angustifolium*) polyphenols during simulated in vitro gastrointestinal digestion. *Food Chem.* 165, 522–531. doi: 10.1016/j.foodchem.2014.05.135

D'Auria, J. C. (2006). Acyltransferases in plants: a good time to be BAHD. *Curr. Opin. Plant Biol.* 9, 331–340. doi: 10.1016/j.pbi.2006.03.016

Diaz-Garcia, L., Covarrubias-Pazaran, G., Schlautman, B., and Zalapa, J. (2016). GiNA, an efficient and high-throughput software for horticultural phenotyping. *PLoS One* 11:e0160439. doi: 10.1371/journal.pone.0160439

Doligez, A., Bertrand, Y., Farnos, M., Grolier, M., Romieu, C., Esnault, F., et al. (2013). New stable QTLs for berry weight do not colocalize with QTLs for seed traits in cultivated grapevine (*Vitis vinifera* L.). *BMC Plant Biol.* 13:217. doi: 10.1186/1471-2229-13-217

Fleschhut, J., Kratzer, F., Rechkemmer, G., and Kulling, S. E. (2006). Stability and biotransformation of various dietary anthocyanins in vitro. *Eur. J. Nutr.* 45, 7–18. doi: 10.1007/s00394-005-0557-8

Georgi, L., Johnson-Cicalese, J., Honig, J., Das, S. P., Rajah, V. D., Bhattacharya, D., et al. (2013). The first genetic map of the American cranberry: exploration of synteny conservation and quantitative trait loci. *Theor. Appl. Genet.* 126, 673–692. doi: 10.1007/s00122-012-2010-8

Giovanelli, G., and Buratti, S. (2009). Comparison of polyphenolic composition and antioxidant activity of wild Italian blueberries and some cultivated varieties. *Food Chem.* 112, 903–908. doi: 10.1016/j.foodchem.2008.06.066

Giusti, M. M., and Wrolstad, R. E. (2003). Acylated anthocyanins from edible sources and their applications in food systems. *Biochem. Eng. J.* 14, 217–225. doi: 10.1016/S1369-703X(02)00221-8

Grace, M. H., Xiong, J., Esposito, D., Ehlenfeldt, M., and Lila, M. A. (2019). Simultaneous LC-MS quantification of anthocyanins and non-anthocyanin phenolics from blueberries with widely divergent profiles and biological activities. *Food Chem.* 277, 336–346. doi: 10.1016/j.foodchem.2018.10.101

Gündüz, K., Serçe, S., and Hancock, J. F. (2015). Variation among highbush and rabbiteye cultivars of blueberry for fruit quality and phytochemical characteristics. *J. Food Composit. Anal.* 38, 69–79. doi: 10.1016/j.jfca.2014.09.007

Hancock, J. F., Lyrene, P., Finn, C. E., Vorsa, N., and Lobos, G. A. (2008). Blueberries and cranberries. *Temp. Fruit Crop Breed. Germplasm Genom.* 290, 115–149. doi: 10.1007/978-1-4020-6907-9-4

Hancock, J. F., Olmstead, J. W., Itle, R. A., Callow, P. W., Neils-Kraft, S., Wheeler, E. J., et al. (2018). Performance of an elite, hybrid family of a northern x southern highbush cross ('Draper' x 'Jewel'). *Euphytica* 214:95.

Jaakola, L. (2013). New insights into the regulation of anthocyanin biosynthesis in fruits. *Trends Plant Sci.* 18, 477–483. doi: 10.1016/j.tplants.2013.06.003

Jaakola, L., Määttä, K., Pirttilä, A. M., Törrönen, R., Kärenlampi, S., and Hohtola, A. (2002). Expression of genes involved in anthocyanin biosynthesis in relation to Anthocyanin, Proanthocyanidin, and Flavonol levels during bilberry fruit development. *Plant Physiol.* 130, 729–739. doi: 10.1104/pp.006957

Kalt, W., McDonald, J. E., Ricker, R. D., and Lu, X. (1999). Anthocyanin content and profile within and among blueberry species. *Can. J. Plant Sci.* 79, 617–623. doi: 10.4141/p99-009

Kalt, W., Ryan, D. A. J., Duy, J. C., Prior, R. L., Ehlenfeldt, M. K., and Vander Kloet, S. P. (2001). Interspecific variation in anthocyanins, phenolics, and antioxidant capacity among genotypes of highbush and lowbush blueberries (*Vaccinium* section *Cyanococcus* spp.). *J. Agric. Food Chem.* 49, 4761–4767. doi: 10.1021/jf010653e

Krikorian, R., Shidler, M. D., Nash, T. A., Kalt, W., Vinqvist-Tymchuk, M. R., Shukitt-Hale, B., et al. (2010). Blueberry supplementation improves memory in older adults. *J. Agric. Food Chem.* 58, 3996–4000. doi: 10.1021/jf9029332

Kurilich, A. C., Clevidence, B. A., Britz, S. J., Simon, P. W., and Novotny, J. A. (2005). Plasma and urine responses are lower for acylated vs nonacylated anthocyanins from raw and cooked purple carrots. *J. Agric. Food Chem.* 53, 6537–6542. doi: 10.1021/jf050570o

Lê, S., Josse, J., and Husson, F. (2008). FactoMineR: an R package for multivariate analysis. *J. Statist. Softw.* 25, 1–18.

Le Roy, J., Huss, B., Creach, A., Hawkins, S., and Neutelings, G. (2016). Glycosylation is a major regulator of phenylpropanoid availability and biological activity in plants. *Front. Plant Sci.* 7:735. doi: 10.3389/fpls.2016.00735

Li, D., Li, B., Ma, Y., Sun, X., Lin, Y., and Meng, X. (2017). Polyphenols, anthocyanins, and flavonoids contents and the antioxidant capacity of various cultivars of highbush and half-high blueberries. *J. Food Composit. Anal.* 62, 84–93. doi: 10.1016/j.jfca.2017.03.006

Li, L., Zhang, H., Liu, Z., Cui, X., Zhang, T., Li, Y., et al. (2016). Comparative transcriptome sequencing and de novo analysis of *Vaccinium corymbosum* during fruit and color development. *BMC Plant Biol.* 16:223. doi: 10.1186/s12870-016-0866-5

Lin, Y., Wang, Y., Li, B., Tan, H., Li, D., Li, L., et al. (2018). Comparative transcriptome analysis of genes involved in anthocyanin synthesis in blueberry. *Plant Physiol. Biochem.* 127, 561–572. doi: 10.1016/j.plaphy.2018.04.034

Lobos, G. A., and Hancock, J. F. (2015). Breeding blueberries for a changing global environment: a review. *Front. Plant Sci.* 6:782. doi: 10.3389/fpls.2015.00782

Lourenço, V. M., Rodrigues, P. C., Pires, A. M., and Piepho, H.-P. (2017). A robust DF-REML framework for variance components estimation in genetic studies. *Bioinformatics* 33, 3584–3594. doi: 10.1093/bioinformatics/btx457

Lyrene, P. M., Vorsa, N., and Ballington, J. R. (2003). Polyploidy and sexual polyploidization in the genus *Vaccinium*. *Euphytica* 133, 27–36. doi: 10.1023/A:1025608408727

Martineau, L. C., Couture, A., Spoor, D., Benhaddou-Andaloussi, A., Harris, C., Meddah, B., et al. (2006). Anti-diabetic properties of the Canadian Lowbush blueberry *Vaccinium angustifolium* Ait. *Phytomedicine* 13, 612–623. doi: 10.1016/j.phymed.2006.08.005

Matera, R., Gabbanini, S., Berretti, S., Amorati, R., De Nicola, G. R., Iori, R., et al. (2015). Acylated anthocyanins from sprouts of *Raphanus sativus* cv. sango: isolation, structure elucidation and antioxidant activity. *Food Chem.* 166, 397–406. doi: 10.1016/j.foodchem.2014.06.056

Matsuda, F., Nakabayashi, R., Yang, Z., Okazaki, Y., Yonemaru, J., Ebana, K., et al. (2015). Metabolome-genome-wide association study dissects genetic architecture for generating natural variation in rice secondary metabolism. *Plant J.* 81, 13–23. doi: 10.1111/tpj.12681

McDougall, G. J., Fyffe, S., Dobson, P., and Stewart, D. (2007). Anthocyanins from red cabbage–stability to simulated gastrointestinal digestion. *Phytochemistry* 68, 1285–1294. doi: 10.1016/j.phytochem.2007.02.004

Mengist, M. F., Alves, S., Griffin, D., Creedon, J., McLaughlin, M. J., Jones, P. W., et al. (2018). Genetic mapping of quantitative trait loci for tuber-cadmium and zinc concentration in potato reveals associations with maturity and both overlapping and independent components of genetic control. *Theor. Appl. Genet.* 131, 929–945. doi: 10.1007/s00122-017-3048-4

Noguchi, A., Horikawa, M., Fukui, Y., Fukuchi-Mizutani, M., Iuchi-Okada, A., Ishiguro, M., et al. (2009). Local differentiation of sugar donor specificity of flavonoid glycosyltransferase in lamiales W. *Plant Cell* 21, 1556–1572. doi: 10.1105/tpc.108.063826

Norberto, S., Silva, S., Meireles, M., Faria, A., Pintado, M., and Calhau, C. (2013). Blueberry anthocyanins in health promotion: a metabolic overview. *J. Funct. Foods* 5, 1518–1528. doi: 10.1016/j.jff.2013.08.015

Oliveira, H., Perez-Gregório, R., de Freitas, V., Mateus, N., and Fernandes, I. (2019). Comparison of the in vitro gastrointestinal bioavailability of acylated and non-acylated anthocyanins: purple-fleshed sweet potato vs red wine. *Food Chem.* 276, 410–418. doi: 10.1016/j.foodchem.2018.09.159

Prencipe, F. P., Bruni, R., Guerrini, A., Rossi, D., Benvenuti, S., and Pellati, F. (2014). Metabolite profiling of polyphenols in *Vaccinium berries* and determination of their chemopreventive properties. *J. Pharmaceut. Biomed. Anal.* 89, 257–267. doi: 10.1016/j.jpba.2013.11.016

Retamales, J. B., and Hancock, J. F. (2018). *Blueberries*. Wallington: CABI.

Ribera, A. E., Reyes-Diaz, M., Alberdi, M., Zuñiga, G. E., and Mora, M. L. (2010). Antioxidant compounds in skin and pulp of fruits change among genotypes and maturity stages in highbush blueberry (*Vaccinium corymbosum* L.) grown in southern Chile. *J. Soil Sci. Plant Nutr.* 10, 509–536. doi: 10.4067/s0718-95162010000200010

Rodriguez-Mateos, A., Cifuentes-Gomez, T., Tabatabaee, S., Lecras, C., and Spencer, J. P. E. (2012). Procyanidin, anthocyanin, and chlorogenic acid contents of highbush and lowbush blueberries. *J. Agric. Food Chem.* 60, 5772–5778. doi: 10.1021/jf203812w

Rodriguez-Saona, C., Vincent, C., and Isaacs, R. (2019). Blueberry IPM: past successes and future challenges. *Ann. Rev. Entomol.* 64, 95–114. doi: 10.1146/annurev-ento-011118-112147

Scalzo, J., Stevenson, D., and Hedderley, D. (2013). Blueberry estimated harvest from seven new cultivars: fruit and anthocyanins. *Food Chem.* 139, 44–50. doi: 10.1016/j.foodchem.2013.01.091

Scalzo, J., Stevenson, D., and Hedderley, D. (2015). Polyphenol compounds and other quality traits in blueberry cultivars. *J. Berry Res.* 5, 117–130. doi: 10.3233/JBR-150097

Schepker, H., and Kowarik, I. (1998). "Invasive north American blueberry hybrids (vaccinium corymbosum x angustifolium) in northern germany," in *Plant Invasions: Ecological Mechanims and Human Responses*, eds U. Starfinger, K. Edwards, M. Kowarik, and M. Williamson (Leiden: Backhuys Publishers).

Schlautman, B., Covarrubias-Pazaran, G., Diaz-Garcia, L. A., Johnson-Cicalese, J., Iorrizo, M., Rodriguez-Bonilla, L., et al. (2015). Development of a high-density cranberry SSR linkage map for comparative genetic analysis and trait detection. *Mol. Breed.* 35, 1–18. doi: 10.1007/s11032-015-0367-5

Schmidt, P., Hartung, J., Bennewitz, J., and Piepho, H.-P. (2019). Heritability in plant breeding on a genotype-difference basis, Genetics. *Genetics* 212, 991–1008. doi: 10.1534/genetics.119.302134

Strauch, R. C., Mengist, M. F., Pan, K., Yousef, G. G., Iorizzo, M., Brown, A. F., et al. (2019). Variation in anthocyanin profiles of 27 genotypes of red cabbage over two growing seasons. *Food Chem.* 301:125289. doi: 10.1016/j.foodchem.2019.125289

Stull, A. J., Cash, K. C., Johnson, W. D., Champagne, C. M., and Cefalu, W. T. (2010). Bioactives in blueberries improve insulin sensitivity in obese, insulin-resistant men and women. *J. Nutr.* 140, 1764–1768. doi: 10.3945/jn.110.125336

Sun, Y., Nemec-Bakk, A. S., Mallik, A. U., Bagchi, A. K., Singal, P. K., and Khaper, N. (2019). Blueberry extract attenuates doxorubicin-induced damage in H9c2 cardiac cells. *Can. J. Physiol. Pharmacol.* 97, 880–884. doi: 10.1139/cjpp-2019-0031

Szymańska, E., Saccenti, E., Smilde, A. K., and Westerhuis, J. A. (2012). Double-check: validation of diagnostic statistics for PLS-DA models in metabolomics studies. *Metabolomics* 8, 3–16. doi: 10.1007/s11306-011-0330-3

Timmers, M. A., Grace, M. H., Yousef, G. G., and Lila, M. A. (2017). Inter- and intra-seasonal changes in anthocyanin accumulation and global metabolite profiling of six blueberry genotypes. *J. Food Composit. Anal.* 59, 105–110. doi: 10.1016/j.jfca.2017.02.019

Wang, H., Wang, C., Fan, W., Yang, J., Appelhagen, I., Wu, Y., et al. (2018). A novel glycosyltransferase catalyses the transfer of glucose to glucosylated anthocyanins in purple sweet potato. *J. Exp. Bot.* 69, 5445–5459. doi: 10.1093/jxb/ery305

Wang, Y., Fong, S. K., Singh, A. P., Vorsa, N., and Johnson-Cicalese, J. (2019). Variation of Anthocyanins, Proanthocyanidins, Flavonols, and organic acids in cultivated and wild diploid blueberry species. *Hortscience* 54, 576–585. doi: 10.21273/hortsci13491-18

Warnes, M. G. R., Bolker, B., Bonebakker, L., and Gentleman, R. (2016). *Package 'gplots.' Various R Programming Tools for Plotting Data*. Available online at: https://github.com/talgalili/gplots (accessed July 28, 2019).

Wei, T., Simko, V., Levy, M., Xie, Y., Jin, Y., and Zemla, J. (2017). Package 'corrplot.'. *Statistician* 56, 316–324.

Wen, W., Li, D., Li, X., Gao, Y., Li, W., Li, H., et al. (2014). Metabolome-based genome-wide association study of maize kernel leads to novel biochemical insights. *Nat. Commun.* 5:3438. doi: 10.1038/ncomms4438

Yang, H., Tian, T., Wu, D., Guo, D., and Lu, J. (2019). Prevention and treatment effects of edible berries for three deadly diseases: cardiovascular disease, cancer and diabetes. *Crit. Rev. Food Sci. Nutr.* 59, 1903–1912. doi: 10.1080/10408398.2018.1432562

Yang, W., Kortesniemi, M., Ma, X., Zheng, J., and Yang, B. (2019). Enzymatic acylation of blackcurrant (*Ribes nigrum*) anthocyanins and evaluation of lipophilic properties and antioxidant capacity of derivatives. *Food Chem.* 281, 189–196. doi: 10.1016/j.foodchem.2018.12.111

Yousef, G. G., Brown, A. F., Funakoshi, Y., Mbeunkui, F., Grace, M. H., Ballington, J. R., et al. (2013). Efficient quantification of the health-relevant anthocyanin and phenolic acid profiles in commercial cultivars and breeding selections of blueberries (*Vaccinium* spp.). *J. Agric. Food Chem.* 61, 4806–4815. doi: 10.1021/jf400823s

Yousef, G. G., Lila, M. A., Guzman, I., Ballington, J. R., and Brown, A. F. (2014). Impact of interspecific introgression on anthocyanin profiles of southern highbush blueberry. *J. Am. Soc. Hortic. Sci.* 139, 99–112. doi: 10.21273/jashs.139.2.99

Zhao, C. L., Yu, Y. Q., Chen, Z. J., Wen, G. S., Wei, F. G., Zheng, Q., et al. (2017). Stability-increasing effects of anthocyanin glycosyl acylation. *Food Chem.* 214, 119–128. doi: 10.1016/j.foodchem.2016.07.073

Zifkin, M., Jin, A., Ozga, J. A., Zaharia, L. I., Schernthaner, J. P., Gesell, A., et al. (2012). Gene expression and metabolite profiling of developing highbush blueberry fruit indicates transcriptional regulation of flavonoid metabolism and activation of abscisic acid metabolism. *Plant Physiol.* 158, 200–224. doi: 10.1104/pp.111.180950

Zong, Y., Kang, H., Fang, Q., Chen, X., Zhou, M., Ni, J., et al. (2019). Phylogenetic relationship and genetic background of blueberry (*Vaccinium* spp.) based on retrotransposon-based SSAP molecular markers. *Sci. Hortic.* 247, 116–122. doi: 10.1016/j.scienta.2018.11.017

Zoratti, L., Jaakola, L., Häggman, H., and Giongo, L. (2015). Anthocyanin profile in berries of wild and cultivated *Vaccinium* spp. along altitudinal gradients in the Alps. *J. Agric. Food Chem.* 63, 8641–8650. doi: 10.1021/acs.jafc.5b02833

Conflict of Interest: The authors declare that the research was conducted in the absence of any commercial or financial relationships that could be construed as a potential conflict of interest.

frontiers in Plant Science

ORIGINAL RESEARCH
published: 08 May 2020
doi: 10.3389/fpls.2020.00538

Methyl Jasmonate Applications From Flowering to Ripe Fruit Stages of Strawberry (*Fragaria* × *ananassa* 'Camarosa') Reinforce the Fruit Antioxidant Response at Post-harvest

*Paz E. Zuñiga[1], Yasna Castañeda[1], Oscar Arrey-Salas[1], Lida Fuentes[2], Felipe Aburto[3] and Carlos R. Figueroa[1]**

[1] Institute of Biological Sciences, Campus Talca, Universidad de Talca, Talca, Chile, [2] Centro Regional de Estudios en Alimentos Saludables, CONICYT-Regional GORE Valparaíso Proyecto R17A10001, Valparaíso, Chile, [3] Laboratorio de Investigación en Suelos, Aguas y Bosques, Facultad de Ciencias Forestales, Universidad de Concepción, Concepción, Chile

OPEN ACCESS

Edited by:
Kevin M. Folta, University of Florida, United States

Reviewed by:
Bruno Mezzetti, Marche Polytechnic University, Italy
Brian Farneti, Fondazione Edmund Mach, Italy

***Correspondence:**
Carlos R. Figueroa
cfigueroa@utalca.cl

Specialty section:
This article was submitted to Crop and Product Physiology, a section of the journal Frontiers in Plant Science

Received: *31 January 2020*
Accepted: *08 April 2020*
Published: *08 May 2020*

Citation:
Zuñiga PE, Castañeda Y, Arrey-Salas O, Fuentes L, Aburto F and Figueroa CR (2020) Methyl Jasmonate Applications From Flowering to Ripe Fruit Stages of Strawberry (Fragaria × ananassa 'Camarosa') Reinforce the Fruit Antioxidant Response at Post-harvest. Front. Plant Sci. 11:538. doi: 10.3389/fpls.2020.00538

Preharvest applications of methyl jasmonate (MeJA) have been shown to improve post-harvest fruit quality in strawberry fruit. However, the effectiveness of consecutive field applications at different phenological stages on the reinforcement of the antioxidant capacity remains to be analyzed. To determine the best antioxidant response of strawberry (*Fragaria* × *ananassa* 'Camarosa') fruit to different numbers and timing of MeJA applications, we performed three differential preharvest treatments (M1, M2, and M3) consisted of successive field applications of 250 μmol L^{-1} MeJA at flowering (M3), large green (M2 and M3), and ripe fruit stages (M1, M2, and M3). Then, we analyzed their effects on fruit quality parameters [firmness, skin color, soluble solids content/titratable acidity (SSC/TA) ratio, fruit weight at harvest, and weight loss] along with anthocyanin and proanthocyanidin (PA) accumulation; the antioxidant-related enzymatic activity of catalase (CAT), guaiacol peroxidase (POX), and ascorbate peroxidase (APX); the total flavonoid and phenolic contents, antioxidant capacity, and ascorbic acid content (AAC) during post-harvest storage (0, 24, 48, and 72 h). We also evaluated the effect on lignin, total carbon and nitrogen (%C and N), lipid peroxidation, and C and N isotopes signatures on fruits. Remarkably, the results indicated that MeJA treatment increases anthocyanin and PA contents as well as CAT activity in post-harvest storage, depending on the number of preharvest MeJA applications. Also, M3 fruit showed a higher AAC compared to control at 48 and 72 h. Noticeably, the anthocyanin content and CAT activity were more elevated in M3 treatment comparing with control at all post-harvest times. In turn, APX activity was found higher on all MeJA-treated fruit independent of the number of applications. Unlike, MeJA applications did not generate variations on fruit firmness and weight, lignin contents,% C and N, and in lipid peroxidation and

water/nitrogen use efficiency according to C and N isotope discrimination. Finally, we concluded that an increasing number of MeJA applications (M3 treatment) improve anthocyanin, PA, AAC, and CAT activity that could play an essential role against reactive oxygen species, which cause stress that affects fruits during post-harvest storage.

Keywords: antioxidants, ascorbate peroxidase (APX), catalase (CAT), flavonoids, *Fragaria* x *ananassa*, preharvest MeJA applications

INTRODUCTION

Strawberry (*Fragaria* × *ananassa* Duch.), a Rosaceae family member, is one of the most popular fruits grown worldwide due to its organoleptic attributes and abundance in nutrients, vitamins, and minerals (Giampieri et al., 2012; Bertioli, 2019). Since the global living standard increases, the improvement of fruit quality at harvest and to maintain it during storage is a current challenge driven by consumers. In this line, scientific research has been focused on finding preharvest treatments with natural compounds to replace chemical post-harvest treatments due to legal restrictions and the negative perception by consumers (García-Pastor et al., 2020). Strawberries have relevant biological activity in human health due to its important content of bioactive compounds, such as vitamin C (58.8 mg per 100 g fresh weight) and phenolic compounds, including anthocyanins (150 to 600 mg/kg of fresh weight) (reviewed by Giampieri et al., 2012). Also, modification in nutrient and phytochemical composition occurs when the fruit is still attached to the plant and during the development and ripening processes (Alvarez-Suarez et al., 2014). Therefore, the improvement of strawberry fruit quality by preharvest management involves considering physicochemical and functional aspects during the fruit development throughout the season in the field.

The jasmonic acid (JA) and its endogenous plant hormone derived methyl jasmonate (MeJA) have been implicated in several physiological processes, mainly modulating plant defense responses, including antioxidant capacity against pathogens and abiotic stresses (Wasternack, 2007; Wasternack and Strnad, 2016) although they play essential roles in fruit growth and ripening regulation (Concha et al., 2013; Serrano et al., 2018). MeJA is a linolenic acid-derived cyclopentanone-based compound, considered an important plant hormone that can mediate intra- and inter-plant communications due to its ability to diffuse through biological membranes and its volatile nature (Reyes-Díaz et al., 2016). MeJA applied as post- or pre-harvest treatment has been shown to have positive effects on increasing fruit bioactive compounds with antioxidant potential, increasing the beneficial health effects as has been demonstrated in lemon fruit (Serna-Escolano et al., 2019). Nevertheless, the effects of exogenous MeJA application in fruit quality are better known on post-harvest treatments (Reyes-Díaz et al., 2016). For instance, MeJA treatment has been shown to induce plant resistance against the negative impacts of storage (chilling and pathogen attacks injuries), increasing the antioxidant capacity and secondary metabolites content. Less known, the MeJA application as preharvest treatments has several effects, depending on the species, cultivar, edaphoclimatic condition, doses, and phenological stage. In this sense, preharvest MeJA applications have been observed as more effective than post-harvest ones in raspberry cultivars (Flores and Ruiz del Castillo, 2014). It has been reported that preharvest MeJA treatment induces an increase in phenolic and anthocyanin concentrations in different climacteric and non−climacteric fruits during ripening (Martínez-Esplá et al., 2014; Zapata et al., 2014; Ozturk et al., 2015; Flores and Ruiz del Castillo, 2016; García-Pastor et al., 2019; Serna-Escolano et al., 2019). In strawberry, MeJA application has been related to an increase of antioxidant capacity and anthocyanin levels. In *F.* × *ananassa* ('Aromas'), during an *in vitro* fruit ripening MeJA assay induces an increase in the red coloration of fruit skin along with anthocyanin levels (Garrido-Bigotes et al., 2018). Other research concluded that preharvest applications of 250 μmol L^{-1} MeJA in the Chilean strawberry fruit [*Fragaria chiloensis* (L.) Mill.] increase antioxidant capacity during post-harvest. Moreover, the antioxidant enzymatic related activity also has been associated with MeJA application. In *Arabidopsis thaliana,* the total activities of catalase (CAT), peroxidase (POX), superoxide dismutase (SOD), and glutathione reductase (GR) increased considerably in response to MeJA (Jung, 2004). In this sense, increased activity of the antioxidant enzymes, together with higher levels of antioxidant compounds, as a result of MeJA treatment reinforce would lead to improving and maintaining fruit quality during the post-harvest time. However, the specificity and effectiveness of consecutive field applications at different phenological stages of strawberry fruit on the reinforcement of the antioxidant capacity remain unclear.

In this study, we performed three differential preharvest treatments consisted of successive field applications of 250 μmol L^{-1} MeJA during strawberry fruit development and ripening. Then, we analyzed their effects mainly on fruit quality parameters, anthocyanins and proanthocyanidins (PAs) accumulation, antioxidant enzymatic, and non-enzymatic activity during four post-harvest storage times. This investigation aimed to determine the best combination between the MeJA application frequency and phenological stage of applications to enhance the antioxidant capacity of strawberry (*F.* × *ananassa* 'Camarosa') fruit. We found that three MeJA applications from flowering to ripe fruit stages improve the antioxidant response of the fruit during post-harvest storage.

MATERIALS AND METHODS

Plant Material and Treatments

Preharvest field treatments were carried out in a commercial strawberry orchard in Pelluhue, Maule Region, Chile (latitude 35° 47′ S; longitude 72° 33′ W). Climatic conditions of this location

are presented in **Supplementary Table 1**. The experiment was arranged in a randomized complete block design. About 100 plants of *F.* × *ananassa* 'Camarosa' distributed in three random plots were used per treatment. Flowers were marked in each plot (n = 180) to analyze the same biological material at each developmental stage planned in the experiment. Methyl jasmonate (MeJA) treatments consisted of different sequential applications as sprays on the plant performed through strawberry fruit development. In this sense, M3 treatment consisted in three different applications at flowering, after 24 days at the large green, and after 7 days at 100% red receptacle fruit stages; M2 treatment consisted in two applications at the large green, and after 7 days at 100% red receptacle; and M1 treatment consisted in one application at 100% red stage (**Supplementary Figure 1**). Each application consisted in 250 μmol L^{-1} MeJA (Sigma-Aldrich, St. Louis, MO, United States) at pH 4.3, and 0.05% (v/v) Tween-20 as surfactant. Distilled water plus 0.05% (v/v) Tween-20 was used as a control (C). The MeJA concentration was chosen as the minimum effective concentration according to previous field experiments on strawberry (Yilmaz et al., 2003; Saavedra et al., 2016, 2017). Harvest was performed at 100% red receptacle after the last MeJA application. Fruits were immediately transported to the laboratory under refrigerated conditions for post-harvest analyses.

Post-harvest Storage

Four times point evaluations were made at 0, 24, 48, and 72 h during post-harvest storage to check the long-term effect of different preharvest MeJA applications. One hundred eight fruits from each preharvest MeJA treatment were selected for the experiment based on uniform size, shape, and absence of surface damage. For each post-harvest time point, 27 fruits per treatment were separated into three groups of nine fruit each and packaged in transparent perforated plastic containers (24 cm width, 16 cm depth, and 12 cm height) and maintained at room temperature (25°C) and 40% relative humidity.

Fruit Quality Assessments

Fruit quality measurements were carried out as previously reported (Delgado et al., 2018; Mora et al., 2019). After harvest, all fruits collected from each plot and treatment were weighed (n = 352) and expressed as grams per fruit (g·$Fruit^{-1}$). Seventeen fruits from each treatment were weighed at each time point (three replicates of nine fruit each) during the post-harvest experiment, and weight loss was expressed as a percentage. Afterward, strawberry skin color from each treatment and post-harvest time point (three replicates of six fruit each) was measured using a colorimeter (model CR-400, Konica Minolta, Tokyo, Japan) and expressed according to the CIELAB scale where L*, a*, and b* values indicate lightness (dark to light), redness [green (−) to red (+)] and yellowness [blue (−) to yellow (+)], respectively. The dimensions of color Chroma [$C = (a^{*2} + b^{*2})^{1/2}$] and Hue angle [$h° = \arctan(b^*/a^*)$] were calculated from numerical values of a* and b* (McGuire, 1992). Two measurements were taken on opposite sides of each fruit on the equatorial side as technical replicates.

Fruit firmness was measured at opposite sides of 18 fruits from each treatment and post-harvest time point (three replicates of six fruit each) using a texture analyzer (model CT3, Brookfield, MA, United States) fitted with a flat 3 mm TA-39 probe suitable for firmness measurement in berries and small fruits. Each fruit was penetrated 3 mm at 1 mm s^{-1} of speed, and the maximum force was recorded in Newton units (N).

Soluble solids content (SSC) and titratable acidity (TA) analyses were conducted according to Saavedra et al. (2016), with some modifications. Nine fruits of 2 g of fruit receptacle from each treatment and post-harvest time point (three replicates of three fruit each) were homogenized in 5 mL of distilled water employing a controlled speed homogenizer (model MicroDisTec^{TM} HOMOGENIZER 125, Kinematica, Lucerne, Switzerland) with a 12 mm rotor, and filtered. For SSC, 150 μL of each sample was measured using a digital refractometer (model HI 96801, Hanna, Nuşfalău, Romania), recorded as Brix degrees (°Bx) and expressed as g of sucrose per 100 g of fresh weight (FW). For TA, aliquots of 2.5 mL of each sample were diluted in distilled water (1:10, v/v) and titrating using semi-automatic titrator (model Digitrate Pro, Jencons Scientific, Ltd., Leighton Buzzard, United Kingdom) with 0.025N NaOH to pH 8.2. Results were calculated as citric acid equivalents (CAE) per 100 g of FW, according to He et al. (2018). Both results were used for the calculation of the SSC/TA ratio.

Carbon, Nitrogen, and Isotopes Analyses

Lyophilized leaf and fruit tissues were oven-dried to a constant weight, milled, and homogenized in a Spex ball micro mill. An aliquot of the milled samples (six fruits or leaves per treatment) was then weighted with a precision of ± 0.001 mg and encapsulated in tin capsules. Total carbon and nitrogen content (in% of dry weight) and carbon and nitrogen isotope composition ($\delta^{13}C$ and $\delta^{15}N$, respectively, in ‰) were determined using a combustion and gas preparation module (EA-GSL Elemental Analyzer, Sercon, United Kingdom), attached to an Isotope Ratio Mass Spectrometer (20–22 IRMS, Sercon, United Kingdom). Combustion and reduction columns were operated at 1000 and 600°C, respectively, and ultra-grade high purity helium was used as the carrier gas. Combusted gas passed through a GC column operated at 100°C. An ultra-grade reference gas (Ultra High-Grade CO_2 and N_2, Indura, Chile) was injected before each analysis for CO_2 and N_2 peak drift correction. Two laboratory standards (Corn Flour SCC2256 and Wheat Flour SC2258 Sercon, United Kingdom) were run every 10 analytical samples to ensure analytical quality. These standards were previously calibrated against international reference materials (USGS-40, USGS-41, IAEA-R045, IAEA-600, IAEA-CH-3, IAEA V9, IAEA-C3). The long-term standard deviation of repeated dual-mode $\delta^{15}N$ and $\delta^{13}C$ measurements of the laboratory standards were ± 0.2 and ± 0.4‰, for $\delta^{13}C$ and $\delta^{15}N$, respectively.

Determination of Membrane Lipid Peroxidation

The level of lipid peroxidation in cell membranes was measured in terms of malondialdehyde (MDA), using 2-thiobarbituric

acid-reactive substances (TBARS) method described by Cai et al. (2015), with modification. Fruit receptacle (500 mg) from each treatment and post-harvest time point (three replicates of three fruit each) was homogenized with 2 mL 0.1% (w/v) cold trichloroacetic acid (TCA) and centrifuged at 5000 rpm for 20 min at 4°C. Then, a 0.4 mL aliquot of the supernatant fraction was mixed with 1 mL of 20% (w/v) TCA containing 0.67% (w/v) thiobarbituric acid (TBA). The mixture was heated at 100°C for 30 min, quickly cooled in an ice bath, and centrifugated at 15,000 rpm for 15 min. The absorbance of the supernatants was recorded at 532 and 600 nm for the correction of non-specific background absorbance. The MDA concentration was calculated using its molar extinction coefficient (155 mM cm^{-1}). The results were expressed as micromoles of MDA per g of FW.

Antioxidant Capacity, Total Flavonoid Content, and Total Phenolic Content

Antioxidant Compounds Extraction

Pooled fruit receptacle (2 g) of each treatment were homogenized in 40 mL of acetone/water/acetic acid (70:29.5:0.5; AWA) solution (Speisky et al., 2012). The resulting mixture was incubated at 30°C for 40 min, with vortexing for 30 s every 10 min, and centrifuged at 5000 rpm for 10 min at 15°C. The supernatant was filtered through a 70 μm nylon cell strainer (Falcon, Corning, NY, United States) and kept at −20°C. The three independent extractions were subjected to the total flavonoid content (TFC), total phenolic content (TPC), and antioxidant capacity determinations.

Total Flavonoid Content Determination

Total flavonoid content (TFC) was determined, according to Chang et al. (2002), using quercetin-3-glucoside as the standard. AWA extract from each treatment and post-harvest time point (three replicates of three fruit each) was diluted in methanol:water (1:1) solution and 500 μL of diluted extracts were mixed with 1.5 mL of 95% ethanol, 100 μL of 10% $AlCl_3$, 100 μL of 1M CH_3CO_2K, and 2.8 mL of distilled water. After incubation at room temperature for 30 min, the OD of the reaction mixture was measured at 415 nm in a UV/Vis spectrophotometer (model V-630, Jasco, Tokyo, Japan), and the results were expressed as mg of quercetin equivalents (QE) per 100 g of FW.

Total Phenolic Content Determination

Total phenolic content (TPC) was determined by Singleton and Rossi (1965) method, with modifications suggested by Galati et al. (2003) using gallic acid (GA) as the standard. AWA extract from each treatment and post-harvest time point (three replicates of three fruit each) was diluted in methanol:water (1:1) solution, and 500 μL of the diluted extract was mixed with 3.75 mL of distilled water, 250 μL Folin-Ciocalteu reagent diluted 1:1 in water, and 500 μL of 10% (w/v) sodium carbonate. The mix was homogenized and incubated at room temperature for 1 h. The OD was measured at 760 nm in a UV/Vis spectrophotometer (Model V-630, Jasco), and the results were expressed as mg of GA equivalents (GAE) per 100 g of FW.

Antioxidant Capacity Determination

The antioxidant capacity was measured by oxygen-radical absorbing capacity (ORAC) method and assayed for each AWA extract from each treatment and post-harvest time point (three replicates of three fruit each) as described by Speisky et al. (2012) using 2,2′-azobis(2-amidinopropane) dihydrochloride (AAPH) as a source of peroxyl radicals and fluorescein as a source of peroxyl radicals as and the oxidizable probe, respectively. In brief, 20 μL of AWA extract (diluted in 75 mM phosphate buffer, pH 7.4) was transferred to 96-well microplates, each containing 75 μL of APPH (18 mM) and 200 μL of fluorescein (108 nM). The plates were placed measured in a Multi-Mode Microplate Reader (Synergy/HTX, Biotek Instruments, Winooski, VT, United States) and incubated at 37°C for 60 min with shaking every 3 min. During the incubation, the fluorescence was monitored at 485 nm Ex/538 nm Em every 3 min throughout the experiment. The analysis of each sample was performed in triplicate. The results of the ORAC activity were estimated based on a standard curve of Trolox using a quadratic regression equation obtained between the net area under the fluorescence decay curve and the Trolox concentration and the net area under the fluorescence decay curve. ORAC activity was expressed as micromoles of Trolox equivalents (TE) per 100 g of FW.

Determination of Non-enzymatic Antioxidants

Anthocyanin, Proanthocyanidin, and Lignin Contents

Total anthocyanin content (AC) was quantified by the pH differential method (Lee et al., 2005; Debnath and Ricard, 2009), with some modifications (Delgado et al., 2018). Fruit receptacle (2.5 g) was homogenized using 10 mL of absolute ethanol and 1.5N HCl (85:15 v/v) as an extraction solution, incubated overnight at 4°C, and centrifuged for 10 min at 12,000 rpm at 4°C. Two aliquots from the ethanolic phase of each sample were diluted (1:4) with two different buffers: a pH 1 buffer (0.025 M KCl) and a pH 4.5 buffer (0.4 M sodium acetate). Finally, absorbances were quantified at 516 and 700 nm. Extraction solution diluted with each pH buffer were used as blanks. Total anthocyanin content was calculated based on the Lambert-Beer law, using the coefficient of molar extinction for the pelargonidin-3-glucoside (31,620 $M^{-1}cm^{-1}$) reported by Swain (1965). Results from each treatment and post-harvest time point (three replicates of three fruit each) were expressed as μg of pelargonidin-3-glucoside equivalent per g of FW.

Total proanthocyanidin content (PA) was quantified by 4-dimethylaminocinnamaldehyde (DMAC) colorimetric method (Prior et al., 2010; Delgado et al., 2018), with some modifications. Fruit receptacle (0.2 g) were ground with liquid nitrogen, homogenized in 1 mL of 80% acetone, and sonicated for 30 min. Aliquots of 70 μL of diluted (1:50) samples were incubated for 20 min with 210 μL of 0.1% DMAC in 80% acidified ethanol and measured at 640 nm using a 96-well microplate reader (model M200, Tecan Trading AG, Switzerland). Ethanol acidified was used as a blank. Total proanthocyanidin content was calculated using linear regression of a calibration curve (0–15.625 μg mL^{-1})

of catechin as standard. Results from each treatment and post-harvest time point (three replicates of three fruit each) were expressed as μg of catechin equivalent per g of FW.

Total lignin content was quantified, according to Saavedra et al. (2016). Fruit receptacle (0.25 g) was ground with liquid nitrogen and hydrolyzed as previously described (Meyer et al., 1998; Franke et al., 2002). Extractable cell wall complexes were obtained by the thioglycolic acid (TGA) method (Campbell and Ellis, 1992). The insoluble lignin pellet was dissolved in 1 mL of 1N NaOH, and UV-absorbance was measured at 280 nm using a 96-well plate reader (model M200, Tecan Trading AG). Total lignin content was calculated using linear regression of a calibration curve (0–20 $\mu g\ mL^{-1}$) of hydrolytic lignin (Sigma-Aldrich) as standard. Results from each treatment and 0, 24, and 48 h post-harvest time point (three replicates of three fruit each) were expressed as μg of lignin per g of FW.

Ascorbic Acid Content

Ascorbic acid content (AAC) was quantified using the 2,6-dichloroindophenol titrimetric method, according to AOAC method 967.21 (Horwitz, 2002; Fuentes et al., 2016). Fruit extracts were prepared from 2 g frozen samples from each treatment and post-harvest time point (three replicates of one fruit each) using 4 mL 3% metaphosphoric acid, homogenized, and centrifuged at 5000 rpm for 15 min. The supernatant was diluted first to 10 ml with 3% metaphosphoric acid and then to 100 mL with ultrapure water. AAC determination was performed through a calibration curve of L-ascorbic acid (Sigma–Aldrich). Measurements were performed four times, and results were expressed as mg of ascorbic acid per 100 g of FW.

Determination of Antioxidant-Related Enzymatic Activities

The determination of enzyme activities was performed through spectrophotometric activity assays at 25°C. Fruit receptacle (1 g) from each treatment at each post-harvest time point (three replicates of three fruit each) were ground with liquid nitrogen and homogenized in 5 mL of extraction buffer containing 100 mM potassium phosphate buffer (pH 7.8), 1 mM EDTA (pH 7.0) and 5% (w/w) polyvinylpolypyrrolidone (PVPP). Then, the homogenate was centrifuged for 15 min at 10,000 rpm at 4°C. The supernatant was taken as a crude enzyme extract and was used for estimated enzymatic activities, as described below.

Catalase (CAT, EC 1.11.1.6)

The CAT activity was determined following the hydrogen peroxide (H_2O_2, $\varepsilon = 36\ mM^{-1}\ cm^{-1}$) breakdown at 240 nm, as previously described (Garcìa-Limones et al., 2002; García-Limones et al., 2009). The reaction mixture contained 30 μL 500 mM potassium phosphate buffer (pH 7.0) and 40 μL of crude fruit protein extract in a 232 μL-volume. The reaction started by adding 68 μL of 88 mM H_2O_2. Results were expressed as mmoles of H_2O_2 decomposed per g of FW.

Guaiacol Peroxidase (POX, EC 1.11.1.7)

The POX activity was determined through the oxidation of guaiacol by measure the rate of tetraguaiacol formation at 470 nm ($\varepsilon = 26{,}600\ mM^{-1}\ cm^{-1}$) (Rao et al., 1996). The assay mixture contained 60 μL 500 mM potassium phosphate buffer (pH 7.0), 2.5 μL 10 mM EDTA (pH 7.0), 16 mM guaiacol, and 16.2 μL 88 mM H_2O_2, in a 195 μL-volume. The reaction was initiated by adding 105 μL of crude fruit protein extract. Results were expressed as mmoles of tetraguaiacol per g of FW.

Ascorbate Peroxidase (APX, EC 1.11.1.11)

The APX activity was determined following the H_2O_2-dependent oxidation of ascorbate by measure the rate of dehydroascorbate (DHA) formation at 290 nm ($\varepsilon = 2.8\ mM^{-1}\ cm^{-1}$) (Garcìa-Limones et al., 2002; García-Limones et al., 2009) with a few modifications. The reaction mixture contained 60 μL 500 mM potassium phosphate buffer (pH 7.0), 20 μL 5 mM L-ascorbic acid (Sigma-Aldrich), 20 μL 10 mM EDTA (pH 7.0), and 20 mL of crude fruit protein extract in a 300 μL-volume. The reaction started by adding 1.2 μL 88 mM H_2O_2. Results were expressed as mmoles of DHA per g of FW.

Statistical Analysis

The experiment was performed using a randomized complete block design. All the measurements were conducted at triplicate and expressed as mean ± standard deviation (SD) (tables) or ± standard error of the mean (SEM) (figures). Data were analyzed by analysis of variance (ANOVA) using Infostat software (version 2016) (Rienzo et al., 2016). Tukey *post hoc* test was used to evaluate the significance between treatments at each post-harvest time point (0, 24, 48, and 72 h). Values of $p \leq 0.05$ were considered statistically significant. Principal component analysis (PCA) was used for all variables to discriminate between treatments and post-harvest times points, using the R software with the ggplot2 package (Wickham, 2016).

RESULTS

Fruit Quality Assessments

Different field MeJA applications seem to have little or no impact on fruit firmness and weight attributes. Regarding that, no differences between treatments on strawberry (*F.* × *ananassa* 'Camarosa') firmness (**Table 1**) or fruit weight at harvest (**Figure 1A**) were observed. Fruit weight loss increased during post-harvest in all treatments (**Figure 1B**), but results showed a significant difference at 72 h on M1 and M2 treatments declining fruit weight loss compared to control fruits ($p \leq 0.05$).

The SSC/TA ratio gradually decreased during post-harvest in all treatments, but higher values of SCC/TA ratio were found in MeJA-treated fruits at 0 (M2), 24 (M3), and 48 h (M2) compared with control, which means that MeJA treatments impact this important parameter in strawberry flavor by increasing SSC and reducing TA values (**Table 1** and **Supplementary Table 2**). In turn, differences in fruit color were found at 0 and 24 h between MeJA-treated and control fruits (**Table 1**). In this sense, significant differences in luminosity (L^* index) were observed between control (28.92 ± 1.83) and M2 (30.97 ± 2.38) treatments at 0 h and a constant decrease from 0 to 72 h during post-harvest storage in M2 and M3 treatments. We observed an

TABLE 1 | Changes in firmness, soluble solids content/titratable acidity (SSC/TA) ratio, and color parameters during post-harvest storage (0, 24, 48, and 72 h) of strawberry (*Fragaria* × *ananassa* 'Camarosa') fruits treated with three different sequential applications of 250 μmol L^{-1} methyl jasmonate (M1, M2, and M3) or water (control) during preharvest.

Post-harvest storage (h)	Treatment	Firmness (N)	SSC/TA ratio	Color parameters				
				L*	a*	b*	Chroma	Hue angle (h°)
0	Control	0.26 ± 0.10^{Aa}	12.76 ± 1.70^{Ac}	28.92 ± 1.83^{Aa}	27.59 ± 2.74^{Ab}	15.13 ± 2.80^{Ab}	31.53 ± 3.38^{Cb}	28.62 ± 3.53^{Aab}
	M1	0.28 ± 0.12^{Aa}	12.35 ± 1.41^{Ab}	29.22 ± 1.95^{Ab}	28.40 ± 2.47^{Ab}	14.99 ± 2.98^{Aa}	32.18 ± 3.23^{ACb}	27.62 ± 3.79^{Aa}
	M2	0.36 ± 0.17^{Aa}	13.97 ± 1.30^{Bb}	30.97 ± 2.38^{Bc}	30.74 ± 2.19^{Bb}	16.43 ± 3.28^{Ab}	34.93 ± 3.15^{Bb}	27.90 ± 3.89^{Aa}
	M3	0.34 ± 0.15^{Aa}	12.60 ± 2.66^{Abc}	30.15 ± 2.33^{ABc}	30.23 ± 2.43^{Bc}	16.29 ± 3.19^{Ac}	34.40 ± 3.38^{ABc}	28.10 ± 3.62^{Ab}
24	Control	0.47 ± 0.20^{Ab}	10.19 ± 2.26^{Aab}	28.60 ± 1.96^{Ba}	24.43 ± 2.88^{Aa}	12.34 ± 2.52^{Aa}	27.61 ± 3.26^{ABa}	26.46 ± 3.95^{ABab}
	M1	0.47 ± 0.15^{Ab}	11.83 ± 1.18^{ABb}	27.24 ± 2.39^{ABa}	24.63 ± 2.78^{ABa}	13.06 ± 2.84^{Aa}	27.74 ± 3.73^{ABa}	27.90 ± 3.16^{Ba}
	M2	0.41 ± 0.13^{Aa}	10.93 ± 1.92^{Aa}	28.03 ± 1.76^{ABa}	24.05 ± 3.26^{Aa}	13.34 ± 2.30^{Aa}	29.77 ± 2.98^{Ba}	26.51 ± 2.77^{ABa}
	M3	0.38 ± 0.13^{Aa}	13.37 ± 3.02^{Bc}	26.69 ± 1.69^{Aa}	26.58 ± 2.39^{Ba}	11.26 ± 2.77^{Aa}	26.60 ± 3.92^{Aa}	24.84 ± 3.56^{Aa}
48	Control	0.41 ± 0.18^{Ab}	11.40 ± 1.87^{Ab}	30.23 ± 2.60^{Aa}	26.82 ± 3.08^{Aab}	14.99 ± 3.02^{Ab}	30.77 ± 3.96^{Ab}	28.99 ± 3.11^{Ab}
	M1	0.44 ± 0.19^{Ab}	12.90 ± 3.15^{ABb}	29.44 ± 2.39^{Ab}	26.51 ± 3.45^{Aab}	14.03 ± 3.53^{Aa}	30.08 ± 4.28^{Aab}	27.61 ± 4.69^{Aa}
	M2	0.44 ± 0.21^{Aa}	13.14 ± 1.47^{Bb}	29.93 ± 2.32^{Abc}	28.21 ± 2.99^{Aa}	14.98 ± 3.09^{Aab}	32.01 ± 3.72^{Aa}	27.81 ± 3.90^{Aa}
	M3	0.43 ± 0.17^{Aa}	11.62 ± 0.88^{Aab}	29.58 ± 2.36^{Abc}	28.40 ± 3.51^{Abc}	14.03 ± 3.28^{Ab}	31.73 ± 4.39^{Abc}	26.03 ± 3.51^{Aab}
72	Control	0.43 ± 0.13^{Ab}	9.71 ± 0.52^{Ba}	29.25 ± 2.55^{Aa}	27.38 ± 3.69^{Ab}	13.60 ± 3.43^{Aab}	30.63 ± 4.63^{Ab}	26.11 ± 3.65^{Aa}
	M1	0.39 ± 0.17^{Aab}	8.72 ± 0.87^{Aa}	29.55 ± 2.00^{Ab}	27.50 ± 2.80^{Ab}	13.47 ± 2.97^{Aa}	30.69 ± 3.52^{Ab}	25.90 ± 3.81^{Aa}
	M2	0.41 ± 0.12^{Aa}	10.27 ± 1.38^{Ba}	28.87 ± 2.16^{Aab}	27.42 ± 3.94^{Aa}	13.15 ± 3.26^{Aa}	30.54 ± 4.18^{Aa}	25.60 ± 5.95^{Aa}
	M3	0.44 ± 0.12^{Aa}	10.29 ± 2.34^{Ba}	28.54 ± 2.25^{Ab}	26.78 ± 3.06^{Ab}	12.39 ± 2.89^{Aab}	29.58 ± 3.64^{Ab}	24.63 ± 4.03^{Aa}

Data show mean values ± SD of three replicates (three fruits by replicate for SSC/TA ratio, and six fruits by replicate for firmness and color parameters). For each parameter, different capital letters indicate a significant difference between treatments within each post-harvest time point, and different lower-case letters indicate significant differences of each treatment between time points during post-harvest ($p \leq 0.05$). For experimental details (see section "Materials and Methods").

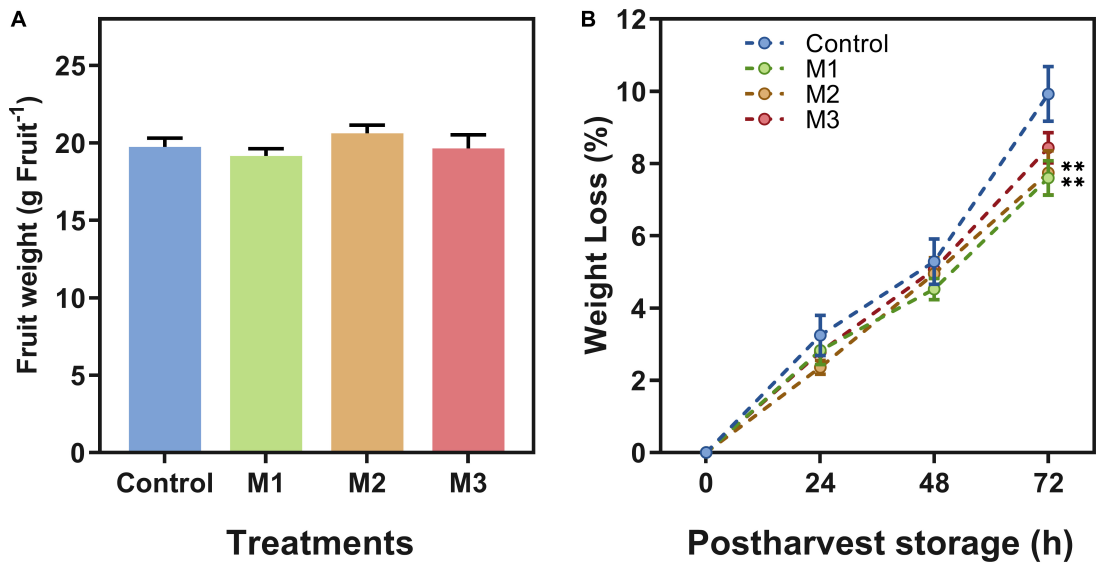

FIGURE 1 | Changes in weight of preharvest methyl jasmonate (MeJA) treated strawberry (*Fragaria* × *ananassa* 'Camarosa') fruit at post-harvest. Effect of different MeJA treatments (M1, M2, and M3) or water (control) on strawberry **(A)** fruit weight (g·$Fruit^{-1}$) at harvest (0 h post-harvest), and **(B)** fruit weight loss (%) during post-harvest storage (0, 24, 48, 72 h). Data represent mean ± SEM (n = 352 for fruit weight; n = 27 for fruit weight loss). Differences between treatments were determined by ANOVA and Tukey test. Asterisks indicate significant differences (**$p \leq 0.01$).

increase in redness (a* index) in M2 (30.74 ± 2.19) and M3 (30.23 ± 2.43) treatments at 0 h compared with control (27.59 ± 2.74), although this index decrease through storage time in those treatments. At 24 h of storage, results showed significant differences between control (28.60 ± 1.96) and M3 treatment (26.69 ± 1.69) in luminosity, and between control (24.43 ± 2.88) and M3 treatment (26.58 ± 2.39) in redness. No significant differences were observed at 48 and 72 h of post-harvest storage in any of the color parameters analyzed. The results on fruit skin luminosity and redness indicate that MeJA treatments could

increase luminosity (whiter) and redness in fruits at 0 h, although this effect is loss from 24 to 72 h post-harvest storage (**Table 1**).

Additionally, with the aim to verify if MeJA alters essential constituents of plants we measured the carbon (C) and nitrogen (N) contents (as% of dry weight) and estimated the C:N ratio in leaf (**Figures 2A,C,E**) and fruit (**Figures 2B,D,F**) of MeJA-treated strawberries at harvest. No alterations in C, N, and C:N ratio were observed both in leaf and fruit tissues, which could imply no changes in main metabolic pathways as results of MeJA preharvest applications.

Isotope Analyses and Lipid Peroxidation Determination

In the present study, we study the changes in C and N isotopes ($\delta^{13}C$ and $\delta^{15}N$) in leaf and fruit at harvest and in lipid peroxidation during post-harvest fruit storage as measurements indicative of stress in different MeJA-treated samples. No differences were found in $\delta^{13}C$ and $\delta^{15}N$ stable isotope composition, used as a proxy for water use efficiency (WUE) and differential nutrient source/allocation, respectively, both in fruits or leaves (**Figures 3A–D**). Additionally, there were no significant differences in strawberry fruit lipid peroxidation (expressed total MDA) during post-harvest storage between treatments (**Figure 3E**). These results suggest that MeJA treatments do not alter the stress status of leaf and fruit at harvest and fruits at post-harvest storage in comparison to control samples.

Determination of Non-enzymatic Antioxidants

Total Flavonoid Content, Total Phenolic Content, and Antioxidant Capacity

The TFC, TPC, and antioxidant capacity of preharvest MeJA treatment fruit during post-harvest storage are shown in **Table 2**. In the present work, no differences were found between control and MeJA treatments on antioxidant capacity and no variation was observed through post-harvest storage in all treatments. Alongside that, no significant differences were found on TFC, where values were spread from 5.4 ± 0.9 to 11.2 ± 1.0 for M3-treated, and from 6.7 ± 1.7 to 10.4 ± 0.7 for control fruits. The TPC values showed no significant changes between treatments either with 157.87 ± 32.01 and 146.22 ± 4.74 mg GAE·100 g^{-1} FW for control and M3 treatment at 0 h, respectively. However, we noted a significant decrease of TFC in MeJA treatments from 24 to 48 h (M1 and M3) and from 0 to 48 h (M2) of post-harvest storage (**Table 2**).

Anthocyanin, Proanthocyanidin, and Lignin Contents

Results indicated an increment in total anthocyanin content (**Figure 4A**) in M3 MeJA-treated fruits respect to control at all time points during post-harvest. The highest anthocyanin content showed by M3 treatment at 24 h, supports the higher a* index observed in MeJA-treated fruits at that time point (**Table 1**), unlike that observed at 0 h. None of the MeJA-treated fruits decreases their anthocyanin content during post-harvest storage; contrary to what happened with the control fruits (**Figure 4A**). Otherwise, differences in total proanthocyanidin content were only noted at 0 h (**Figure 4B**), being M3-treated fruits, which presented higher levels than those exhibited by the other treatments. All treatments increase their proanthocyanidin contents up to the end of post-harvest storage (**Figure 4B**). Additionally, no differences were found related to lignin content between MeJA and control treatments during post-harvest storage (**Supplementary Figure 2**).

Ascorbic Acid Content

The AAC is shown in **Figure 5**. M1-treated fruits had markedly higher values than the control treatment at 24 h, but an increase of AAC was observed for all MeJA treated fruits at 48 h. Remarkably, AAC on M3-treated strawberries was higher than control at 48 h ($p = 0.0016$) and remained higher at 72 h ($p = 0.0092$) with an increase of 63.8 and 53.3%, respectively. However, no significant difference was found for M1 and M2 treatments concerning control at 72 h. Moreover, AAC values of M2 and M3 treatments remain stable during storage time points (**Figure 5**).

Determination of Antioxidant Enzymatic Activities

The effect of preharvest MeJA treatment on strawberry fruit antioxidant enzymatic activity of catalase (CAT), guaiacol peroxidase (POX), and ascorbate peroxidase (APX) is shown in **Figure 6**. Results revealed a significant increase in CAT activity in strawberry fruits (**Figure 6A**) depending on the number of preharvest MeJA applications (M2 and M3) compared to control fruits ($p < 0.0001$). Higher values were found on M3 treatment fruits at 0, 24, 48, and 72 h compared to control (5.2-, 6.1-, 9.4-, and 12.8-fold increases, respectively). Also, CAT activity increased two-fold during the post-harvest storage period between 0 and 72 h for M3 treatment. Along with it, M2 treatment remained approximately 4-fold higher than control at all time points during the post-harvest storage. Nevertheless, no differences were found between M1 and control fruits. Related to POX activity (**Figure 6B**), a similar response of M2 and M3 treatment at each time points were observed, but an unclear effect of preharvest MeJA applications was identified. No significant differences at 24 and 72 h between MeJA treatments and control were found, although a significant increase of POX activity on all MeJA treatments comparing with control was observed at 48 h. In contrast to CAT, we noticed a constant decrease in POX activity of M2 and M3 treatments during post-harvest storage time. Regarding APX activity (**Figure 6C**), even though no difference was observed between MeJA treatments, a higher increase was observed during post-harvest storage on all MeJA treatments, independent of the number of applications, compared to control. The average values of MeJA treatments showed a 15.0-, 15.3-, 22.3-, and 9.4-fold increases in relation to control at 0, 24, 48, and 72 h, respectively.

Finally, the complete dataset was analyzed by PCA (**Supplementary Figure 3**) to identify the major sources of variation responsible for the differences between treatments. The first two principal components (PC1 and PC2) explain 98% of the variability in the data set. In general, control and MeJA-treated fruits were grouped separately along the first and second axes,

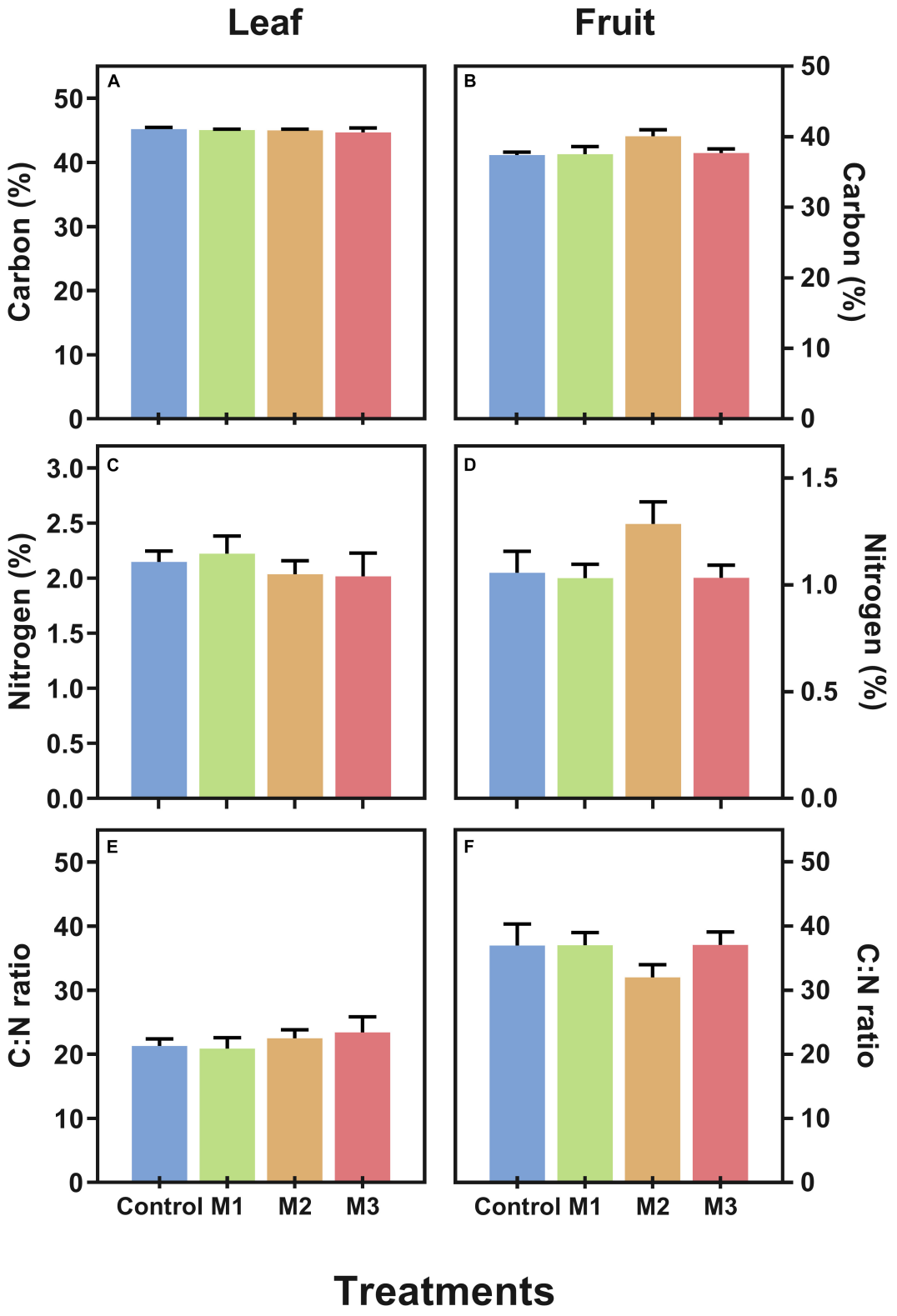

FIGURE 2 | Changes in carbon (C) and nitrogen (N) contents of preharvest methyl jasmonate (MeJA) treated strawberry (*Fragaria* × *ananassa* 'Camarosa') leaf and fruit at harvest. Effect of different MeJA treatments (M1, M2, and M3) or water (control) on **(A)** leaf carbon content (%), **(B)** fruit carbon content (%), **(C)** leaf nitrogen content (%), **(D)** fruit nitrogen content (%), **(E)** leaf C:N ratio, and **(F)** fruit C:N ratio of MeJA-treated strawberry plants at harvest.% of dry weight. Data represent mean ± SEM (n = 6).

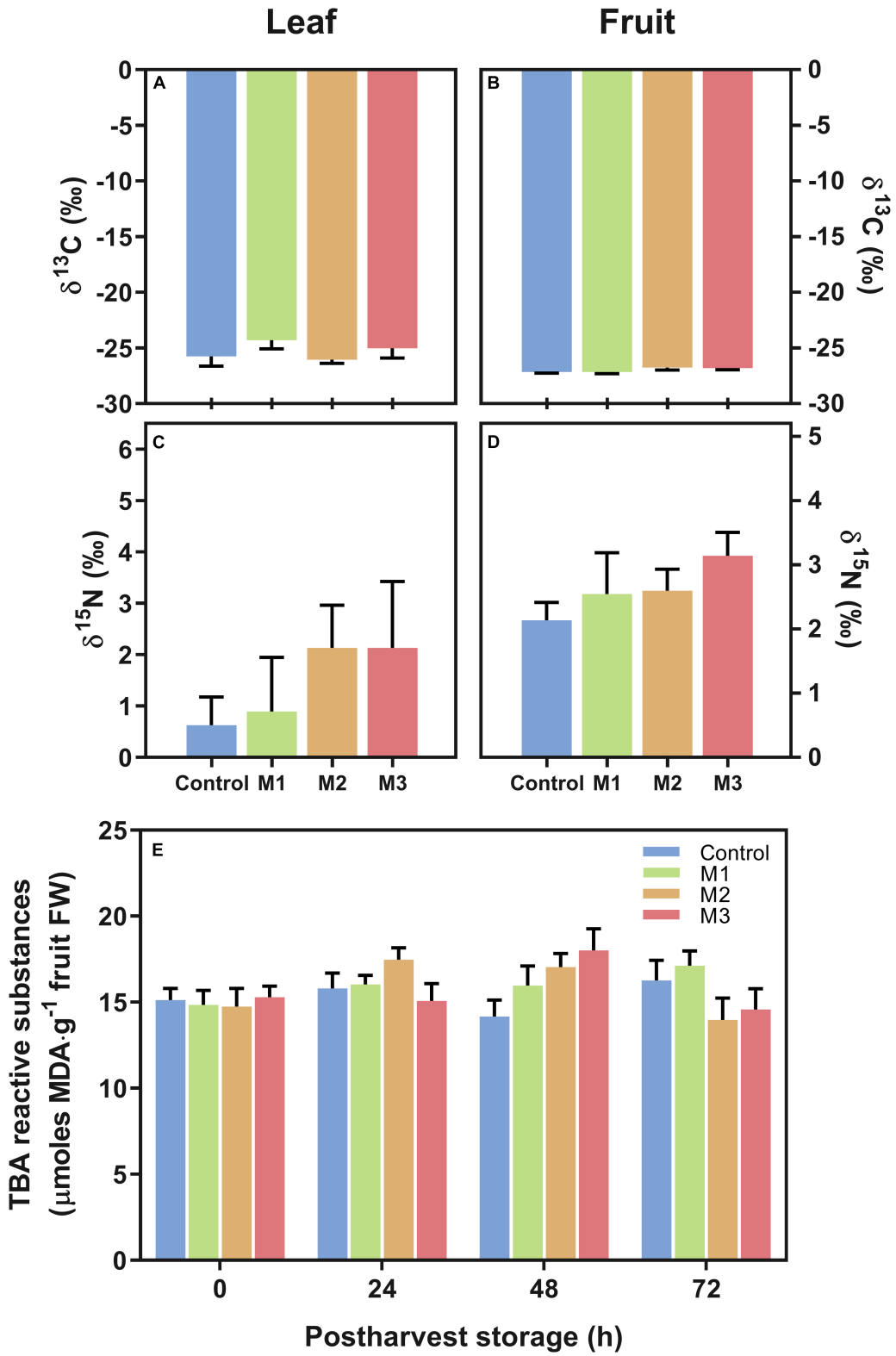

FIGURE 3 | Changes in carbon (C) and nitrogen (N) corresponding isotopes ($\delta^{13}C$ and $\delta^{15}N$) and in malondialdehyde (MDA) content of preharvest methyl jasmonate (MeJA) treated strawberry (*Fragaria* × *ananassa* 'Camarosa') samples. Effect of different MeJA treatments (M1, M2, and M3) or water (control) on **(A)** leaf $\delta^{13}C$ (‰), **(B)** fruit $\delta^{13}C$ (‰), **(C)** leaf $\delta^{15}N$ (‰), **(D)** fruit $\delta^{15}N$ (‰), and **(E)** fruit lipid peroxidation during post-harvest storage (μmoles MDA per g of fresh weight). Data represent mean ± SEM (n = 6) and mean± SEM (n = 9) for isotope and lipid peroxidation analyses, respectively.

TABLE 2 | Changes in total flavonoid content (TFC), total phenolic content (TPC), and antioxidant capacity determined by Oxygen Radical Absorbance Capacity (ORAC) during post-harvest storage (0, 24, 48, and 72 h) of strawberry fruits treated with three different sequential applications of 250 μmol L^{-1} methyl jasmonate (M1, M2, and M3) or water (control) during preharvest.

Post-harvest storage (h)	Treatments	TFC (mg QE ·100 g^{-1} FW)	TPC (mg GAE ·100 g^{-1} FW)	Antioxidant capacity (μmoles TE 100 g^{-1} FW)
0	Control	8.76 ± 2.36^{Aa}	157.87 ± 32.01^{Aa}	3902.67 ± 214.65^{Aa}
	M1	8.76 ± 0.68^{Abc}	138.41 ± 8.01^{Aa}	4340.00 ± 2203.34^{Aa}
	M2	9.94 ± 1.76^{Ab}	133.73 ± 8.90^{Aa}	4309.67 ± 819.29^{Aa}
	M3	10.79 ± 0.56^{Ab}	146.22 ± 4.74^{Aab}	4768.67 ± 468.84^{Aa}
24	Control	10.41 ± 0.65^{Aa}	142.98 ± 7.15^{Aa}	3866.50 ± 1091.07^{Aa}
	M1	9.64 ± 1.39^{Ac}	137.94 ± 8.29^{Aa}	4341.67 ± 683.73^{Aa}
	M2	9.41 ± 1.33^{Aab}	131.77 ± 33.85^{Aa}	3544.33 ± 1032.03^{Aa}
	M3	11.24 ± 0.99^{Ab}	132.13 ± 12.43^{Aa}	3913.67 ± 629.51^{Aa}
48	Control	6.72 ± 1.66^{Aa}	152.23 ± 4.44^{Aa}	3405.00 ± 758.08^{Aa}
	M1	6.12 ± 0.87^{Aa}	155.61 ± 14.80^{Aa}	3878.67 ± 896.53^{Aa}
	M2	6.17 ± 1.28^{Aa}	161.17 ± 20.84^{Aa}	4010.00 ± 1059.49^{Aa}
	M3	6.56 ± 0.52^{Aa}	157.54 ± 17.76^{Aab}	4243.67 ± 1067.63^{Aa}
72	Control	7.17 ± 0.26^{Aa}	171.92 ± 7.04^{Aa}	5086.00 ± 960.98^{Aa}
	M1	6.61 ± 0.88^{Aab}	166.88 ± 11.46^{Aa}	4021.00 ± 210.72^{Aa}
	M2	7.02 ± 0.21^{Aab}	167.74 ± 9.22^{Aa}	2614.33 ± 808.62^{Aa}
	M3	5.37 ± 0.89^{Aa}	161.96 ± 3.06^{Ab}	3174.67 ± 1591.72^{Aa}

Data show mean values ± SD of three replicates (three fruits by replicate). For each parameter, different capital letters indicate a significant difference between treatments within each post-harvest time point, and different lower-case letters indicate significant differences of each treatment between time points during post-harvest ($p \leq 0.05$). FW, fresh weight; QE, quercetin equivalents; GAE, gallic acid equivalent; TE, Trolox equivalent. For experimental details (see section "Materials and Methods").

but no discrimination was observed based on the number of MeJA preharvest applications.

DISCUSSION

In the present research, we report a significant impact of different preharvest MeJA treatments on different fruit quality parameters such as weight loss, soluble solids content/titratable acidity (SSC/TA) ratio, skin color, total anthocyanin (AC), total proanthocyanidin (PA) and ascorbic acid contents (AAC) accumulation, and antioxidant enzymatic activities of catalase (CAT) and ascorbate peroxidase (APX) during post-harvest storage (**Figure 7**). It is known that climatic conditions can influence fruit quality parameters in strawberry (Krüger et al., 2012) since we informed about climactic conditions during the field experiment (**Supplementary Table 1**). As far as we know, this is the first report about the effects of different MeJA preharvest applications on strawberry (*F.* × *ananassa* 'Camarosa') fruit quality parameters during post-harvest storage, and it can be useful to understand the mechanism involved in hormonal field application and its effect on the storability of soft fruits.

Concerning classical fruit quality parameters, we observed changes in weight loss, color, and SSC/TA ratio in preharvest MeJA-treated fruit during post-harvest. Previous reports suggest that MeJA applications during post-harvest of different fruits have an impact on declining the usual increment of fruit weight loss on treated blueberries (at 50 and 100 μmol L^{-1} MeJA) (Wang et al., 2019), apricots (at 200 μmol L^{-1} MeJA) (Ezzat et al., 2017), and strawberries (at 8 and 16 μmol L^{-1} MeJA) (Asghari and Hasanlooe, 2016; Ezzat et al., 2017; Wang et al., 2019). In the present study, the preharvest application of 250 μmol L^{-1} MeJA in large green and 100% red receptacle (M2 treatment) and in 100% red receptacle (M1 treatment) stages of strawberry (*F.* × *ananassa* 'Camarosa') fruit showed an effect on this attribute during post-harvest storage (**Figure 1B**) and could have a substantial impact on maintaining a critical commercial fruit quality attribute as weight.

In turn, fruit skin color is an essential trait for strawberry quality and has been associated with anthocyanin content and flavonoid composition (Fernández-Lara et al., 2015). In this sense, our results showed higher L* and a* values in MeJA-treated fruits (M2 and M3) than control at 0 and 24 h, indicating a brighter red color in 'Camarosa' fruits at the beginning of the post-harvest storage as a result of the preharvest treatment (**Table 1**). In other Rosaceae species such as apple (*Malus domestica* 'Fuji'), preharvest application of MeJA also increased skin red color during fruit development (Rudell et al., 2005). Previous reports in strawberry, using exogenous MeJA applied in an *in vitro* ripening system, indicate a promoter role of this hormone in the acquisition of red coloration in fruit of commercial strawberry (*F.* × *ananassa* 'Aromas') (Delgado et al., 2018; Garrido-Bigotes et al., 2018), and Chilean strawberry (*F. chiloensis*) (Concha et al., 2013). All these antecedents suggest that MeJA could be used as a coloring promotor of strawberry, including field applications.

Another essential quality attribute of strawberry fruit is the flavor. In several fruits, an increase in the SSC and a concomitant reduction of the TA are observed during fleshy fruit ripening, which determine final fruit flavor and acceptance of fruit (Stevens et al., 1979; Cherian et al., 2014; Batista-Silva et al., 2018).

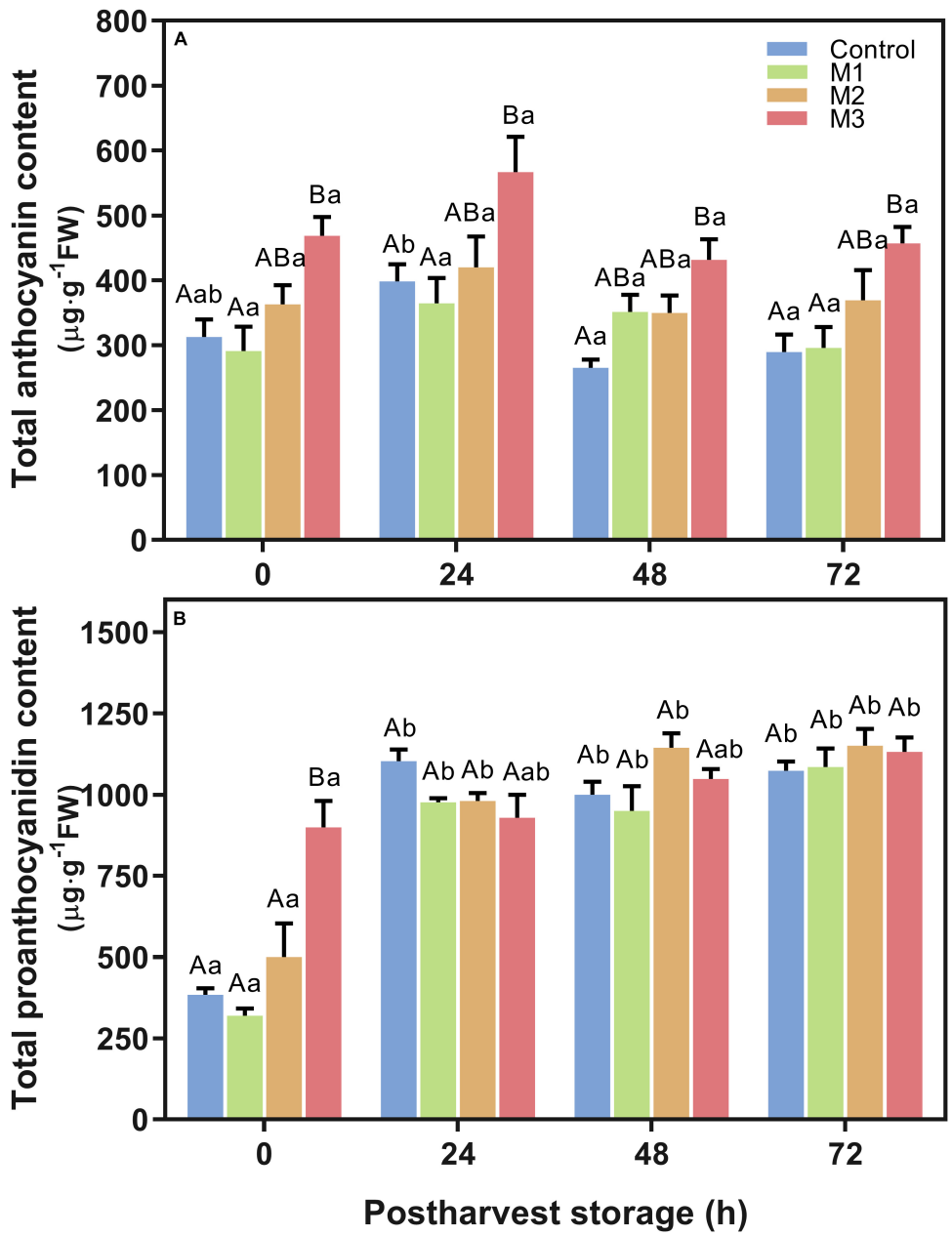

FIGURE 4 | Changes in total anthocyanin and proanthocyanidin contents of preharvest methyl jasmonate (MeJA) treated strawberry (*Fragaria* × *ananassa* 'Camarosa') fruit at post-harvest. Effect of different MeJA treatments (M1, M2, and M3) or water (control) on strawberry **(A)** total anthocyanin content (μg pelargonidin-3-glucoside equivalent per g of FW), and **(B)** total proanthocyanidin content (μg catechin equivalent per g of FW) during post-harvest storage. Data represent mean ± SEM (n = 9). Differences between treatments were determined by ANOVA and Tukey test. Different capital letters indicate a significant difference between treatments within each post-harvest time point, and different lower-case letters indicate significant differences of each treatment between time points during post-harvest ($p \leq 0.05$).

Changes in the SSC/TA ratio by preharvest field MeJA applications have been reported in cultivars of blackberries (Wang et al., 2008), red raspberry (Wang and Zheng, 2005), and Chilean strawberry (Saavedra et al., 2016), but no effect has been observed in commercial strawberry ('Tufts' and 'Cruz' cultivars) at different MeJA concentrations (250, 500, and 1000 μmol L^{-1}) applied at flowering (Yilmaz et al., 2003). Here, we found higher values of the SCC/TA ratio in M2 (at 0 and 48 h) and M3 (at 24 h) fruits compared with control (**Table 1**). In each case, the high SCC/TA ratio was explained by both, an increment on SSC and a diminution on TA of MeJA-treated fruits (**Supplementary Table 1**). In accordance with Yilmaz et al. (2003), which suggest that one MeJA application is not enough for modifying SSC/TA ratio (at 250, 500, or 1000 μmol L^{-1} MeJA), our results point

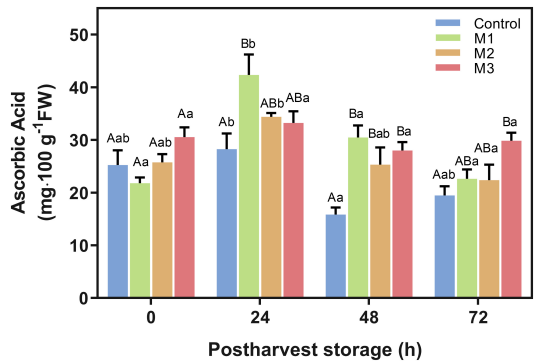

FIGURE 5 | Changes in ascorbic acid content of preharvest methyl jasmonate (MeJA) treated strawberry (*Fragaria* × *ananassa* 'Camarosa') fruit at post-harvest. Effect of different MeJA treatments (M1, M2, and M3) or water (control) on strawberry ascorbic acid content (AAC) during post-harvest storage. Data represent mean ± SEM (n = 3). Differences between treatments were determined by ANOVA and Tukey test. Different capital letters indicate a significant difference between treatments within each post-harvest time point, and different lower-case letters indicate significant differences of each treatment between time points during post-harvest ($p \leq 0.05$).

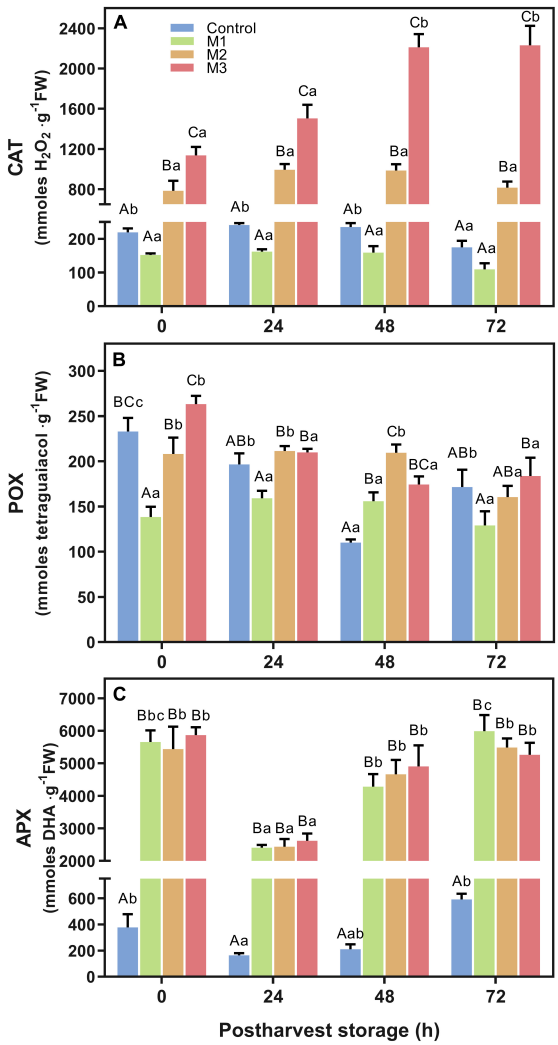

FIGURE 6 | Changes in antioxidant-related enzymatic activities of preharvest methyl jasmonate (MeJA) treated strawberry (*Fragaria* × *ananassa* 'Camarosa') fruit at post-harvest. Effect of different MeJA treatments (M1, M2, and M3) or water (control) on strawberry antioxidant enzymatic activities of **(A)** catalase (CAT), **(B)** guaiacol peroxidase (POX), and **(C)** ascorbate peroxidase (APX) during post-harvest storage. Data represent mean ± SEM (n = 9). Differences between treatments were determined by ANOVA and Tukey test. Different capital letters indicate a significant difference between treatments within each post-harvest time point, and different lower-case letters indicate significant differences of each treatment between time points during post-harvest ($p \leq 0.05$).

out that at least two successive applications of 250 μmol L^{-1} MeJA since flowering (M3) or early fruit developmental (M2) stages are required on commercial strawberry to increase that parameter. Along with this, raspberry fruits treated with foliage-berry spray of 100 μmol L^{-1} MeJA at the early light pink stage with two consecutive sprayings, had higher SSC and lower TA and therefore a higher ratio of SSC/TA than control fruits or those treated with less MeJA concentrations (Wang and Zheng, 2005; Wang et al., 2008). Also, the highest fruit fructose and glucose contents and reduced fruit citric acid and malic acid contents were found in raspberry cultivars treated with MeJA (100 μmol L^{-1}) (Wang and Zheng, 2005). The role of MeJA on the sugar content increase has been associated with the accumulation of anthocyanins and other phenolic compounds in the fruit, as has been shown in grapevine berries (Pirie and Mullins, 1976). However, the mechanism of the jasmonate-associated sugar accumulation should be uncovering in strawberry fruit.

In relation to metabolic changes suggested by changes in N (%) and C:N ratio (**Figure 2**), the MeJA applications assayed in the current study did not significantly modify nitrogen allocation and stoichiometry either in leaves or fruits of 'Camarosa' cultivar. In contrast, in other fruit species such as tomato, considering a biotic stress-related context, MeJA treatment induced a change in the allocation of resources (as C and N) (Gómez et al., 2010). As low nitrogen supply has been associated with an increase in anthocyanin levels in grape berry (Soubeyrand et al., 2014), we did not find an association with N content with the anthocyanin content in strawberry fruit. Therefore, our results suggest that MeJA applied to the whole strawberry plant during the fruit development period did not affect the allocation of N, and that the increment in fruit-related anthocyanin content (**Figure 4A**) could be promoted directly by MeJA application.

Regarding stress associated indicators, the analyses of $\delta^{13}C$ and $\delta^{15}N$ isotopes has been reported for the support that the application of MeJA could induce a more significant water use efficiency (WUE) and a differential allocation of nutrients, respectively, in fruits and leaves of different species as a defense mechanism to face both in biotic and abiotic stresses (Van Dam and Baldwin, 2001; Gómez et al., 2010). In this sense, the non-existence of differences in $\delta^{13}C$ and $\delta^{15}N$ between treatments both in leaves and fruits of MeJA-treated plants (**Figures 3A–D**), indicate that all plants were under the same irrigation and nitrogen fertilization management, and that MeJA did not interfere when the plant is in a non-stressed environment as has

been previously shown in sugar beet and *Nicotiana attenuata* plants (Van Dam and Baldwin, 2001; Fugate et al., 2018). Moreover, we did not observed changes in malondialdehyde (MDA) levels in fruits treated with MeJA during post-harvest storage (**Figure 3E**), as an indicator of lipid peroxidation (Halliwell, 1987) and as has been reported in rice after MeJA application (Hung et al., 2006), which suggest the absence of oxidative stress at least in a high level. The lack of differences in our study suggests that these ranges of MeJA applications did not affect the level of lipid peroxidation in cell membranes at levels that cannot be compensated. Conversely, the MeJA applications could be associated with specific parameters of ripening and fruit quality. Nevertheless, additional research is needed to better understand the effect of field MeJA applications on the nutrient status (i.e., an experiment with differentiated N doses) and membrane integrity in strawberry.

The antioxidant systems in plants include antioxidant enzymes such as CAT, guaiacol peroxidase (POX), and APX, along with non-enzymatic antioxidants such as phenolic compounds, flavonoids, ascorbic acid among others, which are produced as secondary metabolites exerting various protective roles (Dixon and Paiva, 1995; Rice-Evans et al., 1996, 1997; Apel and Hirt, 2004). So, the content of these molecules and the activity of these enzymes can change by different growing conditions in several cultivars of *F.* × *ananassa* (Wang and Zheng, 2001; Wang et al., 2002). Phytohormones regulate many of these changes. Indeed, in different cultivars of blackberries, raspberries, black currants, plums, apples, and pomegranate fruits, MeJA treatment at preharvest increases the antioxidant capacity, total phenolic, and anthocyanin contents during post-harvest in a dependent concentration with a positive correlation between these values (Wang and Zheng, 2005; Wang et al., 2008; García-Pastor et al., 2020). In the present research, MeJA field applications on strawberry (*F.* × *ananassa* 'Camarosa') did not show a relation with those previously reported effects on the antioxidant capacity, total flavonoids content or total polyphenol content values up to 72 h of post-harvest storage. Similar results have been reported in post-harvest MeJA-treated strawberry (*F.* × *ananassa* 'Coral') since no differences in total phenolic content and antioxidant capacity was observed up to 5 days after treatment (de la Peña Moreno et al., 2010). Furthermore, we observed interesting changes in specific antioxidant-related mechanisms. It is known that MeJA application can increase anthocyanin accumulation in *F. chiloensis* and *F.* × *ananassa* 'Camarosa' and 'Aromas' cultivars in an *in vitro* ripening systems (Pérez et al., 1997; Concha et al., 2013; Delgado et al., 2018), because of a stimulatory effect on its biosynthesis through the activation of JA signaling that mean the upregulation of *FaMYC2* and *FaJAZ*s genes, increasing bioactive JA (jasmonoyl-isoleucine, JA-Ile) biosynthesis (Garrido-Bigotes et al., 2018), and consequently upregulating the regulatory (*FaMYB10*) and structural (*FaANS*, *FaUFGT*) genes related to anthocyanin biosynthesis pathway of strawberry (*F.* × *ananassa* 'Aromas') (Concha et al., 2013; Delgado et al., 2018). In the present research, we observed an accumulation of total anthocyanin content proportionally to the number of preharvest MeJA applications (**Figure 4A**) probably by means of the activation of JA signaling. Similarly, in *F.* × *ananassa* ('Coral') fruit treated with MeJA vapor at post-harvest, the anthocyanin content increased at 5 and 7 days post-harvest, being pelargonidin-3-glucoside, cyanidin-3-glucoside and pelargonidin-3-rutinoside the main augmented anthocyanins (de la Peña Moreno et al., 2010). In raspberry, preharvest MeJA treatment (100 μmol L^{-1}) raised anthocyanins such as cyanidin 3-glucoside and cyanidin 3-rutinoside, respectively (Wang and Zheng, 2005). Besides, total proanthocyanidin content increase in M3 fruits but only at 0 h post-harvest (**Figure 4B**). Considering that the fruit color differences -darker red color or bright red color- in cultivars and selections of strawberry result from the content of anthocyanins (Hong and Wrolstad, 1990; Garzón and Wrolstad, 2002; da Silva et al., 2007; Kelebek and Selli, 2011; Song et al., 2015), our results suggest that, along with SCC/TA ratio, MeJA applications from flowering to ripe fruit stages have an essential impact on physiological characteristics during post-harvest storage, especially for the increase of anthocyanin levels during post-harvest and the coloring change (bright red color) at harvest of strawberry fruits.

Ascorbic acid is a non-enzymatic antioxidant that has an essential role in oxidative defense metabolism, maintaining cellular redox status, and scavenging over-production of reactive oxygen species (ROS) (Akram et al., 2017). In strawberry, ascorbic acid, along with anthocyanins, are responsible for between 55-70% (depending on the cultivar) of the total antioxidant capacity (Tulipani et al., 2008). Interestingly, we observed that the preharvest field MeJA applications (M1, M2, and M3) significantly enhanced the AAC during post-harvest (**Figure 5**). This finding was consistent with previous studies on strawberry (*F.* × *ananassa* 'Selva' and 'Queen Elisa' cultivars) (Lolaei et al., 2013), blueberry (Wang et al., 2019), and loquat fruit (Cai et al., 2011). Experiments on plant cell suspensions reports than MeJA can enhance the transcription of genes involved in the *de novo* biosynthesis of ascorbic acid (Wolucka et al., 2005). Besides to the non-enzymatic changes observed in the present study, preharvest MeJA field applications show an increase of antioxidant-related enzymatic activities of CAT and APX on strawberry (*F.* × *ananassa* 'Camarosa') fruits during post-harvest, being the M3 treatment that reached the highest levels of CAT activity at all post-harvest times (**Figure 6A**). Similar behavior was also reported on grape and blueberries, where post-harvest MeJA-treated fruits exhibited significantly higher APX and CAT activities during the storage (Modesti et al., 2018; Wang et al., 2019). Previously reported post-harvest treatment of 8 μmol L^{-1} MeJA on strawberry fruits (*F.* × *ananassa* 'Sabrosa') notified an increased CAT and POX activities (Asghari and Hasanlooe, 2016). Additionally, this effect is also shown on strawberry seedling leaves treated with 250 μmol L^{-1} MeJA (Faghih et al., 2017). In turn, preharvest MeJA treatments (100 μmol L^{-1}) increase CAT, POX, and APX activities during lemon fruit development (Serna-Escolano et al., 2019). In general, we observed that an increase in CAT activity requires MeJA applications from flowering to ripe fruit stages, while APX activity can reach maximum values with just one application at ripe fruit stage (**Figure 6C**). Probably, the MeJA applications increase the levels of hydrogen peroxide (H_2O_2) in the strawberry

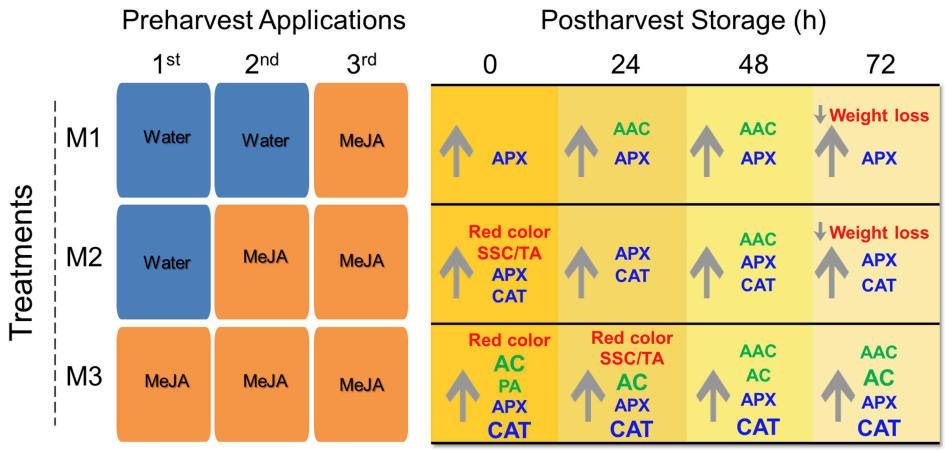

FIGURE 7 | Post-harvest quality attributes of strawberry (*Fragaria* × *ananassa* 'Camarosa') fruit influenced by different preharvest methyl jasmonate (MeJA) treatments. Effect of different MeJA treatments (M1, M2, and M3) compared to control during post-harvest storage (0, 24, 48, 72 h). The same fruits were sprayed at flowering (M3), large green (M3 and M2), and 100% red receptacle (M3, M2, and M1) with 250 μmol L^{-1} MeJA. Upward and downward arrows indicate an increment and a decrease respect to control, respectively. In red font weight loss, red color (based on index a*), SSC/TA ratio; in green font non-enzymatic antioxidants AAC, AC, PA; and in blue font enzymatic antioxidant activities (APX, CAT). Larger font size in CAT indicates significant higher values in M3 respect to M2 treatments. AAC, ascorbic acid content; AC, total anthocyanin content; APX, ascorbate peroxidase; CAT, catalase; PA, total proanthocyanidin content; SSC, soluble solids content; TA, titratable acidity. For experimental details (see section "Materials and Methods").

plants, as has been early shown in several plant species (Orozco-Cardenas and Ryan, 1999). This increment could increase the activity of CAT and APX enzymes and thus inducing tolerance against oxidative stress, as has been demonstrated in tobacco plants (Gechev et al., 2002).

Finally, as the PCA analysis shows differentiation between control and MeJA-treated fruits (**Supplementary Figure 3**) and according to the summary scheme of our research (**Figure 7**) we conclude that MeJA treatment has significant beneficial effects on fruit quality at post-harvest storage, and three successive preharvest MeJA applications in different developmental strawberry (*F.* × *ananassa* 'Camarosa') fruit stages (flowering, large green, and 100% red) can markedly improve fruit quality and reinforce the antioxidant capacity that suggests a better status of the fruit to deal with oxidative stress during post-harvest. It is important to note that the results presented in the current research are related to the Camarosa cultivar, and these could be different using other varieties. All strawberry cultivars present fruits with a different composition of antioxidants (Diamanti et al., 2012a,b) that could interact with MeJA treatments in a different aspect as has been reported for black currant and raspberry cultivars (Flores and Ruiz del Castillo, 2015). By any means, preharvest MeJA applications could be incorporated into the integrated management programs for strawberry cultivation to get a better strawberry fruit quality for consumers. However, the use of an alternative source to analytical methyl jasmonate should be considered for cost reasons for strawberry growers (see **Supplementary Table 3** for an estimate of the application cost per hectare based on the analytical compound used in the present study). Our interest in future research is to explore the MeJA-mediated regulation mechanism of the antioxidant-related enzymatic activity.

DATA AVAILABILITY STATEMENT

The datasets generated for this study are available on request to the corresponding author.

AUTHOR CONTRIBUTIONS

CF designed the research, supervised experiments, and acquired the funding. PZ, YC, OA-S, LF, and FA performed the experiments. PZ, OA-S, LF, FA, and CF analyzed the data. PZ, LF, and CF wrote the manuscript.

FUNDING

This research was funded by the National Research and Development Agency (ANID, Chile), FONDECYT/Regular 1181310.

ACKNOWLEDGMENTS

PZ acknowledges to Universidad de Talca for a doctoral scholarship. We thankfully acknowledge to Felipe Valenzuela-Riffo and Luis Morales-Quintana by their support in the field experiment.

SUPPLEMENTARY MATERIAL

The Supplementary Material for this article can be found online at: https://www.frontiersin.org/articles/10.3389/fpls.2020.00538/full#supplementary-material

REFERENCES

Akram, N. A., Shafiq, F., and Ashraf, M. (2017). Ascorbic Acid-A potential oxidant scavenger and its role in plant development and abiotic stress tolerance. *Front. Plant Sci.* 8:613. doi: 10.3389/fpls.2017.00613

Alvarez-Suarez, J. M., Mazzoni, L., Forbes-Hernandez, T. Y., Gasparrini, M., Sabbadini, S., and Giampieri, F. (2014). The effects of pre-harvest and post-harvest factors on the nutritional quality of strawberry fruits: a review. *J. Berry Res.* 4, 1–10. doi: 10.3233/JBR-140068

Apel, K., and Hirt, H. (2004). Reactive oxygen species: metabolism, oxidative stress, and signal transduction. *Ann. Rev. Plant Biol.* 55, 373–399. doi: 10.1146/annurev.arplant.55.031903.141701

Asghari, M., and Hasanlooe, A. R. (2016). Methyl jasmonate effectively enhanced some defense enzymes activity and total antioxidant content in harvested "Sabrosa" strawberry fruit. *Food Sci. Nutr.* 4, 377–383. doi: 10.1002/fsn3.300

Batista-Silva, W., Nascimento, V. L., Medeiros, D. B., Nunes-Nesi, A., Ribeiro, D. M., Zsögön, A., et al. (2018). Modifications in organic acid profiles during fruit development and ripening: correlation or causation? *Front. Plant Sci.* 9:1689. doi: 10.3389/fpls.2018.01689

Bertioli, D. J. (2019). The origin and evolution of a favorite fruit. *Nat. Genet.* 51, 372–373. doi: 10.1038/s41588-019-0365-3

Cai, Y., Cao, S., Yang, Z., and Zheng, Y. (2011). MeJA regulates enzymes involved in ascorbic acid and glutathione metabolism and improves chilling tolerance in loquat fruit. *Postharvest Biol. Technol.* 59, 324–326. doi: 10.1016/j.postharvbio.2010.08.020

Cai, Z., Yang, R., Xiao, H., Qin, X., and Si, L. (2015). Effect of preharvest application of *Hanseniaspora uvarum* on postharvest diseases in strawberries. *Postharvest Biol. Technol.* 100, 52–58. doi: 10.1016/j.postharvbio.2014.09.004

Campbell, M. M., and Ellis, B. E. (1992). Fungal elicitor-mediated responses in pine cell cultures. *Planta* 186, 409–417. doi: 10.1007/bf00195322

Chang, C. C., Yang, M. H., Wen, H. M., and Chern, J. C. (2002). Estimation of total flavonoid content in propolis by two complementary colorimetric methods. *J. Food Drug Analy.* 10, 178–182.

Cherian, S., Figueroa, C. R., and Nair, H. (2014). 'Movers and shakers' in the regulation of fruit ripening: a cross-dissection of climacteric versus non-climacteric fruit. *J. Exp. Bot.* 65, 4705–4722. doi: 10.1093/jxb/eru280

Concha, C. M., Figueroa, N. E., Poblete, L. A., Oñate, F. A., Schwab, W., and Figueroa, C. R. (2013). Methyl jasmonate treatment induces changes in fruit ripening by modifying the expression of several ripening genes in *Fragaria chiloensis* fruit. *Plant Physiol. Biochem.* 70, 433–444. doi: 10.1016/j.plaphy.2013.06.008

da Silva, F. L., Escribano-Bailón, M. T., Pérez Alonso, J. J., Rivas-Gonzalo, J. C., and Santos-Buelga, C. (2007). Anthocyanin pigments in strawberry. *LWT Food Sci. Technol.* 40, 374–382. doi: 10.1016/j.lwt.2005.09.018

de la Peña Moreno, F., Monagas, M., Blanch, G. P., Bartolomé, B., and Ruiz del Castillo, M. L. (2010). Enhancement of anthocyanins and selected aroma compounds in strawberry fruits through methyl jasmonate vapor treatment. *Eur. Food Res. Technol.* 230, 989–999. doi: 10.1007/s00217-010-1243-5

Debnath, S. C., and Ricard, E. (2009). ISSR, anthocyanin content and antioxidant activity analyses to characterize strawberry genotypes. *J. Appl. Hortic.* 11, 83–89.

Delgado, L. D., Zúñiga, P. E., Figueroa, N. E., Pastene, E., Escobar-Sepúlveda, H. F., Figueroa, P. M., et al. (2018). Application of a JA-Ile biosynthesis inhibitor to methyl jasmonate-treated strawberry fruit induces upregulation of specific MBW complex-related genes and accumulation of proanthocyanidins. *Molecules* 23:1433. doi: 10.3390/molecules23061433

Diamanti, J., Capocasa, F., Balducci, F., Battino, M., Hancock, J., and Mezzetti, B. (2012a). Increasing strawberry fruit sensorial and nutritional quality using wild and cultivated Germplasm. *PLoS One* 7:e46470. doi: 10.1371/journal.pone.0046470

Diamanti, J., Capocasa, F., Denoyes, B., Petit, A., Chartier, P., Faedi, W., et al. (2012b). Standardized method for evaluation of strawberry (Fragaria × ananassa Duch.) germplasm collections as a genetic resource for fruit nutritional compounds. *J. Food Composit. Analy.* 28, 170–178. doi: 10.1016/j.jfca.2012.07.007

Dixon, R. A., and Paiva, N. L. (1995). Stress-induced phenylpropanoid metabolism. *Plant Cell* 7, 1085–1097. doi: 10.1105/tpc.7.7.1085

Ezzat, A., Ammar, A., Szabó, Z., Nyéki, J., and Holb, I. J. (2017). Postharvest treatments with methyl jasmonate and salicylic acid for maintaining physico-chemical characteristics and sensory quality properties of apricot fruit during cold storage and shelf-life. *Pol. J. Food Nutr. Sci.* 67, 159–166. doi: 10.1515/pjfns-2016-0013

Faghih, S., Ghobadi, C., and Zarei, A. (2017). Response of strawberry plant cv. 'Camarosa' to salicylic Acid and Methyl Jasmonate application under salt stress condition. *J. Plant Growth Regul.* 36, 651–659. doi: 10.1007/s00344-017-9666-x

Fernández-Lara, R., Gordillo, B., Rodríguez-Pulido, F. J., Lourdes González-Miret, M., del Villar-Martínez, A. A., Dávila-Ortiz, G., et al. (2015). Assessment of the differences in the phenolic composition and color characteristics of new strawberry (Fragaria x ananassa Duch.) cultivars by HPLC–MS and Imaging *Tristimulus* colorimetry. *Food Res. Intern.* 76, 645–653. doi: 10.1016/j.foodres.2015.07.038

Flores, G., and Ruiz del Castillo, M. L. (2014). Influence of preharvest and postharvest methyl jasmonate treatments on flavonoid content and metabolomic enzymes in red raspberry. *Postharvest Biol. Technol.* 97, 77–82. doi: 10.1016/j.postharvbio.2014.06.009

Flores, G., and Ruiz del Castillo, M. L. (2015). Variations in ellagic acid, quercetin and myricetin in berry cultivars after preharvest methyl jasmonate treatments. *J. Food Composit. Analy.* 39, 55–61. doi: 10.1016/j.jfca.2014.11.007

Flores, G., and Ruiz del Castillo, M. L. (2016). Accumulation of anthocyanins and flavonols in black currants (*Ribes nigrum* L.) by pre-harvest methyl jasmonate treatments. *J. Sci. Food Agric.* 96, 4026–4031. doi: 10.1002/jsfa.7595

Franke, R., Hemm, M. R., Denault, J. W., Ruegger, M. O., Humphreys, J. M., and Chapple, C. (2002). Changes in secondary metabolism and deposition of an unusual lignin in the ref8 mutant of *Arabidopsis*. *Plant J.* 30, 47–59. doi: 10.1046/j.1365-313X.2002.01267.x

Fuentes, L., Valdenegro, M., Gómez, M. G., Ayala-Raso, A., Quiroga, E., Martínez, J.-P., et al. (2016). Characterization of fruit development and potential health benefits of arrayan (*Luma apiculata*), a native berry of South America. *Food Chem.* 196, 1239–1247. doi: 10.1016/j.foodchem.2015.10.003

Fugate, K. K., Lafta, A. M., Eide, J. D., Li, G., Lulai, E. C., Olson, L. L., et al. (2018). Methyl jasmonate alleviates drought stress in young sugar beet (*Beta vulgaris* L.) plants. *J. Agron. Crop Sci.* 204, 566–576. doi: 10.1111/jac.12286

Galati, E. M., Mondello, M. R., Giuffrida, D., Dugo, G., Miceli, N., Pergolizzi, S., et al. (2003). Chemical characterization and biological effects of sicilian *Opuntia ficus* indica (L.) mill. fruit juice: antioxidant and antiulcerogenic activity. *J. Agric. Food Chem.* 51, 4903–4908. doi: 10.1021/jf030123d

García-Limones, C., Dorado, G., Navas-Cortés, J. A., Jiménez-Díaz, R. M., and Tena, M. (2009). Changes in the redox status of chickpea roots in response to infection by *Fusarium oxysporum* f. sp. ciceris: apoplastic antioxidant enzyme activities and expression of oxidative stress-related genes. *Plant Biol.* 11, 194–203. doi: 10.1111/j.1438-8677.2008.00095.x

García-Pastor, M. E., Serrano, M., Guillén, F., Castillo, S., Martínez-Romero, D., Valero, D., et al. (2019). Methyl jasmonate effects on table grape ripening, vine yield, berry quality and bioactive compounds depend on applied concentration. *Sci. Hortic.* 247, 380–389. doi: 10.1016/j.scienta.2018.12.043

García-Pastor, M. E., Serrano, M., Guillén, F., Giménez, M. J., Martínez-Romero, D., Valero, D., et al. (2020). Preharvest application of methyl jasmonate increases crop yield, fruit quality and bioactive compounds in pomegranate 'Mollar de Elche' at harvest and during postharvest storage. *J. Sci. Food Agric.* 100, 145–153. doi: 10.1002/jsfa.10007

Garcìa-Limones, C., Hervás, A., Navas-Cortés, J. A., Jiménez-Dìaz, R. M., and Tena, M. (2002). Induction of an antioxidant enzyme system and other oxidative stress markers associated with compatible and incompatible interactions between chickpea (*Cicer arietinum* L.) and *Fusarium oxysporum* f. sp.ciceris. *Physiol. Mol. Plant Pathol.* 61, 325–337. doi: 10.1006/pmpp.2003.0445

Garrido-Bigotes, A., Figueroa, P. M., and Figueroa, C. R. (2018). Jasmonate metabolism and its relationship with abscisic acid during strawberry fruit development and ripening. *J. Plant Growth Regul.* 37, 101–113. doi: 10.1007/s00344-017-9710-x

Garzón, G. A., and Wrolstad, R. E. (2002). Comparison of the stability of pelargonidin-based anthocyanins in strawberry juice and concentrate. *J. Food Sci.* 67, 1288–1299. doi: 10.1111/j.1365-2621.2002.tb10277.x

Gechev, T., Gadjev, I., Van Breusegem, F., Inzé, D., Dukiandjiev, S., Toneva, V., et al. (2002). Hydrogen peroxide protects tobacco from oxidative stress by

inducing a set of antioxidant enzymes. *Cell. Mol. Life Sci. CMLS* 59, 708–714. doi: 10.1007/s00018-002-8459-x

Giampieri, F., Tulipani, S., Alvarez-Suarez, J. M., Quiles, J. L., Mezzetti, B., and Battino, M. (2012). The strawberry: composition, nutritional quality, and impact on human health. *Nutrition* 28, 9–19. doi: 10.1016/j.nut.2011.08.009

Gómez, S., Ferrieri, R. A., Schueller, M., and Orians, C. M. (2010). Methyl jasmonate elicits rapid changes in carbon and nitrogen dynamics in tomato. *New Phytol.* 188, 835–844. doi: 10.1111/j.1469-8137.2010.03414.x

Halliwell, B. (1987). Oxidative damage, lipid peroxidation and antioxidant protection in chloroplasts. *Chem. Phys. Lipids* 44, 327–340. doi: 10.1016/0009-3084(87)90056-9

He, Y., Bose, S. K., Wang, W., Jia, X., Lu, H., and Yin, H. (2018). Pre-harvest treatment of chitosan oligosaccharides improved strawberry fruit quality. *Intern. J. Mol. Sci.* 19:2194. doi: 10.3390/ijms19082194

Hong, V., and Wrolstad, R. E. (1990). Characterization of anthocyanin-containing colorants and fruit juices by HPLC/photodiode array detection. *J. Agric. Food Chem.* 38, 698–708. doi: 10.1021/jf00093a025

Horwitz, W. (2002). *Official Methods Of Analysis of AOAC International*. Gaithersburg, MD: AOAC International.

Hung, K. T., Hsu, Y. T., and Kao, C. H. (2006). Hydrogen peroxide is involved in methyl jasmonate-induced senescence of rice leaves. *Physiol. Plant.* 127, 293–303. doi: 10.1111/j.1399-3054.2006.00662.x

Jung, S. (2004). Effect of chlorophyll reduction in Arabidopsis thaliana by methyl jasmonate or norflurazon on antioxidant systems. *Plant Physiol. Biochem.* 42, 225–231. doi: 10.1016/j.plaphy.2004.01.001

Kelebek, H., and Selli, S. (2011). Characterization of phenolic compounds in strawberry fruits by RP-HPLC-DAD and investigation of their antioxidant capacity. *J. Liquid Chromatogr. Relat. Technol.* 34, 2495–2504. doi: 10.1080/10826076.2011.591029

Krüger, E., Josuttis, M., Nestby, R., Toldam-Andersen, T. B., Carlen, C., and Mezzetti, B. (2012). Influence of growing conditions at different latitudes of Europe on strawberry growth performance, yield and quality. *J. Berry Res.* 2, 143–157. doi: 10.3233/JBR-2012-036

Lee, J., Durst, R. W., and Wrolstad, R. E. (2005). Determination of total monomeric anthocyanin pigment content of fruit juices, beverages, natural colorants, and wines by the pH differential method: collaborative study. *J. AOAC Int.* 88, 1269–1278.

Lolaei, A., Zamani, S., Ahmadian, E., and Mobasheri, S. (2013). Effect of methyl jasmonate on the composition of yield and growth of strawberry (Selva and Queen Elisa). *Intern. J. Agric. Crop Sci.* 5, 200–206.

Martínez-Esplá, A., Zapata, P. J., Castillo, S., Guillén, F., Martínez-Romero, D., Valero, D., et al. (2014). Preharvest application of methyl jasmonate (MeJA) in two plum cultivars. 1. Improvement of fruit growth and quality attributes at harvest. *Postharvest Biol. Technol.* 98, 98–105. doi: 10.1016/j.postharvbio.2014.07.011

McGuire, R. G. (1992). Reporting of objective color measurements. *Hortscience* 27, 1254–1255. doi: 10.21273/HORTSCI.27.12.1254

Meyer, K., Shirley, A. M., Cusumano, J. C., Bell-Lelong, D. A., and Chapple, C. (1998). Lignin monomer composition is determined by the expression of a cytochrome P450-dependent monooxygenase in *Arabidopsis*. *Proc. Natl. Acad. Sci. U.S.A.* 95, 6619–6623. doi: 10.1073/pnas.95.12.6619

Modesti, M., Petriccione, M., Forniti, R., Zampella, L., Scortichini, M., and Mencarelli, F. (2018). Methyl jasmonate and ozone affect the antioxidant system and the quality of wine grape during postharvest partial dehydration. *Food Res. Intern.* 112, 369–377. doi: 10.1016/j.foodres.2018.06.061

Mora, F., Zúñiga, P. E., and Figueroa, C. R. (2019). Genetic variation and trait correlations for fruit weight, firmness and color parameters in wild accessions of *Fragaria chiloensis*. *Agronomy* 9:506. doi: 10.3390/agronomy9090506

Orozco-Cardenas, M., and Ryan, C. A. (1999). Hydrogen peroxide is generated systemically in plant leaves by wounding and systemin via the octadecanoid pathway. *Proc. Natl. Acad. Sci. U.S.A.* 96:6553. doi: 10.1073/pnas.96.11.6553

Ozturk, B., Yıldız, K., and Ozkan, Y. (2015). Effects of pre-harvest methyl jasmonate treatments on bioactive compounds and peel color development of "Fuji" apples. *Intern. J. Food Propert.* 18, 954–962. doi: 10.1080/10942912.2014.911312

Pérez, A. G., Sanz, C., Olías, R., and Olías, J. M. (1997). Effect of Methyl jasmonate on in Vitro strawberry ripening. *J. Agric. Food Chem.* 45, 3733–3737. doi: 10.1021/jf9703563

Pirie, A., and Mullins, M. G. (1976). Changes in anthocyanin and phenolics content of grapevine leaf and fruit tissues treated with sucrose, nitrate, and Abscisic Acid. *Plant Physiol.* 58, 468–472. doi: 10.1104/pp.58.4.468

Prior, R. L., Fan, E., Ji, H., Howell, A., Nio, C., Payne, M. J., et al. (2010). Multi-laboratory validation of a standard method for quantifying proanthocyanidins in cranberry powders. *J. Sci. Food Agric.* 90, 1473–1478. doi: 10.1002/jsfa.3966

Rao, M. V., Paliyath, G., and Ormrod, D. P. (1996). Ultraviolet-B- and Ozone-Induced Biochemical changes in antioxidant enzymes of *Arabidopsis thaliana*. *Plant Physiol.* 110, 125–136. doi: 10.1104/pp.110.1.125

Reyes-Díaz, M., Lobos, T., Cardemil, L., Nunes-Nesi, A., Retamales, J., Jaakola, L., et al. (2016). Methyl jasmonate: an alternative for improving the quality and health properties of fresh fruits. *Molecules* 21:567. doi: 10.3390/molecules21060567

Rice-Evans, C., Miller, N., and Paganga, G. (1997). Antioxidant properties of phenolic compounds. *Trends Plant Sci.* 2, 152–159. doi: 10.1016/S1360-1385(97)01018-2

Rice-Evans, C. A., Miller, N. J., and Paganga, G. (1996). Structure-antioxidant activity relationships of flavonoids and phenolic acids. *Free Rad. Biol. Med.* 20, 933–956. doi: 10.1016/0891-5849(95)02227-9

Rienzo, J., Casanoves, F., Balzarini, M., Gonzalez, L., Tablada, M., and Robledo, C. (2016). *InfoStat Versión (Facultad de Ciencias Agropecuarias, Universidad Nacional de Córdoba)*. Córdoba: InfoStat Group.

Rudell, D. R., Fellman, J. K., and Mattheis, J. P. (2005). Preharvest application of methyl jasmonate to 'Fuji' apples enhances red coloration and affects fruit size, splitting, and bitter pit incidence. *Hortscience* 40, 1760–1762. doi: 10.21273/HORTSCI.40.6.1760

Saavedra, G. M., Figueroa, N. E., Poblete, L. A., Cherian, S., and Figueroa, C. R. (2016). Effects of preharvest applications of methyl jasmonate and chitosan on postharvest decay, quality and chemical attributes of *Fragaria chiloensis* fruit. *Food Chem.* 190, 448–453. doi: 10.1016/j.foodchem.2015.05.107

Saavedra, G. M., Sanfuentes, E., Figueroa, P. M., and Figueroa, C. R. (2017). Independent preharvest applications of methyl jasmonate and chitosan elicit differential upregulation of defense-related genes with reduced incidence of gray mold decay during postharvest storage of *Fragaria chiloensis* fruit. *Intern. J. Mol. Sci.* 18:1420. doi: 10.3390/ijms18071420

Serna-Escolano, V., Valverde, J. M., García-Pastor, M. E., Valero, D., Castillo, S., Guillén, F., et al. (2019). Pre-harvest methyl jasmonate treatments increase antioxidant systems in lemon fruit without affecting yield or other fruit quality parameters. *J. Sci. Food Agric.* 99, 5035–5043. doi: 10.1002/jsfa.9746

Serrano, M., Martínez-Esplá, A., Zapata, P., Castillo, S., Martínez-Romero, D., Guillén, F., et al. (2018). "Effects of methyl jasmonate treatment on fruit quality properties," in *Emerging Postharvest Treatment of Fruits and Vegetables*, eds K. Barman, S. Sharma, and M. W. Siddiqui, (Oakville: Apple Academic Press), 85–106.

Singleton, V. L., and Rossi, J. A. (1965). Colorimetry of total phenolics with phosphomolybdic-phosphotungstic acid reagents. *Am. J. Enol. Viticult.* 16, 144–158.

Song, J., Du, L., Li, L., Kalt, W., Palmer, L. C., Fillmore, S., et al. (2015). Quantitative changes in proteins responsible for flavonoid and anthocyanin biosynthesis in strawberry fruit at different ripening stages: a targeted quantitative proteomic investigation employing multiple reaction monitoring. *J. Proteom.* 122, 1–10. doi: 10.1016/j.jprot.2015.03.017

Soubeyrand, E., Basteau, C., Hilbert, G., van Leeuwen, C., Delrot, S., and Gomès, E. (2014). Nitrogen supply affects anthocyanin biosynthetic and regulatory genes in grapevine cv. Cabernet-Sauvignon berries. *Phytochemistry* 103, 38–49. doi: 10.1016/j.phytochem.2014.03.024

Speisky, H., López-Alarcón, C., Gómez, M., Fuentes, J., and Sandoval-Acuña, C. (2012). First Web-based database on total phenolics and oxygen radical absorbance capacity (ORAC) of fruits produced and consumed within the South Andes region of South America. *J. Agric. Food Chem.* 60, 8851–8859. doi: 10.1021/jf205167k

Stevens, M. A., Kader, A. A., and Albright, M. (1979). Potential for increasing tomato flavor via increased sugar and acid content. *J. Am. Soc. Hortic. Sci.* 104, 40–42.

Swain, T. (1965). "Analytical methods for flavonoids," in *Chemistry and Biochemistry Of Plant Pigments*, ed. T. W. Goodwin, (London: Academic Press).

Tulipani, S., Mezzetti, B., Capocasa, F., Bompadre, S., Beekwilder, J., de Vos, C. H. R., et al. (2008). Antioxidants, phenolic compounds, and nutritional

quality of different strawberry genotypes. *J. Agric. Food Chem.* 56, 696–704. doi: 10.1021/jf0719959

Van Dam, N. M., and Baldwin, I. T. (2001). Competition mediates costs of jasmonate-induced defences, nitrogen acquisition and transgenerational plasticity in *Nicotiana attenuata*. *Funct. Ecol.* 15, 406–415. doi: 10.1046/j.1365-2435.2001.00533.x

Wang, H., Wu, Y., Yu, R., Wu, C., Fan, G., and Li, T. (2019). Effects of postharvest application of methyl jasmonate on physicochemical characteristics and antioxidant system of the blueberry fruit. *Sci. Hortic.* 258:108785. doi: 10.1016/j.scienta.2019.108785

Wang, S. Y., Bowman, L., and Ding, M. (2008). Methyl jasmonate enhances antioxidant activity and flavonoid content in blackberries (*Rubus* sp.) and promotes antiproliferation of human cancer cells. *Food Chem.* 107, 1261–1269. doi: 10.1016/j.foodchem.2007.09.065

Wang, S. Y., and Zheng, W. (2001). Effect of plant growth temperature on antioxidant capacity in strawberry. *J. Agric. Food Chem.* 49, 4977–4982. doi: 10.1021/jf0106244

Wang, S. Y., and Zheng, W. (2005). Preharvest application of methyl jasmonate increases fruit quality and antioxidant capacity in raspberries. *Intern. J. Food Sci. Technol.* 40, 187–195. doi: 10.1111/j.1365-2621.2004.00930.x1

Wang, S. Y., Zheng, W., and Galletta, G. J. (2002). Cultural system affects fruit quality and antioxidant capacity in strawberries. *J. Agric. Food Chem.* 50, 6534–6542. doi: 10.1021/jf020614i

Wasternack, C. (2007). Jasmonates: an update on biosynthesis, signal transduction and action in plant stress response, growth and development. *Ann. Bot.* 100, 681–697. doi: 10.1093/aob/mcm079

Wasternack, C., and Strnad, M. (2016). Jasmonate signaling in plant stress responses and development – active and inactive compounds. *New Biotechnol.* 33(5, Part B), 604–613. doi: 10.1016/j.nbt.2015.11.001

Wickham, H. (2016). *Ggplot2: Elegant Graphics for Data Analysis*. New York, NY: Springer International Publishing.

Wolucka, B. A., Goossens, A., and Inzé, D. (2005). Methyl jasmonate stimulates the de novo biosynthesis of vitamin C in plant cell suspensions. *J. Exp. Bot.* 56, 2527–2538. doi: 10.1093/jxb/eri246

Yilmaz, H., Yildiz, K., and Muradoğlu, F. (2003). Effect of jasmonic acid on yield and quality of two strawberry cultivars. *J. Am. Pomol. Soc.* 57, 32–35.

Zapata, P. J., Martínez-Esplá, A., Guillén, F., Díaz-Mula, H. M., Martínez-Romero, D., Serrano, M., et al. (2014). Preharvest application of methyl jasmonate (MeJA) in two plum cultivars. 2. Improvement of fruit quality and antioxidant systems during postharvest storage. *Postharvest Biol. Technol.* 98, 115–122. doi: 10.1016/j.postharvbio.2014.07.012

Conflict of Interest: The authors declare that the research was conducted in the absence of any commercial or financial relationships that could be construed as a potential conflict of interest.

frontiers in Plant Science

ORIGINAL RESEARCH
published: 13 May 2020
doi: 10.3389/fpls.2020.00545

Spatiotemporal Modulation of Flavonoid Metabolism in Blueberries

Catrin Sonja Günther[1], Andrew P. Dare[1], Tony K. McGhie[2], Cecilia Deng[1], Declan J. Lafferty[2,3], Blue J. Plunkett[1], Ella R. P. Grierson[2], Janice L. Turner[4], Laura Jaakola[5,6], Nick W. Albert[2] and Richard V. Espley[1]*

[1] The New Zealand Institute for Plant & Food Research Ltd., Auckland, New Zealand, [2] The New Zealand Institute for Plant & Food Research Ltd., Palmerston North, New Zealand, [3] School of Biological Sciences, The University of Auckland, Auckland, New Zealand, [4] The New Zealand Institute for Plant & Food Research Ltd., Brooklyn, New Zealand, [5] Climate Laboratory Holt, Department of Arctic and Marine Biology, UiT The Arctic University of Norway, Tromsø, Norway, [6] Norwegian Institute of Bioeconomy Research, Norwegian Institute of Bioeconomy Research, Ås, Norway

Blueberries are distinguished by their purple-blue fruit color, which develops during ripening and is derived from a characteristic composition of flavonoid-derived anthocyanin pigments. The production of anthocyanins is confined to fruit skin, leaving the colorless fruit flesh devoid of these compounds. By linking accumulation patterns of phenolic metabolites with gene transcription in Northern Highbush (*Vaccinium corymbosum*) and Rabbiteye (*Vaccinium virgatum)* blueberry, we investigated factors limiting anthocyanin production in berry flesh. We find that flavonoid production was generally lower in fruit flesh compared with skin and concentrations further declined during maturation. A common set of structural genes was identified across both species, indicating that tissue-specific flavonoid biosynthesis was dependent on co-expression of multiple pathway genes and limited by the phenylpropanoid pathway in combination with *CHS*, *F3H*, and *ANS* as potential pathway bottlenecks. While metabolite concentrations were comparable between the blueberry genotypes when fully ripe, the anthocyanin composition was distinct and depended on the degree of hydroxylation/methoxylation of the anthocyanidin moiety in combination with genotype-specific glycosylation patterns. Co-correlation analysis of phenolic metabolites with pathway structural genes revealed characteristic isoforms of *O*-methyltransferases and UDP-glucose:flavonoid-3-*O*-glycosyltransferase that were likely to modulate anthocyanin composition. Finally, we identified candidate transcriptional regulators that were co-expressed with structural genes, including the activators *MYBA*, *MYBPA1*, and *bHLH2* together with the repressor *MYBC2*, which suggested an interdependent role in anthocyanin regulation.

Keywords: anthocyanin, blueberry, flavonoid, fruit maturation, MYB, secondary metabolism, structural genes, phenylpropanoid pathway

OPEN ACCESS

Edited by:
Brian Farneti,
Fondazione Edmund Mach, Italy

Reviewed by:
Lingli Li,
Northwest A&F University, China
Mary Ann Lila,
North Carolina State University, United States
David Rudell,
Agricultural Research Service, United States Department of Agriculture, United States

****Correspondence:***
Catrin Sonja Günther
Catrin.guenther@plantandfood.co.nz

Specialty section:
This article was submitted to Crop and Product Physiology, a section of the journal Frontiers in Plant Science

Received: *04 February 2020*
Accepted: *09 April 2020*
Published: *13 May 2020*

Citation:
Günther CS, Dare AP, McGhie TK, Deng C, Lafferty DJ, Plunkett BJ, Grierson ERP, Turner JL, Jaakola L, Albert NW and Espley RV (2020) Spatiotemporal Modulation of Flavonoid Metabolism in Blueberries. Front. Plant Sci. 11:545. doi: 10.3389/fpls.2020.00545

INTRODUCTION

Blueberries have gained global popularity as high-value fruit and whilst all cultivated species originated from North America, production is growing globally. Northern Highbush (*Vaccinium corymbosum*) and Rabbiteye (*Vaccinium virgatum,* syn. *ashei*) are the economically most important species although blueberries are usually marketed without reference to species or cultivar. Rabbiteye

cultivation is increasing in warmer climates where it was shown to outperform *V. corymbosum* genotypes (Huang and Li, 2015; Medeiros et al., 2018). In addition to Rabbiteye's adaptability to warmer climates, its late flowering season make a valuable extension to the fruit harvest window when combined with Northern Highbush (Scalzo, 2013), thus furthering co-cultivation of these complementary species.

The striking purple/blue skin color is a defining character of blueberries, arising from high concentrations of anthocyanins. Anthocyanins are flavonoids that provide pigmentation to flowers and fruits of many plant species, acting as visual cues to attract pollinators and seed-distributers (Davies et al., 2012). In many fruits, including blueberries, anthocyanins are produced during ripening when fruit have the greatest reward, linking visual attraction with nutritional value. Visual traits like color and appearance are likely the first criteria for assessing blueberry quality prior to consumption and consumer demands on fruit quality traits drive current breeding targets and profitability (Gilbert et al., 2014; Gallardo et al., 2018). The public messaging surrounding blueberries as "superfoods," containing high concentrations of "antioxidants," is recognized by consumers and influences their fruit preferences. While anthocyanin profiles of Northern Highbush genotypes are well researched, comparative studies using Rabbiteye are limited but suggest differences in both anthocyanin content and composition between species when ripe (Lohachoompol et al., 2008; Timmers et al., 2017).

Structurally, anthocyanins are composite molecules consisting of an anthocyanidin (aglycone) moiety linked to a hexoside or pentoside. The coloring of the anthocyanidin varies with the degree and position of hydroxylation and/or methoxylation of their 2-phenyl-ring structure in combination with pH and the presence of co-pigments such as flavonols. In nature, over 500 different anthocyanin structures have been reported, based on over a dozen different anthocyanidins (De Pascual-Teresa and Sanchez-Ballesta, 2008). Amongst these, cyanidin, peonidin, delphinidin, malvidin, and petunidin are most commonly identified in blueberry fruit (Kalt et al., 1999; Lohachoompol et al., 2008). While cyanidin-3-*O*-glycosides (Kong et al., 2003; Fang, 2015), are the predominant anthocyanins in many fruits, delphinidin- and malvidin-3-*O*-glycosides are prevalent at high concentrations in blueberries (Kalt et al., 1999; Veberic et al., 2015), which is uncommon among berries (Suh et al., 2018).

In addition to colorful anthocyanins, blueberry fruits also contain complex profiles of mainly colorless flavonoids, which share precursors with anthocyanins (**Figure 1**). In brief, phenylalanine is transformed into *p*-coumaroyl-CoA by the concerted action of phenylalanine ammonia lyase (PAL), cinnamic acid 4-hydroxylase (C4′H), and 4-coumarate ligase (4CL), known as the phenylpropanoid pathway. The thioester *p*-coumaroyl-CoA is a primary precursor to a range of polyphenolic compounds (Durazzo et al., 2019), namely lignans, coumarins, hydroxycinnamic acids (HCAs), and flavonoids (see Quideau et al., 2011 for definition on polyphenols). Anthocyanins are derived from the flavonoid pathway, together with chalcones, flavones, flavonols, and flavanols (Winkel-Shirley, 2001). The first enzyme specific to the flavonoid pathway is chalcone synthase (CHS). This is followed by a cyclisation step by chalcone isomerase (CHI) and hydroxylation by flavanone 3-hydroxylase (F3H). From here the pathway branches according to the hydroxylation pattern, to produce either di- (flavonoid 3′ hydroxylase, F3′H) or tri-hydroxylated (flavonoid 3′5′ hydroxylase, F3′5′H) dihydroflavanonols, respectively. These precursors are converted to flavonols via flavonol synthase (FLS) or reduced to leucoanthocyanidin, a precursor to both anthocyanidins and proanthocyanidins (PAC), by dihydroflavonol reductase (DFR). Blueberry PACs, are polymers of the flavanols, catechin, epicatechin, and/or gallocatechin. Leucoanthocyanidin reductase (LAR) converts leucocyanidin and leucodelphinidin into catechin and gallocatechin, respectively, while epicatechin is derived from cyanidin via anthocyanidin reductase (ANR). Although delphinidin can be converted into epigallocatechin by ANR (Shi et al., 2018), this flavanol is not usually detected in fruit of Northern Highbush or Rabbiteye blueberry. PACs are often localized to vegetative tissues, the seed coat and unripe fruit (Xu et al., 2015).

The biosynthesis of flavonoids is regulated at the transcriptional level and distinct control over the production of anthocyanins and PACs is proposed as regulated by an "MBW" transcription factor (TF) complex. This complex consists of R2R3 MYB, bHLH and WD-Repeat proteins which were shown to activate the expression of biosynthetic genes (Baudry et al., 2004; González et al., 2008; Albert et al., 2014). Recently, we isolated and characterized an R2R3-MYB gene from blueberry, *VcMYBA* (Plunkett et al., 2018). *VcMYBA* was coexpressed with anthocyanin biosynthetic genes and induced anthocyanin production when expressed *in planta*. However, an additional class of R2R3-MYB protein, exemplified by grape *VviMYBPA1* also regulates anthocyanin and/or PAC biosynthesis in a variety of berries (Bogs et al., 2007; Jaakola et al., 2010; Primetta et al., 2015), although the exact role remains unclear.

While the majority of plant MYBs are involved in transcriptional activation, MYBs with repressive activity also regulate flavonoid biosynthesis. R2R3 and R3 MYB repressors such as AmMYB308, and PhMYBx, repress key branch-points within the pathway by directly or indirectly disrupting the activity of the MBW complex redirecting metabolites to alternative biosynthetic pathways (Tamagnone et al., 1998; Jin et al., 2000; Colquhoun et al., 2011; Albert et al., 2014). These repressors are themselves regulated by the MBW activation complex, providing a feedback repression mechanism (Albert et al., 2014; Zhou et al., 2015; Bond et al., 2016).

Different phases of blueberry fruit development are commonly based on berry expansion and color change (Zifkin et al., 2012; Karppinen et al., 2016; Li et al., 2019b) and it is well established that anthocyanins accumulate in parallel with the expression of structural genes of the flavonoid pathway. Blueberry pigmentation, however, is confined to fruit skin and since our current knowledge is based on whole fruit studies, we do not know whether this is regulated at key points within the pathway or by reduced flavonoid biosynthesis overall. Different mechanisms were suggested to limit anthocyanin production in pigment-deficient genotypes, such as inactivation

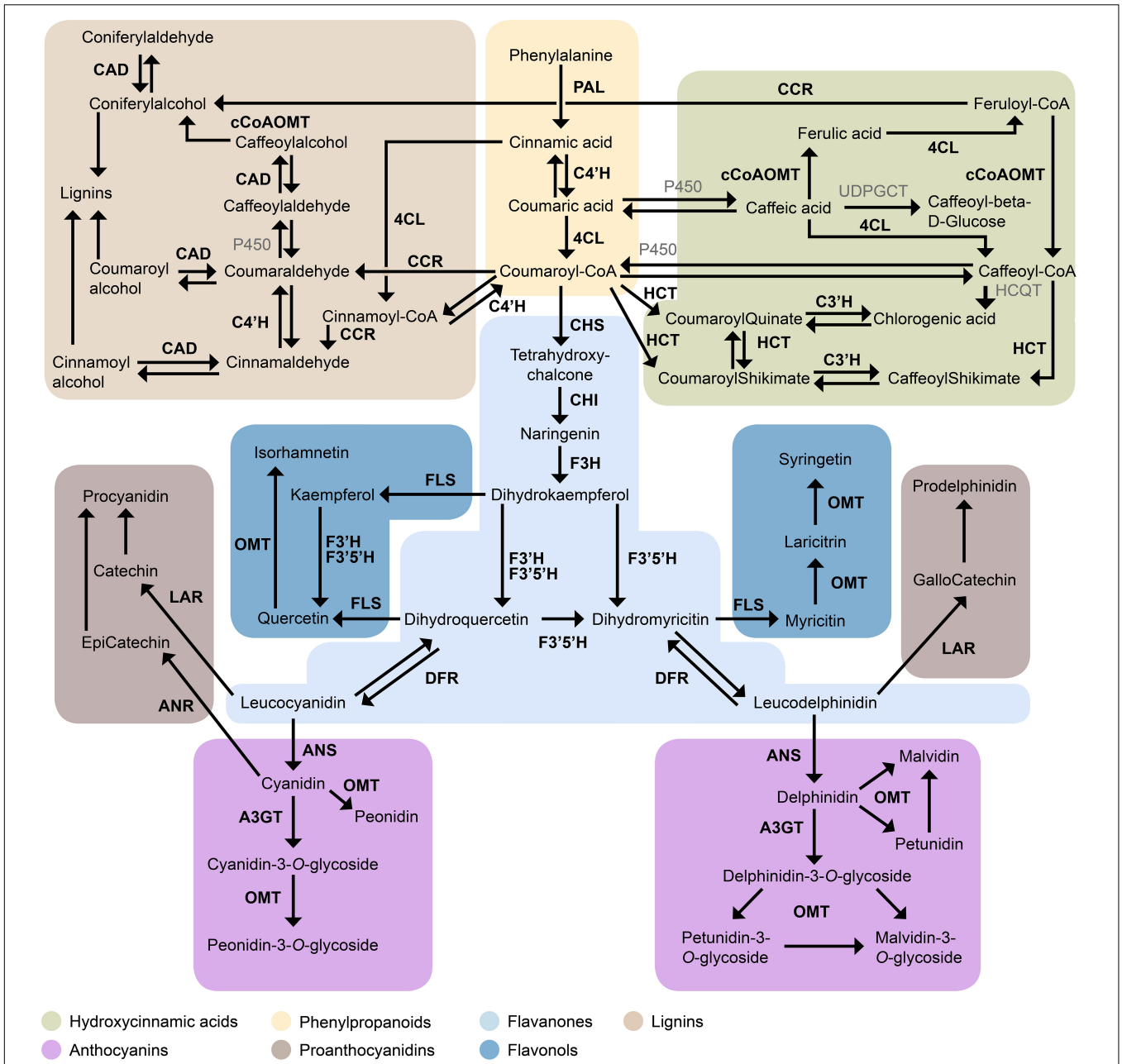

FIGURE 1 | Overview of the metabolic network leading to flavonoid biosynthesis in blueberries. Enzyme abbreviations as follows; PAL, phenylalanine ammonia lyase; C4′H, cinnamate 4-hydroxylase; 4CL, 4-coumarate-CoA ligase; CCR, cinnamoyl-CoA reductase; CAD, cinnamoyl alcohol dehydrogenase; cCoAOMT, Caffeoyl-CoA *O*-methyltransferase; HCT, shikimate *O*-hydroxycinnamoyltransferase; C3′H, 5-*O*-(4-coumaroyl)-D-quinate 3′-monooxygenase; CHS, chalcone synthase; CHI, chalcone isomerase; F3H, flavanone 3-dioxygenase; F3′H, flavonoid 3′ hydroxylase; F3′5′H, flavonoid 3′, 5′ hydroxylase; FLS, flavonol synthase; OMT, *O*-methyltransferase; LAR, leucoanthocyanidin reductase; ANR, anthocyanidin reductase; DFR, dihydroflavonol 4-reductase; ANS, anthocyanidin synthase; A3GT, anthocyanidin 3-*O*-glycosyltransferase.

of anthocyanidin synthase (ANS) in raspberry (Rafique et al., 2016), substrate competition between DFR and FLS in *Petunia* (Davies et al., 2003) and downregulation of multiple structural genes in albino bilberry (Zorenc et al., 2017). To investigate the determinants of spatial anthocyanin production in wild-type blueberries, we employed an interdisciplinary approach, linking targeted analysis of metabolites and gene transcription, to map the dynamic changes in flavonoid biosynthesis during fruit maturation of the commercial cultivars 'Nui' (Northern Highbush) and 'Velluto Blue' (Rabbiteye). Further, we studied how structural genes and their transcriptional regulators affect genotypic flavonoid profiles as a prerequisite for identifying genetic targets that modulate color-related traits.

MATERIALS AND METHODS

Blueberry Fruit Material

Berries were derived from cultivated collections of tetraploid *V. corymbosum* 'Nui' and hexaploid *V. virgatum* 'Velluto Blue' (Plant & Food Research, Motueka, New Zealand). Fruit was harvested between November 2017 and March 2018 at five different developmental stages identified by fruit skin color ranging from green to deep purple (Zifkin et al., 2012). The sampling was replicated at three separate plots within the field (each "plot" comprised two plants). Each biological replicate consisted of approximately 40 berries from each plot per stage and blueberry cultivar. Each replicate was immediately frozen in dry ice and then transferred to a −80°C freezer. Berry skin was separated from the flesh with a scalpel while keeping the fruit frozen on foil-covered dry ice. Seeds were not removed from the fruit flesh. Each frozen tissue sample was homogenized to a fine powder (IKA A11 basic mill) and stored at −80°C for no longer than 3 months.

Extraction of Polyphenols and UHPLC-ESI-QTOF-HRMS

Each sample was freeze dried (Edwards worldwide) and 50 ± 5 mg was extracted with 1.5 mL solvent (ethanol: water: formic acid; 80:20:1) at room temperature for 2.5–3 h in the dark and vortexed several times during this period. The samples were then transferred to 1°C overnight, centrifuged (10.000*g* for 10 min) then diluted (1:10) with 1% formic acid in methanol and stored at −20°C prior to analysis.

Ultra-High-Performance Liquid Chromatography (UHPLC) – Mass Spectrometry (LC-MS) was employed (Henry-Kirk et al., 2018) to measure anthocyanins and polyphenols and data were processed using Target Analysis for Screening and Quantitation software (TASQ, Bruker Daltonics, Bremen, Germany).

Anthocyanins

Anthocyanins were separated using a Luna Omega Polar C18 (100 × 2.1 mm, 1.6 μm) column maintained at 50°C. The mobile phase was composed of solvents: A = 5% formic acid in water and B = 100% acetonitrile at a flow rate of 300 μL/min. The solvent gradient was: initial composition 95% A, 0–0.5 min; linear gradient to 85% A, 0.5–10 min; linear gradient to 60% A, 10–20 min; linear gradient to 5% A, 20–25 min; composition held at 95% A, 25–28 min; linear gradient to 95% A, 28–28.2 min; to return to the initial conditions. The injection volume for samples and standards was 1 μL. The micrOTOF QII parameters were: temperature 225°C; drying N_2 flow 6 L min^{-1}; nebulizer N_2 1.5 bar, endplate offset 500 V, mass range 100–1500 Da, data were acquired at 5 scans s^{-1}. Positive ion electrospray was used with a capillary voltage of 3000 V. All anthocyanins were quantified as cyanidin 3-O-glucoside equivalents (Extrasynthese, Genay, France).

Polyphenols

Polyphenols were separated using a Luna Omega C18 (100 × 2.1 mm, 1.6 μm) column maintained at 40°C. The mobile phase was composed of solvents: A = 0.2% formic acid and B = 100% acetonitrile at a flow rate of 400 μL/min. The solvent gradient was: initial composition 95% A, 0–0.5 min; linear gradient to 85% A, 0.5–7 min; linear gradient to 60% A, 7–13.5 min; linear gradient to 5% A, 13.5–16 min; composition held at 95% A, 16–18 min; linear gradient to 95% A, 18–18.2 min;. The injection volume and the micrOTOF QII parameters were as above. Negative ion electrospray was used with a capillary voltage of 3500 V. Polyphenolic concentrations were calculated by comparison to external calibration curves of authentic compounds (details in **Supplementary Table S1**).

Gene Expression Analysis Using RNAseq

RNA was isolated from fruit tissues (100 mg) using the Spectrum™ Plant Total RNA isolation kit (Sigma-Aldrich) with minor modifications. The modifications made include adding 100 μL of CTAB solution (4% PVP, 4% CTAB) to the 500 μL of lysis buffer at the lysis stage and increased volume (750 μL) of binding buffer. RNA quantity was assessed using a Nanodrop spectrophotometer (Thermo Fisher Scientific). RNA quality was assessed on the Fragment Analyser using the DNF-471 kit (Agilent).

Between 2 and 3 μg of high-quality RNA (A260/280 ratio: 1.8–2, RIN-value of ≥8) per sample was supplied to the Australian Genome Research Facility (AGRF) Ltd. Independent Illumina mRNA libraries were prepared for each biological replicate and sequenced on the Illumina NovaSeq 6000 platform in paired end mode with 150 bp read length.

Raw data was cleaned with Trimmomatic-0.36 (Bolger et al., 2014) then mapped to the *V. corymbosum* reference transcriptome (RefTrans V1) from the Genome Database For Vaccinium (GDV) using bowtie2-2.3.4.3[1]. KEGG annotation of transcripts in RefTrans V1 was performed at GDV using the KEGG/KASS server. When the tetraploid *V. corymbosum* blueberry genome was published (Colle et al., 2019), the best matching genes to the candidate RefTrans V1 sequences were identified through reciprocal ncbi-blast/2.6.0 (Johnson et al., 2008) and considered as candidate genes (see **Supplementary Appendix** for gene sequences). Differentially expressed genes (DEGs) were detected using DESeq2_1.22.2 (Love et al., 2014) in R version 3.5.1. Transcripts with a total read count less than 100 across samples were discarded as a data filtering step for DEG test. Transcripts with adjusted *P*-value (padj) < 0.05 and logFC larger than 2 or smaller than −2 were marked as highly differentially expressed genes (HDEGs).

Predicted amino acid sequences were validated by BLAST searches of the Arabidopsis TAIR database[2] and the NCBI database[3]. Protein coding sequences from each gene family were then aligned with reference genes from Arabidopsis, grape and *Vaccinium* species using Geneious software version 10.9.1 to confirm homology and to identify full-length open reading frames. Gene duplicates were identified by reciprocal blast-search

[1]http://bowtie-bio.sourceforge.net/bowtie2/index.shtml

[2]https://www.arabidopsis.org/

[3]https://blast.ncbi.nlm.nih.gov/Blast.cgi

against Blueberry_MSU_tetraploid_proteins using our in-house sequence server database and removed from the dataset.

Statistical Analyses and Data Visualization

All statistical analyses were conducted using R 3.5.1 version "Feather Spray" (R Core Team, 2018) at $\alpha = 0.05$. Welch test (Welch, 1951) was used for univariate analysis if the data means were normally distributed according the Shapiro–Wilk test (Royston, 1982). If normality was rejected, nonparametric rank sum testing according to Kruskal–Wallis (Hollander and Douglas, 1973) and for pairwise comparisons Mann–Whitney/Wilcoxon (Bauer, 1972) were applied for sample comparisons. For multifactor analysis, analysis of variance (ANOVA) of LOG10-transformed data was used, followed by *post hoc* correction (Tukey–Kramer honest significant difference, Tukey-HSD) (Yandell, 1997). False discovery rate (FDR) adjustment for multiple comparisons were employed for all tests using the Benjamini–Hochberg method (Benjamini and Yekutieli, 2001).

Transcript abundances were normalized using Fragments Per Kilobase of transcript per Million mapped reads (FPKM-values) and genes with >1 FPKM were selected for analysis. Radial heat maps were computed using "*ggplot2*" and "*reshape*" (Wickham, 2007, 2016). The package "*RColorBrewer*" (Neuwirth, 2014) was used to select color schemes for figures. Heatmaps were constructed using the heatmap.2 function as implemented in "gplots" (Warnes et al., 2019).

Spearman rank correlations were performed using the "*Hmisc*" package (Harrell, 2019) for correlation analysis (Best and Roberts, 1975) and plots visualized with "*corrplot*" (Simko and Wei, 2017). To link chemical data with gene expression, regularized canonical correlation analysis (rCCA; Leurgans et al., 1993; González et al., 2008) was employed and Clustered Image Maps (CIM) (González et al., 2012) computed using a hierarchical clustering approach as implemented in "Biocmanager-mixomics" (Le Cao et al., 2009; Le Cao et al., 2016) by the Omics Data integration project. Relevance association networks were displayed for rCCA data according to González et al. (2012).

RESULTS

Anthocyanin Composition Is Distinct Between Blueberries

Anthocyanin concentrations from skin and flesh of 'Nui' (Northern Highbush) and 'Velluto Blue' (Rabbiteye) blueberry were quantified throughout development. Fruit flesh was largely devoid of anthocyanins, which accumulated rapidly in skin between S6 (onset of color change) and S8 (**Figure 2**). In fruit skin, concentrations of total anthocyanins increased to 120 ± 12 mg/g DW in 'Nui' which was marginally higher at S8 (15%, $P = 0.04$) compared with 'Velluto Blue.' Using multifactor analysis we found that developmental stage ($F = 171.1$; $P = 1.5 \times 10^{-9}$) and genotype ($F = 15.9$; $P = 0.002$) both affected anthocyanin concentrations, but their interaction did not ($F = 1.8$; $P = 0.2$), confirming that production rates were comparable between genotypes.

Despite comparable amounts of total anthocyanins in skin of ripe fruit, the composition was distinctly different between the two blueberries (**Figure 2**): While malvidin-3-*O*-glycosides were predominant in both genotypes, concentrations measured for 'Nui' (58.5 ± 5.5 mg/g DW) were 1.6-fold ($P = 0.003$) higher when compared with 'Velluto Blue.' An increased production in 3′5′ hydroxylated/methoxylated ($3'5'OH/OCH_3$) anthocyanins was observed for 'Nui,' whereas 'Velluto Blue' produced twice the amount of cyanidin- (16.9 ± 2.7 mg/g DW) and peonidin-3-*O*-glycosides (14.5 ± 1.9 mg/g DW). Thus, $3'5'OH/OCH_3$ anthocyanins were prevalent in 'Nui' whereas the composition of 'Velluto Blue' was characterized by a more balanced profile with respect to the concentrations of $3'OH/OCH_3$ and $3'5'OH/OCH_3$ anthocyanidins.

The anthocyanin profile was differentiated further by the glycone moiety. Glucosides, galactosides and arabinosides of the five common blueberry anthocyanidins were detected in both genotypes and acetylglucosides were also identified in 'Nui' but not in 'Velluto Blue' (**Figure 2**). In 'Velluto Blue,' up to 75% of anthocyanins were present as galactosides and only up to 15% as glucosides and this glycosylation pattern was largely conserved across the different groups of anthocyanidins (**Supplementary Table S2**). In contrast, the majority (30–40%) of anthocyanidins were linked to glucose in 'Nui' and the proportional glycosylation pattern between aglycones was different: cyanidin and peonidin were predominantly linked with acetylglucose, delphinidin with arabinose, and malvidin with glucose. Thus the major anthocyanin in 'Nui' was malvidin-3-*O*-glucoside and concentrations at S8 were eightfold higher compared with 'Velluto Blue,' which predominantly accumulated malvidin-3-*O*-galactoside.

Spatiotemporal Changes of Polyphenols Are Different Between Genotypes

A further 47 polyphenols were quantified from three distinct chemical classes: HCAs, flavonols (FOL), and PAC. As these metabolites share *p*-coumaroyl-CoA as common precursor (**Figure 1**), their biosynthesis can either divert pathway flux away from or toward anthocyanins as pathway end products.

Across fruit development, the concentrations of measured polyphenolic metabolites were up to fourfold higher in skin compared with flesh ($P_{'Nui'} = 1.7 \times 10^{-5}$; $P_{'Velluto\ Blue'} = 3.1 \times 10^{-6}$) and did not differ significantly between the genotypes when fully mature (skin = 19.6 ± 1.3 mg/g DW, $P = 0.34$; flesh = 5.5 ± 1.5 mg/g DW; $P = 0.07$, **Supplementary Figure S1**), indicating that biosynthetic activity was consistently higher in fruit skin. The spatiotemporal accumulation of polyphenols, however, was different between genotypes: In 'Nui,' maximum concentrations were measured in skin and flesh from unripe berries (S4, **Supplementary Figure S1**), exceeding 'Velluto Blue' concentrations by twofold. While a gradual decline in polyphenols during fruit maturation

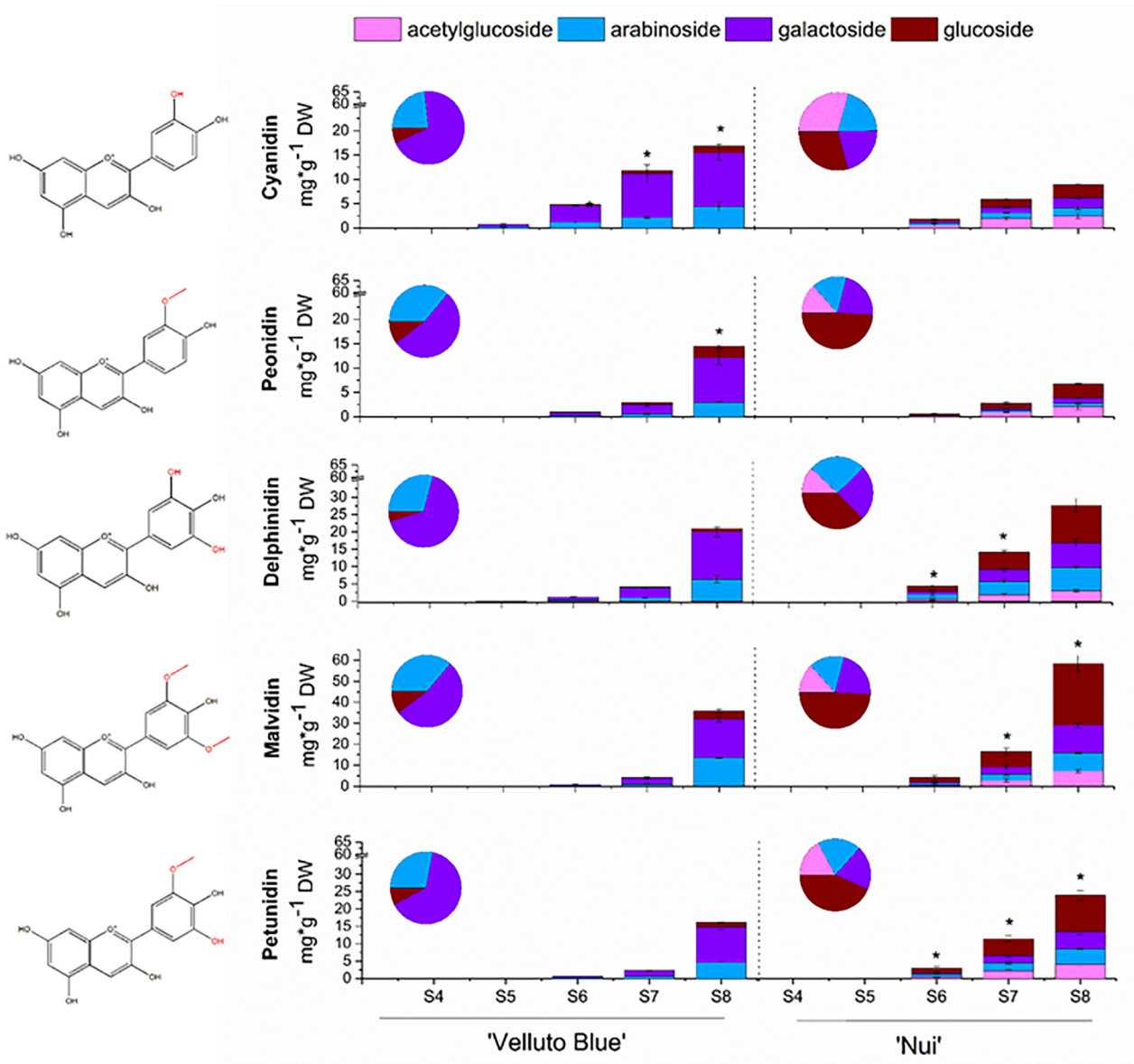

FIGURE 2 | Anthocyanin profiles of *Vaccinium virgatum* 'Velluto Blue' (Rabbiteye) and *V. corymbosum* 'Nui' (Highbush) fruit skin over development (S4-green, unripe -S8 fully ripe, purple). The asterisk (*) indicates significant differences in anthocyanidin concentrations (Welch *t*-test, $\alpha = 0.05$) between blueberries. Proportions of glycosides were averaged across all stages and are displayed in pie charts. Structure of each corresponding aglycone shown on left hand side.

was measured for 'Nui,' this was only observed in 'Velluto Blue' fruit flesh but not skin, where concentrations remained stable across time ($P = 0.27$).

Overall, HCA was the main class of measured polyphenols and during maturation concentrations were consistently higher in skin than flesh for both 'Nui' (2-fold) and 'Velluto Blue' (1.5-fold), respectively. Independent of the genotype, chlorogenic acid (CGA) and its derivatives *cis*-CGA and *neo*-CGA ('Velluto Blue' only) were major compounds and accounted for 44.7 ± 3.3% ($P = 0.2$) and 87.2 ± 1.8% ($P = 0.6$) of measured polyphenols in skin and flesh at S8, respectively. The main difference in HCA production was the pronounced accumulation at S4 in 'Nui' (**Figure 3**), thus contributing to time but not tissue-specific differences between genotypes.

FOLs were the second largest group of non-colored polyphenols (**Figure 3**), with 3′OH quercetin-3-*O*-glycosides accounting for >90% of total FOL in unripe blueberry skin (S4 and S5) besides monohydroxylated kaempferol-3-*O*-glycosides as minor compounds. While quercetin-3-*O*-glycosides remained stable (6.2 ± 0.9 mg/g DW, $P = 0.05$) during maturation in 'Velluto Blue,' concentrations halved in 'Nui' from S4 over development ($P = 1 \times 10^{-4}$) and were comparable between genotypes at S8 ($P = 0.96$). Except for small amounts of quercetin-3-*O*-glycosides in fruit flesh from unripe berries, FOL

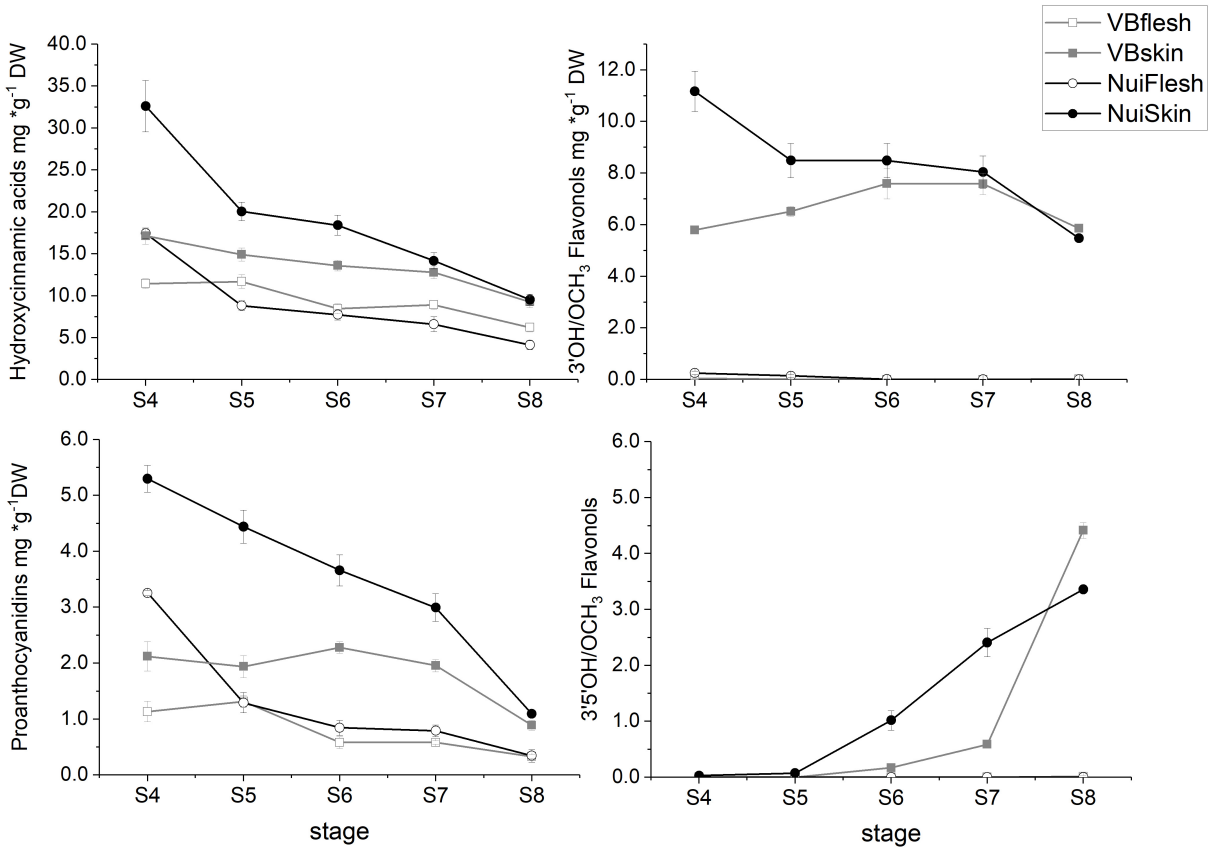

FIGURE 3 | Time course of polyphenolic metabolites in blueberry tissue types during development (S4-green, unripe -S8 fully ripe, purple). Metabolites were grouped according to their chemical class and the mean (± Standard error) is visualized for *Vaccinium virgatum* 'Velluto Blue' (VBflesh, VBskin) and *V. corymbosum* 'Nui' (NuiFlesh, NuiSkin).

biosynthesis appeared confined to fruit skin in both genotypes. In contrast to quercetin- and kaempferol-3-*O*-glycosides, the accumulation of 3′OCH_3 isorhamnetin-3-*O*-glycosides and 3′5′OH/OCH_3 FOL (laricitrin, myricetin-, syringetin-3-*O*-glycosides) coincided with anthocyanin production and increased rapidly from S6–S8 in skin of both genotypes (**Figures 3**, **4**).

Procyanidins (ProCy) were the major group of PAC which were also higher in blueberry skin compared with flesh and reflecting 3′OH FOL accumulation patterns, particularly (**Figure 3**). The condensation of the ProCy monomers catechin (Cat) and epicatechin (epiCat) leads to the formation of ProCy dimers B1 (PCB1, Cat-epiCat) and B2 (PCB2, epiCat-epiCat). ProCy composition was found to be the strongest driver in genotypic profiles: similar to HCA and 3′OH FOL production, concentrations of all measured ProCy, were highest at S4 in 'Nui' (**Supplementary Figure S2**). While Cat and ProCB1 accumulation was consistently at least twofold higher and thus characteristic for 'Nui,' 'Velluto Blue' produced up to fivefold higher concentrations of epiCat (both tissues) and ProCB2 (skin only) during maturation but ProCy concentrations were generally lower when with 'Nui'. In particular, epiCat flux was distinct and increased steadily in skin but decreased in flesh of 'Velluto Blue' berries (**Supplementary Figure S3**). Leucocyanidin (LeucoCy) is a precursor for both cyanidin and ProCy biosynthesis and accumulated in fruit skin from S6–S8 ('Nui') in parallel with anthocyanins when ProCy levels declined, indicating that precursor availability was unlikely limiting ProCy production. Although leucodelphinidin was not detected, its derivative the 3′5′OH PAC gallocatechin (GalCat) increased in parallel with 3′5′OH/OCH_3 FOL in 'Nui' (**Figure 4**) but not in 'Velluto Blue' where GalCat was only detected at S8.

In summary, the production of measured polyphenols was higher in blueberry skin compared with flesh, which almost exclusively accumulated HCA and ProCy. In fruit skin, the production of 3′5′OH/OCH_3 polyphenols and anthocyanins increased rapidly from S6–S8, contrasting the decline of HCA, ProCy and 3′OH FOL. The production of HCA, ProCy and 3′OH FOL was further distinguished between blueberries by pronounced accumulation in unripe berries (S4) in 'Nui' but not 'Velluto Blue.'

Gene Expression Corresponds to Metabolite Dynamics in Blueberry Tissue

Transcript abundances of 20 biosynthetic genes were measured, linking phenylpropanoid-pathway as source for

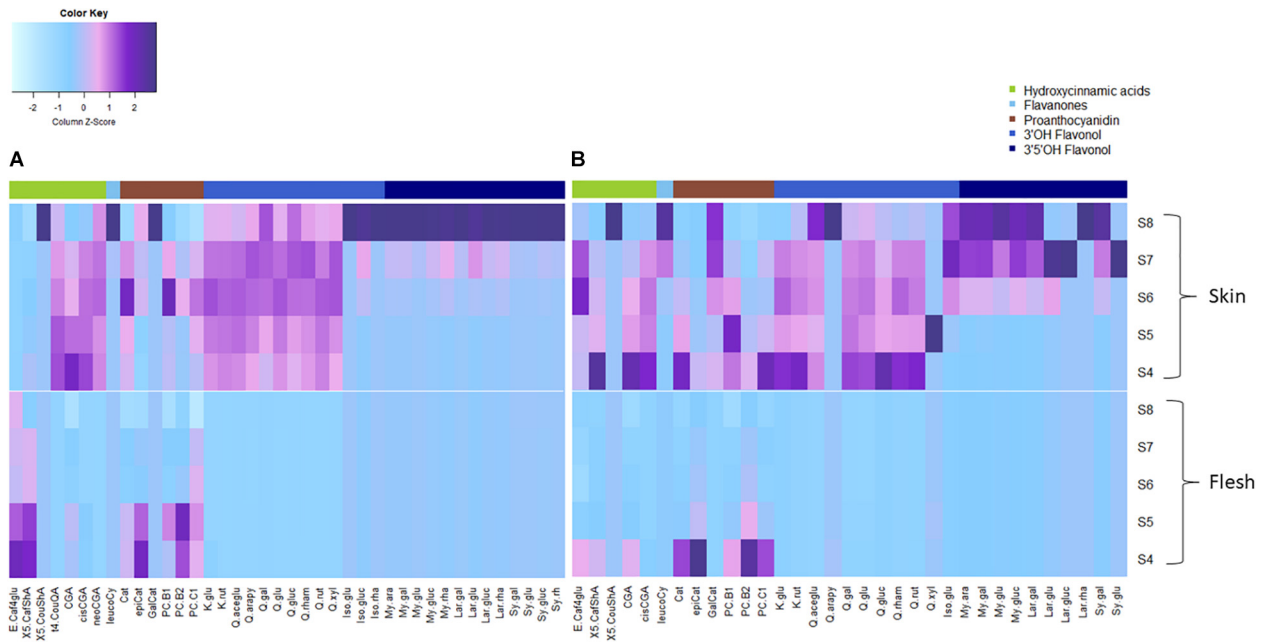

FIGURE 4 | Heatmap of measured polyphenols (mean, *N* = 3) from fruit skin and flesh of **(A)** *Vaccinium virgatum* 'Velluto Blue' and **(B)** *V. corymbosum* 'Nui' berries during maturation (S4-green, unripe -S8 fully ripe, purple). Column scaling was applied for data standardization, visualizing the spatiotemporal distribution of concentrations per compound. The key to compound abbreviations is outlined in l **Supplementary Table S1**.

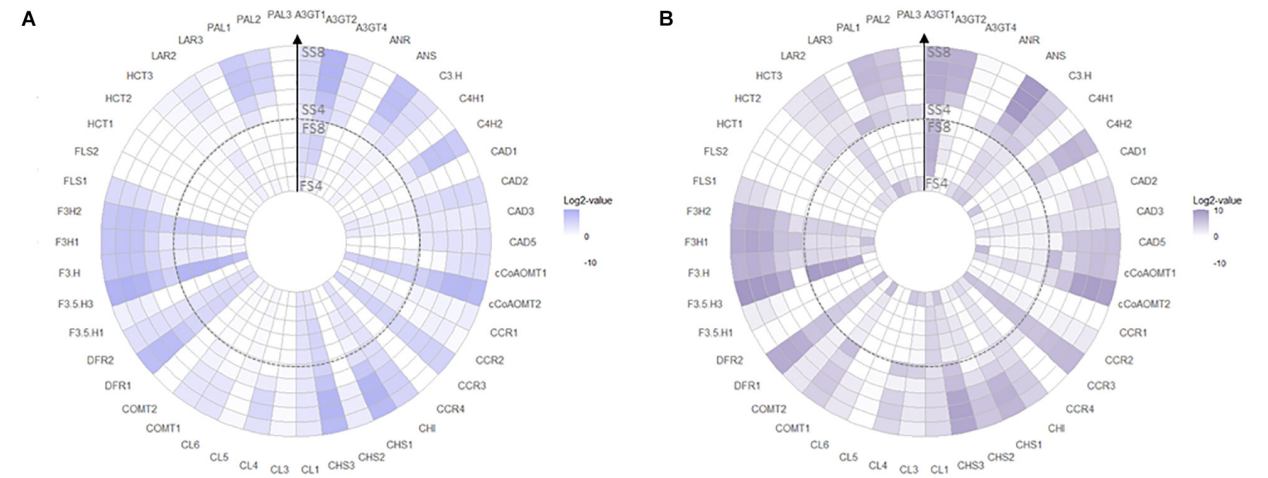

FIGURE 5 | Radial heat map of Log2-transformed gene expression data for *Vaccinium virgatum* 'Velluto Blue' **(A)** and *V. corymbosum* 'Nui' **(B)** tissue types throughout development (FS4: flesh stage 4; FS8: flesh stage 8; SS4: skin stage 4; SS8: skin stage 8). Transcript abundances below 1 FPKM are white. The key to gene abbreviations is presented in **Supplementary Table S3**.

precursors with structural genes of the flavonoid, lignin, and HCA pathway as sinks for substrates (**Figure 1**). Enzymes were encoded by multiple isoforms, except for *CHI*, *F3′H*, *C3′H*, *ANR*, and *ANS* which appeared encoded by a single gene (**Supplementary Table S3**). Transcript abundance was >1 FPKM for 46 genes (**Figure 5**) in both blueberry genotypes which were further included in the analysis. Overall, transcriptional activity in fruit skin was fourfold higher ($P_{\text{'Velluto Blue'}}$ = 0.005; $P_{\text{'Nui'}}$ = 0.007) when compared with flesh and increased sharply in both genotypes from S5 to S7 in fruit skin (**Supplementary Figure S4**), but not in flesh. In fruit flesh, transcripts of the structural genes *CHS3*, *F3H2*, *F3′5′H3*, and *DFR1* were prevalent in addition to *CCR3* (cinnamoyl- CoA reductase 3), accounting for 61% ('Velluto Blue') and 54% ('Nui') proportional abundance across development, suggesting a role in procyanidin formation. Tissue-specific differences in terms of transcript presence/ absence on

TABLE 1 | Overview of highly differentially expressed genes (HDEG) and proportional transcript abundance in *Vaccinium corymbosum* 'Nui' and *V. virgatum* 'Velluto Blue' blueberry.

	***V. corymbosum* 'Nui'**				***V. virgatum* 'Velluto Blue'**			
	HDEG Tissue Skin-flesh S7 Log2FC ± SD	**HDEG Time Skin S5–S6 Log2FC ± SD**	**% Skin S6–S7 AV ± SD**	**% Flesh S6–S7 AV ± SD**	**HDEG Tissue Skin-flesh S7 Log2FC ± SD**	**HDEG Time Skin S5–S6 Log2FC ± SD**	**% Skin S6–S7 AV ± SD**	**% Flesh S6–S7 AV ± SD**
PAL1	7.3 ± 0.9	2.6 ± 1.4	**1.8 ± 0.1**	0.1 ± 0.05	6.4 ± 0.1	2.1 ± 0.1	**2.6 ± 0.2**	0.14 ± 0.03
PAL2	7.8 ± 0.7	3.1 ± 1.5	**1.2 ± 0.1**	0.04 ± 0.02	9 ± 1.9	2.9 ± 0.3	**1.0 ± 0.1**	0.02 ± 0.01
C4.H2	6.2 ± 0.2	2.9 ± 1.7	**2.5 ± 0.1**	0.2 ± 0.06	5.7 ± 0.6	2.2 ± 0.1	**3.1 ± 0.3**	0.3 ± 0.08
CL4	7.2 ± 0.3	2.9 ± 1.5	0.4 ± 0.02	0.02 ± 0.01	6.5 ± 1.4	2.4 ± 0.3	0.5 ± 0.1	0.03 ± 0.01
CL6	8.8 ± 0.3	2.9 ± 0.2	0.08 ± 0.01	nd	4 ± 0.2	2.5 ± 0.1	0.2 ± 0.02	0.05 ± 0.01
CHI	2.7 ± 0.2		0.5 ± 0.05	0.5 ± 0.1			0.8 ± 0.2	0.8 ± 0.1
CHS1	7.5 ± 1.4	2.6 ± 1.1	**2.7 ± 0.2**	0.1 ± 0.1	6.3 ± 0.6	2.3 ± 0.1	**10.4 ± 0.8**	0.7 ± 0.3
CHS2	3.3 ± 0.4		0.8 ± 0.1	0.5 ± 0.1	5 ± 1.6		0.1 ± 0.01	0.02 ± 0.01
CHS3	6.4 ± 0.7		**7.3 ± 0.6**	0.6 ± 0.4	3.9 ± 0.6		**9.3 ± 0.4**	**3.0 ± 1.0**
F3H1	5.4 ± 0.5	2.2 ± 0.9	**6.1 ± 0.2**	0.9 ± 0.3	4.6 ± 0.5	2.2 ± 0.1	**3.0 ± 0.2**	0.6 ± 0.2
F3H2	3.6 ± 0.4		**3.8 ± 0.3**	**1.9 ± 0.6**			**2.8 ± 0.3**	**6.9 ± 0.9**
F3.H	4.3 ± 0.2	2.3 ± 1	**3.3 ± 0.3**	1.0 ± 0.1	4.4 ± 0.7		**2.8 ± 0.3**	0.6 ± 0.2
F3.5.H1	8.1 ± 0.1		0.1 ± 0.02	nd	8.2 ± 3.4		0.1 ± 0.02	nd
FLS1	7.6 ± 1.4	3.5 ± 1.4	0.2 ± 0.04	nd	4.9 ± 0.2		0.3 ± 0.04	0.05 ± 0.01
DFR1	3.1 ± 0.3		**4.3 ± 0.01**	**3.1 ± 0.2**	3.3 ± 0.5		**5.8 ± 1.1**	**2.8 ± 0.5**
ANS	6.4 ± 0.6	2.7 ± 1.5	**17.5 ± 0.5**	**1.4 ± 0.5**	6.3 ± 0.4	2.4 ± 0.2	**4.5 ± 0.1**	0.3 ± 0.1
A3GT2	5.7 ± 0.6		**3.2 ± 0.1**	0.4 ± 0.2	3.8 ± 0.3	2.7 ± 0.2	**11.9 ± 0.5**	**4.1 ± 0.9**
A3GT4			0.02 ± 0.001	0.05 ± 0.01	3.6 ± 0.4		0.2 ± 0.02	0.06 ± 0.03
COMT1	3.4 ± 0.3		0.6 ± 0.06	0.3 ± 0.03	2.6 ± 0.2		0.1 ± 0.01	0.1 ± 0.02
COMT2	3.1 ± 0.8		0.07 ± 0.01	0.05 ± 0.03			0.02 ± 0.01	0.05 ± 0.05
cCoAOMT1	5.1 ± 0.5		1.2 ± 0.2	0.2 ± 0.06			0.3 ± 0.1	0.02 ± 0.01
cCoAOMT2	6.5 ± 0.5	3.3 ± 2.1	**10.3 ± 0.7**	0.7 ± 0.3	2.8 ± 0.2		**8.1 ± 0.4**	**5.4 ± 0.8**
C3.H	2.6 ± 0.2		0.4 ± 0.07	0.4 ± 0.06	3 ± 0.2		0.7 ± 0.1	0.4 ± 0.06
CAD2	2.6 ± 0.3		0.3 ± 0.02	0.3 ± 0.1	3.1 ± 0.3		0.5 ± 0.1	0.3 ± 0.03
CAD5	4.9 ± 0.5		0.9 ± 0.04	0.2 ± 0.04	3.2 ± 0.2		0.1 ± 0.06	0.1 ± 0.02

Only DEG with Log2-fold change (Log2FC) > 2 and Padj < 0.05 are listed. The increase in transcripts in fruit skin vs flesh at stage 7 (S7) is summarized as HDEG Tissue. HDEG Time marks genes which increased in fruit skin during time of color change (S6 compared with S5). Average values and standard deviation (SD) are given. Bold font indicates prominent genes at >1% proportional abundance and italicized genes are suggested candidates in blueberry. nd = not detected.

the gene-family level were primarily noted for *PAL* and *FLS* which were not detected in flesh from the time of berry color change.

Reflecting increased concentrations of polyphenols in unripe 'Nui' berries, transcript abundances of 26 (flesh) and 12 (skin) genes were at least fivefold higher at S4 then S5, in this genotype only. This was particularly striking for *LAR3*, *ANR*, *PAL3*, *CCR4,* and Shikimate O-hydroxycinnamoyltransferase 2 (*HCT2)*, which were only expressed at this early stage (**Figure 5**) in both tissues. A subset of these early genes (*HCT3, PAL1, PAL2, C4′H2, CHS1, CHS3, F3H1, ANS*) decreased only in flesh but increased in skin during maturation.

Consistent for both genotypes, a core set of structural genes was identified using HDEG analysis at the critical time points framing berry color changes (S5–S7). Candidate genes encoding the entire phenylpropanoid pathway (*PAL1, PAL2, C4′H2, CL4, CL6),* specific isoforms of the early flavonoid pathway *(CHS1, F3H1)* in combination with ANS catalyzing the final step of anthocyanidin biosynthesis (**Table 1**), were not only significantly more abundant in pigmented fruit skin compared with flesh but also increased sharply in fruit at S6 compared with S5. The proportional abundance of these candidates was also comparable between genotypes and between 5- and 15-fold higher in skin compared with flesh, thus marking these as main drivers of tissue-specific transcript profiles during pigmentation. Although prominent isoforms were common to both genotypes, HDEG variation was observed for decorating enzymes, catalyzing modifications of the flavonoid structure. Genotypic differences were apparent for 'Nui' showing particularly increased abundance of *cCoAOMT1* and c*CoAOMT2* and 'Velluto Blue' of *A3GT4*.

We went on to co-correlate metabolites with transcripts in fruit skin using rCCA (**Figure 6**). Here, metabolites were grouped according to chemical class when these were correlated (Spearman's rank correlation) over time in both blueberries. Two distinct pathway correlation clusters were identified in both genotypes (**Figures 6A,B**): The first was associated with HCA biosynthesis in 'Velluto Blue' only but co-correlated with ProCy and 3′OH FOL metabolites in addition to HCA in 'Nui.' This cluster was negatively correlated with the second cluster

which visualized strong co-correlations of anthocyanins and 3′5′OH/OCH_3 FOL with *FLS1*, *CHS2*, *F3′5′H3*, *A3GT2*, and *CL6* in both genotypes. In 'Velluto Blue' epiCat production was positively correlated with cyanidin biosynthesis (**Figure 6A**), suggesting simultaneous production of both compounds. In 'Nui' on the contrary, ProCy including Cat and epiCat were associated with HCA and not cyanidin biosynthesis, showing strong negative correlations with structural flavonoid pathway genes, except *PAL3, LAR3,* and *ANR* (**Figure 6B**) with which these metabolites were positively co-correlated.

Possible Role of Transcription Factors in Gene Regulation

MYB TFs together with bHLH and WD-repeat proteins are known to regulate flavonoid biosynthesis and the effect of genotype, tissue, and their interaction on their transcript profiles (**Supplementary Table S4**) was analyzed. Only *bHLH1* was unaffected by these factors ($P > 0.19$), whereas five candidates (*bHLH2, MYB4, MYBA, MYBC2, MYBPA1*) were significantly higher ($P < 6.7 \times 10^{-5}$) in skin and *MYBR3* slightly higher (25%, $P = 9.9 \times 10^{-5}$) in fruit flesh. This was independent of species and factor interaction. In both genotypes transcripts of these five candidates increased steadily during maturation in skin only (**Supplementary Figures S5A–C**), thus resembling tissue-type dependent accumulation patterns of 3′5′OH/OCH_3 polyphenols and anthocyanins.

Genotype had the strongest effect on expression profiles of *bHLH075* (a regulator of fruit ripening (Fasoli et al., 2018)), *WDR1*, *MYBPA2a*, and *MYBPA2b*. *MYBPA2a* and *MYBPA2b* are likely associated with PAC biosynthesis (Terrier et al., 2009) and transcript abundance of both genes were below 1 FPKM in 'Velluto Blue,' whereas *bHLH075* and *WDR1* were each twofold higher ($P < 5 \times 10^{-4}$) compared with 'Nui' (**Supplementary Figures S5A–C**). *MYBPA2a* and *MYBPA2b* were co-expressed with *LAR3,* and *ANR* in 'Nui' which coincided with increased ProCy concentrations at S4.

To identify interactions of these TFs, we correlated gene transcription during fruit maturation (**Figure 7**). In fruit skin, two cohorts were identified of which *bHLH2*, *MYBA*, *MYBC2*, and *MYBPA1* (cohort 1) were co-expressed in skin of both genotypes and negatively correlated with, *MYB4*, *MYBR3*, and *WDR1* (cohort 2). Of these, cohort 1 was expressed in parallel with anthocyanin production during ripening, suggesting a possible function as activators. In fruit flesh, *MYBA*, *MYBPA1*, and *MYBC2* were not co-expressed and fewer significant correlations were apparent overall.

In order to propose a general model for the potential function of TF interactions on polyphenol biosynthesis in blueberry, we further focused on tissue-type dependent TFs only and co-correlated their transcripts with metabolites across both genotypes. The relevance networks (**Figure 8**) visualize strong correlations only (cut-off >0.7) and for fruit flesh (**Figure 8A**) a positive relationship between *MYBPA1*, *bHLH1*, and *MYB4* and metabolites from HCA and PA pathways is suggested. Although *MYB4* is classified as a repressor of gene transcription (Jin et al., 2000), it is unlikely that this MYB acts as a repressor of HCA and PAC pathway genes directly. These same TFs were also strongly correlated to metabolites in fruit skin (**Figure 8B**) where associations with more defined sections of the pathway were apparent. While *bHLH1* was associated with HCA primarily, *MYBPA1*, together with *MYBA* and *MYBC2*, were positively correlated with the accumulation of anthocyanins and 3′5′ substituted polyphenols. In contrast, *MYB4* was negatively correlated suggesting a possible repression of flavonoids in particular.

DISCUSSION

Precursor Limitation as Likely Cause for Flavonoid Deficiency in Fruit Flesh

We studied flavonoid biosynthesis during fruit maturation by correlating metabolite concentrations with gene transcript abundance in 'Velluto Blue' (Rabbiteye) and 'Nui' (Northern Highbush) blueberry. The accumulation of anthocyanins, gallocatechin and flavonols was confined to fruit skin. Procyanidins and HCAs were produced in fruit flesh, although at lower concentrations, and their concentrations declined in both tissues during maturation. In fruit skin, the production of anthocyanins and trihydroxylated flavonoids was strongly co-correlated with structural genes leading to their biosynthesis and negatively correlated with HCAs, thus indicating likely competition for substrates between pathways. This confirms conclusions from previous studies in Highbush and Lowbush blueberries (Gibson et al., 2013; Li et al., 2019b) suggesting that precursors might be increasingly used for flavonoid instead of HCA biosynthesis when fruit ripens. In both tissues, however, HCAs declined in parallel with procyanidin biosynthesis, thus indicating that precursors were shared and pathways might be co-regulated. While a diversion of substrates away from procyanidin biosynthesis toward cyanidins might likely explain the temporal shift observed in fruit skin at the onset of pigmentation, low gene transcription in fruit flesh of the phenylpropanoid pathway in general and *PAL* genes in particular, indicated limited supply of precursors as primary cause for reduced flavonoid production rather than substrate competition. During ripening, at least one isoform of structural flavonoid genes was prevalent in fruit flesh (with the exception of *FLS*) and the integrity of the pathway was therefore not interrupted at any particular step. Instead limited transcription of multiple pathway genes were identified as bottlenecks: In addition to isoforms of the phenylpropanoid pathway (*PAL1-2*, *C4′H2*, *4CL4/6*), structural genes catalyzing formation of flavanone scaffolds (*F3H1*, *CHS1*) in combination with *ANS* were likely restricting anthocyanin formation in fruit flesh. This is in line with previous studies on anthocyanin-deficient raspberry (Rafique et al., 2016) and bilberry (Zorenc et al., 2017). In contrast to our findings, DFR-activity was also reduced in albino bilberry and a concomitant increase in flavonols reported. Substrate competition between DFR and FLS has previously suggested to regulate anthocyanin formation (Davies et al., 2003) but this was unlikely causing the observed lack of pigmentation

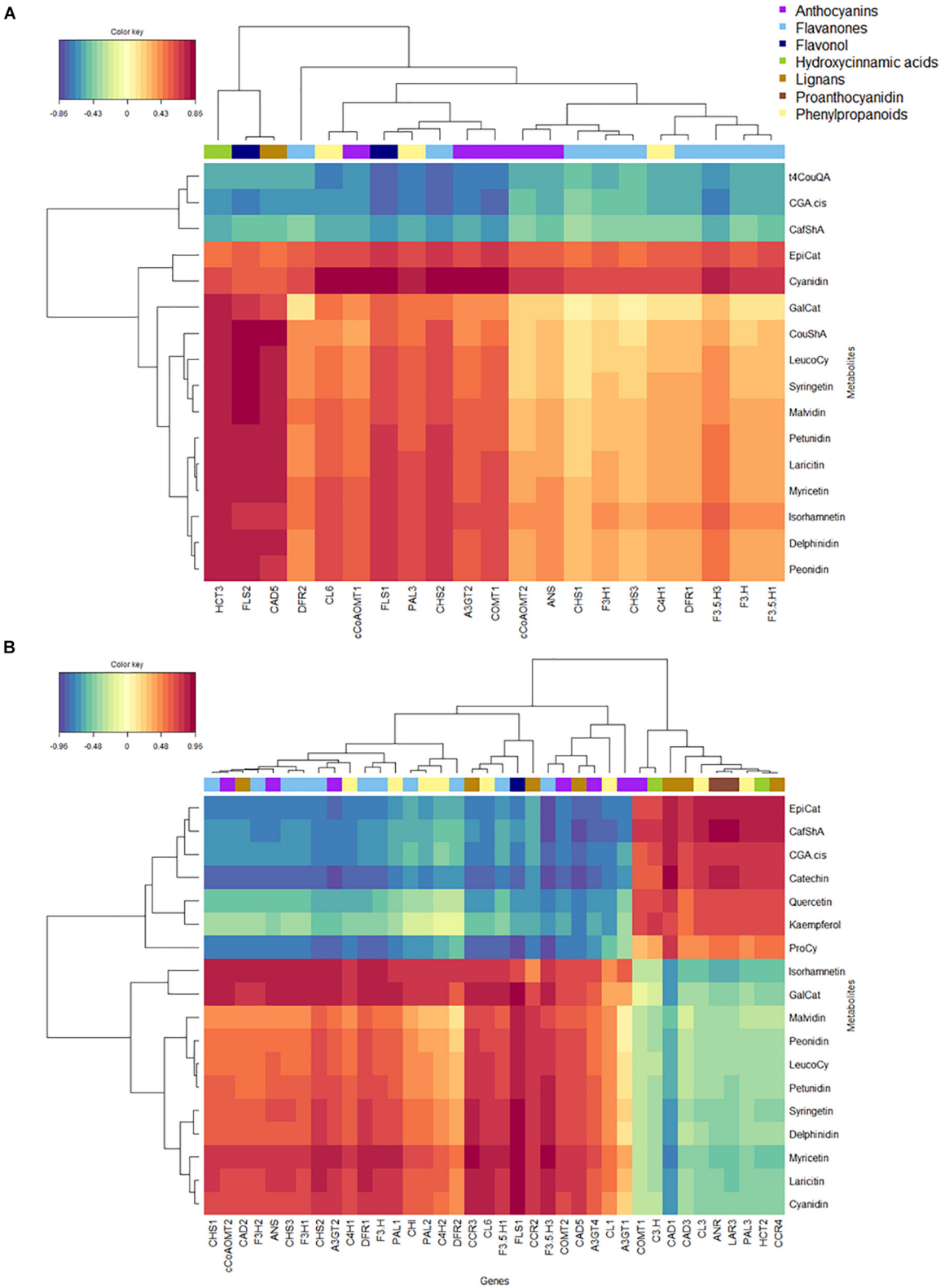

FIGURE 6 | Heatmap of regularized canonical correlations between normalized expression levels of biosynthetic genes and polyphenolic metabolites in fruit skin of **(A)** *Vaccinium virgatum* 'Velluto Blue' and **(B)** *V. corymbosum* 'Nui.' The correlation threshold was set to 0.7. The dendrogram clusters the data (method "Ward") with respect to their correlation strength. Warmer colors (red, orange) indicate positive and cooler colors (blue, green) negative correlations. Biosynthetic genes are grouped by color-bars according to their function.

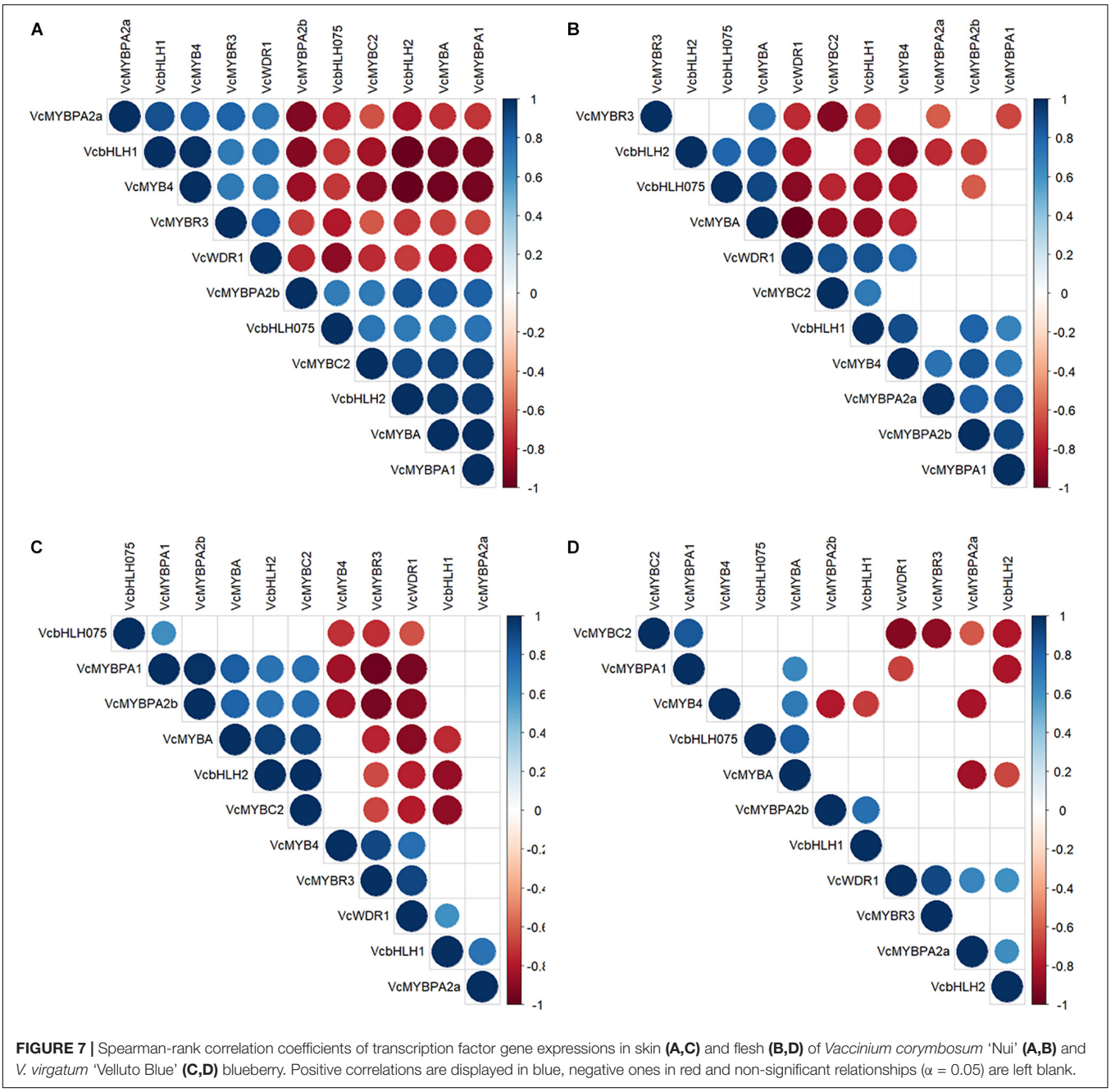

FIGURE 7 | Spearman-rank correlation coefficients of transcription factor gene expressions in skin **(A,C)** and flesh **(B,D)** of *Vaccinium corymbosum* 'Nui' **(A,B)** and *V. virgatum* 'Velluto Blue' **(C,D)** blueberry. Positive correlations are displayed in blue, negative ones in red and non-significant relationships ($\alpha = 0.05$) are left blank.

in our study as blueberry flesh was largely devoid of flavonols and *FLS* gene expression.

Anthocyanin Biosynthesis Was Likely Regulated by Coexpression of Transcriptional Activators MYBA, MYBPA1, and the Repressor MYBC2

Trihydroxylated flavonoids accumulated in parallel with anthocyanins, which was concomitant with expression patterns of transcriptional activators *MYBA* and *MYBPA1* in addition to *bHLH2* and the repressor *MYBC2*. The co-expression of the repressor *MYBC2* with the activators *MYBA* and *MYBPA1* fit proposed models, where the activators regulate repressors to provide feedback repression and fine control of anthocyanin production (Albert et al., 2014). Under these models, the expression of the R2R3-MYB repressor (*MYBC2*) and R3-MYB repressor (*MYBR3*) would be expressed most highly in tissues that accumulate key activators of anthocyanin or proanthocyanidin biosynthesis. Genotype-specific transcriptional regulation was most apparent for proanthocyanidin biosynthesis which was likely regulated by *MYBPA2a* in Northern Highbush fruit while no co-correlations with any of the *MYBPA* TSs were identified in Rabbiteye.

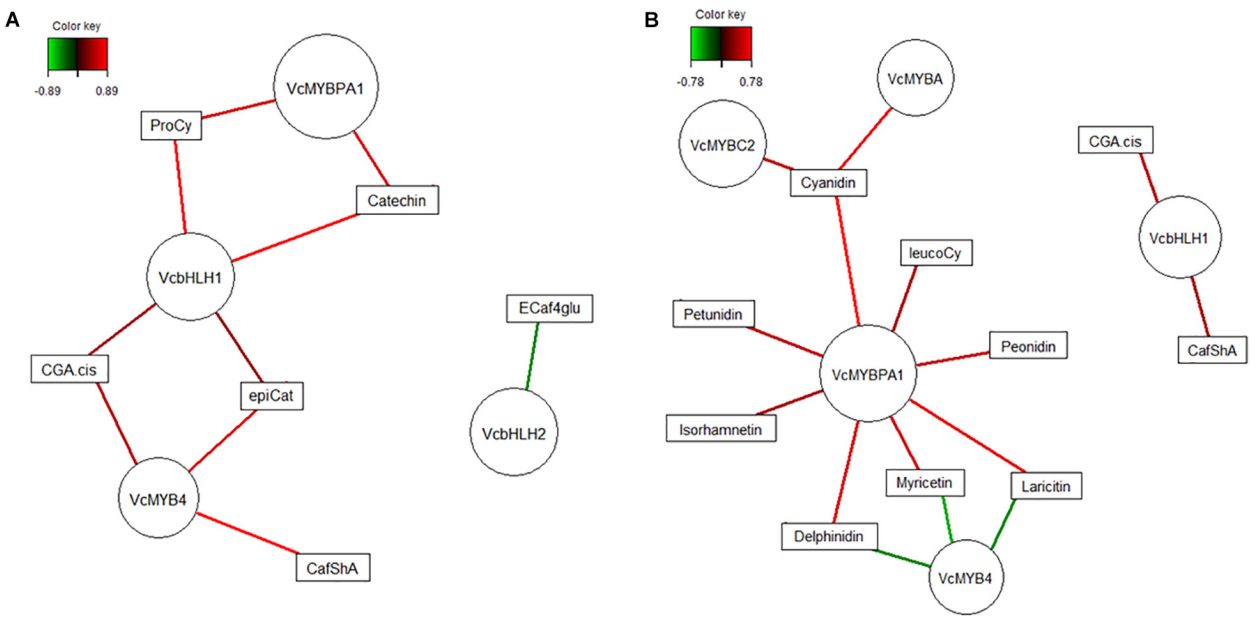

FIGURE 8 | Relevance network graph depicting correlations derived from regularized canonical correlation analysis between polyphenolic metabolites and genotype-independent transcription factors for blueberries (combined data, *Vaccinium virgatum* and *V. corymbosum*) flesh **(A)** and skin **(B)**. Nodes (circles) represent variables and are sized according to number of connections. Lines are colored according to correlation strength with augmented intensity indicating higher strength, green negative and red positive values, correlation threshold were set 0.8 for **(A)** and 0.7 for **(B)**.

Interestingly, the expression of *MYBR3* was not correlated with *MYBA*, *MYBPA1,* or *MYBPA2* transcription as expected, but was more highly expressed in the flesh of berries than skin. In albino bilberry (Zorenc et al., 2017) *MYBR3* was also significantly increased while *MYBC2* and *MYBPA1* were lower compared with the pigmented phenotype. It is, however, unlikely that *MYBR3* is responsible for the lack of anthocyanins in the flesh, because its mode of action is to titrate bHLH proteins (Albert et al., 2014) which would also affect proanthocyanidin biosynthesis. Proanthocyanidins were reduced in fruit flesh compared with skin but not abolished, indicating that *MYBR3* might indeed suppress flavonoid production to some degree but not entirely.

Flavonoid Biosynthesis Is Distinct Between Northern Highbush and Rabbiteye Blueberry in the Early Stages of Fruit Development

In line with our observations, quercetin-3-*O*-glycosides have previously been described as the most abundant flavonols in Northern Highbush blueberry (Häkkinen et al., 1999) and we show tissue-dependent accumulation in fruit skin. Maximum concentrations have been reported at the early stages of berry development when amounts of HCA and PAC were also high (Jaakola et al., 2002; Zifkin et al., 2012). We confirm these trends for the Northern Highbush but not for the Rabbiteye cultivar, where procyanidins and dihydroxylated flavonols were relatively consistent over time and not pronounced at S4. These diverging metabolic profiles correlated well with transcript abundances of structural genes, which remained stable in green Rabbiteye berries but were down-regulated in Northern Highbush after S4. In skin and flesh of Northern Highbush, increased transcription of the phenylpropanoid pathway genes (*PAL, C4′H, 4CL*) was concomitant with *HCT, C3′H*, and *cCoAOMT* at S4, which likely corresponded with the observed early peak in HCA production. In skin, the production of quercetin-3-*O*-glycosides coincided with early expression of *F3′H*, *CHI, CHS,* and *F3H* isoforms but not *FLS*. *DFR* and *ANS* transcripts were also detected at S4 in the absence of anthocyanins, suggesting that *ANS* expression might primarily affect procyanidin biosynthesis as procyanidin accumulation was strongly correlated with the early expression of *LAR3,* and *ANR* in Northern Highbush. Earlier findings in Northern Highbush by Zifkin et al. (2012), postulated that flavan-3-ol synthesis was likely restricted to early stages of fruit development, providing sufficient pools of monomers to drive procyanidin production further into S5 and S6. For Rabbiteye, however, neither procyanidin biosynthesis nor expression of *LAR or ANR* was pronounced early in development. Our data indicate heterogeneity in the expression profile of the *LAR* gene family, with the presence of *LAR2* transcripts in the skin and flesh of both blueberry species well into the later stages of development, suggesting that procyanidin biosynthesis likely continued past berry color change. In fruit skin, the metabolic flux of procyanidins resembled patterns observed for quercetin-3-*O*-glycosides, indicating that precursors were shared between both groups of flavonoids. The prodelphinidin gallocatechin, on the contrary, accumulated in parallel with trihydroxylated flavonols (myricetin- and laricitrin-, syringetin-3-O-glycosides), which was consistent for both species. Differences in proanthocyanidin biosynthesis were not previously identified in blueberry and

our findings suggest prodelphinidin biosynthesis was likely dependent on availability of structurally different substrates in addition to *LAR2* gene transcription.

Genotype-Characteristic Anthocyanin Profiles Were Likely Determined by Flavonoid Flux and Decorating Enzymes

We observed genotypic differences in anthocyanin production, which affected their onset and composition, but not their total amounts or distributions between tissue types. In Northern Highbush, anthocyanins accumulated simultaneously in fruit skin from S6 onward whereas in Rabbiteye the onset of cyanidin production occurred earlier in fruit development (S5), preceding other anthocyanins. Small amounts of anthocyanidin-3-*O*-glycoside have been previously measured in green Northern Highbush berries by Zifkin et al. (2012) and Li et al. (2019b). The use of different experimental techniques, however, challenges conclusions to whether these diverging findings might be based on genetic variation. Since standardized conditions were applied in our comparative study, we suggest that leucocyanidin might have been more efficiently used as precursor for cyanidin instead of procyanidin biosynthesis in Rabbiteye, reflecting low abundance of *LAR3* and *ANR* transcripts. In ripe fruit, the composition of anthocyanins was distinct between the blueberries with Rabbiteye producing significantly higher amounts of 3′ and Northern Highbush of 3′5′ substituted anthocyanins. Although only one genotype per species was analyzed in this study, Lohachoompol et al. (2008) reported similar trends for anthocyanin profiles from ripe fruit based on three Northern Highbush and Rabbiteye genotypes each, indicating that the observed differences in anthocyanin composition are likely to be a species-specific feature.

Fruit-specific anthocyanin profiles are likely genetically predisposed, but plasticity in pigment composition has also been emphasized in response to environmental factors such as light and temperature (Karppinen et al., 2016; Spinardi et al., 2019). As Rabbiteye fruit usually mature toward the later summer months and – as in our case – harvest dates can be months' apart, seasonal effects on anthocyanin accumulation cannot be excluded. Our knowledge of these effects, however, does not sufficiently explain the observed accumulation of cyanidin-based anthocyanins in Rabbiteye compared with Northern Highbush, because delphinidin- and malvidin-based anthocyanins were found to predominantly increase with light wavelength (Zoratti et al., 2014; Zoratti et al., 2015; Spinardi et al., 2019), at least in Northern Highbush and bilberry fruit.

The production of delphinidin-based anthocyanins was shown to depend on *F3′5′H* transgene expression in fruits naturally devoid of trihydroxylated anthocyanins (Brendolise et al., 2017) and in blueberry, accumulation of trihydroxylated anthocyanins was suggested to depend on *F3′5′H* gene expression (Zifkin et al., 2012). Using whole fruit samples, a late induction (S7/S8) in *F3′5′H* gene expression was found by Zifkin et al. (2012) and an increase in F3′5′H proteins was reported during development of Northern Highbush blueberry in a recent study (Li et al., 2019b). Thus making *F3′5′H* a strong candidate for regulating the accumulation of trihydroxylated flavonoids in ripe fruit.

We identified two *F3′5′H* isoforms that co-correlated with trihydroxylated flavonoids in blueberry skin. While *F3′5′H1* transcripts accumulated predominantly in skin, the major isoform *F3′5′H3* was also highly expressed in fruit flesh, reflecting both increased production of dihydroxylated flavonoids in unripe Northern Highbush as well as accumulation of trihydroxylated flavonoids during ripening. While our data confirm that increased *F3′5′H* gene expression was concomitant with increased flavonoid production, we conclude that tissue-specific biosynthesis was unlikely regulated by *F3′5′H* gene expression alone. The formation of trihydroxylated compounds is described as two-step reaction, and F3′5′H is therefore considered to exhibit both F3′H and F5′H activity. Since dihydroxylated flavonoids were predominant in unripe fruit and fruit flesh, even in the absence of *F3′H* gene expression, we postulate that *F3′5′H3* was primarily involved with generating dihydroxylated compounds due to high substrate turnover and formation of trihydroxylated compounds occurred later when excess substrate was available.

While *F3′5′H* expression is undoubtedly necessary for the production of delphinidin-based anthocyanins, *F3′5′H* as well as *F3′H* transcript abundances were within the same range for Northern Highbush and Rabbiteye fruit and therefore unlikely driving observed differences in anthocyanidin composition. We found structural genes linking phenylpropanoid and flavonoid pathways co-expressed and therefore conclude that anthocyanin composition in fruit skin was likely modulated by genotype-specific pathway flux, resembling the concerted action and interaction of each element of the pathway rather than regulated by individual genes. For example, ANS produces precursors for both anthocyanins and PAC, and gene expression was fourfold higher in Northern Highbush, while the actual anthocyanin concentrations were comparable between species. Since procyanidins were also highest in this species, especially during berry development, we suggest that this accumulation might have been at the expense of leucocyanidin, leading to lower cyanidin accumulation compared with Rabbiteye. That substrate competition between LAR and ANS can affect cyanidin concentrations has recently been shown in crabapple (Li et al., 2019a) but how this relationship might affect composition between di-and trihydroxylated anthocyanins has not been explored to date.

Anthocyanins are also structurally modified by methyltransferases, which were indicative for Northern Highbush and increased concentrations of malvidin- and petunidin-3-*O*-glycosides in this species might have been related to 3- and 5-fold higher expression of COMTs and cCoAOMTs, respectively. In addition to methyl transferases, the expression of UDP-glucose: flavonoid-3-*O*-glycosyltransferases was genotype-characteristic and likely to affect characteristic pigment compositions. To our knowledge, specific glycosylation patterns of blueberry anthocyanins have not been focussed on in previous literature, but have been suggested as markers for the authenticity of bilberry products (Primetta et al., 2013). We have shown that Northern Highbush produced 30% more anthocyanidin-3-*O*-glucosides than Rabbiteye, which produced

pigments predominantly linked to galactose. These results are of interest as the bioavailability of anthocyanins was shown to be influenced by the nature of the aglycone in combination with its glycoside. Firstly, systemically, after absorption into the bloodstream, arabinosides were generally less bioavailable than glucosides (McGhie et al., 2003). In addition, methoxylation also improved bioabsorption, and malvidin-3-*O*-glucoside was most efficiently absorbed. Secondly, *in vitro* and gut studies have suggest that glucosides were most efficiently metabolized by the intestinal microflora (Aura et al., 2005).

CONCLUSION

In summary, we conclude that anthocyanin biosynthesis is likely modulated by flavonoid flux within the pathway and fine-tuned by decorating enzymes with respect to structural composition. The control of the pathway, however, involves multiple pathway steps in association with multiple TFs in an interdependent manner.

DATA AVAILABILITY STATEMENT

The full raw sequence reads used for comparative RNAseq-based transcriptomics analyses have been made available on NCBI. PRJNA591951: *Vaccinium virgatum* 'Velluto Blue' (TaxID: 1493660) https://www.ncbi.nlm.nih.gov/bioproject/PRJNA591951. PRJNA591663: *Vaccinium corymbosum* 'Nui' (TaxID: 69266) https://www.ncbi.nlm.nih.gov/bioproject/PRJNA591663. The raw data supporting the conclusions of this article will be made available by the authors, without undue reservation, to any qualified researcher.

AUTHOR CONTRIBUTIONS

RE, AD, and NA conceived the experimental design and supervised all aspects of the study. CG performed the experiments, analyzed the data, and wrote the manuscript. CD was leading Bioinformatics of RNA sequencing. DL contributed to the data analysis and manuscript writing with respect to transcription factors. LJ provided academic advice on all sections of the manuscript. TM performed the LC-MS experiments, metabolite identification, and quantification. EG, JT, and BP provided support in sample collection, sample processing, and preparation of the manuscript.

FUNDING

This study was supported by the New Zealand Ministry of Business, Innovation, and Employment contract C11X1704 "Filling the Void: boosting the nutritional content of NZ fruit."

ACKNOWLEDGMENTS

We acknowledge Rebecca Kirk for the excellent coordination of the program and Minna Pesonen for the graphical design of **Figure 1**. We greatly appreciate Lenka James for help with fruit sampling, and Chethi Waite, Sarah Moss, Steve Arathoon, and Kui Lin-Wang for supporting the blueberry peeling. We further thank Jessica Rodrigues, Andy Allan, and Kevin Davies for constructive feedback on the manuscript. Access to the *V. corymbosum* genome was kindly granted by Patrick Edgar before public release. Lastly, we are grateful for the CRAN project for open source R.

SUPPLEMENTARY MATERIAL

The Supplementary Material for this article can be found online at: https://www.frontiersin.org/articles/10.3389/fpls.2020.00545/full#supplementary-material

FIGURE S1 | Concentrations of total measured polyphenols in blueberry fruit tissues during.

FIGURE S2 | Differences in procyanidin composition between blueberries.

FIGURE S3 | Epicatechin accumulation in blueberry tissues during fruit maturation.

FIGURE S4 | Combined transcript counts of biosynthetic genes and transcription factors in blueberry tissues during fruit maturation.

FIGURE S5A–C | Gene expression profiles of *bHLH*, *MYB* and *WDR1* transcription factors in blueberry tissue types during fruit maturation.

TABLE S1 | Summary of compound identification from blueberry tissues using LC-MS.

TABLE S2 | Glycosylation patterns of anthocyanidins from blueberry (*Vaccinium*) skin.

TABLE S3 | Overview of gene mapping results and functional annotation.

TABLE S4 | Summary of factorial ANOVA testing the effect of blueberry genotype, tissue, and interaction on gene expression of candidate transcription factors.

APPENDIX | Coding sequences of genes listed in **Supplementary Table S3**.

REFERENCES

Albert, N. W., Davies, K. M., Lewis, D. H., Zhang, H., Montefiori, M., Brendolise, C., et al. (2014). A conserved network of transcriptional activators and repressors regulates anthocyanin pigmentation in eudicots. *Plant Cell* 26, 962–980.

Aura, A. M., Martin-Lopez, P., O'Leary, K. A., Williamson, G., Oksman-Caldentey, K. M., Poutanen, K., et al. (2005). In vitro metabolism of anthocyanins by human gut microflora. *Eur. J. Nutr.* 44, 133–142.

Baudry, A., Heim, M. A., Dubreucq, B., Caboche, M., Weisshaar, B., and Lepiniec, L. (2004). TT2, TT8, and TTG1 synergistically specify the expression of BANYULS and proanthocyanidin biosynthesis in *Arabidopsis thaliana*. *Plant J.* 39, 366–380.

Bauer, D. F. (1972). Constructing confidence sets using rank statistics. *J. Am. Statist. Assoc.* 67, 687–690.

Benjamini, Y., and Yekutieli, D. (2001). The control of the false discovery rate in multiple testing under dependency. *Ann. Statist.* 29, 1165–1188.

Best, D. J., and Roberts, D. E. (1975). The upper tail probabilities of Spearman's Rho. *J. R. Stat. Soc. Ser. C Appl. Stat.* 24, 377–379. doi: 10.2307/2347111

Bogs, J., Jaffe, F. W., Takos, A. M., Walker, A. R., and Robinson, S. P. (2007). The grapevine transcription factor VvMYBPA1 regulates proanthocyanidin synthesis during fruit development. *Plant Physiol.* 143, 1347–1361.

Bolger, A. M., Lohse, M., and Usadel, B. (2014). Trimmomatic: a flexible trimmer for Illumina sequence data. *Bioinformatics* 30, 2114–2120.

Bond, D. M., Albert, N. W., Lee, R. H., Gillard, G. B., Brown, C. M., Hellens, R. P., et al. (2016). Infiltration-RNAseq: transcriptome profiling of Agrobacterium-mediated infiltration of transcription factors to discover gene function and expression networks in plants. *Plant Methods* 12:41.

Brendolise, C., Espley, R. V., Lin-Wang, K., Laing, W., Peng, Y. Y., McGhie, T., et al. (2017). Multiple copies of a Simple MYB-Binding site confers trans-regulation by specific flavonoid-related R2R3 MYBs in diverse species. *Front. Plant Sci.* 8:1864. doi: 10.3389/fpls.2017.01864

Colle, M., Leisner, C. P., Wai, C. M., Ou, S., Bird, K. A., Wang, J., et al. (2019). Haplotype-phased genome and evolution of phytonutrient pathways of tetraploid blueberry. *Gigascience* 8:giz012.

Colquhoun, T. A., Kim, J. Y., Wedde, A. E., Levin, L. A., Schmitt, K. C., Schuurink, R. C., et al. (2011). PhMYB4 fine-tunes the floral volatile signature of Petunia x hybrida through PhC4H. *J. Exp. Bot.* 62, 1133–1143.

Davies, K. M., Albert, N. W., and Schwinn, K. E. (2012). From landing lights to mimicry: the molecular regulation of flower colouration and mechanisms for pigmentation patterning. *Funct. Plant Biol.* 39, 619–638.

Davies, K. M., Schwinn, K. E., Deroles, S. C., Manson, D. G., Lewis, D. H., Bloor, S. J., et al. (2003). Enhancing anthocyanin production by altering competition between flavonol synthase and dihydroflavonol 4-reductase. *Euphytica* 131, 259–268.

De Pascual-Teresa, S., and Sanchez-Ballesta, M. T. (2008). Anthocyanins: from plant to health. *Phytochem. Rev.* 7, 281–299.

Durazzo, A., Lucarini, M., Souto, E. B., Cicala, C., Caiazzo, E., Izzo, A. A., et al. (2019). Polyphenols: a concise overview on the chemistry, occurrence, and human health. *Phytother. Res.* 33, 2221–2243.

Fang, J. (2015). Classification of fruits based on anthocyanin types and relevance to their health effects. *Nutrition* 31, 1301–1306.

Fasoli, M., Richter, C. L., Zenoni, S., Bertini, E., Vitulo, N., Dal Santo, S., et al. (2018). Timing and order of the molecular events marking the onset of berry ripening in grapevine. *Plant Physiol.* 178, 1187–1206.

Gallardo, R. K., Zhang, Q., Dossett, M., Polashock, J. J., Rodriguez-Saona, C., Vorsa, N., et al. (2018). Breeding trait priorities of the blueberry industry in the United States and Canada. *Hortscience* 53, 1021–1028.

Gibson, L., Rupasinghe, H. P. V., Forney, C. F., and Eaton, L. (2013). Characterization of changes in polyphenols, antioxidant capacity and physico-chemical parameters during lowbush blueberry fruit ripening. *Antioxidants* 2, 216–229.

Gilbert, J. L., Olmstead, J. W., Colquhoun, T. A., Levin, L. A., Clark, D. G., and Moskowitz, H. R. (2014). Consumer-assisted selection of blueberry fruit quality traits. *Hortscience* 49, 864–873.

González, I., Cao, K.-A. L., Davis, M. J., and Déjean, S. (2012). Visualising associations between paired 'omics' data sets. *Biodata Min.* 5:19.

González, I., Dejean, S., Martin, P. G. P., and Baccini, A. (2008). CCA: An R package to extend canonical correlation analysis. *J. Statist. Softw.* 23, 1–14.

Häkkinen, S. H., Karenlampi, S. O., Heinonen, I. M., Mykkanen, H. M., and Torronen, A. R. (1999). Content of the flavonols quercetin, myricetin, and kaempferol in 25 edible berries. *J. Agr. Food Chem.* 47, 2274–2279. doi: 10.1021/jf9811065

Harrell, F. E. Jr. (2019). *Hmisc: Harrell Miscellaneous. R Package Version 4.2–0*.

Henry-Kirk, R. A., Plunkett, B., Hall, M., McGhie, T., Allen, A. C., Wargent, J. J., et al. (2018). Solar UV light regulates flavonoid metabolism in apple (Malus x domestica). *Plant Cell Environ.* 41, 675–688.

Hollander, M. A. W., and Douglas, A. (1973). *Nonparametric Statistical Methods*. New York, NY: John Wiley & Sons, 115–120.

Huang, S. H., and Li, K. T. (2015). Dormant season fertigation promotes photosynthesis, growth, and flowering of 'Blueshower' rabbiteye blueberry in warm climates. *Hortic. Environ. Biotechnol.* 56, 756–761.

Jaakola, L., Määttä, K., Pirttilä, A. M., Törrönen, R., Kärenlampi, S., and Hohtola, A. (2002). Expression of genes involved in anthocyanin biosynthesis in relation to anthocyanin, proanthocyanidin, and flavonol levels during bilberry fruit development. *Plant Physiol.* 130, 729–739.

Jaakola, L., Poole, M., Jones, M. O., Kamarainen-Karppinen, T., Koskimaki, J. J., Hohtola, A., et al. (2010). A SQUAMOSA MADS box gene involved in the regulation of anthocyanin accumulation in bilberry fruits. *Plant Physiol.* 153, 1619–1629.

Jin, H. L., Cominelli, E., Bailey, P., Parr, A., Mehrtens, F., Jones, J., et al. (2000). Transcriptional repression by AtMYB4 controls production of UV-protecting sunscreens in *Arabidopsis*. *EMBO J.* 19, 6150–6161.

Johnson, M., Zaretskaya, I., Raytselis, Y., Merezhuk, Y., McGinnis, S., and Madden, T. L. (2008). NCBIBLAST: a better web interface. *Nucleic Acids Res.* 36, W5–W9.

Kalt, W., McDonald, J. E., Ricker, R. D., and Lu, X. (1999). Anthocyanin content and profile within and among blueberry species. *Can. J. Plant Sci.* 79, 617–623.

Karppinen, K., Zoratti, L., Nguyenquynh, N., Häggman, H., and Jaakola, L. (2016). On the developmental and environmental regulation of secondary metabolism in *Vaccinium* spp. Berries. *Front. Plant Sci.* 7:655. doi: 10.3389/fpls.2016.00655

Kong, J. M., Chia, L. S., Goh, N. K., Chia, T. F., and Brouillard, R. (2003). Analysis and biological activities of anthocyanins. *Phytochemistry* 64, 923–933.

Le Cao, K. A., Gonzalez, I., and Dejean, S. (2009). integrOmics: an R package to unravel relationships between two omics datasets. *Bioinformatics* 25, 2855–2856.

Le Cao, K. A., Gonzalez, I., Dejean, S., Gautier, B., Bartolo, F., Monget, P., et al. (2016). *mixOmics: Omics Data Integration Project. R Package Version 6.1.1*.

Leurgans, S. E., Moyeed, R. A., and Silverman, B. W. (1993). Canonical Correlation Analysis when the data are curves. *J. R. Statist. Soc. Ser. B* 55, 725–740.

Li, H., Tian, J., Yao, Y.-Y., Zhang, J., Song, T.-T., Li, K.-T., et al. (2019a). Identification of leucoanthocyanidin reductase and anthocyanidin reductase genes involved in proanthocyanidin biosynthesis in Malus crabapple plants. *Plant Physiol. Biochem.* 139, 141–151.

Li, X., Jin, L., Pan, X., Yang, L., and Guo, W. (2019b). Proteins expression and metabolite profile insight into phenolic biosynthesis during highbush blueberry fruit maturation. *Food Chem.* 290, 216–228.

Lohachoompol, V., Mulholland, M., Srzednicki, G., and Craske, J. (2008). Determination of anthocyanins in various cultivars of highbush and rabbiteye blueberries. *Food Chem.* 111, 249–254.

Love, M. I., Huber, W., and Anders, S. (2014). Moderated estimation of fold change and dispersion for RNA-seq data with DESeq2. *Genome Biol.* 15:550.

McGhie, T. K., Ainge, G. D., Barnett, L. E., Cooney, J. M., and Jensen, D. J. (2003). Anthocyanin glycosides from berry fruit are absorbed and excreted unmetabolized by both humans and rats. *J. Agric. Food Chem.* 51, 4539–4548.

Medeiros, J. G. S., Biasi, L. A., de Bona, C. M., and Cuquel, F. L. (2018). Phenology, production and quality of blueberry produced in humid subtropical climate. *Rev. Bras. Frutic.* 40:10.

Neuwirth, E. (2014). *ColorBrewer Palettes. R Package Version 1.1–2*.

Plunkett, B. J., Espley, R. V., Dare, A. P., Warren, B. A. W., Grierson, E. R. P., Cordiner, S., et al. (2018). MYBA from blueberry (*Vaccinium* section *Cyanococcus*) is a subgroup 6 type R2R3 MYB transcription factor that activates anthocyanin production. *Front. Plant Sci.* 9:1300. doi: 10.3389/fpls.2018.01300

Primetta, A. K., Jaakola, L., Ayaz, F. A., Inceer, H., and Riihinen, K. R. (2013). Anthocyanin fingerprinting for authenticity studies of bilberry (*Vaccinium myrtillus* L.). *Food Control* 30, 662–667.

Primetta, A. K., Karppinen, K., Riihinen, K. R., and Jaakola, L. (2015). Metabolic and molecular analyses of white mutant *Vaccinium* berries show down-regulation of MYBPA1-type R2R3 MYB regulatory factor. *Planta* 242, 631–643.

Quideau, S., Deffieux, D., Douat-Casassus, C., and Pouysegu, L. (2011). Plant polyphenols: chemical properties, biological activities and synthesis. *Angewandte Chem. Intern. Edn.* 50, 586–621.

R Core Team (2018). *R: A Language And Environment For Statistical Computing*. Vienna: R Foundation for Statistical Computing.

Rafique, M. Z., Carvalho, E., Stracke, R., Palmieri, L., Herrera, L., Feller, A., et al. (2016). Nonsense mutation inside anthocyanidin synthase gene controls pigmentation in yellow raspberry (*Rubus idaeus* L.). *Front. Plant Sci.* 7:1892. doi: 10.3389/fpls.2018.01892

Royston, J. P. (1982). An extension of shapiro and wilk-W test for normality to large samples. *J. R. Statist. Soc. Ser. C Appl. Statist.* 31, 115–124.

Scalzo, J. (2013). 'Velluto Blue': a new late-cropping Rabbiteye blueberry cultivar. *Hortscience* 48, 392–393.

Shi, L. Y., Cao, S. F., Chen, X., Chen, W., Zheng, Y. H., and Yang, Z. F. (2018). Proanthocyanidin synthesis in chinese bayberry (*Myrica rubra* Sieb. et Zucc.) fruits. *Front. Plant Sci.* 9:212. doi: 10.3389/fpls.2018.00212

Simko, V., and Wei, T. (2017). *R Package "Corrplot": Visualization of a Correlation Matrix (Version 0.84)*.

Spinardi, A., Cola, G., Sebastiano Gardana, C., and Mignani, I. (2019). Variation of ANthocyanin content and profile throughout fruit development and ripening of Highbush blueberry cultivars grown at two different altitudes. *Front. Plant Sci.* 10:1045. doi: 10.3389/fpls.2019.01045

Suh, D. H., Jung, E. S., Lee, G. M., and Lee, C. H. (2018). Distinguishing six edible berries based on metabolic pathway and bioactivity correlations by non-targeted metabolite profiling. *Front. Plant Sci.* 9:1462. doi: 10.3389/fpls.2018.01462

Tamagnone, L., Merida, A., Parr, A., Mackay, S., Culianez-Macia, F. A., Roberts, K., et al. (1998). The AmMYB308 and AmMYB330 transcription factors from antirrhinum regulate phenylpropanoid and lignin biosynthesis in transgenic tobacco. *Plant Cell* 10, 135–154.

Terrier, N., Torregrosa, L., Ageorges, A., Vialet, S., Verries, C., Cheynier, V., et al. (2009). Ectopic expression of VvMybPA2 promotes proanthocyanidin biosynthesis in grapevine and suggests additional targets in the pathway. *Plant Physiol.* 149, 1028–1041.

Timmers, M. A., Grace, M. H., Yousef, G. G., and Lila, M. A. (2017). Inter- and intra-seasonal changes in anthocyanin accumulation and global metabolite profiling of six blueberry genotypes. *J. Food Composit. Anal.* 59, 105–110.

Veberic, R., Slatnar, A., Bizjak, J., Stampar, F., and Mikulic-Petkovsek, M. (2015). Anthocyanin composition of different wild and cultivated berry species. *Lwt Food Sci. Technol.* 60, 509–517.

Warnes, G. R., Bolker, B., Bonebakker, L., Gentleman, R., Huber, W., Liaw, A., et al. (2019). *Gplots: Various R Programming Tools for Plotting Data. R Package Version 3.0.1.1*.

Welch, B. L. (1951). On the comparison of several mean values - an alternative approach. *Biometrika* 38, 330–336.

Wickham, H. (2007). Reshaping data with the reshape package. *J. Statist. Softw.* 21:122505.

Wickham, H. (2016). *Ggplot2: Elegant Graphics For Data Analysis*. New York, NY: Springer-Verlag.

Winkel-Shirley, B. (2001). Flavonoid biosynthesis. A colorful model for genetics, biochemistry, cell biology, and biotechnology. *Plant Physiol.* 126, 485–493.

Xu, W., Dubos, C., and Lepiniec, L. (2015). Transcriptional control of flavonoid biosynthesis by MYB–bHLH–WDR complexes. *Trends Plant Sci.* 20, 176–185.

Yandell, B. S. (1997). *Practical Data Analysis For Designed Experiments*. London: Chapman & Hall.

Zhou, H., Lin-Wang, K., Wang, H., Gu, C., Dare, A. P., Espley, R. V., et al. (2015). Molecular genetics of blood-fleshed peach reveals activation of anthocyanin biosynthesis by NAC transcription factors. *Plant J.* 82, 105–121.

Zifkin, M., Jin, A., Ozga, J. A., Zaharia, L. I., Schernthaner, J. P., Gesell, A., et al. (2012). Gene expression and metabolite profiling of developing highbush blueberry fruit indicates transcriptional regulation of flavonoid metabolism and activation of abscisic acid metabolism. *Plant Physiol.* 158, 200–224.

Zoratti, L., Jaakola, L., Häggman, H., and Giongo, L. (2015). Anthocyanin profile in berries of wild and cultivated *Vaccinium* spp. along altitudinal gradients in the alps. *J. Agric. Food Chem.* 63, 8641–8650.

Zoratti, L., Sarala, M., Carvalho, E., Karppinen, K., Martens, S., Giongo, L., et al. (2014). Monochromatic light increases anthocyanin content during fruit development in bilberry. *BMC Plant Biol.* 14:377. doi: 10.1186/s12870-014-0377-1

Zorenc, Z., Veberic, R., Slatnar, A., Koron, D., Miosic, S., Chen, M.-H., et al. (2017). A wild 'albino' bilberry (*Vaccinium myrtillus* L.) from Slovenia shows three bottlenecks in the anthocyanin pathway and significant differences in the expression of several regulatory genes compared to the common blue berry type. *PLoS One* 12:e0190246. doi: 10.1371/journal.pone.0190246

Conflict of Interest: The authors declare that the research was conducted in the absence of any commercial or financial relationships that could be construed as a potential conflict of interest.

frontiers in Plant Science

ORIGINAL RESEARCH
published: 25 May 2020
doi: 10.3389/fpls.2020.00490

The Synergism of 1-Methylcyclopropene and Ethephon Preserves Quality of "Laiyang" Pears With Recovery of Aroma Formation After Long-Term Cold Storage

Pan Shu, Dedong Min, Jingxiang Zhou, Wen Ai, Jiaozhuo Li, Zilong Li, Xinhua Zhang, Zedong Shi, Yingjie Sun, Fujun Li*, Xiaoan Li and Yanyin Guo*

School of Agricultural Engineering and Food Science, Shandong University of Technology, Zibo, China

OPEN ACCESS

Edited by:
Brian Farneti, Fondazione Edmund Mach, Italy

Reviewed by:
Nicola Busatto, Fondazione Edmund Mach, Italy
Claudio Bonghi, University of Padua, Italy
Jordi Giné-Bordonaba, Institute of Agrifood Research and Technology (IRTA), Spain

***Correspondence:**
Xinhua Zhang
zxh@sdut.edu.cn
Fujun Li
lifujun@sdut.edu.cn

Specialty section:
This article was submitted to Crop and Product Physiology, a section of the journal Frontiers in Plant Science

Received: *03 January 2020*
Accepted: *01 April 2020*
Published: *25 May 2020*

Citation:
Shu P, Min D, Zhou J, Ai W, Li J, Li Z, Zhang X, Shi Z, Sun Y, Li F, Li X and Guo Y (2020) The Synergism of 1-Methylcyclopropene and Ethephon Preserves Quality of "Laiyang" Pears With Recovery of Aroma Formation After Long-Term Cold Storage. Front. Plant Sci. 11:490. doi: 10.3389/fpls.2020.00490

A "Laiyang" pear is a climacteric fruit with a special taste and nutritional value but is prone to a post-harvest aroma compound loss and a loss in fruit quality. In this study, pears were pretreated with 0.5 μl L^{-1} 1-methylcyclopropene (1-MCP) at 20°C for 12 h and then stored at 0 ± 1°C for 150 days to evaluate the influence of 1-MCP on fruit quality and the changes in components of volatile aromas. In addition, pears were further treated with 2 mmol L^{-1} ethephon. The effects of ethephon on the recovery of aroma production were investigated during the 150 day storage at 0 ± 1°C and the subsequent 7 day shelf life at 20 ± 1°C. Treatment with 1-MCP inhibited firmness loss, increased electrical conductivity, reduced respiration and ethylene production rates as well as the contents of soluble solids, and maintained the storage quality of the fruits. However, 1-MCP treatment inhibited the emission of volatile aromas in pear fruits by decreasing the activities of various enzymes, such as lipoxygenase (LOX), hydroperoxide lyase (HPL), alcohol dehydrogenase (ADH), pyruvate carboxylase (PDC), and alcohol acetyltransferase (AAT). During the shelf-life, activities of the above mentioned enzymes were significantly enhanced, and a higher content of volatile aromas were found in fruits treated with 1-MCP + ethephon, while other qualities were not compromised. These results showed that 1-MCP treatment could effectively maintain the quality of the "Laiyang" pear during cold storage, and the additional application of ethephon on fruits during shelf-life may be a promising way to restore volatile aromas in pear fruits after long-term storage.

Keywords: aroma, pear (*Pyrus bretschneideri* Reld), aroma recovery, ethephon, 1-methylcyclopropene, cold storage

INTRODUCTION

"Laiyang" pears (*Pyrus bretschneideri* Reld), important fruits produced on a commercial scale in China for many years, are favorable for their special flavor, nutritional and medicinal functions (Liu et al., 2013; Fan et al., 2016). However, physiological disorders easily occur in this fruit at room temperature no more than 1 month after harvest, resulting in a significant loss of aroma compounds

and quality deterioration, leading to great economical losses during post-harvest storage periods (Liu et al., 2013). Therefore, how to effectively control the quality deterioration and to prolong the fruit's post-harvest life becomes a critical factor affecting the future development of this fruit.

The "Laiyang" pear has been recognized as a climacteric fruit since its ripening process is accompanied by ethylene and a respiration burst (Nath and Panwar, 2018). Methylcyclopropene (1-MCP), a strong inhibitor of ethylene perception, can effectively prevent ethylene biosynthesis, reduce tissue browning, and delay ripening of fruits and vegetables by permanently binding to ethylene receptors. 1-MCP has been successfully applied in commercial post-harvest operations to extend the storage life of climacteric and non-climacteric fruit (Blankenship and Dole, 2003; Li F. et al., 2013, Li L. et al., 2016; Liu et al., 2018). In "Huangguan" pears, the application of 1-MCP decreased the production of ethylene and respiration rates, and reduced the browning index (Xu et al., 2020). The positive role of 1-MCP had also been confirmed in the "Yali" pear. The pear fruit treated with 1.0 μl L^{-1} 1-MCP retained a higher firmness, titratable acidity (TA), and lower core browning (Cheng et al., 2019). Although, the positive roles of 1-MCP in maintaining a fruit's physiology have been well demonstrated in various fruits, the negative effects on the formation of aroma cannot be ignored. In "d" Anjou' pears, 1-MCP treatment decreased the prevalence of scald and internal disintegration but interfered with the "d" Anjou' pear's ability to ripen normally after storage (Argenta et al., 2003; Xie et al., 2014). In addition, the treatment with 1-MCP at the early ripening stage of the pear fruit, caused a failure in ripening so that the fruit did not attain the desirable taste and flavor, and did not develop a buttery texture (Moya-León et al., 2006; Hendges et al., 2018). In apples, 1-MCP treatment significantly inhibited and delayed the volatile production such as α-farnesene, alcohols, and esters (Yang et al., 2016). The volatile production evaluation demonstrated that 1-MCP treatment significantly suppressed the synthesis of saturated and unsaturated esters derived from ethylene-dependent fatty acid metabolism in papaya (Sundaram and Prabhakaran, 2017). Balbontin et al. (2007) reported that the development of ethylene-dependent flavor processes in fruit was blocked by 1-MCP treatment. Therefore, in spite of the aforementioned benefits, unfavorable influences in 1-MCP treatment on fruit aroma and ripening have also been reported.

The formation of aroma is closely related to fruit maturity and mainly involves three pathways: amino acid, fatty acid, and terpenoid metabolic pathways. Ethylene as a plant hormone participates in many ripening-related processes favorable for the synthesis of aromas (Saltveit, 1999). Wang et al. (2018) reported that most flavor-relevant compounds that accumulated the most in red-ripe tomato fruit were regulated by ethylene. Treatment of cold-stored kiwifruit with ethephon effectively enhanced the "tropical" and "fruit candy" aromas, while the "green" aroma was less obvious (Günther et al., 2015). In "Eureka" lemon, ethephon treatment significantly increased the volatile compounds in the fruit peel about 1-fold compared to the control (Zhang and Zhou, 2019). In apples, total volatiles as well as individual compounds, mainly associated with alcohols and esters, were significantly increased by ethylene treatment. Ethylene not only regulated the genes related to fatty acid synthesis and metabolism but also regulated the synthesis of esters by promoting alcohol acetyltransferase activity (Defilippi et al., 2005; Yang et al., 2016). The production of most esters in papaya was also dependent on ethylene, and the application of ethephon during fruit ripening promoted the production of esters (Balbontin et al., 2007). In addition, ethylene also played an important role in regulating the production of methyl-branched and aromatic volatile compounds from the catabolism of amino acids (Li Y. et al., 2016). However, exogenous application of ethylene or ethephon and excessive endogenous ethylene can easily lead to fruit over-ripening and senescence.

Recent studies have revealed that the simultaneous application of 1-MCP and ethylene at harvest has been tested as a strategy to recover ripening capacity of banana (Musa spp.) fruit (Botondi et al., 2014; Zhu et al., 2015) and the "Conference" pear (Chiriboga et al., 2011; Neuwald et al., 2015). However, there is no available information on the effects of 1-MCP and ethylene treatment on the aroma recovery of pear fruit during their shelf-life. The study aims to investigate the effect of 1-MCP treatment on the quality of the "Laiyang" pear during the cold storage period, and the effect of ethephon on the recovery of aroma formation of the "Laiyang" pear fruit during the shelf-life.

MATERIALS AND METHODS

Fruit Material and Treatments

Pear fruits (*Pyrus bretschneideri* Reld cv. Laiyang) were harvested from homogeneous trees (400 fruits per tree) in a commercial orchard (fruit weight: 168.28 ± 9.71 g; soluble solids content: 12.26 ± 0.14% and firmness: 40.83 ± 1.89 N) in Laiyang, Shandong Province, China, and then immediately transported to the laboratory. Trees were grafted in 1995 on Duli (*Pyrus Betulaefolia* Bunge) rootstock, with a tree spacing of 6 m × 4 m. Fruit with similar sizes, free of mechanical damage, were selected as materials.

The pear fruits were randomly divided into two groups of 240 fruits each and subjected to the following treatments: (1) 1-MCP treatment: the fruits were fumigated with 0.5 μl L^{-1} 1-MCP at 20 ± 1°C for 12 h in a sealed container. (2) CK treatment: the fruit were sealed in a container at 20 ± 1°C for 12 h without 1-MCP. After treatment, all pear fruits were immediately transferred and stored at 0 ± 1°C with 90–92% relative humidity. At 1-month intervals, for a total storage time of 5 months, fruits were removed and allowed to equilibrate at 20°C overnight for measurements of ethylene production rate, respiration rate, aroma, and fruit quality immediately, or frozen in liquid nitrogen and stored at −80°C for enzyme assays. All treatments were conducted with three replications.

After 150 days of storage, 40 fruit from each treatment of each replicate were randomly selected from CK or 1-MCP treatment and divided into two portions, each containing 20 fruit for soaking with either 2 mmol L^{-1} ethephon (marked as CK + ethephon or 1-MCP + ethephon) or distilled water (which served as the control for ethephon treatment, marked as CK + H_2O or 1-MCP + H_2O) for 2 min. After

drying, all fruits were stored at room temperature for 7 days before being measured.

Determination of Ethylene Production Rate and Respiration Rate

The respiration rate and ethylene production were determined according to the method of Both et al. (2016). Five fruits from each treatment were sealed in a 4-L airtight container. After 1 h, 1 ml of the headspace gas was sampled from the container and injected into a gas chromatograph (Agilent 6890N, United States) to assay the ethylene production. The temperatures of the oven, injector, and detector were 110, 50, and 150°C, respectively. The flow rates for nitrogen, hydrogen, and compressed air were, respectively, 50, 50, and 400 ml min^{-1}. The respiration rate was measured using a combined CO_2/O_2 analyzer (CheckMate 9900, PBI-Dansensor, Denmark). The result was expressed as nmol kg^{-1} s^{-1} for ethylene production rate, and as nmol kg^{-1} s^{-1} CO_2 for respiration rate.

Determination of Fruit Quality

Fruit firmness was measured using a destructive method on opposing sides of the equator region of 10 fruit per treatment with a handheld electrometer (GY-1, Mudan River, China), and the firmness was automatically calculated. Values were expressed as newton (N). After determination of firmness, the remaining parts were assessed for titratable acidity (TA) and soluble solids content (SSC). TA was determined using a base buret by titrating the juice with 0.01 mol L^{-1} NaOH up to pH 8.1. The results were expressed as g kg^{-1} of malic acid by fresh weight. SSC was measured by a manual refractometer (WYT-J, Chendu Optical Apparatus Co., Ltd., China) and the results were expressed as percentage (%).

Electrical conductivity (EC) was determined according to our previous studies with minor modifications (Zhang et al., 2013). Five pieces of fruit tissue from five fruits were obtained by steel core borer (10 mm diameter, 1 mm thick), rinsed three times and immersed in 20 ml distilled water at 25°C for 1 h. The initial EC (C_0) was determined by DDS-307A conductivity meter (Leici Inc., Shanghai, China). Then, the fruit disks were boiled for 5 min, cooled to room temperature, and the total EC (C_1) was monitored. The EC was defined as $C_0/C_1 \times 100\%$.

Extraction and Determination of Aroma-Related Enzyme Activities

Lipoxygenase (LOX) activity was determined according to Lara et al. (2003) with minor modifications. Frozen tissue (2 g) was homogenized with 6 ml phosphate buffer containing 2 mM dithiothreitol (DTT) (pH 7.5), 1% (w/v) polyvinyl pyrrolidone (PVP) and 0.1% (V/V) Triton X-100. Then, the homogenate was centrifuged at 12 000 × *g* for 20 min at 4°C, and the supernatants were used for enzyme assays. The reaction mixture comprised of 1.5 ml of 0.1 M phosphate buffer saline (PBS), 400 μl substrate solution (8.6 mM linoleic acid, 0.25% (v/v) Tween-20, 10 mM NaOH), and 100 μl enzyme extraction. LOX activity was determined by measuring the absorbance at 234 nm for 60 s at 25°C. One unit of LOX activity was defined as an increasing of 0.01 at OD_{234} per minute.

Alcohol acetyltransferase (AAT) activity was determined as described by Pérez et al. (1996) with some modifications. Frozen tissue (2 g) was extracted in 3 ml extraction buffer containing 0.5 M Tris–HCl (pH 8.0), 0.1% (v/v) Triton X-100, and 1% (w/v) PVP. The homogenate was centrifuged at 12 000 × *g* for 20 min at 4°C, and the supernatants were used for the enzyme assays. The reaction solution contained 2 ml of 5 mM $MgCl_2$, 150 μl of 5 mM acetyl-CoA, 50 μl of 200 mM butanol, 100 μl of 10 mM 5, 5′-dithiobis-bis-2-nitrobenzoic acid and 200 μl enzyme solution. AAT activity was determined by measuring the absorbance at 412 nm for 60 s at 25°C. One unit of AAT activity was defined as the increase in one unit of absorbance at 412 nm per minute.

Hydroperoxide lyase (HPL) activity was analyzed according to Vick (1991) with some modifications. Frozen tissue (2g) was extracted in 4 ml of extraction buffer containing 2-(N-morpholino) ethanesulfonic acid (MES), pH 6.5; 2 mM DTT, 1% (v/v) PVP. Then the homogenate was centrifuged at 12 000 × *g* for 20 min at 4°C. The reaction mixture contained 0.75 ml linoleate sodium hydroperoxide, 1.5 ml of 1.6 mM nicotinamide adenine dinucleotide (NAD), 0.1 ml adenine dinucleotide, and 0.5 ml crude enzyme extraction. The mixture was incubated at 30°C and then determined at 340 nm for 60 s. One unit of HPL activity was defined as an increase of 0.01 at OD_{340} per minute.

Alcohol dehydrogenase (ADH) and pyruvate carboxylase (PDC) activities were determined according to the method of Lara et al. (2003) with slight modifications. Frozen tissue (2 g) was homogenized with 4 ml MES buffer containing 2 mM DTT, 1% (w/v) PVP. Then the homogenate was centrifuged at 12 000 × *g* for 20 min at 4°C, and the supernatants were used for the enzyme assays. The ADH reaction mixture contained 0.8 ml of 100 mM MES-Tris (pH 6.5), 1.5 ml of 1.6 mM NAD, 0.05 ml of 80 mM acetaldehyde, and 0.1 ml enzyme extraction. The PDC reaction mixture contained 0.45 ml of 100 mM MES-Tris (pH 6.5), 0.1 ml of 5 mM thiamine pyrophosphate (TPP), 100 μl of 50 mM $MgCl_2$, 50 μl of 1.6 mM NADH, ADH (1600U), 100 μl of 50 mM pyruvate, and 100 μl enzyme extraction. ADH and PDC activity was determined by measuring the absorbance at 340 nm for 2 min at 25°C. One unit of ADH and PDC activities was defined as an increase of 0.01 at OD_{340} per minute.

Protein content in the enzyme extracts was determined according to the method of Bradford (1976), using bovine serum albumin as a standard. Specific activities of the enzymes were expressed as units per milligram protein.

Aroma Volatiles Analysis

Fresh fruit (10 g) containing peel from equator was homogenized with 3 ml saturated sodium chloride, and then transferred to a 30 ml vial. Before sealing of the vials, 2 μl of a solution of 0.82 g/l 3-non-anone solution was added as an internal standard. The aroma volatile compounds of pear fruits were determined using GC-MS (QP2010, Shimadzu, Japan) fitted with RTX-5 column (30 m × 0.25 mm × 0.25 μm, Agilent, United States) and based on solid-phase micro-extraction (SPME), according to a method of Cai et al. (2018). A fiber coated with 65 μm of polydimethylsiloxane and divinylbenzene (PDMS/DVB) (Supelco, Bellefonte, United States) was used for volatile compound extraction at 50°C for 30 min. The

chromatographic conditions were set as follows: The furnace temperature was first maintained at 40°C for 2 min, increased at a rate of 4°C min^{-1} to 60°C and kept for 1 min, and then increased at a rate of 2°C min^{-1} to 150°C, and finally increased at a rate of 10°C min^{-1} to 210°C and kept for 5 min. Helium was used as carrier gas at a flow rate of 1.03 ml min^{-1}. Electronic ionization was used at 70 eV. Detection was performed from 45 to 450 mass units. The GC-MS data processing was dealt with using Thermo XCALIBUR^{TM} 2.2 software. At the same time, retention indices (RI) were calculated by analyzing a series of n-alkanes (C_5-C_{24}) under the same conditions. The volatile aroma compounds in our experiment were identified by comparing their mass spectra with the National Institute for Standards and Technology (NIST) (Zhang et al., 2009) and by comparing it with RI reported in research. Results were expressed as μg g^{-1}, and were used for hierarchical clustering heatmap analysis after homogenization.

Statistical Analysis

Each treatment comprised three independent biological replicates. All data were expressed as the means ± standard deviation (SD) and were analyzed statistically, using one-way analysis of variance (ANOVA) and Ducan's multiple range tests with SPSS 19.0 (SPSS Inc., Chicago, IL, United States). Volatile compound data from the four treatments were submitted to a principal component analysis (PCA), using the Origin 2018 software. In order to visualize the differences in volatile aroma composition, a hierarchical clustering heatmap was created with the heatmap3 R package.

RESULTS

Effects of 1-MCP Treatment on Quality Traits of Pear

The "Laiyang" pear is a climacteric fruit with a clear peak respiration rate. During the cold storage period, the respiration rate of CK fruit first increased and then decreased, which shows a similar level at the end of storage time in comparison to beginning. A significant suppression of respiration rate was observed in 1-MCP-treated fruit compared to CK fruit. The respiratory climacteric peak of 1-MCP-treated fruit was significantly delayed by 30 days and decreased by 34.4% compared to CK fruit (**Supplementary Figure S1a**). A similar change was observed in ethylene production. As shown in **Supplementary Figure S1b**, the ethylene production in 1-MCP-treated fruit was always lower than that in the CK fruit during the storage period. The ethylene production peaks of 1-MCP-treated fruit was also delayed by 30 days and decreased by 34.3% compared to CK fruit.

In the course of the cold storage period, the firmness of the pear fruit, without treatment, decreased. As shown in **Supplementary Figure S1c**, the treatment with 1-MCP significantly suppressed the reduction of firmness in comparison to CK. The firmness of 1-MCP-treated fruit was 23.6 N, which was 40.6% higher than that of the CK fruit (16.8 N) at the end of storage. TA in both CK and 1-MCP treated fruit gradually increased within 90 days (**Supplementary Figure S1d**) and then decreased during the remaining storage time. 1-MCP treatment inhibited the decline of TA compared to CK, especially in the later storage period. The SSC of CK fruits increased to a peak value on day 30, whereas 1-MCP treatment inhibited the increase and delayed the peak to day 90. The SSC content in the 1-MCP treatment group was 7.9% lower than that in CK fruits at the end of storage (**Supplementary Figure S1e**). EC in the CK fruits gradually increased from 27.9% at the beginning of storage to 89.3% after 150 days of storage. The significant changing trend of EC was mitigated by 1-MCP treatment. The EC in CK fruits on day 60 of the storage period increased to 76.0%, while that value was only 54.5% in 1-MCP-treated fruits (**Supplementary Figure S1f**).

Effects of 1-MCP Treatment on Aroma-Related Enzyme Activities of Pear

Lipoxygenase activity increased significantly in the first 60 days of the cold storage period and then declined sharply in CK fruits, which exhibited a higher LOX activity than that in 1-MCP treated fruits (**Figure 1A**). As shown in **Figures 1B,C**, the activities of HPL and ADH were also inhibited by 1-MCP treatment, and significantly higher contents of HPL and ADH were found in CK fruits, except on days 30 and 150 ($P < 0.05$). Compared with the CK fruits, 1-MCP treatment also significantly inhibited PDC activity, which with a value of 18.8%, is lower than that in the CK fruits at the end of storage time (**Figure 1D**). The AAT activity in CK fruits gradually increased and reached the peak on day 120, whereas 1-MCP treatment significantly inhibited the increase of AAT activity, except on days 30 and 150. In particular, on day 120, the AAT activity in CK fruits was 43.6% higher than that in 1-MCP-treated fruits (**Figure 1E**) ($p < 0.05$).

Effects of 1-MCP Treatment on Aroma Components of Pear

In CK fruits, 21, 27, 26, 27, 27, and 24 aroma components were respectively detected on days 0, 30, 60, 90, 120, and 150, whereas the number of aroma components detected in 1-MCP-treated fruits on days 30, 60, 90, 120, and 150 were decreased by 4, 1, 4, 3, and 3, respectively (**Supplementary Table S1**). Thirty aroma-related compounds were identified in the "Laiyang" pear fruit, including five alcohols, three acids, 10 esters, three ketones, three alkanes, three aldehydes, and three other aroma-related compounds in this study (**Supplementary Table S2**).

As shown in **Figure 2** and **Supplementary Table S2**, the treatment with 1-MCP significantly suppressed the aroma compounds. 2-methyl-1-hexadecanol is the most abundant alcohols in the "Laiyang" pear fruit and shows a higher content in CK fruits ($p < 0.05$). Contents of ethanol, 3,7,11-trimethyl-1-dodecanol, 1-pentanol, and 1-heptanol in the 1-MCP treatment group were also relatively lower as compared with CK fruits. Total acids displayed a fluctuation during cold storage (**Supplementary Table S2**). 2-ethyl-heptanoic acid accounted for the major part of these three acids and its content in CK fruits was 841% higher than that in 1-MCP-treated fruits at the end of the storage period. Total esters increased before day 90 (CK) or day

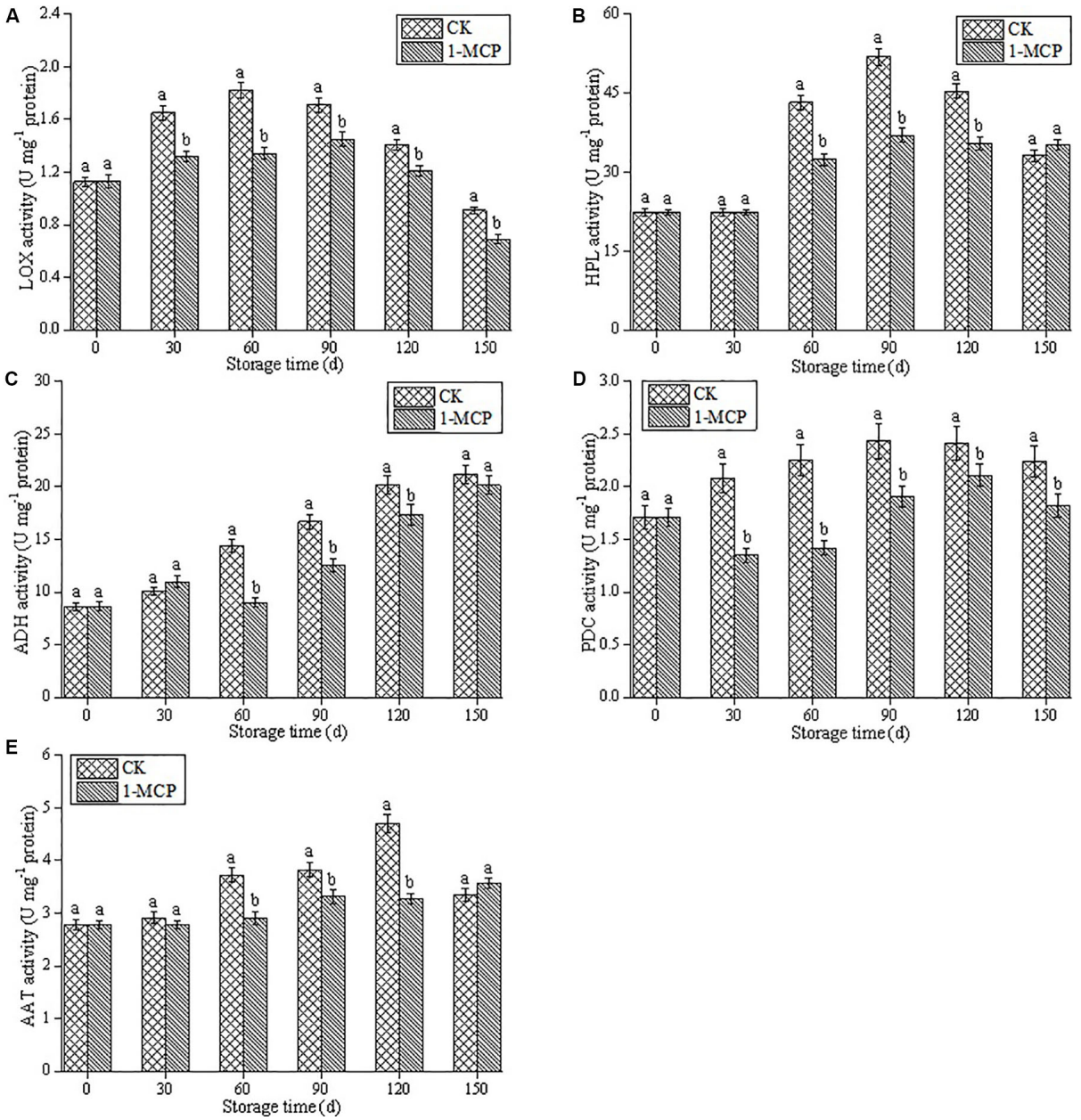

FIGURE 1 | Effects of 1-MCP on LOX activity **(A)**, HPL activity **(B)**, ADH activity **(C)**, PDC activity **(D)** and AAT activity **(E)** in pear fruit during storage at 0 ± 1°C. Vertical bars represent the standard errors of the means. Means followed by different letters at the same time differ significantly at $P < 0.05$ by Duncan's multiple range test.

150 (1-MCP treatment group). Acetic acid hexyl ester, dimethyl phthalate, and diethyl phthalate accounted for the major part of all detected ester components and their contents in CK fruits were significantly higher than those in 1-MCP-treated fruits ($p < 0.05$) (**Supplementary Table S2**). Total ketones increased before day 90 and then decreased, and the contents of these ketones in CK fruits were significantly higher than those in 1-MCP-treated fruits. Three alkanes, such as dodecamethyl-cyclohexasiloxane, 2,6,10-trimethyl-Tetradecane, and tetrapentacontane were detected in "Laiyang" pear fruits. As observed for ketones, total alkanes contents in 1-MCP-treated fruits were much lower than that in CK fruits. Aldehydes including hexanal, (E)-2-hexenal, and pentanal were identified in this study. The content of (E)-2-hexenal in CK fruits first increased and then decreased during the storage period. The content of (E)-2-hexenal in CK fruits on days 30 and 60 was significantly higher than that in 1-MCP-treated fruits ($p < 0.05$) (**Figure 2**). The contents of pentanal, both in 1-MCP-treated and CK fruit, were only detected on day 60 during the storage time. In addition, there were three other aromas including alpha-farnesene, heptanoic acid anhydride, and

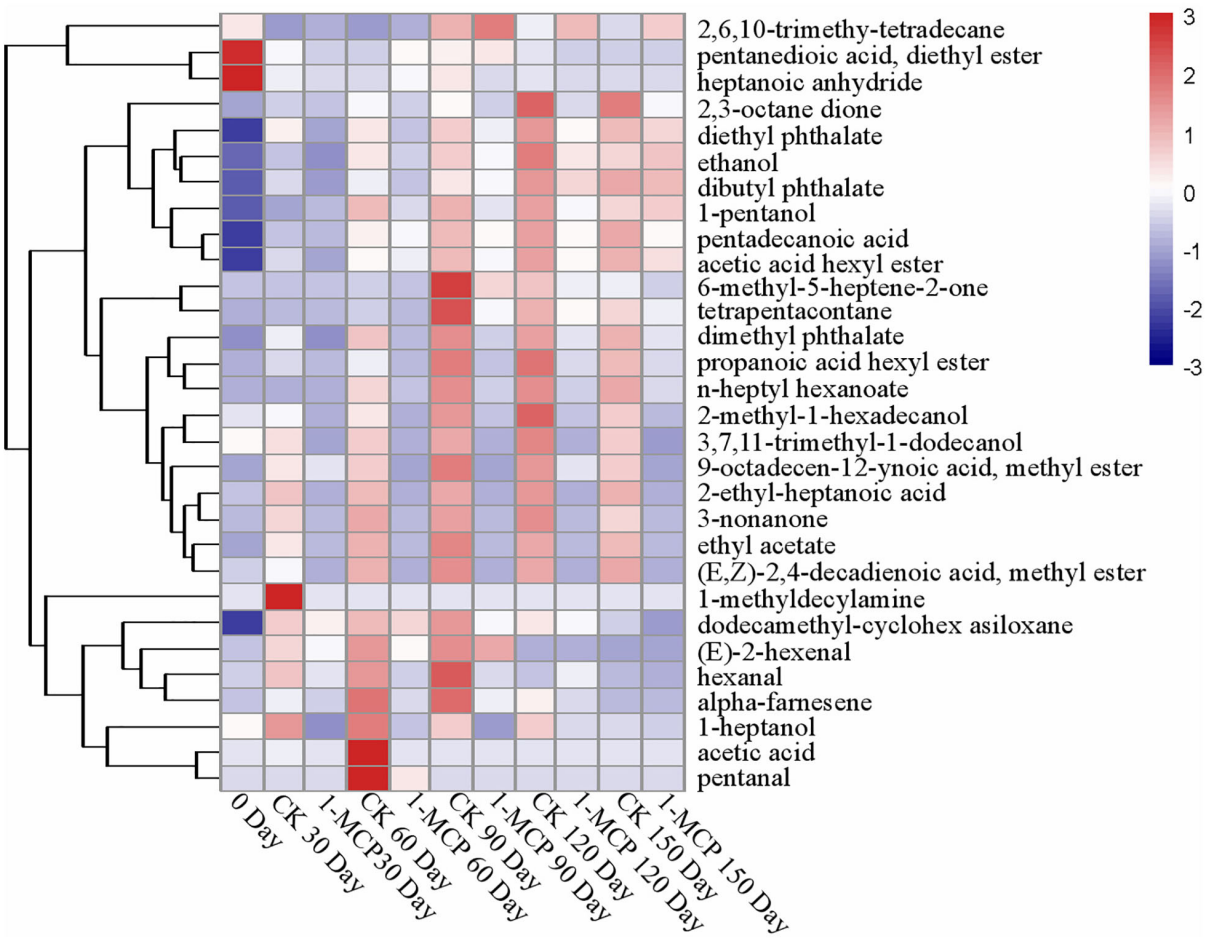

FIGURE 2 | Hierarchical clustering of a heatmap depicting the aroma (**Supplementary Table S2**) among CK and 1-MCP. The different treatments were shown in columns, and volatile aroma compounds were shown in rows. The color box for each compound indicates the abundance of the compound. The red color annotates higher abundance while the blue color annotates the lower abundance.

1-methyldecylamine, which were only detected at specific storage times (**Figure 2**).

Effects of Ethephon Treatment on Quality Traits in Pears Treated With or Without 1-MCP, After 150 Days of Cold Storage and 7 Days of Shelf-Life

As shown in **Figure 3A**, there were no significant changes observed in the firmness of fruit not treated by ethephon during the shelf life period, while the fruit firmness significantly reduced in both CK + ethephon or 1-MCP + ethephon treatment compared with those in CK or 1-MCP-treated fruits, respectively. During the 7 days shelf-life, the SSC increased by 37.1% in the 1-MCP + ethephon treatment group, but no significant difference was found among the other three treatments (**Figure 3B**). The titrate acid of CK fruit dropped sharply at the shelf-life period after treatment with ethephon, whereas no significant differences were found in the fruits treated with 1-MCP + H_2O, and 1-MCP + ethephon (**Figure 3C**).

Effect of Ethephon Treatment on Aroma-Related Enzyme Activities in Pear Treated With or Without 1-MCP After 150 Days Cold Storage and 7 Days Shelf-Life

During the shelf-life, the LOX activity in the fruits treated with 1-MCP alone or 1-MCP + ethephon was significantly higher than that in CK fruits. In addition, the LOX activity in the 1-MCP + ethephon treatment group was 63.1% higher than that in the 1-MCP + H_2O treatment group during the shelf-life, whereas the LOX activity in the CK + ethephon treatment group was 7.8% lower than that in the CK + H_2O treatment group during the shelf-life (**Figure 4A**).

As shown in **Figures 4B,C**, treatment with ethephon significantly promoted the increase of PDC and HPL activities, no matter whether the fruits were treated with 1-MCP or not. The activities of PDC and HPL in the 1-MCP + ethephon treatment group were, respectively, 44.8 and 56.4% higher than those in the 1-MCP + H_2O treatment group during the shelf-life.

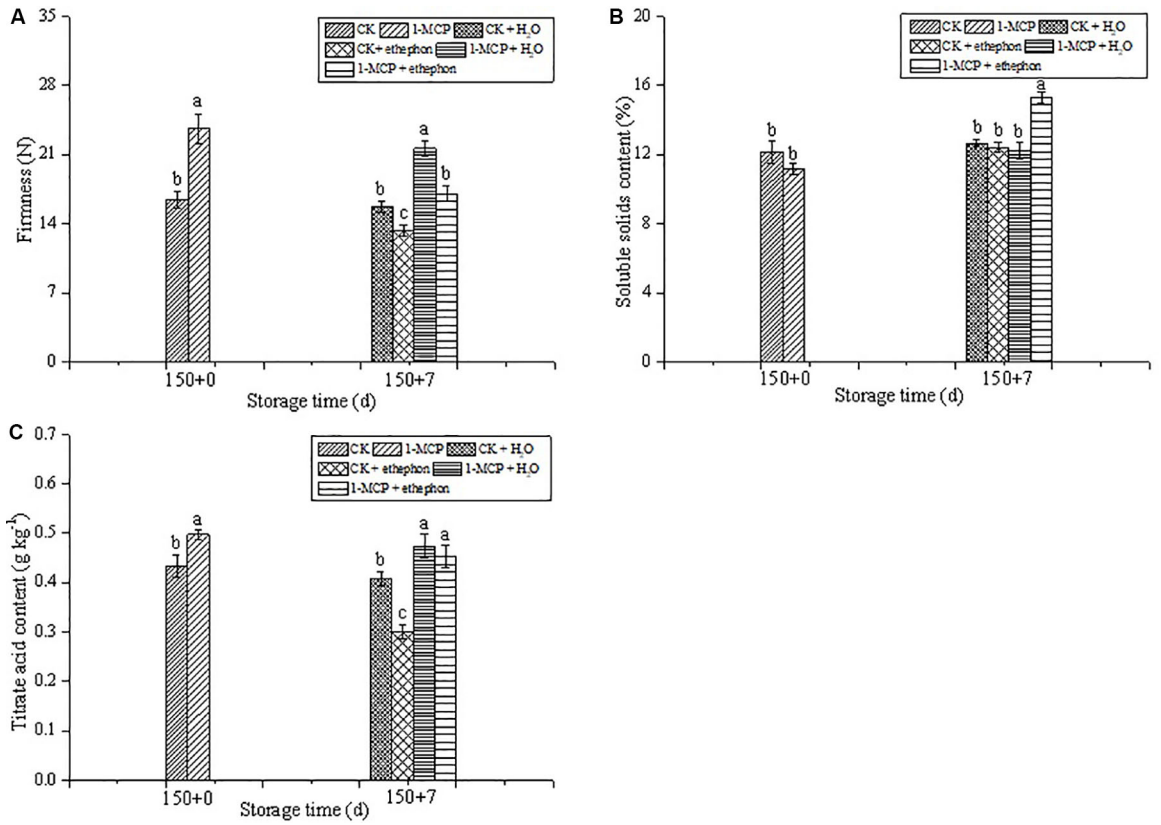

FIGURE 3 | Effects of ethephon treatment on firmness **(A)**, soluble solids content **(B)**, and titrate acid content **(C)** in pear after cold storage for 150 days + 7 days of shelf-life at 20 ± 1°C. Vertical bars represent the standard errors of the means. Means followed by different letters at the same time differ significantly at $P < 0.05$ by Duncan's multiple range test.

The PDC and HPL activities in the CK + ethephon treatment group were, respectively, 21.6 and 66.4% higher than those in the CK + H_2O treatment group. In addition, the activity of PDC in the CK + ethephon treated fruit was higher than that in the 1-MCP + H_2O group.

During the shelf-life, the highest ADH activity was observed in the 1-MCP + ethephon treatment group. No significant difference of ADH activity was found between the CK + H_2O and 1-MCP + H_2O treatment groups, whereas ADH activity in CK fruits treated with ethephon was slightly decreased (**Figure 4D**). The AAT activity of the 1-MCP group treated with or without ethephon was significantly increased during the shelf-life, but no significant difference was found in the CK groups (**Figure 4E**). In addition, the highest activity of AAT was also found in the 1-MCP + ethephon treatment group.

Effect of Ethephon Treatment on Aroma Components of Pear Treated With or Without 1-MCP After 150 Days Cold Storage and 7 Days Shelf-Life

The total alcohol contents in the CK + H_2O, 1-MCP + H_2O, and 1-MCP + ethephon treatment groups were all increased during the shelf-life. The highest total alcohol content was found in the 1-MCP + ethephon treatment group, followed by the CK + H_2O, 1-MCP + H_2O, and CK + ethephon treatment groups. Five alcohols identified in fruits during the shelf life were also found during the cold storage period. 2-methyl-1-hexadecanol was the major alcohol in pears. 2-methyl-1-hexadecanol content was the highest, amongst all the treatment groups, in the 1-MCP + ethephon treatment group. Most notably, the contents of another four alcohols including 3,7,11-trimethyl-1-dodecanol, 1-pentanol, ethanol, and 1-heptanol in the 1-MCP + ethephon treatment group increased significantly during the shelf-life and were much higher than those in the other three treatment groups. The acids were all significantly increased in the 1-MCP + H_2O/ethephon treatment group during the shelf-life period (**Supplementary Table S3**).

The total ester contents in the 1-MCP treatment group and CK treatment group, during the 150 days storage at 0 ± 1°C, were lower than that in the 1-MCP + H_2O and 1-MCP + ethephon treatment groups in the shelf life, but higher than that in the CK + H_2O and CK + ethephon treatment group in the shelf life (**Supplementary Table S3**). Acetic acid hexyl ester, dimethyl phthalate, and diethyl phthalate were the three major esters found and all increased sharply in the 1-MCP + ethephon treatment group during the shelf-life period, the contents of which were the highest in the 1-MCP + ethephon treatment group, with

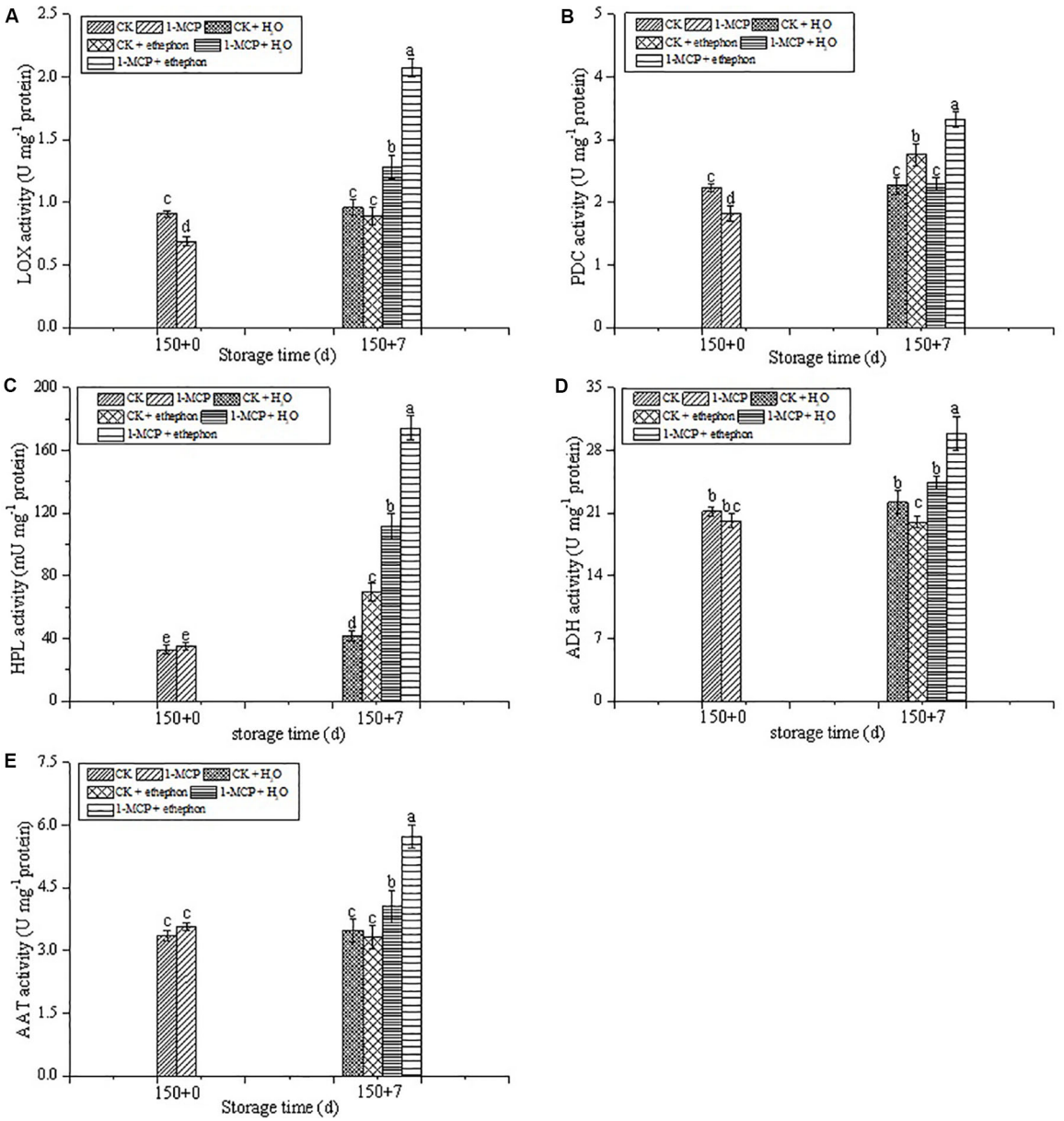

FIGURE 4 | Effects of ethephon treatment on the activities of LOX **(A)**, PDC **(B)**, HPL **(C)**, ADH **(D)**, and AAT **(E)** in pear after cold storage for 150 days + 7 days of shelf-life at 20 ± 1°C. Vertical bars represent the standard errors of the means. Means followed by different letters at the same time differ significantly at $P < 0.05$ by Duncan's multiple range test.

a value about 63.3, 80.1, and 51.7% higher than those in the 1-MCP + H_2O, CK + ethephon and CK + H_2O treatment groups. Total ketones in all the treatment groups showed a similar changing trend to the esters during the shelf-life, but the total content of ketones was much lower than that of esters (**Supplementary Table S3**).

The total content of alkanes in all the treatment groups during the shelf life was higher than that in the fruits during the 150 days storage period at 0 ± 1°C. The highest total content of alkanes found amongst all the treatment groups was in the 1-MCP + ethephon treatment group. 2,3-octane dione and 6-methyl-5-heptene-2-one were the two main alkanes identified. All three alkanes were increased during the shelf-life, except for dodecamethyl-cyclohexasiloxane, which was not detected in the CK + ethephon or 1-MCP + ethephon treatment group during the shelf-life (**Supplementary Table S3**).

Aldehydes were only detected in a specific treatment. As for (E)-2-hexeanl, no significant difference was found between the CK + H_2O and CK + ethephon treatment groups. The compound of pentanal was only detected in the CK + ethephon and 1-MCP + ethephon treatment groups. In addition, alpha-farnesene and heptanoic acid anhydride were also detected in

all treated fruits during the shelf-life, the content of which were also highest in the 1-MCP + ethephon treatment group (**Supplementary Table S3**).

Principal Component Analysis (PCA) and Hierarchical Clustering Heatmap Analysis

The effect of ethephon treatment on the aroma production in fruits during the shelf-life period (**Supplementary Table S3**) was also clearly depicted in the PCA plot (**Figure 5A**). The PCA highlighted the distribution of the samples in a hyperspace defined by two principal components (PC1: 61.0% and PC2: 22.0%), which accounted for 83.0% of the entire variability in the aroma components during the shelf life. The distinct profile of aroma components in the 1-MCP + ethephon treatment group was observed in the PCA plot (**Figure 5A**). CK, CK + H_2O, 1-MCP, and 1-MCP + H_2O treatment groups were located in the PC1 negative area of the plot, and the 1-MCP + ethephon treatment group was located in the extreme region of the PC1 positive quadrant. In addition, the CK + ethephon treatment group was also located in the PC1 positive quadrant but near the positive/negative boundary. Remarkably, the second principal component (PC2) distinguished the 1-MCP and 1-MCP + H_2O treatment groups from the CK and CK + H_2O treatment groups in the PC1 negative area of the plot. The 1-MCP + ethephon and the CK + ethephon treatment group in the PC1 positive area of the plot were also distinguished from each other by the PC2. The CK and 1-MCP + ethephon treatment groups were clearly discriminated from all other samples. 2-methyl-1-hexadecanol (S1), (E,Z)-2,4-decadienoic acid, methyl ester (S14), 9-octadecen-12-ynoic acid, methyl ester (S17), 3-nonanone (S19), and 2,3-octane dione (S20) contributed more to the aroma components of the CK group. On the other hand, acetic acid (S6), 2,6,10-trimethyl-tetradecane (S23), pentanedioic acid, diethyl ester (S18), heptanoic anhydride (S29), hexanal (S25), tetrapentacontane (S24), alpha-farnesene (S28), dibutyl phthalate (S16), ethanol (S4), pentanal (S27), 3,7,11-trimethyl-1-dodecanol (S2), 1-pentanol (S3), 1-heptanol (S5), pentadecanoic acid (S8), propanoic acid hexyl ester (S11), diethyl phthalate (S15), acetic acid hexyl ester (S10), n-heptyl hexanoate (S13), 6-methyl-5-heptene-2-one (S21), and ethyl acetate (S9) contributed more to the aroma components of the 1-MCP + ethephon treatment group.

The specific content of aromas was furthermore graphically reordered with a hierarchical clustering heatmap (**Figure 5B**) that showed a gradual and linear shift of aroma components from the CK to 1-MCP + ethephon treatment group. The cluster of aromas with lower content in 1-MCP was significantly increased in the 1-MCP + ethephon treatment group, while, on the contrary, the aroma with a higher content in CK resulted in a strong decrease in the CK + ethephon treatment group.

DISCUSSION

1-MCP as a competitive inhibitor, binding irreversibly to the ethylene receptor, blocks ethylene action and influences ethylene biosynthesis through feedback inhibition in a broad range of horticultural crops. Therefore, post-harvest application of 1-MCP is a common and effective technology for the quality maintenance of various fruits and vegetables (Cai et al., 2006; Façanha et al., 2019; Massolo et al., 2019). Previous research on "d" Anjou' pears (Argenta et al., 2003), "William's" pears (Xie et al., 2014), "Red Clapp's" pears (Calvo and Sozzi, 2004), and "Packham's Triumph" pears (Moya-León et al., 2006) showed that 1-MCP treatment had tremendous potential for maintaining the quality of pear fruits and significantly inhibited the development of physiological disorders during storage. Our previous results also demonstrated that 0.5 μl L^{-1} 1-MCP treatment effectively prevented fruit core browning and maintained Vc contents and flesh color of the "Laiyang" pear fruit (Li F. et al., 2013). On this basis, we further explored its effects on fruit quality and aroma components in the present study. The results demonstrated that treatment with 0.5 μl L^{-1} 1-MCP significantly delayed fruit senescence, as shown in **Supplementary Figure S1**. Although the firmness and titratable acidity were not affected by 1-MCP within 90 days, 1-MCP treatment significantly inhibited the decline of firmness and titratable acidity at the later stage of storage. In the study, we also found that the accumulation of aroma volatile compounds in "Laiyang" pear fruits was inhibited by 1-MCP during the cold storage. Previous research found that volatile compounds were produced through several biosynthetic pathways, and fatty acid metabolism was a key pathway for aroma volatile biosynthesis in most fruits, which comprises four key enzymes, including LOX, HPL, ADH, and AAT (Bartley et al., 1985; Dudareva et al., 2013). LOX and HPL are essential for the formation of aldehydes, which are reduced to alcohols in ADH-catalyzed reactions (Defilippi et al., 2009; Dudareva et al., 2013). AAT catalyzes the biosynthesis of esters and a significant correlation between AAT activity and ester formation has been reported in pears (*Pyrus ussuriensis* Maxim) (Li G. et al., 2013). In the study, the contents of aldehydes increased before 90 days and then decreased. Analysis of the activities of LOX and HPL found that the change trend of the enzymes was similar to that of the aldehydes content. Production of total esters aroma compounds are very low in fruits treated with 1-MCP in comparison to CK. According to Rizzolo et al. (2005) ethyl acetate was identified as an important volatile in the "Conference" pear aroma. We found that ethyl acetate, acetic acid hexyl ester, dimethyl phthalate, diethyl phthalate and (E,Z)-2,4-Decadienoic acid, and methyl ester accounted for most of the ester aroma of "Laiyang" pears. These ester aroma compounds were also detected in "Conference," "Alexander Lucas," and "Nanguoli" pears (Li G. et al., 2013; Hendges et al., 2018). In addition, dimethyl phthalate and diethyl phthalate were also detected in "Laiyang" pears in our study, which have not been reported in other pear varieties, but which have been reported in other fruits such as longans and peaches (Chen et al., 2010; Xu et al., 2012). The highest content of esters was found in CK fruit after being stored for 120 days, which was closely related the activity of AAT (**Figure 1E**). Particularly, 1-MCP treatment significantly suppressed the increase of ethyl acetate, propanoic acid hexyl ester, dimethyl phthalate, n-heptyl hexanoate, (E,Z)-2,4-Decadienoic acid methyl ester, and 9-octadecen-12-ynoic acid methyl ester. In addition, though the

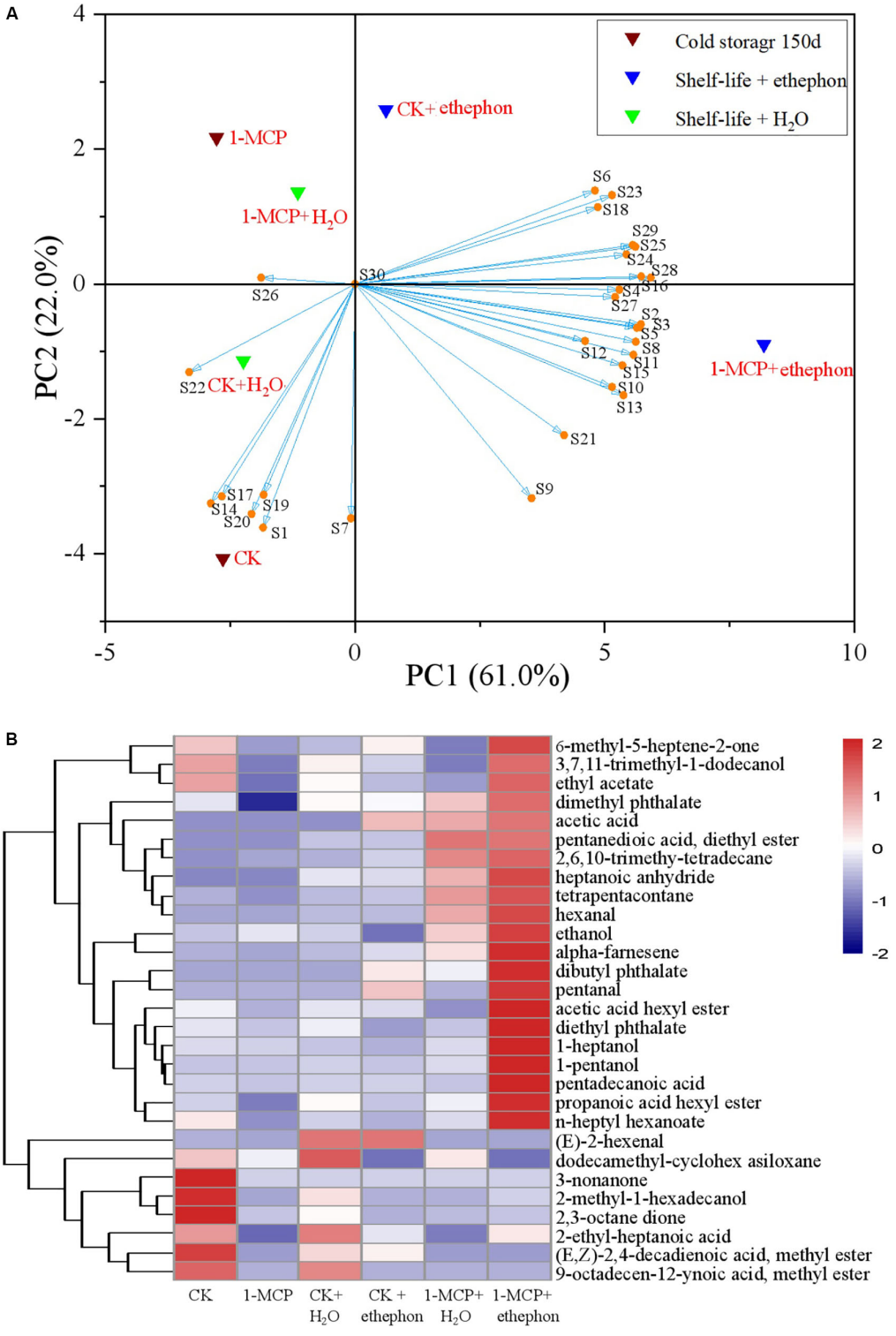

FIGURE 5 | Principal component analysis (PCA) biplot **(A)** of the first two principal components (PC1 and PC2) and hierarchical cluster analysis **(B)** of the aroma compounds in different treatment pears. **(A)** Control or pear fruit treated with 1-MCP during cold storage for 150 days are indicated as CK and 1-MCP, respectively. During 7 days of shelf life, the fruit further treated with 2 mmol L^{-1} ethephon (marked as CK + ethephon or 1-MCP + ethephon) or distilled water (marked as CK + H_2O or 1-MCP + H_2O). Compounds represented in S from **Supplementary Table S3**. **(B)** Hierarchical clustering of a heatmap depicting the aroma (**Table 3**) among CK, 1-MCP, CK + H_2O, 1-MCP + H_2O, CK + ethephon and 1-MCP + ethephon treatments. The different treatments were shown in columns, and volatile aroma compounds were shown in rows. The color box for each compound indicates the abundance of the compound. The red color annotates higher abundance while the blue color annotates the lower abundance.

activities of ADH, HPL, and AAT showed no significant difference between CK and 1-MCP on day 30, the aroma compounds of alcohols, aldehydes and esters were higher in CK. The contents of 1-pentanol, ethanol, n-heptyl hexanoate, dibutyl phthalate, and dodecamethyl-cyclohexasiloxane showed no significant difference according to the activities of ADH, HPL, and AAT. Previous research also noted that 1-MCP treatment reduced the characteristic aroma in "Nanguo" Pears (Dong et al., 2010). A lower production of alcohols, aldehydes, and esters was found in d'Anjou pears treated with 1-MCP (Argenta et al., 2003). Hendges et al. (2018) found lower levels of 1-butanol, butyl, and hexyl acetates in "Conference" pears which were harvested from the first maturity stage and treated with 1-MCP before cold storage. Therefore, although 1-MCP could delay the post-harvest senescence of pear fruits, its negative effects on the formation of aroma compounds should not be overlooked. How to maintain the physiological quality of the fruit and how to reduce the loss of aroma has become a problem that needs to be solved.

The mechanisms of 1-MCP inhibition of aroma formation were reportedly due to the suppression of the expression of genes involved in volatiles synthesis, including *LOX*, *HPL*, *ADH*, and *AAT* in fruits (Li G. et al., 2016; Cai et al., 2018). In our study, the significant depression of the activities of aroma-related enzymes (LOX, HPL, ADH, PDC, and AAT) was found in the 1-MCP treatment group. Despite the fact that an inhibitory effect of 1-MCP on volatile aroma has been discovered in fruit, the way to restore aroma has seldomly been reported. It is well known that ethylene plays an important role in the ripening of climacteric fruits and initiating and coordinating diverse processes including the aroma formation (Torregrosa et al., 2020). Günther et al. (2015) also reported that a reduction in the rate of ethylene production during refrigerated storage resulted in a decrease in the production of volatile aroma compounds. Ethephon influences several metabolic pathways of climacteric fruits and plays an important role in the formation of aroma compounds (Xu et al., 2015; Li Y. et al., 2016; Wang et al., 2016). Schaffer et al. (2007) showed that a transgenic line of apple with no detection of ethylene had very low aroma levels. We explored the role of ethylene in aroma recovery by measuring the effect of ethephon on the aroma component and content of pears under different treatments. Combined with the detection of aroma related enzymes, we found that activities of aroma-related enzymes (LOX, HPL, ADH, PDC, AAT) in 1-MCP + ethephon, improved significantly compared to other treatments. Moreover, we found that the activity of PDC in CK + ethephon was higher than that in 1-MCP + H_2O. Analysis of aldehydes showed that (E)-2-hexenal and pentanal were higher in CK + ethephon. In addition, the ester aroma compounds such as acetic acid hexyl ester, propanoic acid hexyl ester, dimethyl phthalate, n-heptyl hexanoate, diethyl phthalate, dibutyl phthalate, pentanedioic acid, and diethyl ester (**Figure 5B**) improved significantly in 1-MCP + ethephon fruits. We analyzed the results and found that the enhanced ester aroma compounds may be related to the increase of AAT activity, which was similar to the results reported by Li G. et al. (2013). Moreover, Li Y. et al. (2016) reported that the level of acetate, hexanoate, and hexyl esters and the activities of LOX, ADH, and AAT in sweet melon were significantly increased by ethephon. The hexanal and pentanal are two main aldehydes which increased 12.16 and 5.09 times, respectively, in 1-MCP + ethephon treated fruits compared with 1-MCP treated fruits. These results suggested that the additional application of ethephon during shelf-life was a promising way to allow recovery of aroma components after long-term cold storage of "Laiyang" pears.

In conclusion, compared with the storage at 0 ± 1°C without any treatment, 1-MCP treatment more effectively controlled ripening and senescence of Laiyang pear fruits under cold storage conditions. However, the activities of aroma-related enzymes, such as LOX, PDC, HPL, ADH, and AAT, as well as the important aroma volatiles, such as esters and ketone, were negatively influenced by 1-MCP treatment during the cold storage period. During the shelf-life period after 150 days of cold storage, the application of ethephon could significantly increase the activities of aroma-related enzymes (LOX, PDC, HPL, ADH, and AAT) and the aroma components. Moreover, compared with the CK group, without being treated with 1-MCP or ethephon, 1-MCP + ethephon treatment had no effect on fruit firmness, but it increased the contents of SSC and TA in fruits during the shelf-life period. Therefore, the application of ethephon during shelf-life has the potential for commercial application to allow recovery of aroma components after long-term cold storage of "Laiyang" pears.

DATA AVAILABILITY STATEMENT

All datasets generated or analyzed for this study are included in the article.

AUTHOR CONTRIBUTIONS

XZ and FL conceived and designed the research. PS drafted the manuscript and analyzed all data. DM, JZ, WA, JL, and ZL carried out most of the experiments together, with close supervision from XZ, XL, and YG. ZS and YS performed the quality indexes analysis. All authors read and approved the manuscript.

FUNDING

This work was supported by the National Natural Science Foundation of China (Nos. 31772024 and 31101587).

ACKNOWLEDGMENTS

We are grateful to the Toppaper (http://www.toppaper.cn) for language polishing in the manuscript.

SUPPLEMENTARY MATERIAL

The Supplementary Material for this article can be found online at: https://www.frontiersin.org/articles/10.3389/fpls.2020.00490/full#supplementary-material

REFERENCES

Argenta, L. C., Fan, X., and Mattheis, J. P. (2003). Influence of 1-methylcyclopropene on ripening, storage life, and volatile production by d\"Anjou cv. pear fruit. *J. Agric. Food Chem.* 51, 3858–3864. doi: 10.1021/jf034028g

Balbontin, C., Gaete-Eastman, C., Vergara, M., Herrera, R., and Moya-León, M. A. (2007). Treatment with 1-MCP and the role of ethylene in aroma development of mountain papaya fruit. *Postharvest Biol. Tech.* 43, 67–77.

Bartley, I. M., Stoker, P. G., Martin, A. D. E., Hatfield, S. G. S., and Knee, M. (1985). Synthesis of aroma compounds by apples supplied with alcohols and methyl esters of fatty acids. *J. Sci. Food Agr.* 36, 567–574.

Blankenship, S. M., and Dole, J. M. (2003). 1-Methylcyclopropene: a review. *Postharvest Biol. Tech.* 28, 1–25.

Both, V., Thewes, F. R., Brackmann, A., Ferreira, D. D. F., Pavanello, E. P., and Wagner, R. (2016). Effect of low oxygen conditioning and ultralow oxygen storage on the volatile profile: ethylene production and respiration rate of 'Royal Gala' apples. *Sci. Hortic.* 209, 156–164.

Botondi, R., De Sanctis, F., Bartoloni, S., and Mencarelli, S. (2014). Simultaneous application of ethylene and 1-MCP affects banana ripening features during Storage. *J. Sci. Food Agric.* 94, 2170–2178. doi: 10.1002/jsfa.6599

Bradford, M. M. (1976). A rapid and sensitive method for the quantitation of microgram quantities of protein utilizing the principle of protein-dye binding. *Anal. Biochem.* 72, 248–254. doi: 10.1006/abio.1976.9999

Cai, C., Chen, K. S., Xu, W. P., Zhang, W. S., Li, X., and Fergusan, L. (2006). Effect of 1-MCP on postharvest quality of loquat fruit. *Postharvest Biol. Tech.* 40, 155–162.

Cai, H., An, X., Han, S., Jiang, L., Yu, M., Ma, R., et al. (2018). Effect of 1-MCP on the production of volatiles and biosynthesis-related gene expression in peach fruit during cold storage. *Postharvest Biol. Tech.* 141, 50–57.

Calvo, G., and Sozzi, G. O. (2004). Improvement of postharvest storage quality of 'Red Clapp's' pears by treatment with 1-methylcyclopropene at low temperature. *J. Hortic. Sci. Biotech.* 79, 930–934.

Chen, F. X., Wu, S. H., Zheng, S. X., Sheng, S. L., Li, Y. Y., et al. (2010). The preliminary determination of volatile constituents of Longan arillus, epicarpium and seeds by gas chromatography-mass spectrometry coupled with solid-phase microextraction. *Acta Hortic.* 863, 653–658.

Cheng, Y., Liu, L., Feng, Y., Dong, Y., and Guan, J. (2019). Effects of 1-MCP on fruit quality and core browning in 'Yali' pear during cold storage. *Sci. Hortic.* 243, 350–356.

Chiriboga, M., Schotsmans, W. C., Dupille, E., Larrigaudière, C., Dupille, E., and Recasens, I. (2011). How to prevent ripening blockage in 1-MCP-treated 'Conference' pear. *J. Sci. Food Agric.* 91, 1781–1788. doi: 10.1002/jsfa.4382

Defilippi, B. G., Kader, A. A., and Dandekar, A. M. (2005). Apple aroma: alcohol acyltransferase, a rate limiting step for ester biosynthesis, is regulmed by ethylene. *Plant Sci.* 168, 1199–1210.

Defilippi, B. G., Manríquez, D., Luengwilai, K., and González-Agüero, M. (2009). Aroma volatiles: biosynthesis and mechanisms of modulation during fruit ripening. *Adv. Bot. Res.* 50, 1–37.

Dong, P., Xin, G., Zhang, B., Feng, F., and Chun, L. T. (2010). Effect of 1-MCP treatment on fruit aroma components in Nanguo pears during storage at 20 oC. *Food Sci.* 109, 477–479.

Dudareva, N., Klempien, A., Muhlemann, J. K., and Klpan, I. (2013). Biosynthesis, function and metabolic engineering of plant volatile organic compounds. *New Phytol.* 2013, 16–32. doi: 10.1111/nph.12145

Façanha, R. V., Spricigo, P. C., Purgatto, E., Purgatto, E., and Jacominoa, A. P. (2019). Combined application of ethylene and 1-methylcyclopropene on ripening and volatile compound production of 'Golden' papaya. *Postharvest Biol. Tech.* 151, 160–169.

Fan, M., Li, W., Hu, X., Sun, Y., Yu, G., and Zhang, X. (2016). Effect of micro-vacuum storage on active oxygen metabolism, internal browning and related enzyme activities in Laiyang pear (*Pyrus bretschneideri* Reld). *LWT-Food Sci. Technol.* 72, 467–474.

Günther, C. S., Marsh, K. B., Winz, R. A., Harkera, R. F., Wohlersa, M. W., Whitea, A., et al. (2015). The impact of cold storage and ethylene on volatile ester production and aroma perception in 'Hort16A' kiwifruit. *Food Chem.* 169, 5–12. doi: 10.1016/j.foodchem.2014.07.070

Hendges, M. V., Neuwald, D. A., Steffens, C. A., Vidrih, R., Zlatić, E., and do Amarantea, C. V. T. (2018). 1-MCP and storage conditions on the ripening and production of aromatic compounds in Conference and Alexander Lucas pears harvested at different maturity stages. *Postharvest Biol. Tech.* 146, 18–25.

Lara, I., Miró, R. M., Fuentes, T., Sayez, G., Graell, J., and López, M. L. (2003). Biosynthesis of volatile aroma compounds in pear fruit stored under long-term controlled-atmosphere conditions. *Postharvest Biol. Tech.* 29, 29–39.

Li, F., Zhang, X., Song, B., Li, J., Shang, Z., and Guan, J. (2013). Combined effects of 1-MCP and MAP on the fruit quality of pear (*Pyrus bretschneideri* Reld cv. Laiyang) during cold storage. *Sci. Hortic.* 164, 544–551.

Li, G., Jia, H., Wu, R., and Teng, Y. (2013). Changes in volatile organic compound composition during the ripening of 'Nanguoli'pears (*Pyrus ussuriensis* Maxim) harvested at different growing locations. *J. Hortic. Sci. Biotechnol.* 88, 563–570.

Li, L., Lichter, A., Chalupowicz, D., Gamrasni, D., Goldberg, T., Nerya, O., et al. (2016). Effects of the ethylene-action inhibitor 1-methylcyclopropene on postharvest quality of non-climacteric fruit crops. *Postharvest Biol. Tech.* 111, 322–329.

Li, Y., Qi, H., Jin, Y., Tian, X., Sui, L., and Qiu, Y. (2016). Role of ethylene in biosynthetic pathway of related-aroma volatiles derived from amino acids in oriental sweet melons (*Cucumis melo* var. makuwa Makino). *Sci. Hortic.* 201, 24–35.

Li, G., Jia, H., Li, J., Li, H., and Teng, Y. (2016). Effects of 1-MCP on volatile production and transcription of ester biosynthesis related genes under cold storage in 'Ruanerli' pear fruit (*Pyrus ussuriensis* Maxim.). *Postharvest Biol. Tec.* 111, 168–174.

Liu, H., Jiang, W., Cao, J., and Ma, L. (2018). A combination of 1-methylcyclopropene treatment and intermittent warming alleviates chilling injury and affects phenolics and antioxidant activity of peach fruit during storage. *Sci. Hortic.* 229, 175–181.

Liu, R., Lai, T., Xu, Y., and Tian, S. (2013). Changes in physiology and quality of Laiyang pear in long time storage. *Sci. Hortic.* 150, 31–36.

Massolo, J. F., Zarauza, J. M., Hasperué, J. H., Rodoni, L. M., and Vicente, A. R. (2019). Maturity at harvest and postharvest quality of summer squash. *Pesqui. Agropecu. Bras.* 54, 1–10.

Moya-León, M. A., Vergara, M., Bravo, C., Montes, M. E., and Moggia, C. (2006). 1-MCP treatment preserves aroma quality of 'Packham\"s Triumph' pears during long-term storage. *Postharvest Biol. Tech.* 42, 185–197.

Nath, A., and Panwar, A. S. (2018). *"Postharvest Biology and Technology of Pear." Postharvest Biology and Technology of Temperate Fruits*. Cham: Springer, 245–271.

Neuwald, D. A., Streif, J., and Kittemann, D. (2015). Effects of 1-MCP treatment in combination with ethylene on storage behavior and fruit ripening of 'Conference' pears. *Acta. Hortic.* 1079, 459–464.

Pérez, A. G., Sanz, C., Olías, R., Ríos, J. J., and Olías, J. M. (1996). Evolution of strawberry alcohol acyltransferase activity during fruit development and storage. *J. Agric. Food Chem.* 44, 3286–3290.

Rizzolo, A., Cambiaghi, P., Grassi, M., and Eccher Zerbini, P. E. (2005). Influence of 1-methylcyclopropene and storage atmosphere on changes in volatile compounds and fruit quality of Conference pears. *J. Agric. Food Chem.* 53, 781–789. doi: 10.1021/jf051339d

Saltveit, M. E. (1999). Effect of ethylene on quality of fresh fruits and vegetables. *Postharvest Biol. Tech.* 15, 279–292. doi: 10.1021/jf904540m

Schaffer, R. J., Friel, E. N., Souleyre, E. J. F., Bolitho, K., Thodey, K., Ledger, S., et al. (2007). A genomics approach reveals that aroma production in apple is controlled by ethylene predominantly at the final step in each biosynthetic pathway. *Plant Physiol.* 144, 1899–1912. doi: 10.1104/pp.106.093765

Sundaram, S., and Prabhakaran, J. (2017). Effect of 1-methylcyclopropene (1-MCP) on volatile compound production in papaya (*Carica papaya* L.) fruit. *Pharm. Innovat. J.* 6, 532–536.

Torregrosa, L., Echeverria, G., Illa, J., Torres, R., and Giné-bordonaba, J. (2020). Spatial distribution of flavor components and antioxidants in the flesh of 'Conference' pears and its relationship with postharvest pathogens susceptibility. *Postharvest Biol. Tech.* 159, 111004.

Vick, B. A. (1991). A spectrophotometric assay for hydroperoxide lyase. *Lipids* 26, 15–320.

Wang, L., Luo, W., Sun, X., and Qian, C. (2018). Changes in flavor-relevant compounds during vine ripening of tomato fruit and their relationship with ethylene production. *Hortic. Environ. Biotech.* 59, 787–804.

Wang, R. H., Yuan, X. Y., Meng, L. H., Zhu, B. Z., Zhu, H. L., Luo, Y. B., et al. (2016). Transcriptome analysis provides a preliminary regulation route of the ethylene signal transduction component, SlEIN2, during tomato ripening. *PLoS One* 11:e168287. doi: 10.1371/journal.pone.0168287

Xie, X., Song, J., Wang, Y., and Sugar, D. (2014). Ethylene synthesis, ripening capacity, and superficial scald inhibition in 1-MCP treated 'd'Anjou' pears are affected by storage temperature. *Postharvest Biol. Tech.* 97, 1–10.

Xu, C., Wang, C., Ju, L., Zhang, R., Biggs, A. R., Tanaka, B. E., et al. (2015). Multiple locus genealogies and phenotypic characters reappraise the causal agents of apple ring rot in China. *Fungal Divers.* 71, 215–231.

Xu, F., Dong, S., Xu, Q., and Liu, S. (2020). Control of brown heart in Huangguan pears with 1-methylcyclopropene microbubbles treatment. *Sci. Hortic.* 259:108820.

Xu, Z. H., Jia, J. H., Lv, X. L., Peng, Y. J., Xu, T., and Hong, G. (2012). Effect of high hydrostatic pressure and heat sterilization on volatile components in peach juice. *Food Sci.* 33, 25–27.

Yang, X., Song, J., Du, L., Forney, C., Leslie, C. H., Sherry, F., et al. (2016). Ethylene and 1-MCP regulate major volatile biosynthetic pathways in apple fruit. *Food. Chem.* 194, 325–336. doi: 10.1016/j.foodchem.2015.08.018

Zhang, P., and Zhou, Z. (2019). Postharvest ethephon degreening improves fruit color, flavor quality and increases antioxidant capacity in 'Eureka' lemon (*Citrus limon* (L.) Burm. f.). *Sci. Hortic.* 248, 70–80.

Zhang, X., Shen, L., Li, F., Meng, D., and Sheng, J. (2013). Amelioration of chilling stress by arginine in tomato fruit: changes in endogenous arginine catabolism. *Postharvest Biol. Tech.* 76, 106–111.

Zhang, Y., Gao, B., Zhang, M. W., Shi, J., and Xu, Y. J. (2009). Headspace solid-phase microextraction–gas chromatography–mass spectrometry analysis of the volatile components of longan (*Dimocarpus longan* Lour.). *Eur. Food Res. Technol.* 229, 457–465. doi: 10.1007/s00217-009-1076-2

Zhu, X., Shen, L., Fu, D., Si, Z., Wu, B., Chen, W., et al. (2015). Effects of the combination treatment of 1-MCP and ethylene on the ripening of harvested banana fruit. *Postharvest Biol. Tech.* 107, 23–32.

Conflict of Interest: The authors declare that the research was conducted in the absence of any commercial or financial relationships that could be construed as a potential conflict of interest.

frontiers in Plant Science

ORIGINAL RESEARCH
published: 09 June 2020
doi: 10.3389/fpls.2020.00707

Trunk Girdling Increased Stomatal Conductance in Cabernet Sauvignon Grapevines, Reduced Glutamine, and Increased Malvidin-3-Glucoside and Quercetin-3-Glucoside Concentrations in Skins and Pulp at Harvest

Giuliano E. Pereira[1,2], Emily M. T. Padhi[3], Raul C. Girardello[2], Cristina Medina-Plaza[2], Dave Tseng[2], Robert C. Bruce[2], Jesse N. Erdmann[2], Sahap K. Kurtural[2], Carolyn M. Slupsky[3,4] and Anita Oberholster[2]**

[1] Brazilian Agricultural Research Corporation-Embrapa Grape & Wine, Bento Goncalves, Brazil, [2] Department of Viticulture and Enology, University of California, Davis, Davis, CA, United States, [3] Department of Food Science and Technology, University of California, Davis, Davis, CA, United States, [4] Department of Nutrition, University of California, Davis, Davis, CA, United States

OPEN ACCESS

Edited by:
Francesco Emanuelli,
Fondazione Edmund Mach, Italy

Reviewed by:
Chiara Pastore,
University of Bologna, Italy
Marianna Fasoli,
E. & J. Gallo Winery, United States

***Correspondence:**
Giuliano E. Pereira
giuliano.pereira@embrapa.br
Anita Oberholster
aoberholster@ucdavis.edu

Specialty section:
This article was submitted to Crop and Product Physiology, a section of the journal Frontiers in Plant Science

Received: 26 November 2019
Accepted: 05 May 2020
Published: 09 June 2020

Citation:
Pereira GE, Padhi EMT, Girardello RC, Medina-Plaza C, Tseng D, Bruce RC, Erdmann JN, Kurtural SK, Slupsky CM and Oberholster A (2020) Trunk Girdling Increased Stomatal Conductance in Cabernet Sauvignon Grapevines, Reduced Glutamine, and Increased Malvidin-3-Glucoside and Quercetin-3-Glucoside Concentrations in Skins and Pulp at Harvest. Front. Plant Sci. 11:707. doi: 10.3389/fpls.2020.00707

Girdling is a traditional horticultural practice applied at fruit set or other phenological stages, and is used mostly as a vine management. In grapevines, it is used primarily for table grapes to improve berry weight, sugar content, color, and to promote early harvest. The objective of this study was to evaluate the effect of trunk girdling applied at veraison, in 'Cabernet Sauvignon' wine grapes (*Vitis vinifera* L.), on agronomical and physiological parameters during vine development from the onset of ripening (veraison) to harvest, and additionally to quantify the effect of girdling on primary and secondary metabolism. Girdling was applied 146 days after pruning (dap) at veraison, when berry sampling for metabolomics and agronomical evaluations commenced, with a further three sampling dates until harvest, at 156 dap (30% maturation, 10 days after girdling-dag), 181 dap (70% maturation, 35 dag), and 223 dap (commercial harvest, 77 dag). Skin/pulp and seed tissues were extracted separately and metabolomics was performed using one-dimensional proton nuclear magnetic resonance (1D ^{1}H NMR) spectroscopy and high performance liquid chromatography (HPLC-DAD). At harvest, girdling significantly increased stomatal conductance (g_s) in vines, decreased glutamine concentrations, and increased anthocyanin and flavonol concentrations in the skin/pulp tissues of grape berries. Berry weight was reduced by 27% from 181 dap to harvest, and was significantly higher in grapes from girdled vines at 181 dap. Sugars, organic acids, and other amino acids in skin/pulp or seeds were not significantly different, possibly due to extra-fascicular phloem vessels transporting metabolites from leaves

to the roots. Using a metabolomics approach, differences between skin/pulp and seeds tissues were meaningful, and a greater number of secondary metabolites in skin/pulp was affected by girdling than in seeds. Girdling is a simple technique that could easily be applied commercially on vine management to improve berry color and other phenolics in 'Cabernet Sauvignon' grapes.

Keywords: amino acids, biosynthesis, grape and wine, ^{1}H NMR spectroscopy, metabolome, organic acids, phenolic compounds and sugars, *Vitis vinifera* L.

INTRODUCTION

'Cabernet Sauvignon,' originating from France, is the most important grape variety used for red wines, varietal, or blended in all winegrowing regions worldwide. In Napa Valley, California, the hot and dry Mediterranean climate, defined by mountain ranges and influenced by its proximity to the Pacific Ocean, is propitious for grapes and other fruits to reach a high maturity level (Cayan et al., 2008). In these conditions, grapes at harvest present with high concentrations of sugars, phenolic compounds, high pH, and low acidity. These characteristics require that wineries make adjustments to balance components in order to lower the wine pH to levels suitable for commercial red wines. In most cases, grapes at harvest in Napa Valley are overripe and are sometimes shriveled, resulting in a loss of profitability due to lower berry weights/yield and final volume by concentration, which in turn influences the balance of metabolites in wine (Keller, 2015). Vine management practices should be evaluated for their ability to reduce cycle and harvest time in order to retain grapes with optimal characteristics, which include a high concentration of sugars and phenolics, balanced acidity and pH, and reduced volume loss due to shriveling. Girdling is a simple and easily implemented technique that might improve the quality of grapes intending for winemaking in the Napa Valley region (Williams et al., 2000; Williams and Ayars, 2005).

Girdling is a traditional horticulture practice that involves removing a strip of bark, phloem, and cambium around the trunk or cane of some fruit trees such as mango and vine (Harrell and Williams, 1987; Roper and Williams, 1989; Urban et al., 2004; Ferrara et al., 2014; Gallo et al., 2014; Böttcher et al., 2018). Physiologically, the phloem is responsible for the movement of carbohydrates (sugars and starches) produced by photosynthesizing leaves to developing organs (including the fruit and roots). Phloem sugar is unloaded into the cell vacuole via an apoplastic mechanism requiring the intervention of hexose transporters, and an osmotic gradient translocates phloem to the berries during ripening (Hunter and Ruffner, 2001; Terrier et al., 2005). Removal of a portion of the phloem through girdling prevents the translocation of carbohydrates to the root system, thus supplying more nutrients for fruit growth until the girdle heals (Keller, 2010). The immediate causal effect for plants is to stop the basipetal movement of assimilates through the phloem, which results in an accumulation of carbohydrates above the girdle (Urban et al., 2004). In coniferous trees for wood, girdling is applied at different phenological stages, before, during, or after stem growth, acting as a C sink, and can reveal the dependency of root growth and wood development on current photosynthates throughout the growing season (Rainer-Lethaus and Oberhuber, 2018). Indeed, girdling causes changes in the net rate of CO_2 assimilation, which is reflected in changes to stomatal conductance (g_s) and consequently on the behavior of plant performance (Von Caemmerer and Farquhar, 1981; Buckley and Mott, 2013). Stomata exert control over the fluxes of H_2O vapor and CO_2 between the leaf and the atmosphere, and adjust their aperture in response to a number of environmental factors, such as girdling, gibberellic acid application, water regimes and seasonal effect on vines. It can be estimated using different parameters, including leaf porometer, thermal imagery and chambers, used at a leaf or whole-plant scale (Roper and Williams, 1989; Leinonen et al., 2006; Buckley and Mott, 2013; Douthe et al., 2018). In grapevines, girdling is normally applied at fruit set or veraison, depending on whether the objective is to increase berry size (at fruit set), reduce cycle duration, or promote metabolite accumulation (at veraison) (Harrell and Williams, 1987; Roper and Williams, 1989; Böttcher et al., 2018). This technique is typically used for table grapes sold as fresh fruit; however, to our knowledge, the influence of girdling on grapevine development, berry weight, and primary and secondary metabolism in 'Cabernet Sauvignon' grapes intended for winemaking has not yet been investigated. The application of this technique to winemaking grapevines at veraison should increase the concentration of phenolic compounds and sugars in grape berries, and reduce the growing season to allow for early harvest, thus avoiding volume loss during the winemaking process (Keller et al., 2006).

In wine grapes, metabolites are found mainly in the skin, pulp (or flesh), and seeds of the berries, including sugars, organic acids, amino acids, and some polyphenols such as flavonols and hydroxycinnamic acids (Ollat et al., 2002; Ribéreau-Gayon et al., 2006; Carbonneau et al., 2015). In non-teinturier grape varieties, anthocyanins are only found in the skins, as well as flavanols (also called flavan-3-ols) and flavonols, while the largest portion of the flavanols are located in the seeds (Kennedy et al., 2000; Cerpa-Calderón and Kennedy, 2008; Ali et al., 2010). Flavan-3-ols are present as monomers and various oligomers called proanthocyanidins, collectively called grape tannins. The accumulation of the primary metabolite sugars and organic acids is well known in the literature; however, less is known regarding the development of secondary metabolites in different grape tissues, as these processes are regulated by different genes and pathways (Coombe and McCarthy, 2000; Hunter and Ruffner, 2001; Ollat et al., 2002; Keller, 2010; Cohen et al., 2012; Rienth et al., 2014). Previous studies have shown that tannin biosynthesis occurs mostly during the early stages

of berry development, while the ripening phase is characterized by polymerization reactions and other alterations to existing tannin units (Downey et al., 2006; Keller, 2010). Furthermore, study of the grape ripening process is difficult, due to the heterogeneity of berries in the grape bunches (Kuhn et al., 2014; Reshef et al., 2019). Viticulturists and enologists can optimize the composition of sugars, organic acids, and amino acids in wine grapes by adjusting management practices during vine development or during winemaking (Ribéreau-Gayon et al., 2006; Carbonneau et al., 2015).

Metabolomics describes the metabolic composition of samples present at diverse concentrations, while the term metabolome is the multivariate sum of these components (Fiehn, 2002; Zhang et al., 2011; Nicholson et al., 2012; Xia et al., 2015). These analyses are considered quantitative measurements of the dynamic multiparametric metabolic response of living systems to environmental stimuli or genetic modification (Fiehn et al., 2000; Roessner et al., 2001; Holmes et al., 2019). Metabolic phenotyping involves the comprehensive analysis of biological fluids or tissue samples (Roullier-Gall et al., 2014).

Different analytical methods have been used to study the influence of natural or induced factors on model plants, vine development, and metabolic compounds in grapes/wines by gas chromatography mass spectroscopy (GC-MS) (Fiehn et al., 2000), proton nuclear magnetic resonance (^{1}H NMR) spectroscopy (Krishnan et al., 2005; Pereira et al., 2006a,b; Lima et al., 2010; Zhang et al., 2012; Gallo et al., 2014; Peterson and Waterhouse, 2016; Cassino et al., 2019), and high performance liquid chromatography (HPLC) (Peng et al., 2002; Oberholster et al., 2013; Hernández-Hierro et al., 2014; Garrido-Bañuelos et al., 2019a). ^{1}H NMR spectroscopy is a powerful tool that allow for the simultaneous determination of metabolites from different groups of organic compounds, such as sugars, organic acids, amino acids, some polyphenols, and vitamins in a single run, and uses a targeted or non-targeted approach to describe metabolic profiles from different conditions and experiments (Pereira et al., 2006a; Fotakis et al., 2013; Godelmann et al., 2013; Lloyd et al., 2015; Pinu, 2018). ^{1}H NMR spectroscopy is also used to quantify metabolites in cell or tissue extracts without the necessity of *a priori* knowledge of the sample composition (Gallo et al., 2014). However, the determination of most phenolic compounds is difficult using one dimension ^{1}H NMR spectroscopy, due to their molecular complexity (Pereira et al., 2006b). Instead, HPLC is largely used to determine phenolics in grapes and wines, with easy identification of the anthocyanins, flavonols, flavanols and hydroxycinnamic acids in a single run at different wavelengths (Peng et al., 2002; Oberholster et al., 2013; Garrido-Bañuelos et al., 2019b; Girardello et al., 2019).

The purpose of this study was to evaluate the effect of trunk girdling, applied at veraison, on agronomical and physiological parameters during vine development, and to determine how primary and secondary metabolites in the skin/pulp and seed tissues of 'Cabernet Sauvignon' grapes are altered over four different phenological stages, using a metabolomics approach. It is expected that trunk girdling will increase the content of sugars and phenolic compounds at harvest, which may enable an earlier harvest date in the future, due to potential earlier ripening, thereby avoiding volume losses and must/juice corrections by wineries associated with the long growing season in Napa Valley.

MATERIALS AND METHODS

Field Procedure and Agronomical Parameters

This study was carried out during the 2018 growing season at the University of California Experimental Station in Oakville, Napa County, CA, United States (38°25′ N; 122°24′ W). The vineyard was planted in 2012 with *V. vinifera* L. 'Cabernet Sauvignon' FPS 08 (Foundation Plant Services, UC Davis), grafted onto rootstock 110R. Plant spacing was 2.0 × 2.4 m (vine × row) in Northeast-Southwest oriented rows. Grapevines were trained to bilateral cordons and vertical-shoot-positioned trellis, and the vineyard was drip-irrigated with two pressure compensating emitters per plant delivering 2.0 L h^{-1} each.

The vineyard was composed of 12 rows containing 25 vines per row, and 8 vines were selected randomly per treatment (8 biological replicates for girdled and 8 for non-girdled vines), in different parts of the plot, to account for soil variability. Vines were pruned on March 7th 2018 and evaluations began at veraison, on July 31st 2018, 146 days after pruning (dap), when the first girdle was applied (**Figure 1A**). An entire ring of bark was removed, approximately 1 cm of thickness, all around the trunk, 10 cm below bilateral arms formation of the vines. Berry samples were collected (40 berries/vine, and 320 berries per treatment) for analyses, kept on ice in a cooler, then put in the liquid nitrogen prior storage in a freezer at −80°C, as described in sample preparation. The second sampling of 40 berries was carried out at 30% of berry maturation, on August 10th, 156 dap, 10 days after girdling (dag), as described previously. The second girdling was applied on August 31st, thirty days after first girdling, in order to ensure the girdling technique was initiated correctly and to avoid photo-assimilated transportation to the roots (Rainer-Lethaus and Oberhuber, 2018). The third sampling took place on September 4th, 181 dap (35 dag) at 70% of berry maturation, and the fourth and last sampling took place at harvest, on October 16th, 223 dap (77 dag) (**Figures 1B,C**). Stomatal conductance (g_s) was measured at all four phenological stages described before, with a leaf porometer (METER Group, Inc., Pullman, WA, United States), and was evaluated in two different leaves per vine, or 16 leaves per treatment. Two fully expanded sun exposed leaves from the top of the canopy were measured as previously described (Roper and Williams, 1989; Williams and Ayars, 2005).

Chemicals and Standards

Ethanol (96%), methanol (reagent grade), acetonitrile (HPLC grade), (+)-catechin hydrate (98%), (−) epicatechin (90%), p-coumaric acid (98%), ferulic acid (99%), caffeic acid (98%), quercetin (95%), gallic acid monohydrate (99%), syringic acid (98%), and vanillic acid (97%) were purchased from Sigma Aldrich (St. Louis, MO, United States). Malvidin-3-O-glucoside (95%) was purchased from Extrasynthese (Genay, France). Phosphoric acid (88%) (HPLC grade) was purchased from

FIGURE 1 | Experimental procedures conducted at UCDavis. **(A)** example of a 1 cm thick girdle made on *Vitis vinifera* L. vines 146 days after pruning (dap). **(B)** a non-girdled vine at harvest. **(C)** a girdled vine at harvest.

Fisher Scientific (Pittsburgh, PA, United States). Deionized water was prepared in-house to a final purity of 18.2 MΩ·cm. D_2O (99.9%) was purchased from Cambridge Isotope Laboratories, Inc. (Tewksbury, MA, United States). 3-(trimethylsilyl)-1-propanesulfonic acid-d6 (DSS-d6) was purchased from Chenomx (Edmonton, Alberta, Canada). NMR tubes were purchased from Bruker BioSpin (Billerica, MA, United States). Internal standard 2,2,3,3,4,4-d6-3-(trimethylsilyl)-1-propane sulfonic acid (DSS-d6) and sodiumazide (NaN3) in D_2O was from Chenomx Inc. (Edmonton, Alberta, Canada). Sodium hydroxide and hydrochloric acid solutions were purchased from Fisher Scientific (Fair Lawn, NJ, United States).

Sample Preparation

From the 40 'Cabernet Sauvignon' berries initially collected per vine per phenological stage of each treatment, 20 berries were used to determine pH, total soluble solids, total acidity, and berry weight on the same day as collection. The remaining berries were put in the liquid nitrogen then stored at −80°C until further analysis.

Berry Tissue Extraction

Of the remaining 20 berries stored at −80°C, 10 berries were used for metabolomics analyses (^{1}H NMR and HPLC). The remaining 10 berries were kept at −80°C for long-term storage, and eventually were discarded. First, ten berries were weighed and then split in half with a scalpel to separate seeds from the skin/pulp. Both tissues (skin/pulp and seeds) were weighed, seeds were counted, and both tissues were ground separately with ethanol for 3 min using a T18 digital ULTRA-TURRAX® (IKA® Works, Inc., Wilmington, NC, United States). Each sample was placed inside a cooler and mixed (1 h, 10°C) with a magnetic multiple stirrer with external control unit (2mag Magnetic Motion, Muenchen, Germany) (Pereira et al., 2006a,b). Then, samples were centrifuged at 4000 rpm (1792 relative centrifugal force-rcf) for 10 min and stored at −80°C until metabolomics analyses by ^{1}H NMR spectroscopy and HPLC-DAD.

1D ^{1}H NMR Spectroscopy

Aliquots (1 mL) of ethanolic extracts containing ground skins/pulp or seeds were dried under vacuum for 24 h at room temperature (20°C ± 2). Then, samples were suspended with 1 mL of D_2O and dried again under vaccuum for 24 h to remove/reduce ethanol and water signals. Samples were dissolved in 1 mL of 10 mM potassium phosphate buffer (pH 6.8 ± 0.1) and centrifuged (5 min, 4°C, 14 krcf) using an Eppendorf® Model 5415R microcentrifuge (Eppendorf North America, Hauppauge, NY, United States). A portion of the supernatant (585 µL) was combined with 65 µL of internal standard containing 5 mM 3-(trimethylsilyl)-1-propanesulfonic acid-d6 (DSS-d_6), NaN_3, and D_2O. The final concentrations were 0.5 mM DSS-d6, 0.02% NaN3, and ∼10% D_2O. The pH of the sample was adjusted to 6.8 ± 0.1 with 1 N NaOH or HCl and 600 µL of the subsequent mixture was transferred to 5 mm NMR tubes and stored at 4°C until ^{1}H NMR data were acquired (within 24 h of sample preparation) (Chin et al., 2014). The 1D ^{1}H NMR spectra of the aqueous samples of skins/pulp and seeds were acquired at 298 K using the Bruker "noesypr1d" experiment on a Bruker Avance 600 MHz NMR spectrometer equipped with a SampleJet. The acquisition parameters were: 12 ppm sweep width, 2.5 s acquisition time, 2.5 s relaxation delay, and 100 ms mixing time. Water saturation was applied during the relaxation delay and mixing time. The resulting spectra were zero-filled to 128,000 data points and an exponential apodization function corresponding to a line-broadening of 0.5 Hz was applied. Spectra were processed for metabolite identification and quantification using the Chenomx Inc. NMR Suite Processor version 8.2

(Edmonton, AB, Canada). Each spectrum was acquired in approximately 12 min.

HPLC-DAD

Ethanolic extracts (1 mL) of skins/pulp and seeds were centrifuged (5 min, 4°C, 10 krcf), and the resulting supernatant was transferred to HPLC vials for analysis by HPLC-DAD (Peng et al., 2002; Oberholster et al., 2013). For the skins/pulp, four wavelengths were used in the same run, at 280 nm, to determine flavanols, 320 nm for hydroxycinnamic acids, 360 nm for flavonols and 520 nm for anthocyanins. Seeds were analyzed at 280 nm to identify and quantify flavanols (Girardello et al., 2019). Samples were analyzed by RP-HPLC using an Agilent 1260 Infinity equipped with a PLRP-S 100A 3 μM 150 × 4.6 mm column (Agilent Technologies, Santa Clara, CA, United States) at 35°C, an auto sampler with temperature control at 8°C and diode array detector, according to previous studies (Peng et al., 2002; Oberholster et al., 2013). Each chromatogram was acquired in approximately 105 min, and peaks were identified and qualified using ChemStation software (B.04.03, 2011).

Statistical Analyses

All results acquired from agronomical, physiological, physicochemical, NMR, and HPLC data were evaluated for normality using histograms and the Shapiro−Wilk test. Differences between girdling (G+) and non-girdled (G-) groups were evaluated using the Mann-Whitney *U*-test and results were considered significant if $p < 0.05$. Principal components analysis (PCA) was performed with mean centering and unit variance scaling. The quality of the models was judged by the goodness-of-fit parameter (R^2X or R^2Y). For ^1H NMR data, the chemical shifts and metabolite identifications were assigned with literature and the Chenomx Inc. database (Chin et al., 2014; Kortesniemi et al., 2016). All figures and statistical procedures were carried out in R Version 3.5.1 (R Core Team, 2012).

RESULTS

Agronomical Data

Agronomical parameters evaluated in vines, berries, clusters, and shoots at different phenological stages are shown in **Table 1**. Significant differences were observed for stomatal conductance of the vines (g_s) at 181 dap (35 dag, or 70% maturation) and 223 dap (77 dag, or harvest date), and pH at harvest (223 dap). At 70% maturation g_s was higher in G(−), while at harvest, G(+) presented the highest values (190 mmol H_2O m^{-2} s^{-1}, vs. 128 mmol H_2O m^{-2} s^{-1} for G(−). The pH of grapes at harvest from G(+) was slightly but significantly lower than pH of grapes from G(−). No differences were found for°Brix, total acidity, berry weight, number of berries per cluster, weight of berry clusters, number and weight of shoots, and Ravaz Index at harvest.

Primary and Secondary Metabolites Determined Through 1D ^1H NMR Spectroscopy

Twenty metabolites were identified and quantified in skins/pulp of Cabernet Sauvignon grapes, including sugars, organic acids, carboxylic acids, amino acids, phenolics, and one vitamin (**Table 2**). Except for carboxylic acids, small but significant differences were observed in all classes of primary and secondary metabolites, at different phenological stages, including fructose and glucose at 30% maturation (156 dap, and 10 dag), tartaric acid (156 dap), malic acid (181 dap, 35 dag), glutamine (156 dap and 10 dag, and 223 dap and 77 dag), threonine (146 and 181 dap), epicatechin (223 dap). Twenty-one metabolites were identified and quantified in seed extracts, including sugars, organic acids, carboxylic acids, amino acids, phenolics, and one vitamin (**Table 3**). Compared to skin/pulp, fewer significant results were observed in seeds. There were no differences in sugars, except for glucose at 181 dap, which was reduced in G(+)

TABLE 1 | Agronomical parameters measured in 'Cabernet Sauvignon' vines, grapes, clusters, and shoots at different phenological stages[1], from two groups[2].

	146		156		181		223	
	G(+)	G(−)	G(+)	G(−)	G(+)	G(−)	G(+)	G(−)
Stomatal conductance (g_s)[3]	213 (69)	176 (43)	441 (51)	405 (52)	219 (88)[b]	311 (95)[a]	190 (51)[a]	128 (46)[b]
pH	2.5 (0)	2.5 (0)	2.9 (0)	2.9 (0)	3 (0)	3 (0)	3.3 (0)[b]	3.4 (0)[a]
Brix	7 (1)	7 (1)	13 (1)	12.5 (1)	20 (1)	20 (1)	26 (1)	26 (0)
Total acidity (g L^{-1})	34 (4)	40 (3)	16 (2)	17 (4)	7 (1)	7 (1)	6.8 (0)	6.2 (1)
Berry weight (g) (n = 20)	10 (2)	11 (1)	16 (1)	16 (2)	26 (1)[a]	25 (2)[b]	19 (2)	18 (3)
No. clusters	ND	ND	ND	ND	ND	ND	57 (18)	51 (6)
Cluster weight (Kg $vine^{-1}$)	ND	ND	ND	ND	ND	ND	7 (4)	7 (1)
No. shoots	ND	ND	ND	ND	ND	ND	28 (2)	27 (3)
Shoot weight (Kg $vine^{-1}$)	ND	ND	ND	ND	ND	ND	1 (1)	1.1 (0)
Yield (Kg ha^{-1})	ND	ND	ND	ND	ND	ND	14 (7)	14 (2)
Ravaz Index	ND	ND	ND	ND	ND	ND	7.1 (1)	6 (1)

[1]Phenological stages represented as days after pruning (DAP), where 146, veraison; 156, 30% maturation; 181, 70% maturation; 223, harvest; [2]Grapevines received girdling application, G(+), or were non-girdled control, G(−); [3]Stomatal conductance measured in mmol H_20 $m^{-2}s^{-1}$. ND, not determined. Measures of cluster weight, number and shoot weight, yield, and Ravaz index were collected at harvest (223 DAP) only. Values are median (interquartile range, IQR). Differences between groups at each phenological stage were evaluated using the Mann Whitney U-test. Shaded groups with different letters are statistically significant ($p < 0.05$).

TABLE 2 | Metabolite profiling determined by 1D ^{1}H NMR spectroscopy in skin/pulp of 'Cabernet Sauvignon' grapes[1] at different phenological stages[2], from two treatments[3].

	146		156		181		223	
	G(+) *n* = 8	G(−) *n* = 8	G(+) *n* = 8	G(−) *n* = 8	G(+) *n* = 7‡	G(−) *n* = 8	G(+) *n* = 8	G(−) *n* = 8
Fructose	7343 (3242)	6439 (4375)	34317 (4450)[b]	37293 (1352)[a]	61695 (1541)	62269 (2823)	85309 (5086)	85900 (4031)
Glucose	12879 (2601)	11612 (5275)	39787 (4783)[b]	42550 (771)[a]	65842 (878)	66106 (2564)	87102 (6507)	89318 (4682)
Sucrose	96 (83)	107 (48)	1151 (276)	1315 (246)	2569 (1095)	2418 (1351)	4746 (1398)	4280 (915)
Total sugars	20318	18158	75255	81158	130106	130793	177157	179498
Malic	12127 (1438)	12982 (977)	4966 (1188)	4767 (609)	824 (68)[b]	1042 (189)[a]	353 (142)	417 (92)
Tartaric	4898 (699)	4807 (721)	2507 (246)[a]	1995 (481)[b]	539 (144)	500 (113)	376 (169)	421 (217)
Total organic acids	17025	17789	7473	6762	1363	1542	729	838
Formic	1 (0)	1 (0)	1 (0)	1 (0)	2 (0)	2 (0)	2 (0)	2 (0)
Succinic	13 (5)	12 (2)	7 (1)	7 (1)	1 (0)	2 (1)	1 (0)	1 (1)
Total carboxylic acids	14	13	8	8	3	4	3	3
Alanine	11 (4)	11 (2)	11 (3)	10 (2)	14 (2)	12 (1)	6 (2)	7 (3)
Arginine	7 6)	7 (3)	10 (5)	9 (4)	10 (5)	8 (3)	6 (6)	8 (3)
GABA	26 (8)	26 (14)	32 (9)	37 (7)	39 (5)	38 (7)	39 (8)	45 (12)
Glutamine	30 (8)	24 (2)	24 (8)[b]	30 (7)[a]	13 (4)	11 (4)	4 (2)[b]	7 (1)[a]
Isoleucine	1 (0)	1 (0)	2 (1)	2 (1)	4 (1)	2 (1)	12 (1)	13 (2)
Leucine	1 (0)	1 (0)	2 (1)	2 (1)	3 (2)	2 (1)	11 (1)	12 (3)
Proline	4 (4)	6 (3)	29 (24)	42 (15)	349 (89)[a]	309 (79)[b]	841 (152)	927 (117)
Threonine	22 (7)[a]	12 (5)[b]	15 (3)	15 (3)	19 (4)[a]	12 (1)[b]	14 (4)	13 (2)
Tyrosine	2 (1)	2 (1)	3 (1)	3 (1)	4 (1)	4 (1)	17 (6)	15 (4)
Valine	1 (1)	2 (0)	3 (1)	3 (1)	7 (2)	5 (1)	21 (3)	21 (3)
Total amino acids	105	92	131	153	462	403	971	1068
Epicatechin	2 (1)	2 (1)	3 (2)	4 (1)	–	–	3 (0)[a]	2 (1)[b]
Gallic acid	2 (1)	2 (0)	1 (0)	1 (0)	–	–	1 (0)	1 (1)
Total phenolics	4	4	4	5	–	–	4	3
Choline	5 (2)	5 (4)	14 (2)	14 (1)	15 (1)	15 (2)	18 (2)	18 (1)

[1]Values are median (interquartile range, IQR) mg Kg^{-1} of skin/pulp fresh weight; [2]Phenological stages represented as days after pruning (DAP), where 146, veraison; 156, 30% maturation; 181, 70% maturation; 223, harvest; [3]Grapevine received girdling application, G(+), or were non-girdled control, G(−). Differences between groups at each phenological stage were evaluated using the Mann Whitney U-test. Shaded groups with different letters are statistically significant ($p < 0.05$). ‡One sample was lost during processing.

grapevines. Other small differences in tartaric acid, pyruvic acid, succinic acids, and alanine were also observed.

Secondary Metabolites Determined by HPLC-DAD

Twenty-three phenolic metabolites were identified and quantified in skin/pulp, with two unknown compounds (**Table 4**). Significant differences were observed in all classes of phenolics, but at different phenological stages. Concentrations of the flavanol epicatechin gallate were higher in G(−) vines at veraison, and lower at 156 dap, but not at harvest. The flavonols quercetin-3-glucose, quercetin-3-glucuronide and quercetin-3-galactoside were higher in G(+) vines at 156 dap, while quercetin-3-glucose (26.3 vs. 19.2 mg/kg fresh weight) and an unknown flavonol-1 (7.3 vs. 5.8 mg/kg fresh weight) were higher in G(+) at harvest. The response of the anthocyanins was varied, as some metabolites were higher in non-girdled vines, while others in girdled vines, at different phenological stages. The compounds cyanidin-3-glucoside, delphinidin-3-glucoside, peonidin-3-glucoside, petunidin-3-glucoside, and the acetyl acetylated and p-coumaroyl acylated forms of delphinidin-3-glucoside, were significantly higher in non-girdled vines at 70% maturation, but no differences were found at harvest. The most important anthocyanin in *Vitis vinifera* L. is malvidin-3-glucoside, and girdling appeared to increase the concentration of this compound at harvest (181.7 vs. 167.1 mg/kg fresh weight). A similar finding was observed in G(+) vs G(−) vines for malvidin-3-acetylglucoside (73.1 vs. 63.4 mg/kg fresh weight), and p-coumaroyl acylated forms (36.5 vs. 17.7 mg/kg fresh weight). Berries grown on girdled grapevines also presented with higher concentrations at different phenological stages and at harvest of peonidin-p-coumaroyl acetylated (4.8 vs. 4.2 mg/kg fresh weight), hydroxycinamic acid caftaric (6.1 vs. 4.0 mg/kg fresh weight), as well as polymeric phenol (1092.6 vs. 671.8 mg/kg fresh weight) (**Table 4**). Six phenolic compounds were identified and quantified in seeds, none of which were significant, except for compound procyanidin "B1" at 146 dap (**Table 5**).

Multivariate Statistical Analysis

Metabolites from ^{1}H NMR spectroscopy and HPLC-DAD data were visualized using principal components analysis (PCA)

TABLE 3 | Metabolite profiling determined by 1D ^{1}H NMR spectroscopy in seeds of 'Cabernet Sauvignon' grapes[1] at different phenological stages[2], from two treatments[3].

	146		156		181		223	
	G(+) *n* = 8	G(–) *n* = 8	G(+) *n* = 8	G(–) *n* = 8	G(+) *n* = 7‡	G(–) *n* = 8	G(+) *n* = 8	G(–) *n* = 8
Fructose	2132 (592)	2167 (441)	7000 (1370)	6843 (1194)	10030 (382)	10936 (855)	25063 (3301)	23615 (3042)
Glucose	1913 (554)	1916 (619)	5934 (534)	6027 (1384)	9510 (883)[b]	11311 (809)[a]	25529 (2356)	24576 (3985)
Sucrose	5001 (1146)	5175 (1349)	8852 (2492)	9524 (1209)	15845 (2055)	16084 (2794)	12774 (2351)	12626 (891)
Total sugars	9046	9258	21786	22394	35385	38331	63366	60817
Malic	113 (19)	107 (10)	86 (21)	82 (31)	48 (7)	44 (15)	40 (14)	33 (7)
Tartaric	132 (52)	162 (43)	128 (45)	135 (38)	130 (11)[b]	163 (50)[a]	280 (80)	199 (44)
Total organic acids	245	269	214	217	178	207	320	232
Formic	–	–	5 (5)	3 (1)	114 (26)	132 (14)	179 (59)	196 (15)
Pyruvic	3 (1)[b]	5 (1)[a]	4 (1)	5 (1)	4 (2)	4 (3)	5 (2)	5 (2)
Succinic	18 (4)[a]	14 (5)[b]	44 (14)	44 (4)	42 (5)	41 (9)	13 (5)	15 (4)
Total carboxylic acids	21	19	53	52	160	177	197	216
Alanine	146 (25)[a]	115 (22)[b]	175 (34)	198 (33)	114 (25)	115 (37)	50 (29)	44 (14)
Arginine	11 (5)	12 (3)	13 (6)	13 (6)	9 (2)	10 (2)	14 (4)	15 (3)
GABA	184 (18)	154 (59)	166 (33)	169 (37)	140 (33)	160 (38)	123 (90)	109 (72)
Glutamine	283 (86)	348 (96)	96 (21)	127 (44)	51 (11)	65 (29)	36 (14)	38 (5)
Isoleucine	–	–	3 (2)	3 (1)	1 (1)	2 (1)	2 (1)	3 (1)
Leucine	52 (11)	53 (5)	47 (10)	44 (9)	20 (5)	22 (8)	20 (5)	15 (4)
Phenylalanine	42 (12)	44 (9)	31 (9)	30 (9)	35 (2)	38 (3)	31 (5)	28 (5)
Proline	37 (13)	48 (9)	70 (11)	78 (25)	129 (29)	134 (36)	306 (57)	271 (36)
Threonine	26 (11)	26 (4)	27 (7)	27 (6)	24 (3)	22 (5)	16 (3)	13 (5)
Tyrosine	128 (20)	128 (15)	110 (16)	100 (18)	30 (5)	35 (5)	28 (14)	19 (4)
Valine	45 (12)	45 (4)	51 (12)	47 (9)	46 (8)	42 (11)	41 (7)	37 (9)
Total amino acids	954	973	789	736	599	645	667	592
Epicatechin	1665 (254)	1615 (232)	1377 (352)	1595 (545)	581 (206)	567 (150)	284 (41)	271 (103)
Choline	4 (1)	3 (1)	15 (5)	14 (2)	23 (4)	27 (9)	23 (6)	24 (5)

[1]Values are median (interquartile range, IQR) mg Kg^{-1} of seeds fresh weight; [2]Phenological stages represented as days after pruning (DAP), where 146, veraison; 156, 30% maturation; 181, 70% maturation; 223, harvest; [3]Grapevine received girdling application, G(+), or were non-girdled control, G(–). Differences between groups at each phenological stage were evaluated using the Mann Whitney U-test. Shaded groups with different letters are statistically significant ($p < 0.05$). ‡One sample was lost during processing.

in order to identify which compounds had correlations and were most influenced by girdling. Metabolites in both tissues were strongly separated by maturation level, as was expected, while the effect of girdling was secondary. The best separation between girdled and non-girdled vine samples was observed with secondary metabolites (phenolics) determined in skins + pulp tissue, followed by phenolics in seeds (both determined using HPLC). Less separation was observed for primary and secondary metabolites determined in skins + pulp and seeds identified using ^{1}H NMR spectroscopy.

DISCUSSION

Impact of Girdling on Agronomical Data

According to the agronomical parameters evaluated, stomatal conductance (g_s) was significantly different between girdled and non-girdled vines. In both groups, the trend in g_s was an increase from veraison (146 dap, 0 dag) to 30% maturation (156 dap, 10 dag), followed by a reduction at 70% maturation (181 dap, 35 dag). At harvest, g_s was reduced further for (G-) at harvest and was significantly lower than G(+) (**Figure 2**). These findings demonstrate that girdled vines had higher rates of carbon dioxide entering or water vapor exiting through the stomata of the leaves at harvest, suggesting higher physiological activity. By using a leaf porometer, Roper and Williams (1989) showed that g_s was significantly lower for girdled table grape vines throughout most of the day, 4 weeks after girdling was applied. In the present study, we also showed reduced g_s for girdled vines at 70% berry maturation (181 dap), 35 days after girdling. However, at harvest (77 dag) results were contrary and girdled vines presented higher g_s as compared to non-girdled vines. These findings suggest higher stress and physiological activity for girdled vines close to harvest compared to non-girdled vines. Douthe et al. (2018) demonstrated that measurements of water and carbon fluxes at the whole-plant level under conditions mimicking the field presented results contrary to what occurs at the leaf scale. Stomatal conductance is helpful for studying interactions at the leaf scale as well as whole-plant-leaf dynamics (Buckley and Mott, 2013). As mentioned previously, the focus and objectives of this experiment was a metabolomics approach, which resulted in fewer eco-physiological measures being made, and future field studies should evaluate carbon fluxes of girdled and non-girdled vines using whole-plants.

TABLE 4 | Phenolic compounds determined by HPLC-DAD in skin/pulp of 'Cabernet Sauvignon' grapes[1] at different phenological stages[2], from two treatments[3].

	146		156		181		223	
	G(+) *n* = 8	G(−) *n* = 8	G(+)*n* = 8	G(−) *n* = 8	G(+)*n* = 7‡	G(−) *n* = 8	G(+)*n* = 8	G(−) *n* = 8
Catechin	17.7 (6.5)	19.2 (3.9)	2.5 (1.5)	2.6 (1.2)	4.1 (0.7)	4.7 (0.4)	6.9 (0.7)	8.0 (1.4)
Epicatechin	3.0 (0.7)	2.7 (0.7)	2.0 (0.3)	1.9 (0.4)	7.5 (2.2)	6.7 (2.4)	26.3 (2.6)	26.3 (4.9)
Epicat. gallate	6.2 (1.7)[b]	7.8 (1.3)[a]	2.8 (1.6)[a]	1.3 (0.6)[b]	2.1 (0.7)	1.5 (0.6)	3.1 (1.2)	2.5 (0.3)
Epigallocatechin	4.9 (1.7)	5.0 (1.3)	1.6 (0.4)	1.3 (0.3)	2.3 (0.8)	2.1 (2.2)	4.0 (2.0)	4.7 (2.5)
Total Flavanols	31.8	34.7	8.9	7.4	15.9	15.1	40.4	41.6
Querc-3-gluc.	6.5 (4.7)	5.4 (3.4)	7.9 (2.8)[a]	3.9 (2.9)[b]	13.9 (5.0)	11.5 (3.4)	26.3 (6.1)[a]	19.2 (3.0)[b]
Quer-glucur.	33.2 (2.7)	30.67 (7.4)	25.4 (7.9)[a]	13.8 (8.6)[b]	11.7 (3.8)	9.9 (2.9)	17.3 (4.7)	14.4 (1.9)
Querc-galact.	1.8 (1.1)	1.6 (0.7)	2.9 (0.5)[a]	1.9 (0.9)[b]	4.4 (1.1)	4.8 (0.8)	7.4 (1.8)	6.5 (1.0)
Quer-rhamn.	0.3 (0.6)	0.4 (0.2)	0.8 (0.4)	0.6 (0.5)	3.7 (1.1)	3.4 (0.9)	8.7 (2.2)	7.1 (0.9)
Unknown 1	0.6 (0.2)	0.5 (0.1)	0.9 (0.3)	1.0 (0.3)	3.6 (0.8)	3.7 (0.4)	7.3 (1.0)[a]	5.8 (1.9)[b]
Unknown 2	ND	ND	3.9 (1.8)	3.3 (1.8)	14.4 (1.7)	13.0 (2.8)	26.1 (3.7)	24.9 (4.9)
Total Flavonols	42.5	38.5	39.5	24.7	51.7	446.4	93.3	78.16
Cya-3-gluc.	–	–	2.1 (2.1)	2.6 (1.7)	1.9 (0.4)[b]	3.4 (0.8)[a]	3.1 (1.3)	4.2 (0.9)
Delph-3-gluc.	–	-	7.3 (5.2)	8.4 (3.3)	21.3 (3.7)[b]	27.1 (1.5)[a]	32.9 (5.1)	38.8 (9.8)
Malv-3-gluc.	–	–	23.2 (3.7)	24.3 (6.6)	78.4 (10.4)	84.9 (8.1)	181.7 (8.1)[a]	167.1 (22.1)[b]
Peo-3-gluc.	–	–	6.6 (5.2)	6.9 (3.3)	11.6 (1.6)[b]	14.3 (0.7)[a]	21.5 (2.8)	23.8 (4.7)
Pet-3-gluc.	–	–	5.4 (3.2)	5.9 (2.0)	13.85 (2.4)[b]	16.4 (0.7)[a]	23.6 (2.0)	26.7 (6.7)
Delph-3-acet.	–	–	2.8 (2.2)	4.1 (1.2)	6.8 (1.8)[b]	9.8 (1.0)[a]	11.0 (2.3)	12.7 (3.3)
Malv-3-acet.	–	–	13.6 (1.8)	16.0 (2.9)	36.7 (8.1)	38.7 (4.1)	73.1 (2.9)[a]	63.4 (4.2)[b]
Peo-3-acet.	–	–	3.3 (1.6)	3.6 (1.1)	4.1 (0.8)	5.5 (0.6)	6.7 (1.0)	7.3 (1.1)
Pet-3-acet.	–	–	2.6 (1.6)	3.4 (0.9)	5.8 (1.3)	7.7 (0.6)	9.7 (0.9)	11.1 (2.3)
Delph-3-pcoum.	–	–	1.0 (0.5)	1.1 (0.3)	2.3 (0.4)[a]	2.8 (0.2)[a]	3.7 (0.3)	3.8 (0.8)
Malv-3-pcoum.	–	–	5.2 (0.7)	4.9 (0.8)	14.6 (2.1)	13.8 (1.1)	36.5 (3.3)[a]	17.7 (10.8)[b]
Peo-3-pcoum.	–	–	2.8 (1.0)	2.5 (0.8)	3.6 (0.8)	3.9 (0.5)	4.8 (1.3)[a]	4.2 (0.6)[b]
Pet-3-pcoum.	–	–	0.3 (0.1)	0.3 (0.1)	0.6 (0.1)	0.6 (0.3)	1.6 (0.2)	1.5 (0.2)
Total Anthocyanins	–	–	76.5	84.3	201.7	221.2	410.2	382.4
Caftaric acid	47.5 (27.1)	44.8 (10.8)	14.8 (3.5)[a]	11.9 (2.8)[b]	3.1 (1.0)	2.9 (1.7)	6.1 (0.6)[a]	4.0 (1.4)[b]
Polymeric phenols	1350.99 (342.1)[a]	1052.2 (275.2)[b]	866.3 (113.8)	533.2 (106.5)	600.9 (144.3)[a]	370.1 (42.7)[b]	1092.6 (178.1)[a]	671.8 (222.4)[b]
Polymeric pigments	1.9 (0.9)	1.6 (0.6)	0.7 (0.1)	0.9 (0.3)	1.4 (0.3)	1.3 (0.1)	4.7 (0.6)	4.1 (0.9)
∑ all phenolics	1550	1246	1131	781	1152	947	2206	1697

[1]Values are median (interquartile range, IQR) mg Kg^{-1} of skin/pulp fresh weight; [2]Phenological stages represented as days after pruning (DAP), where 146, veraison; 156, 30% maturation; 181, 70% maturation; 223, harvest; [3]Grapevine received girdling application, G(+), or were non-girdled control, G(−). Differences between groups at each phenological stage were evaluated using the Mann Whitney U-test. Shaded groups with different letters are statistically significant ($p < 0.05$). ‡One sample was lost during processing.

TABLE 5 | Phenolic compounds determined by HPLC-DAD in seeds of 'Cabernet Sauvignon' grapes[1] at different phenological stages[2], from two treatments[3].

	146		156		181		223	
	G(+) *n* = 8	G(−) *n* = 8	G(+) *n* = 8	G(−) *n* = 8	G(+) *n* = 7‡	G(−) *n* = 8	G(+) *n* = 8	G(−) *n* = 8
Catechin	907.9 (177.8)	812.4 (87.2)	572.4 (198.2)	592.3 (129.9)	166.3 (33.9)	210.3 (39.8)	82.9 (37.9)	104.7 (44.8)
Procyanidin B1	20.6 (8.2)[a]	10.8 (4.3)[b]	15.1 (1.2)	16.2 (3.2)	14.0 (1.2)	13.5 (3.8)	8.8 (1.6)	7.8 (2.2)
Epicatechin	354.0 (62.5)	342.7 (36.5)	300.4 (48.1)	347.2 (28.8)	158.5 (32.9)	181.4 (27.5)	99.8 (39.0)	108.8 (15.9)
Procyanidin B2	12.6 (4.3)	10.9 (1.3)	13.0 (2.4)	11.2 (4.3)	25.6 (3.7)	27.2 (10.2)	19.7 (3.9)	16.5 (3.6)
Epicatechin gallate	679.2 (31.1)	658.5 (48.0)	437.1 (93.5)	408.2 (101.0)	70.9 (7.2)	84.9 (18.9)	26.7 (13.2)	25.5 (4.9)
Polymeric Phenols	4227.9 (745.6)	4518.7 (236.1)	3958.9 (508.0)	4066.8 (152.4)	5122 (820.8)	5350.9 (725.6)	4964.3 (750.3)	5364.2 (495.3)
Total flavanols	6203	6355	5296	5441	5220	5868	5203	5629

[1]Values are median (interquartile range, IQR) mg Kg^{-1} of seeds fresh weight; [2]Phenological stages represented as days after pruning (DAP), where 146, veraison; 156, 30% maturation; 181, 70% maturation; 223, harvest; [3]Grapevine received girdling application, G(+), or were non-girdled control, G(−). Differences between groups at each phenological stage were evaluated using the Mann Whitney U-test. Shaded groups with different letters are statistically significant ($p < 0.05$). ‡One sample was lost during processing.

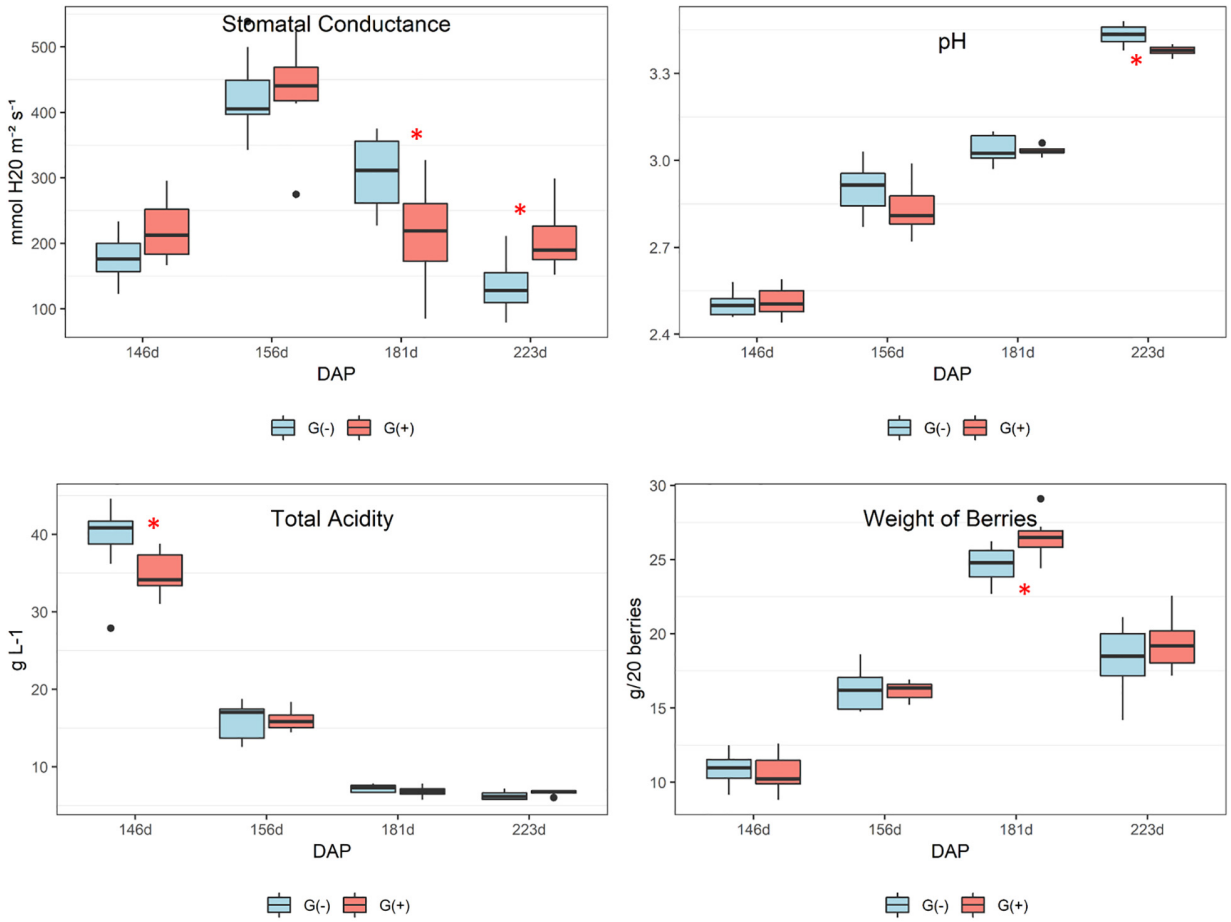

FIGURE 2 | Agronomical parameters evaluated in leaves and grapes of 'Cabernet Sauvignon' at different phenological stages, from two treatments, girdled – G(+); and non-girdled – G(–) vines. Stomatal conductance was determined in vine leaves (g_s); pH and total acidity were measured in grape berries. DAP = days after pruning, where: 146 corresponds to veraison; 156 to 30% maturation; 181 to 70% maturation; and 223 corresponds to harvest. Box plots show median, interquartile range (IQR), minimum/maximum, and strong outliers (>1.5 IQR). Differences between groups at each phenological stage were evaluated using the Mann Whitney *U*-test. Groups marked with (*) are statistically significant ($p < 0.05$).

Stomatal conductance behavior in most plants is regulated by hydraulic and chemical signaling, influencing guard cell physiology in response to water deficits and stress from other treatments, which is linked to abscisic acid and leaf water potential (Comstock, 2002). In one study, girdling reduced g_s in Canary Island pine (*Pinus canariensis*) at 140 dag, showing that the plant response to girdling may depend on the species (López et al., 2015). In this case, the authors suggested that the inhibitive effect of girdling on photosynthesis was primarily due to changes in the electron transport rate rather than changes in g_s. Their two likely explanations for the negative feedback on photosynthesis was due either to an excess of starch grains leading to physical damage of thylakoids and the subsequent decrease of chlorophyll levels, or through the inhibition of photosynthetic genes regulated by carbohydrate content. The authors also found that girdling changed the concentration and ratio of photosynthetic pigments (chlorophyll concentrations progressively decreased in girdled plants), in addition to observing an acceleration of chlorosis in mature girdled leaves. In the current study, chlorosis was observed in both treatments and was more pronounced in leaves obtained from girdled vines at harvest (**Figure 1**, middle and bottom images).

The pH of grapes from G(−) was slightly higher than G(+) and values increased from veraison to harvest (**Figure 2**). This suggests differences in berry acidity, however, even though total acidity declined from veraison to harvest date, girdling did not influence total acidity in grapes. It is possible that other compounds may have influenced the pH of berries at harvest, such as organic acids, or that the balance of ions, titratable protons, and monovalent metal cations, such as potassium and sodium were altered (Boulton, 1980). Finally, berry weight increased from veraison (146 dap) to 181 dap (70% maturation), then decreased at harvest (no significant differences between girdled vs. non-girdled vines), with some shriveling observed. In the plots used for the current study, and in the majority of wineries throughout Napa Valley, grape harvesting occurs when sugars reach a minimum of 25°Brix. According to the boxplots of berry weights, shown in **Figure 2**, harvesting could

be initiated 1–2 weeks earlier, or around 209–216 days after pruning, which could avoid volume losses associated with berry shriveling. Brar et al. (2008) showed that girdling at fruit set increased berry weight in table grapes, while Kennedy et al. (2000) showed that berries attained their maximum size approximately 30 days prior to harvest (24°Brix is considered commercially mature), with no evidence of berry contraction. The differences between our results and those from these authors are that the girdling in our study was applied at veraison and not at frut set, avoiding berry weight increases for wine grapes, as well as that in previous studies berries were harvested earlier before shriveling occurred. However, most Californian wineries harvest 'Cabernet Sauvignon' grapes later than this. Depending on harvest criteria, most commercial harvests may actually be taking place when fruit is overripe (>27°Brix), which would result in shriveled berries. Some authors showed that the volume loss in berries occurs due to declining phloem influx into the berries and cuticular berry transpiration (Coombe and McCarthy, 2000; Keller et al., 2006). It is possible that a similar effect occurred in the present study as a result of grapevine girdling, whereby phloem influx was reduced in order to balance water efflux; however, differences in berry weight between groups were not found in the current study.

Impact of Girdling on Primary Metabolites in Skin/Pulp

Although all sugars (glucose, fructose, and sucrose) increased from veraison to harvest, there were no significant differences between groups at harvest in terms of sugars, organic acids, and carboxylic acids. Girdling was expected to increase the sugar content of berries, but no differences were found which may suggest the development of secondary phloem vessels that enabled sap movement from leaves to roots, as shown by others (Zhang et al., 2000). Zhang et al. (2000) showed that fascicular phloem is largely responsible for sugar transport, whereas the extra-fascicular phloem may function in signaling, defense, and the transport of other metabolites. Another study using a genomics approach showed leaf girdling induced leaf senescence

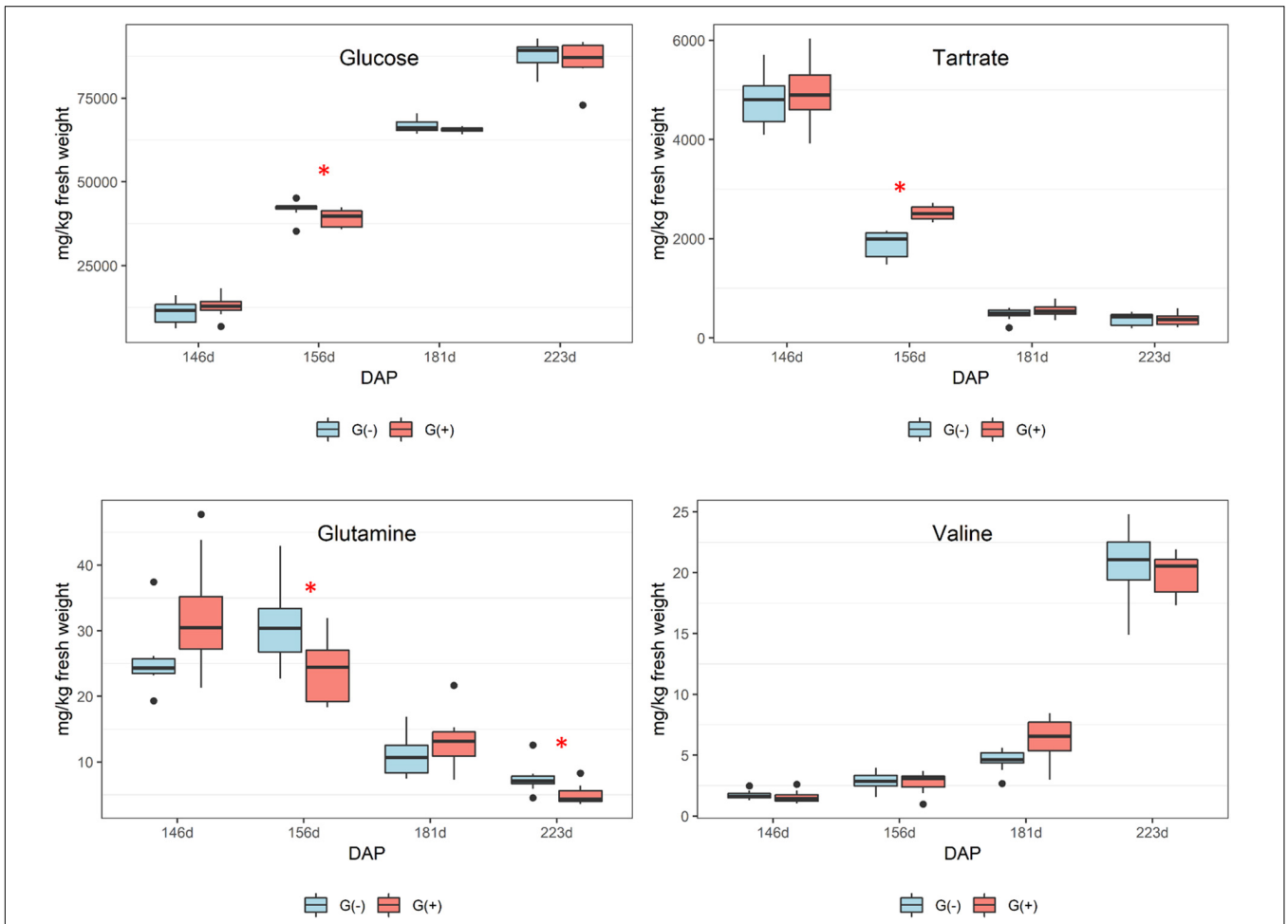

FIGURE 3 | Metabolites determined by 1D ^{1}H NMR spectroscopy in skin/pulp of 'Cabernet Sauvignon' grapes at different phenological stages, from two treatments, girdled – G(+); and non-girdled – G(–) vines. DAP = days after pruning, where: 146 corresponds to veraison; 156 to 30% maturation; 181 to 70% maturation; and 223 corresponds to harvest. Box plots show median, interquartile range (IQR), minimum/maximum, and strong outliers (>1.5 IQR). Differences between groups at each phenological stage were evaluated using the Mann Whitney *U*-test. Groups marked with (*) are statistically significant ($p < 0.05$).

and carbohydrate accumulation (Parrott et al., 2007), and girdling of a single leaf is observed to be sufficient for inhibiting photosynthesis and promoting starch accumulation, which in turn influences plant primary and secondary metabolism (Zhang et al., 2015). In addition, a study by Gallo et al. (2014) showed that agronomical practices such as girdling applied to table grapes affected primary metabolites, and increased the concentrations of sugar and the amino acid arginine.

No differences in organic acids were found between treatments at harvest, and no clear trend was apparent. As expected, **Figure 3** shows declining tartaric acid in skin/pulp from veraison to harvest, which likely occurred as a result of dilution, as shown in previous studies (Ollat et al., 2002). Significant differences in amino acids were only found for glutamine and threonine (**Table 2**). From veraison to harvest, glutamine was reduced in both groups, but girdling was shown to reduce glutamine concentrations at harvest. Some authors have shown that N composition of the phloem sap, particularly the glutamine content, may vary according to O_2 diffusion and nitrogenase activity (Neo and Layzell, 1997). These authors showed evidence that the N content of phloem sap plays a role in the feedback regulation of nitrogenase activity, and that glutamine acts as a signal molecule regulating metabolism. Parrott et al. (2007) showed that genes associated with N metabolism, including glutamine synthetase, glutamate synthase, asparagine synthetase and several aminotransferase genes, were upregulated in girdled leaves. In tobacco leaves, glutamine was shown to be a precursor for the synthesis of proline via glutamate, and in the phloem played a major role as a key metabolite synthesized in response to water stress (Brugière et al., 1999).

In the current study, there was a trend toward higher amounts of proline, GABA, and other amino acids (results did not reach statistical significance) in non-girdled vines (**Table 2**). This could suggest the involvement of an alternate pathway for proline accumulation, which is one of the most important amino acids in grapes (Huang and Ough, 1991). Valine concentrations increased substantially from veraison to harvest, but no significant differences were found between treatments (**Figure 3** and **Table 2**). Leucine, isoleucine, and tyrosine also substantially increased from veraison to harvest, contrary to the results shown by Lamikanra and Kassa (1999). This could be related to differences in demand for amino acids involved in protein synthesis that occur during grape ripening. Amino acids are known as important precursors for volatile and phenolic compounds (Gourieroux et al., 2016), and although high concentrations of amino acids can produce defective qualities in wines, they add complexity to wines at lower concentrations (Ardö, 2006).

Impact of Girdling on Primary Metabolites in Seeds

Smaller variations were observed in seeds as compared to skin/pulp. Sugars accumulated from veraison in both treatments (**Figure 4**), but there were no differences between groups, except at 181 dap, in which glucose concentrations were observed to be higher in grapes grown on girdled vines. Others have shown that grape seeds are less influenced by abiotic factors than the skin and pulp tissues (Adams, 2006; Braidot et al., 2008; Carbonneau et al., 2015; Blancquaert et al., 2019). According to the ^{1}H NMR spectroscopy data, the concentrations of organic acids and tartaric acid in grape seeds were stable from veraison to 181 dap, and then increased to harvest for both treatments (**Figure 4**), and tartaric acid concentrations were higher in G(−) vines at 181 dap as compared to G(+) vines (**Table 3**). Malic acid decreased from veraison to harvest, with no differences found between treatments. Bobeica et al. (2015) showed that the organic acids are less responsive to carbon limitation at harvest. Lamikanra and Kassa (1999) showed that amino acids content in skin, seed, pulp and grape berries presented different metabolite profiling from fruit set to harvest. A similar observation was made in the current study, in which alanine increased from veraison to 156 dap, but was reduced at harvest. Conversely, amino acids in skin/pulp trended toward increased proline, GABA, and other amino acids in girdled vines (**Table 3**).

Impact of Girdling on Secondary Metabolites in Skin/Pulp

Secondary metabolites were more influenced by girdling than primary metabolites as a greater number of significant results were found in skin/pulp grape extracts. Phenolics are complex compounds and are difficult to identify using 1D ^{1}H NMR spectroscopy due to heterogeneous polymerization products and various hydrogen and carbon bonds (Fotakis et al., 2013; Lloyd et al., 2015). However, epicatechin concentrations, as determined by NMR spectroscopy, were higher in girdled compared to non-girdled vines. The HPLC data presented more significant findings as significant differences were observed for all phenolics at different phenological stages (**Figure 5** and **Table 4**). Caftaric acid is a hydrocinnamic acid, specifically caffeic acid conjugated with tartaric acid, that was significantly higher in girdled vines at 30% maturation and at harvest. Some authors have reported a strong decrease in caftaric acid from veraison to harvest, and this metabolite is believed responsible for browning in raisins and wines (Singleton et al., 1985; Ali et al., 2010; Sun et al., 2017).

According to these results, it is important to highlight that girdled vines presented higher stomatal conductance at harvest, lower amounts of glutamine, a trend toward lower concentrations of other amino acids, and higher concentrations of the most important anthocyanins and flavonols in grapes, malvidin-3-glucoside and quercetin-3-glucoside, respectively. Many authors showed that lower fertilization and inputs of N for vines can be related to higher amounts of phenolic compounds in grapes and wines, and that abiotic factors can increase phenolics, with increased gene expression (Keller and Hrazdina, 1998; Bell and Henschke, 2005; Terrier et al., 2005; Keller et al., 2006; Van Leeuwen and Seguin, 2006; Braidot et al., 2008; Roullier-Gall et al., 2014; Sun et al., 2017). In the present study we can confirm a link between glutamine, a key signal regulating N accumulation, and the pathway

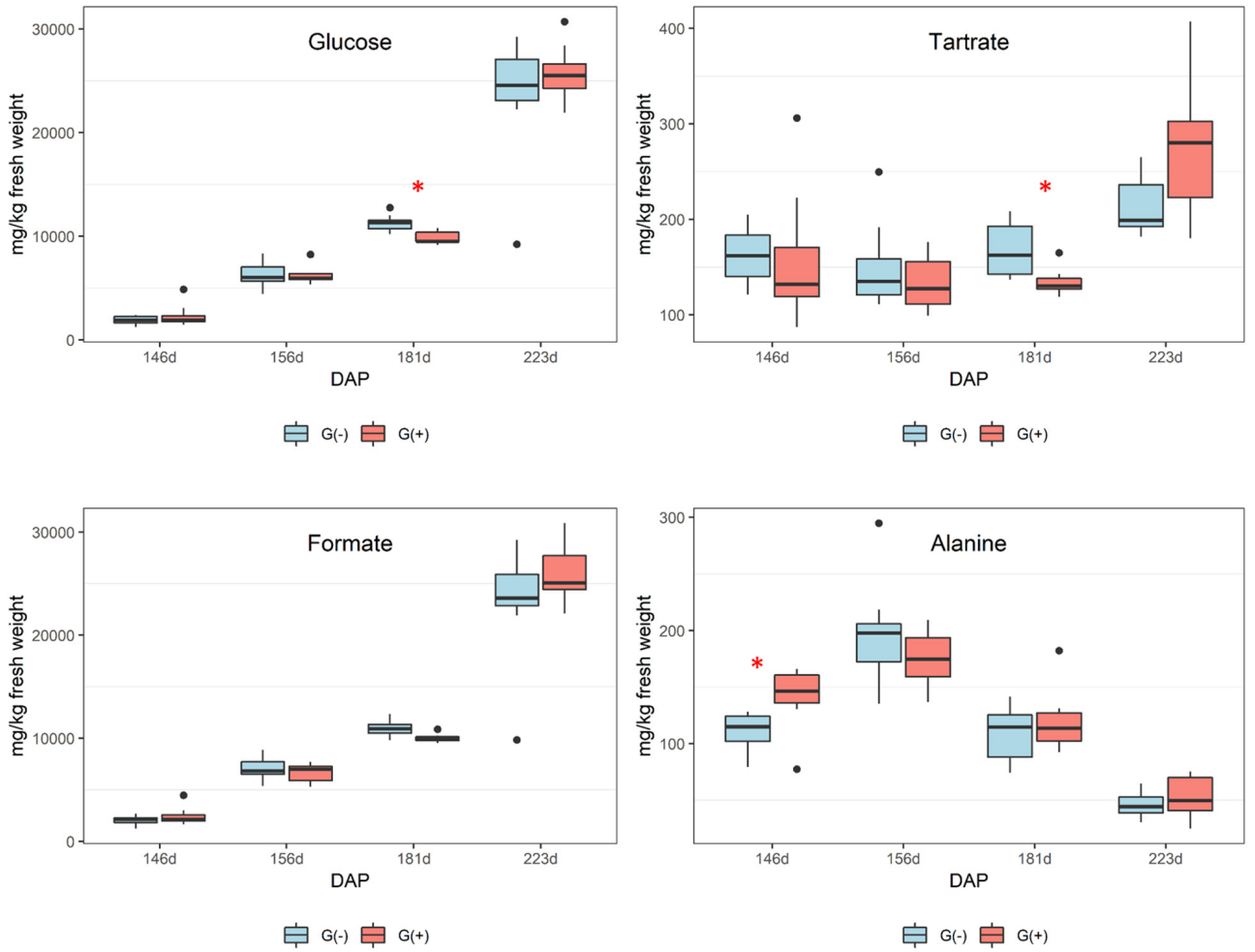

FIGURE 4 | Metabolites determined by 1D ^{1}H NMR spectroscopy in seeds of 'Cabernet Sauvignon' grapes at different phenological stages, from two treatments, girdled – G(+); and non-girdled – G(–) vines. DAP = days after pruning, where: 146 corresponds to veraison; 156 to 30% maturation; 181 to 70% maturation; and 223 corresponds to harvest. Box plots show median, interquartile range (IQR), minimum/maximum, and strong outliers (>1.5 IQR). Differences between groups at each phenological stage were evaluated using the Mann Whitney *U*-test. Groups marked with (*) are statistically significant ($p < 0.05$).

involved in the biosynthesis of phenolic compounds, with higher concentrations of anthocyanins and flavonols in skin/pulp of 'Cabernet Sauvignon' grapes at harvest. Surprisingly, girdling did not affect sugar concentrations in mature 'Cabernet Sauvignon' grapes, potentially due to the development of extrafascicular vessels issued in the trunk zone; however, girdling did increase the concentration of phenolics. This increase was due to stress caused by girdling, because increased synthesis of phenolic compounds, including flavonoids and phenylpropanoid pathways, is a common plant response to stresses during grape ripening (Dixon and Paiva, 1995; Fortes et al., 2011).

Impact of Girdling on Secondary Metabolites in Seeds

In seeds, only epicatechin was identified and quantified by ^{1}H NMR spectroscopy, and differences between girdled and non-girdled vines were not observed. For HPLC, flavan-3-ols were quantified in seed extracts of the treatments G(+) and G(−) from veraison to harvest, and similar to ^{1}H NMR spectroscopy, significant differences were not observed for any metabolites (**Table 5**). There was a large decrease in catechin and epicatechin, while procyanidin B2 increased from veraison to 181 dap, followed by a decrease at harvest (**Figure 6**). Additional research is needed to identify this unknown compound, possibly using LC-MS or 2D NMR. Kennedy et al. (2000) also reported a dramatic decrease of 90% for flavan-3-ols during ripening and 60% for proanthocyanidins. The accumulation and alterations in skin and seed tannins are less understood, although it is clear that biosynthesis occurs mostly during the early stages of berry development, while the ripening phase is characterized by polymerization reactions and other alterations to existing tannin units (Keller et al., 2006). Different studies have shown that tannin concentrations differ according to grape variety (Ristic and Iland, 2005). Cadot et al. (2006) showed histologically that seed lignification is achieved at veraison, with

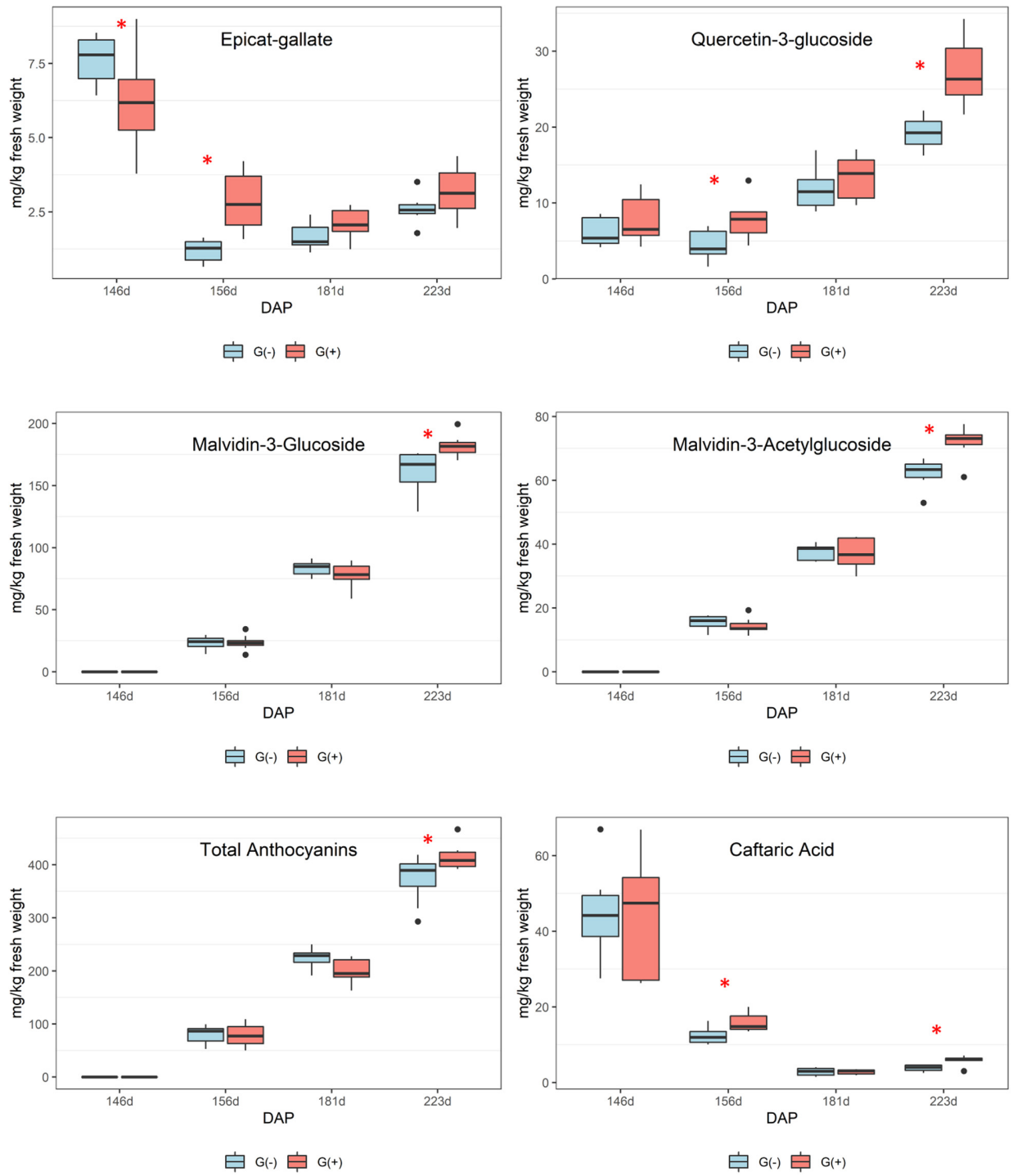

FIGURE 5 | Metabolites determined by HPLC-DAD in skin/pulp of 'Cabernet Sauvignon' grapes at different phenological stages, from two treatments, girdled – G(+); and non-girdled – G(–) vines. DAP = days after pruning, where: 146 corresponds to veraison; 156 to 30% maturation; 181–70% maturation; and 223 corresponds to harvest. Box plots show median, interquartile range (IQR), minimum/maximum, and strong outliers (>1.5 IQR). Differences between groups at each phenological stage were evaluated using the Mann Whitney *U*-test. Groups marked with (*) are statistically significant ($p < 0.05$).

proanthocyanidins localized in the epidermis while flavan-3-ol localization was linked with changes in cell walls of the outer integument.

In this study, girdling was applied at veraison and repeated after thirty days to increase the likelihood of the treatment being effective. We observed that it does not achieve additional

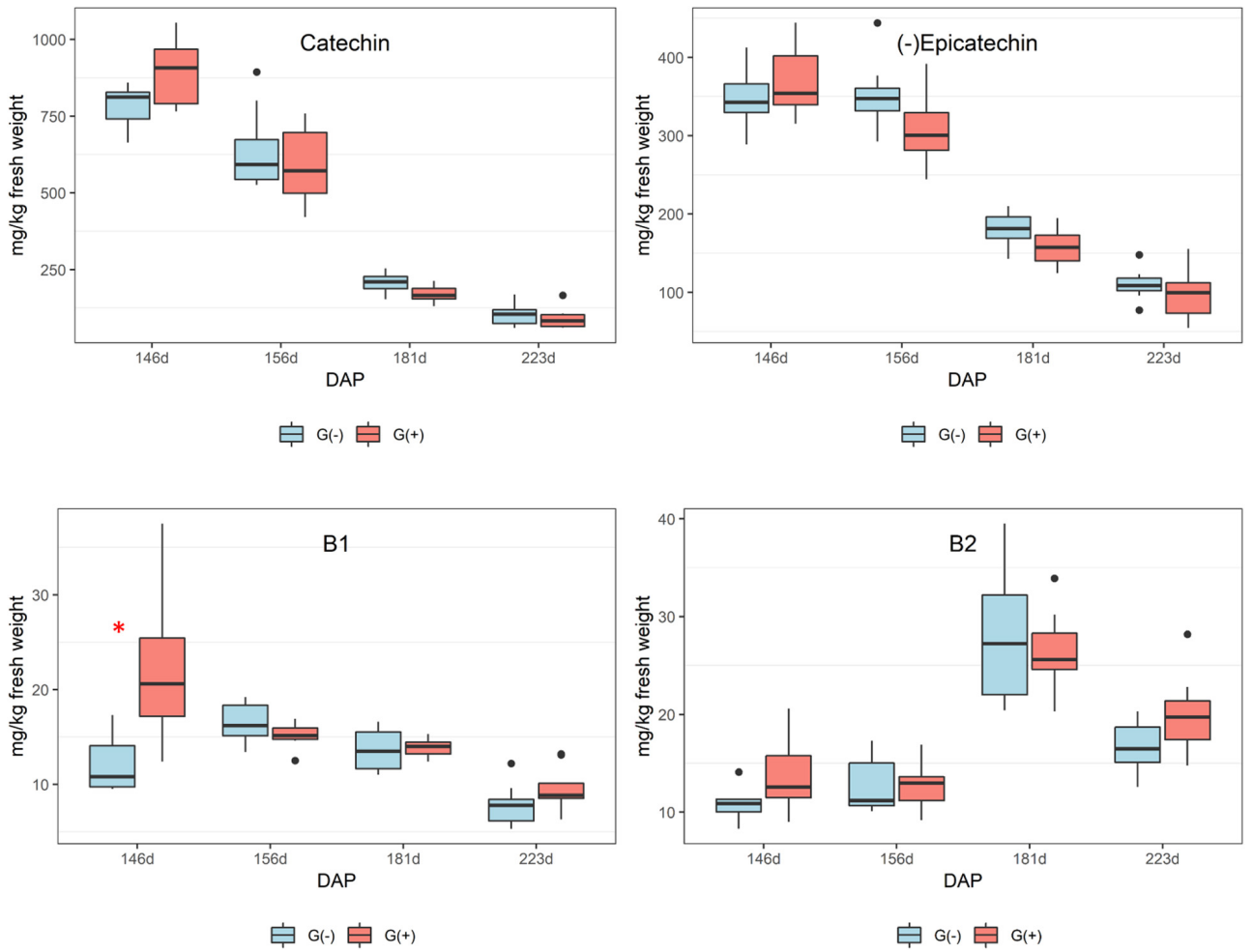

FIGURE 6 | Phenolic compounds determined by HPLC-DAD in seeds of 'Cabernet Sauvignon' grapes from different phenological stages. DAP = days after pruning, where: 146 corresponds to veraison; 156 to 30% maturation; 181 to 70% maturation; and 223 corresponds to harvest. Box plots show median, interquartile range (IQR), minimum/maximum, and strong outliers (>1.5 IQR). Differences between groups at each phenological stage were evaluated using the Mann Whitney *U*-test. Groups marked with (*) are statistically significant ($p < 0.05$).

gains in berry size and sugar level, but does fruit coloration (anthocyanins) and flavonols.

Impact of Girdling on Metabolites by Multivariate Statistical Analysis

According to the multivariate statistical analysis, PCA of skins + pulp data derived from the HPLC analysis showed that the first PC was responsible for 96.15% of total variability (**Figure 7A**). The most important factor responsible for sample discrimination was phenological stage, with samples at veraison (146 dap) separating strongly from samples collected at 30% maturation (156 dap), 70% maturation (181 dap), and harvest (223 dap). The main compounds driving separation were malvidin-3-glucoside and its derivatized forms, with higher concentrations on the right side of PC1. **Figure 7B** shows the PCA of metabolites in seeds derived from HPLC data. PC1 accounted for 93.59% of total variability, with grapes sampled at 146 and 156 dap separating from 181 and 223 dap. The metabolites driving this separation were epicatgallate, catechin and epicatechin, which were higher in grapes sampled from less mature vines (146 and 156 dap). **Figure 7C** shows the PCA of metabolites in skins + pulp tissue identified by ^{1}H NMR spectroscopy. PC1 explained 86.84% of total variability, and once again strong separation was observed between samples from 146 dap and 156 dap and those from 181 dap and 223 dap. The main metabolites explaining sample variability for less mature grapes (146 and 156 dap) were malic acid, tartaric acid, and succinic acid, and glutamine, while proline, sucrose and valine were important for more mature grapes (181 and 223 dap). The PCA obtained from metabolites determined in seeds using ^{1}H NMR spectroscopy was similar to skins + pulp data in that PC1 explained 86.16% of total variability and samples from 146 and 156 dap separated from grapes sampled at181 and 223 dap (**Figure 7D**). The main metabolites

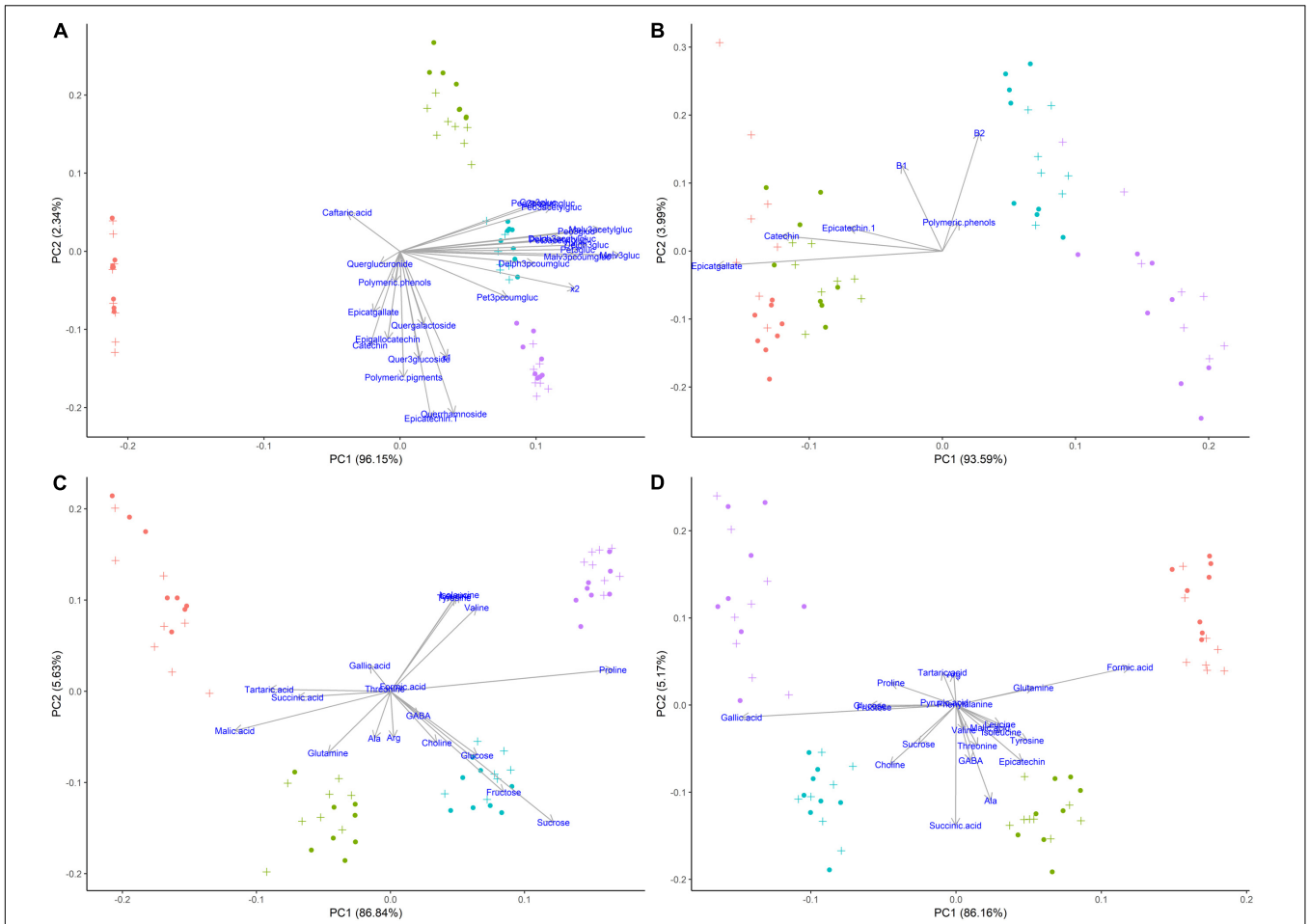

FIGURE 7 | Principal component analyses of metabolites determined by HPLC-DAD and ^{1}H NMR spectroscopy in different tissues of 'Cabernet Sauvignon' grapes at different phenological stages, from two treatments, girdled-G(+) and non-girdled vines- G(–). **(A)** HPLC-DAD of skin/pulp; **(B)** HPLC-DAD of seeds; **(C)** ^{1}H NMR spectroscopy of skin/pulp; **(D)** ^{1}H NMR spectroscopy of seeds. ● = veraison (146 days after pruning, DAP); ● = 30% maturation (156 DAP); ● = 70% maturation (181 DAP); ● = harvest (223 DAP); + = G(+); ● = G(–).

accounting for sample variability were formic acid and glutamine characterizing samples from veraison (146 dap), and gallic acid characterizing samples from harvest date (223 dap). Strongest separation was observed in secondary metabolites determined by HPLC in skins and pulps, followed by seeds. The main compounds driving separation were malvidin-3-glucoside and its derivatized forms. PCA of ^{1}H NMR data shows that malic acid, tartaric acid, and succinic acid were driving separation early in the phenological development, and that proline and sucrose are of importance as grapes ripen. Hernández-Hierro et al. (2014) also showed that the most important factor discriminating polyphenols in grape samples harvested at different times and contents of soluble solids was the degree of ripeness.

Principal components analysis were also generated for each phenological stage, as ripening was the main driver for differences among samples when evaluating the whole sample set (**Figure 7**). **Figure 8** shows the PCA of HPLC-DAD and ^{1}H NMR spectroscopy generated data from grape tissue at harvest (223 dap). PCA of the other periods (146, 156 and 181 dap) did not show additional information. PCA of phenolic skins + pulp data (HPLC) showed treatment separation (girdled vs. non-girdled) in PC2, responsible for 31.37% of total variability (**Figure 8A**). PC1 showed only the sample variability. Treatment separation was due to cyanidin-3-glucoside and epigallocatechin, characterizing non-girdled skin/pulp at the top, while malvidin-p-coumaroylglucoside and caftaric acid characterized girdled samples, on the bottom of the graph. These results can be confirmed in **Table 4**. **Figure 8B** shows the PCA of phenolic metabolites in the seeds (HPLC), but clear separation due to treatment were not obtained, similar to skin + pulp and seed metabolites determined by ^{1}H NMR spectroscopy (**Figures 8C,D**). Results indicate that girdling impacted mainly the secondary metabolites in the skin + pulp.

The metabolomics approach carried out in this study provided further information regarding vine development and skin, flesh/pulp and seed metabolite accumulation in Cabernet

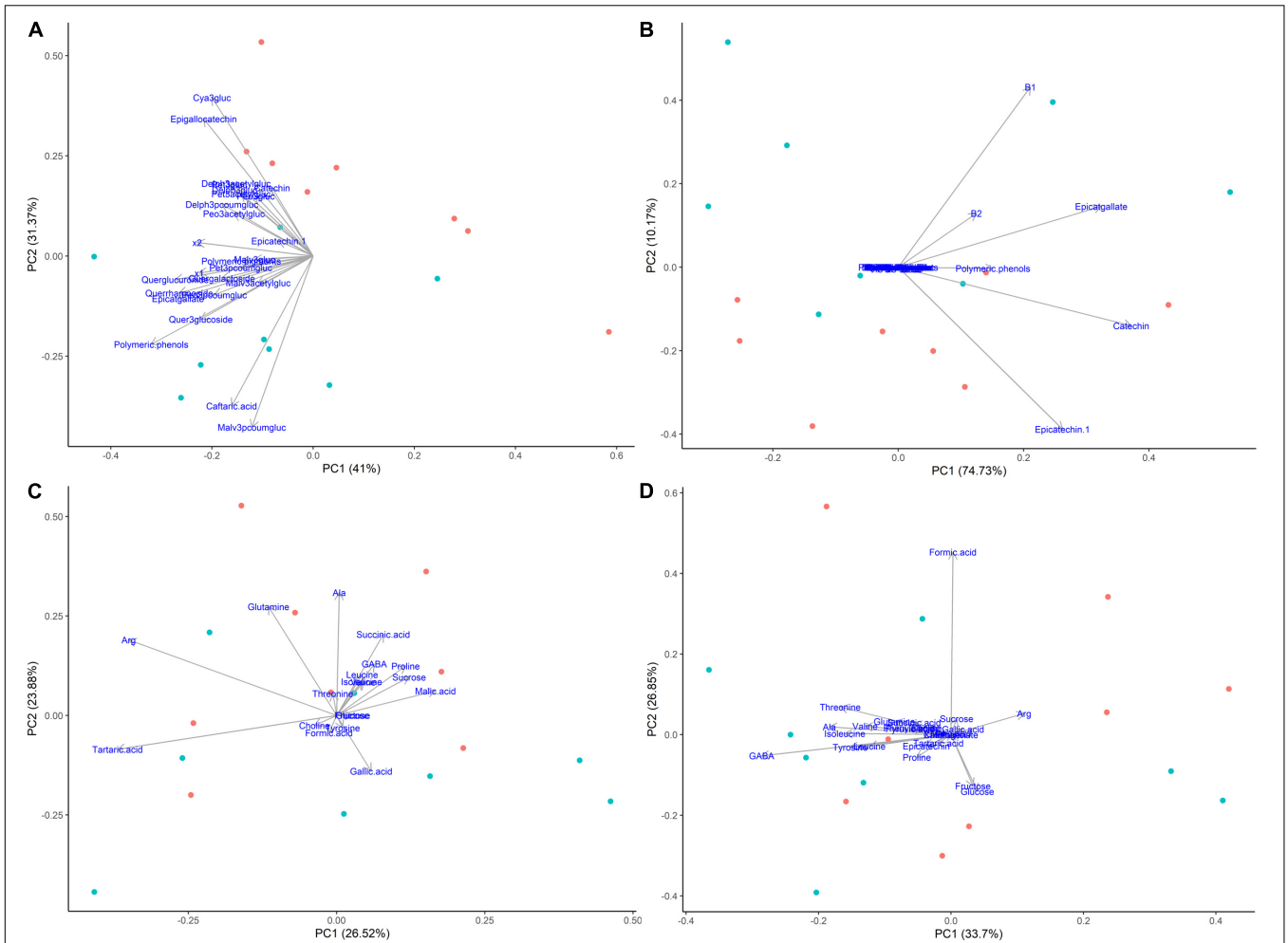

FIGURE 8 | Principal component analyses of metabolites determined by HPLC-DAD and ^{1}H NMR spectroscopy in different tissues of Cabernet Sauvignon grapes collected at harvest (223 days after pruning, DAP) from two treatments, girdled – G(+) and non-girdled vines - G(–). **(A)** HPLC-DAD of skin/pulp; **(B)** HPLC-DAD of seeds; **(C)** ^{1}H NMR spectroscopy of skin/pulp; **(D)** ^{1}H NMR spectroscopy of seeds. ● = G(+); ● = G(–).

Sauvignon grapes from veraison to harvest. Additional research should be carried out (i) to evaluate the use of girdling at fruit set with the aim of achieving greater balance in the composition of sugars, a higher anthocyanins and tannins contents, and to harvest an earlier crop. New studies could also evaluate (ii) the effect of girdling on volatile compounds using GC-MS. Further, studies are needed (iii) to determine the optimal date for harvest, in terms of berry weight reduction versus wine characteristics. For this, focus should be placed on larger sample sizes at the period of 70% maturation to harvest. Also, (iv) several unidentified compounds in skins/pulp and seeds could be elucidated with the use of 2D NMR (^{1}H-^{1}H and/or ^{1}H-^{13}C). Finally (v), future work could utilize genomic approaches to identify genes involved in primary and secondary pathways in grape berries after girdling, between veraison and harvest. Future research should also investigate the impact of girdling over multiple seasons and cultivars, as a metabolic effect has been shown.

CONCLUSION

A metabolomics approach was used to evaluate the effect of grapevine girdling on vine development, and metabolite accumulation in the skins/pulp and seeds of 'Cabernet Sauvignon' grapes, from veraison to harvest. Girdling at veraison increased stomatal conductance in vines at harvest, decreased glutamine, and increased anthocyanin and flavonol concentrations in skin/pulp tissues of grape berries, while primary metabolites such as sugars, organic acids, and other amino acids in skin/pulp and seeds were not dramatically affected. We hypothesize that this is due to extrafascicular phloem vessels transporting metabolites from leaves to the roots in vines. Girdling is a simple technique that could be used commercially for vine management to improve berry enological potential, particularly in terms of promoting the development of anthocyanins and flavonols in 'Cabernet Sauvignon' grapes.

DATA AVAILABILITY STATEMENT

All datasets generated for this study are included in the article/supplementary material.

AUTHOR CONTRIBUTIONS

SK and AO provided the experiment plan. GP, RG, DT, RB, CM-P, JE, and AO carried out agronomical and physiological measurements, berry samplings, and harvest. GP performed the extractions on grape berries. CS provided ^{1}H NMR spectroscopy sample preparation support. GP and EP analyzed the 1D ^{1}H NMR spectroscopy data. GP and CM-P performed the HPLC analysis. EP performed the statistical analyses. GP, AO, and EP interpreted the results. GP wrote the manuscript. AO and EP edited the manuscript. All authors read and approved the final manuscript.

ACKNOWLEDGMENTS

We are grateful to the UC Davis Oakville Experimental Station (SKK) for the grapes supplied.

REFERENCES

Adams, D. O. (2006). Phenolics and ripening in grape berries. *Am. J. Enol. Vitic.* 57, 249–256.

Ali, K., Maltese, M., Choi, Y. H., and Verpoorte, R. (2010). Metabolic constituents of grapevine and grape-derived products. *Phytochem. Rev.* 9, 357–378. doi: 10.1007/s11101-009-9158-0

Ardö, Y. (2006). Flavour formation by amino acid catabolism. *Biotechnol. Adv.* 24, 238–242. doi: 10.1016/j.biotechadv.2005.11.005

Bell, S.-J., and Henschke, P. A. (2005). Implications of nitrogen nutrition for grapes, fermentation and wine. *Aust. J. Grape Wine Res.* 11, 242–295.

Blancquaert, E. H., Oberholster, A., Ricardo-da-Silva, J. M., and Deloire, A. J. (2019). Effects of abiotic factors on phenolic compounds in the grape berry - a review. *S. Afr. J. Enol. Vitic.* 40, 779–784.

Bobeica, N., Poni, S., Hilbert, G., Renaud, C., Gomès, E., Delrot, S., et al. (2015). Differential responses of sugar, organic acids and anthocyanins to source-sink modulation of Cabernet Sauvignon and Sangiovese grapevines. *Front. Plant Sci.* 6:382. doi: 10.3389/fpls.2015.00382

Böttcher, C., Boss, P. K., Harvey, K. E., Burbidge, C. A., and Davies, C. (2018). Peduncle-girdling of Shiraz (*Vitis vinifera* L.) bunches and sugar concentration at the time of girdling affect wine volatile compounds. *Aust. J. Grape Wine Res.* 24, 206–218. doi: 10.1111/ajgw.12319

Boulton, R. (1980). The general relationship between potassium, sodium and pH in grape juice and wine. *Am. J. Enol. Vitic.* 31, 182–186.

Braidot, E., Zancani, M., Petrussa, E., Peresson, C., Bertolini, A., Patui, S., et al. (2008). Transport and accumulation of flavonoids in grapevine (*Vitis vinifera* L.). *Plant Signal. Behav.* 3, 626–632. doi: 10.4161/psb.3.9.6686

Brar, H. S., Singh, Z., Swinny, E., and Cameron, I. (2008). Girdling and grapevine leafroll associated viruses affect berry weight, colour development and accumulation of anthocyanins in 'Crimson Seedless' grapes during maturation and ripening. *Plant Sci.* 175, 885–897. doi: 10.1016/j.plantsci.2008.09.005

Brugière, N., Dubois, F., Limami, A. M., Lelandais, M., Roux, Y., Sangwan, R. S., et al. (1999). Glutamine synthetase in the phloem plays a major role in controlling proline production. *Plant Cell* 11, 1995–2011. doi: 10.1105/tpc.11.10.1995

Buckley, T. N., and Mott, K. A. (2013). Modelling stomatal conductance in response to environmental factors. *Plant Cell Environ.* 36, 1691–1699. doi: 10.1111/pce.12140

Cadot, Y., Miñana-Castelló, M. T., and Chevalier, M. (2006). Anatomical, histological, and histochemical changes in grape seeds from *Vitis vinifera* L. cv Cabernet franc during fruit development. *J. Agric. Food Chem.* 54, 9206–9215. doi: 10.1021/jf061326f

Carbonneau, A., Deloire, A., Torregrosa, L., Jaillard, B., Pellegrino, A., Métay, A., et al. (2015). *Traité de la Vigne: Physiologie, Terroir, Culture*. Paris: Dunod.

Cassino, C., Tsolakis, C., Bonello, F., Gianotti, V., and Osella, D. (2019). Wine evolution during bottle aging, studied by 1H NMR spectroscopy and multivariate statistical analysis. *Food Res. Intern.* 116, 566–577. doi: 10.1016/j.foodres.2018.08.075

Cayan, D. R., Maurer, E. P., Dettinger, M. D., Tyree, M., and Hayhoe, K. (2008). Climate change scenarios for the California region. *Clim. Change* 87, S21–S42.

Cerpa-Calderón, F. K., and Kennedy, J. A. (2008). Berry integrity and extraction of skin and seed proanthocyanidins during red wine fermentation. *J. Agric. Food Chem.* 56, 9006–9014. doi: 10.1021/jf801384v

Chin, E. L., Mishchuk, D. O., Breksa, A. P., and Slupsky, C. M. (2014). Metabolite signature of *Candidatus* liberibacter asiaticus infection in two citrus varieties. *J. Agric. Food Chem.* 62, 6585–6591. doi: 10.1021/jf5017434

Cohen, S. D., Tarara, J. M., Gambetta, G. A., Matthews, M. A., and Kennedy, J. A. (2012). Impact of diurnal temperature variation on grape berry development, proanthocyanidin accumulation, and the expression of flavonoid pathway genes. *J. Exp. Bot.* 63, 2655–2665. doi: 10.1093/jxb/err449

Comstock, J. P. (2002). Hydraulic and chemical signalling in the control of stomatal conductance and transpiration. *J. Exp. Bot.* 53, 195–200. doi: 10.1093/jexbot/53.367.195

Coombe, B. G., and McCarthy, M. G. (2000). Dynamics of grape berry growth and physiology of ripening. *Aust. J. Grape Wine Res.* 6, 131–135. doi: 10.1111/j.1755-0238.2000.tb00171.x

Dixon, R. A., and Paiva, N. L. (1995). Stress-induced phenylpropanoid metabolism. *Plant Cell* 7, 1085–1097. doi: 10.1105/tpc.7.7.1085

Douthe, C., Medrano, H., Tortosa, I., Escalona, J. M., Hernández-Montes, E., and Pou, A. (2018). Whole-plant water use in field grown grapevine: seasonal and environmental effects on water and carbon balance. *Front. Plant Sci.* 9:1540. doi: 10.3389/fpls.2018.01540

Downey, M. O., Dokoozlian, N. K., and Krstic, M. P. (2006). Cultural practice and environmental impacts on the flavonoid composition of grapes and wine: a review of recent research. *Am. J. Enol. Vitic.* 57, 257–268.

Ferrara, G., Mazzeo, A., Netti, G., Pacucci, C., Matarrese, A. M. S., Cafagna, I., et al. (2014). Girdling, gibberellic acid, and forchlorfenuron: effects on yield, quality, and metabolic profile of table grape cv. Italia. *Am. J. Enol. Vitic.* 65, 381–387. doi: 10.5344/ajev.2014.13139

Fiehn, O. (2002). Metabolomics-the link between genotypes and phenotypes. *Plant Mol. Biol.* 48, 155–171. doi: 10.1023/A:1013713905833

Fiehn, O., Kopka, J., Dörman, P., Altmann, T., Trethewey, R. N., and Willmitzer, T. L. L. (2000). Metabolite profiling for plant functional genomics. *Nat. Biotechnol.* 18, 1157–1161. doi: 10.1038/81137

Fortes, A. M., Agudelo-Romero, P., Silva, M. S., Ali, K., Sousa, L., Maltese, F., et al. (2011). Transcript and metabolite analysis in Trincadeira cultivar reveals novel information regarding the dynamics of grape ripening. *BMC Plant Biol.* 11:149. doi: 10.1186/1471-2229-11-149

Fotakis, C., Kokkotou, K., Zoumpoulakis, P., and Zervou, M. (2013). NMR metabolite fingerprinting in grape derived products: an overview. *Food Res. Int.* 54, 1184–1194. doi: 10.1016/j.foodres.2013.03.032

Gallo, V., Mastrorilli, P., Cafagna, I., Nitti, G. I., Latronico, M., Longobardi, F., et al. (2014). Effects of agronomical practices on chemical composition of table grapes evaluated by NMR spectroscopy. *J. Food Comp. Anal.* 35, 44–52. doi: 10.1016/j.jfca.2014.04.004

Garrido-Bañuelos, G., Buica, A., Schückel, J., Zietsman, A. J. J., Willats, W. G. T., Moore, J. P., et al. (2019a). Investigating the relationship between grape cell wall polysaccharide composition and the extractability of phenolic compounds into Shiraz wines. Part I: vintage and ripeness effects. *Food Chem.* 278, 36–46. doi: 10.1016/j.foodchem.2018.10.134

Garrido-Bañuelos, G., Buica, A., Schückel, J., Zietsman, A. J. J., Willats, W. G. T., Moore, J. P., et al. (2019b). Investigating the relationship between cell wall polysaccharide composition and the extractability of grape phenolic compounds into Shiraz wines. Part II: extractability during fermentation into wines made from grapes of different ripeness levels. *Food Chem.* 278, 26–35. doi: 10.1016/j.foodchem.2018.10.136

Godelmann, R., Fang, F., Humpfer, E., Schütz, B., Bansbach, M., Schäfer, H., et al. (2013). Targeted and nontargeted wine analysis by 1H NMR spectroscopy combined with multivariate statistical analysis. Differentiation of important parameters: grape variety, geographical origin, year of vintage. *J. Agric. Food Chem.* 61, 5610–5619. doi: 10.1021/jf400800d

Girardello, R. C., Cooper, M. L., Smith, R. J., Lerno, L., Bruce, R. C., Eridon, S., and Oberholster, A. (2019). Impact of grapevine red blotch disease on grape composition of *Vitis vinifera* cabernet sauvignon, merlot and chardonnay. *J. Agric. Food Chem.* 67, 5496–5511. doi: 10.1021/acs.jafc.9b01125

Gourieroux, A. M., Holzapfel, B. P., Scollary, G. R., McCully, M. E., Canny, M. J., and Rogiers, S. Y. (2016). The amino acid distribution in rachis xylem sap and phloem exudates of *Vitis vinifera* 'Cabernet Sauvignon' bunches. *Plant Physiol. Biochem.* 105, 45–54. doi: 10.1016/j.plaphy.2016.04.010

Harrell, D. C., and Williams, L. E. (1987). Net CO2 assimilation rate of grapevine leaves in response to trunk girdling and gibberellic acid application. *Plant Physiol.* 83, 457–459. doi: 10.1104/pp.83.3.457

Hernández-Hierro, J. M., Quijada-Morín, N., Martínez-Lapuente, L., Guadalupe, Z., Ayestarán, B., Rivas-Gonzalo, J. C., et al. (2014). Relationship between skin cell wall composition and anthocyanin extractability of *Vitis vinifera* L. cv. Tempranillo at different grape ripeness degree. *Food Chem.* 146, 41–47. doi: 10.1016/j.foodchem.2013.09.037

Holmes, E., Wilson, I. D., and Lindon, J. C. (2019). "An overview of metabolic phenotyping and its role in systems biology," in *The Handbook of Metabolic Phenotyping*, eds J. C. Lindon, and J. K. Nicholson, (Oxford: Elsevier), 1–51.

Huang, Z., and Ough, C. S. (1991). Amino acid profiles of commercial grape juices and wines. *Am. J. Enol. Vitic.* 42, 261–267. doi: 10.1111/1567-1364.12222

Hunter, J. J., and Ruffner, H. P. (2001). Assimilate transport in grapevines – effect of phloem disruption. *Aust. J. Grape Wine Res.* 7, 118–126. doi: 10.1111/j.1755-0238.2001.tb00198.x

Keller, M. (2010). Managing grapevines to optimise fruit development in a challenging environment: a climate change primer for viticulturists. *Aust. J. Grape Wine Res.* 16, 56–69. doi: 10.1111/j.1755-0238.2009.00077.x

Keller, M. (2015). *The Science of Grapevines: Anatomy and Physiology*, 2nd Edn. New York, NY: Academic Press.

Keller, M., and Hrazdina, G. (1998). Interaction of nitrogen availability during bloom and light intensity during veraison. II. Effects on anthocyanin and phenolic development during grape ripening. *Am. J. Enol. Vitic.* 49, 341–349.

Keller, M., Smith, J. P., and Bondada, B. R. (2006). Ripening grape berries remain hydraulically connected to the shoot. *J. Exp. Bot.* 11, 2577–2587. doi: 10.1093/jxb/erl020

Kennedy, J. A., Matthews, M. A., and Waterhouse, A. L. (2000). Changes in grape seed polyphenols during fruit ripening. *Phytochemistry* 55, 77–85. doi: 10.1016/s0031-9422(00)00196-5

Kortesniemi, M., Slupsky, C. M., Ollikka, T., Kauko, L., Spevacek, A. R., Sjövall, O., et al. (2016). NMR profiling clarifies the characterization of Finnish honeys of different botanical origins. *Food Res. Int.* 86, 83–92. doi: 10.1016/j.foodres.2016.05.014

Krishnan, P., Kruger, N. J., and Ratcliffe, R. G. (2005). Metabolite fingerprinting and profiling in plants using NMR. *J. Exp. Bot.* 56, 255–265. doi: 10.1093/jxb/eri010

Kuhn, N., Guan, L., Dai, Z. W., Wu, B. H., Lauvergeat, V., Gomès, E., et al. (2014). Berry ripening: recently heard through the grapevine. *J. Exp. Bot.* 65, 4543–4559. doi: 10.1093/jxb/ert395

Lamikanra, O., and Kassa, A. K. (1999). Changes in the free amino acid composition with maturity of the noble cultivar of *Vitis rotundifolia* Michx. grape. *J. Agric. Food Chem.* 47, 4837–4841. doi: 10.1021/jf981085e

Leinonen, I., Grant, O. M., Tagliavia, C. P. P., Chaves, M. M., and Jones, H. G. (2006). Estimating stomatal conductance with thermal imagery. *Plant Cell Environ.* 29, 1508–1518.

Lima, M. R. M., Felgueiras, M. L., Gracxa, G., Rodrigues, J. E. A., Barros, A., Gil, A. M., et al. (2010). NMR metabolomics of esca disease-affected *Vitis vinifera* cv. Alvarinho leaves. *J. Exp. Bot.* 61, 4033–4042. doi: 10.1093/jxb/erq214

Lloyd, N., Johnson, D. L., and Herderich, M. J. (2015). Metabolomics approaches for resolving and harnessing chemical diversity in grapes, yeast and wine. *Aust. J. Grape Wine Res.* 21, 723–740. doi: 10.1111/ajgw.12202

López, R., Brossa, R., Gil, L., and Pita, P. (2015). Stem girdling evidences a trade-off between cambial activity and sprouting and dramatically reduces plant transpiration due to feedback inhibition of photosynthesis and hormone signaling. *Front. Plant Sci.* 6:285. doi: 10.3389/fpls.2015.00285

Neo, H. H., and Layzell, D. B. (1997). Phloem glutamine and the regulation of O2 diffusion in legume nodules. *Plant Physiol.* 113, 259–267. doi: 10.1104/pp.113.1.259

Nicholson, J. K., Holmes, E., Kinross, J. M., Darzi, A. W., Takats, Z., and Lindon, J. C. (2012). Metabolic phenotyping in clinical and surgical environments. *Nature* 491, 384–392. doi: 10.1038/nature11708

Oberholster, A., Carstens, L. M., and Du Toit, W. (2013). Investigation of the effect of gelatine, egg albumin and cross-flow microfiltration on the phenolic composition of Pinotage wine. *Food Chem.* 138, 1275–1281. doi: 10.1016/j.foodchem.2012.09.128

Ollat, N., Diakou-Verdin, P., Carde, J.-P., Barrieu, F., Gaudillère, J.-P., and Moing, A. (2002). Grape berry development: a review. *J. Int. Sci. Vigne Vin* 36, 109–131. doi: 10.20870/oeno-one.2002.36.3.970

Parrott, D. L., McInnerney, K., Feller, U., and Fischer, A. M. (2007). Steam-girdling of barley (*Hordeum vulgare*) leaves leads to carbohydrate accumulation and accelerated leaf senescence, facilitating transcriptomic analysis of senescence-associated genes. *New Phytol.* 176, 56–69. doi: 10.1111/j.1469-8137.2007.02158.x

Peng, Z., Iland, P. G., Oberholster, A., Sefton, M. A., and Waters, E. J. (2002). Analysis of pigmented polymers in red wine by reverse phase HPLC. *Aust. J. Grape Wine Res.* 8, 70–75. doi: 10.1111/j.1755-0238.2002.tb00213.x

Pereira, G. E., Gaudillere, J.-P., Van Leeuwen, C., Hilbert, G., Maucourt, M., Deborde, C., et al. (2006a). ^{1}H NMR metabolite fingerprints of grape berry: comparison of vintage and soil effects in Bordeaux grapevine growing areas. *Anal. Chim. Acta* 563, 346–352. doi: 10.1016/j.aca.2005.11.007

Pereira, G. E., Gaudillere, J.-P., Van Leeuwen, C., Hilbert, G., Maucourt, M., Deborde, C., et al. (2006b). Microclimate influence on mineral and metabolic profiles of grape berries. *J. Agric. Food Chem.* 54, 6765–6775. doi: 10.1021/jf061013k

Peterson, A. L., and Waterhouse, A. L. (2016). 1H NMR: a novel approach to determining the thermodynamic properties of acetaldehyde condensation reactions with glycerol, (+)-catechin, and glutathione in model wine. *J. Agric. Food Chem.* 64, 6869–6878. doi: 10.1021/acs.jafc.6b02077

Pinu, F. R. (2018). Grape and wine metabolomics to develop new insights using untargeted and targeted approaches. *Fermentation* 4:e92. doi: 10.3390/fermentation4040092

R Core Team, (2012). *R: A Language and Environment for Statistical Computing*. Vienna: R Foundation for Statistical Computing.

Rainer-Lethaus, G., and Oberhuber, W. (2018). Phloem girdling of Norway spruce alters quantity and quality of wood formation in roots particularly under drought. *Front. Plant Sci.* 9:392. doi: 10.3389/fpls.2018.00392

Reshef, N., Fait, A., and Agam, N. (2019). Grape berry position affects the diurnal dynamics of its metabolic profile. *Plant Cell Environ.* 42, 1897–1912. doi: 10.1111/pce.13522

Ribéreau-Gayon, P., Glories, Y., Maujean, A., and Dubourdieu, D. (2006). *Handbook of Enology. The Chemistry of Wine. Stabilization and Treatments*, Vol. 2. Hoboken, NJ: John Wiley & Sons.

Rienth, M., Torregrosa, L., Kelly, M. T., Luchaire, N., Pellegrino, A., Grimplet, J., et al. (2014). Is transcriptomic regulation of berry development more important at night than during the day? *PLoS One* 9:e88844. doi: 10.1371/journal.pone.0088844

Ristic, R., and Iland, P. G. (2005). Relationships between seed and berry development of *Vitis Vinifera* L. cv Shiraz: developmental changes in seed morphology and phenolic composition. *Aust. J. Grape Wine Res.* 11, 43–58. doi: 10.1111/j.1755-0238.2005.tb00278.x

Roessner, U., Luedemann, A., Brust, D., Fiehn, O., Willmitzer, T. L. L., and Fernie, A. R. (2001). Metabolic profiling allows comprehensive phenotyping of genetically or environmentally modified plant systems. *Plant Cell* 13, 11–29. doi: 10.1105/tpc.13.1.11

Roper, T. R., and Williams, L. (1989). Net CO2 assimilation and carbohydrate partitioning of grapevine leaves in response to trunk girdling and gibberellic

acid application. *Plant Physiol.* 89, 1136–1140. doi: 10.1104/pp.89.4.1136

Roullier-Gall, C., Boutegrabet, L., Gougeon, R. D., and Schmitt-Kopplin, P. (2014). A grape and wine chemodiversity comparison of different appellations in Burgundy: vintage vs terroir effects. *Food Chem.* 152, 100–107. doi: 10.1016/j.foodchem.2013.11.056

Singleton, V. L., Salgues, M., Zaya, J., and Trousdale, E. (1985). Caftaric acid disappearance and conversion to products of enzymic oxidation in grape must and wine. *Am. J. Enol. Vitic.* 36, 50–56.

Sun, R., Cheng, G., Li, Q., He, Y., Wang, Y., Lan, Y.-B., et al. (2017). Light-induced variation in phenolic compounds in Cabernet Sauvignon grapes (*Vitis vinifera* L.) involves extensive transcriptome reprogramming of biosynthetic enzymes, transcription factors, and phytohormonal regulators. *Front. Plant Sci.* 8:547. doi: 10.3389/fpls.2017.00547

Terrier, N., Glissant, D., Grimplet, J., Barrieu, F., Abbal, P., Couture, C., et al. (2005). Isogene specific oligo arrays reveal multifaceted changes in gene expression during grape berry (*Vitis vinifera* L.) development. *Planta* 222, 832–847. doi: 10.1007/s00425-005-0017-y

Urban, L., Léchaudel, M., and Lu, P. (2004). Effect of fruit load and girdling on leaf photosynthesis in *Mangifera indica* L. *J. Exp. Bot.* 55, 2075–2085. doi: 10.1093/jxb/erh220

Van Leeuwen, C., and Seguin, G. (2006). The concept of terroir in viticulture. *J. Wine Res.* 17, 1–10. doi: 10.1080/09571260600633135

Von Caemmerer, S., and Farquhar, G. D. (1981). Some relationships between the biochemistry of photosynthesis and the gas Exchange of leaves. *Planta* 153, 376–387. doi: 10.1007/BF00384257

Williams, L., and Ayars, J. E. (2005). Water use of Thompson Seedless grapevines as affected by the application of gibberellic acid (GA3) and trunk girdling - practices to increase berry size. *Agric. For. Meteorol.* 129, 85–94. doi: 10.1016/j.agrformet.2004.11.007

Williams, L. E., Retzlaff, W. A., Yang, W., Biscay, P. J., and Ebisuda, A. N. (2000). Effect of girdling on leaf gas exchange, water status, and non-structural carbohydrates of field-grown *Vitis vinifera* L. (cv. Flame Seedless). *Am. J. Enol. Vitic.* 51, 49–54.

Xia, J., Sinelnikov, I. V., Han, B., and Wishart, D. S. (2015). MetaboAnalyst 3.0-making metabolomics more meaningful. *Nucleic Acids Res.* 43, W251–W257. doi: 10.1093/nar/gkv380

Zhang, B., Tolstikov, V., Turnbull, C., Hicks, L. M., and Fiehn, O. (2000). Divergent metabolome and proteome suggest functional independence of dual phloem transport systems in cucurbits. *Proc. Natl. Acad. Sci. U.S.A.* 107, 13532–13537. doi: 10.1073/pnas.0910558107

Zhang, X., Breksa, A. P., Mishchuk, D. O., Fake, C. E., O'Mahony, M. A., and Slupsky, C. M. (2012). Fertilisation and pesticides affect mandarin orange nutrient composition. *Food Chem.* 134, 1020–1024. doi: 10.1016/j.foodchem.2012.02.218

Zhang, X., Breksa, A. P., Mishchuk, D. O., and Slupsky, C. M. (2011). Elevation, rootstock, and soil depth affect the nutritional quality of mandarin oranges. *J. Agric. Food Chem.* 59, 2672–2679. doi: 10.1021/jf104335z

Zhang, Y., Ding, Z., Ma, F., Chauhan, R. D., Allen, D. K., Brutnell, T. P., et al. (2015). Transcriptional response to petiole heat girdling in cassava. *Sci. Rep.* 5:e8414. doi: 10.1038/srep08414

Conflict of Interest: GP was employed by company Brazilian Agricultural Research Corporation-Embrapa Grape & Wine.

The authors declare that the research was conducted in the absence of any commercial or financial relationships that could be construed as a potential conflict of interest.

frontiers in Plant Science

ORIGINAL RESEARCH
published: 14 August 2020
doi: 10.3389/fpls.2020.01140

Development of a Novel Phenotypic Roadmap to Improve Blueberry Quality and Storability

Brian Farneti[1]*, *Francesco Emanuelli*[1], *Iuliia Khomenko*[2], *Matteo Ajelli*[1], *Franco Biasioli*[2] *and Lara Giongo*[1]

[1] Genomics and Biology of Fruit Crop Department, Fondazione Edmund Mach, Trento, Italy, [2] Food Quality and Nutrition Department, Fondazione Edmund Mach, Trento, Italy

Improved fruit quality and prolonged storage capability are key breeding traits for blueberry (*Vaccinium* spp.) fruit. Until now, breeding selection was mostly oriented on the amelioration of agronomic traits, such as flowering time, chilling requirement, or plant structure. Up until now, however, the storage effect on fruit quality has not been extensively studied, mostly because objective and handy phenotyping tools to evaluate quality traits were not available. In this study we are proposing a novel phenotyping protocol to support breeding selection and quality control within the entire blueberry production chain. Volatile organic compounds (VOCs) and texture traits, were measured by Proton Transfer Reaction- Time of Flight- Mass Spectrometry (PTR-ToF-MS) and a texture analyzer respectively, taking into consideration the influence of prolonged storage. The exploitation of the genetic variability existing within the investigated blueberry germplasm collection (including both southern and northern highbush, hybrids, and rabbiteyes) allowed the identification of the best performing cultivars, based on texture and VOCs variability, to be used as superior parental lines for future breeding programs. The comprehensive characterization of blueberry aroma allowed the identification of a wide array of spectrometric features, mostly related to aldehydes, alcohols, terpenoids, and esters, that can be used as putative biomarkers to rapidly evaluate the blueberry aroma variations related to genetic differences and storability. In addition, this study revealed a lack of straightforward relationship between harvest and postharvest quality features, that might be genotype-dependent.

Keywords: *Vaccinium* spp., texture, aroma, Proton Transfer Reaction-Time of Flight-Mass Spectrometry, breeding, storage

OPEN ACCESS

Edited by:
Claudio Bonghi,
University of Padua, Italy

Reviewed by:
Anish Malladi,
University of Georgia, United States
Jessica Scalzo,
Costa, Corindi Beach, Australia
Lisa Jeannine Rowland
Agricultural Research Service, United States

***Correspondence:**
Brian Farneti
brian.farneti@fmach.it

Specialty section:
This article was submitted to Crop and Product Physiology, a section of the journal Frontiers in Plant Science

Received: *26 April 2020*
Accepted: *14 July 2020*
Published: *14 August 2020*

Citation:
Farneti B, Emanuelli F, Khomenko I, Ajelli M, Biasioli F and Giongo L (2020) Development of a Novel Phenotypic Roadmap to Improve Blueberry Quality and Storability. Front. Plant Sci. 11:1140. doi: 10.3389/fpls.2020.01140

INTRODUCTION

Worldwide blueberry (*Vaccinium* spp.) production, for both processed and fresh market, has increased over the last decade making blueberry becoming the second most important soft fruit species after strawberry (Romo-Muñoz et al., 2019). Fresh market production, for instance, rose from about 270,000 tons to 370,000 tons in only 4 years (2012-2016, https://www.internationalblueberry.org/). Nonetheless, this progression mostly concerns certain production

areas, situated for the most part in Peru, Mexico, Spain, Poland, South Africa, and China (Romo-Muñoz et al., 2019). The development of new blueberry accessions, suitable for cultivation under different climate conditions and for prolonged storage, is thus fundamental to guarantee a year-round supply of blueberries to cover the rising market demand, and with shipped fruit being in the best possible conditions upon delivery.

Initially, blueberry breeding programs were focused on developing cultivars to withstand conditions in the northern United States, including, among the major traits, disease resistance and broad ripening times (Hancock, 2009). Later, certain breeding programs became focused on the development of genotypes adapted to climatic conditions in the southern United States by hybridizing *V. corymbosum* with other species like *V. darrowii* and *V. elliottii* (Lyrene et al., 2003). Today, key breeding traits are a larger harvest window, improved fruit quality, and better storage capability (Gallardo et al., 2018).

Although trait relevance highly depends on supply chain, addressing high and distinguishable fruit quality is essential for capturing consumer preferences. Recent studies (Gilbert et al., 2015; Gallardo et al., 2018) disclosed that flavor, texture, and prolonged shelf-life are the most appreciated quality traits for both blueberry industry and consumers. Notably, consumers identify typical blueberry flavor and sweetness as positive quality traits, and unpleasant texture attributes, such as mealy and pasty, as negative ones. Both textural and flavor attributes decline during storage but a generic aim of shelf-life extension may have unintended negative consequences on other fruit quality traits, for instance aroma, as already suggested for several horticultural products, like strawberry, peach, apple, or tomato (Goff and Klee, 2006; Klee, 2010; Rambla et al., 2014; Farneti et al., 2017a; Tieman et al., 2017). The chance of this quality decline may be heightened by the fact that breeding selection for aroma has occurred almost without analytical assistance, since aroma is still not considered as a discriminating trait in the early breeding selection phase (Klee and Tieman, 2018). This is also strengthened by the complex and time-consuming phenotyping protocols ordinarily used, which make the analytical screening of wide germplasm unfeasible.

Blueberry aroma depends on the interaction of dozens of volatile compounds (VOCs) synthesized by fruit during ripening (Du et al., 2011; Beaulieu et al., 2014; Du and Rouseff, 2014; Gilbert et al., 2015; Farneti et al., 2017b). As most secondary plant metabolites, VOCs are detectable in blueberry fruit with high variability according to genetic and environmental differences and, above all, to the biological ripening stage of the fruit at the time of analysis (Farneti et al., 2017b). Most of compounds responsible for blueberry aroma are synthesized by the fruit in the full ripe stage, such as linalool and majority of monoterpenes, (Z)-2-hexen-1-ol, and hexanal, or at the pink stage of ripening, such as (E)-2-hexenal (Farneti et al., 2017b). Esters, although being present in lower average concentration, strongly affect blueberry aroma, especially "sweet" and "fruity" fragrances. A large fraction of esters, such as ethyl acetate, methyl isovalerate, ethyl isovalerate, methyl 2-methylbutanoate, are exclusively synthesized in the last phase of ripening and magnified in overripe fruit (Farneti et al., 2017b).

In order to satisfy consumer demands more effort and attention need to be devoted, from a scientific and practical background, to improve and optimize blueberry quality upon delivery to the consumers. The key attributes of quality may vary with context and depend on the intended use of the product and the available or affordable technology (Abbott, 1999). Defining and quantifying quality properties of blueberry fruit, in relation to distinct segments of the production chain, needs comprehensive investigations.

While taste traits (sweetness and sourness) are relatively well explained by the sugar content and titratable acidity, the prediction of aroma and texture traits seems more uncertain (Blaker et al., 2014; Gilbert et al., 2015; Ferrão et al., 2020) because of the lack of precision in the instrumental measures and the high interactions among traits (Folta and Klee, 2016). Breeders need selection criteria, both efficient and easy to assess, for supporting organoleptic quality breeding. Physical and chemical traits could be an alternative approach for routine measurements of some of the quality traits, but molecular markers will provide more efficient tool for selecting improved genotypes (Folta and Klee, 2016). The genetic dissection of these complex processes would permit a more systematic approach to plant improvement than has been possible previously (Klee and Tieman, 2018). An important component that has to be studied more accurately, also from a genetic perspective, is the fruit quality deterioration during storage and the resistance of fruit to several postharvest biotic and abiotic disorders. The achievement of this goal will only be possible with a more accurate and objective quality traits phenotyping, ideally combined with multivariate prediction models of quality perception.

In this study, a wide blueberry germplasm collection, including southern and northern highbush, hybrids and rabbiteyes, was employed and assessed for both texture and aroma traits applying advanced phenotyping strategies preliminarily developed in Giongo et al. (2013) and Farneti et al. (2017b). The aims of this work were i) to estimate the potential genetic variability among blueberry cultivars for both quality traits and ii) to evaluate how post-harvest cold storage may influence this quality variability. Knowing of the genetic variability existing within the blueberry germplasm could allow a precise identification of the best performing cultivars to be used as superior parental lines for future breeding program aimed to improve blueberry fruit quality. In addition, results of this study might be useful in defining an objective phenotyping protocol to apply in the selection breeding phases of blueberry.

MATERIALS AND METHODS

Plant Material and Sampling

Forty-six *Vaccinium* accessions (**Table 1**) were chosen from the experimental field of Edmund Mach Foundation Research and Innovation Centre at Pergine (Trento), located in the northern Italy (Trentino Alto Adige region). At the time of the analysis,

TABLE 1 | List of the *Vaccinium* spp. cultivars employed in this study.

	CULTIVAR			CULTIVAR	
1	Aron	*V. angustifolium, V. uliginosum*	**24**	Jubilee	*V. corymbosum, V. darrowii, V. elliotti*
2	Atlantic	*V. corymbosum*	**25**	Legacy	*V. corymbosum, V. darrowii*
3	Aurora	*V. corymbosum*	**26**	Liberty	*V. corymbosum*
4	Azur	*V. corymbosum*	**27**	Marimba	*V. corymbosum, V. darrowii, V. ashei*
5	Berkeley	*V. corymbosum*	**28**	Misty	*V. corymbosum, V. darrowii*
6	Biloxi	*V. corymbosum, V. virgatum, V. darrowii*	**29**	Mondo	-
7	Blue Crop	*V. corymbosum*	**30**	North Blue	*V. corymbosum, V. angustifolium*
8	Blue Moon	*V. corymbosum*	**31**	Northland	*V. corymbosum, V. angustifolium*
9	Brigitta Blue	*V. corymbosum*	**32**	Nui	*V. corymbosum*
10	Centra Blue	*V. virgatum*	**33**	O'Neal	*V. corymbosum, V. darrowii, V. ashei*
11	Centurion	*V. virgatum*	**34**	Ozark Blue	*V. corymbosum*
12	Chandler	*V. corymbosum*	**35**	Poppins	*V. corymbosum, V. ashei*
13	Compact	*V. corymbosum*	**36**	Primadonna	*V. corymbosum hybrid*
14	Cosmopolitan	-	**37**	Puru	*V. corymbosum*
15	Coville	*V. corymbosum*	**38**	Roxy Blue	*V. corymbosum, V. darrowii, V. elliotti*
16	Darrow	*V. corymbosum*	**39**	Rubel	*V. corymbosum*
17	Early Blue	*V. corymbosum*	**40**	Safir	*V. corymbosum*
18	Elizabeth	*V. corymbosum*	**41**	Simultan	*V. corymbosum*
19	Elliott	*V. corymbosum*	**42**	Sky Blue	*V. virgatum*
20	Emerald	*V. corymbosum, V. darrowii, V. elliotti*	**43**	Southern Belle	*V. corymbosum, V. darrowii*
21	Goldtraube	*V. corymbosum, V. lamarkii*	**44**	Star	*V. corymbosum, V. darrowii, V. ashei*
22	Jersey	*V. corymbosum*	**45**	Top Hat	*V. angustifolium*
23	Jewel	*V. corymbosum, V. darrowii, V. elliotti*	**46**	Toro	*V. corymbosum*

plants were in the full production phase, between 7 and 10 years old. Bushes were maintained following standard pruning and surface bark mulching renewal. In the plot, each of the accessions was represented by at least five plants. To avoid both misnaming and redundant genotypes each accessions employed in the study was checked with molecular markers.

Fruit were harvested at maturity stage assessed according to the method described by Giongo et al. (2013), coincident with the commercial harvest. Homogeneous fruit, free from external damages or irregularities, were sampled immediately at harvest and divided into two batches, of about 80 fruit each. Analyses were carried out at harvest and after 6 weeks of storage, at 2°C (RH 85%). Each fruit batch was subsequently re-divided into two subsets for texture and VOC analysis, respectively.

DNA Extraction

Plant material of 46 blueberry accessions (**Table 1**) was collected from young leaves, stored at -20°C and then vacuum lyophilized (72 h) prior to DNA extraction. DNA was extracted in triplicate using the DNeasy 96 Plant Kit (Qiagen GmbH, Germany) according to the manufacturer's protocol. DNA was re-suspended in 200 ul AE buffer (Qiagen GmbH, Germany) and was diluted 1:10 for use in PCR. The quality and concentration of all DNA samples was visually checked on agarose gels and estimated using a NanoDrop ND-8000 spectrophotometer. Six SSRs (**Table S1**) were chosen as proposed by Boches et al. (2006) and were grouped into two separate multiplexed reactions, MVA and MVB, and used to screen all genotypes. Each specific forward primer was connected with one of the 5′ universal primer sequence tails (Missiaggia and Grattapaglia, 2006; Ge et al., 2014) which were T7 (5′-TAATACGACT CACTATAGGG), M13 (5′-TGTAAAACGACGGCCAGT), M13R (5′-CAGGAAACAGCTATGACC), or D12S1090f (5′-CTATAGGGCACGCGTGGT) (**Table S2**).

The stand alone universal primers M13, D12S1090f, M13R and T7 were fluorescently labeled with FAM, VIC, NED, and PET respectively. All primers were ordered from Life Technologies and dissolved in TE (10 mM Tris, 1 mM EDTA, pH 8.0) to produce a 20 μM stock solution for fluorescently-labeled universal primer and locus-specific reverse primer and a 10μM stock solution of locus-specific forward primer with universal tail (moles of tailed forward primer: reverse primer: dye-labeled universal primer= 1:2:2). Primer mix here designated Pmixlocus (three primers were mixed for each specific locus). Each Multiplex included equimolar amounts of the Pmixlocus.

Multiplexed reactions (MVA and MVB) were carried out in 10ul reactions using Type-it^{TM} Microsatellite PCR kit (Qiagen) according to the manufacturer instructions. Thermal cycling conditions for MVA were as follow: initial 3 min denaturation step at 94°C, eight touch-down cycles comprising a 30 s denaturation at 94°C followed by 90 s of annealing starting at 64°C and decreasing, 0.5°C per cycle, down to 60°C and 60 s of extension at 72°C. Subsequently, 25 more identical cycles were conducted with and annealing temperature of 60°C followed by a final 30 min extension step at 60°C. Thermal conditions for MVB changed only for the annealing temperature, starting at 60°C and decreasing 0.5°C per cycle, down to 60°C. Subsequently, 25 more identical cycles were conducted with an annealing temperature of 56°C followed by a final 30 min extension step at 60°C. Products from multiplexed reactions were checked on agarose gels and then diluted 1:50 prior to analysis and separated by electrophoresis on an ABI3730XL genetic analyzer (Applied Biosystems).

Data generated were then acquired and analysed using the GENEMAPPER (Applied Biosystems) software and checked

visually. Final allele sizes were thus obtained per locus and per blueberry accession after removing the length of each universal tail sequence.

Genetic Structure Analysis

To investigate the genetic relationships between blueberry genotypes, the microsatellite dataset was analyzed using the Poppr package (Kamvar et al., 2014) in R (3.1.3 version, https://www.r-project.org).

Initially, the molecular profile for the 6-SSRs was examined by using the discriminant analysis of principal components (DAPC) implemented in the Adegenet package ver. 2.0.1 (Jombart, 2008; Jombart et al., 2010). Prior clusters were identified by a sequential K-means clustering algorithm ("find.clusters" function) after data transformation by Principal Component Analysis (PCA). Then, a discriminant analysis (DA) used part of the principal components (PCs) to describe the clusters. K-means was run with K varying from 1 to 20 and, to ensure convergence, we increased the number of starting points to 200. The number of clusters was chosen based on the Bayesian Information Criterion (BIC) (Schwarz, 1978). To avoid retaining too many dimensions at the DA step, the optimal number of PCs was determined using both "optim.a.score" and "xvalDapc" functions from Adegenet. The final cluster assignment was obtained after the DA step (posterior assignment of the DAPC analysis).

Once each genotype was assigned to a specific cluster, a dendrogram was established using Bruvo's distance (Bruvo et al., 2004) and Neighbour Joining (NJ) clustering (Paradis et al., 2004). Bruvo's distance takes into account the mutational process of microsatellite loci and is well adapted to populations with mixed ploidy levels and is therefore suitable for the study of the blueberry collection used in this work that included both autotetraploid (*V. corymbosum*) and hexaploid cultivars (*V. virgatum*, "Rabbiteye"). The ''bruvo.boot'' command (Kamvar et al., 2014) with bootstrap support of 1000 replication was used to produce a neighbor joining tree with the ''njs'' algorithm from the ape package ver. 5.0 (Paradis et al., 2004).

Texture Analysis

Texture assessment was performed for each cultivar on 20 homogenous fruit at harvest and after storage. Texture was determined by a texture analyser (Zwick Roell, Ulm, Germany), which profiled a mechanical force displacement using a 5 kg loading cell and a cylindrical flat head probe with a diameter of 4 mm entering into the berry flesh from the sagittal side (for more details see Giongo et al., 2013). The mechanical profile was defined by two fundamental variables: force (N) and distance (strain, %). The force was measured with the following instrumental settings: test speed of 100 mm min^{-1}, post-test speed of 300 mm min^{-1}, auto force trigger of 2 g, and stop plot at target position. Each berry was compressed until deformation of 90%. Data of the mechanical profiles were acquired with a resolution of 500 points per second. On the force displacement profile, seven parameters were computed: maximum force, final force, area, maximum deformation, minimum deformation, maximum force strain, and gradient (or imitative Young's module, also known as elasticity module). All data were analyzed by TaxtExpertII software (Zwick Roell, Ulm, Germany).

VOC Analysis by PTR-ToF–MS

Three biological replicates of 1 g of powdered frozen sample, each obtained by five fruit, were inserted into 20 ml glass vials equipped with PTFE/silicone septa (Agilent, Cernusco sul Naviglio, Italy) and mixed with 1 ml of deionized water, 400 mg of sodium chloride, 5 mg of ascorbic acid, and 5 mg of citric acid (Farneti et al., 2017b). Measurements of blueberry VOCs were performed in three biological replicates with a commercial PTR-ToF–MS 8000 apparatus (Ionicon Analytik GmbH, Innsbruck, Austria; Farneti et al., 2017b). The drift tube conditions were as follows: 110°C drift tube temperature, 2.25 mbar drift pressure, 550 V drift voltage. This leads to an E/N ratio of about 140 Townsend (Td), with E corresponding to the electric field strength and N to the gas number density (1 Td = 10-17 Vcm2). The sampling time per channel of ToF acquisition was 0.1 ns, amounting to 350,000 channels for a mass spectrum ranging up to m/z = 400. The sample headspace was withdrawn through PTR-MS inlet with 40 sccm flow for 60 cycles resulting in an analysis time of 60 s/sample. Pure nitrogen was flushed continuously through the vial to prevent pressure drop. Each measurement was conducted automatically after 20 min of sample incubation at 40°C and 2 min between each measurement was applied in order to prevent memory effect. All steps of measurements were automated by an adapted GC autosampler (MPS Multipurpose Sampler, GERSTEL) coupled to PTR-ToF-MS.

The analysis of PTR-ToF–MS spectra proceeded as described in Farneti et al., 2017b.

Data and Statistical Analysis

The array of masses detected with PTR-ToF-MS was reduced by applying noise and correlation coefficient thresholds. The first removed peaks were not significantly different from blank samples; the latter excluded peaks with over 99% correlation, which correspond for the most part to isotopes of monoisotopic masses (Farneti et al., 2017b).

For all quality parameters, both texture and volatiles, a storage index (SI) was computed using the formula proposed by Giongo et al., 2013, $SI = \log_2(Qi_{PH}/Qi_H)$, where Qi_H is the value of the i-th quality parameter measured at harvest, and Qi_{PH} is the value of the same parameter measured after cold storage. Positive SI values indicate a quality trait enhancement, while negative values highlight a loss of the quality trait during storage.

R.3.4.1. R Foundation for Statistical Computing, Vienna, Austria) internal statistical functions and the external packages "mixOmics", "FactoMineR", and "ggplot2" were used for the multivariate statistical methods (PCA, MFA, hierarchical clustering, and definition of significant cluster numbers) employed in this work.

RESULTS

Genetic Variability of *Vaccinium* Germplasm

MVA and MVB multiplexed reactions failed for two blueberry accessions ['Azur' (#4) and 'Southern Belle' (#43)] out of 46 samples and thus these accessions were not included in the genetic analysis. The obtained 44 molecular profiles were further used to identify K-clusters by successive K-means, resulting in the definition of four clusters (**Figure1A**, **Table S3**). Then, SSR profiles were used for the construction of a dendrogram reflecting the genetic proximity between genotypes. The method was based on Bruvo's distance and NJ and was chosen for being reliable and suitable for populations with mixed ploidy levels. Again, the germplasm collection clustered into four main genetic groups with a good level of accordance to the DAPC grouping (**Figure 1C**). As expected, the hexaploid accessions ("Rabbiteye") were clustered distinctively (Group 1) and displayed a large genetic distance to the tetraploid cultivars as previously reported by Bian et al. (2014). Tetraploid accessions were clustered into three groups. Those that clustered into three distinct groups by DAPC also displayed a closer genetic proximity in the NJ dendrogram. This result reflects the different and complex pedigree of southern highbush blueberry

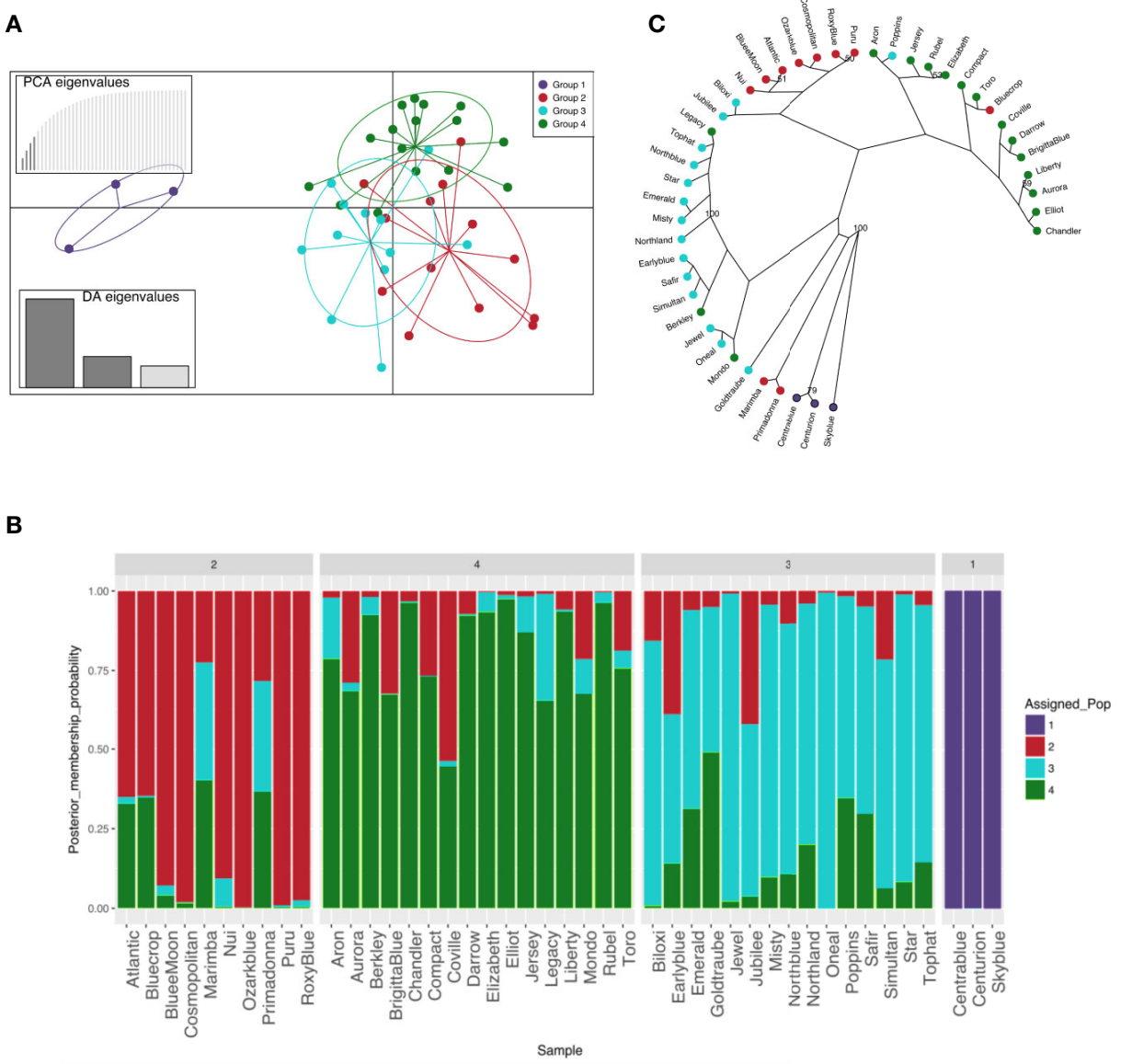

FIGURE 1 | Genetic structure of the 44 blueberry samples evaluated with six SSR. **(A)** Discriminant analysis of principal components (DAPC). **(B)** STRUCTURE-like plot of DAPC analysis for a global picture of the clusters composition. Each individual is represented by a vertical coloured line. Same colour in different individuals indicates that they belong to the same cluster. **(C)** Radial dendrogram based on Bruvo's distance.

[i.e. 'Biloxi' (#6), 'Jubilee' (#24) and 'Misty' (#28)], half-high blueberry [i.e. 'Top Hat' (#45), 'Northland' (#31)] clustering mainly in group 3 and northern highbush blueberry (group 2 and group 4). However, there were some cases of disagreement ['Legacy' (#25), 'Bluecrop' (#7), 'Poppins' (#35), 'Berkley' (#5), 'Mondo' (#29), 'Primadonna' (#36), and 'Marimba' (#27)]. These accessions, despite being assigned to a specific group in the DAPC analysis, showed a certain degree of admixture in the assignment plot (**Figure 1B**). In particular, admixture appeared to be the strongest in 'Marimba' (#27) and 'Primadonna' (#36) which grouped distinctively in the NJ dendrogram.

Advanced Texture Phenotyping of *Vaccinium* Germplasm

The broad genetic variability revealed in our *Vaccinium* germplasm collection may lead to a high phenotypic variance that can be enhanced and altered by prolonged cold storage. Phenotypic variance for texture qualities and for their alteration during cold storage (**Table 2**), is represented by a PCA plot (**Figure 2**) defined by the first two PCs (PC1: 53% and PC2: 35%). Textural differences related to cold storage are mostly explainable by the second component (PC2) variability for mostly correlated with force strain and gradient (Young's module). Indeed, storage index values of maximum force strain and gradient were, on average, +0.31 and -0.95, respectively (**Table 2**). Differences among *Vaccinium* genotypes are predominantly related to the first component (PC1) that is highly correlated to the deformation forces, both maximum and minimum. In accordance with the results presented in Giongo et al. (2013) the gradient is orthogonally oriented to the force related parameters and almost oppositely oriented to deformation strains. The perception of a gummy berry is associated with an increased deformation strain at the maximum force caused by a lower turgidity and a high resistance against the force required to break the skin (Paniagua et al., 2013; Blaker et al., 2014). Based on these textural parameters blueberry fruit can be categorized into three main groups. The first group, mostly distinguished based on high gradient values, is characterized by turgid fruit with a high internal turgor pressure while the second group is mostly

TABLE 2 | Texture parameters detected by a texture analyzer at harvest and after storage, over 46 *Vaccinium* spp. cultivars.

		HARVEST			POST HARVEST			STORAGE INDEX		
		min	***max***	***average***	***min***	***max***	***average***	***min***	***max***	***average***
Gradient	*MPa*	0.99	2.22	1.46	0.41	1.33	0.77	-1.59	0.01	-0.95
Maximum force strain	*%*	2.60	5.08	3.98	3.95	6.41	4.92	0.07	0.70	0.31
Minimum force strain	*%*	4.55	6.66	5.83	5.37	9.29	6.89	0.01	0.55	0.24
Max Force	*N*	2.58	5.13	3.58	1.94	5.41	3.80	-0.41	0.51	0.07
Min Force	*N*	0.50	1.38	0.81	0.44	1.68	0.96	-0.56	0.82	0.21
Area	*N%*	114.08	256.81	157.08	82.29	243.76	170.34	-0.53	0.52	0.10
Final Force	*N*	0.85	2.39	1.43	0.64	2.31	1.60	-0.43	0.69	0.14

For each parameter the average (20 replicates for each cultivar), minimum and maximum values are reported. In addition, the change fold values between harvest and storage assessments (expressed as SI index) are reported.

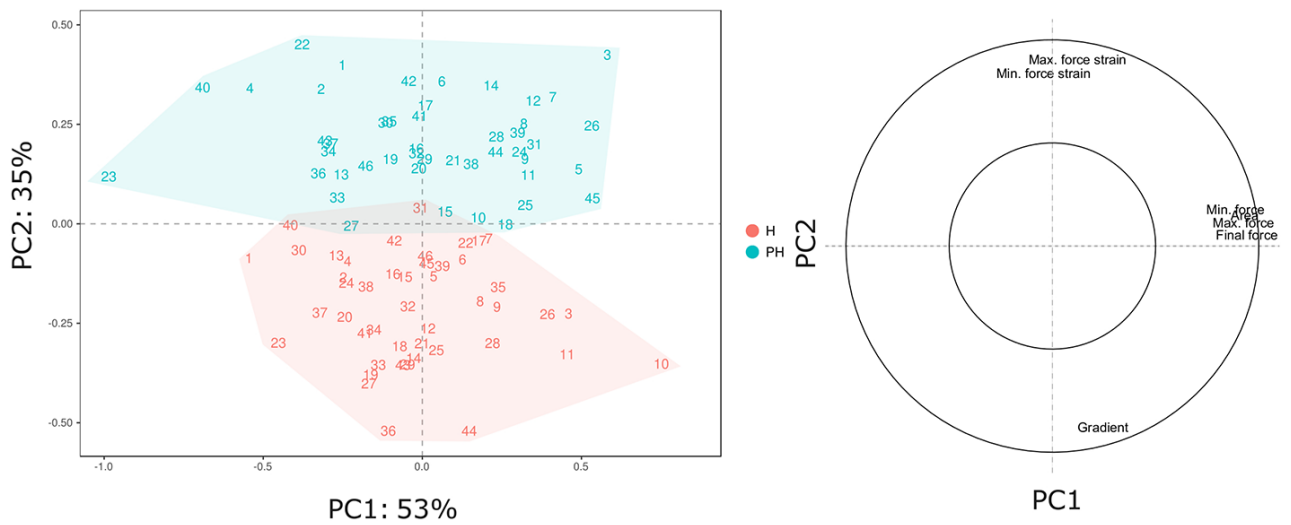

FIGURE 2 | PCA and loading plot of the texture profile of 46 *Vaccinium* spp. cultivars, assessed by texture analyzer at harvest and after storage. Each point of the PCA plot is the average of 20 measurements.

composed of firm, rather than turgid, fruit. The last group is instead defined by low texture performance berries, for both the deformation modulus and deformation forces, leading to the perception of gumminess.

The complexity of the blueberry texture analysis can be reduced to only three variables: deformation strain at maximum force, maximum force, and gradient. All three textural parameters, assessed at harvest and after storage, disclosed a high variability between *Vaccinium* cultivars (**Figure 3**, **Figure S1**). Nevertheless, a strict correlation between texture values assessed at harvest and after storage is not found. This indicated a strong cultivar-storage interaction that cannot be fully estimated considering only the assessment at harvest.

Deformation at maximum force (**Figure 3A**, **Figure S1**) ranged from around 2.6 ['Star' (#44)] to 5% ['Safir' (#40)] at harvest. After 6 weeks of storage, the deformation of all cultivars increased, without any significant relation with the values recorded at harvest. Several accessions, such as 'Star' (#44), 'Elliott' (#19), or 'Chandler' (#12), were defined by low deformation levels at harvest and remarkably high after storage. Differently, other cultivars characterised by low deformation at harvest, like 'Centra Blue' (#10), did not considerably change during storage. Accessions defined by

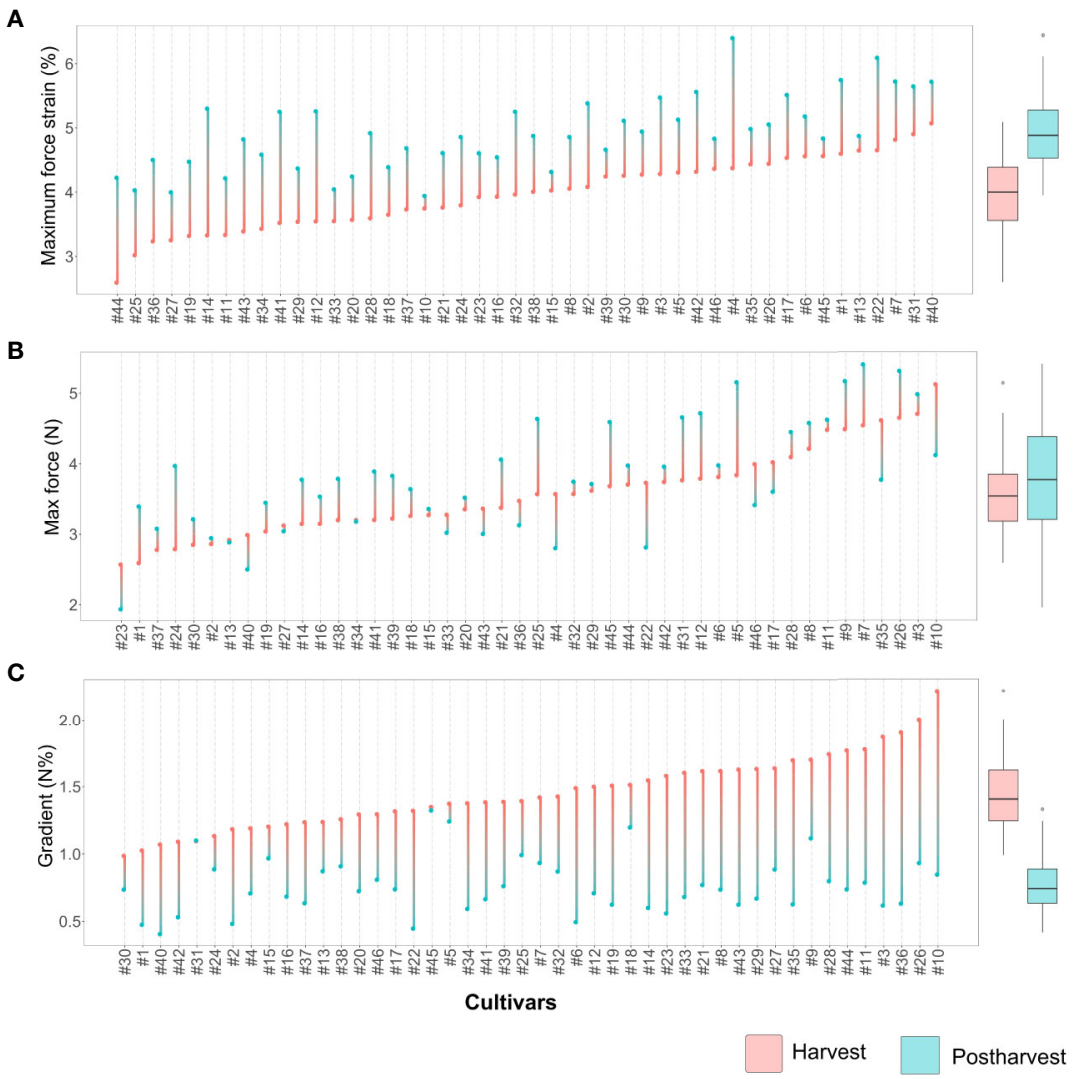

FIGURE 3 | Lollipop graph and box plot of three texture parameters: **(A)** Maximum force strain, **(B)** Maximum force, **(C)** Gradient. Each graph illustrates the average value (of 20 measurements) recorded at harvest and after 6 weeks of storage, for each cultivar (names of the cultivars are reported in **Table 1**). For graphical purpose, cultivars of each graph are ordered based on the trait level recorded at harvest. The box plot, reported next to each lollipop graph, summarise the differences between fruit assessed at harvest and after storage. Lollipop graphs, together with distribution plots and box plots of all 7 texture parameters, are reported in **Figure S1**.

high deformation at harvest also showed the same variability, with cultivars stable during storage, like 'Biloxi' (#6) and 'Compact' (#13), or very unstable ones like 'Jersey' (#22) and 'Azur' (#4). The overall increase in deformation caused by prolonged storage can be mostly explained by a turgidity decrement of blueberries that lost between 6 to 15% of water during storage. However, no significant correlation was found between fruit weight loss and deformation fold changes (R^2 = 0.12, **Figure S2**).

Maximum force variability of fruit assessed at harvest (**Figure 3B**) ranged from around 2.7 ['Jewell' (#23)] to 5.1 N ['Centra Blue' (#10)]. Differently from the deformation results, the maximum force variability, assessed after storage, increased. This high variability is mostly explainable by both positive and negative variations during storage. Among the accessions that showed low force values at harvest, "Jewell" (#23) decreased the force after storage, while 'Jubilee' (#24) more than doubled its value. Among those accessions defined by high force level at harvest, the force level decreased for 'Centra Blue' (#10) fruit, while increased for 'Brigitta Blue' (#9). In addition, several accessions, like 'Biloxi' (#6) and 'Centurion' (#11), showed a very stable force level during storage with minimal modifications.

The gradient values were highly negative correlated with deformation (R^2: 0.47; **Figure S2**) as it was previously evidenced by the PCA analysis (**Figure 2**). Therefore, changes among blueberry cultivars, at harvest and during storage, were comparable with the deformation ones (**Figure 3C**). Gradient module ranged from around 1.0 ['Northblue' (#30)] to 2.2 N% ['Centra Blue' (#10)] at harvest. After storage, the gradient module of all cultivars decreased, without any significant relation with the values recorded at harvest. Although several cultivars revealed similar trends for both Young's module and deformation during storage, such as 'Coville' (#15), 'Top Hat' (#45), or 'Star' (#44), for other cultivars, as 'Centra Blue' (#10), 'Biloxi' (#6), or 'O'Neal' (#33), these values were not comparable. For instance, 'Centra Blue' (#10) was the cultivar with the strongest gradient decrement during storage and, at the same time, one with the lowest deformation change. That resulted in a weak correlation (R^2 = 0.1) between the storage index values of the deformation strain and deformation (**Figure S2**).

Cultivar Characterization Based on Storage Textural Modification

Texture profiling of the blueberry germplasm collection was further analysed at harvest and after storage separately, in order to characterize each cultivar more accurately. In addition, cultivar stability during storage was estimated based on the Storage Index (SI) computed on each texture parameter. As for the PCA based on the whole texture database (**Figure 2**), the total variance of each PCA—based on the texture profiles at harvest, storage, and SI- was mostly entirely explained by the first two components (**Figure 4**, **Figure S3**, **Table S3**).

Four distinct clusters were statistically distinguished at harvest based exclusively on texture (**Figure 4A**). Most of variability (68%) is explainable by the first PC, that is highly correlated with the maximum and minimum forces, the total area, and the gradient (**Figure S3**). The deformation at maximum and minimum forces is rather related with the second component, accounting for 22% of the explained variability. Accessions belonging to the first two clusters ("Cl_1", and "Cl_2") were mostly distinguished based on forces and gradient. Cultivars of the first cluster, such as 'Jewell' (#23), 'Emerald' (#20), or 'Ozark Blue' (#34), were defined by low forces and gradient while the four accessions of the second cluster ['Centurion' (#11), 'Centra Blue' (#10), 'Aurora' (#2), and 'Liberty' (#26)] by high deformation forces and gradient values. The last two clusters ("Cl_3", "Cl_4"), both characterized by intermediate values of force and gradient, were mostly separated based on deformation. Cultivars of the third cluster, such as 'Bluecrop' (#7), 'Brigitta Blue' (#9), or 'Biloxi' (#6), were defined by high deformation values, while cultivars of the fourth cluster, such as 'Star' (#44), 'O'Neal' (#33), and 'Legacy' (#25), by low deformation.

Three clusters of cultivars were statistically distinguished after storage based on texture assessment (**Figure 4B**). These clusters were distributed according to the first component variation, that is highly correlated with the force displacement and gradient and it explained the 76% of the texture profiling variability. The second PC, mostly related with fruit deformation, explains only 11% of the variance. Based on this classification, the first cluster ("Cl_1") included few blueberry accessions, such as 'Jewell' (#23), 'Safir' (#40), or 'Jersey' (#22), defined by extremely low force displacement and gradient values. Cultivars of the opposite cluster ("Cl_2"), such as 'Brigitta Blue' (#9), 'Bluecrop' (#7) and 'Liberty' (#26), were defined by positive values of the first component, as a result of higher values of deformation forces and gradient.

The PCA related to the Storage Index (**Figure 4C**) is intended to describe the potential storability of each accession based on textural characteristics. The SI provides valuable information related to the magnitude of the variation of each texture parameter during storage, rather than an absolute value. The 88% of this variability was explained by the first two components (PC1 68%, PC2 20%). Three distinct clusters of cultivars were statistically distinguished mostly based on the PC1 variability. The first cluster ("Cl_1") was characterized by cultivars, such as 'Aurora' (#3), 'Chandler' (#12), or 'Star' (#44), with high fold changes of deformation at the maximum force, low delta of the gradient, and an intermediate delta of the forces. Accessions of the second cluster ("Cl_2"), such as 'Biloxi' (#6), 'Centra Blue' (#10), or 'Jersey' (#22), showed low fold change values of maximum force, and intermediate ones of the deformation at maximum force and of the gradient. Cultivars of the last cluster ("Cl_3"), such as 'Jubilee' (#24), 'Northland' (#31), or 'Top Hat' (#45), showed high changes of gradient values and forces, and low changes of the deformation at maximum force.

The texture profiling assessed at both harvest and after postharvest storage did not reveal any significant association with the genetic molecular profile based on six SSRs (**Figure S1**; **Figure S3**).

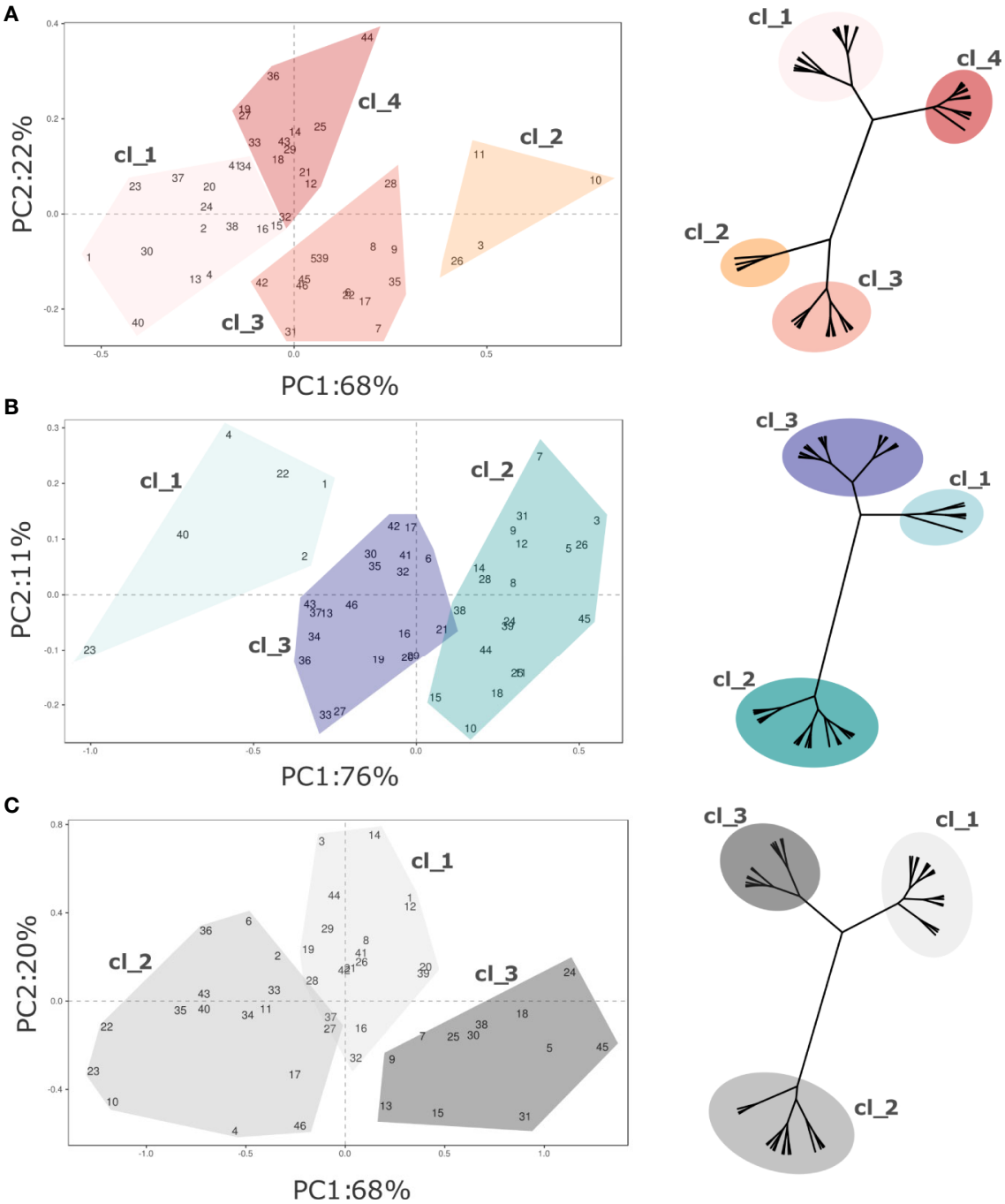

FIGURE 4 | PCA and hierarchical clustering (based on Ward distances) of 46 *Vaccinium* spp cultivars based on texture profile assessed at **(A)** harvest and **(B)** postharvest, and on the calculated storage index **(C)**. Each point of the PCA plot is the average of 20 fruit. Loading plots of each PCA are reported in **Figure S3**. Clusters highlighted in each PCA plot corresponds to the clusters identified by Ward clustering.

Phenotyping of *Vaccinium* Germplasm Volatilome

Blueberry VOC profile was assessed at harvest and after storage in triplicate by PTR-ToF-MS analysis as described in Farneti et al. (2017b). Mass peaks from the raw PTR-ToF-MS spectra were reduced from 285 to 134, applying noise and correlation coefficient thresholds. Tentative identification of each mass, detected by PTR-ToF-MS, was based on comparison with pure standards and gas chromatographic results previously presented in Farneti et al., 2017b (**Table 3**).

VOC profile, assessed at harvest, was characterised by mass peaks tentatively identified (t.i.) as methanol (*m/z* 33.033),

TABLE 3 | Volatile organic compounds detected by PTR-ToF-MS at harvest and after storage, over 46 *Vaccinium* spp. cultivars.

m/z	Formula	tentative Identification	HARVEST			POSTHARVEST			STORAGE INDEX		
			min	*Max*	*average*	*Min*	*max*	*average*	*min*	*max*	*average*
27.0263	C2H3+		0.07	1.49	0.22	0.12	2.81	0.58	-1.14	3.4	1.21
28.0184			0.09	0.24	0.16	0.07	0.24	0.15	-1.5	0.72	-0.16
28.0314			0.03	0.13	0.07	0.04	0.95	0.19	-1.36	3.44	1.03
30.0435			0.01	0.19	0.05	0.06	12.08	1.76	0.34	7.76	4.06
30.9952			0.81	1.14	0.93	0.97	1.14	1.05	-0.18	0.46	0.18
31.0455			0	0.35	0.05	0.01	0.17	0.06	-2.8	4.47	0.46
33.0331	CH4OH+	Methanol	502.07	5790.87	2228.26	647.91	11096.53	3956.04	-2.13	3.76	0.77
34.9958	H2SH+	Hydrogen sulfide	0.07	4.79	1.17	0.01	0.35	0.15	-5.49	1.53	-1.82
39.0228	C3H3+	common fragment	2.29	17.68	5.3	3.34	14.16	6.21	-1.31	1.74	0.27
41.0386	C3H5+	common fragment	6.83	51.65	12.26	7.38	46.6	16.97	-1.01	2.01	0.4
42.0101	C2H2O+		0.01	0.14	0.05	0.02	0.83	0.16	-0.81	4.04	1.41
42.0225			0.07	0.82	0.23	0.09	1.39	0.39	-1.41	3.41	0.74
43.0153	C2H3O+	common fragment	9	45.61	21.83	11.32	1388.15	68.48	-1.16	5.24	0.69
43.0576	C3H7+	common fragment	2.6	53.65	6.06	3.58	48.84	9.95	-1.07	3.14	0.71
44.058			0.08	1.71	0.2	0.1	1.53	0.34	-1.13	2.97	0.75
45.0319	C2H4OH+	Acetaldehyde	17.71	515	80.78	158.07	1448.6	651.28	0.09	5.02	3.21
47.0102	CH3O2+	Formic acid	2.93	6.56	4.38	2.29	6.11	3.98	-1.17	0.54	-0.16
47.0193			4.63	5.63	5.08	1.9	5.95	4.49	-1.41	0.36	-0.22
47.0436	C2H6OH+	Ethanol	0.48	21.56	2.44	9.92	2534.48	341.28	2.34	11.32	6.68
49.0112	CH4SH+	Methanethiol	0.03	6.61	0.59	0.02	0.47	0.09	-4.79	1.61	-1.59
49.0277			0.02	0.13	0.06	0.02	0.45	0.12	-1.16	3.44	0.84
49.9991			0.31	0.54	0.42	0.41	0.55	0.48	-0.27	0.66	0.2
51.0059			0.05	0.35	0.1	0.05	0.24	0.11	-1.41	1.74	0.15
51.0431	CH3OH*H3O+	Methanol cluster	10.53	120.38	45.71	13.65	258.95	81.27	-2.12	3.76	0.77
53.0039			0.03	0.3	0.06	0.02	0.12	0.06	-1.75	1.15	-0.07
53.0396	C4H5+	common fragment	0.71	4.81	1.91	0.93	3.49	1.77	-1.49	1.59	-0.02
55.0171	C3H3O+		0.09	0.56	0.32	0.1	1.77	0.33	-1.54	1.83	-0.06
55.0542	C4H7+	common fragment	13.66	110.63	43.32	16.34	75.46	38.92	-1.89	1.54	-0.06
57.0334	C3H4OH+	common fragment	63.22	414.55	205.7	10.81	311.75	149.17	-3.61	1.19	-0.57
57.0697	C4H9+	1-Octanol, high alcohol fragment	2.61	6.59	3.43	2.75	45.53	9.01	-0.45	3.57	1.08
60.0214			0	0.04	0.02	0.01	0.43	0.04	-2.28	8.52	0.9
61.0233	C2H4O2H+	Acetic acid, common ester fragment	4.56	46.19	14.04	6.08	2146.05	87.91	-1.88	7.19	1.24
63.0083			0.17	0.73	0.42	0.28	0.99	0.51	-0.69	2.06	0.39
63.0329	C2H6SH+	Dimethyl sulfide, Ethanethiol	0.75	2.63	1.62	1.27	14.32	2.88	-0.53	3.31	0.79
63.0425	C2H4O*H3O+	Ethanol cluster	0	1.3	0.07	0.09	4.92	1.6	-0.6	15.21	10.79
65.02			0.14	0.31	0.21	0.12	0.34	0.2	-1.01	0.91	-0.11
67.056	C5H7+		0.57	2.21	1.32	0.66	2.04	1.11	-1.16	0.76	-0.23
69.0333	C4H4OH+	Furan	0.15	0.69	0.32	0.15	0.64	0.25	-1.52	1.33	-0.34
69.0699	C5H9+	Aldehyde fragment	2.36	8.22	5.31	2.55	8.04	4.07	-1.28	0.41	-0.37
71.0491	C4H6OH+	Butenal	0.96	2.82	1.74	0.87	5.52	1.63	-1.25	1.15	-0.16
71.0854	C5H11+	3-methyl-1-butanol + 2-methyl-1-butanol, Pentanol	0.66	3.58	1.39	0.59	11.71	2.23	-1.46	2.33	0.48
73.0298	C3H4O2H+		0.88	1.87	1.09	0.8	3.52	1.1	-0.91	1.84	-0.04
73.0646	C4H8OH+	Butanale, isobutyraldehyde	1.07	2.43	1.62	2.13	12.14	4.31	0.1	3.09	1.31
75.0436	C3H6O2H+	Methyl acetate	1.09	21.3	5.6	1.28	244.82	19.06	-3.29	5.08	0.75
75.0803			0	0.14	0.02	0	0.36	0.04	-13.08	9.25	0.32
77.0223			0.07	0.37	0.22	0.17	0.4	0.23	-0.65	1.39	0.09
78.0465	C6H6+		1.61	2.62	2.01	1.7	1.96	1.83	-0.54	0.18	-0.12
79.0374	C6H7+	Benzene	0.02	2.1	0.41	0.05	10.51	0.55	-4.58	6.61	0.55
79.0739			0	0.52	0.1	0.01	2.15	0.37	-2.87	13.2	3.73
80.0559	C5[13]CH7+		0.25	1.64	0.52	0.16	2.19	0.48	-2.51	2.42	-0.23
81.0701	C6H9+	Fragment of aldehydes (Hexenals); fragment of terpenes (Linalool)	25.34	450.16	109.22	4.9	159.48	51.31	-4.93	0.89	-1
83.0492	C5H6OH+	Methylfuran	0.39	1.39	0.88	0.37	1.26	0.75	-1.19	0.88	-0.21
83.0858	C6H11+	(E)-3-Hexen-1-ol, (Z)-3-Hexen-1-ol, (Z)-2-Hexen-1-ol, Hexanal, 2-Hexanone	10.84	85.36	34.12	13.09	65.7	32.36	-1.76	1.65	0.02
85.028	C4H4O2H+	Furanone	0.13	0.23	0.17	0.11	0.21	0.16	-0.96	0.63	-0.12
85.0647	C5H8OH+	(E)-2-Pentenal	1.14	7.94	3.81	1.21	6.98	3.11	-1.37	1.02	-0.27
85.1008	C6H13+	Hexanol	0.2	0.99	0.43	0.7	7.59	2.02	0.34	4.04	2.14
87.0442	C4H6O2H+	Butyrolactone	0.56	18.83	1.77	0.55	37.82	1.99	-3.84	5.2	-0.25
87.081	C5H10OH+	2-methyl butanal+3-methyl butanal	0.5	1.45	0.89	0.5	5.08	1.26	-0.71	2.14	0.29

(Continued)

TABLE 3 | Continued

m/z	Formula	tentative Identification	HARVEST			POSTHARVEST			STORAGE INDEX		
			min	*Max*	*average*	*Min*	*max*	*average*	*min*	*max*	*average*
89.055	C4H8O2H+	Ethyl acetate	0.24	1.76	0.7	0.45	755.64	25.74	-0.96	9.32	2.52
89.1408			0	0.01	0.01	0	0.15	0.01	-2.42	6.32	0.99
89.201			0	0.02	0.01	0	0.16	0.01	-8.61	6.42	-0.11
89.2685			0	0.02	0.01	0	0.34	0.02	-9.71	5.53	0.49
91.068	C7H7+	Benzyl Alcohol	0.33	2.63	0.57	0.44	6.41	1.16	-2.38	3.87	0.76
93.0379	C3H8OSH+	2-(Methylthio)ethanol	1.1	4.01	2.22	1.89	5.72	2.8	-0.62	1.86	0.38
93.9552			0.14	0.3	0.2	0.15	0.23	0.2	-0.72	0.51	-0.03
94.0932			0.01	0.24	0.06	0.01	0.27	0.06	-4.44	2.43	-0.12
95.0188			0.33	1.12	0.62	0.52	1.04	0.72	-0.58	1.35	0.25
95.0489	C6H6OH+	Phenol	1.51	1.87	1.64	1.38	3.04	1.98	-0.32	1	0.23
95.0873	C7H11+	(E)-2-Heptenal, Monoterpene fragment	1	6.75	2.61	0.77	4.53	1.65	-1.82	0.22	-0.61
97.0274	C5H4O2H+	Furfural	0.3	0.49	0.37	0.28	0.47	0.35	-0.44	0.43	-0.06
97.0652	C6H8OH+	(E,Z)-2,4-Hexadienal, (E,E)-2,4-Hexadienal	0.34	2.3	1.01	0.26	1.54	0.57	-2.29	0.78	-0.76
99.0803	C6H10OH+	(Z)-3-Hexenal, (E)-2-Hexenal	28.44	172.73	92.5	3.38	145.1	65.19	-4.05	1.19	-0.61
101.023			0.13	0.2	0.16	0.12	0.18	0.15	-0.49	0.43	-0.13
101.061	C5H8O2H+	2,3-Pentanedione, 2-Butenoic acid methyl ester	0.25	0.58	0.36	0.29	1.38	0.47	-0.39	2.11	0.33
101.096	C6H12OH+	Hexanal	1.4	12.4	4.99	1.26	8.24	3.88	-2.33	1.86	-0.29
103.076	C5H10O2H+	Ethyl Propanoate	0.24	2.88	1.04	0.32	34.21	4.43	-1.83	4.6	1.44
105.064	C8H9+	Phenetyl Alcohol. Styrene	0.1	0.31	0.17	0.14	0.59	0.27	-0.56	2.14	0.69
106.08			0.03	0.41	0.09	0.04	0.63	0.12	-2.48	3.18	0.32
107.07	C7H6OH+	Benzaldehyde	0.1	0.9	0.29	0.2	2.86	0.59	-1.45	3.5	0.91
107.087	C8H10H+	Ethyl Benzene, p-Xylene, m-Xylene	1.93	39.61	7.62	1.58	52.78	8.76	-4.14	3.94	0
108.958			0.65	0.81	0.72	0.67	0.89	0.77	-0.15	0.27	0.1
109.034			0.09	0.29	0.18	0.12	0.19	0.15	-1.31	1.01	-0.16
109.102	C8H13+	2-Octenal (E)	1.31	7.75	3.28	2.17	7.97	3.71	-0.59	1.13	0.2
111.044			0.12	0.24	0.15	0.09	0.15	0.12	-1.13	0.18	-0.36
111.081	C7H10OH+	(E,E)-2,4-Heptadienal	0.26	0.96	0.57	0.22	0.83	0.41	-1.47	0.51	-0.45
111.117	C8H15+	(E)-2-Octenal, Octanal,1-Octen-3-ol	0.31	0.57	0.41	0.3	0.76	0.46	-0.55	1.07	0.14
113.06	C6H8O2H+	Sorbic acid	0.14	1.83	0.53	0.15	0.69	0.25	-3.36	1.01	-0.9
113.098	C7H12OH+	(E)-2-Heptenal	0.21	0.92	0.52	0.31	0.9	0.5	-0.99	0.79	-0.04
115.076	C6H10O2H+	Ethyl Crotonate, Ethyl (2E)-2-butenoate	0.2	0.45	0.29	0.24	1.73	0.57	-0.31	2.79	0.85
115.114	C7H14OH+	2-Heptanone, Heptanal	0.09	2.98	0.88	0.13	1.76	0.55	-2.78	2.07	-0.48
117.092	C6H12O2H+	Ethyl Isobutanoate, Methyl-2-methyl butanoate, Methyl Isovalerate, Ethyl Butyrate, Hexanoic Acid	0.25	5.59	0.85	0.57	56.58	10.09	-0.19	6.65	2.66
118.05			0	0.09	0.02	0	0.29	0.02	-10.62	4.12	-0.42
118.981			0	0.02	0.01	0	0.2	0.04	-0.47	5.03	1.57
119.074	C9H11+	3-Phenylpropanol	0.18	0.33	0.23	0.19	0.56	0.33	-0.25	1.23	0.47
121.068	C8H8OH+	Acetophenone, Phenylacetaldehyde	0.67	1.59	1.14	0.53	3.75	1.83	-1.16	2.48	0.47
123.048			0.11	0.21	0.17	0.14	0.33	0.19	-0.29	0.93	0.18
123.118	C9H15+	2-Nonenal, (E)-2-Nonenal	0.23	0.69	0.41	0.24	0.54	0.37	-0.89	0.65	-0.12
123.946			0.12	0.2	0.16	0.13	0.2	0.16	-0.29	0.43	0.04
125.1	C8H12OH+	6-Methyl-3,5-heptadien-2-one	0.19	0.5	0.34	0.24	1.01	0.4	-0.58	1.46	0.21
125.96			0.15	0.22	0.18	0.17	0.24	0.2	-0.2	0.46	0.12
126.904			0.3	1.84	1	0.55	1.14	0.81	-1.57	1.74	-0.02
127.072			0.08	0.4	0.16	0.07	0.16	0.11	-1.61	0.64	-0.4
127.113	C8H14OH+	1-octen-3-one, 6-methyl-5-hepten-2-one, (E)-2-Octenal.	0.48	2.86	1.39	0.85	2.68	1.48	-0.53	0.92	0.11
129.092	C8H16OH+	2-octanone, Octanal, 1-Octen-3-ol	0.12	0.18	0.15	0.15	0.68	0.26	-0.1	2.21	0.65
131.107	C7H14O2H+	Ethyl-2-methyl butanoate, Ethyl Isovalerate	0.1	2.08	0.23	0.2	32.86	4.04	0.31	7.25	3.14
133.103	C10H13+	Thymol	0.2	4.13	0.7	0.18	1.48	0.52	-2.11	2.04	-0.33
135.115	C10H15+	HO-Trienol	0.26	11.04	2.42	0.21	9.78	1.41	-3.3	0.98	-0.81
136.024			0.09	0.31	0.18	0.09	0.17	0.12	-1.78	0.67	-0.52
136.99			0	0.02	0.01	0.01	0.07	0.02	-1.06	4.18	0.76
137.134	C10H17+	1.8-cineole, Linalool, 4-Terpineol, alpha Terpineol, Nerol, Geraniol* Beta myrcene, Limonene, (E)-Beta Ocimene, Alpha Terpinolene	1.42	22.44	8.30	0.62	16.06	3.63	-3.21	0.51	-1.15
139.076	C8H10O2H+	5,5-Dimethyl-2-cyclohexen-1,4-dione	0.2	0.46	0.31	0.13	1.05	0.49	-1.33	2.36	0.47
139.117	C9H14OH+		0.16	0.43	0.25	0.16	0.56	0.24	-0.86	0.64	-0.05
141.094	C9H16OH+	2-Nonenal, (E)-2-Nonenal, Ethyl sorbate	0.15	0.24	0.19	0.14	0.27	0.2	-0.57	0.65	0.06
143.109	C8H14O2H+	(Z)-3-Hexenyl Acetate, 2-Hexenyl Acetate	0.21	0.34	0.28	0.2	0.39	0.28	-0.55	0.58	0.01
143.145	C9H18OH+	2-Nonanone, Nonanal	0.18	2.13	0.62	0.17	1.23	0.38	-1.93	0.54	-0.62

(Continued)

TABLE 3 | Continued

m/z	Formula	tentative Identification	HARVEST			POSTHARVEST			STORAGE INDEX		
			min	*Max*	*average*	*Min*	*max*	*average*	*min*	*max*	*average*
144.915			0.1	1.5	0.74	0.47	0.92	0.66	-1.53	2.78	0.52
145.124	C8H16O2H+	Ethyl Hexanoate, Hexyl Acetate, Octanoic Acid	0.25	0.51	0.37	0.32	0.66	0.46	-0.41	1	0.34
147.111			0.04	0.13	0.07	0.04	0.18	0.08	-0.66	1.65	0.27
151.113			0.11	0.4	0.21	0.13	0.3	0.18	-1.08	0.67	-0.21
157.122	C9H16O2H+	γ-Nonalactone	0.07	0.15	0.1	0.08	0.47	0.13	-0.39	1.6	0.39
157.16	C10H20OH+	Decanal	0.07	0.18	0.12	0.06	0.22	0.12	-1.12	1.38	-0.09
159.14	C9H18O2H+	Nonanoic Acid	0.42	1.16	0.75	0.61	1.41	1.07	-0.44	1.49	0.54
161.107			0.03	0.08	0.05	0.04	0.1	0.06	-0.66	0.97	0.17
163.088			0.04	0.13	0.06	0.05	0.25	0.08	-0.97	1.99	0.24
165.094			0.05	0.16	0.1	0.09	0.23	0.14	-0.39	1.63	0.45
169.126			0.05	0.11	0.08	0.05	0.11	0.07	-0.59	0.74	-0.04
171.138	C10H18O2H+	Linalool oxide, 2-Octenyl Acetate, gamma-Decalactone	0.06	0.31	0.12	0.06	0.32	0.11	-1.15	0.72	-0.08
171.177			0.05	0.53	0.13	0.02	0.25	0.06	-3.27	1.9	-0.93
173.156	C10H20O2H+	Decanoic Acid	0.07	0.3	0.18	0.11	0.39	0.25	-0.63	1.75	0.55
174.908			0.01	0.24	0.04	0.05	0.37	0.1	-0.41	3.13	1.51
175.116			0.02	0.05	0.03	0.02	0.05	0.03	-0.7	1.14	0.15
177.111	C13H21+	Geranyl Acetone	0.01	0.03	0.02	0.02	0.11	0.03	-0.51	2.32	0.3
179.111			0.02	0.06	0.04	0.03	0.67	0.14	-0.59	4.39	1.2
187.167			0.02	0.05	0.03	0.02	0.07	0.04	-1.08	1.27	0.22

Each mass peak is tentatively identified based on GC-MS analysis reported in Farneti et al. (2017b). Mass peaks values are reported as concentration (μg Kg−1). The average (three replicates for each cultivar). Minimum and maximum values are reported. In addition, the change fold values between harvest and storage assessments (expressed as SI index) are reported.

acetaldehyde (*m/z* 45.031), C6-aldehydes (i.e. *m/z* 99.08; 101.09; 83.08; 81.07), monoterpenes (*m/z* 137.13), benzoic compounds (*m/z* 107.087), butyrolactone (*m/z* 87.04), and sulfuric compounds (*m/z* 34.99; 49.011; 63.033). In agreement with Farneti et al., 2017b, concentration of mass peaks related with ester compounds (i.e. *m/z* 75.043; 89.055; 103.07; 117.09; 131.107; 145.124) was very low.

VOC profile changed significantly during storage; however, any additional mass peaks were not revealed solely after cold storage. Aldehydes and terpenes decreased during storage, as confirmed by the masses *m/z* 81.07 (common fragment of C6-aldehydes and terpenes; SI: -1.00), *m/z* 99.08 (hexenal isomers; SI: -0.61), *m/z* 101.096 (hexanal; SI: -0.29), *m/z* 133.103 (thymol; SI:-033), and *m/z* 137.134 (monoterpenes; SI: -1.15). In contrast, fruit storage significantly enhanced the content of several alcohols (*m/z* 33.033, 47.043, 57.069, 71.085, 85.100) and esters (*m/z* 75.043, 89.055, 103.076, 115.076, 117.092, 131.107). Ethanol (*m/z* 47.043) was one of the compounds that increased most (SI: + 6.68), followed by acetaldehyde (*m/z* 45.031; SI: + 3.21), and by masses related with ester compounds in particular *m/z* 131.107 (t.i. as ethyl isovalerate; SI: + 3.14), *m/z* 117.092 (t.i. as ethyl isobutanoate; SI: + 2.66), or *m/z* 89.055 (t.i as ethyl acetate; SI: + 2.52).

The VOC variability, assessed at harvest and after 6 weeks of 2°C storage, is represented by a PCA plot (**Figure 5**) defined by the first two PCs (PC1: 55% and PC2: 12%). VOC differences related to cold storage are mostly explainable by the first component (PC1) variability, that is for the most part related with differences in concentrations of esters and alcohols. Differences among *Vaccinium* genotypes, especially at harvest, are mostly related to the second component (PC2). In contrast with the outcome of texture assessment (**Figure 2**), that revealed a stronger influence of genetic variability over the storage effect, blueberry VOC profile seemed to be mostly influenced by the storage condition, but still with a significant interaction with genetic variability. As a result, blueberry cultivars, at harvest and after storage, are evidently clustered into two groups (**Figure 5**) based on PC1 variability, with only three cultivars ['Centra Blue' (#10), 'Centurion' (#11), and 'Sky Blue' (#42)] characterized by a VOC profile at harvest more similar to the one detected after postharvest. These cultivars are the only three *Vaccinium* hexaploid accessions ("Rabbiteye", *V. virgatum*) taken into consideration in this study. These results confirmed that the VOC profile of "Rabbiteye" blueberry cultivars is distinguishable from other *Vaccinium* species, particularly from *V. corymbosum*, for the most part due to a higher content of esters and alcohols (Du et al., 2011; Beaulieu et al., 2014; Farneti et al., 2017b).

Results of this study revealed a strong interaction between genotype and storage treatment. Being the last products of fruit metabolic pathways, VOC emissions are highly controlled by both genetic and environmental factors, such as storage conditions. Indeed, cold storage conservation amplified VOC profile differences between cultivars, as confirmed by the increased variability in PC1 and PC2 values. For instance, cultivars characterized by a similar VOC profile at harvest, like 'Star' (#44) or 'Northland' (#31), are considerably different after storage. These differences may be the consequence of both ripening and senescence processes.

Methanol (*m/z* 33.033, **Figure 6A** and **Figure S3**), being a direct product of cell wall degradation (Dorokhov et al., 2018), is commonly considered as a marker compound for fruit ripening and senescence. The content variability among the *Vaccinium*

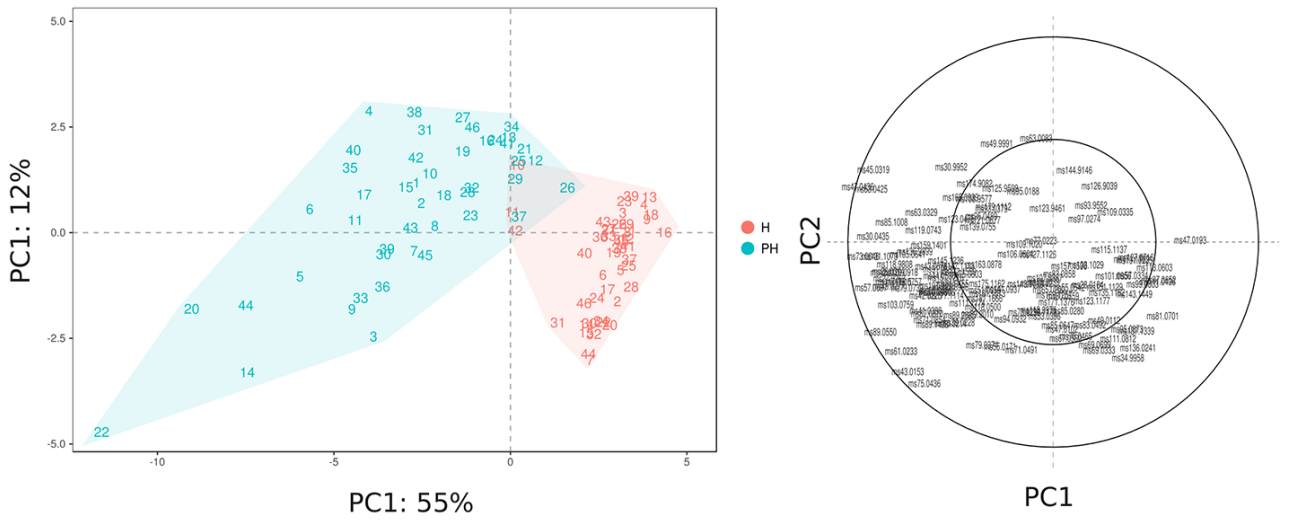

FIGURE 5 | PCA and loading plot of the VOC profile of 46 *Vaccinium* spp. cultivars, assessed by PTR-ToF-MS at harvest and after storage. Each point of the PCA plot is the average of three replicates.

germplasm is remarkably high at both harvest and storage assessments, without any well-defined trend due to fruit conservation. Several cultivars, such as 'Compact' (#13), 'Centra Blue' (#10), and 'Jubilee' (#24), showed very low concentration of methanol at both stages, while others, such as 'Azur' (#4), 'Jersey' (#22), and 'Star' (#44), are characterized by a severe increase due to storage, independently from the concentration assessed at harvest. On the contrary, several cultivars with high methanol content at harvest, such as 'Toro' (#46), 'Liberty' (#26), and 'Top Hat' (#45), significantly reduced their content after storage.

Ethanol is another VOC ordinarily considered as a reliable marker of fruit senescence (Pesis, 2005). After storage, only 15 cultivars of our germplasm selection had an elevated (over 250 ppb) concentration of ethanol (*m/z* 47.043, **Figure 6C**, **Figure S4**). Among them, 'Jersey' (#22), 'Emerald' (#20), 'Biloxy' (#6), and 'Star' (#44), are the cultivars with the highest ethanol concentration.

Variation of methanol and ethanol after storage did not show any significant correlation with the texture parameters previously presented (**Figure S5**). Indeed, among cultivars with the highest ethanol production, only 'Jersey' (#22) revealed a higher deterioration of the textural parameters (gradient, maximum force, and force strain) while 'Emerald' (#20), 'Biloxy' (#6), and 'Star' (#44) showed average textural parameters with almost any substantial alterations of Max force values.

Another VOC related to fruit ripening and senescence is acetaldehyde (Pesis, 2005). Results of this study confirmed that acetaldehyde content increased in blueberry fruit during cold storage, as previously demonstrated on a reduced genotype collection by Farneti et al. (2017b). All germplasm accessions of this study increased in acetaldehyde content (*m/z*/45.031, **Figure 6B**, **Figure S4**) during storage. Most of the cultivars, except the *V. virgatum* ones ['Centra Blue' (#10), 'Centurion' (#11), and 'Sky Blue' (#42)], presented an extremely low concentration of acetaldehyde at harvest. Variation during storage is related to genotypes: results of this experiment showed cultivars with a low increase, such as 'Centra Blue' (#10), 'Liberty' (#26), and 'Aurora' (#3), and others with a more predominant increase, such as 'Jersey' (#22), 'Star' (#44), and 'Safir' (#40). Cultivars with a high acetaldehyde production had also a high content of methanol and ethanol, but no statistically significant positive correlation was found. Nevertheless, a significant positive correlation is obtained linking SI values of ethanol and acetaldehyde (**Figure S5**), suggesting that acetaldehyde is synthetized in blueberry fruit from ethanol by alcohol dehydrogenases activity as for many other fruit species (Chervin et al., 1999; Tadege et al., 1999; Pesis, 2005).

Postharvest storage significantly improved the concentration of ester compounds, particularly the ones identified with the mass peaks *m/z* 75.043, 89.055, 103.076, 115.076, 117.092, and 131.107. Most of these esters were assessed only in trace amount at harvest; remarkably, only some cultivars significantly enhanced their concentration after storage. All these ester compound mass peaks were not strictly correlated to each other (**Figure S5**), indicating different metabolic pathways involved in their synthesis as well as an evident effect of genotype. Mass peak *m/z* 117.092, tentatively identified as C6 esters, such as ethyl isobutanoate, methyl-2-methyl butanoate, methyl isovalerate, and ethyl butyrate, increased during storage in more than half of the cultivars (**Figure 6E**, **Figure S4**). Notably, for most of the cultivars [i.e. 'North Blue' (#30), 'Bluecrop' (#7), and 'Brigitta Blue' (#9),] the increase of m/z 117.092 concentration was not correlated with the variation of

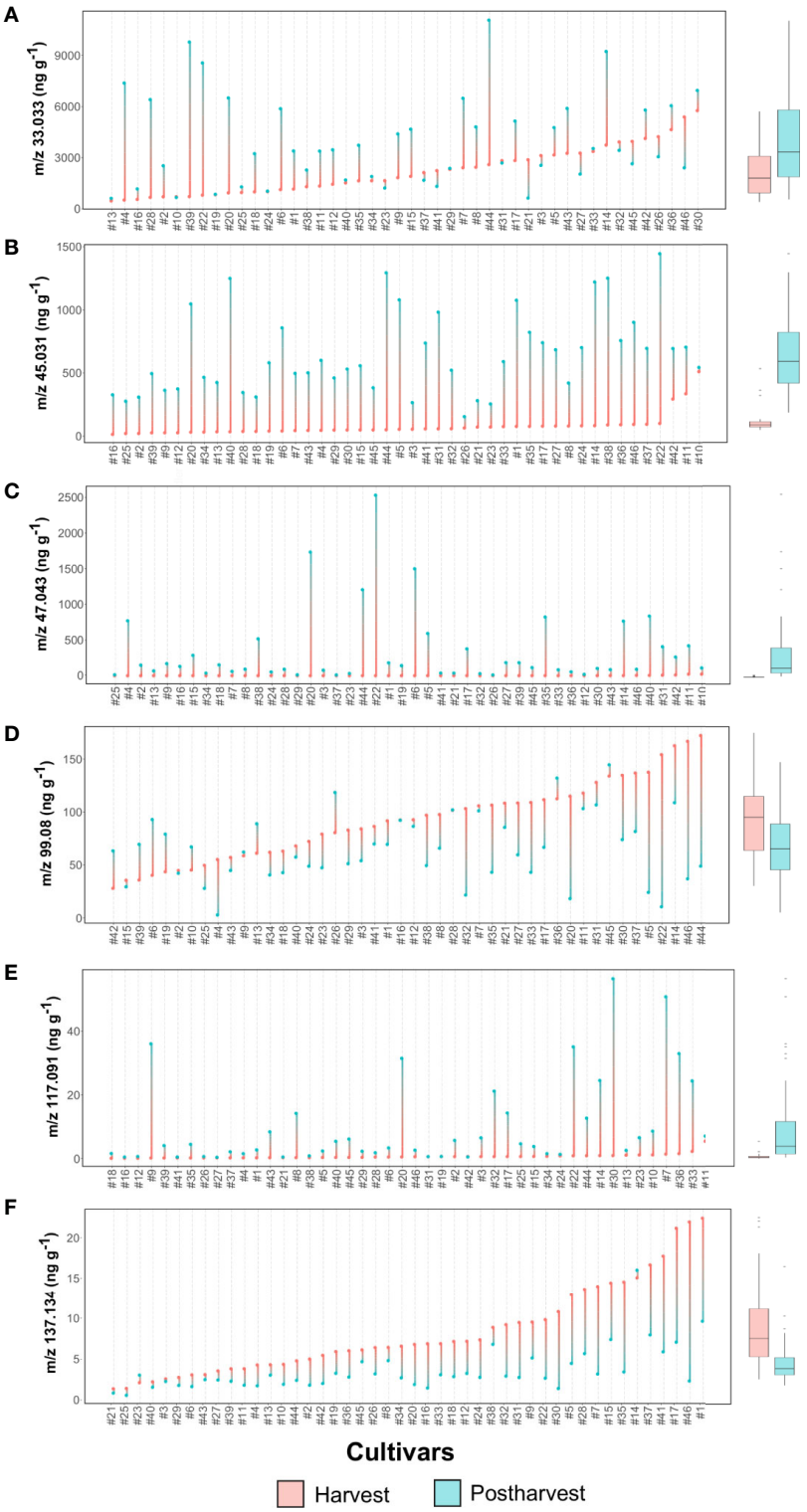

FIGURE 6 | Lollipop graph and box plot of six VOC mass peaks (out of 134 detected in total by PTR-ToF-MS: **(A)** *m/z* 33.033, **(B)** *m/z* 45.031, **(C)** *m/z* 47.043, **(D)** *m/z* 99.08, **(E)** *m/z* 117.091, **(F)** *m/z* 137.134. Each graph illustrates the average value (of three measurements) recorded at harvest and after 6 weeks of storage, for each cultivar (names of the cultivars are reported in **Table 1**). For graphical purpose, cultivars of each graph are ordered based on the trait level recorded at harvest. The box plot, reported next to each lollipop graph, summarize the differences between fruit assessed at harvest and after storage. Lollipop graphs, together with distribution plots and box plots of all 134 VOC mass peaks, are reported in **Figure S4**.

neither ethanol and methanol, nor textural properties (**Figure S5**).

Ethyl acetate (*m/z* 89.055) is another ester compound measured at high concentration after storage, but only in a limited number of accessions (**Figure S4**). As it has already been reported in several fruit species, ethyl acetate content is often highly correlated with ethanol and acetaldehyde levels (Knee and Hatfield, 1981; Larsen, 1995). In this study, high concentrations of *m/z* 89.055 are positively correlated with the content of ethanol and methanol as evidenced in the cultivars 'Jersey' (#22), 'Emerald' (#20), 'Cosmopolitan' (#14), 'Berkeley' (#5), and 'Star' (#44) (**Figure S5**).

Aldehyde and terpene content normally decrease during the last ripening phases of blueberry fruit, as previously demonstrated by Farneti et al. (2017b). In this study, decay of these compounds was evident also for fruit after storage, with variations in concentration that are evidently cultivar dependent. C6 aldehydes, for most hexenal isomers (*m/z* 99.08) and hexanal (*m/z* 101.096), diminished during storage in a genotype dependent manner with cultivars, such as 'Jersey' (#22), 'Toro' (#46), 'Star' (#44), or 'Berkeley' (#5) characterized by a SI lower than -2, and, on the contrary, several nearly stable cultivars, such as 'Darrow' (#16), 'Misty' (#28), or 'Bluecrop' (#7) (**Figure 6D**, **Figure S4**). Hexenal isomers and hexanal contents were highly correlated at both harvest and storage phases, even if these compounds are derived by different free fatty acid precursors, linolenic and linoleic acid respectively (Klee and Tieman, 2018; Ferrão et al., 2020). Based on these outcomes, it is impossible to predict C6 aldehyde content after storage of a blueberry cultivar based solely on the assessment at harvest. Several cultivars, such as 'Berkeley' (#5), 'Emerald' (#20), 'Jersey' (#22), 'Star' (#44), or 'Toro' (#46), were characterized by the lowest content of hexenal isomers (*m/z* 99.08) despite their high values at harvest. On the contrary, other cultivars with low values at harvest, like 'Biloxy' (#6), 'Centra Blue' (#10), 'Eliott' (#19), 'Rubel' (#39), or 'Sky Blue' (#42), showed positive SI values and the highest concentrations after storage. In addition, reinforcing the high variability among the *Vaccinium* germplasm, there were also accessions with stable hexenal content during storage, independent of the concentration assessed at harvest, such as 'Atlantic' (#2), 'Bluecrop' (#7), 'Brigitta Blue' (#9), 'Chandler' (#12), 'Darrow' (#16), or 'Northblue' (#30).

Monoterpenes (*m/z* 137.133) were the VOC class most negatively affected by fruit storage (**Figure 6F**, **Figure S4**). The high variability in monoterpenes content assessed at harvest was extremely reduced after storage. Indeed, cultivars, like 'Aron' (#1), 'Toro' (#46), 'Early Blue' (#17), 'Simultan' (#41) or 'Puru' (#37) showed very low monoterpene content after storage in spite of the high concentration assessed at harvest. Among monoterpene high-ranking cultivars at harvest, only 'Cosmopolitan' (#14) was stable after storage.

Another relevant mass peak for the characterization of blueberry VOC profile was *m/z* 107.086 (**Figure S4**), that is the characteristic fragment of compounds containing a benzoic ring, like ethyl benzene or xylene. No significant differences were detectable based on average values obtained at harvest and after storage, suggesting a stability of this trait during cold storage. Nevertheless, SI values showed an extremely high variability between genotypes, with values ranging between -4 to +4. For instance, cultivars like 'Centurion' (#11), 'Aurora' (#3), 'Mondo' (#29), or 'Elizabeth' (#18), revealed high concentration of *m/z* 107.086 after storage despite the very low concentration at harvest. On the contrary, cultivars like 'Southern belle' (#43), 'Rubel' (#39), 'Nui' (#32), 'Hortblue Poppins' (#35), or 'Atlantic' (#2) were highly ranked at harvest but showed very low values after storage.

Cultivar Characterization Based on Storage VOC Modification

VOC profiling of the blueberry germplasm collection was further analyzed by separately considering the assessments at harvest and after storage, as formerly described for texture. Differently from texture results, the overall VOC profile variability was only partially explained by considering the first two principle components (**Figure 7** and **Figure S6**; Harvest 49%; Postharvest, 61%; SI, 39%).

Nevertheless, *Vaccinium* cultivars were divided into statistically significant clusters, based on Ward hierarchical clustering of the VOC profile, according to the moment of assessment (harvest and post-harvest) and to the storage index (SI). Due to the high multidimensionality of VOC profiles, clusters, based on Euclidean's distances, were not always properly separated over the bidimensional space produced by PCA analysis. In addition, excluding the three *Vaccinium* virgatum accessions, the profiling based on VOC production did not reveal any significant association with the genetic molecular profile based on six SSRs (**Figure S4** and **Figure S6**).

Five clusters of cultivars were statistically distinguishable at harvest based on VOC composition (**Figure 7A**; **Figure S4** and **Figure S6**). Since only 49% of the overall VOC variability is explained by the first two components, the graphical clusters separation in the PCA plot is not sufficiently effective. For instance, the separation of clusters "Cl_2" and "Cl_5" is clearly distinguishable only after adding the third dimension (data not shown). The variability expressed by the first two components is mostly associated with a reduced VOC array, for the most part related to C6 aldehydes and alcohols (*m/z* 81.07, 83.085, 99.08, 101.096), terpenes (*m/z* 137.134), methanol (*m/z* 33.033) and methyl acetate (*m/z* 75.043). Clusters "Cl_1" and "Cl_4" were composed by cultivars with high content of C6 aldehydes and terpenes, such as 'Toro'(#46), 'Northland'(#31), 'Puru' (#37), 'Cosmopolitan' (#14) or 'Jersey'(#22). On the contrary, accessions belonging to "Cl_3" and "CL_2", for instance 'Atlantic' (#2), 'Biloxi' (#6), 'Southern Belle' (#43), or 'Legacy' (#25), had a less intense VOC profile. The three *V. virgatum* accessions which clustered into "Cl_5", namely 'Centra Blue' (#10), 'Centurion' (#11), and 'Sky Blue' (#42), were characterized by very low concentration of terpenes and C6 aldehydes, and high content of acetaldehyde (*m/z* 45.031), ethanol (*m/z* 47.043) and esters (*m/z* 61.023 75.043, 117.091, 131.107).

After fruit storage, the VOC variability expressed by the first two components of the PCA analysis increased up to 61%

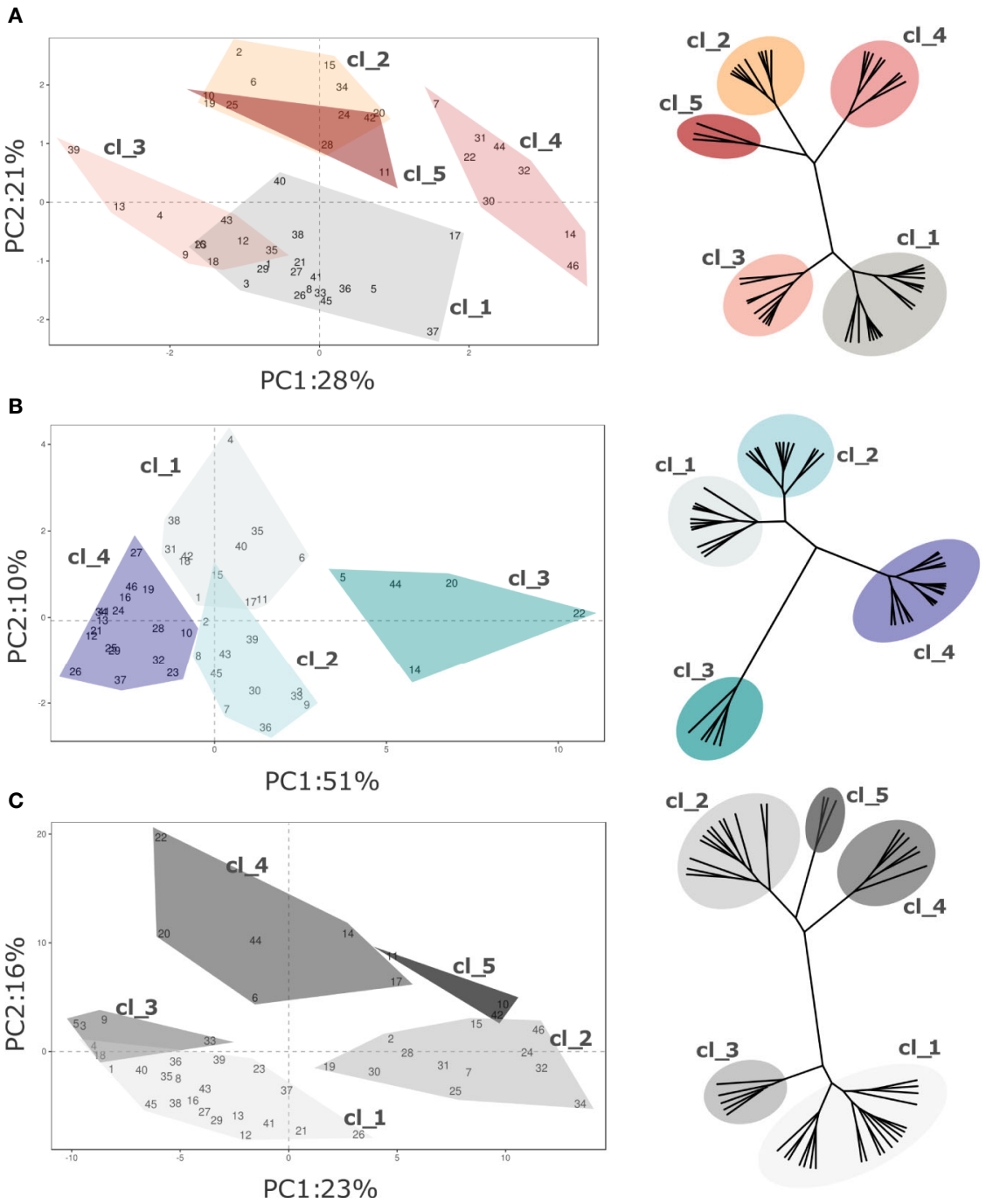

FIGURE 7 | PCA and hierarchical clustering (based on Ward distances) of 46 *Vaccinium* spp cultivars based on VOC profile assessed at **(A)** harvest and **(B)** postharvest, and on the calculated storage index **(C)**. Each point of the PCA plot is the average of three measurements. Loading plots of each PCA are reported in the supplementary **Figure 6**. Clusters highlighted in each PCA plot corresponds to the clusters identified by Ward clustering.

(**Figure 7B**, **Figure S4** and **Figure S6**). Most of this variability was covered by the first component (PC1, 51%), that is highly interrelated with C6 aldehydes (*m/z* 81.070, 99.08, 101.096), C6 alcohols (*m/z* 83.085, 85.100), terpenes (*m/z* 137.134), and with VOCs that were not so relevant to discern cultivars at harvest, principally ethanol (*m/z* 47.043), acetaldehyde (*m/z* 45.031), and several ester compounds (*m/z* 61.023, 75.043, 89.055, 103.076, 117.091, 131.107). Based on that, *Vaccinium* accessions of this study were grouped into four clusters. Accessions with the most modified VOC profile were clustered into "Cl_3". That cluster is

composed only of five accessions, namely 'Berkeley'(#5), 'Cosmopolitan'(#14), 'Emerald'(#20), 'Jersey'(#22), and 'Star'(#44), characterized by the highest concentrations of ethanol, acetaldehyde, methyl acetate (*m/z* 75.043) and ethyl acetate (*m/z* 89.055). This alteration of the VOC profile after postharvest storage may be linked to a raise in fermentation processes due to fruit overripening. Differently, VOC profile of "Cl_2" accessions was for the most part characterized by low concentrations of ethanol and acetaldehyde together with high contents of some ester compounds (*m/z* 75.043, 103.076, 117.091, 131.107), especially the cultivars 'Aurora'(#3), 'Brigitta Blue' (#9), 'North Blue'(#30), 'O'Neal' (#33), and 'Rubel'(#39). Cultivars of the two remaining clusters, "Cl_1" and "Cl_4", were defined by low concentrations of most compounds, except for C6 aldehydes (*m/z* 81.070, 99.08, 101.096) and C6 alcohols (*m/z* 83.085, 85.100).

The first two PCA components, assessed over the SI values, explained only 39% of the VOC profile variability (**Figure 7C**). This low percentage is mostly due to the high statistical noise of the dataset, introduced by the SI calculation (logarithmic of the molecule concentration ratio assessed before and after fruit storage). Based on that, several molecules that were assessed at extremely low concentration, most probably far below their threshold level, might have a significantly high relevance in the statistical analysis (i.e. minimum and maximum concentration of *m/z* 89.201 ranging between 0.00 and 0.16 ppb, resulting in SI values between -8.61 and +6.42). Nonetheless, *Vaccinium* accessions considered in this study were statistically divided into five clusters based on Euclidean's distances (**Figure 7C**, **Figure S4** and **Figure S6**). Clusters "Cl_1" and "Cl_2" grouped cultivars with a more stable VOC profile during storage, such as 'Aron'(#1), 'Blue Moon' (#8), 'Chandler'(#12), 'Northland'(#31), or 'Ozark Blue'(#34). Accessions belonging to cluster "Cl_1" differed by a higher average SI value of some ester related masses (*m/z* 43.015, 61.023, 75.043, 89.055, 103.076). Clusters "Cl_3" and "Cl_4" grouped cultivars (i.e. 'Biloxi' (#6), 'Brigitta Blue' (#9), 'Emerald' (#20), 'Jersey'(#22), or 'Star' (#44)) characterized by high SI values of masses related to esters (*m/z* 43.015, 61.023, 75.043, 89.055, 103.076, 117.091, 131.107), acetaldehyde (*m/z* 45.031), and ethanol (*m/z* 47.043), but low SI values of C6 aldehydes (*m/z* 81.070, 99.08, 101.096). The latter cluster, "Cl_5", included only the three *V. virgatum* cultivars ['Centra Blue' (#10), 'Centurion' (#11), and 'Sky Blue' (#42)] that differed from the other accessions for the higher stability of C6 aldehydes (*m/z* 99.08, 101.096), C6 alcohols (*m/z* 83.085 and 85.100), ethanol (*m/z* 47.043), and acetaldehyde (*m/z* 45.031).

DISCUSSION

Until now, as for many horticultural fruit species (Folta and Klee, 2016; Klee and Tieman, 2018) blueberry breeding selection has been mostly oriented on the amelioration of agronomic traits, such as flowering time, chilling requirements or plant structure, and on standardising the physical-chemical quality traits of the fruit at the time of harvest, ignoring the possible storage effect (Gilbert et al., 2014). Indeed, quality assessments at harvest revealed a limited variability, especially for VOC content, in comparison with the high genetic variability of the *Vaccinium* accessions employed in this study. For this reason, an accurate and objective post-harvest characterization of each accession, based on each quality trait, is necessary for the selection of the optimal parental choice and the best progenies oriented towards distinct market sectors.

The genetic analysis of the plant materials showed that the individuals under investigation are unique genotypes and that the hexaploid *Vaccinium* accessions are genetically diverse and cluster distinctly compared to the tetraploid accessions. On the other hand, there is no evidence of strong genetic structure among the tetraploid cultivars even if distinct clusters for northern and southern highbush blueberry cultivars can be clearly defined. Results of the cluster analysis agreed to what it is reported so far in blueberry (Boches et al., 2006; Bassil et al., 2020). The grouping of highbush blueberry in two main clusters of southern and northern highbush was also visible, as expected, despite some exceptions for which the limiting factor could be also the number of SSRs. In addition, Bassil et al. (2020) recently proposed two new set of markers (5 to 10) including some of the SSRs used in this paper to solve blueberry genotypes, and they showed that the 5-set markers failed in discriminating only two genotypes out of 367 accessions of the USDA germplasm. However, in our study, this genetic clustering could not be correlated, for most of the accessions, either to fruit texture parameters, or to fruit VOCs. Indeed, the choice of parental lines based uniquely on accession's pedigree or genetic similarities, based on six SSRs, is not enough for a parental choice aimed to improve fruit quality. Moreover, that suggests an overall standardization of blueberry fruit quality that has been reached by breeding activity during these years. However, textural and VOC variability among accessions increased after storage, with clusters of cultivars being more distinguishable based on textural and VOC attributes. For instance, concerning texture results, we could identify cultivars that became more turgid and harder after storage while others lost their turgidity and became softer. Regarding VOCs, instead, several cultivars preserved their profile similarly to the one assessed at harvest, while others considerably altered their VOC profile for the most part enhancing the concentration of esters and other compounds associated with fruit fermentation and deterioration, like ethanol and acetaldehyde (Pesis, 2005). Since blueberry fruit is mostly consumed after storage, often after long transcontinental shipments, these findings raised the importance for breeders to evaluate new varieties' quality also after a storage period that simulates commercial requirements.

This high variability on quality traits observed after storage might be determined by genetic differences that regulate fruit physiological, chemical and physical features. According to published studies (Giongo et al., 2013) and ongoing experiments on both segregating population and broad germplasm collection, this lack of straightforward relationship between harvest and postharvest quality features seems to be genotype-dependent. Physiological changes associated with ripening, such as firmness

decay and flavours and off flavours production, are coordinated by a complex network of endogenous hormones, for the most ethylene and ABA. Nevertheless, there is still no consensus on whether blueberry is a climacteric fruit or not (MacLean and Scott NeSmith, 2011). Although a peak in respiration and ethylene production has been observed in blueberry in some studies (Windus et al., 1976; El-Agamy et al., 1982), this was not conclusive in others (Frenkel, 1972). Recent studies confirmed a complex interaction between ethylene softening and sucrose metabolism in blueberry fruit (Wang et al., 2018; Wang et al., 2020). This complexity is evident in the number and type of cell wall-modifying genes (i.e. VcPE and VcPG) and the different ways in which they are regulated. On the contrary, other studies revealed an important role of ABA on fruit ripening regulation (Karppinen et al., 2018; Oh et al., 2018). Post-harvest ABA treatment during bilberry (*Vaccinium myrtillus*) fruit ripening led to the induction in the expression of genes associated with cell wall modifications (Karppinen et al., 2018). Among these, ABA induced genes encoding pectin-modifying enzymes (i.e. VmPL, VmRGLyase, VmβGAL1, and VmβGAL2) as well as genes involved in depolymerization of hemicellulose (i.e.VmXTH and VmCEL) and expansins (i.e. VmEXP1, VmEXP2, and VmEXP3).

Taking into account the high genetic variability considered in this study, we aimed to uncover most of the blueberry texture and VOC variability. However, without a detailed sensory analysis, quantifying the relevance of each trait might be too speculative, especially for VOCs, bearing also in mind the non-linear interaction of these molecules in determining the consumer preference. For this reason, in order to reduce any possible statistical bias in the result interpretation, all data were analysed with unsupervised multivariate statistical methodologies (PCA and hierarchical clustering). Nonetheless, considering each quality trait independently (i.e. **Figure S1** and **Figure S4**) might be useful for the backcross breeding approach, aimed to introduce, or improve, a distinct quality trait to an elite breeding line. To simplify the application of these results, we limited the number of texture and VOC traits that have to be considered (**Figure S7**), according to the loading plots of the principle component analysis and to the results of previously published articles (Giongo et al., 2013; Farneti et al., 2017b). The content of each trait was grouped based on the distribution quantile (low: 0%-25%; middle-low: 25%-50%; middle-high:50%-75%; high:75%-100%), calculated for both harvest and postharvest assessment (**Figure S7**). Accessions employed in the study can be consequently sorted and clustered according to the content of the trait of interest, that can be arbitrarily chosen.

Until now only the research of Ferrão et al. (2020) reports results on employing molecular markers in the selection of blueberry fruit for flavour. Indeed, metabolite genome-wide association analysis (GWAS) elucidated the genetic architecture and demonstrated that blueberry VOC synthesis can be accurately predicted using genomic information. Nonetheless results of that investigation were only based on blueberry quality traits recorded at harvest. Moreover VOCs, for which their genomic regions were detected, showed an extremely low (i.e. linalool) or even negative (i.e. eucalyptol) correlation with consumer taste preferences (Gilbert et al., 2015; Ferrão et al., 2020). Considering that no molecular markers are yet available to predict VOC and texture variations during blueberry storage, the application of reliable phenotyping techniques is still essential to support breeding activity.

Analytical methodologies considered in this study may result in powerful tools for phenotyping quality traits and, at the same time, in developing genetic markers that help to screen blueberry populations. The phenotyping approach suggested in our research, detailed in **Figure 8**, provides the opportunity to use fast and high-throughput techniques to assess a broad number of samples by relatively unskilled personnel, and to follow fruit quality changes during storage. Storage requirements, for instance time length, temperature or atmospheric gas composition, must be optimized according to the breeding objectives (i.e. selection for local market or for overseas exportation). In our case, we established the postharvest assessment after 6 weeks of storage since this prolonged storability is one of the breeding targets requested to extend the Italian blueberry supply.

Analytical detection of traits concerning fruit taste perception, for most part acidity and sweetness, can still be based on refractometer and titrator. Despite the simplicity and lack of sophistication, results obtained by these techniques are properly linked with consumer perception (Gilbert et al., 2015). Nonetheless, it is desirable, in the near future, to use more accurate and high-performance mass spectrometric analytic techniques based, in our opinion, on direct analysis, such as DART-MS (Chen et al., 2007; Guo et al., 2017). Therefore, beside a better identification of compounds determining taste perception, a rapid quantification of blueberry nutraceutical compounds might also be possible.

Fruit texture, is also one of the main quality traits driving consumer preference (Gilbert et al., 2015; Ferrão et al., 2020). In our opinion, being blueberry texture determined by several physical constrains, such as cell turgor, peel elasticity, and cell wall structure, the destructive evaluation of blueberry fruit by texturometer is preferable than the non-destructive assessments based on fruit compression (i.e. Firmtech II; Li et al., 2011; Giongo et al., 2019), laser induced method (Li et al., 2011), hyperspectral imaging (Hu et al., 2015), or Vis-NIR spectroscopy (Hu et al., 2018). Application limits of these non-destructive techniques are still the need of a constant updated calibration of the predictive multivariate algorithm, and the low spatial and spectral resolution (Li et al., 2019). Moreover, for the phenotyping pipeline that we proposed (**Figure 8**) the destructive assessment of texture is not a limiting factor, since analysed fruit can be employed for the analysis of other quality traits, such as total soluble solids, titratable acidity, and VOCs. In that case, the instant freezing of samples using liquid nitrogen, is essential to preserve the organoleptic characteristics of the fruit, that, on the contrary, might be altered by fruit cutting and air exposure.

Bearing in mind that the aim of VOC assessment is to obtain an objective estimation of the aroma perceived by the

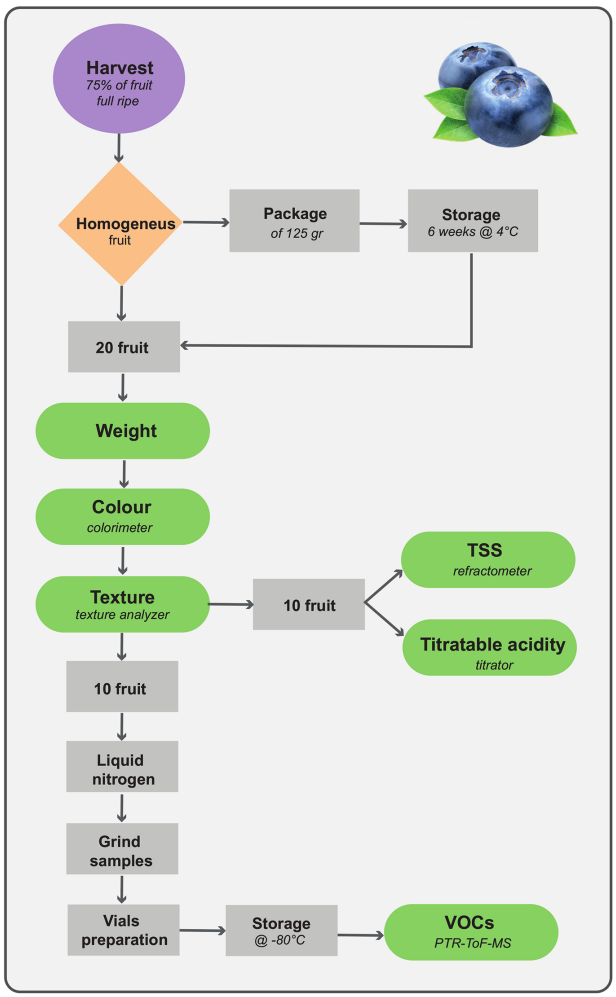

FIGURE 8 | Phenotyping assessment of quality traits applicable for blueberry breeding screening.

consumer during fruit consumption, we consider worthless the application of too aggressive chemical extraction methodologies (i.e. liquid-liquid extraction with hexane or dichloromethane). These methodologies are only necessary for the quantification of compounds at extremely low concentrations that, in case of blueberry fruit, might be under the perception threshold of the consumer. Furthermore, we need high resolution analytical techniques, able to identify and quantify, at once, molecules with different polarity and molecular weight (i.e. methanol and sesquiterpenes) present in a broad concentration range (from ppt to ppm). The extreme complexity of food aroma composition is a challenging issue for any existing analytical technology. The rapid development of mass spectrometry (MS) application in metabolomic studies had a significant impact in the field of VOC analysis. Most of the progresses of MS techniques are focused on instrumental improvements of mass resolution, mass accuracy, sensitivity, and enhanced reproducibility. PTR-MS is particularly suited to develop reliable food VOC fingerprints because it provides handier analytical information (concentration estimation and reduced fragmentation) in comparison with the application of MS-e-noses based on electron impact ionization (Biasioli et al., 2011). PTR-ToF-MS, equipped with multipurpose auto-samplers, provides a rich, informative, and high-throughput fingerprint. This study supports the results of Farneti et al. (2017b), confirming that blueberry VOC profile can be accurately assessed by direct injection techniques. One of the aims of this research was the untargeted analysis by PTR-ToF-MS to disclose VOC differences among blueberry accessions due to genetic differences and prolonged fruit storage, while in the previous research (Farneti et al., 2017b) we mostly focused on differences related with blueberry fruit ripening. Pulling together results of these two investigations, the array of mass peaks suitable to describe most of blueberry VOC variability can be considerably reduced. This information can be applied to target VOC assessment for both breeding selection and quality control within the entire production chain, by adopting less performing, but more handy and inexpensive, direct-injection instruments with a quadrupole mass spectrometer (i.e. PTR-MS or SIFT-MS; Vendel et al., 2019).

This investigation, together with recent findings on blueberry flavour (Ferrão et al., 2020), suggests an accurate and objective road map for *Vaccinium* flavor improvement. A better understanding of genes and enzymes involved in the VOC production and textural modification is still needed. This could lead to genetic and environmental manipulations to optimize aroma at the time of consumption, following shipping and marketing. To this end, future breeding programs focused of prolonged fruit post-harvest storage need to consider blueberry VOC modification. This can be achieved only with a more informed and precise identification of the best performing cultivars to be used as superior parental lines in combination with a reliable phenotyping methodology and molecular markers.

DATA AVAILABILITY STATEMENT

All datasets presented in this study are included in the article/ **Supplementary Material**.

AUTHOR CONTRIBUTIONS

BF designed the research, analyzed and interpreted data, and wrote the manuscript. FM carried out the genetic structure analysis. IK helped with PTR-ToF-MS data analysis. MA assessed the texture analysis and sampled the blueberries. FB guided the PTR-ToF-MS analysis and edited the manuscript. LG coordinated the work design and edited the manuscript.

FUNDING

This work was financially supported by the AdP of the PAT (Provincia Autonoma di Trento) and partially by the project AppleBerry (L6/99 of the PAT).

SUPPLEMENTARY MATERIAL

The Supplementary Material for this article can be found online at: https://www.frontiersin.org/articles/10.3389/fpls.2020.01140/full#supplementary-material

REFERENCES

Abbott, J. A. (1999). Quality measurement of fruits and vegetables. *Postharvest Biol. Technol.* 15 (3), 207–225. doi: 10.1016/S0925-5214(98)00086-6

Bassil, N., Bidani, A., Nyberg, A., Hummer, K., and Rowland, L. J. (2020). Microsatellite markers confirm identity of blueberry (Vaccinium spp.) plants in the USDA-ARS National Clonal Germplasm Repository collection. *Genet. Resour. Crop Evol.* 67, 393–409. doi: 10.1007/s10722-019-00873-8

Beaulieu, J. C., Stein-Chisholm, R. E., and Boykin, D. L. (2014). Qualitative analysis of volatiles in rabbiteyeblueberry cultivars at various maturities using rapid solid-phase microextraction. *J. Am. Soc. Hortic. Sci.* 139, 167–177

Biasioli, F., Yeretzian, C., Märk, T. D., Dewulf, J., and Van Langenhove, H. (2011). Direct-injection mass spectrometry adds the time dimension to (B)VOC analysis. *Trends Anal. Chem.* 30 (7), 1003–1017. doi: 10.1016/j.trac.2011.04.005

Blaker, K. M., Plotto, A., Baldwin, E. A., and Olmstead, J. W. (2014). Correlation between sensory and instrumental measurements of standard and crisp-texture southern highbush blueberries (*Vaccinium* corymbosum L. interspecific hybrids). *J. Sci. Food Agric.* 94 (13), 2785–2793. doi: 10.1002/jsfa.6626

Bian, Y., Ballington, J., Raja, A., Brouwer, C., Reid, R., Burke, M., et al. (2014). Patterns of simple sequence repeats in cultivated blueberries (Vaccinium section Cyanococcus spp.) and their use in revealing genetic diversity and population structure. *Mol. Breed.* 34, 675–689

Boches, P. S., Bassil, N., and Rowland, L. (2006). Genetic diversity in the highbush blueberry evaluated with microsatellite markers. *J. Am. Soc. Hortic. Sci.* 131, 674–686. doi: 10.21273/JASHS.131.5.674

Bruvo, R., Michiels, N. K., D'souza, T. G., and Schulenburg, H. (2004). A simple method for the calculation of microsatellite genotype distances irrespective of ploidy level. *Mol. Ecol.* 13, 2101–2106.

Chen, H., Sun, Y., Wortmann, A., Gu, H., and Zenobi, R. (2007). Differentiation of Maturity and Quality of Fruit Using Noninvasive Extractive Electrospray Mass Spectrometry. *Anal. Chem.* 79 (4), 1447–1455. doi: 10.1021/ac061843x

Chervin, C., Truett, J. K., Speirs, J., Industry, C. P., Unit, H., Box, P. O., et al. (1999). Alcohol Dehydrogenase Expression and Alcohol Production during Pear Ripening. *J. Am. Soc. Hortic. Sci.* 124 (1), 71–75. doi: 10.21273/JASHS.124.1.71

Dorokhov, Y. L., Sheshukova, E. V., and Komarova, T. V. (2018). Methanol in Plant Life. *Front. Plant Sci.* 9, 1–6. doi: 10.3389/fpls.2018.01623

Du, A., Plotto, E. V., Song, M., Olmstead, J., Rouse, R., and States, U. (2011). Volatile composition of four southern highbush blueberry cultivars and effect of growing location and harvest date. *J. Agric. Food Chem.* 59, 8347–8357. doi: 10.1021/jf201184m

Du, X., and Rouseff, R. (2014). Aroma active volatiles in four southern highbush blueberry cultivars determined by gas chromatographyolfactometry (GC-O) and gas chromatography-mass spectrometry (GC-MS). *J. Agric. Food Chem.* 62, 4537–4543. doi: 10.1021/jf500315t

El-Agamy, S., Aly, M. M., and Biggs, R. H. (1982). Fruit maturity as related to ethylene in 'Delite' blueberry. *Proc. Fla. State Hortic. Soc* 95, 245–246.

Farneti, B., Di Guardo, M., Khomenko, I., Cappellin, L., Biasioli, F., Velasco, R., et al. (2017a). Genome-wide association study unravels the genetic control of the apple volatilome and its interplay with fruit texture. *J. Exp. Bot.* 68 (7), 1467–1478. doi: 10.1093/jxb/erx018

Farneti, B., Khomenko, I., Grisenti, M., Ajelli, M., Betta, E., Algarra, A. A., et al. (2017b). Exploring blueberry aroma complexity by chromatographic and direct-injection spectrometric techniques. *Front. Plant Sci.* 8:617. doi: 10.3389/fpls.2017.00617

Ferrão, L. F. V., Johnson, T. S., Benevenuto, J., Edger, P. P., Colquhoun, T. A., and Munoz, P. R. (2020). Genome-wide association of volatiles reveals candidate loci for blueberry flavor. *New Phytol.* 266 (6), 1725–1737. doi: 10.1111/nph.16459

Folta, K. M., and Klee, H. J. (2016). Sensory sacrifices when we mass-produce mass produce. *Horticult. Res.* 3, 16032. doi: 10.1038/hortres.2016.32

Frenkel, C. (1972). Involvement of peroxidase and indole-3-acetic acid oxidase isozymes from pear, tomato, and blueberry fruit in ripening. *Plant Physiol.* 49, 757–763. doi: 10.1104/pp.49.5.757

Gallardo, R. K., Dossett, M., Development, B. C. B. C., Agriculture, C. O., Vm, B. C., Polashock, J. J., et al. (2018). Breeding Trait Priorities of the Blueberry Industry in the United States and Canada. *HortScience* 53, 7, 1021–1028. doi: 10.21273/HORTSCI12964-18

Ge, C., Cui, Y.-N., Jing, P.-Y., and Hong, X.-Y. (2014). An Alternative Suite of Universal Primers for Genotyping in Multiplex PCR. *PLoS ONE* 9 (3), e92826. doi: 10.1371/journal.pone.0092826

Gilbert, J. L., Olmstead, J. W., Colquhoun, T. A., Levin, L. A., Clark, D. G., and Moskowitz, H. R. (2014). Consumer-assisted selection of blueberry fruit quality traits. *HortScience* 49 (7), 864–873. doi: 10.21273/HORTSCI.49.7.864

Gilbert, J. L., Guthart, M. J., Gezan, S. A., De Carvalho, M. P., Schwieterman, M. L., Colquhoun, T. A., et al. (2015). Identifying breeding priorities for blueberry flavor using biochemical, sensory, and genotype by environment analyses. *PloS One* 10 (9), 1–21. doi: 10.1371/journal.pone.0138494

Giongo, L., Poncetta, P., Loretti, P., and Costa, F. (2013). Texture profiling of blueberries (*Vaccinium* spp.) during fruit development, ripening and storage. *Postharvest Biol. Technol.* 76, 34–39. doi: 10.1016/j.postharvbio.2012.09.004

Giongo, L., Ajelli, M., Poncetta, P., Ramos-García, M., Sambo, P., and Farneti, B. (2019). Raspberry texture mechanical profiling during fruit ripening and storage. *Postharvest Biol. Technol.* 149, 177–186. doi: 10.1016/j.postharvbio.2018.11.021

Goff, S. A., and Klee, H. J. (2006). Plant volatile compounds: Sensory cues for health and nutritional value? *Science* 311 (5762), 815–819. doi: 10.1126/science.1112614

Guo, T., Yong, W., Jin, Y., Zhang, L., Liu, J., Wang, S., et al. (2017). Applications of DART-MS for food quality and safety assurance in food supply chain. *Mass Spectrom. Rev.* 36 (2), 161–187. doi: 10.1002/mas.21466

Hancock, J. F. (2009). Highbush blueberry breeding.*HortScience* 41 (2), 20–21.

Hu, M., Dong, Q., Liu, B., Linus, U., and Chen, L. (2015). Postharvest Biology and Technology Estimating blueberry mechanical properties based on random frog selected hyperspectral data. *Postharvest Biol. Technol.* 106, 1–10. doi: 10.1016/j.postharvbio.2015.03.014

Hu, M., Zhai, G., Zhao, Y., and Wang, Z. (2018). Uses of selection strategies in both spectral and sample spaces for classifying hard and soft blueberry using near infrared data. *Sci. Rep.* 8, 1–10. doi: 10.1038/s41598-018-25055-x

Jombart, M. (2008). adegenet: a R package for the multivariate analysis of genetic markers. *Bioinformatics* 24, 1403–1405

Jombart, T., Devillard, S., and Balloux, F. (2010). Discriminant analysis of principal components: A new method for the analysis of genetically structured populations. *BMC Genet.* 11, 94. doi: doi: 10.1186/1471-2156-11-94

Kamvar, Z. N., Tabima, J. F., and Grünwald, N. J. (2014). Poppr: an R package for genetic analysis ofpopulations with clonal, partially clonal, and/or sexual reproduction. *PeerJ* 2, e281.

Karppinen, K., Tegelberg, P., Häggman, H., and Jaakola, L. (2018). Abscisic acid regulates anthocyanin biosynthesis and gene expression associated with cell wall modification in ripening bilberry (*Vaccinium myrtillus* L.) fruits. *Front. Plant Sci.* 9, 1259. doi: 10.3389/fpls.2018.01259

Klee, H. J., and Tieman, D. M. (2018). The genetics of fruit flavour preferences. *Nat. Rev. Genet.* 19, 347–356. doi: 10.1038/s41576-018-0002-5

Klee, H. J. (2010). Improving the flavor of fresh fruits: Genomics, biochemistry, and biotechnology. *New Phytol.* 187 (1), 44–56. doi: 10.1111/j.1469-8137.2010.03281.x

Knee, M., and Hatfield, S. G. S. (1981). The Metabolism of Alcohols by Apple Fruit Tissue. *J. Sci. Food Agric.* 32, 593–600. doi: 10.1002/jsfa.2740320611

Larsen, M. (1995). Firmness and concentrations of acetaldehyde, ethyl acetate and ethanol in strawberries stored in controlled and modified atmospheres. *Postharvest Biol. Technol.* 5, 39–50. doi: 10.1016/0925-5214(94)00012-H

Li, C., Luo, J., and MacLean, D. (2011). A novel instrument to delineate varietal and harvest effects on blueberry fruit texture during storage. *J. Sci. Food Agric.* 91 (9), 1653–1658. doi: 10.1002/jsfa.4362

Li, S., Luo, H., Hu, M., Zhang, M., Feng, J., and Liu, Y. (2019). Arti fi cial Intelligence in Agriculture Optical non-destructive techniques for small berry fruits: A review. *Artif. Intell. Agric.* 2, 85–98. doi: 10.1016/j.aiia.2019.07.002

Lyrene, P. M., Vorsa, N., and Ballington, J. R. (2003). Polyploidy and sexual polyploidization in the genus. *Vaccinium* 133, 27–36. doi: 10.1023/A:1025608408727

MacLean, D. D., and Scott NeSmith, D. (2011). Rabbiteye Blueberry Postharvest Fruit Quality and Stimulation of Ethylene Production by 1-Methylcyclopropene, HortScience horts. *HortScience* 46 (9), 1278–1281. doi: 10.21273/HORTSCI.46.9.1278

Missiaggia, A., and Grattapaglia, D. (2006). Plant microsatellite genotyping with 4-color fluorescent detection using multiple-tailed primers. *Genet. Mol. Res.* 5, 72–78

Oh, H. D., Yu, D. J., Chung, S. W., Chea, S., and Lee, H. J. (2018). Abscisic acid stimulates anthocyanin accumulation in 'Jersey' highbush blueberry fruits during ripening. *Food Chem.* 244, 403–407. doi: 10.1016/j.foodchem.2017.10.051

Paniagua, A. C., East, A. R., Hindmarsh, J. P., and Heyes, J. A. (2013). Moisture loss is the major cause of firmness change during postharvest storage of blueberry. *Postharvest Biol. Technol.* 79, 13–19. doi: 10.1016/j.postharvbio.2012.12.016

Paradis, E., Claude, J., and Strimmer, K. (1994) APE: Analyses of Phylogenetics and Evolution in R language. *Bioinformatics* 20, 289–290.

Pesis, E. (2005). The role of the anaerobic metabolites, acetaldehyde and ethanol, in fruit ripening, enhancement of fruit quality and fruit deterioration. *Postharvest Biol. Technol.* 37 (1), 1–19. doi: 10.1016/j.postharvbio.2005.03.001

Rambla, J. L., Tikunov, Y. M., Monforte, A. J., Bovy, A. G., and Granell, A. (2014). The expanded tomato fruit volatile landscape. *J. Exp. Bot.* 65 (16), 4613–4623. doi: 10.1093/jxb/eru128

Romo-Muñoz, R. R., Dote-pardo, J. D., and Garrido-henríquez, H. G. (2019). Blueberry consumption and healthy lifestyles in an emerging market. *Span. J. Agric. Res.* 17 (4), e0111. doi: 10.5424/sjar/2019174-14195

Schwarz, G. (1978). Estimating the dimension of a model. *Ann. Stat.* 6, 461–464. doi: 10.1214/aos/1176344136

Tadege, M., Dupuis, I., and Kuhlemeier, C. (1999). Ethanolic fermentation: new functions for an old pathway. *Trends Plant Sci.* 4 (8), 320–325. doi: 10.1016/S1360-1385(99)01450-8

Tieman, D., Zhu, G., Resende, M. F. R., Lin, T., Nguyen, C., Bies, D., et al. (2017). A chemical genetic roadmap to improved tomato flavor. *Science* 355 (6323), 391–394. doi: 10.1126/science.aal1556

Vendel, I., Hertog, M., and Nicolaï, B. (2019). Fast analysis of strawberry aroma using SIFT-MS: A new technique in postharvest research. *Postharvest Biol. Technol.* 152, 127–138. doi: 10.1016/j.postharvbio.2019.03.007

Wang, S. Y., Zhou, Q., Zhou, X., Wei, B. D., and Ji, S. J. (2018). The effect of ethylene absorbent treatment on the softening of blueberry fruit. *Food Chem.* 246, 286–294. doi: 10.1016/j.foodchem.2017.11.004

Wang, S., Zhou, Q., Zhou, X., Zhang, F., and Ji, S. (2020). Ethylene plays an important role in the softening and sucrose metabolism of blueberries postharvest. *Food Chem. 2020;* 310, 125965. doi: 10.1016/j.foodchem.2019.125965

Windus, N. D., Shutak, V. G., and Gough, R. E. (1976). CO2 and C2H4 evolution by highbush blueberry fruit. *HortScience* 11, 515–517.

Conflict of Interest: The authors declare that the research was conducted in the absence of any commercial or financial relationships that could be construed as a potential conflict of interest.

Advantages of publishing in Frontiers

OPEN ACCESS
Articles are free to read for greatest visibility and readership

FAST PUBLICATION
Around 90 days from submission to decision

HIGH QUALITY PEER-REVIEW
Rigorous, collaborative, and constructive peer-review

TRANSPARENT PEER-REVIEW
Editors and reviewers acknowledged by name on published articles

Frontiers
Avenue du Tribunal-Fédéral 34
1005 Lausanne | Switzerland

Visit us: www.frontiersin.org
Contact us: info@frontiersin.org | +41 21 510 17 00

REPRODUCIBILITY OF RESEARCH
Support open data and methods to enhance research reproducibility

DIGITAL PUBLISHING
Articles designed for optimal readership across devices

FOLLOW US
@frontiersin

IMPACT METRICS
Advanced article metrics track visibility across digital media

EXTENSIVE PROMOTION
Marketing and promotion of impactful research

LOOP RESEARCH NETWORK
Our network increases your article's readership